

Physiology and Electrochemistry of Nerve Fibers

Ichiji Tasaki

Laboratory of Neurobiology
National Institute of Mental Health
National Institutes of Health
Bethesda, Maryland

1982



ACADEMIC PRESS

A Subsidiary of Harcourt Brace Jovanovich, Publishers

New York London

Paris San Diego San Francisco São Paulo Sydney Tokyo Toronto

**BIOPHYSICS AND
BIOENGINEERING SERIES**

A Series of Monographs and Edited Treatises

EDITOR

ABRAHAM NOORDERGRAAF

*Department of Bioengineering D2
University of Pennsylvania
Philadelphia, Pennsylvania*

- 1** ABRAHAM NOORDERGRAAF. *Circulatory System Dynamics*. 1978
- 2** MARY PURCELL WIEDEMAN, RONALD F. TUMA, AND
HARVEY NORMAN MAYROVITZ
An Introduction to Microcirculation. 1981
- 3** ICHIJI TASAKI. *Physiology and Electrochemistry of Nerve Fibers*. 1981

In preparation

- 4** L. L. HENCH AND E. C. ETHRIDGE.
Biomaterials: An Interfacial Approach. 1982

264017

615

TAS e2

ALL RIGHTS RESERVED.
NO PART OF THIS PUBLICATION MAY BE REPRODUCED OR TRANSMITTED IN ANY FORM OR BY ANY MEANS, ELECTRONIC OR MECHANICAL, INCLUDING PHOTOCOPY, RECORDING, OR ANY INFORMATION STORAGE AND RETRIEVAL SYSTEM, WITHOUT PERMISSION IN WRITING FROM THE PUBLISHER.

ACADEMIC PRESS, INC.
111 Fifth Avenue, New York, New York 10003

United Kingdom Edition published by
ACADEMIC PRESS, INC. (LONDON) LTD.
24/28 Oval Road, London NW1 7DX

Library of Congress Cataloging in Publication Data

Tasaki, Ichiji, Date.
Physiology and electrochemistry of nerve fibers.

(Biophysics and bioengineering series ; v. 3)
Includes bibliographies and index.
1. Neural conduction. 2. Action potentials (Electrophysiology) 3. Electrochemistry. I. Title. II. Series.
QP363.T325 599.01'88 81-20486
ISBN 0-12-683780-5 AACR2

PRINTED IN THE UNITED STATES OF AMERICA

82 83 84 85 9 8 7 6 5 4 3 2 1

686491°

Contents

<i>Preface</i>	xiii
1 Introduction	
Text	1
2 The Dawn of Electrophysiology	
A. Early Studies of Animal Electricity	5
B. The Discovery of Injury and Action Current	8
C. The First Measurement of the Rate of Nerve Conduction	10
D. du Bois–Reymond’s Theory of Nerve Excitation	13
E. Pflüger’s Rule of Excitability and Anodal Block of Nerve Conduction	14
F. The Membrane Hypothesis	16
References	19

3	The Rise and Fall of Theories of Nerve Excitation	
	A. The Downfall of du Bois–Reymond’s Theory of Excitation	22
	B. Nernst’s Semipermeable Membrane Theory	24
	C. The Colloid Chemical Theory of Loeb and Höber	27
	D. The Strength–Duration Relation and Chronaxie	28
	E. The Two Factor Theory	30
	F. Rushton’s Concept of Liminal Length	32
	References	34
4	Early Observations of Saltatory Conduction of Nerve Impulses	
	A. Isolation of Single Myelinated Nerve Fibers	37
	B. Measurement of Threshold along a Myelinated Nerve Fiber	39
	C. Tripolar Stimulation of a Nerve Fiber	43
	D. The Electric Resistance of the Nodal Membrane	45
	E. Propagation of Nerve Impulses across Inexcitable Nodes	47
	F. The Pathway of the Local Current	51
	G. The Capacitor-like Behavior of the Myelin Sheath	53
	H. Further Studies of the Action Currents of Myelinated Nerve Fibers	55
	I. Microelectrode Recording of Electric Responses from Myelinated Nerve Fibers.	57
	References	59
5	Conduction of Impulses in Myelinated Nerve Fibers	
	A. The All-or-None Behavior of the Node of Ranvier	62
	B. Refractory Period	65
	C. Abolition of Action Potential	66
	D. The Fall of the Membrane Resistance during Nerve Excitation	69
	E. The Resistance and Capacity of the Myelin Sheath and of the Nodal Membrane	71

F. Effect of Polarizing Current on Nerve Conduction	74
G. Nerve Conduction during the Relatively Refractory Period	77
H. Nerve Conduction in the Anesthetized Region of Nerve Fiber	80
I. Experimental Demyelination	85
J. The Relation between Fiber Diameter and Conduction Rate	87
References	90
6 Electric Excitation of Single Myelinated Fibers	
A. Consideration of the Ultrastructure of the Myelin Sheath	93
B. The Cable Equation	95
C. The Strength–Latency Relation	98
D. Latent Addition	100
E. The Limiting Quantity of Electricity	102
F. Superposition of Threshold Depression	104
G. Strength–Duration Relation and Latent-Addition Curve	107
H. Strength–Frequency Relation for High-Frequency AC	109
I. Variation of Rheobase and Chronaxie along the Nerve Fiber	111
References	112
7 Accommodation in Myelinated Nerve Fibers	
A. Excitation by Linearly Rising Voltage Pulses	114
B. Exponentially Rising Voltage Pulses	116
C. Exponentially Rising Voltage with Superposed DC and Double Condenser Pulses	119
D. Excitation by Low-Frequency AC	120
E. Repetitive Firing of Action Potentials	122
F. Cathodal Depression and the Minimal Gradient	125
G. Break Excitation	127
References	128

8 Emergence of the Squid Giant Axon

A. Nonmyelinated Nerve Fibers	130
B. Intracellular Recording of Action Potentials	131
C. Fall of Membrane Resistance during Excitation	133
D. Potassium Ion and the Membrane Potential	136
E. Sodium Ion and Excitability	140
F. Intracellular Wiring of Squid Giant Axons	143
G. The Voltage Clamp Procedure	146
H. The Hodgkin–Huxley Theory of Nerve Excitation	148
References	152

9 Morphology and Biochemistry of the Squid Giant Axon

A. The Ultrastructure of the Sheath Components	155
B. Electrolytes, Proteins, and Lipids in the Axoplasm	157
C. The Ultrastructure of the Ectoplasm	160
D. Release of Submembranous Proteins during Excitation	162
E. Chemical Modification of Proteins in the Axon	164
F. Models of the Plasma Membrane	168
G. Binding of Tetrodotoxin to the Nerve Membrane	169
References	173

10 Further Electrophysiological Studies of Intact Squid Axons

A. The Relation between Axon Diameter and Conduction Velocity	177
B. Intracellular Injection of Tetraethylammonium Salt	179
C. Abolition of a Prolonged Action Potential	181
D. Hyperpolarizing Responses in Potassium-Rich Media	182
E. Chemical Stimulation of Nerve Fibers	185
F. Monnier's Phenomena of Pararesonance	187
G. Periodic Miniature Responses	189
H. The Discreteness of Miniature Responses	191
I. Classification of Chemical Stimulants	193
J. Miniature Responses Generated by Electric Currents	195
K. Effects of TTX and TEA on Miniature Responses	198

L. Membrane Noise and Miniature Responses	201
References	203

11 Squid Giant Axons under Internal Perfusion

A. Techniques of Intracellular Perfusion	206
B. Effects of Anions inside the Axon	208
C. Substitution of External Na-Ion with Polyatomic Univalent Cations	210
D. Substitution and Dilution of External Divalent Cation Salts	213
E. Dilution of the Intracellular Potassium Salt Solution	215
F. Substitution of Na for Internal K on Membrane Potential	216
G. Prolongation of Action Potential Duration by Substitution of Na for Internal K	219
H. The Resistance-Flux Product	219
I. Influx of Calcium Ion	223
J. Effects of Changing the Internal pH	225
K. Effects of Ca-Ion on the Duration of Prolonged Action Potentials	228
References	229

12 Macromolecular Transitions

A. Bi-Ionic Action Potentials	232
B. Action Potentials Observed with Na-Ion Internally	234
C. Bi-Ionic Action Potential Observed with K-Ions Internally	236
D. Polyatomic Univalent Cations in the Axon Interior	238
E. The Effect of External Na-Salt on Bi-Ionic Action Potentials	239
F. Abrupt Depolarization	242
G. Hyperpolarizing Responses in Internally Perfused Axons	244
H. Cyclic Changes in Membrane Properties—Hysteresis	246
I. Instability Observed near the Critical Point for Transition	248
J. Macromolecular Transitions under Voltage Clamp	250
K. Demonstrations of Domains in Excited and Resting States	252
References	254

13 A Physicochemical Approach and a Model

A. Early Relation between Physical Chemistry and Physiology	256
B. Unstirred Diffusion Layer	258
C. An Example of Current–Voltage Relations	260
D. Intramembrane Concentration Profiles	263
E. A Macromolecular Model of Two Discrete States of Nerve Membrane	265
F. A Physicochemical Theory of Conformational Transition	267
G. Initiation, Termination, Abolition, and Repetitive Firing of Action Potentials under Bi-Ionic Conditions	269
H. A Macromolecular Interpretation of Excitation Processes in Intact Axons	272
I. Domains of the Membrane in Its Excited State	275
References	278

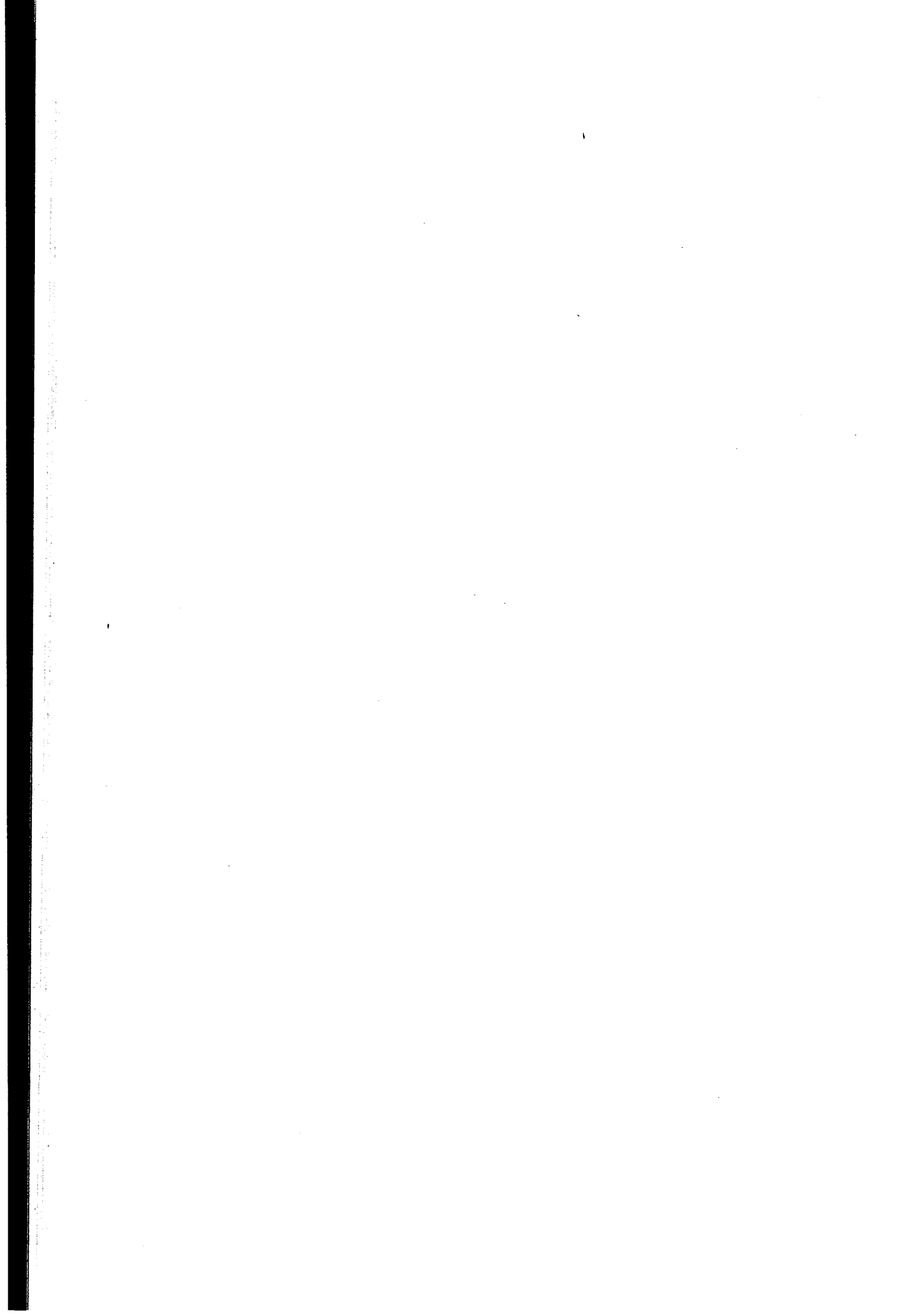
14 Electrochemical Considerations of the Classical Membrane Theory

A. Electrochemical Properties of the Squid Axon: Recapitulation	281
B. Polarization of the Axon Membrane	282
C. Sodium Influx and Production of an Action Potential	285
D. Measurements of Ion Permeability with Radioisotopes of Na- and K-Ions	287
E. Accumulation of K-Salts in Protoplasm	290
F. Single Ion Conductances in Equivalent Circuit Membrane Model	293
G. Determination of EMF by Voltage Clamping	296
H. Liquid Membranes and Porous Membranes	298
References	301

15 Optical Studies of the Axon Membrane

A. Nonelectrical Signs of Nerve Excitation	304
B. Small Movements of the Axon Surface during Action Potential	305

C. Ectoplasm and Birefringence Response	308
D. Optical Responses Produced by Expansion of Dye-Loaded Endoplasm	310
E. Transient Change in Light Absorption Associated with Excitation of Vially Stained Nerve	312
F. Spectra of Light Absorption Responses	316
G. Mathematical Expressions for Spectra of Optical Responses	318
H. Analyses of Light Absorption Responses	323
I. Relation between Optical Responses and the Membrane Potential	328
J. Optical Setup for Detection of Transient Changes in Extrinsic Fluorescence	329
K. Physicochemical Factors Affecting Production of AmNS Fluorescence Responses	331
L. Spectral Analysis of Fluorescence Responses	333
M. Fluorescence Polarization Studies	336
N. General Comment on Optical Studies	338
References	340
<i>Index</i>	343



Preface

This book is written for students of biology and medicine who are interested in investigating the properties of nerve fibers. A great number of experimental facts known to us at present are described and interpreted on the basis of our present level of understanding of morphology, biochemistry, and physical chemistry of the nerve fiber. Old theories, which were once popular, are also discussed in some detail, for the experimental bases of those theories are still meaningful and ought not to be forgotten. Throughout this volume, effort is made to trace the origins of the concepts that are important in studying the physiology of the nerve fibers.

Historically, evolution of the study of physiology of nerve fibers is linked closely with that of electrochemistry. The foundations were laid by prominent physical chemists: Hermann Helmholtz (1850), Wilhelm Ostwald (1890), Walther Nernst (1899), and others. In addition, many important discoveries in physical chemistry were made by investigators known as biologists or physiologists (see Chapter 13). Thus, great efforts were made in classical physiology to explain properties of nerve fibers in physicochemical terms.

With the advent of the age of electronic engineering, however, the traditionally close tie between physical chemistry and physiology was weakened considerably. Driven by the increasing need for advanced knowledge of various electronic devices employed in their experiments, investigators of physiology started to interpret physiological findings in terms of electronic engineers' concepts, e.g., positive feedback, channels, gates, equivalent circuits,

and less emphasis was placed, in recent years, on physicochemical approaches. I have therefore made a conscious effort to "translate" modern electrophysiological terms into physicochemical language.

One of the difficulties encountered in writing this book has been that many students of biology and medicine are not sufficiently familiar with the basic concepts in thermodynamics and electrochemistry. To alleviate this difficulty, an effort has been made to refer to textbooks and papers where the concepts employed to explain electrophysiological data are explained.

This book consists of five general areas of investigation. In Chapter 1, the significant events that led us to the present state of understanding of the behavior of nerve fibers are given in chronological order. In Chapters 2 and 3, the properties of the frog sciatic nerve, known before the advent of the single-fiber technique, are described. An historical account of the discoveries of the action current and conduction velocity and old theories of nerve excitation are presented. Chapters 4 through 7 deal with properties of isolated myelinated nerve fibers. The process of saltatory conduction and experimental facts concerning electrical excitation are explained. In Chapters 8 to 14, old and recent experiments on squid giant axons are discussed. I have focused on experimental results obtained by using the techniques of intracellular perfusion. The experimental results obtained were interpreted on the basis of the theory developed by Jacques Loeb (1900) and Cremer (1906) and combined with the concept of stability of the membrane. In Chapter 15, I have directed the discussion toward the experimental findings obtained by recording nonelectrical signs of nerve excitation. The behavior of dye molecules in and near the axon membrane has yielded useful information about the state of membrane macromolecules during nerve excitation.

I express my sincere gratitude to Nobuko Tasaki and Patricia Kenny for the preparation of figures and charts. I also wish to thank Zelda Wolk, Mary Clampitt, Irma Zimmerman, and Sandra Means, who prepared the manuscript of this book for publication. I thank Professors Torsten Teorell and Akira Watanabe, Drs. Paul Maclean and Jorgen Fex, and members of the Laboratory of Neurobiology who read portions of the manuscript and gave me valuable suggestions. I am also grateful to the many physiologists who permitted me to reproduce various figures and tables: Professor A. L. Hodgkin, Dr. K. S. Cole, Professor A. F. Huxley, Dr. P. Rosenberg, and Dr. B. G. Uzman.

Ichiji Tasaki

Physiology and Electrochemistry of Nerve Fibers

1. Introduction

In this book, a large number of experiments on physiological properties of nerve fibers are described and the results are analyzed from a physicochemical point of view. It is shown that physiology and electrochemistry of nerve fibers have developed to the present level in three, more-or-less discrete, stages. The discovery of the action current and of the conduction velocity of a nerve impulse marked the opening of the first stage. The second stage started when electrophysiological methods for examining properties of individual nerve fibers were devised. The invention of the technique of intracellular perfusion laid the foundation for the third stage. Studies of nonelectrical signs of nervous activity furnished, from time to time, valuable information concerning the physicochemical nature of excitation processes. It is emphasized that every significant achievement in the field has been invariably preceded by advancements in allied sciences.

The significant events that contributed to the development of our present knowledge about the properties of nerve fibers are listed below in chronological sequence.

- 1746: Leiden jar was invented; physiological action of electric shocks was widely recognized.
- 1791–1800: The Galvani–Volta controversy aroused great interest in studies of electricity; Volta’s pile—a continuous source of electricity—was invented.
- 1808: Na, K, Ca, Mg, etc., were discovered by electrolysis (Davy).
- 1822: Galvanometer was invented (Ampère and Babinet).
- 1828–1840: Injury current of the muscle was recognized (Nobili, Matteucci).
- 1843–1848: Action current of the muscle and nerve was discovered (du Bois-Reymond).
- 1850: The velocity of nerve conduction was determined (Helmholtz).
- 1855: Fick’s diffusion equation was published.
- 1871: The all-or-none property of the cardiac muscle was described (Bowditch).
Node of Ranvier was discovered (Ranvier).

- 1879: Cable properties of the nerve were examined and the local current theory was proposed (Hermann).
- 1880: Effect of K ion on electric properties of the muscle was discovered (Biedermann).
- 1882–1886: Salt solution for maintaining the normal contractility of the heart muscle was described (Ringer).
- 1883: Dissociation of electrolytes in water was demonstrated (Arrhenius).
- 1885: The mobilities of ions were determined (Kohlrausch).
- 1890: The concept of ionic (charged) membranes, physical and biological, was formulated (Ostwald).
- 1889–1890: The Nernst–Planck electrodiffusion equations were formulated and the origin of emf's in electrolyte solutions was clarified.
- 1899–1910: The theory of nerve excitation of Nernst and Hill overshadowed the old theory of du Bois-Reymond.
- 1899–1912: Attempts were made at explaining bioelectric phenomena on the basis of the Nernst–Planck equations (Nernst, Cremer, Bernstein).
- 1900–1920: The importance of Ca ion in excitation and contraction was recognized, and the colloid–chemical (macromolecular) theory of nerve excitation was proposed (Loeb, Höber, Bethe).
- 1911: Donnan's paper on membrane equilibrium was published.
- 1926–1928: Electric responses of single myelinated nerve fibers were recorded by using electronic amplifiers (Adrian, Zotterman, Bronk).
- 1934: The importance of Ranvier nodes in excitation and conduction was recognized (Kubo, Ono, Tasaki, Erlanger, Blair).
- 1934–1939: Intrinsic rhythmicity of the nerve fiber was studied (Monnier, Fessard, Arvanitaki).
- 1935–1936: The Teorell–Meyer–Sievers membrane theory was formulated.
- 1937–1940: The validity of the local circuit theory was established (Rushton, Hodgkin, Tasaki, Katz, Schmitt).
- 1939: The fall of the membrane impedance during action potentials was demonstrated (Cole and Curtis).
- 1939–1941: Intracellular recording of the resting and action potentials was accomplished (Hodgkin, Huxley, Cole, Curtis).
- 1939–1942: The role of the myelin sheath and the node of Ranvier in nerve excitation and conduction was clarified (Tasaki).

- 1949: The importance of extracellular Na ion in nerve excitation was emphasized (Hodgkin and Katz).
The method of space clamping of squid giant axons was invented (Marmont).
- 1952: The process of nerve excitation was explained on the basis of an equivalent electric circuit (Hodgkin and Huxley).
- 1961–1962: The technique of intracellular perfusion was invented (Baker, Hodgkin, Shaw, Tasaki, Watanabe, Takenaka).
- 1967–1969: Action potentials were recorded from axons with only a Na-salt solution internally and a Ca-salt solution externally (Watanabe, Tasaki, Lerman). Bistability of the nerve membrane was emphasized (Tasaki).
- 1967–1971: Assumption of spatial independence of Na and K channels was popularized by a number of investigators.
- 1968: Changes in turbidity and in birefringence during action potentials were discovered (Cohen, Keynes, Hille).
Optical signals were recorded from vitally stained nerve fibers (Tasaki, Watanabe, Sandlin, Carnay).
- 1980: Swelling of nerve fibers during action potentials was demonstrated (Tasaki and Iwasa).

At present, the field of investigation with which we are concerned is not exactly in a rapidly developing stage. Nevertheless, a number of investigators are making attempts at advancing the frontier of our knowledge. In recent years, electrophysiological properties of "single ion channels" have been pursued on the premise that there are two discrete conformational states in the macromolecular elements of the membrane. Vigorous efforts are being made also toward elucidating the organization of various macromolecular elements in and near the axon membrane by using biochemical, electron microscopic, and immunological techniques.

Currently, a few studies are being conducted indicating that ion channels for different alkali ions in the nerve membrane are not independent. However, it seems unlikely that the proponents of the independence hypothesis will be convinced by the new and the old studies which refute the hypothesis that there is an independent channel for each of Na-, K-, and Ca-ions.

Reflecting on the difficulty of convincing his opponents, Max Planck once remarked that, in physics, a new idea is not usually accepted by convincing one's opponents step by step, but rather, it is accepted when the opponents die out and the new generation accepts the idea from the outset (see p. 267 in "Wege zur physikalischen Erkenntnis," Hirzel, Leipzig, 1933). In the field of physiology and medicine, the factors that determine the acceptability and

popularity of new ideas are undoubtedly more complicated than in physics. Furthermore, it is far more difficult in this field to make plausible conjectures as to the future development. Nevertheless, there is no doubt that, in the future, new epoch-making discoveries will be made by young investigators who refuse to complacently accept the majority view. The goal of this book is to supply these investigators with selected but unadulterated experimental facts.

2. The Dawn of Electrophysiology

A. EARLY STUDIES OF ANIMAL ELECTRICITY

In the mid eighteenth century, a number of simple, but important, observations on electricity brought about substantial progress in our understanding of the nature of the imponderable "electric fluid." The great achievements made in the field of physics had a profound impact on physiology and medicine at that time. The philosophical speculation that electricity might be playing a crucial role in various aspects of animal functions was a natural product of the scientific atmosphere of the period.

Luigi Galvani's celebrated memoir on animal electricity was published in 1791. It is very interesting to inquire into the circumstances that led Galvani to his observations and interpretation. Hence, we shall digress for a moment from our main subject, the animal electricity, and briefly describe what was known about electricity in general at the time of Galvani. The major source of the following accounts is Joseph Priestley's brilliant and widely circulated book, "The History of Electricity," first published in 1767.

From *ηλεκτρον*, the Greek name for amber, is derived the term "electricity." Early in the eighteenth century, glass, sealing wax, sulfur, etc., as well as amber, were known to be "electric," namely, to have the property of attracting light objects when rubbed. During the fourth decade of the century, metals and the human body were found to conduct electricity (Gray, 1735–1736). Shortly afterward, electric machines for rubbing glass tubes or globes with woolen cloth were invented (Winkler, 1744–1745). Understandably, the general concept of electricity was still hazy and controversial.

The Leiden jar for accumulating electricity was invented in about 1745 (see Muschenbroeck, 1746). Following this invention electricity became a household word in Europe: public shows were held in many countries demonstrating frightening sensations produced by electric shocks (see p. 85 in Priestley, 1767). Soon, Benjamin Franklin (1751) demonstrated, using a small electrified object fixed at the end of a fine silk thread, that the sign of the electricity accumulated inside a Leiden jar is opposite to that on the exter-

nal surface of the jar. Another great event that aroused considerable public attention on electricity was the publication of Franklin's experiments demonstrating the identity of electricity and the matter of lightning and thunder (Franklin, 1751). Immediately, studies of the atmospheric electricity were carried out in many parts of Europe. The well-known tragic incident in the history of electricity, the death of Professor G. W. Richman of Petersburg (Leningrad), who was struck by lightning during his experiments on the atmospheric electricity, took place in 1753.

Medical and biological application of electric shocks also followed the invention of the Leiden jar. Patients with a variety of diseases were treated by physicians and physicists who had large electric machines (see p. 408 in Priestley, 1767). Electricity was believed to quicken the growth of plants. The effects of electric shocks on frog muscles and other animal tissues were studied by physicists, including Priestley. Powerful stimulating effects of electricity on the nerve-muscle preparation of the frog were noted by M. A. Caldani, Galvani's immediate predecessor as Professor of Anatomy at Bologna (see p. 145 in Caldani, 1760).

Galvani's memoir (1791) consists of four parts. In Part I he showed that a frog nerve-muscle preparation on a table could be stimulated by a sparking electric machine on the same table when he touched the nerve with a piece of metal held by hand. He saw twitches of the muscle whenever he brought the edge of his scalpel in contact with the nerve. Obviously, there was a flow of electricity (by the process which we now call capacitive coupling) from the machine to the ground through the nerve-muscle preparation. Although flow of electricity between two spatially separated conductors was known among physicists studying electricity (see pp. 253 and 438 in Priestley, 1767), Galvani did not know it and was completely puzzled by his finding. In Part II, he described his observation on the effect of atmospheric electricity on the nerve-muscle preparation. He put up an iron wire connecting the roof of his house to a frog preparation on a table near the house. He saw powerful twitches of the muscle when, in stormy weather, lightning and dark clouds approached his house. Since a study of the atmospheric electricity had been carried out also in Italy (see p. 357 in Priestley, 1767), Galvani could have anticipated his results. Nevertheless, he was astonished by the high sensitivity of the frog preparation to atmospheric electricity.

In Part III, Galvani described his finding that a nerve-muscle preparation could be stimulated by a bimetallic arc with its one end making contact with the nerve or the spine and the other with the muscle or the leg (see Fig. 2.1). He also saw that a unimetallic arc or a bimetallic arc with an intercalated nonconducting material is ineffective in stimulating the nerve. Nevertheless, Galvani explained this finding by assuming that muscle fibers were analogous to electrified Leiden jars and that the metallic arc brought about a dis-

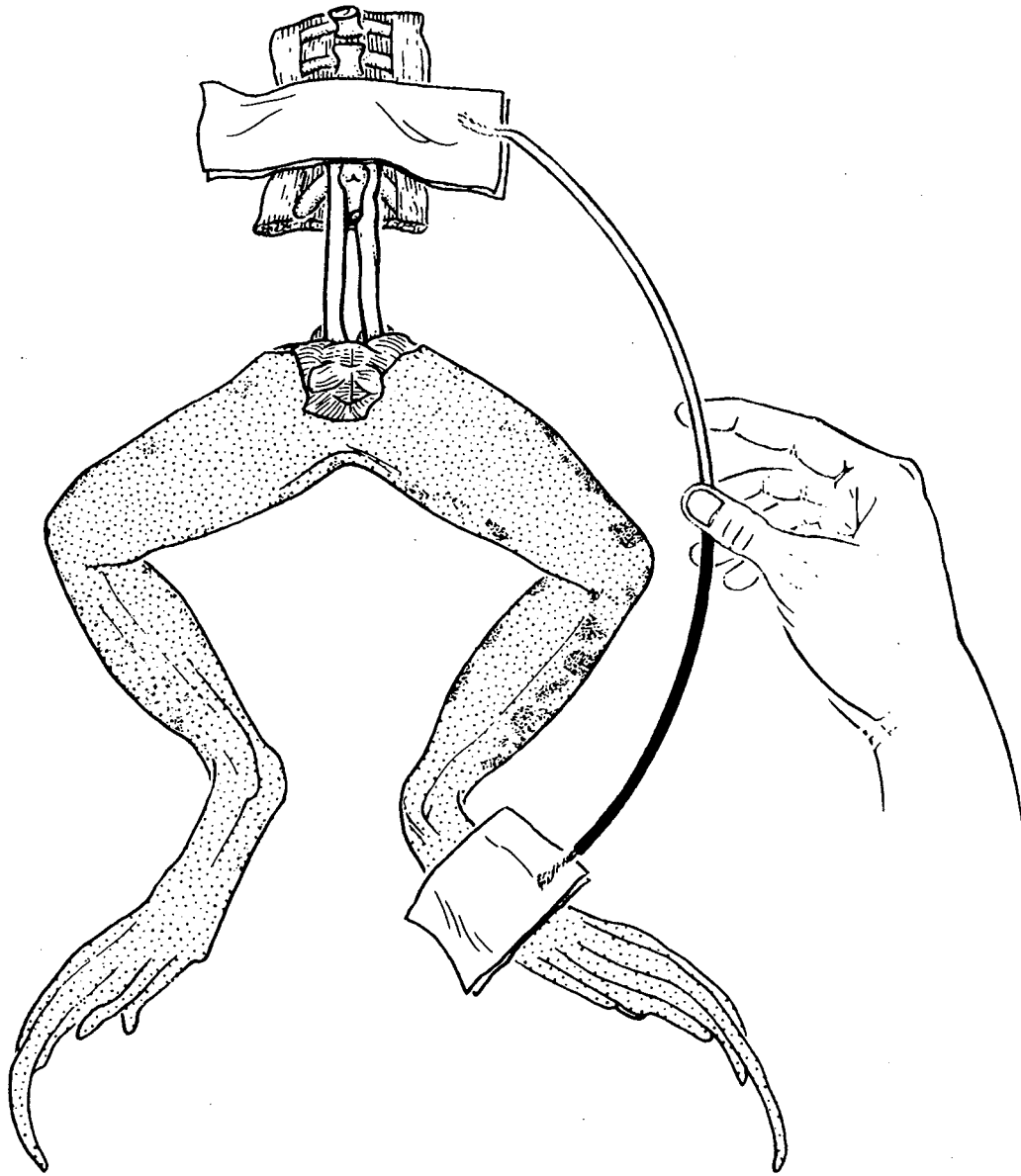


Fig. 2.1 One of Galvani's experimental setups used to demonstrate twitches of frog muscles produced by "conducting animal electricity" through an arc made of iron and silver. (Adapted from Fig. 9 of Galvani's "Commentary.")

charge of this animal electricity (Part IV). Later, Volta (1800) showed that the bimetallic arc is a source of continuous electric current and that none of Galvani's experiments can be regarded as evidence for the existence of animal electricity.

According to Matteucci (1847, p. 3), a bimetallic arc was used by Swammerdam to stimulate a nerve-muscle preparation of the frog in the middle of the seventeenth century. More significantly, Sulzer (1752, 1762) showed that the sensory nerve of the tongue could be stimulated by a bimetallic arc. Apparently, Galvani was not aware of these previous findings.

Galvani's memoir and Volta's objection to Galvani's interpretation of the

experiments on animal electricity created great excitement in the scientific community! To present-day students of physics and physiology, it might seem inconceivable that these simple and almost trivial observations of Galvani appeared so important and exciting. The reason for the excitement appears to be that many romantic investigators and laymen of that period were fascinated by the experiments attempting to interpret various aspects of life phenomena as being electrical in nature (see p. 144 in Rothschild, 1973). Galvani was aware of the situation that the hypothesis of animal electricity, already prevalent at that time, did not have a sound experimental basis. Indefatigably, Galvani attempted to replace the age-old "animal spirit" with "animal electricity" (see p. 169 in Hoff, 1936). Extending Galvani's hypothesis of animal electricity, some physicians claimed that electricity had mysterious curative effects on a variety of diseases (see p. 244 in Fulton and Cushing, 1936).

Later on, in an anonymous tract, it was shown that a nerve-muscle preparation could be excited without metal, simply by bringing the nerve in contact with another muscle (see p. 260 in Fulton and Cushing, 1936; see also Mauro, 1969). Shortly afterward, it was shown further that, when the nerve of a muscle-nerve preparation was placed quickly between the freshly cut surface and the intact portion of a muscle, weak twitches of the muscle could be observed repeatedly (see p. 367 in Humboldt, 1797). The twitch without metal may be regarded as evidence for stimulation by animal electricity. (Note that the potential difference between the cut surface and the intact part of the gastrocnemius muscle falls quickly to 35–50 mV; the potential difference required to stimulate a normal sciatic nerve is about 30 mV. The effectiveness may vary depending on how the nerve is brought in contact with the muscle.)

In conclusion, one might say that electrophysiology had a glamorous, but confusing, beginning. First, powerful stimulating effects of electricity on nerves and muscles became known to physiologists. Next, the phenomenon that may be regarded as a sign of stimulation of the nerve by animal electricity was vaguely recognized by Galvani and his followers.

B. THE DISCOVERY OF INJURY AND ACTION CURRENT

Volta's invention of his pile, a stable and continuous source of electric current (Volta, 1800), opened up a new era in physics and chemistry. Soon, Davy (1808) succeeded in isolating, by electrolysis, many biologically important elements including sodium, potassium, calcium, and magnesium. Soon after Oersted's (1820) discovery of the mechanical effect of a continuous electric current on a magnetic needle, Ampère and Babinet (1822, p. 29) constructed an astatic moving-magnet galvanometer by using two simi-

lar magnetized needles fixed in reversed relative positions. Employing a galvanometer of this type, Nobili (1828) and Matteucci (1840, 1844, 1845) studied the "frog currents" and "muscle currents," which are now called injury currents of the muscle. Matteucci (1847) also made an extraordinary observation indicating the possibility of stimulating a frog nerve by the electric current developed by a twitching muscle.

In 1843, one of the most important discoveries in the history of physiology was made. Emil du Bois-Reymond, a 25-year-old student of Johannes Müller in Berlin, succeeded in demonstrating the "action currents" of the nerve. He constructed a moving-magnet galvanometer which was far more sensitive than those employed previously by the Italian physicists, Nobili and Matteucci. The galvanometer was connected to a pair of platinum electrodes immersed in a concentrated solution of common salt and the nerve was brought into contact with the salt solution by means of moistened blotting paper and a small piece of animal tissue (see Fig. 2.2). [Note that Ringer's (1883) and Locke's (1894) solutions were not available for many decades to come.] du Bois-Reymond found that the galvanometer was traversed by a

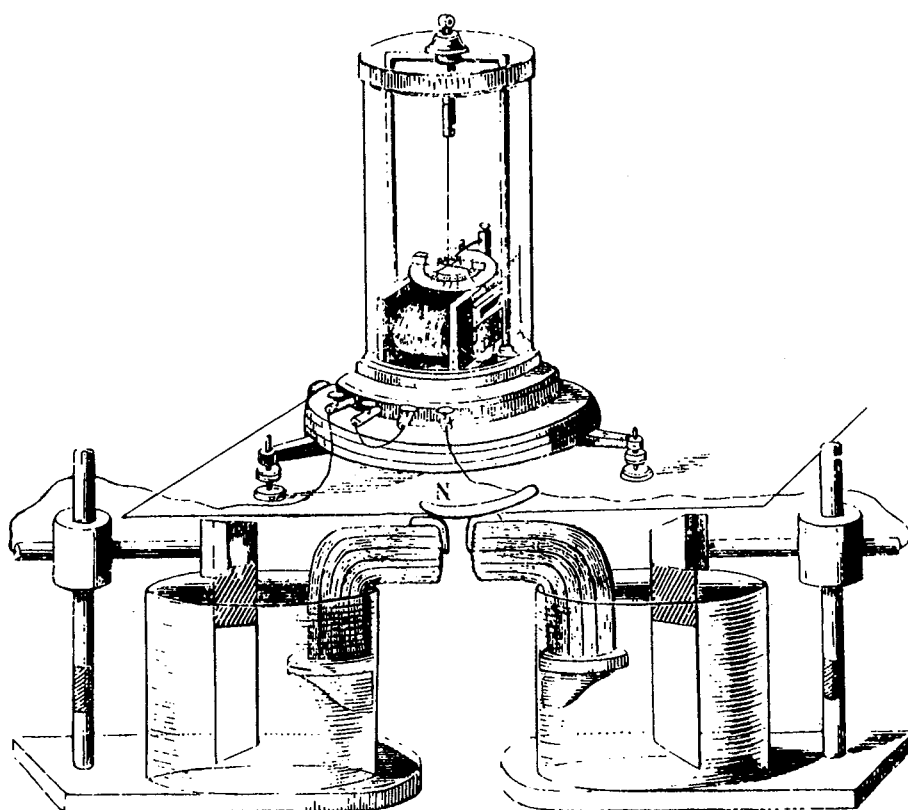


Fig. 2.2 The experimental setup used by du Bois-Reymond in his demonstration of the action current of a nerve. N represents a frog sciatic nerve. The nerve is in contact with small pieces of animal tissue placed on pads of blotting paper moistened with salt solution. Two large platinum plates are immersed in the salt solution in the glass vessels shown in the lower part of the figure. The sensitivity of the moving-magnet galvanometer shown in the upper part is estimated to be about 10^{-8} A or slightly higher. (Adapted from Fig. 9 in Ludwig's textbook of physiology published in 1852.)

steady current flowing from the intact portion to the cut end of a frog nerve. When he repeatedly excited the nerve by connecting the stimulating electrodes alternately to the terminals of a battery one way and then the other, he observed that the magnetic needle of the galvanometer moved toward the origin. He called the change in the current associated with responses of the nerve to electric stimuli a "negative variation." Much later the term "action current" was introduced by Hermann (1868) to replace "negative variation." For a very long time to come, the action current remained as the sole sign of physiological activity of an isolated nerve.

In his early experiments, du Bois-Reymond observed action current using platinum electrodes which could present serious problems. When an electric current traverses platinum electrodes immersed in a salt solution, a counterelectromotive force develops as a result of an accumulation of salts near the metal surface. Strong electric currents through platinum electrodes can produce, by electrolysis of the salt, alkali or acid which is toxic to biological tissues. For the purpose of circumventing these problems, du Bois-Reymond (1859) constructed "nonpolarizable electrodes" using a zinc rod immersed in a saturated solution of zinc sulfate. Contact between the electrodes and the nerve was made with a thick layer of a semisolid mixture of kaolin and a NaCl solution. No irreversible electrochemical reaction takes place on the surface of the metal under these conditions. Much later, calomel electrodes replaced the Zn-ZnSO₄ electrodes.

According to Rothschild (1973), the progress of physiology in the middle of the nineteenth century was strongly motivated by the antivitalistic, anti-teleological way of thinking among young physiologists. For the first time in the history of physiology, young brilliant physiologists of the time, represented by Ludwig, du Bois-Reymond, and Helmholtz, could completely dissociate themselves from the old notion that the laws governing the properties of living organisms are fundamentally different from those governing the inanimate world. In accordance with their firm belief, they proceeded to measure various physical quantities as functions of time. Volume II of du Bois-Reymond's book (see Fig. 89) contains one of the first curves in which physiological quantities are registered as ordinate against time as abscissa.

C. THE FIRST MEASUREMENT OF THE RATE OF NERVE CONDUCTION

In 1850, Hermann Helmholtz, a young professor of physiology at Königsberg and a close friend of du Bois-Reymond, succeeded in measuring the rate at which the effect of nerve stimulation travels along the nerve. For a full appreciation of the significance of Helmholtz's success, it is necessary to un-

derstand how the leading physiologists at that time visualized the mysterious process that travels along the nerve with an immense velocity. For this purpose, quoted below is an excerpt from a handbook of physiology written by his teacher, Johannes Müller (1834), shortly before Helmholtz's measurements.

It is yet uncertain whether nervous action, which is propagated with such immeasurable rapidity, is owing to the passage of an imponderable matter along the nerve . . . , or nervous action consists merely in oscillations or vibrations in an imponderable nervous principle present in the nerve (p. 652 in Baly's translation, 1840).

The attempts made to estimate the velocity of nervous action have not been founded on sound experimental bases. . . . As the galvanic principle and the nervous principle were regarded as identical, the rate at which the latter acts was calculated from the rapidity with which electricity is transmitted through electric conductors. We shall probably never attain the power of measuring the velocity of nervous action, for we have not the opportunity of comparing its propagation through immense space as we have in the case of light (p. 653).

By the words "immense space," Johannes Müller was undoubtedly referring to the space between the planets Jupiter and Earth, namely, to the distance required at that time to estimate the light velocity. Obviously, he believed that it would be impossible to measure the rate of nerve conduction because of the limitation of the length available. Helmholtz must have heard the news from France that immense space is no longer required to measure the light velocity: Fizeau's (1849) paper describing the result of a new measurement of the light velocity using a rotating cogwheel appeared immediately before Helmholtz's measurement.

To measure the velocity of nerve action, Helmholtz (1850a,b) used nerve-muscle preparations of the frog. He employed two different methods for determining the interval between the moment of delivery of a brief induction shock to the sciatic nerve and the onset of a twitch of the innervated gastrocnemius muscle. In his first series of measurements, he adopted Pouillet's method of measuring short time intervals with a ballistic galvanometer: an electric circuit involving a battery and a galvanometer was closed at the moment when the shock was delivered and was opened by the onset of the resulting twitch of the muscle (see Fig. 2.3). The size of the galvanometer deflection was taken as the measure of the time interval. He found that the time interval measured was definitely shorter when the shock was delivered to a point on the nerve near the muscle than when it was applied far away from the muscle. From this difference in the time interval, he arrived at an average value of 28.4 m/sec for nerve conduction at room temperature.

In the second series of experiments, Helmholtz adopted a much simpler method. He registered the time course of twitches of the muscle with a lever on a moving cylindrical surface. When an induction shock was delivered to a point on the nerve close to the muscle, the twitch was found to start sooner than when the shock was applied far from the muscle. The difference in the

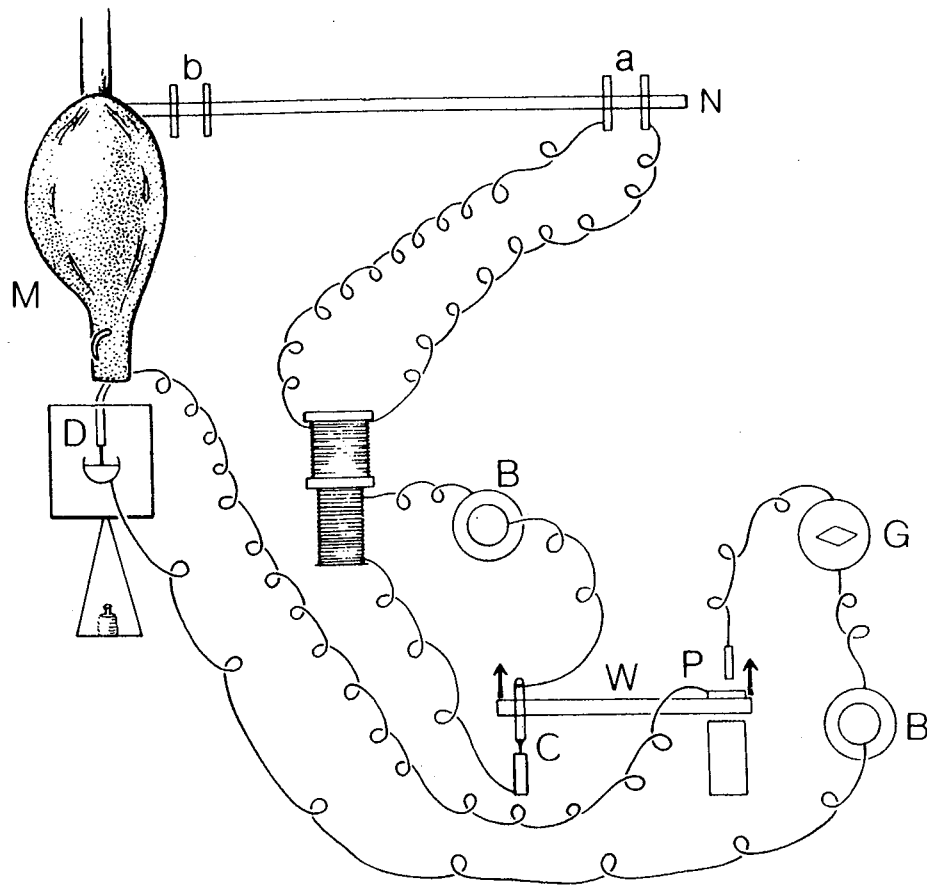


Fig. 2.3 Experimental arrangement used by Helmholtz for measuring the velocity of nerve impulses. N, nerve; M, muscle; B, batteries; G, a galvanometer; C, an electric contact that was broken at the moment when an induction shock is delivered to the nerve; D, a contact that was interrupted by muscle contraction. The distance between the two pairs of stimulating electrodes, a and b, was about 50 mm. (Adapted from Fig. 161 in Biedermann's *Electrophysiologie*, 1895.)

latency of the twitch was found to correspond to $\frac{1}{514}$ sec. The length of the nerve involved was 53 mm; the rate was then 27.3 m/sec. Thus, he found that this simple method yielded results that were consistent with those obtained by the previous method. Furthermore, he showed that the conduction velocity decreases with a fall in the ambient temperature, as do other physiological processes.

Helmholtz made this remarkable discovery at the age of 28. At that time, however, he had already achieved a high reputation among both physicists and physiologists because of his earlier publication on the conservation of energy (Helmholtz, 1847) and on the results of measurement of heat production in the muscle (Helmholtz, 1848).

A long time after Helmholtz's discovery, Julius Bernstein (1868), who later became known for his membrane hypothesis, raised the following question: At what rate does the negative variation discovered by du Bois-Reymond

spread along the nerve? Bernstein constructed a special device, called a differential rheotome, with which the time interval between the delivery of an electric shock to the nerve and the appearance of a negative variation at the end of the nerve could be measured. The rate of propagation of the negative variation found by this method agreed very well with the value found by Helmholtz. He thus concluded that "the electric state-change in the nerve propagates at the same rate as the excitation process" (see p. 40 in Bernstein, 1912). By using the same instrument, Bernstein also found that the action current has a rapid rising phase and a slow falling phase.

D. DU BOIS-REYMOND'S THEORY OF NERVE EXCITATION

In Volume I of his monograph (p. 258), du Bois-Reymond (1848) noted that a nerve-muscle preparation of the frog responds to a long pulse of constant current only at the beginning and at the end of the current. No twitch of the muscle is usually observed while the nerve is traversed by a constant current. He also saw that a slowly increasing current (obtained by means of a sliding contact on a stretched wire connected to a battery) is far less effective as a stimulus than a suddenly applied current. In his own words, "it is not the current density at each moment that produces a response in the nerve (which evokes a twitch of the innervated muscle); instead, it is a change in the current intensity that determines the effectiveness, a more rapidly changing current being more effective."

du Bois-Reymond described his theory of excitation in terms of the following mathematical expressions. Denoting the current density by i , he described the excitatory effect, $d\eta$, produced by the current during an infinitesimal period of time dt by

$$d\eta = F(di/dt) dt$$

where $F(di/dt)$ represents a function of the rate of current rise, di/dt . If it is assumed that η is simply proportional to di/dt , the effect produced between t_1 and t_2 is then described by

$$\eta = A[i(t_2) - i(t_1)]$$

where A is the proportionality constant, and $i(t_1)$ and $i(t_2)$ are the current densities at moment t_1 and t_2 , respectively. In this theory, only the importance of the rate of rise of the applied current is stressed. The effects of the intensity and duration of the stimulating current were left completely unresolved.

It is interesting to note that du Bois-Reymond's theory was formulated only shortly after the discovery of electric (mutual) induction (Faraday,

1831), which is the clearest case where the rate of change in the current intensity plays a crucial role. Obviously, the electric instruments at du Bois-Reymond's disposal were quite limited. He used induction coils, but not extensively. Neither he nor his contemporaries employed condenser-discharge pulses or rectangular current pulses of variable durations for stimulation. [Quantitative measurements of the effectiveness of such pulses in exciting a nerve were carried out much later (see Chapter 3).]

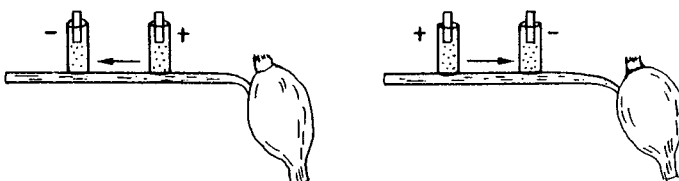
It is interesting to note that many of the outstanding physiologists at that time, including H. Helmholtz (1821–1894), E. Brücke (1819–1892), and E. du Bois-Reymond (1818–1896), belonged to the school of Johannes Müller (1801–1858) in Berlin. According to the "History of Physiology" written by Rothsuh (1973), the following physiologists, whose names frequently appear on the following pages of the present book, are listed as belonging to the next generation of the same school: E. Pflüger (1829–1910), L. Hermann (1838–1914), J. Bernstein (1839–1917), J. von Kries (1853–1928), M. Verworn (1863–1923), and others. Consequently, many ideas originating in Müller's school had a lasting effect on the course of the development of physiology.

E. PFLÜGER'S RULE OF EXCITABILITY AND ANODAL BLOCK OF NERVE CONDUCTION

In connection with the excitatory effect of a constant current on the nerve, Pflüger (1859) described a set of experimental facts which was known as his "rule of excitability" (*Zuckungsgesetz*). His rule had been explained in almost all the textbooks of physiology published before the early part of the present century and was used as a diagnostic tool for neurological diseases in man (see, e.g., Waller and Wattenville, 1882).

It is easy to demonstrate Pflüger's rule using a frog nerve–muscle preparation. A pair of nonpolarizable electrodes are placed on the nerve of the preparation. The source of electric currents is provided with a device to vary the intensity and direction of the current, as well as with a switch to initiate and terminate the current. A battery with an emf of a few volts and a low-resistance potential divider may be used for the required purpose.

Pflüger's rule is illustrated in Fig. 2.4. The left column in the figure represents the results obtained with applied current directed away from the muscle, and the right column those obtained with currents directed toward the muscle. When the current is barely effective ("weak"), a muscle twitch is observed only at the onset of the current (see the columns marked "on"). In the intermediate range of the current intensity, twitches are observed both at the onset and at the end of the current, namely, in the "on" and "off" phase



ELECTRIC CURRENT	ASCENDING		DESCENDING	
	ON	OFF	ON	OFF
WEAK	twitch	no twitch	twitch	no twitch
MEDIUM	twitch	twitch	twitch	twitch
STRONG	no twitch	twitch	twitch	no twitch ?

Fig. 2.4 Pflüger's rule of excitability (*Zuckengesetz*). The diagram on the top illustrates the positions of the stimulating nonpolarizable electrodes, cathode (–) and anode (+), relative to the innervated muscle. The presence of muscle contraction was taken as an index of a nerve impulse arriving at the muscle.

of the current. Usually, the muscle remains relaxed during the period in which a current of a constant intensity is passing through the nerve. With a strong current flowing away from the muscle ("ascending"), no twitch is observed at the onset of the current. With a strong current directed toward the muscle ("descending"), the break response of the muscle becomes either very weak or absent.

At a glance, the experimental facts mentioned above may seem complicated. Actually, however, this rule is easy to understand, and Pflüger himself gave a correct interpretation of the phenomenon. In classical physiology, the state of the portion of a nerve around the sink (cathode) of the applied constant current—the depolarized or cathodally polarized state in the present-day terminology—is called "catelectrotonus"; similarly, the state of hyperpolarization (or anodally polarized state) is called "anelectrotonus." Since the old terms may sound unfamiliar to most modern physiologists, the modern terms are used in the following interpretation.

Pflüger's rule indicates that (1) with a weak current, a propagated response of the nerve is evoked at the onset of cathodal polarization or depolarization, (2) with currents of medium intensities, termination of hyperpolarization also produces a propagated nerve impulse (break excitation), and (3) a region of strong anodal polarization, and, to some extent, a region under the influence of suddenly terminated depolarization, can block conduction of a nerve impulse. In other words, the absence of twitch in the bottom row in the figure is explained as resulting from conduction block in the

anodal region of the nerve impulse initiated in the cathodal region of the nerve. Much later, the mechanism of anodal block of nerve conduction was examined by using isolated single nerve fibers (see Chapter 5, Section F). The process of break excitation is discussed in detail later (see Chapter 7, Section G). The theory of nerve excitation deals specifically with the process of initiation of a nerve impulse at the onset of depolarization.

F. THE MEMBRANE HYPOTHESIS

Late in the nineteenth century, dissociation of electrolytes in water (Arrhenius, 1883) was established and the mobilities of ions were determined (Kohlrausch, 1885). Based on the newly acquired knowledge of ions in water, both the process of nerve excitation and generation of bioelectricity were linked directly with the "nerve membrane" on physicochemical grounds. It was Wilhelm Ostwald (1890) who proposed first that bioelectric potentials might arise from the semipermeable membrane in muscle and nerve fibers. In an article entitled, "Electric properties of semipermeable partitions," he pointed out the similarity between his precipitation-membrane (made of copper ferrocyanide) and the membranes which enclose living protoplasm. Both of these membranes were found to be permeable to water but not to solutes (Pfeffer, 1877). After investigating properties of inanimate semipermeable membranes, Ostwald stated: "Not only the current in muscles and nerves but also the enigmatic action of electric fish can be explained in terms of the properties of the semipermeable membranes" (Ostwald, 1890, p. 80).

Ostwald's paper was preceded by Walther Nernst's famous article, "The electromotive action of ions," in which the well-known equation for the potential difference between two solutions of a uni-univalent electrolyte at different concentrations was derived (Nernst, 1889). The potential difference V is related to the concentrations of the two solutions, c' and c'' , by the following equations:

$$V = \frac{u - v}{u + v} \frac{RT}{F} \ln \frac{c'}{c''} \quad (1.1)$$

where R is the gas constant, T the absolute temperature, F the Faraday constant, and u and v the mobilities of the cation and anion in the solution, respectively. It is important to note that this equation is derived under the condition of *electroneutrality*. In the case where v is negligibly small as compared with u , this equation is reduced to

$$V = \frac{RT}{F} \ln \frac{c'}{c''} \quad (2.2)$$

Shortly afterward, Max Planck (1890) published his famous papers on the potential difference between two electrolyte solutions. He solved the equations for electrodiffusion for univalent ions under the condition of *electroneutrality* and obtained his equation for the diffusion potential. Planck's treatment includes a special case where the total salt concentration is constant and the potential gradient across the diffusion zone is independent of the space coordinate (constant field). In this special case, the potential difference V is described by

$$V = \frac{RT}{F} \ln \frac{u_1 c'_1 + u_2 u'_2 + \dots + v_i c''_i + v_j c''_j + \dots}{u_1 c''_1 + u_2 c''_2 + \dots + v_i c'_i + v_j c'_j + \dots} \quad (2.3)$$

where u 's and v 's represent the mobilities of cations and anions (univalent), respectively, and c'_i and c''_i are the concentrations of the ion species i in the two solutions. Later on, Nernst and Riesenfeld (1902) discussed the behavior of the potential difference across the phase boundary between two immiscible solvents.

The first attempt to explain a bioelectric phenomenon on a quantitative basis was made in 1899 by Nernst. He argued that a semipermeable membrane must exist at the surface of biological cells, because a large difference in the electrolyte composition is maintained between the cell interior and the external fluid medium (Nernst, 1899). He inferred that concentration polarization of this membrane plays a crucial role in the process of nerve excitation (see Chapter 3, Section B).

In 1900, Cremer expressed the view that bioelectric phenomena can be explained in terms of emf which depends on the concentration difference and the properties of ions. In the same year, Macdonald (1900) studied the effect of dilution of the saline solution on the intensity of injury currents of mammalian nerves and suggested the possibility that the source of "demarkation" (or injury) currents might be a "concentration cell." He also examined the effects of temperature changes on the injury current. Then, in 1902, Bernstein published a paper devoted exclusively to the effects of temperature changes on the injury current of the muscle. He explained his results in terms of Nernst's equation for concentration cells by assuming the preexistence of a concentration difference across the living plasma membrane.

Shortly afterward, Cremer (1906, 1909) developed a comprehensive theory of bioelectric potentials, again emphasizing the importance of the semipermeable membrane in bioelectric phenomena. He did not limit his arguments to concentrations cells. He examined the possibility of explaining the emf in the nerve in terms of Planck's Eq. (2.3) and Nernst's Eq. (2.1), as well as on the basis of the equation of Nernst and Riesenfeld for phase-boundary potentials. He regarded the membrane as a thin, water-immiscible layer and treated the membrane potential as consisting of three components, namely,

potential differences across the two phase-boundaries and a diffusion potential. [This treatment may be considered as the forerunner of the modern membrane theories (see Chapter 8, Section D).] He also discussed the possibility that biological membranes may be composed of two distinct layers. He had to assume the existence of an unknown process responsible for the maintenance of the differences in the ion concentrations across the membrane. He also explained the process of production of action currents in terms of a change in the "electrolyte battery" produced by the appearance of new ions or by an alteration of the layer acting as the solvent for the ions involved (see p. 878 in Cremer, 1909). From the present-day point of view, the argument developed by Cremer has to be considered as thorough and logical.

Bernstein's well-known monograph, "Electrobiologie," appeared in 1912. In his monograph, 73-year-old Bernstein developed practically no new concepts. Bernstein's diagram illustrating the origin of the injury current is reproduced in Fig. 2.5. In explaining the change in the membrane potential associated with excitation, he thought that the potential change was produced by "unification of the positive ions on the external surface of the membrane with the negative ions inside" as in the case of condenser discharge (see Bernstein, 1912, p. 105). Apparently, Bernstein was trying to explain Galvani's Leiden jar analog of the muscle fiber (see Section A) in terms of the Nernst-Planck theory of electrodiffusion. However, he did not realize that, in the Nernst-Planck theory, the electric potential difference was calculated under the electroneutrality condition, namely, without assuming ac-

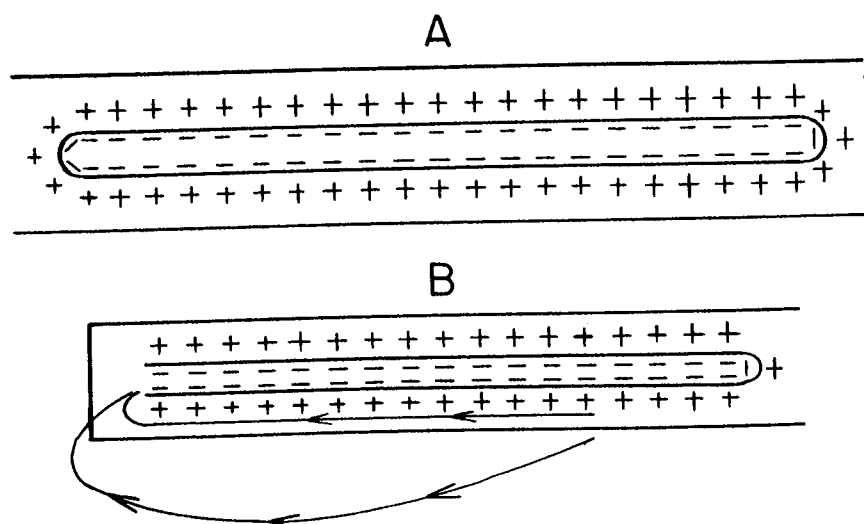


Fig. 2.5 Diagram illustrating Bernstein's notion as to the source of injury currents in muscles and nerves. (A) An intact fiber; (B) how an injury current is generated when one end of the fiber is cut. Bernstein assumed that there is an accumulation of anions on the inner surface and cations on the outer surface of his membrane. (Adapted from p. 94 in *Elektrobiologie*, 1912.)

cumulation of net charge to be neutralized anywhere in the system. [The significance of the electroneutrality condition will be discussed in detail later (see Chapter 14, Section B).] Bernstein calculated the membrane potential of the muscle by assuming either a high mobility of the internal K ion, which he designated as $(K_2H)^{3+}$, or a low mobility of the external Na ions (p. 94 and p. 99). He assumed that the semipermeable membrane was located *underneath* the sarcolemma (or axolemma) or the surface of individual myofibrils (or neurofibrils). In his monograph, Bernstein also made wild attempts at interpreting the process of secretion, cell division, etc., in terms of bioelectricity.

We now summarize what has been discussed in this section in the following manner. The mechanism of generation of electromotive forces in biological membrane was placed on an electrochemical basis predominantly by Ostwald and Cremer. The importance of phase boundaries and the possibility of the presence of a multilayer structure in the nerve membrane were first suggested by Cremer.

Although the membrane hypothesis of Cremer and Bernstein was formulated around the turn of the century, the importance of the nerve membrane was not fully recognized for many decades to come. One of the main reasons for this slow recognition of the importance of the "membrane" appears to be related to the structural complexity of frog motor nerve fibers. The long, cylindrical mass of protoplasm, called axis-cylinder, of these fibers is covered with myelin sheath which is interrupted at regular intervals (Ranvier, 1871). In the axis-cylinder, there are fibrous elements which old histologists called "neurofibrils." Almost solely on histological grounds, many physiologists assumed that neurofibrils were the ultimate structure along which nerve conduction takes place [Apáthy (1897); see also Parker (1929)]. Because of the popularity of the neurofibril hypothesis, there has been a lingering suspicion that the surface of individual neurofibrils might be the location of the "membrane." In Chapter 4, we shall see how and why the neurofibril hypothesis was abandoned.

Further developments of the membrane hypothesis will be discussed in later chapters.

REFERENCES

- Ampère, A. M., and Babinet, J. (1822). "Exposé des Nouvelles Découvertes sur l'Électricité et le Magnétisme," 91 pp. Paris, Méquignon-Marvis.
- Apáthy, S. (1897). Das leitende Element des Nervensystems und seine topographischen Beziehungen zu den Zellen. *Mitt. Zoolog. Station Neapel*. **12**, 495–748.
- Arrhenius, S. (1883). "Untersuchungen über die galvanische Leitfähigkeit der Elektrolyte," 147 pp. Engelmann, Leipzig reprinted in 1907.

- Baly, W. (1840). "Elements of Physiology by J. Müller." University College, London.
- Bernstein, J. (1868). Ueber den zeitlichen Verlauf der negativen Schwankung des Nervenstroms. *Arch. Gesamte Physiol. Menschen Tiere* **1**, 173–207.
- Bernstein, J. (1902) Untersuchungen zur Thermodynamik der bioelektrischen Ströme. *Pfluegers Arch. Gesamte Physiol. Menschen Tiere* **92**, 521–562.
- Bernstein, J. (1912). "Elektrobiologie," 88 pp. Friedr. Vieweg & Son, Braunschweig.
- Caldani, M. A. (1760). Lettre á Mr. Albert de Haller: In "Haller: Mémoires sur les Parties Sensibles et Irritables du Corps Animal," v. iii; 1–156. Lausanne.
- Cremer, M. (1900). Ueber den Begriff des Kernleiters und der physiologische Polarization. *Sitzungsber. Ges. Morphol. Physiol.* **16**, 124–127.
- Cremer, M. (1906). Über die Ursache der elektromotorischen Eigenschaften der Gewebe, zugleich ein Beitrag zur Lehre von den polyphasischen Elektrolytketten. *Z. Biol. (Munich)* **47**, 562–608.
- Cremer, M. (1909). Die allgemeine Physiologie der Nerve, in Nagel's *Handbuch der Physiologie des Menschen*. Vol IV, 793–992.
- Davy, H. (1808). The Bakerian Lecture on some new phenomena of chemical changes produced by electricity, particularly the decomposition of fixed alkalies, and the exhibition of the new substances which constitute their bases and on the general nature of alkaline bodies. *Phil. Trans. R. Soc. London* 1–44 (see also pp. 333–370).
- du Bois-Reymond, E. (1848). "Untersuchungen über Thierische Elektrizität," Vol. I, 743 pp., (1849) Vol. II(1) 608 pp. Reiner, Berlin.
- du Bois-Reymond, E. (1859). "Gesammelte Abhandlungen zur allgemeinen Muskel- und Nervenphysik." Bd. I, 42–79. Verlag von Veit & Comp., Leipzig, 1875.
- Faraday, M. (1831). In "Experimental Researches in Electricity." London. 1839. Vol. I, 574 pp. (see pp. 1–16).
- Fizeau, H. (1849). Sur une expérience relative à la vitesse de propagation de la lumière. *C. R. Acad. Sci.* **29**, 90–92.
- Franklin, B. (1751). "Experiments and Observations on Electricity Made at Philadelphia in America," 85 pp. E. Cave, London.
- Fulton, J. F., and Cushing, H. (1936). A bibliographical study of the Galvani and the Aldini writings on animal electricity. *Ann. Sci.* **1**, 239–268.
- Galvani, L. (1791). "Commentary on the Effect of Electricity on Muscular Motion," translated by R. M. Green, Waverly Press, Inc., Baltimore, 1953.
- Gray, S. (1735–1736). Experiments relating to electricity. *Phil. Trans. R. Soc. London* **39**, 16–24, 166–170, 400–403.
- Helmholtz, H. (1847). "Über die Erhaltung der Kraft." 60 pp. G. Reiner, Berlin.
- Helmholtz, H. (1848). Über die Wärmeentwicklung bei der Muskelaction. *Arch. Anat. Physiol.* **1848**, 144–164.
- Helmholtz, H. (1850a). Vorläufige Bericht über die Fortpflanzungsgeschwindigkeit der Nervenreizung. *Arch. Anat. Physiol.* **1850**, 71–73.
- Helmholtz, H. (1850b). Messungen über den zeitlichen Verlauf der Zuckung animalischer Muskeln und die Fortpflanzungsgeschwindigkeit der Reizung in den Nerven. *Arch. Anat. Physiol.* **1850**, 276–364.
- Hermann, L. (1868). "Untersuchungen zur Physiologie der Muskeln und Nerven." III Heft. August Hirschwald, Berlin (see p. 61).
- Hoff, H. E. (1936). Galvani and the pre-Galvanian electrophysiologists. *Ann. Sci.* **1**, 157–172.
- Humboldt, F. A. von (1797). "Versuche über die gereizte Muskel- und Nervenfasern," Vol. 1, 495 pp. Posen, Berlin.
- Kohlrausch, F. (1885). Ueber das Leitungsvermögen einiger Electrolyte in äusserst verdünnter wässriger Lösung. *Ann. Phys. Chem.* **26**, 161–227.

- Locke, F. S. (1894). Notiz über den Einfluss physiologischer Kochsalzlösung auf die electrische Erregbarkeit von Muskeln und Nerven. *Contraibl. Physiol.* **8**, 166–167.
- Macdonald, J. S. (1900). The demarcation current of mammalian nerve. III. The demarcation source and the concentration law. *Proc. R. Soc. (London)* **67**, 325–328.
- Matteucci, C. (1840). "Essai sur les Phénomènes Électriques des Animaux," 88 pp. Paris.
- Matteucci, C. (1844). "Traité de Phénomènes Électro-physiologique des Animaux," 272 pp. Paris.
- Matteucci, C. (1845). The muscle current. *Phil. Trans. R. Soc. London*, **1**, 283–296.
- Matteucci, C. (1847). "Lectures on the physical phenomena of living beings" (translated by J. Pereira), 435 pp. Longman, Brown, Green and Longmans, London.
- Mauro, A. (1969). The role of the voltaic pile in the Galvani-Volta controversy concerning animal vs. metallic electricity. *J. Hist. Med. Allied Sci.* **24**, 140–150.
- Müller, J. (1834). "Handbuch der Physiologie des Menschen." I. J. Hölscher, Coblenz.
- Musschenbroeck, P. van (1746). Part of a letter from Mr. Trembley to Martin Folkes. *Phil. Trans. R. Soc. London* **44**, 58–60.
- Nernst, W. (1889). Die elektromotorische Wirksamkeit der Ionen. *Z. Phys. Chem.* **4**, 129–181.
- Nernst, W. (1899). Zur Theorie der elektrischen Reizung. *Königl. Ges. Wiss. Göttingen, Nachrichten.* 104–108.
- Nernst, W., and Riesenfeld, E. H. (1902). Ueber elektrolytische Erscheinungen an der Grenzfläche zweier Lösungsmittel. *Ann. Phys.* **8**, 600–608.
- Nobili, L. (1828). Comparaison entre des deux galvanomètres des plus sensibles, la grenouille et le multiplicateur à deux aiguilles, suivie de quelques résultats nouveaux. *Ann. Chim. Phys.* **38**, 225–245.
- Oersted, H. C. (1820). Galvanic magnetism. *Philos. Mag.* **56**, 394.
- Ostwald, W. (1890). Elektrische Eigenschaften halbdurchlässiger Scheidewände. *Z. Phys. Chem.* **6**, 71–82.
- Parker, G. H. (1929). The neurofibril hypothesis. *Q. Rev. Biol.* **4**, 155–178.
- Pfeffer, W. (1877). "Osmotische Untersuchungen: Studien zur Zellmechanik," 236 pp. Engelmann, Leipzig.
- Pflüger, E. (1859). "Untersuchungen über die Physiologie des Electrotonus." August Hirschwald, Berlin.
- Planck, M. (1890). Ueber die Erregung von Electricität and Wärme, in Electrolyten. *Ann. Phys. Chem.* **39**, 161–186. See also **40**, 561–576.
- Priestley, J. (1967). The History and Present State of Electricity, 3rd ed. (1775), London (Johnson Reprint Corp., New York, 1966).
- Ranvier, L. (1871). Contributions à l'histologie et à la physiologie des nerfs périphériques. *C. R.* **73**, 1168–1171.
- Ringer, S. (1883). A further contribution regarding the influence of the different constituents of the blood on the contraction of the heart. *J. Physiol. (London)* **4**, 29–42.
- Rothschub, K. E. (1973). "History of Physiology," 379 pp. R. E. Krieger Publishing Co., Huntington, New York.
- Sulzer, J. G. (1752). p. 356 in "Recherches sur l'origine des sentiments agréables et désagréables." Histoire de l'Académie Royale des Sciences de Berlin. (*Theorie der angenehmen und unangenehmen Empfindungen*, 1762, Berlin.)
- Volta, A. (1800). On the electricity excited by the mere contact of conducting substances of different kinds. *Phil. Trans. R. Soc. London* **90**, 403–431.
- Waller, A., and Wattenville, A. de (1882). On the influence of galvanic current on the excitability of motor nerves of man. *Phil. Trans. R. Soc. London* **1882**, 961–991.
- Winkler, J. H. (1744–1745). Of electricity. *Phil. Trans. R. Soc. London* **43**, 307–315.

3. The Rise and Fall of Theories of Nerve Excitation

A. THE DOWNFALL OF DU BOIS-REYMOND'S THEORY OF EXCITATION

Since the dawn of electrophysiology, the process of excitation of a nerve by application of electricity has had an irresistible fascination for many investigators. Many theories were proposed to explain how nerve impulses are generated by electric currents. In the present chapter, major theories enunciated before World War II are described. All these theories are based on indisputable experimental facts. Nevertheless, we shall see that many of these immensely popular theories were abandoned when new methods of investigation were devised.

In the theory of nerve excitation proposed by du Bois-Reymond, it was assumed that an electric current exerted its excitatory effect on the nerve or muscle only when its intensity was varied (see Chapter 2, Section D). According to this theory, a pulse of constant current is capable of exciting a nerve only at the beginning and at the end of a current pulse, but not during the period of steady flow. If this is true, the threshold strength (i.e., the lowest current strength that excites a nerve) should be totally independent of the duration of the current pulse. Neither the absolute value of the current intensity nor the quantity of electricity transported through the nerve plays an important role in du Bois-Reymond's theory.

On the basis of this theory, how can the effect of current intensity described in Pflüger's rule of excitability (Chapter 2, Section E) be understood? A constant current can, under certain circumstances, evoke sustained repetitive responses (see p. 38 and 47 in du Bois-Reymond, 1849, Vol. II(1); von Frey, 1883). How can this fact be reconciled with the notion that a constant current exerts no excitatory effect during the period of steady flow? Is there any definite amount of energy or quantity of electricity required for nerve excitation? All these questions were left unanswered.

In spite of these serious defects, du Bois-Reymond's theory had not been seriously challenged for many decades. Many physiologists working on the

subject of nerve excitation quoted this theory as "the fundamental law of excitation" and made every effort to explain their new experimental data on the basis of this theory.

Some physiologists constructed ingenious mechanoelectric devices which served to reexamine the law of electric excitation. Fick (1863, 1864), for example, employed an instrument called a "spring rheotome" and showed that the duration of a current pulse is an important factor in excitation. Then, he made the following confusing remark: "For a given level of current variation, the current has to be maintained for a certain period of time in order to be effective" (Fick, 1863, p. 52). He observed also that some invertebrate muscles remain in the state of steady contraction as long as a current is maintained (without any variation in its intensity). The existence of such sustained responses of the muscle is in direct contradiction with du Bois-Reymond's fundamental law. However, Fick said: "A basically new formulation of the law of muscle excitation is not yet considered" (p. 44).

In 1882, von Kries published a remarkable experimental finding. He employed sinusoidally alternating current (AC) for the first time and determined the threshold amplitude as a function of frequency. He found that the threshold for a nerve or a muscle of the frog shows a minimum at a certain frequency (100–200 Hz); it rises on both higher and lower sides of the optimum frequency (see Fig. 3.1). The rise of threshold in the low frequency range might have been expected from du Bois-Reymond's fundamental law. However, the rise in the high frequency range is totally inconsistent with the

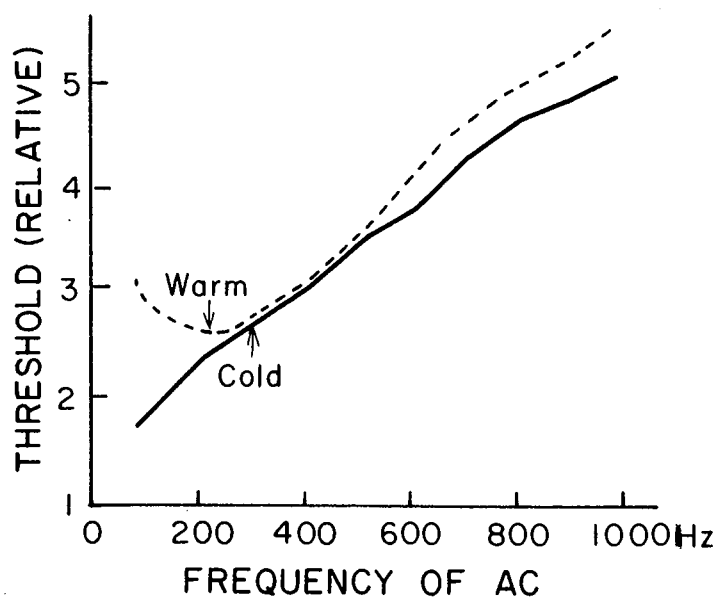


Fig. 3.1 The dependence of threshold amplitudes of alternating currents (AC) on the frequency. The continuous line represents the data obtained from a frog sciatic nerve kept at about 0°C; the broken line was obtained from the same nerve kept at about 37°C. (Adapted from von Kries, 1882.)

accepted law. Nevertheless, von Kries (1882, p. 194) tried to interpret his results on the basis of du Bois-Reymond's mathematical formula.

Toward the end of the last century, physiologists started determining the relationship between the duration of a stimulating current pulse and the threshold strength. Using condenser-discharge pulses of variable durations, Hoorweg (1892, 1894) in Utrecht, the Netherlands, carried out an extensive experimental study and arrived at the following empirical formula relating the threshold voltage, V , to the capacity C :

$$V = aR + b/C \quad (3.1)$$

where R represents the resistance of the circuit, and a and b are constants. According to his result, the voltage required to excite a nerve rises as the capacity is decreased. The quantity of electricity required for stimulation, VC , decreases with a reduction of C and approaches a finite limiting value as C tends to zero. The electric energy, $\frac{1}{2}CV^2$, on the contrary, reaches a definite minimum at a particular intermediate duration. In his conclusion, Hoorweg said: "The nerve excitation does not derive from variations in the current intensity, di/dt . . . ; the excitation process is only a function of the current intensity $i(t)$ " (Hoorweg, 1894, p. 104). This statement appears to be the first definite criticism of du Bois-Reymond's law. Hoorweg's results were confirmed and extended by other investigators (see Chapter 6, Section E).

Strangely, the majority of physiologists at the time of Hoorweg did not realize that essentially the same relationship between the capacity and the threshold strength was obtained by Volta (1803) by taking the pricking sensation caused by an electric shock to his own finger as an index. The popularity of de Bois-Reymond's theory must have clouded the old observation of Volta.

Shortly afterward, Nernst (1899; see Chapter 2) announced his theory of nerve excitation based on an entirely new concept (see below). As a consequence, there was a rapid downfall of the popularity of du Bois-Reymond's theory of nerve excitation at about the turn of the century.

B. NERNST'S SEMIPERMEABLE MEMBRANE THEORY

In 1908 Walther Nernst published a 40-page article explaining his theory of nerve excitation to physiologists. The physicochemical basis of his theory appeared to be quite sound and the treatment of his experimental data was regarded by many physiologists as the best exemplar of a quantitative biological research. Since this was the first highly quantitative theory in physiology, the impact of this article on physiologists was very great. Even in the 1930s I knew of several professors of physiology in Japan who dedicated their lives to the extension of Nernst's theory.

Nernst started his theory by pointing out the observation that high frequency alternating current is far less effective as a stimulus to nerves than low frequency AC (see Fig. 3.1). It was known that, at frequencies over 10^4 Hz, strong AC which can light an electric bulb fails to arouse any sensation or muscle twitches in human subjects (d'Arsonval, 1898; Einthoven, 1900). Next, he emphasized that an electric current passing through a homogeneous electrolytic solution brings about no change in the ionic composition. (He noted that the number of ions entering into every volume element of a homogeneous solution at any moment is equal to that of the same ion species leaving the same volume element.) He argued that a semipermeable membrane that prevents free diffusion of ions is responsible for the maintenance of the difference in electrolyte composition between the inside and outside of the nerve. When a current passes through this semipermeable membrane, a change is produced in the electrolyte composition in the vicinity of the membrane.

Nernst did not specify the ion species that penetrate the semipermeable membrane. Nor did he speculate about physicochemical properties of the nerve membrane. Nevertheless, he emphasized that the passage of a current through such a membrane brings about a rise in the salt concentration on one side and a fall (or desalinization) on the other side and that, aside from heat production, this concentration change is the only effect that an electric current can produce in the electrolyte solution in biological tissues. (To stress the validity of the electroneutrality condition, Nernst used the term "salt-concentration"—and not "ion-concentration"—throughout.) The rate of salt accumulation is proportional to the current intensity. The salt accumulated on the surface of the membrane is carried by diffusion away from the surface of the membrane.

The equation describing the diffusion process is

$$\frac{\partial c}{\partial t} = k \frac{\partial^2 c}{\partial x^2} \quad (3.2)$$

where c , the salt concentration, is a function of time t and distance x from the membrane and k is the diffusion coefficient (determined by the mobilities of the anions and cations involved). The boundary condition (at $x = 0$) is

$$-k \frac{\partial c}{\partial x} = \nu i$$

where i is the current density and ν the proportionality constant. At $x = \infty$, c is constant and equal to c_0 . When the current intensity varies sinusoidally with time, namely, when

$$i = a \sin nt$$

n being the angular frequency and a the amplitude, the solution of the diffusion equation is given by

$$c - c_0 = \frac{av}{\sqrt{nk}} \exp[-\sqrt{n/(2k)} x] \sin [nt - \sqrt{n/(2k)} x - \frac{1}{4}]$$

For the current to be effective in exciting the nerve, the salt concentration at the membrane surface has to exceed a certain critical value. From this consideration, it follows that the relationship between the frequency f of the AC ($2\pi f = n$) and the threshold strength of i is given by

$$i\sqrt{f} = \text{constant} \quad (3.3)$$

When rectangular current pulses are used for stimulation, the following relationship is obtained between the threshold strength i and the duration t :

$$i\sqrt{t} = \text{constant}$$

Nernst made an extensive comparison between the theoretical results and the experimental data (obtained by his own collaborators and by other physiologists). In the range of frequency, f , higher than 100 Hz, he obtained an excellent agreement between the theory and experiment. When rectangular current pulses were used instead of AC, there was good agreement between the theoretical and experimental values within a limited range of duration. He attributed the deviation observed with pulses with long durations to "accommodation" (see Chapter 3, Section E and Chapter 7, Section A).

Soon after the publication of Nernst's paper, A. V. Hill (1910) derived an equation for the strength-duration relation by solving the same differential Eq. 3.2 under the assumption that in the nerve fiber there are two "transverse" membranes separated by a short distance. Hill did not speculate about the location of these two imaginary transverse membranes which are assumed to play a crucial role in nerve excitation. Nevertheless, his equation, which contained three adjustable parameters, yielded better agreement between calculated and observed data over a wider range of pulse durations. Lucas (1910) discussed the significance of the three adjustable parameters in Hill's equation by determining i to t relations under a variety of experimental conditions.

In spite of its immense popularity, Nernst's theory of excitation was found later to be untenable on both experimental and theoretical grounds. The nerves used in Nernst's experiments contain a large number of nerve fibers. When single nerve fiber preparations (see Chapter 6, Section H) were used instead of nerve trunks, the frequency-dependence of the threshold was found to be far more pronounced than what was predicted by Nernst's equation. Furthermore, it was found that the effectiveness of AC in stimulation is determined by the cable property of the myelin sheath rather than by the excitable membrane at nodes of Ranvier (see Chapter 6, Sections B and H).

In summary, the shortcoming of the theories of nerve excitation proposed by Nernst and by Hill lies in the fact that they completely ignored the real structure of the nerve. These theories, which were very popular for many decades, have little or no value at present.

C. THE COLLOID CHEMICAL THEORY OF LOEB AND HÖBER

Jacques Loeb's (1900) theory was formulated on the basis of his own experiments in which the effects of various inorganic ions on excitable tissues were compared with their effects on a number of biocolloids. At that time, Ringer (1880) and Locke (1894; see Chapter 2) had already published their recipes of saline solutions which are favorable for maintaining the excitability of excised muscles and nerves. To explain the effects of Ca ions on excitable tissues, Loeb introduced the concept of "ion-antagonism." In an article subtitled, "The poisonous character of a pure NaCl solution," Loeb pointed out that the salt solutions containing Na-ions only cannot maintain excitability and that the poisonous effect of Na-ions can be antagonized by Ca-ions. The following paragraphs are taken directly from his papers (1900) and his monograph (1906).

The salts, or electrolytes in general, do not exist in living tissues as such exclusively, but are partly in combination with proteins or fatty acids. The salts or electrolytes do not enter into this combination as a whole, but through ions. The great importance of these ion-proteid compounds (or soaps) lies in the fact that, by the substitution of one ion for another, the physical properties of the proteid compound change. We thus possess in these ion-proteid or soap compounds essential constituents of living matter, which can be modified as desired, and hence enable us to vary and control the life phenomena themselves (Loeb, 1900, p. 327).

The normal irritability of animal tissues depends upon the presence in these tissues of Na, K, Ca and Mg ions in the right proportion; . . . any sudden change in the relative proportions of these ion lipoids or ion proteids or ion carbohydrates alters the properties of the tissues and give rise to an activity or an inhibition of the activity . . . (Loeb, 1906, p. 95).

The quotient of the concentration of the Na ion over the Ca ions, C_{Na}/C_{Ca} , becomes therefore of importance for phenomena of irritability (Loeb, 1906, p. 79).

It is not impossible that a substitution of K for Ca, or vice-versa, in ion colloid actually occurs at the cathode, while a constant current flows through the nerve (Loeb, 1906, p. 102).

It would be unwarranted to say that Ca or any other ions are the cause of, or the stimulus for, the rhythmical contraction. . . . It would be much nearer the truth to assume that for the possibility of rhythmical contractions, the Na, Ca and K ions must exist in definite proportions in the tissue . . . (Loeb, 1900, p. 394).

Loeb's theory is only qualitative. Probably for this reason, Loeb's theory never gained much popularity among physiologists. We see repeatedly that physiologists prefer mathematically formulated theories of excitation, even when the quantities which are treated in their theories are of dubious physicochemical significance. Nevertheless, the basis of Loeb's theory is quite

sound and has been exploited, often unknowingly, by many recent investigators. It is quite evident that he had a clear concept of ion-exchange processes taking place in the nerve membrane.

Loeb's theory was expanded to a considerable extent by Höber (1905, 1926). He found, on the basis of his experiments on muscles, that the magnitude of the effect of ions on the excitability follows the lyotropic series. The ion effects on the nerve were explained also in terms of the lyotropic series (see Höber, 1926, p. 659). [The significance of the lyotropic series (Hofmeister, 1888) will be discussed later (Chapter 9, Section D and Chapter 11, Section B).] Furthermore, Höber (1905) showed that dyes like toluidine blue intensely stain a nerve soaked in a K-rich medium, while they only poorly stain a highly excitable nerve immersed in a normal, Ca-rich saline solution. Höber explained this parallelism between the stain-ability and the excitability in terms of "loosening" (*Auflockerung*) and "tightening" (*Verdichtung*) of the colloidal plasma membrane. In a potassium-rich medium, the plasma membrane was thought to swell and become loosened because of increased hydration; a reverse process could take place in a Ca-rich medium.

It is important to note that, in most of the experiments carried out by Loeb and Höber, properties of frog nerve-muscle preparations and of heart muscles were examined by taking muscular contraction as an index of effective stimulation. Hence, the results obtained were frequently confusing. Nevertheless, with slight modifications, Loeb and Höber's notion can be used to explain the results of most recent observations on the effects of ions on excitable systems (see Chapters 12 and 13).

D. THE STRENGTH-DURATION RELATION AND CHRONAXIE

The apparent rigor of the mathematicophysical theory of nerve excitation proposed by Nernst and Hill inspired great enthusiasm among physiologists for making precise measurements of the strength-duration relation in nerves and muscles. In years just preceding and following the turn of the century, it was not easy to generate brief rectangular current pulses of known durations. A pendulum or a spring was frequently employed for this purpose in order that two points in an electric circuit could be broken successively. The durations of the pulses thus obtained had to be calibrated by a tedious procedure using a slowly moving galvanometer.

Using the method of breaking two wires in an electric circuit successively by a bullet fired by a gun, Weiss (1901) obtained rectangular current pulses. After a careful study of the strength-duration relations obtained by this method, he proposed a simple, but useful, empirical formula relating the current strength, i , to the duration t :

$$i = \frac{a}{t} + b \quad (3.1)$$

where a and b are constants. Other investigators confirmed Weiss' result by using the method of breaking two points in a circuit successively by a swing of a pendulum.

Figure 3.2 illustrates the strength-duration relation expressed by Weiss' empirical formula. In the range of very short durations, the pulse intensity required for exciting a nerve is roughly inversely proportional to the duration. As the duration is made sufficiently long, the threshold intensity approaches a constant value, b . Lapicque (1909) named the threshold intensity for pulses with an infinitely long duration the "rheobase," and the critical duration for a pulse intensity of twice the rheobase the "chronaxie." In Weiss' formula, the constant b represents the rheobase and the ratio a/b corresponds to the chronaxie. When a bundle of many nerve fibers is used, as was always the case at that time, the absolute value of the rheobase has little significance, because it is strongly affected by the thickness of the fluid medium in the surrounding connective tissue and in the intercellular space. The chronaxie of the frog motor nerve fiber was found to be of the order of 0.3 msec.

Lapicque believed that the chronaxie was an important quantity characterizing the physiological property of an excitable tissue. He collected the values of chronaxie measured on a variety of excitable tissues under diversified experimental conditions (Lapicque, 1926). He thought that the block of

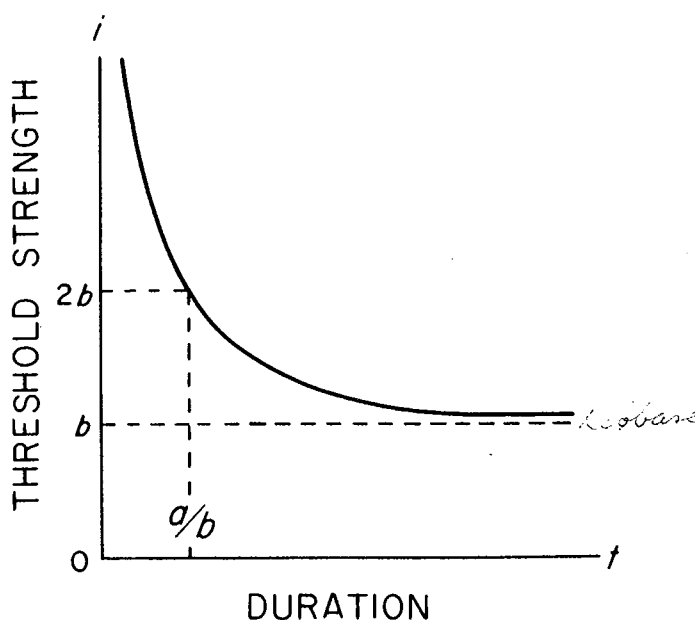


Fig. 3.2 A diagram illustrating Weiss' formula for the strength-duration relation in threshold excitation of a nerve. The threshold strength for long-duration current pulses (i.e., rheobase) is denoted by b . The chronaxie, namely, the required duration for a pulse with strength $2b$, is denoted by a/b .

transmission across a neuromuscular junction by curare, a South American arrowhead poison, was brought about by a change in the chronaxie of the muscle. Many investigators, who were favorably impressed by the quantitative aspect of Lapicque's theory or charmed by the sophisticated technique of measuring chronaxie, attempted to interpret complex phenomena in the central nervous system on the basis of Lapicque's concept.

It should be noted, however, that even at the peak of the popularity of chronaxie measurements, there were a few papers questioning the significance of such measurements. Davis (1923), for example, pointed out that the chronaxie of a muscle measured with large electrodes is much longer than the value obtained with a small stimulating cathode. Much later, Rush-ton (1935) also emphasized the dependence of the chronaxie on the arrangement of the electrodes used for stimulation and put a damper on the popularity of chronaxie.

When a current pulse is delivered to a nerve trunk, a change in the potential is produced across the nerve membrane. Since the time of Hermann (1879, 1899) and Hoorweg (1898), it has been known that the nerve membrane surrounding the axis-cylinder (i.e., core) can be represented by a series of leaky capacitors. This feature of a nerve is called the "core-conductor properties" or "cable properties." As has been pointed out by Cremer (1929, 1932), the mathematical equation which describes the spread of electricity along a core-conductor (see Chapter 6, Section B) is identical with the diffusion equation used by Nernst to derive his theoretical strength-duration relation. It is possible to derive a strength-duration relation on the assumption that the threshold is reached when this capacitor is charged to a critical level (Hill, 1932; Erlanger and Gasser, 1937). Because of the cable property of the nerve fiber, it is not surprising that the strength-duration relation for an excitable tissue is profoundly affected by the experimental arrangement utilized for delivering the pulses (see Chapter 6, Section I).

There is no doubt that the strength-duration relation gives some information about the electric properties of the excitable tissue. However, measurements of the relation with a high degree of precision do not yield much useful information about the tissue. When this limitation of studies of the strength-duration relation was realized, the initial enthusiastic support given to the theories of Lapicque, Hill, Lucas, and others gradually faded.

E. THE TWO FACTOR THEORY

During the middle part of the 1930s, mathematically oriented physiologists were interested in describing the process of nerve excitation by using one or two differential equations. The leading proponents of this approach

were Blair (1932), Rashevsky (1933), Monnier (1934), and Hill (1936). The proposed equations described time-dependent changes of "something" produced in the nerve by a stimulating electric current. French investigators called the quantity described by the equations "l'état d'excitation"; Hill and others called it "local potential." It is important to note that the physico-chemical nature of this quantity was not specified. Only the alleged law governing the rise and fall of this quantity was expressed by the differential equations. Different authors employed slightly different mathematical expressions to describe the process. Again, it was assumed that threshold was reached when the local excitatory state reached a certain critical level.

Let us follow the formulation developed by A. V. Hill (1936). The rate of rise of the local potential, V , is assumed to be proportional to the intensity of the current, i . At the same time, V spontaneously decays; the rate of this decay is proportional to $(V - V_0)$, where V_0 is the value of V before the onset of the stimulating current pulse. Thus, the law governing the rise and fall of V is described by

$$\frac{dV}{dt} + \frac{(V - V_0)}{k} = bi$$

where b and k are constants. The critical value of V required for excitation of the nerve is U . Furthermore, it was assumed that U rises slowly when long current pulses were used for stimulation

$$\frac{dU}{dt} + \frac{(U - U_0)}{\beta} = \frac{(V - V_0)}{\lambda}$$

where β and λ are also constants. This is a formal description of the process of "accommodation." The simultaneous differential equations can be solved for rectangular current pulses ($i = \text{constant}$) and for exponentially decaying (i.e., condenser discharge) pulses. The solutions of these equations were found to agree very well with the observed strength-duration relation when the adjustable constants in the equations were properly chosen.

The agreement between the theory and the experimental results does not necessarily prove the legitimacy of the theory. When there are a sufficient number of adjustable parameters in the equations, it is not difficult to fit the observed data satisfactorily. Concerning the number of adjustable parameters, Lopicque once quoted, with biting sarcasm, Joseph Bertrand's remark: "Allow me four, then I shall portray an elephant; give me five and the elephant will raise his trunk (see p. 15 in Lopicque, 1926).

Why did this pure formalism appear so attractive to biophysicists? And why was this approach completely abandoned later and without having made any positive contribution to the progress which took place in the fol-

lowing decade? I would like to quote Heilbrunn's opinion (p. 431 in Heilbrunn, 1938) on mathematical theories of nerve excitation.

Because of their deep admiration of the science of physics, biologists are often too enthusiastic about the application of the mathematical method to problems of excitation. If a mathematical physicist were asked to develop equations for a process involving unknown chemical substances acting in a system whose physical properties are largely unknown, he would presumably feel rather hesitant about making any attempt at mathematical analysis. Some of the mathematicians who have worked in the field of excitation have been but little aware of the complexities of biological material; often enough they have too little understanding of what it is they are trying to explain.

F. RUSHTON'S CONCEPT OF LIMINAL LENGTH

Shortly before World War II, a dramatic revival of one of the old concepts in physiology took place. By applying Hermann's old concept of "re-stimulation by local currents" (see p. 194 in Hermann, 1879), Rushton (1937) predicted the existence of a small area of the membrane in the excited state (i.e., localized response) in a nerve fiber subjected to a subthreshold stimulating current.

The diagram shown in Fig. 3.3A is adapted from Hermann's handbook of physiology published in 1879. Symbol E in the figure represents the portion of the nerve thrown into the excited state directly by the stimulating current. The surface membrane of this portion is traversed by an *inwardly* directed current. In the neighboring zones, there are *outwardly* directed currents which tend to excite these resting zones. The inwardly directed current through the excited membrane area tends to throw this area back to the resting state. These currents, which are produced by the difference in membrane potential between the excited (i.e., active) area and the resting zone, are called "*local currents*" (*Strömchen*). Hermann postulated that nerve

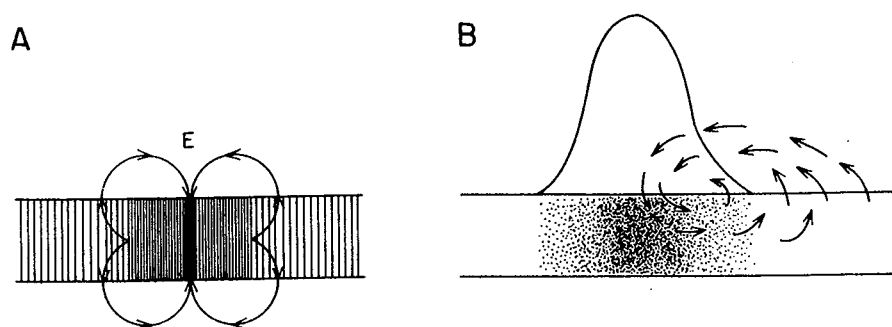


Fig. 3.3 (A) Diagram illustrating Hermann's concept of the process of restimulation by action currents. (Adapted from Fig. 25 of *Handbook of Physiology*, published in 1879). (B) Diagram illustrating the mechanism of propagation of an "activation wave" in Ostwald-Lillie's iron wire nerve analog. (Adapted from Fig. 5 of Lillie's monograph published in 1932.)

conduction is brought about by successive excitation of the resting zones by the local currents generated at the boundary between the resting area and the excited zone.

Figure 3.3B is reproduced from a figure in Lillie's monograph published in 1932, illustrating his conception of the local current. He based his entire argument on the similarity in electric behavior between a passive iron wire in nitric acid and a nerve. The passive iron wire model of a nerve fiber was introduced originally by Wilhelm Ostwald: his student, Heathcote (1901, 1907) examined this model extensively. Later on, Ralph Lillie (1932, p. 389) greatly popularized the model. It is interesting to note that the excited region of the nerve in this figure is represented by discrete stipples.

With the pictures of local currents in mind, Rushton developed the following argument. The area of the membrane excited directly by the applied stimulus is expected to increase with the stimulus intensity. When the area is large enough, a propagated all-or-none nerve impulse is initiated by the stimulus. If, on the contrary, the stimulating current pulse is weak, the area excited directly by the applied stimulating pulse is small, and, consequently, the local current generated is too weak to initiate a propagated nerve impulse. Thus, the condition for initiation of the nerve impulse is, to use Rushton's expression, that "*an action potential should arise over a region great enough to generate an action current sufficient to stimulate the neighboring region.*" In other words, if the local currents are acting as a restimulating agent, there should be, in the nerve membrane, a small electric response localized at the site of (subthreshold) stimulation. In order to facilitate his mathematical analysis, Rushton assumed that the primary excited area is delineated sharply, as shown in Hermann's diagram, by two lines perpendicular to the long axis of the axon. However, there is no reason why the excited area cannot be irregular or patchy, as hinted in Lillie's figure (Fig. 3.3B). Rushton was convinced that the experiment carried out by Hodgkin (1937), the youngest member of his laboratory, indicated the validity of Hermann's local current theory. Soon after Rushton's prediction, Hodgkin (1938) actually succeeded in demonstrating the existence of small, graded electric responses at the site of subthreshold stimulation.

In this connection, it is interesting to note that graded, subthreshold responses can be demonstrated easily in an iron wire model of nerve (Matsumoto *et al.*, 1958). When a subthreshold current pulse is applied to a passive iron wire, small, discrete, "active" patches and spots can be seen to appear on the passive surface. The number of active spots and patches increases with the current strength. These spots and patches disappear quickly when the applied current is terminated. When the fraction of the surface covered by these spots and patches reaches a certain critical value, the entire surface of the iron is thrown into the active state. This observation strongly suggests

the possibility of the existence of active spots and patches in the nerve membrane (see Chapter 13, Section I).

It was soon realized that, in analyzing excitation processes in frog nerve fibers, the structural factors, arising from the existence of nodes of Ranvier and myelin sheath, have to be taken into consideration. As we shall see in the following chapters, Tasaki and his collaborators have demonstrated that the myelin sheath is a good electric insulator (particularly to DC) and that the process of excitation is localized at nodes of Ranvier. Furthermore, nerve impulses were shown to propagate from one node to the next as the result of restimulation by local currents, the rate of propagation being determined almost exclusively by the cable property of the myelin sheath. At the same time, it became very clear that the use of vertebrate nerve fibers for studies of excitation processes per se presents various kinds of difficulties arising from the smallness of the fiber diameter. Soon thereafter, neurophysiology plunged into a new era in which much larger invertebrate nerve fibers were used for analysis of excitation processes. The experimental findings obtained by using giant nerve fibers will be discussed in later chapters.

REFERENCES

- Blair, H. A. (1932). On the intensity-time relations for stimulation by electric currents. *J. Gen. Physiol.* **15**, 709–729.
- Cremer, M. (1929). Erregungsgesetze des Nerven. In "Handbuch norm. u. pathol. Physiol." (A. Bethe ed.), Vol. 9, 244–284. Julius Springer, Berlin.
- Cremer, M. (1932). Ein neues Erregungsgesetz. *Scientia* **51**, 145–156.
- d'Arsonval, A. (1898). Action physiologique et therapeutique des courants a haute fréquence. *Ann. Électrobiol.* **1**, 1–28.
- Davis, H. (1923). The relationship of the "Chronaxie" of muscle to the size of the stimulating electrode. *J. Physiol. (London)* **57**, 81–82.
- Einhoven, W. (1900). Ueber Nervenreizung durch frequente Wechselströme. *Pfluegers Arch. Gesamte Physiol. Menschen Tiere* **82**, 101–133.
- Erlanger, J., and Gasser, H. S. (1937). "Electrical Signs of Nervous Activity." Univ. of Pennsylvania Press, Philadelphia.
- Fick, A. (1863). "Beiträge zur vergleichenden Physiologie der irritablen Substanzen." In *Gesammelte Schriften von Adolf Fick*. III Band. Stahel'sche Verlags-Anstalt, Würzburg. Friedrich Vieweg and Sohn, Braunschweig.
- Fick, A. (1864). "Untersuchungen über elektrische Nerven Reizung." Friedrich Vieweg and Sohn, Braunschweig.
- Heathcote, H. L. (1901). Vorläufiger Bericht über Passivierung, Passivität und Aktivierung des Eisens. *Z. Phys. Chem.* **37**, 368–373.
- Heathcote, H. L. (1907). The passivifying, passivity, and activifying of iron. *J. Soc. Chem. Ind., London* **26**, 899–917.
- Heilbrunn, L. V. (1938). "An Outline of General Physiology." Saunders, Philadelphia.

- Hermann, L. (1879). Allgemeine Nervenphysiologie. In "Handbuch der Physiologie." Ister Theil, 1-196, F. C. W. Vogel, Leipzig.
- Hermann, L. (1899). Zur Theorie der Erregungsleitung und der elektrischen Erregung. *Pfluegers Arch. Gesamte Physiol. Menschen Tiere* **75**, 574-590.
- Hill, A. V. (1910). A new mathematical treatment of changes of ionic concentration in muscle and nerve under the action of electric currents, with a theory as to their mode of excitation. *J. Physiol. (London)* **40**, 190-224.
- Hill, A. V. (1932). "Chemical Wave Transmission in Nerve." Cambridge Univ. Press, London and New York.
- Hill, A. V. (1936). Excitation and accommodation in nerve. *Proc. R. Soc. London, Ser. B* **119**, 305-355 (see also 440-453).
- Höber, R. (1905). Ueber den Einfluss neutraler Alkalisalze auf die Erregbarkeit und Färbbarkeit der peripheren Nervenfasern vom Frosch. *Zentralbl. Physiol.* **19**, 390-392.
- Höber, R. (1926). "Physikalische Chemie der Zelle und der Gewebe," 955 pp., 6th ed. Leipzig, Wilhelm Engelmann.
- Hodgkin, A. L. (1937). Evidence for electrical transmission in nerve. *J. Physiol. (London)* **90**, 183-232.
- Hodgkin, A. L. (1938). The subthreshold potentials in a crustacean nerve fibre. *Proc. R. Soc. London, Ser. B.* **126**, 87-121.
- Hofmeister, R. (1888). Zur Lehre von der Wirkung der Salze. Ueber Regelmässigkeiten in der eiweiss-fallenden Wirkung der Salze und ihre Beziehung zum physiologischen Verhalten derselben. *Arch Exp. Pathol. Pharmacol.* **24**, 247-260.
- Hoorweg, J. L. (1892). Ueber die elektrische Nervenerregung. *Pfluegers Arch. Gesamte Physiol. Menschen Tiere* **52**, 87-108.
- Hoorweg, J. L. (1894). Ueber die Nervenerregung durch Condensatorentladungen. *Pfluegers Arch. Gesamte Physiol. Menschen Tiere* **57**, 427-436.
- Hoorweg, J. L. (1898). Über die elektrische Eigenschaften der Nerven. *Pfluegers Arch. Gesamte Physiol. Menschen Tiere* **71**, 128-157.
- Lapicque, L. (1909). Définition expérimentale de l'excitabilité. *C. R. Soc. Biol.* **67**, 280-283.
- Lapicque, L. (1926). "L'Excitabilité en Fonction du Temps: La Chronaxie, sa signification et sa mesure." 365 pp. Presses Universitaires de France, Paris.
- Lillie, R. S. (1932). "Protoplasmic Action and Nervous Action," 2nd ed. 417 pp. Univ. of Chicago Press, Chicago, Illinois.
- Loeb, J. (1900). On ion-proteid compounds and their role in the mechanics of life phenomena. I. The poisonous character of a pure NaCl solution. *Am. J. Physiol.* **3**, 327-338.
- Loeb, J. (1906). "The Dynamics of Living Matter." Columbia Univ. Press, New York.
- Lucas, K. (1910). An analysis of changes and differences in the excitatory process of nerves and muscles based on the physical theory of excitation. *J. Physiol. (London)* **40**, 225-249.
- Matumoto, M., Iwaya, T., Fukuda, M., and Ishihara, H. (1958). Role of H-ion in excitation and excitation conduction in electrochemical model of excitation. *Gunma J. Med. Sci.* **7**, 29-37.
- Monnier, A. M. (1934). "L'Excitation Électriques des Tissus" Hermann and Cie, Paris.
- Nernst, W. (1908). Zur Theorie des elektrischen Reizes. *Pfluegers Arch. Gesamte Physiol. Menschen Tiere* **122**, 275-314.
- Rashevsky, N. (1933). Outline of a physico-mathematical theory of excitation and inhibition. *Protoplasma* **20**, 42-56.
- Ringer, S. (1880). Concerning the influence exerted by each of the constituents of the blood on the contraction of the ventricle. *J. Physiol. (London)* **3**, 380-393.
- Rushton, W. A. H. (1935). The time factor in electrical excitation. *Biol. Rev.* **10**, 1-17.

- Rushton, W. A. H. (1937). Initiation of the propagated disturbance. *Proc. R. Soc. London, Ser. B.* **124**, 210–243.
- Volta, A. (1803). Fortgesetzte Versuche über die Electricität. *Ann. Phys. (Leipzig)* **14**, 257–263.
- von Frey, M. (1883). Ueber die tetanisch Erregung von Froschnerven durch den constanten Strom. *Arch. Anat. Physiol. Leipzig, Physiol. Abt.* 43–56.
- von Kries, J. (1882). Ueber die Erregung des motorischen Nerven durch Wechselströme. *Ber. Naturforsch. Ges., Freiburg* **8**, 170–204.
- Weiss, G. (1901). Sur la possibilité de rendre comparables entre eux les appareils servant à l'excitation électrique. *Arch. Ital. Biol.* **35**, 413–446.

4. Early Observations of Saltatory Conduction of Nerve Impulses

A. ISOLATION OF SINGLE MYELINATED NERVE FIBERS

From the dawn of electrophysiology until the 1930s, sciatic nerves of the frog had been the most favorable material used by physiologists for investigating excitability phenomena. As is well known, a vertebrate nerve has a rather complex structure. It contains a great number of myelinated nerve fibers, large and small, as well as many nonmyelinated fibers. These fibers are bound together by a common connective tissue sheath.

Electrophysiological properties of the sciatic nerve reflect the structural complexity of the tissue. There is a systematic difference in physiological characteristics between small and large nerve fibers (Lapicque and Legendre, 1913; Gasser and Erlanger, 1927). A long time ago, Hermann (1872) showed that the electric resistivity of a nerve (trunk) is anisotropic, namely, that the resistance in the transverse direction is several times as high as that in the longitudinal direction. The resistance of a nerve is not purely ohmic. The potential drop produced within a nerve by a constant current is highly time dependent due to "internal polarization" (Hermann, 1905; Ebbecke, 1926; Bishop, 1928). The action potential (i.e., the potential drop produced by the action currents passing through the fluid medium within a nerve trunk) is strongly affected by the reactive and anisotropic properties of the nerve trunk. It is evident, therefore, that investigation of the properties of individual nerve fibers by using nerve trunks is of a very indirect character. The use of isolated nerve fibers could obviate most of the problems associated with studies of electrophysiological properties of nerve trunks.

In 1928, taking advantage of the advancement of electronics, Adrian and Bronk succeeded in recording small action potentials developed by individual nerve fibers. By reducing the number of fibers in the phrenic nerve of the rabbit by dissection, they could record distinct signs of nerve impulses traveling along individual nerve fibers. Following this success in England, Kaku

(presently known as J. Kwak) in Kato's laboratory in Tokyo developed a surgical technique for isolating single motor nerve fibers innervating the gastrocnemius muscle of the toad. The usefulness of such single-fiber muscle preparations became apparent when Kubo and Ono demonstrated a distinct variation in the electric threshold along a single nerve fiber (see Kato, 1934).

Motor nerve fibers of the toad are 10 to 15 μm in diameter and are heavily myelinated. In these fibers, the myelin sheath which covers the protoplasmic gel (called axis-cylinder) is interrupted at more-or-less regular intervals of about 2 mm. The regions of a nerve fiber devoid of the myelin sheath, namely, nodes of Ranvier, are very narrow (about 1 μm or less).

It may be of some interest to see how the state of our knowledge about the role of myelin sheath was at the time when direct experiments on isolated single fibers were begun. Ranvier (1871; Chapter 3), the discoverer of the nodes (see Fig. 4.1) believed that the axis-cylinder receives its nutrition through these gaps in the myelin sheath. Later, some investigators expressed the view that the lipid in the myelin sheath might be contributing to insulation of the axis-cylinder (see Göthlin, 1910; Lillie, 1925; Gerard, 1931). However, in Bethe's "Handbook of Physiology" published in 1929, Cremer stated absolutely nothing about the possible role of nodes of Ranvier. It is also interesting to note that Lillie (1932; see Chapter 3), who previously studied saltatory conduction in an iron-wire analog of the nerve (Lillie, 1925), completely ignored the existence of the myelin sheath and nodes of Ranvier in his monograph published in 1932.

In a review written in 1931, Gerard said: "The relation of myelin to nerve function has been a matter of even greater uncertainty than that of the (neuro-)fibrils, and the significance of the nodes of Ranvier has been particularly elusive (p. 69 in Gerard, 1931)." Without any experimental support, Gerard speculated further on the role of the nodes of Ranvier in the following manner: "If the stimulating action currents are in fact effective from node to node, the constriction of the axis-cylinder with reduction of axoplasm at just these points would render the neurofibrils especially open to activation by them (p. 71)." Evidently, physiologists at that time were misled by the popular, but erroneous, notion that there were no nodes of Ranvier in the central nervous system (see p. 47 in Ranson, 1927) and that neurofibrils were the ultimate element that carry nerve impulses (see Apáthy, 1897; see Chapter 3). In the history of neurophysiology (see Chapter 3), there are many cases in which widely accepted notions and theories are later proved to be erroneous. The neurofibril theory is another example of such cases.

It is important to note in this connection that at about the time when the properties of the nodes of Ranvier were examined by using isolated single nerve fibers, the role of the myelin sheath in nerve conduction was investigated by Erlanger and Blair (1934) through an entirely different method. They employed the method of "anodal polarization" applied to a small

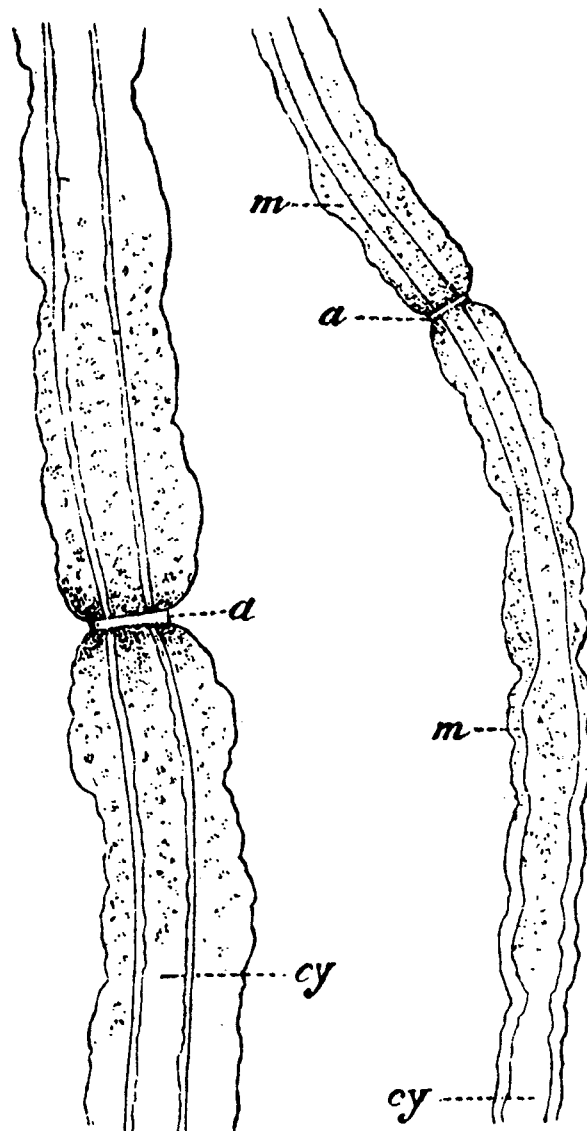


Fig. 4.1 Large myelinated nerve fibers isolated from a rabbit sciatic nerve in 1% picocarmine solution. *a*, nodes; *m*, myelin sheath; *cy*, axis-cylinder. The largest part of the fiber was about $15\ \mu\text{m}$ in diameter. (Reproduced from Fig. 235 in Ranvier's "Traite d'Histologie," 1889.)

branch of a nerve trunk. Since this method is somewhat indirect and the interpretation of the result obtained is rather complex, we defer the description of this experiment until Chapter 5, Section F.

B. MEASUREMENT OF THRESHOLD ALONG A MYELINATED NERVE FIBER

A single nerve fiber used for these threshold measurements was floating in a thin layer of Ringer's solution on a glass plate. The stimulating electrodes were relatively small; they were usually between 10 and $50\ \mu\text{m}$ in diameter. The stimulating cathode of these electrodes was moved stepwise within the

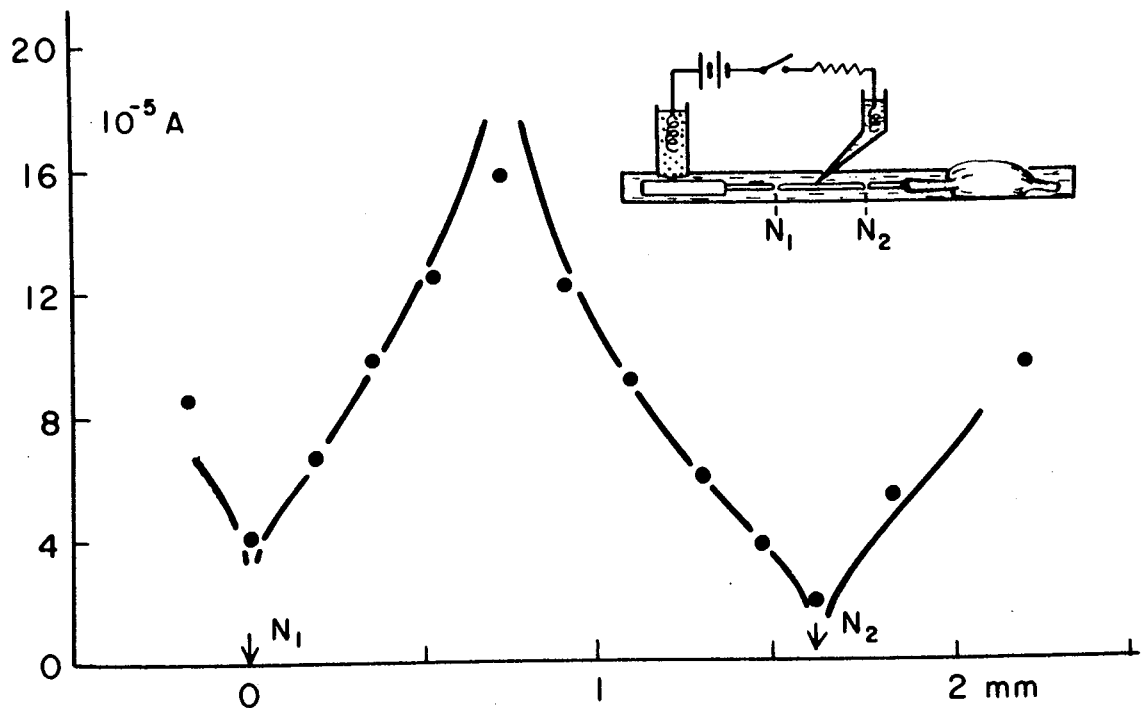


Fig. 4.2 Circles: The threshold strength of a long stimulating current pulse (expressed in amperes) plotted against the distance from a node of Ranvier. A glass-pipette electrode, about $100 \mu\text{m}$ in diameter, was used to measure the threshold along the fiber (from Tasaki, 1953). Continuous lines: Threshold current intensities calculated by the use of Eq. (4.4) with the value of κ chosen to fit the observed threshold for each of the two nodes of Ranvier involved.

layer of Ringer's solution and, at every position of the electrode, the current intensity necessary to evoke a twitch of the innervated gastrocnemius muscle was determined. The stimulating anode was, as a rule, kept stationary at one position in Ringer's solution. It was found that the threshold showed a distinct and sharp minimum at every node of Ranvier.

The significance of this finding was immediately clarified on the basis of an analysis of the potential field in the two-dimensional conducting fluid medium (Tasaki in Kato, 1934 and 1936). It was found possible to calculate the observed threshold variation on the assumption that the myelin sheath is a perfect electric insulator. In early studies, the threshold was measured with brief induction shocks applied through polarizable platinum electrodes. Later, more reliable results were obtained by the use of long rectangular current pulses delivered through a small nonpolarizable electrode (see Fig. 4.2).

Now it is well known that the field of electric potential produced by a sink of an electric current in a thin, two-dimensional fluid medium, $\phi(r)$, is given by

$$\phi(r) = -\frac{\rho I}{2\pi d} \ln r + \text{constant} \quad (4.1)$$

where r is the distance from the sink, ρ the resistivity of the fluid medium, d its thickness, and I the current intensity. The contribution of a source of current to the potential field is described by Eq. (4.1) with the sign of the current reversed. The nerve fiber under study is exposed to the net potential field given by superposition of the contributions of both the sink and source of the applied current (see Fig. 4.2). The presence of a single motor nerve fiber in the medium is considered not to disturb this potential distribution.

Next, the effect of this potential field on the nerve fiber is considered under the assumption that the myelin sheath is a perfect insulator for DC. The electric potentials in the medium at the positions of three successive nodes of Ranvier, N_0 , N_1 , and N_2 , are denoted by ϕ_0 , ϕ_1 , and ϕ_2 , respectively. The current which flows in the axis-cylinder between N_0 and N_1 is proportional to the potential difference $(\phi_0 - \phi_1)$. Similarly, the current in the fiber between N_2 and N_1 is proportional to $(\phi_2 - \phi_1)$. The intensity of the outwardly directed current through node N_1 can then be given by superposition of these two currents. Therefore, the condition for threshold excitation of the nerve fiber is given by

$$\frac{\phi_0 - \phi_1}{W} + \frac{\phi_2 - \phi_1}{W} = i_0 \quad (4.2)$$

where i_0 is the intensity of the outwardly directed current required to excite node N_1 and W the effective resistance of the internodal segment. This threshold condition can be rewritten explicitly as a function of the positions of the sink and the source by the use of Eq. (4.1).

We now treat a special case where the anode (source) is fixed at a point far away from the nerve fiber and the stimulating cathode (sink) is moved along the nerve fiber (Fig. 4.3). The distance between the cathode and node N_1 is denoted by x , the distance between N_2 and the cathode by $(l - x)$ and that between N_0 and the sink by $(l + x)$, where l represents the internodal distance. Thus, Eq. (4.2) can be written as

$$\frac{\rho I}{2\pi W d} [\ln(l - x) + \ln(l + x) - 2 \ln x] = i_0 \quad (4.3)$$

or

$$I = \frac{\kappa}{\ln[(l^2 - x^2)/x^2]} \quad (4.4)$$

where κ is equal to $(2\pi i_0 W d / \rho)$ and is independent of x . This is the desired relationship between the threshold intensity of the applied current I and the distance x between a node and the stimulating cathode. It was found that Eq. (4.4) explains the observed relationship between I and x satisfactorily.

Similar calculations were carried out under the condition that the stimu-

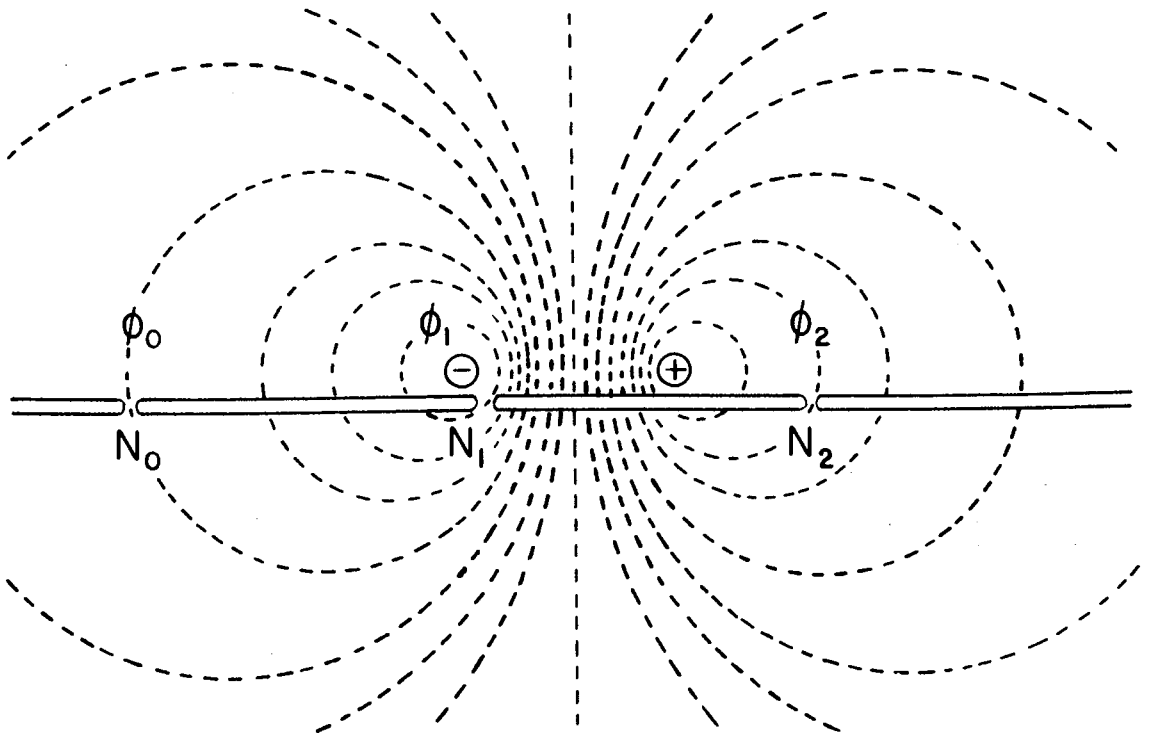


Fig. 4.3 The field of electric potential generated by a sink and a source of current in a thin layer of Ringer's solution. The equipotential lines which intercept nodes N_0 , N_1 , and N_2 are indicated by symbols ϕ_0 , ϕ_1 , and ϕ_2 .

lating cathode was moved in the direction perpendicular to the nerve fiber. In all cases, the results of calculation based on the assumption that the myelin sheath is a perfect insulator for DC gave good agreement with the experimental data.

An isolated single nerve fiber floating in a large volume of Ringer's solution was also used for threshold measurements. The threshold for DC (i.e., the rheobase) was found to vary more markedly in such a fiber than in fibers immersed in a shallow pool of Ringer's solution (Tasaki, 1950b). The potential field produced by the stimulating current in a three-dimensional electrolytic conductor varies inversely with the distance from the tip of the stimulating electrode. The rheobase is then expected to vary, in the vicinity of a node of Ranvier, directly with the distance between the node and the electrode tip (i.e., the sink of the current). In fact, it was found that this is actually the case.

In spite of the success of the theoretical treatment described above, it was soon realized that the accuracy of the threshold condition described by Eq. (4.2) is somewhat limited. In the following sections we shall see (1) that the myelin sheath cannot be treated as a perfect insulator when brief current pulses are used for stimulation, and (2) that the electric current through a node (e.g., N_1) is affected to some extent by the potential difference across remote internodal segments (e.g., the internode between N_2 and N_3). We

shall see later that the limitation of Eq. (4.2) derives from a "capacitative" flow of electricity through the myelin sheath, as well as from a relatively high electric resistance of the plasma membrane at the node of Ranvier.

C. TRIPOLAR STIMULATION OF A NERVE FIBER

An isolated nerve fiber floating in a pool of Ringer's solution is a very difficult object to investigate, for both stimulating and action currents are short-circuited by the conducting fluid medium outside the fiber. This difficulty can be obviated by dividing the fluid medium outside the fiber into two portions using some insulating material. Vaseline, paraffin, or a glass tubing coated with melted paraffin may be used to partition the Ringer's solution outside the fiber. When the portion of the fiber between two neighboring nodes of Ranvier is placed across such a "ridge" made of insulating material, it is possible to excite the fiber with a pair of large stimulating electrodes immersed in the pools of Ringer's solution divided by the ridge.

It is also possible to use a narrow (about 0.1 mm wide) air gap to divide the Ringer's solution into two separate pools. As long as all the nodes of the fiber are kept in Ringer's solution, measurements of the threshold of the fiber with the electrodes in the pools yield highly reproducible results. Under these circumstances, the entire space occupied by each pool of Ringer's solution is practically equipotential. Therefore, it is more convenient to express the threshold strength in applied voltage rather than in current intensity.

It is easy to divide the Ringer's solution around the fiber into three independent pools with a pair of ridges or air gaps. In large motor nerve fibers of the bullfrog or the toad, nodes of the fiber are separated by a distance of about 2.5 mm. If the width of the middle pool is about 2 mm, it is easy to introduce a single node of Ranvier in the middle pool (see Fig. 4.4). To control the potential along a nerve fiber, three electrodes, one in each of the three pools, are required. This electrode arrangement is similar to that employed by Danilewsky (1895) and by Rushton (1928) in their tripolar stimulation experiments on a nerve trunk.

The experimental result expected from this tripolar arrangement is very simple. If a nerve fiber is perfectly insulated by the myelin sheath except nodes of Ranvier, the voltage applied between the left-hand and middle pools, u , should correspond to the potential difference between node N_0 and N_1 , namely, $(\phi_0 - \phi_1)$. Similarly, the voltage between the right-hand and middle pools, v , should correspond to $(\phi_2 - \phi_1)$. We rewrite Eq. 4.2 in the following form:

$$u + v = v_0 \quad (4.5)$$

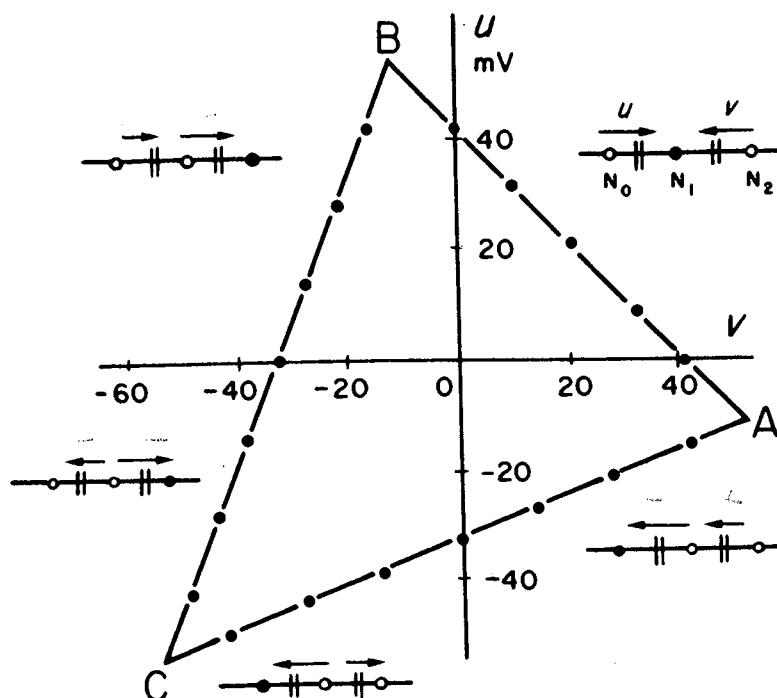


Fig. 4.4 Tripolar stimulation of a single myelinated nerve fiber immersed in pools of Ringer's solution divided by two "bridge insulators." A single node of Ranvier was introduced into the middle pool. u , The strengths of the voltage pulses applied between the proximal and middle pools; v , the strengths of the pulses applied between the distal and middle pools. These two pulses started and ended simultaneously. Straight line AB corresponds to the threshold conditions described by Eq. (4.5). Straight lines BC and AB are described by Eqs. (4.10) and (4.11), respectively. The primary sites of excitation are marked with black circles in the diagrams. (From Tasaki, 1939a.)

where v_0 is a constant. This relationship between u and v for threshold excitation represents a straight line intersecting both the u - and v - axes at 45° .

An example of the results of actual threshold measurements with long voltage pulses is shown in the first quadrant of the u - v plane in Fig. 4.4. In these measurements, the value of u was varied stepwise in the subthreshold range and the magnitude of v sufficient to excite the fiber was determined. These measurements revealed that Equation (4.5) describes the observed data extremely accurately. Note that the electrode in the middle pool is acting as a sink and those in the two lateral pools as the source of the stimulating currents.

The finding described in this section is quite consistent with the view that *the myelin sheath is a nearly perfect insulator for DC*, and consequently, that both voltage pulses u and v produce an outwardly directed current through the node in the middle pool, N_1 . Since the current generated by voltage pulse u in the axis-cylinder is opposite to that generated by voltage pulse v , the only possible site where the effects of u and v summate is at the surface membrane at node N_1 .

D. THE ELECTRIC RESISTANCE OF THE NODAL MEMBRANE

The tripolar arrangement of stimulating a single myelinated nerve fiber was used for disclosing another important property of the node of Ranvier. With this arrangement, it was demonstrated that the surface membrane at the node has a relatively high electric resistance. The principle of this resistance measurement was derived from the old concept of "electrotonic" spread of electric current along the nerve (Hermann, 1872; Cremer, 1900; see Chapter 2).

When the fluid medium outside a single nerve fiber is divided into three pools as shown in Fig. 4.4 (top), two independently adjustable voltage pulses, which start and end simultaneously, can be applied to two neighboring internodal segments. Again, the voltage pulse applied between nodes N_0 and N_1 is denoted by u and the pulse delivered between N_2 and N_1 is designated by v . The convention of the sign of these pulses is such that positive pulses produce outwardly directed currents through the node in the middle pool, N_1 . We have seen in the preceding section that, with positive pulses, the primary site of excitation is node N_1 .

The experimental results shown in Fig. 4.4 include the data obtained under the condition in which u is positive while v is negative (see the second quadrant in the figure), both u and v are negative (third quadrant), and u is negative while v is positive (fourth quadrant). It is seen in the figure that the values of u and v that satisfy the threshold condition lie on three distinct straight lines. Now, it is clear that all the observed points on straight line AB represent the threshold condition for the node on the middle pool, N_1 . When u is small and negative, voltage v has to be raised to override the inwardly directed current generated by u at node N_1 . Similarly, when v is small and negative, the threshold value of u for excitation of node N_1 is larger than v_0 .

Next, the significance of the straight lines in other quadrants, BC and AC , is considered. When v is negative and u is null, the threshold is reached when the outwardly directed current through N_2 reaches the critical value. If the voltage pulse applied between N_0 and N_1 does not generate any current through N_2 , the threshold voltage measured with v (< 0) is expected to remain totally unaffected by u . Actually, however, the slope of straight line BC clearly indicates that the voltage applied between N_0 and N_1 does affect node N_2 . This finding can easily be understood on the assumption that the surface membrane at N_1 has a relatively high electric resistance.

In treating the spread of DC, a myelinated nerve fiber can be represented adequately by the simple network of resistors shown in Fig. 4.5. Here, the resistance of the nodal membrane is represented by R and the resistance of

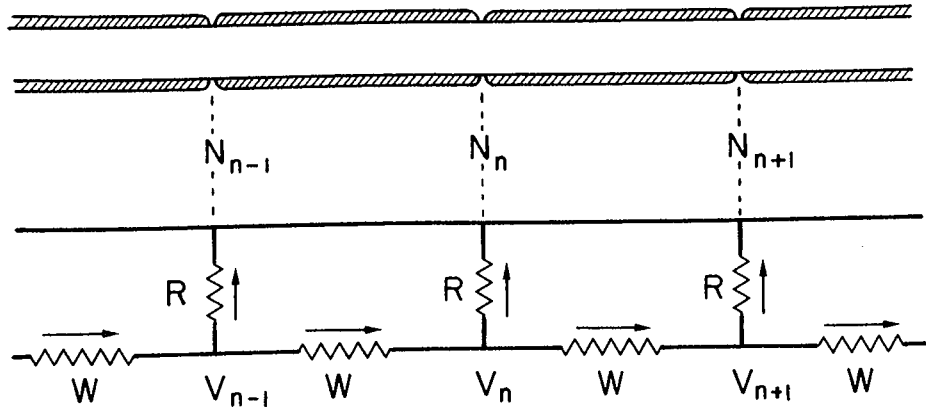


Fig. 4.5 Electric network designed to explain the spread of DC along a myelinated nerve fiber. W , the resistance of the axis-cylinder between two adjacent nodes of Ranvier; R , the resistance of the nodal membrane. The spread of electric potential along a network of this type is described by difference Eq. (4.7) in the text.

the axis-cylinder between two successive nodes by W . The resistance of the external medium is regarded as being negligibly small. The emf of the membrane at rest is omitted in this figure, because it is assumed to be constant. The spread of potentials and currents along this network can readily be analyzed by the use of a *difference equation*. We denote the potential inside the n th node referred to the potential of the external fluid medium by V_n . We now apply the well-known Kirchhoff law to the junction of the electric network at node N_n :

$$\frac{V_{n-1} - V_n}{W} - \frac{V_n - V_{n+1}}{W} = \frac{V_n}{R} \quad (4.6)$$

where V_{n-1} and V_{n+1} represent the potential inside node N_{n-1} and N_{n+1} , respectively. The terms in this equation can be rearranged to obtain the following difference equation:

$$V_{n-1} - \left(2 + \frac{W}{R}\right) V_n + V_{n+1} = 0 \quad (4.7)$$

This equation solved under the condition that the potential at $n = \infty$ is null has the following form:

$$V_n = V_0 e^{-\gamma n} \quad n = 1, 2, 3, \dots \quad (4.8)$$

where γ is determined by

$$\cosh \gamma = 1 + \frac{W}{2R} \quad (4.9)$$

Thus, it is found that the potential inside the nerve fiber is attenuated by a factor of $e^{-\gamma}$ per internode. When R is negligibly small as compared to W , the attenuation factor, $e^{-\gamma}$, is close to zero. The observed slope of straight

line BC indicates that the resistance of the nodal membrane, R , is not negligible as compared with the internodal resistance, W .

From these considerations, straight line BC , representing the threshold condition for long rectangular voltage pulses u and v , is described by

$$ue^{-\gamma} - v = v_0 \quad (4.10)$$

where v_0 represents the threshold value of v under the condition $u = 0$. Analogously, straight line AC is described by

$$ve^{-\gamma} - u = v_0 \quad (4.11)$$

With rectangular voltage pulses longer than about 1 msec, the observed value of $e^{-\gamma}$ is approximately 0.4. By introducing this value into Eq. (4.9), it is found that the DC resistance of the nodal membrane, R , is roughly 1.1 times the internodal resistance, W . The absolute values of these resistances are discussed later (see Chapter 5, Section E).

It is possible to widen the middle pool of Ringer's solution and to introduce two nodes of Ranvier. Tripolar stimulation of a nerve fiber under those conditions was found to yield the results expected from the argument developed above. Under these conditions, we have four different nodes as the primary sites of stimulation. The observed relationship between u and v which satisfies the threshold condition was found to fall on four distinct straight lines intersecting the axes roughly at predicted angles (Tasaki, 1939a). When only a myelinated portion of a nerve fiber is introduced into the middle pool the observed relationship between u and v was found to lie, as expected, on two straight lines (Tasaki, 1940).

Originally, the properties of a myelinated nerve fiber described above were disclosed by taking a contraction of the muscle innervated by the fiber as an index of excitation. As expected, the experiments carried out by taking action currents of the fiber as an index were found to yield the same results (Tasaki, 1953). Parenthetically, it may be pointed out that difference equations (4.7) can readily be solved under a variety of boundary conditions. When voltage v is applied externally between nodes N_1 and N_2 , for example, the voltage across the surface membrane at N_1 is found to be given by $V_1 = vR(1 - e^{-\gamma})/[W + 2R/(1 - e^{-\gamma})]$.

E. PROPAGATION OF NERVE IMPULSES ACROSS INEXCITABLE NODES

With the tripolar arrangement described above, it is easy to anesthetize the short portion of a nerve fiber in the middle pool keeping the neighboring regions in normal Ringer's solution. Figure 4.6 shows an example of the results of threshold measurements conducted before and after introduction of

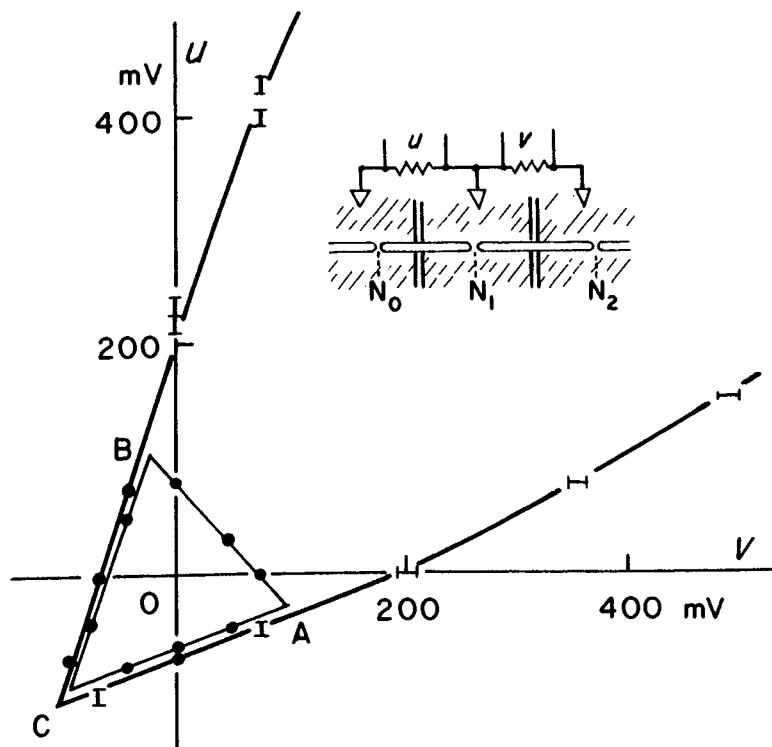


Fig. 4.6 Tripolar stimulation of a nerve fiber with one completely inexcitable node of Ranvier. The experimental arrangement used is shown by the diagram on the top. Note that the straight line (AB) representing threshold excitation of node N_1 , disappeared after introduction of cocaine into the middle pool. Note also that straight lines BC and AC remained practically unaffected by the anesthetic. (From Tasaki, 1939b.)

a 3 mM cocaine–Ringer’s solution into the middle pool. This concentration of cocaine is high enough to render a nerve trunk completely inexcitable. In fact, immediately after introduction of the anesthetizing solution, the threshold for the node in the middle pool, N_1 , was found to rise to an unmeasurably high level. Under these conditions, extensions of the threshold $u-v$ relationships for the nodes in the lateral pools, N_0 and N_2 , were observed in the first quadrant of the diagram. These results lend a straightforward confirmation of the conclusion stated in the preceding section.

It was noted immediately, however, that a nerve fiber under these conditions is capable of conducting impulses from one end to the other. When a brief electric current pulse was applied near the proximal end of the nerve fiber, the muscle innervated by the fiber was found to twitch. Even when the results of threshold measurements indicated that the node in the middle pool was completely inexcitable, nerve impulses were found to travel across the anesthetized region. The important implication of this finding was recognized at once.

At the time when this observation was made, most physiologists assumed that nerve impulses travel continuously along the axis-cylinder. On the basis

of this assumption, the effect of anesthetics diffusing into the axis-cylinder through nodes of Ranvier was discussed; the effect of cooling of the internodal segment was also examined from the same standpoint (Kato, 1934, 1936). Erlanger, who made a remarkable observation on segmentation of myelinated nerve fibers (Erlanger and Blair, 1934) was also in favor of the view that nerve impulses travel continuously along the axis-cylinder (p. 126 in Erlanger and Gasser, 1937). An important question arose immediately: If nerve conduction is a continuous process transmitted along the axis-cylinder, how can a nerve impulse travel across one completely inexcitable node of Ranvier?

Further examinations on the effects of anesthetics on single nerve fibers revealed the following additional facts:

1. When only a myelinated portion of a nerve fiber is immersed in the middle pool, namely, when there is no node of Ranvier in the middle pool, the anesthetic in the middle pool produces practically no change in the threshold $u-v$ relationship.
2. With a single node in the middle pool, nerve conduction across the anesthetized zone in the middle pool is maintained as long as the normal structure of the fiber is kept intact. When the structure of the fiber in the middle pool is destroyed, either osmotically or mechanically, conduction across the portion of the middle pool is suspended.
3. If a portion of a nerve fiber involving two successive nodes is exposed to the anesthetizing solution in the middle pool, conduction across the middle pool is blocked in some preparations. With three nodes in the middle pool, conduction across the anesthetized zone can never be observed.

It was not difficult to offer a reasonable explanation of all these experimental facts. Shortly before these observations on single nerve fibers were conducted, Hodgkin (1937; see Chapter 3) interpreted his results on compression block of a frog nerve (trunk) in terms of Hermann's hypothesis (see Chapter 3, Section F) that the action current is the agent that excites the resting area in front of the active zone. It was recognized that the experimental results obtained with single myelinated nerve fibers can readily be explained on the assumption that *the action current developed in the normal zone of a nerve fiber is strong enough to excite normal (i.e., unanesthetized) nodes of Ranvier beyond the anesthetized zone.*

When an action current spreads along a portion of a nerve fiber involving two inexcitable nodes, the current intensity is expected to be attenuated to a level of $\frac{1}{2}$ or less [see Eq. (4.8)]. It is therefore necessary to postulate that the action current is about 5 times the threshold value at the entrance of the an-

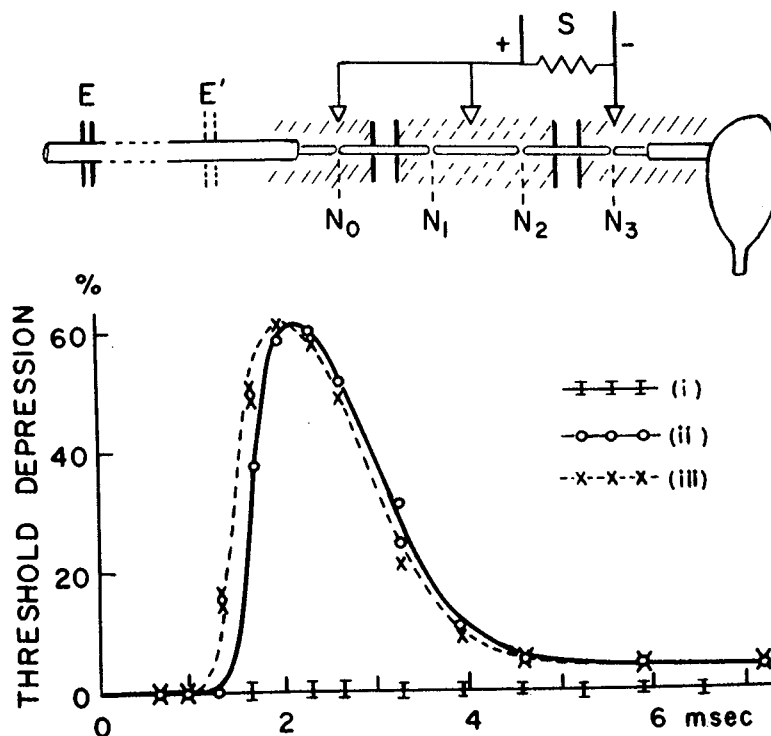


Fig. 4.7 Demonstration of the subthreshold stimulating effects of the action current spreading beyond two inexcitable nodes of Ranvier. Nerve conduction across the anesthetized region was suspended by slightly raising the threshold of the node in the distal pool with calcium chloride. The first electric shock (applied near the proximal end of the fiber) was (i) subthreshold (90%), (ii) barely suprathreshold (110%), and (iii) twice the threshold. The threshold strengths of the second shocks (applied between the middle and distal pools) were determined as a function of the interval between the two shocks. (From Tasaki, 1939b.)

esthetized zone. When this current amplitude is reduced to a level subthreshold for the excitable node beyond the anesthetized zone, conduction across the middle pool can no longer take place.

The effect of this spreading action current can be detected by delivering brief current pulses to the distal excitable node at about the time of the arrival of the action current. Figure 4.7 shows an example of the results in which the threshold current intensity for node N_3 was measured as a function of time after the delivery of a brief stimulating pulse to the nerve fiber through electrode E in the figure. As was expected from Hodgkin's experimental results, the threshold depression was found to closely resemble that of the action current developed by the node in the proximal pool, N_0 . This finding indicates the legitimacy of the interpretation mentioned above. The relationship between the threshold depression and the change in the membrane potential will be discussed later in Chapter 6, Section F.

F. THE PATHWAY OF THE LOCAL CURRENT

The physiologists who founded and developed the local circuit theory of nerve conduction [Hermann, 1879 (see Chapter 3); Cremer, 1929] were quite vague about the pathway of the local current. The term "sheath" (*Hülle*) was often used without specifying what the sheath was. Erlanger appeared to be reluctant to accept the possibility that the pathway might include the external fluid medium. He said (see p. 126 in Erlanger and Gasser, 1937): "But if progression in nerve is from node to node, it would have to be accomplished through restimulation by eddy currents flowing from node to node outside of the segments. . . . In other words the process that determines impulse propagation in a fiber would have to operate through structures that are foreign to the fiber. From the standpoint of teleology it is hard to believe that this is the case."

In this section, experimental evidence is presented that the pathway of the local current actually includes the electrolytic conductor outside the fiber (Tasaki, 1939b). At about the time when the following experiment was carried out on isolated myelinated fibers, Hodgkin (1939) also obtained convincing evidence that the pathway of the local current in the nonmyelinated fiber involves the external fluid medium.

The experimental setup employed for examining the pathway of the local current was the same as that described in the preceding section (see Fig. 4.8A). A single motor nerve fiber was mounted on a nerve chamber provided with two air gaps. Into the middle pool, two nodes of Ranvier were introduced. The three pools of Ringer's solution were kept at the same potential by means of a nonpolarizable electrode immersed in each pool. The

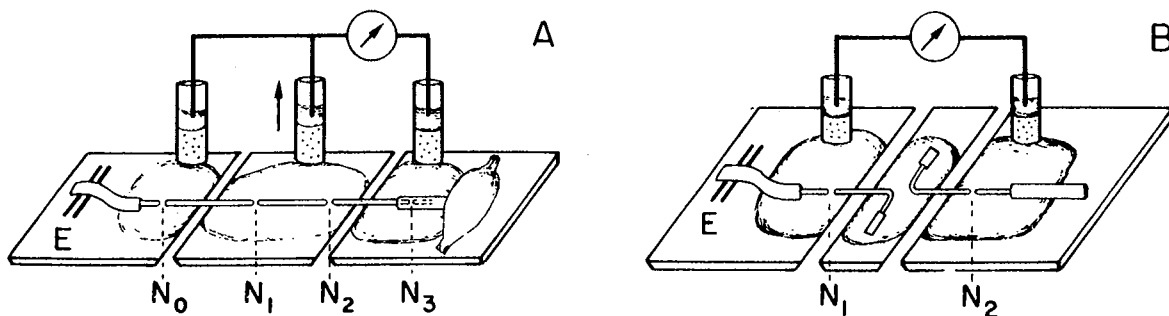


Fig. 4.8 (A) The experimental setup used for demonstrating that the pathway of the local current involves the external fluid medium. Conduction of the nerve impulse evoked by a shock delivered with electrode *E* was suspended by introducing a cocaine-Ringer's solution into the middle pool. Conduction was restored when the middle electrode was disconnected from the pool in the middle. (From Tasaki, 1939b.) (B) The arrangement used for demonstrating excitation of one nerve fiber by the action current developed by another. Note that the action current developed by node *N*₁ of the fiber on the left flows through the circuit involving node *N*₂ of the fiber on the left and the two electrodes. (From Tasaki and Tasaki, 1950.)

electrode in the middle was held by a micropositioner so that the electrode could be raised and its electric contact with the fluid medium could be broken when desired. Then, the normal Ringer's solution in the middle pool was replaced with 3 mM cocaine-Ringer's solution, which often brought about suspension of nerve conduction across the anesthetized zone. If nerve conduction was still maintained after introduction of the anesthetic into the middle pool, a slight increase in the CaCl_2 concentration in the distal (right-hand) pool was sufficient to bring about conduction block.

It was found that, when the middle pool was electrically isolated by raising the electrode, conduction of nerve impulses across the middle pool was immediately restored. When the middle electrode was again brought in contact with the fluid in the middle, nerve conduction across the anesthetized zone was immediately suspended. This effect of electric isolation of the middle pool was perfectly reproducible.

Electric isolation of the middle pool is expected to reduce the outward flow of electricity through the nodes in the middle pool, resulting in an increase in the outward current through N_3 . Thus, under the condition that node N_3 was traversed by a barely subthreshold electric current when the middle electrode was in contact with the pool, the current through N_3 becomes suprathreshold when the middle pool is electrically isolated. It is practically impossible to offer an alternative interpretation to this simple observation.

In the experiments just mentioned, the portion of the nerve fiber in the middle pool is acting simply as an inert conductor of electricity. We have also argued that the action current deriving from the normal (i.e., nonanesthetized) zone of a fiber is far stronger than the current intensity required for excitation (Section E). If there is no mistake in this line of argument, it should be possible to excite a single nerve fiber by an action current developed by another fiber. The air gap method offers an effective means of leading electric currents from one fiber to another.

Figure 4.8B shows the experimental arrangement used for demonstrating a "jump" of a nerve impulse from one myelinated nerve fiber to another. Two motor nerve fiber preparations were arranged in such a manner that both the distal end of one fiber and the proximal end of the other fiber were immersed in the small pool of Ringer's solution in the middle. During manipulation of these nerve fibers, the fluid in the middle pool was connected to the fluid in other pools by means of nonpolarizable electrodes. One of the fibers was excited by brief current pulses applied near its proximal end. The response of the other fiber was monitored either by observing contraction of the innervated muscle or the appearance of an action current.

With this experimental arrangement, it was possible to demonstrate that the action current developed by a single nerve fiber can excite another nerve

fiber. When the middle pool was electrically isolated from the lateral pools of Ringer's solution, the second fiber was found to be excited by the action current developed by the first fiber. As expected, transmission of a nerve impulse from one nerve fiber to another was found to take place only when electric coupling between the two fibers is very effective (Tasaki, 1950a).

From the experimental findings described above, it is expected that propagation of a nerve impulse should be blocked when the external electric resistance across one internodal segment is raised to a sufficiently high level. However, it is extremely difficult, if not impossible, to demonstrate conduction block in myelinated fibers by such a procedure. In order to reduce the local current effectively, the external resistance between two neighboring nodes has to be raised to a level well above 100 M Ω . Furthermore, if contraction of the innervated muscle is taken as an index of nerve conduction, the electric capacity of the muscle itself makes a large contribution toward closing the pathway of the local currents for a short period of time.

The internal resistance of a vertebrate myelinated nerve fiber is very high (see Chapter 5). Therefore, a nerve impulse traveling along one fiber in a normal nerve trunk is never transmitted to other fibers. In this sense, conduction of nerve impulses along individual nerve fibers is *isolated*.

G. THE CAPACITOR-LIKE BEHAVIOR OF THE MYELIN SHEATH

A long time before direct electrical measurements were carried out on isolated myelinated nerve fibers, Lillie (1925) made a very interesting observation on his iron wire model. He immersed, in a solution of concentrated nitric acid, a long iron wire covered segmentally with glass tubing. He found that a wave of activation of the oxidized surface layer travels from a break in the glass tubing to the next. He also showed that the wave of activation travels much faster along such a model than in the same wire without glass covering. Later, Rashevsky (1938) discussed the possible implication of Lillie's model under the assumption that the myelin sheath is a perfect insulator of electricity.

It is true that Lillie's model mimics some aspects of the behavior of real nerve fibers. However, it is important to note that the similarity between Lillie's model and the nerve fiber is quite limited. Above all, the space occupied by the iron wire is practically equipotential because of the high conductivity of the metal; in a nerve fiber carrying a nerve impulse, a large potential gradient exists only inside the fiber. Furthermore, electrical properties of glass tubing are very different from those of the myelin sheath. Shortly after the first demonstration of saltatory conduction in the myelinated nerve

fiber, it was found that *the myelin sheath of a nerve fiber behaves like a leaky capacitor* (Tasaki, 1940; see also Chapter 5, Section E). There is no doubt that the myelin sheath shows a high resistance to DC; but, when the potential difference across the myelin sheath suddenly changes, there is a rather strong, transient flow of electricity through the sheath.

When a nerve impulse travels along a nerve fiber, there is a large variation in the potential difference across the myelin sheath. It is therefore expected that a sizable capacitative flow of electricity takes place through the myelin sheath during nerve conduction. This expectation was verified by the use of the experimental setup diagrammatically shown in Fig. 4.9A (top) (see Tasaki and Takeuchi, 1941, 1942). Here, a 1-mm long myelinated portion of a nerve fiber was introduced into the middle pool of a nerve chamber with a pair of narrow air gaps. The electrodes immersed in the two lateral pools were directly grounded; and the electrode in the middle pool was connected to the other electrodes through a relatively low resistance. With this arrangement, a current through the portion of myelin sheath in the middle pool produces a potential drop across the inserted resistance. This potential drop was recorded with a cathode ray oscillograph through an amplifier.

The left-hand record in the figure represents the membrane current which was observed when the nerve fiber was excited by an electric shock applied to the nerve fiber near its proximal end. It is seen that there are two peaks in the current which traverses the myelin sheath during nerve conduction. The time interval between the peaks was found to be roughly 0.1 msec. Since the conduction rate in these motor nerve fibers is, at room temperature, about 25 m/sec and since the internodal distance is close to 2.5 mm, the interval between the two peaks corresponds to the "internodal conduction time." Hence, the first peak in the record was explained as representing a capacitative current associated with the appearance of an action potential at the proximal node, N_1 . Similarly, the second peak was explained as being produced by an action potential at the distal node, N_2 . (Here, the term "action potential" is used to denote a sudden change in the emf evoked by a stimulus.) This interpretation is supported by the experimental fact that anesthetization of node N_2 suppresses the second peak without affecting either the position or the amplitude of the first peak. A dilute anesthetizing solution introduced into the middle pool was found, as expected, not to produce any change in either the intensity of the current or the interval between the two peaks.

Figure 4.9B shows the membrane current recorded from a portion of a nerve fiber including a single node of Ranvier. The length of the portion of the fiber in the middle pool was the same as in the experiment of Fig. 4.9A. Hence, the recorded current includes the component passing through the myelin sheath. The important difference between Records A and B lies in the

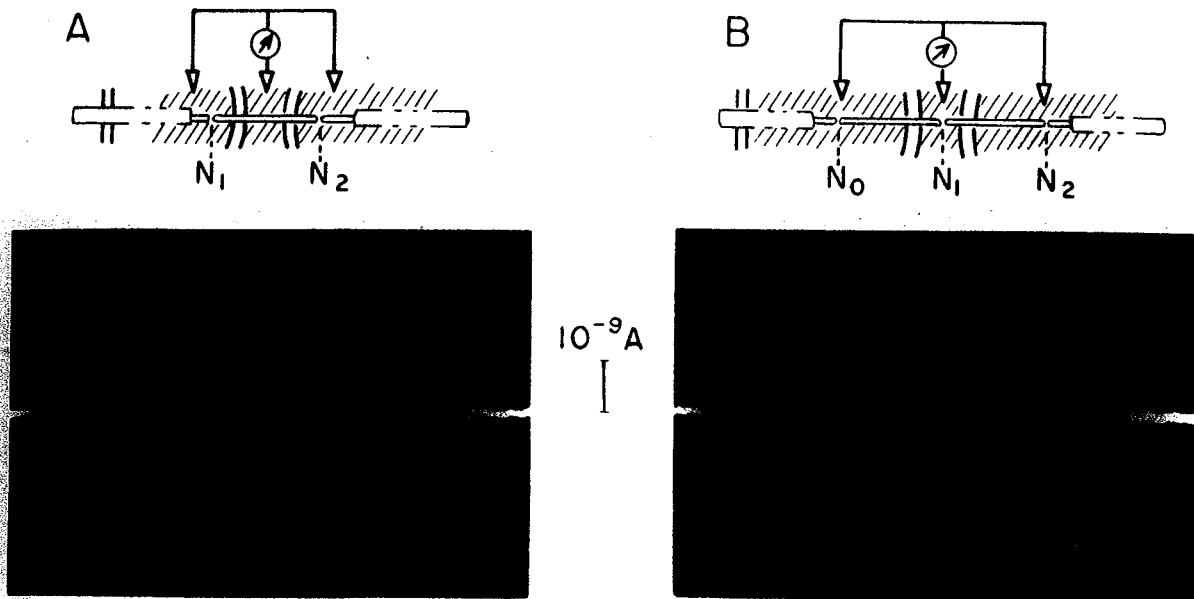


Fig. 4.9 (A) Membrane current led through a 1-mm long myelin covered portion of a toad motor nerve fiber. (B) Membrane current recorded from a 1-mm long portion of a motor nerve fiber including one node of Ranvier. A nerve impulse was evoked by a brief electric shock applied to the fiber through the electrodes placed near the proximal end of the fiber. (From Tasaki, 1958.)

fact that there is a large negative deflection in Record B while the fast deflections in Record A are purely positive. The negative deflection in Record B indicates that the nodal membrane at N_1 is traversed by an inwardly directed current. This inward current is expected to start immediately after the onset of the action potential at node N_1 and to cease when node N_2 is also thrown into excitation. The relationship between the electric capacity of the myelin sheath and the internodal conduction time will be discussed further in Chapter 5, Section E.

H. FURTHER STUDIES OF THE ACTION CURRENTS OF MYELINATED NERVE FIBERS

The major portion of the experimental findings described in the preceding sections were published shortly before and during the early period of World War II. Several years after the end of the war, Huxley and Stämpfli (1949) devised a new method of recording action currents from different parts of the myelinated nerve fiber. This method consisted in passing a single nerve fiber through a small hole in a celluloid partition in a nerve chamber filled with Ringer's solution. By means of electrodes placed in the two pools of Ringer's solution, action currents could be recorded at any point along the fiber. The

nerve fiber could be displaced stepwise at short intervals in the longitudinal direction of the fiber. By subtracting the action current recorded at one point from that taken at a neighboring point graphically, the current passing through a short portion of the surface membrane of the fiber could be obtained. With this method, it was possible to record membrane currents from several segments within one internode.

The results of these measurements are reproduced in Fig. 4.10. Again, the current through the myelin sheath was found to have two peaks separated by an interval of about 0.1 msec. The current through a short segment involving

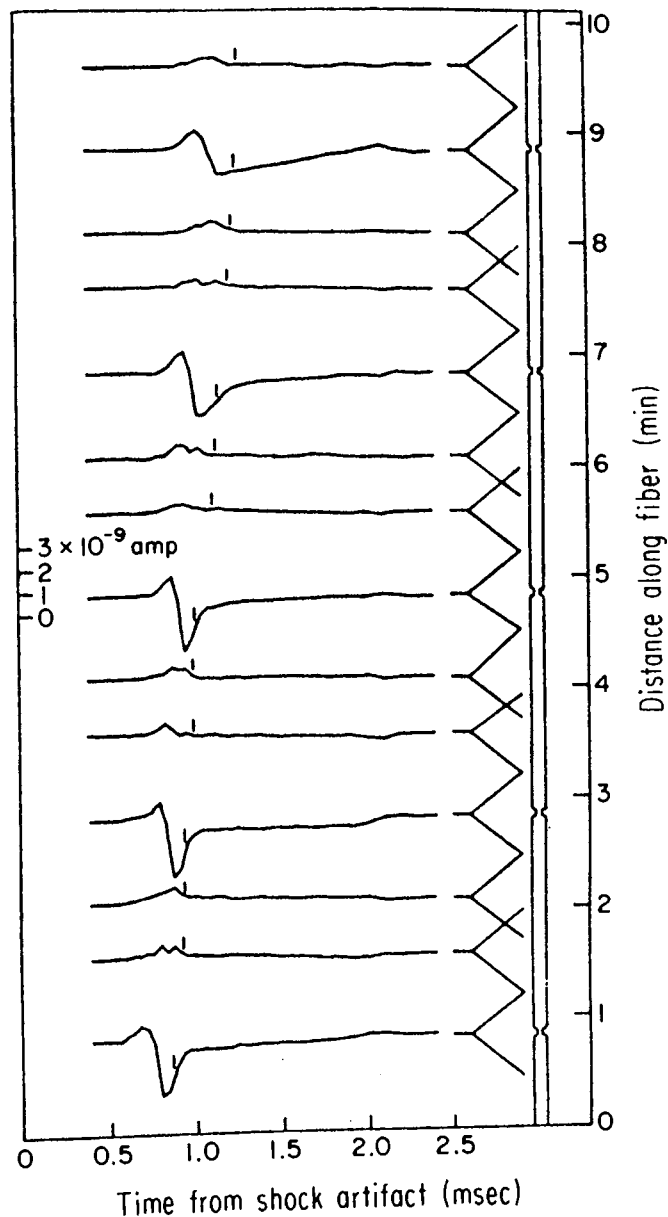


Fig. 4.10 Membrane currents obtained by the subtraction method. Each curve shows the difference between the two longitudinal currents at two points 0.75 mm apart on the fiber. The positions of those two points relative to the nodes are indicated on the diagrammatic fiber on the left. (From Huxley and Stämpfli, 1949.)

a single node of Ranvier was found to show a clear indication of an inward current.

The inward current through the node could also be detected without using any insulating partitions (Tasaki and Tasaki, 1950). The method employed for this purpose was to place a single nerve fiber in a shallow pool of Ringer's solution. A fine platinized platinum electrode held by means of a micromanipulator was used for recording. The reference electrode was placed far away from the fiber. Under these conditions, the amplitude of the potential variation, V , observed at the peak of inward current through a node is expected to vary with the logarithm of the distance, r , from the node (cf. Section B):

$$V = \frac{l\rho}{2\pi d} \ln r + \text{constant} \quad (4.12)$$

where ρ is the resistivity and d the thickness, respectively, of the thin conducting fluid medium.

The observed potential variation showed a sharp negative peak when the recording electrode was located in the immediate vicinity of each node of Ranvier. As the recording electrode was moved away from a node, the observed potential variation was found to decrease to a level which was roughly independent of the direction in which the electrode was displaced. Furthermore, the amplitude of the potential variation agreed, within the uncertainty of the estimation the thickness, d , with the value predicted by Eq.(4.12).

It may be added in this connection that Frankenhaeuser (1952) obtained the sign of inward current through the node of Ranvier in single nerve fibers *within* a nerve trunk. The electric impedance of a nerve trunk is highly anisotropic and is dependent on the frequency of the AC used for measurement. Therefore, the potential variation produced by the action currents of single fibers within a nerve trunk is very different from that observed in simple electrolytic conductors. Nevertheless, we may conclude, from Frankenhaeuser's observation and from Lussier and Rushton's (1952) experiment on the excitability of a single nerve fiber in an intact nerve trunk, that there is no fundamental difference between surgically isolated nerve fibers and those buried in a nerve trunk.

I. MICROELECTRODE RECORDING OF ELECTRIC RESPONSES FROM MYELINATED NERVE FIBERS

In classical neurophysiology, the term "action potential" is used to denote a potential variation which appears on the surface of a nerve trunk when fibers within the trunk carry nerve impulses (see Erlanger and Gasser, 1937).

Since individual fibers in a nerve trunk are surrounded by a highly conductive tissue fluid, the potential variation generated by the action currents of the fibers on the surface of the nerve trunk is usually very small; it is less than a few millivolts in amplitude under ordinary experimental conditions.

In 1950, by using hyperfine glass-pipette electrodes devised by Ling and Gerard (1949), Nastuk and Hodgkin (1950) succeeded in recording action potentials from the interior of individual frog muscle fibers. Shortly afterward, A. F. Huxley and I. Tasaki found, in Cambridge, England, that this method of recording action potentials can be applied to myelinated nerve fibers. The following is a brief description of the results of a further study carried out in St. Louis, Missouri (Tasaki, 1952).

Again, large motor nerve fibers of the frog were used. An isolated single nerve fiber was mounted on a chamber provided with a narrow air gap (see Fig. 4.11, top). The air gap served to immobilize the fiber and to facilitate penetration of the fiber with a microelectrode. Simultaneously, it was used for recording action currents of the fiber by means of a pair of large electrodes immersed in the pools of Ringer's solution in the chamber. A micro-manipulator was employed to push the microelectrode diagonally into the myelinated portion of the nerve fiber.

It was found by this method that, when the tip of a microelectrode is pushed deep into the myelin sheath of a nerve fiber, a small positive potential variation appears on the screen of an oscillograph connected to the microelectrode (see Record A). At this moment, the DC output of the microelectrode is not significantly different from that observed when the microelectrode tip is immersed in the Ringer's solution outside the fiber. As the microelectrode is pushed deeper into the nerve fiber, the amplitude of the recorded action potential is increased. With frog motor nerve fibers of about $10\ \mu\text{m}$ in outside diameter, action potentials that exceed about 50 mV in amplitude can be observed by this method.

It is interesting to note that even when the top of the microelectrode is pushed clearly into the axis-cylinder, the oscillograph trace displaying the microelectrode output often shows no clear sign of a DC shift. Under these conditions, the tip of the microelectrode appears to be covered with a very thin layer of lipid material. It was found also that, when a distinct negative shift appears in the DC output of the microelectrode, the action current recorded across the air gap starts to deteriorate (Record C). Shortly after the appearance of a DC shift, a "notch" appears at the top of the action potential, indicating a large increase in the conduction time across the injured internode (Record D). Soon, the separation between the two peaks of the action potential starts to increase (Record E); finally, the second peak of the action potential drops out, indicating that nerve conduction across the injured internode is suspended (Record F).

This method of recording action potentials can be applied to nerve fibers

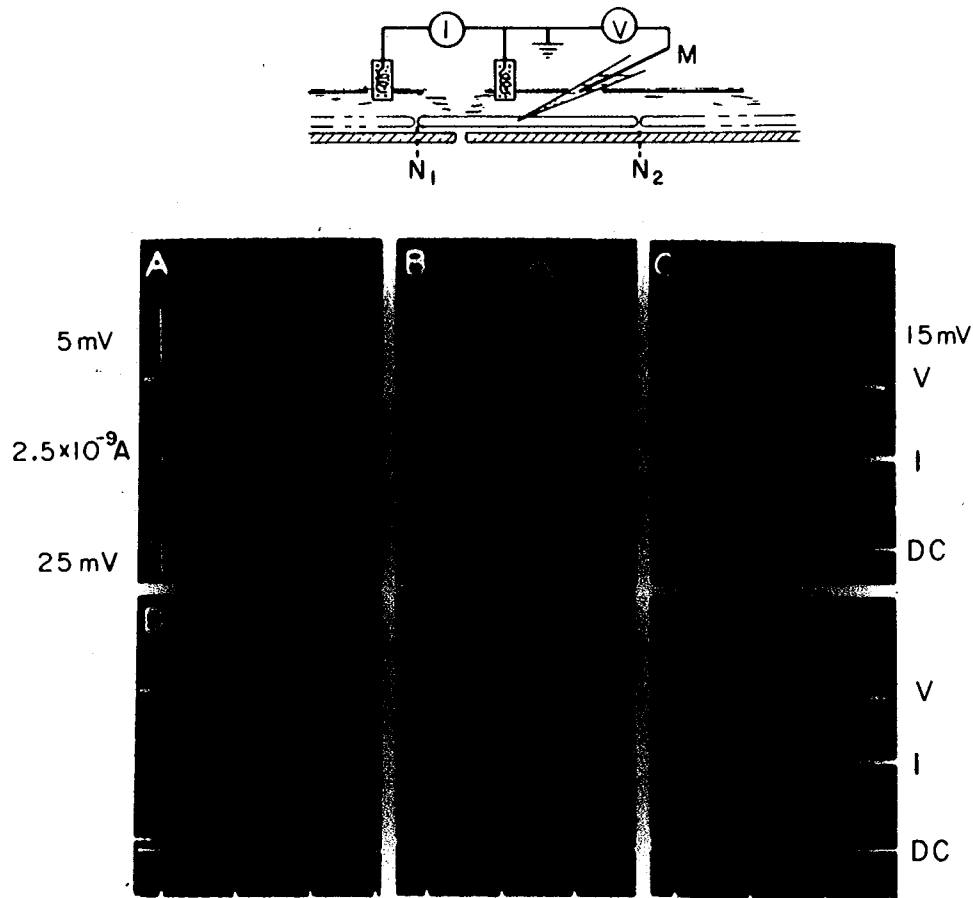


Fig. 4.11 V, Action potentials recorded with a hyperfine microelectrode pushed into the myelinated portion of a motor nerve fiber. I, Action currents simultaneously recorded from the same internode mounted across a bridge-insulator. DC, the resting potential recorded with the microelectrode. Record A was taken when the microelectrode pushed in the myelin sheath began to pick up action potentials. B was taken after pushing the microelectrode deeper into the myelin sheath. C, D, and E show progressive deterioration of the fiber. Time marker, 1 msec apart. (From Tasaki, 1952.)

within intact nerve trunks (Woodbury, 1952). This is a very convenient method of tracing the pathway of nerve impulses and of examining the pattern of impulse discharges. However, for a quantitative study of electrical properties of the nodal membrane, this method is totally inadequate because of the injurious effect of microelectrode penetration. Later, a new method of recording action potential of a single node of Ranvier was developed (see Chapter 5, Section A).

REFERENCES

- Adrian, E. D., and Bronk, D. W. (1928). The discharge of impulses in motor nerve fibres. I. Impulses in single fibres of the phrenic nerve. *J. Physiol. (London)* **66**, 81–101.
- Bishop, G. H. (1928). The effect of nerve reactance on the threshold of nerve during galvanic current flow. *Am. J. Physiol.* **85**, 417–431.

- Cremer, M. (1929). Erregungsgesetze des Nerven. "Handbuch d. norm. u. pathol. Physiol" (A. Bethe, ed.), Vol. 9, pp. 244–284. Julius Springer, Berlin.
- Danilewsky, B. (1895). Über die tripolare elektrische Reizung der Nerven. *Centralblatt Physiol.* **9**, 390–398.
- Ebbecke, U. (1926). Ueber die Polarisation im Nerven und muskel und ihre Messung. *Pfluegers Arch. Gesamte Physiol. Menschen Tiere* **212**, 121–135.
- Erlanger, J., and Blair, E. A. (1934). Manifestation of segmentation in myelinated axons. *Am. J. Physiol.* **110**, 287–311.
- Erlanger, J., and Gasser, H. S. (1937). "Electrical Signs of Nervous Activity" 216 pp. Univ. of Pennsylvania Press, Philadelphia.
- Frankenhaeuser, B. (1952). Saltatory conduction in myelinated nerve fibres. *J. Physiol. (London)* **118**, 107–112.
- Gasser, H. S., and Erlanger, J. (1927). The role played by the sizes of the constituent fibers of a nerve trunk in determining the form of its action potential wave. *Am. J. Physiol.* **80**, 522–547.
- Gerard, R. W. (1931). Nerve conduction in relation to nerve structure. *Q. Rev. Biol.* **6**, 59–83.
- Göthlin, G. F. (1910). Untersuchungen über Kapazität, Isolationswiderstand, Leitungswiderstand und Propagationsgeschwindigkeit für elektrische Stromstöße bei den Nervenfasern im Corpus callosum des Rindes. *Pfluegers Arch. Gesamte Physiol. Menschen Tiere* **133**, 87–144.
- Hermann, L. (1872). Ueber eine Wirkung galvanischer Ströme auf Muskeln und Nerven. *Pfluegers Arch. Gesamte Physiol. Menschen Tiere* **6**, 312–360.
- Hermann, L. (1905). Beiträge zur Physiologie und Physik des Nerven. *Pfluegers Arch. Gesamte Physiol. Menschen Tiere* **109**, 95–144.
- Hodgkin, A. L. (1939). The relation between conduction velocity and the electrical resistance outside a nerve fibre. *J. Physiol. (London)* **94**, 560–570.
- Huxley, A. F., and Stämpfli, R. (1949). Evidence for saltatory conduction in peripheral myelinated nerve fibres. *J. Physiol. (London)* **108**, 315–339.
- Kato, G. (1934). "Microphysiology of Nerve." Maruzen, Tokyo.
- Kato, G. (1936). On the excitation, conduction, and narcotisation of single nerve fibres. *Cold Spring Harbor Symp. Quant. Biol.* **4**, 202–213.
- Lapicque, L., and Legendre, R. (1913). Relation entre le diamètre des fibres nerveuses et leur rapidité fonctionnelle. *C. R. Acad. Sci.* **157**, 1163–1166.
- Lillie, R. S. (1925). Factors affecting transmission and recovery in the passive iron nerve model. *J. Gen. Physiol.* **7**, 473–507.
- Ling, G., and Gerard, R. W. (1949). The normal membrane potentials of frog sartorius fibers. *J. Cell. Comp. Physiol.* **34**, 383–396.
- Lussier, J. J., and Rushton, W. A. H. (1952). The excitability of a single fibre in a nerve trunk. *J. Physiol. (London)* **117**, 87–108.
- Nastuk, W. L., and Hodgkin, A. L. (1950). The electrical activity of single muscle fibers. *J. Cell. Comp. Physiol.* **35**, 39–74.
- Ranson, S. W. (1927). "The Anatomy of the Nervous System," 3rd ed. Saunders, Philadelphia, Pennsylvania. (see p. 47)
- Ranvier, L. (1889). "Traité technique d'Histologie," 2nd ed. Paris, Libraire F. Savy.
- Rashevsky, N. (1938). "Mathematical Biophysics." Univ. of Chicago Press, Chicago, Illinois.
- Rushton, W. A. H. (1928). Nerve excitation by multipolar electrodes. *J. Physiol. (London)* **66**, 217–230.
- Tasaki, I. (1939a). Electric stimulation and the excitatory process in the nerve fiber. *Am. J. Physiol.* **125**, 380–395.
- Tasaki, I. (1939b). The electrosaltatory transmission of the nerve impulse and the effect of narcosis upon the nerve fiber. *Am. J. Physiol.* **127**, 211–227.

- Tasaki, I. (1940). Microphysiologische untersuchungen über die Grundlage der Erregungsleitung in der markhaltigen Nervenfasern. *Pfluegers Arch. Gesamte Physiol. Menschen Tiere* **244**, 125–141.
- Tasaki, I. (1950a). Excitation of single nerve fiber by action current from another single fiber. *J. Neurophysiol.* **13**, 177–183.
- Tasaki, I. (1950b). Nature of the local excitatory state in the nerve fiber. *Jpn. J. Physiol.* **1**, 75–85.
- Tasaki, I. (1952). Properties of myelinated fibers in frog sciatic nerve and in spinal cord as examined with microelectrodes. *Jpn. J. Physiol.* **3**, 73–94.
- Tasaki, I. (1953). "Nervous Transmission." Thomas, Springfield, Illinois.
- Tasaki, I. (1958). Conduction of the nerve impulse. In "Handbook of Physiology" (J. Field, H. W. Magoun, and V. E. Hall, eds.), Vol. 1, Chap. III. American Physiological Society, Bethesda.
- Tasaki, I., and Takeuchi, T. (1941). Der am Ranvierschen Knoten entstehende Aktionsstrom und seine Bedeutung für die Erregungsleitung. *Pfluegers Arch. Gesamte Physiol. Menschen Tiere* **244**, 696–711.
- Tasaki, I., and Takeuchi, T. (1942). Weitere Studien über den Aktionsstrom der markhaltigen Nervenfasern und ueber die elektrosaltatorische Uebertragung des Nervenimpulses. *Pfluegers Arch. Gesamte Physiol. Menschen Tiere* **245**, 764–782.
- Tasaki, I., and Tasaki, N. (1950). The electric field which a transmitting nerve fiber produces in the fluid medium. *Biochim. Biophys. Acta* **5**, 335–342.
- Woodbury, J. W. (1952). Direct membrane resting and action potential from single myelinated nerve fibers. *J. Cell. Comp. Physiol.* **39**, 323–340.

5. Conduction of Impulses in Myelinated Nerve Fibers

A. THE ALL-OR-NONE BEHAVIOR OF THE NODE OF RANVIER

In this chapter we deal first with the electrophysiological properties of individual nodes of Ranvier under a variety of experimental conditions. Next, we analyze the mechanism of nerve conduction under normal and abnormal conditions on the basis of the saltatory theory. We start this chapter by describing the all-or-none behavior of the electric response of a single node of Ranvier.

The discovery of the "all-or-none law" is very old. Even in the mid-eighteenth century (see Chapter 2, Section A), some Italian physiologists had a rather clear understanding of this law. In 1757, Felice Fontana proposed the well-known gun power analogy of the stimulus-response relationship; he compared a strong contraction of the heart muscle produced by a weak stimulus to a powerful explosion of gun powder ignited by a small spark (see p. 236 in Haller, 1760). In 1871 Henry P. Bowditch, an American doctor of medicine who was working in Carl Ludwig's laboratory in Leipzig, Germany, examined the magnitude of contraction of the nonbeating heart muscle as a function of the strength of the induction shock used for stimulation. He found that, in the range of stimulus strength higher than the threshold, the magnitude of muscular contraction did not increase with the stimulus strength; instead, it remained constant irrespective of the stimulus strength.

Much later, Gotch (1902) argued that the impulses conducted along individual nerve fibers in a nerve trunk might be of the "all-or none" character. When Adrian and Zotterman (1926) and, later, Adrian and Bronk (1928; see Chapter 4) succeeded in recording electrical responses from individual nerve fibers, it became quite clear that *the electric sign of a propagated nerve impulse obeys the all-or-none law.*

In the preceding chapter, we have seen that nerve conduction in the myelinated nerve fiber is nothing more than successive excitation of nodes of Ranvier through the mediation of local currents. We regard excitation of a

single node as a unitary process that is more basic than the process of conduction of a nerve impulse. It is therefore important to examine the relationship between the stimulus strength and the response of a single node of Ranvier. In order to examine the behavior of the nodal membrane without being disturbed by the responses of the neighboring nodes, it is necessary to physiologically isolate a single node of Ranvier.

Physiological isolation of a single node was accomplished first by the use of the tripolar arrangement (see Fig. 4.4) in which the portions of the fiber in the two lateral pools were rendered inexcitable with an anesthetic (Tasaki and Takeuchi, 1941; see Chapter 4). Later, by combining anesthetics with electric insulation, a new method of recording action potentials of a single node was devised (Tasaki, 1956; see also Frankenhaeuser, 1957).

The diagram on the top of Fig. 5.1 illustrates the experimental arrangement used for recording potential changes of a node (referred to the potential of the external fluid medium) produced by rectangular current pulses applied to the node. With this arrangement, the myelin sheath between node N_1 and node N_2 in the diagram may be regarded as a "microelectrode" connecting the interior of node N_1 to the input of the potential recording device. Although there is some uncertainty as to the absolute DC level observed with this device, the potential variations brought about by the applied current pulses are considered to be reliable.

Examples of the records taken with this experimental arrangement are shown in the lower part of the figure. It is seen that action potentials are initiated when the intracellular potential level was raised to about 20 mV above the resting potential. In a wide range of duration of the stimulating pulse, the threshold membrane potential was found to be independent of the duration. The constancy of the "electrotonic potential" in threshold excitation had been suggested a long time before direct measurements of the membrane potential became possible (see Schaefer, 1936).

It was also found by the method described above that the amplitude of the action potential developed by a normal node is about 110 mV and is practically independent of the stimulus strength when the pulse duration is relatively short. The nodal membrane behaves in an all-or-none manner when excited with brief shocks.

It is seen in the figure that the action potentials evoked by long rectangular current pulses of barely suprathreshold strengths are somewhat smaller than those produced by brief pulses. These relatively small action potentials are preceded by a gradual rise in the membrane potential, or a "foot" of the action potential. This gradual potential rise is interpreted as the sign of "subthreshold responses" predicted by Rushton (see Chapter 3, Section F). We thus find that the action potentials preceded by a distinct subthreshold response are slightly smaller than those which rise to the peak swiftly.

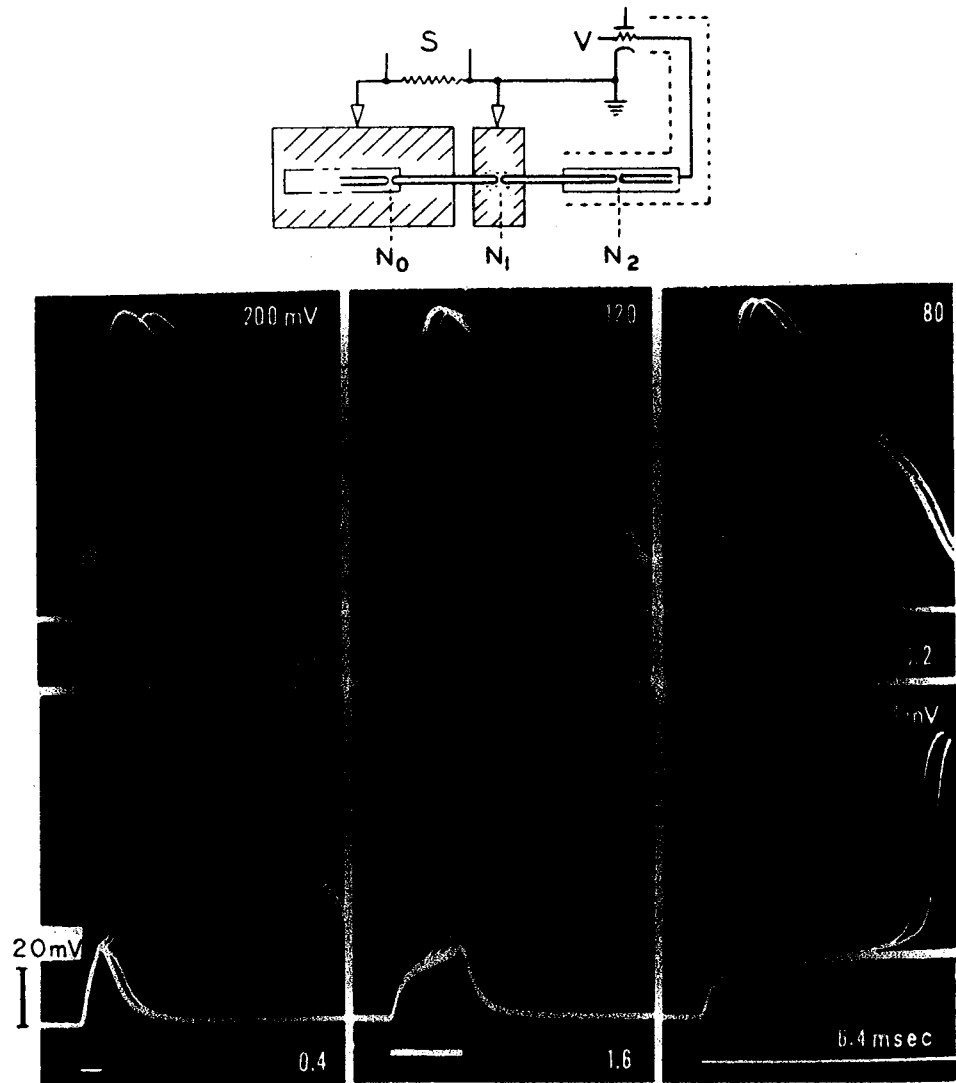


Fig. 5.1 Action potentials of a single node of Ranvier evoked by rectangular current pulses. Node N_1 is immersed in normal Ringer's; N_0 and N_2 are made inexcitable. Stimulating current pulses (S) are applied between N_0 and N_1 . V indicates a high input-impedance recording system. The durations of the applied pulses are indicated. Note that the action potentials evoked by long pulses are slightly smaller than those produced by brief pulses. A toad nerve fiber at 10°C . (From Tasaki, 1956.)

Hence, we may conclude that a *single node of Ranvier obeys the all-or-none law only approximately*.

The deviation of the electric response of a single node from the all-or-none behavior becomes more distinct when the excitability of the node is partially suppressed with a dilute anesthetizing solution or simply by mechanical injury. Poor excitability of a node is characterized by a low amplitude of the action potential, associated sometimes with a relatively high threshold current strength.

A brief comment may be made of the subthreshold response of the node of Ranvier. The nodal membrane is of the form of a narrow ring; its width is

estimated to be between 0.5 and 1 μm and its diameter to be slightly smaller than 10 μm . It seems impossible that subthreshold excitation of such a structure involves an even narrower, sharply delineated piece of membrane as depicted by Rushton (see Chapter 3, Section F). Observations of subthreshold responses in the Ostwald–Lillie nerve analog suggest the possibility that a subthreshold response represents the appearance of small spots or patches in the membrane in the excited state. This possibility will be considered in detail in Chapter 10, Section H.

B. REFRACTORY PERIOD

The term “refractory period” was introduced by Marey to describe the ineffectiveness of induction shocks delivered a short period after initiation of a contraction in the cardiac muscle (Marey, 1876). This property of the heart muscle had long been known among Italian physiologists. In 1785, Fontana wrote: “In the contracting or just relaxing muscle, external stimuli evoke no response, because the heart is not then irritable and has not yet reached the state which is necessary for a new response” (translation by Hoff, 1942, p. 642). Obviously, the refractoriness of the cardiac muscle is directly related to the all-or-none character of its contractility.

In a nerve trunk of the frog, demonstration of its refractory period is complicated by the presence of a large number of fibers with different properties. Using a capillary electrometer connected to a frog sciatic nerve, Gotch and Burch (1899) found that a second induction shock delivered shortly after the first produces no added action potential. They demonstrated also that lowering of the temperature markedly prolongs the refractory period.

There is an important rule as to the relationship between the duration of the action potential and the refractory period. Adrian (1921) found that when a second shock is delivered to a nerve shortly after the end of its first action potential, a subnormal response could be evoked if the shock is strong enough. Adrian and Lucas (1912) named the period during which a subnormal response can be evoked by a strong stimulus the “*relatively refractory period*.” A second electric shock delivered before the end of the action potential evoked by the first shock was found to be totally ineffective. The period during which the second shock is completely ineffective is called the “*absolutely refractory period*.” In an isolated myelinated nerve fiber, it is very easy to show that the *absolutely refractory period coincides with the duration of the action potential* (Tasaki and Takeuchi, 1942, see Chapter 4; Tasaki, 1949; 1956).

Figure 5.2 illustrates the course of recovery from the refractoriness of a single node of Ranvier following production of an action potential. The con-

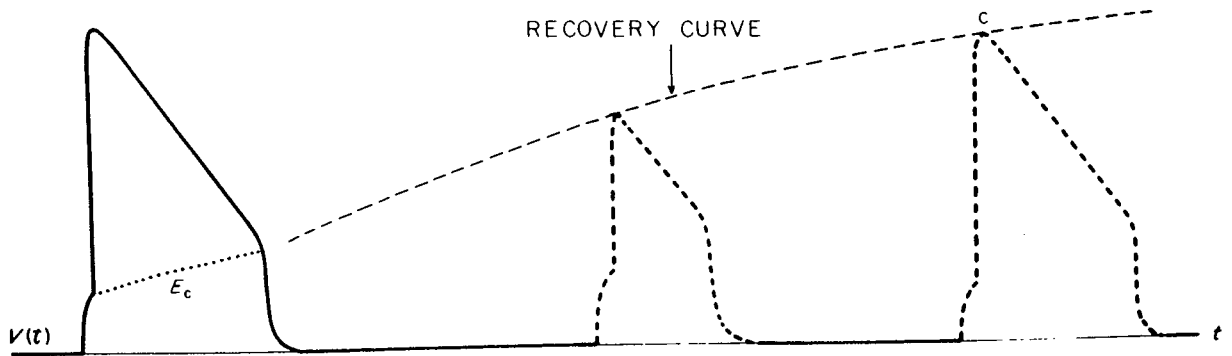


Fig. 5.2 Recovery of the action potential amplitude during the relatively refractory period. The continuous line represents the action potential produced by the first stimulating pulse. The thin broken line marked "recovery curve" represents the curve obtained by connecting the peaks of the action potentials produced during the relatively refractory period (shown by the broken lines).

tinuous line in the figure indicates the action potential of the node produced by the first stimulating pulse alone. The broken line shows the responses to the second stimulus; these responses are roughly all-or-none. The thin smooth line marked "recovery curve" indicates the peak levels of the second action potentials evoked at widely varied intervals. It is seen that the amplitude of the second action potential increases gradually after the end of the first action potential. It is important to note that, immediately after the end of the first action potential, the peak level of the second action potential is very close to the level of the "shoulder" of the first action potential. The significance of this fact will be discussed in Chapter 13, Section H.

C. ABOLITION OF ACTION POTENTIAL

The term "abolition of an action potential" was introduced to denote premature, all-or-none termination of an electric response of a single node of Ranvier (Tasaki, 1956). Originally, the phenomenon of abolition was observed by Weidmann (1951) in a spontaneously beating cardiac muscle fiber of which the electric responses lasted as long as 500 msec. In classical electrophysiology, suppression of a mechanical response of the cardiac muscle with an inward current was clearly recognized by Biedermann (see p. 223–224 in Biedermann, 1895).

Figure 5.3 shows examples of the tracings of action potentials of a single node of Ranvier abolished by brief pulses of inward current. It is seen that, when an inward current pulse applied to the node is weak, the membrane potential returns, after the end of the applied pulse, roughly back to the level that would have been reached in the absence of the applied pulse. When the

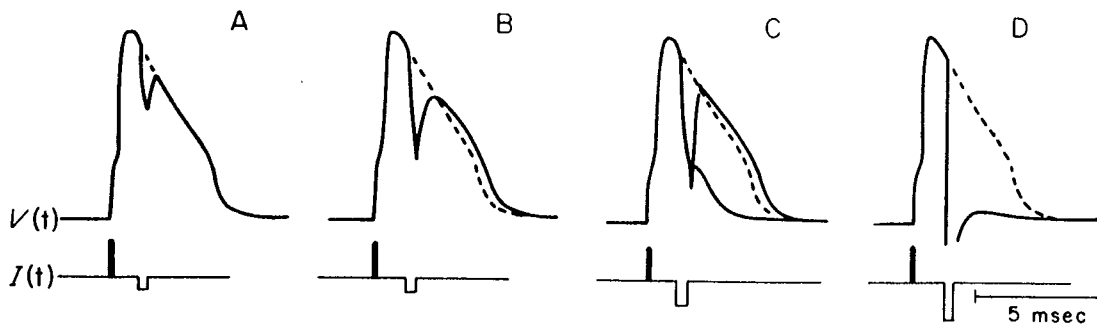


Fig. 5.3 Abolition of the action potential of a single node by a pulse of inward membrane current. The lower oscillograph trace indicates the time course of the voltage applied between N_0 and N_1 in the diagram of Fig. 5.1. (From Tasaki, 1956.)

current intensity reaches a certain critical value, the membrane potential does not rise after the end of the pulse; instead, it falls rapidly toward the resting level of the membrane potential. In other words, the action potential is prematurely terminated by a pulse of inward current in a roughly all-or-none manner.

These abolition experiments revealed one more important fact that is worth pointing out. The intensity of the current pulse required to abolish an action potential at its peak is very high. During the falling phase of the action potential, there is a continuous fall in the threshold for abolition. The action potential can readily be terminated by an extremely weak current pulse when applied near the shoulder. One might say therefore that natural (i.e., spontaneous) termination of an action potential occurs at the moment when the current intensity required for abolition reaches zero (see Chapter 10, Section C).

Abolition of an action potential has a striking effect on the relative refractoriness left behind the action potential. When it is abolished at its peak, the node can be reexcited as readily as in the resting state and the amplitude of the second response is as large as the first. In other words, the refractoriness left behind the first action potential is completely wiped out by abolition in this case. This point is shown in the superposed records in Fig. 5.4. When an action potential is abolished at a point halfway between the peak and the resting level, the amplitude of the second action potential that can be evoked after abolition starts its recovery from this halfway level. When abolition is performed near the shoulder of an action potential, the relative refractoriness left behind the first action potential is not seriously affected by abolition.

Qualitatively, it is not difficult to understand the phenomenon mentioned above on a physicochemical basis. We shall see in the following section that there is a large increase in the ion mobilities within the nodal membrane during the action potential. Consequently, the rate of cation interdiffusion is

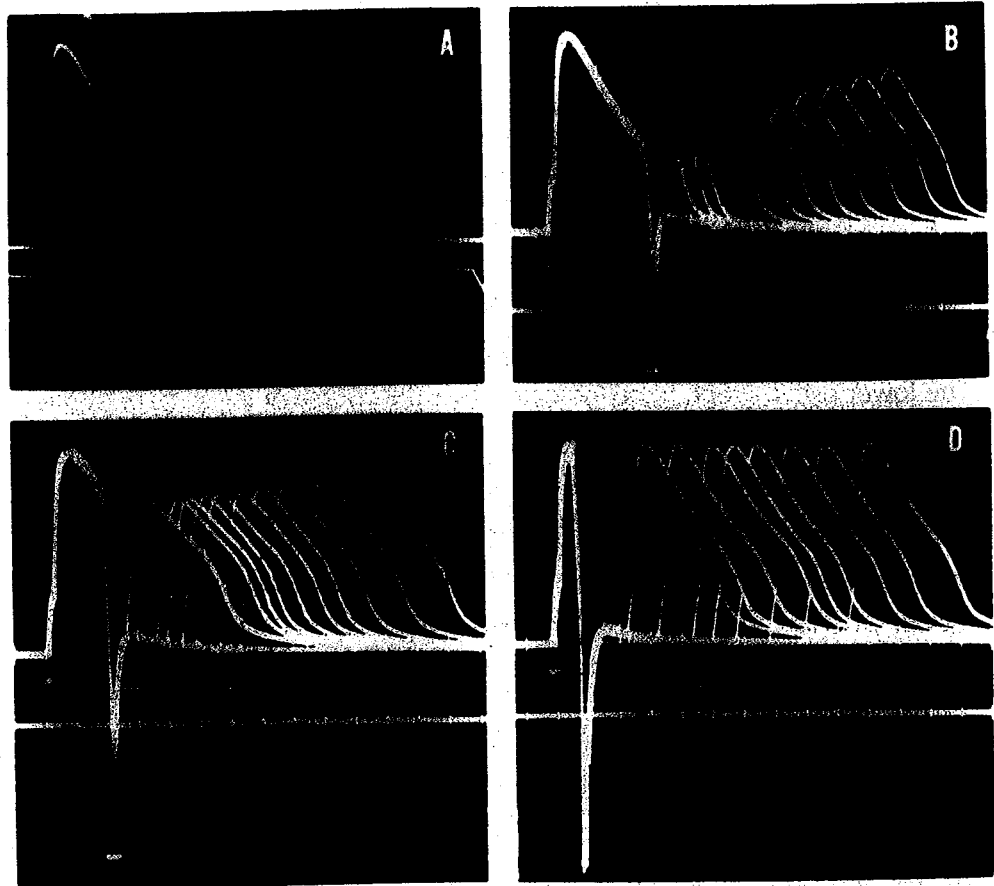


Fig. 5.4 (A and B) Superposed recordings showing that the recovery process is not affected appreciably by abolition of the action potential near the shoulder. (C and D) Recovery after an action potential abolished at its peak; note that the second action potentials in (D) are full-sized (From Tasaki, 1956.)

profoundly enhanced during the excited state of the nodal membrane. Therefore, one might visualize the refractoriness of the nodal membrane as being brought about by accumulation of the salts of external cations on the inner side of the membrane and of the salts of internal cations on the external surface. When an action potential is abolished, this process of salt accumulation is also prematurely terminated and the recovery starts from the level reached at the time of abolition. The recovery may then be interpreted as representing a reverse process representing the disappearance (by transport) of the accumulated substances. The recovery process is known to be strongly affected by the passage of electric current through the nodal membrane.

Electrochemists who deal with inanimate membranes are fully aware of the difficulties involved in the mathematical treatment of time-dependent (i.e., transient) phenomena. The use of a complex biological membrane, in place of inanimate membranes, makes a quantitative treatment of rapidly changing electrochemical processes even more difficult. For this reason, our

interpretation of the effect of abolition of an action potential on the refractoriness is only qualitative.

D. THE FALL OF THE MEMBRANE RESISTANCE DURING NERVE EXCITATION

It has long been thought that the permeability of the nerve membrane rises during excitation. For example, Bernstein's argument along this line is as follows. A dead region of a nerve is negative (acting as a sink of current) relative to its intact surface (acting as a source); the excited region of the nerve is also negative. Therefore, the membrane must have as high a permeability in the excited region as in the dead region (p. 103 in Bernstein, 1912; see Chapter 2). Much later, Lillies (1930) saw that the AC impedance of a frog sciatic nerve trunk falls when the intensity of the measuring AC is increased above the threshold. Lillie compared a fall in the polarizability of the nerve membrane during excitation with a similar change in his iron wire model (p. 358 in Lillie, 1932; see Chapter 3). However, until Cole and Curtis (1939) showed the temporal relationship between the fall of the membrane impedance and the action potential in squid giant axons (see Chapter 8, Section C), the evidence for a change in the membrane resistance during excitation was quite nebulous. Obviously, the structural complexity and the small sizes of the myelinated nerve fibers in a sciatic nerve had been causing serious difficulties in previous measurements.

The first demonstration of a fall of the resistance of the nodal membrane during excitation was based on the following reasoning: Consider a nerve fiber with a series of nodes of Ranvier, N_0, N_1, N_2, \dots . Now, suppose node N_2 and the following nodes are rendered inexcitable by application of an anesthetizing solution. Let us assume for a moment that the action current is produced by a change in the emf at N_1 without being accompanied by a change in the membrane resistance. Then, the action current observed between N_1 and N_2 should be about 50% stronger when both N_1 and N_0 are excited simultaneously than when only N_1 is thrown into excitation. When the action current produced by excitation of N_1 was measured before and after anesthetization of N_0 , it was found that the loss of excitability of N_0 brings about no detectable change in the action current intensity measured between node N_1 and N_2 . Thus, it was concluded that there is a large fall in the resistance of the nodal membrane during excitation (Tasaki and Takeuchi, 1941; see Chapter 4).

Much later, it was found possible (Tasaki and Mizuguchi, 1949) to carry out impedance measurements on single myelinated fibers in a manner similar to those performed by Cole and Curtis. Again, a bridge insulator was used

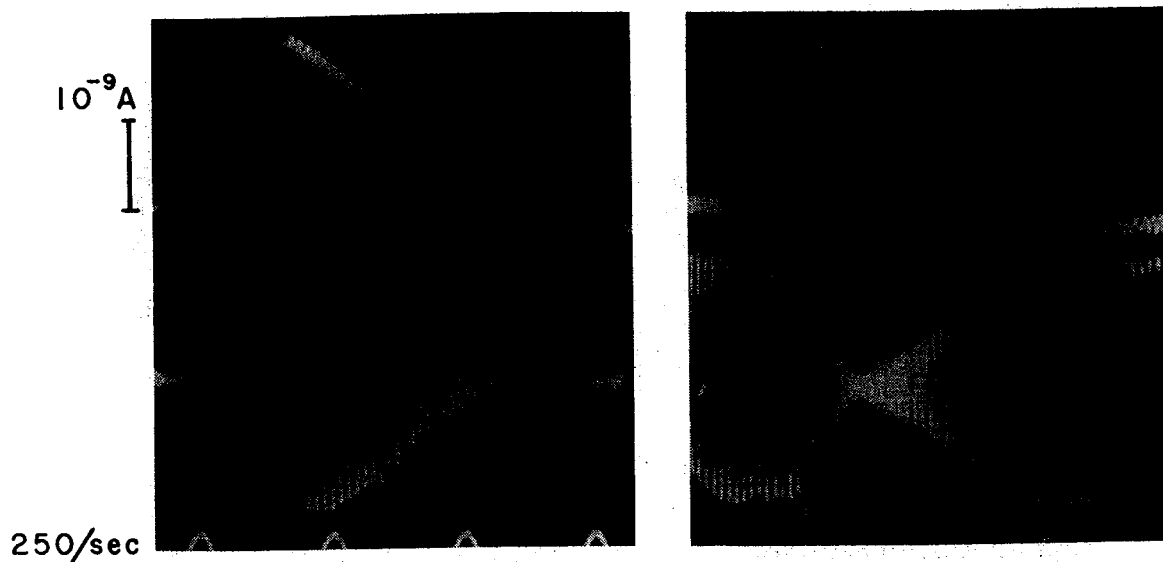


Fig. 5.5 Simultaneous recording of the electric response of a single node of Ranvier and the associated change in the membrane impedance. The left-hand record was taken with the impedance bridge balanced for the impedance at rest. The right-hand record was obtained with the bridge adjusted to give the best balance at the peak of excitation. (From Tasaki and Freygang, 1955.)

in order to reduce the shunting effect of the external medium. At a low temperature (about 4°C) the duration of the response of a toad motor nerve fiber is very long (6–7 msec); therefore, a bridge AC frequency between 2 and 3 kHz could be used for impedance measurements. The impedance of a single fiber at rest was well over $50\text{ M}\Omega$. Nevertheless, it was possible to demonstrate that there is a close parallelism between the change in the emf and the impedance loss during excitation.

Figure 5.5 shows two examples of the records obtained by this method. The upper oscillograph trace in each record represents the electric response of a single node of Ranvier; the lower trace represents the output of the AC impedance bridge displayed after passing through an amplifier tuned roughly to the frequency of the bridge AC. The left-hand record was taken with the bridge balanced for the impedance of the fiber at rest. It is seen that the envelope of the AC is roughly parallel to the deflection of the upper trace. The right-hand record in the figure was taken with the bridge balanced for the impedance of the fiber at the peak of excitation. Again, the envelope of the AC and the electric response of the node are seen to rise and fall nearly simultaneously.

By measuring potential changes produced by current pulses, the membrane resistance of the node was shown to fall, at the peak of excitation, to a level between $\frac{1}{10}$ and $\frac{1}{15}$ of the value at rest (Tasaki and Freygang, 1955). As we shall see in the following section, the resistance of unit area of the nodal membrane is very low as compared with that of the squid giant axon.

Probably, this is the reason why the ratio of the resistance during excitation to that at rest is relatively small in the nodal membrane.

E. THE RESISTANCE AND CAPACITY OF THE MYELIN SHEATH AND OF THE NODAL MEMBRANE

The DC resistance of the myelin sheath is very high (see Chapter 4, Section B). It was found possible to estimate the absolute value of this resistance by a method utilizing collision of two nerve impulses. The principle of the method is as follows. When action potentials are set up simultaneously at the two neighboring nodes of Ranvier, the myelin sheath of the internode is traversed by a strong capacitive flow of electricity during the rising phase of the intracellular potential. During the falling phase, the direction of this capacitive flow is reversed. At the end of the action potential, the total quantity of electricity carried through the capacitive pathway in the myelin sheath returns to zero. The current through the resistive pathway of the myelin sheath remains outwardly directed during the entire period of an action potential. Hence, the total quantity of electricity carried through the myelin sheath during the interval from the beginning to the end of an action potential reflects solely the flow of electricity through the resistive pathway. The resistance of the myelin sheath can then be estimated by integrating the current traversing the myelin sheath during an action potential.

Figure 5.6 schematically illustrates the experimental arrangement used for this estimation. A 1-mm-long portion of the myelin sheath was isolated from the remainder of the nerve fiber by the use of two bridge insulators. Two pulses of stimulating current were applied to the fiber, one pulse near each end of the fiber. The interval between the two pulses was adjusted so that the two nodes, N_1 and N_2 in the figure, were excited simultaneously. The electric current traversing the myelin sheath was amplified, and was displayed on the screen of an oscillograph after integration with respect to time.

We denote the resistance and the capacity of the myelin sheath in the middle pool (Fig. 5.6) by R and C , respectively, and the potential variation in the axis-cylinder by $V(t)$, a function of time, t . Within the limit that allows us to describe the electric behavior by using such a parallel R - C circuit, the current and the quantity of electricity transported through the myelin sheath are given, respectively, by

$$I(t) = C \frac{dV(t)}{dt} + \frac{V(t)}{R} \quad (5.1)$$

and

$$Q(t) = C \int_0^t dV(t) + \frac{1}{R} \int_0^t V(t) dt \quad (5.2)$$

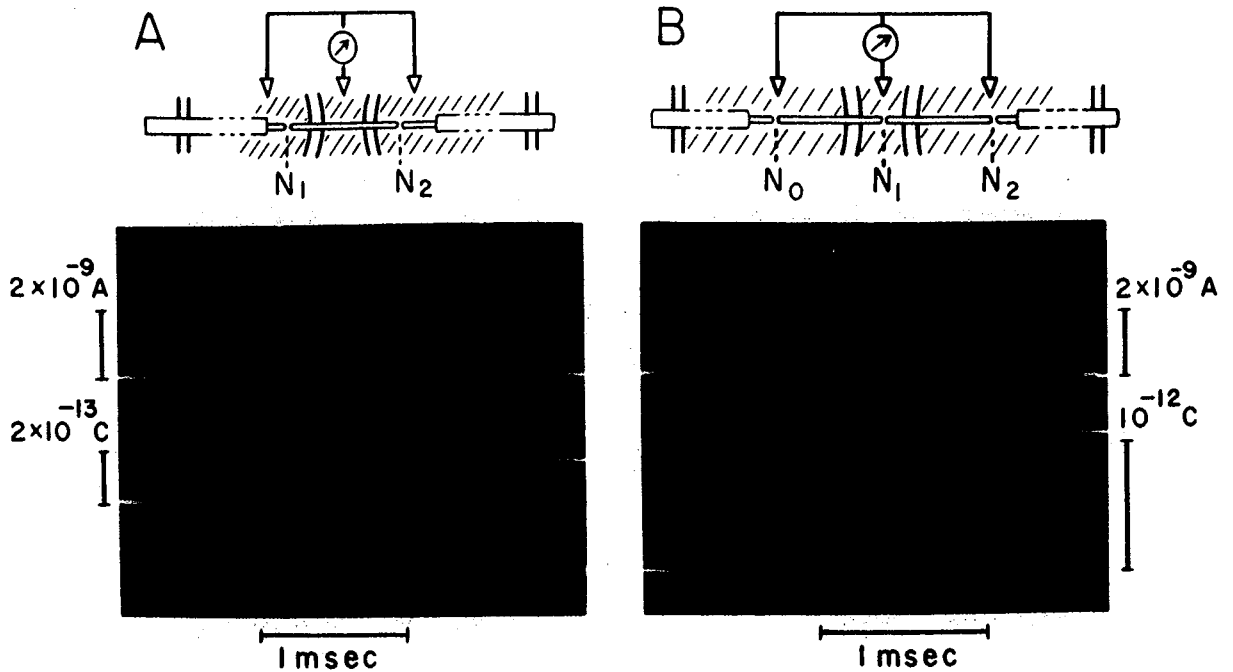


Fig. 5.6 Top: Schematic diagrams showing the experimental arrangement used for estimating the resistance and the capacity of the myelin sheath (A) and of an inexcitable node of Ranvier (B). Bottom: The upper oscillograph trace displays the membrane current, $I(t)$, produced by simultaneous excitation of the two adjacent nodes of Ranvier. The lower trace registers the quantity of electricity, $Q(t)$ in Eq. (5.2), transported through the myelin sheath. (From Tasaki, 1955.)

As the potential inside the myelin sheath rises and then returns to the initial level at the end of an action potential, the first term on the right-hand side of Eq. (5.2) vanishes. The integral in the second term can be approximated by $\frac{1}{2} \tau V_p$, where τ is the duration of the action potential and V_p the peak value of the potential variation. The value of V_p is taken as 0.1 V and the duration of the action potential is 0.9 msec in frog motor nerve fibers at 24°C. The resistance of a myelin sheath can be found immediately by introducing these values into

$$R = \frac{1}{2} \tau V_p / Q_e \quad (5.3)$$

where Q_e represents the quantity of electricity at the end of the action potential. By this method, the resistance of the myelin sheath immersed in a 1-mm-wide middle pool filled with normal Ringer's solution was found to be $290 \pm 38 \text{ M}\Omega$ for frog motor nerve fibers 12–15 μm in diameter. Adopting 13 μm as the average diameter of these fibers, the resistance for unit area is found to be of the order of 100 $\text{k}\Omega/\text{cm}^2$.

Using the value of R thus determined, it is simple to estimate the capacity of the portion of the myelin sheath in the middle pool (Fig. 5.6). The quantity of electricity observed at the peak of the action potential Q_p , is given by: Both Q_p and the integral in the last equation can be determined from the

$$Q_p = CV_p + \frac{1}{R} \int_0^p V(t) dt \quad (5.4)$$

oscillograph records directly. The value of C found by this method was $(1.6 \pm 0.2) \times 10^{-12}$ farad for a 1-mm-long portion of the myelin sheath of frog motor nerve fibers, or $0.0046 \mu\text{farad}/\text{cm}^2$.

According to the results of these measurements, the RC product, or the time constant of the myelin sheath, is 0.46 msec. Thus, it is found that *the time constant of the myelin sheath is far longer than the internodal conduction time* (i.e., time required for a nerve impulse to travel from one node to the next), which is close to 0.1 msec. Because of this cablelike property of the myelin sheath, the effect of a rapid potential variation taking place at one node of Ranvier does *not* reach the next node instantaneously. The electric capacity of the myelin sheath is the major factor which determines the internodal conduction time (see Hodler *et al.*, 1952). There have been widespread misgivings about the mode of conduction of a nerve impulse along a myelinated nerve fiber. A statement like "the action potential jumps from a node to the next instantly" is incorrect. (Records of action currents that seem to support such a statement can be obtained when there is a serious distortion of the currents due to a high input capacity of the recording system.)

The method described above was also used for estimating the resistance and the capacity of the nodal membrane. By introducing a node of Ranvier into the middle pool which was filled with Na-free choline-Ringer's solution (see Fig. 5.6), the current and the quantity of electricity transported through a 1-mm-long portion of the fiber including a node of Ranvier was estimated. The peak value of the potential variation inside this nonresponding node was estimated indirectly from the attenuation constant for stimulating current pulses (see Chapter 4, Section C); the value of 70 mV was adopted. By this method, the capacity and the resistance of a 1-mm long portion of a frog motor nerve fiber including one node of Ranvier was found to be $(3.1 \pm 0.4) \times 10^{-12}$ farad and $(36.3 \pm 5.2) \times 10^6 \Omega$, respectively. By subtracting the capacity of the myelin sheath in the middle pool, the capacity of the nodal membrane was found to be 1.5×10^{-12} farad. Similarly, the resistance of the nodal membrane was found to be $41 \times 10^6 \Omega$. The RC product or the time constant of the nodal membrane at rest is then of the order of 0.062 msec; this value is far smaller than the duration of the action potential.

It is difficult to measure the area of the nodal membrane in its normal, excitable state, because its width is of the order of the wavelength of visible light. It is probably safe to assume that the area is between 2 and $10 \times 10^{-7} \text{ cm}^2$. We then find the resistance of a unit area of the nodal membrane to be between 8 and $40 \Omega \cdot \text{cm}^2$ and the capacity between 1.5 and 7×10^{-6}

F/cm². The area is known to increase when the node is rendered inexcitable by various means.

The effects of several chemicals on the electric resistance of the nodal membrane (as well as on the myelin sheath) were examined by the same method. A few alkaloids (cocaine, bufotenine, sinomenine, etc.) were shown to bring about a significant increase in the membrane resistance at relatively high concentrations. A concentrated NaCl solution (about 0.5 M) was found to reduce the resistance of the myelin sheath appreciably. Lowering the temperature raises the membrane resistance.

F. EFFECT OF POLARIZING CURRENT ON NERVE CONDUCTION

The amplitude of the action potential developed by a node of Ranvier is strongly affected by a constant current traversing the nodal membrane. As long as the current intensity is within a certain limit (which will be discussed in Chapter 7, Section F), the effect of a constant polarizing current may be interpreted qualitatively in the following manner (see Fig. 5.7). In the absence of a constant current, the potential inside the node membrane (relative to that in the external medium) has to be raised to about 20 mV above the resting level. A weak constant current through the nodal membrane shifts the membrane potential roughly in proportion to its intensity. When the applied current is inwardly directed (namely, when the node is under "hyper-

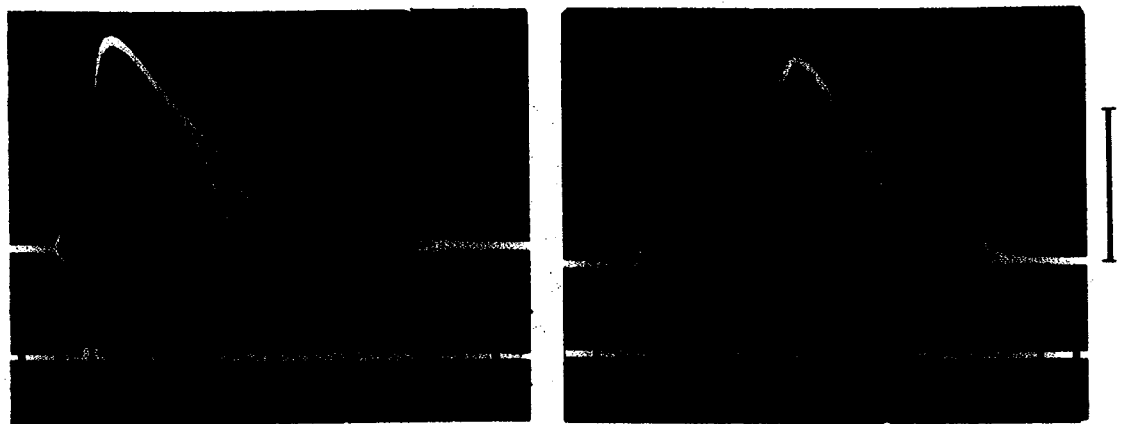


Fig. 5.7 Oscillograph records showing the effects of weak pulses of inward or outward current on the action potential of a single node of Ranvier. The experimental setup illustrated in Fig. 5.1 (top) was used. Long voltage pulses applied between nodes N_0 and N_1 . Both N_0 and N_2 were rendered inexcitable. Brief stimulating pulses were applied 1 msec (left-hand record) or 4 msec (right-hand record) after the onset of the long pulses. Voltage calibration, 50 mV; time markers, 1 msec. A toad nerve fiber at 11°C. (From Tasaki, 1956.)

polarization''), a stronger stimulating pulse has to be superposed on the hyperpolarizing current, because the initial level of the membrane potential is now more than 20 mV below the threshold level. Due to a large fall in the membrane resistance at the peak of excitation (see Chapter 5, Section D), the peak level of the action potential is not significantly affected by the constant current. Hence, both the threshold intensity of the stimulating current pulses and the potential variation associated with excitation are increased by hyperpolarization. A continuous flow of outwardly directed current (i.e., depolarization) produces opposite effects on the threshold current intensity and the action potential amplitude.

Strictly speaking, the simple interpretation of the effect of polarizing current mentioned above is valid only when the intensity of the polarizing current is low and its duration is limited. A strong polarizing current produces complex secondary changes in the electric properties of the node of Ranvier (see Takeuchi and Tasaki, 1942).

The effect of polarizing currents on the process of nerve conduction along a single nerve fiber within a nerve trunk was studied extensively by Erlanger and Blair (1934; see Chapter 4). In fact, their study was the first to demonstrate the discontinuous nature of conduction block in myelinated nerve fibers. However, the original interpretation of the results was not quite correct. Erlanger visualized the myelin sheath as possessing a high electric resistance; but he assumed that the excitation wave travels continuously along the axis-cylinder (see p. 121 and 126 in Erlanger and Gasser, 1937). Later, similar polarization experiments were carried out using isolated nerve fibers, and the results obtained were interpreted based on the theory of saltatory conduction (Takeuchi and Tasaki, 1942).

Figure 5.8 shows the records demonstrating the effect of DC polarization of nerve conduction in an isolated nerve fiber (left) and in a fiber within a small nerve trunk (right). In the experiment illustrated by the left-hand diagram, a constant current was applied between node N_1 and N_2 . To simplify the interpretation of the responses observed, node N_2 was rendered inexcitable with an anesthetizing solution. The nerve fiber was excited by a brief current pulse applied near the proximal end of the fiber, and the action current was recorded between N_1 and N_2 . As the threshold of node N_1 was raised by a polarizing current which was directed inward through N_1 , the time interval from the onset of the action potential at N_0 to that at N_1 was increased; the appearance of a "notch" on the rising limb of the recorded electric response is a reflection of this increase in the time interval. At a critical intensity of polarization, there was a sudden reduction in the action current amplitude, indicating that the response of N_1 had just dropped out. Similar records obtained by Erlanger and Blair (see the right-hand records in the figure) can be explained in the same manner. The loss of the sharpness in the

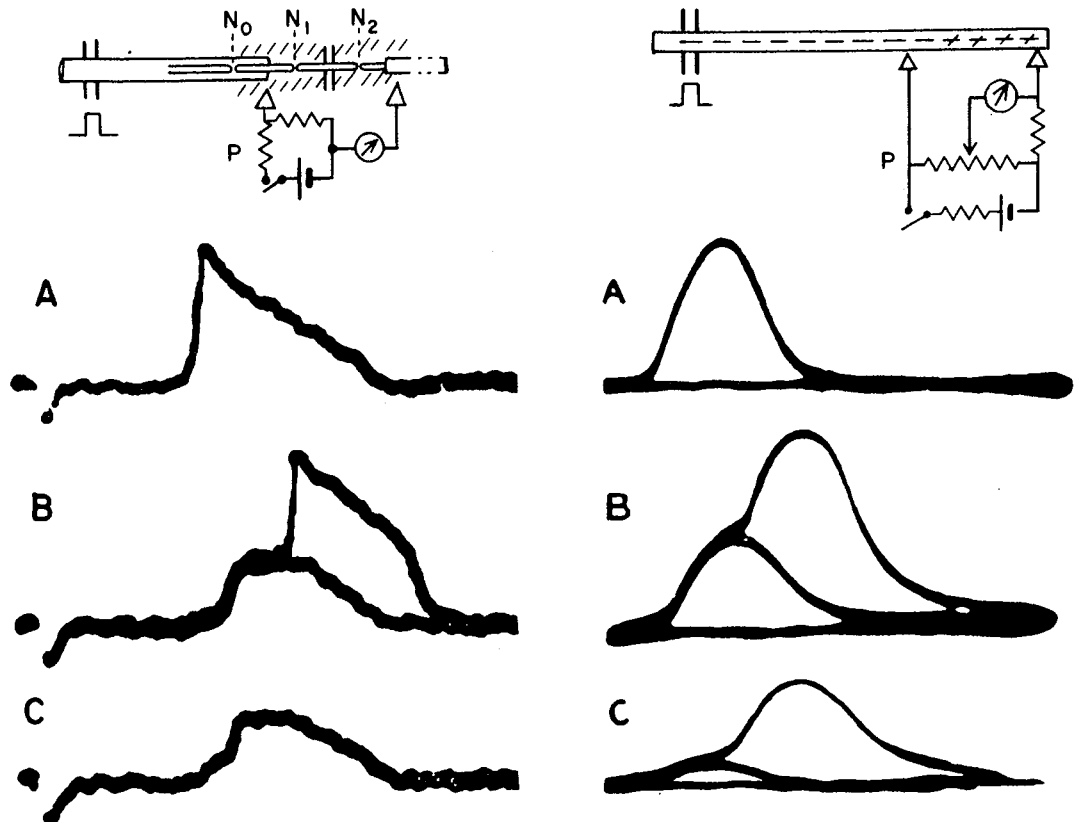


Fig. 5.8 Left: Changes in the time course of an action current produced by anodal polarization of a node (N_1 in the figure). The distal node (N_2) was rendered inexcitable with cocaine. The voltage applied was (from the top) 0 in (A) and 115 mV in (B) (superposed), and 120 mV in (C), respectively. (Taken from Fig. 60, in Tasaki, 1953.) Right: Changes in the configuration of a monophasic action potential of a single nerve fiber in an intact nerve trunk produced by anodal polarization at the proximal recording lead. (A) The normal spike potential. (B) The spike under anodal polarization just strong enough to block at the most accessible node; two action potentials superposed. (C) Further increase in the polarizing current to the next critical strength. (Adapted from Erlanger and Blair, 1934.)

rising phase of the right-hand records is undoubtedly caused by the capacity of the myelin sheath of many nerve fibers present in the nerve trunk.

In connection with the effect of a polarizing current on nerve conduction, a brief mention may be made of an interesting phenomenon first noted by Samoiloff and Kisseleff (1925). When a short portion of a nerve trunk is exposed to a relatively strong DC, nerve conduction across the polarized region becomes unidirectional. The mechanism of this *unidirectional conduction of nerve impulses under DC polarization* can be interpreted in the following manner. Conduction from a depolarized node (which develops a weak action current) to a hyperpolarized node (which has a high threshold) is very unfavorable and can be readily suspended. On the contrary, conduction from a hyperpolarized node (which develops a strong action current) to a depolarized node (which has a low threshold) is always favorable. Under

strong DC polarization of a short stretch of a nerve trunk, therefore, nerve impulses can travel in the direction of the polarizing current in the trunk, but not in the reverse direction. It is easy to demonstrate unidirectional conduction in isolated nerve fibers under DC polarization (Tasaki, 1953).

[In a normal nerve fiber (i.e., without DC polarization), the excitation wave spreads from one node to the next (e.g., from N_1 to N_2) as readily as in the reverse sequence (from N_2 to N_1), for both nodes are capable of developing action potentials of the normal size and have approximately the same threshold.]

There is another interesting phenomenon—discovered a long time ago by Woronzow (1924)—which may be explained in a similar fashion. Nerve conduction blocked by local application of anesthetics or potassium salts can be restored by passage of an electric current if the direction and the intensity of the current are properly chosen. As can be expected from the description of the effect of DC, *restoration of nerve conduction by DC polarization* takes place only when the proximal side of the nerve is connected to the anode and the distal side to the cathode of the polarizing circuit (see p. 115 in Tasaki, 1953).

G. NERVE CONDUCTION DURING THE RELATIVELY REFRACTORY PERIOD

In this section we are concerned with the behavior of a nerve impulse evoked during the relatively refractory period of a myelinated nerve fiber. It has already been pointed out that the relatively refractory period begins immediately after the end of the nodal action potential (Section B). During the following period, the response evoked is smaller and the threshold is higher than in the normal, resting state. The behavior of the nerve impulse propagating along nerve fibers during such a period may readily be interpreted on the basis of our knowledge concerning the properties of the node during the recovery period (see Fig. 5.2).

Using two brief electric pulses with variable intensities, Adrian and Lucas (1912) determined the recovery of excitability of a nerve (trunk) after a stimulus. They adjusted the intensity of the first electric shock to a level strong enough to excite all the motor nerve fibers in a nerve-muscle preparation and measured the threshold intensity of the second brief shock as a function of the interval between the two shocks. They called the curve relating the reciprocal of the threshold of the second shock to the interval the "*recovery curve*." In classical neurophysiology, the term "excitability" was frequently used to denote the reciprocal of the threshold intensity. In this sense, the excitability of the nerve is low during the relatively refractory period. After

the end of the refractory period, the excitability becomes higher than its resting level for a limited period of time. Adrian and Lucas called this period the "supernormal phase." Later, Gasser argued that the supernormal phase is related to the *afterpotential*, namely, to the long-lasting potential shift which is frequently encountered following the production of a full-sized action potential (see p. 151 in Erlanger and Gasser, 1937).

In isolated nerve fibers, the recovery curve can be determined by a similar procedure. In fact, the threshold for the second pulse can be measured more readily in single fiber preparations than in nerve trunks, because the criterion for the presence or absence of a second propagated nerve impulse is totally unambiguous in single fibers. An example of such curves for large motor nerve fibers of the toad is shown in Fig. 5.9. It is seen that the excitability (i.e., the reciprocal of the threshold strength) measured with the second pulse recovers continuously and becomes supernormal. After the *supernormal phase*, it returns smoothly to the normal level. Toward the origin of the abscissa, however, the curve is abruptly terminated. The existence of this sharp break in the recovery curve was not recognized at the time of Adrian and Lucas.

The significance of the discontinuity in the recovery curve is as follows. Suppose that two electric shocks are delivered to a single nerve fiber across an internode between N_0 and N_1 and that the first shock is strong enough to excite node N_1 . Promptly, full-sized action potentials are generated successively at N_1 , N_2 , N_3 , etc., by virtue of strong local currents since all the

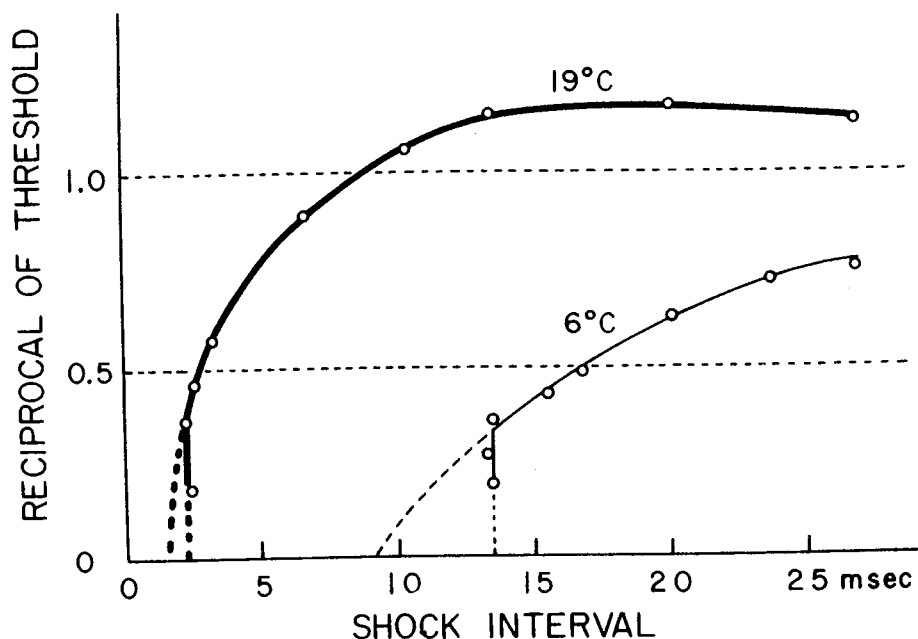


Fig. 5.9 Recovery curves of a toad nerve fiber determined at two different temperatures. The reciprocal of the threshold strength of the second shock was plotted against the interval between two shocks. (From Tasaki, 1949.)

nodes of the fiber are at rest initially. Immediately after the end of the action potential at N_1 , a second action potential can be evoked at N_1 when the second shock is strong enough. The amplitude of this second action potential is small (about $\frac{1}{3}$ of the normal amplitude). At the time when this second action potential is evoked at N_1 , the threshold of node N_2 is well above the normal level. Hence, the local current associated with the second action potential at N_1 fails to excite the adjacent node, N_2 . As the interval between the two shocks is increased, the amplitude of the second action potential of N_1 is enhanced and the excitability of N_2 rises. Thus, at intervals longer than a critical value, a second action potential is generated also at N_2 . The discontinuity in the recovery curve is a reflection of the failure of the second response to propagate along the nerve fiber. The legitimacy of this interpretation has been demonstrated by a direct experiment (Tasaki and Takeuchi, 1942; see Chapter 4).

It is convenient to introduce at this moment the concept of a *safety factor* of nerve conduction. Consider an imaginary procedure by which the amplitude of an action potential of node N_1 is gradually reduced without altering its duration. As the amplitude is reduced, the outwardly directed current through N_2 (which precedes the production of an action potential at this node) decreases. Eventually, a critical state is reached at which the current intensity falls short of the threshold of N_2 . The safety factor is defined as the ratio of the initial action potential amplitude to that at the critical stage. The safety factor of a normal motor nerve fiber of the toad was estimated to be approximately 5. The concept of safety factor is useful in explaining propagation of nerve impulses under abnormal conditions. The break in the recovery curve corresponds to the interval at which the safety factor for the second impulse is equal to unity.

The *least interval*, namely, the shortest interval at which two propagated impulses can be elicited, should be distinguished from the absolutely refractory period. This distinction is important particularly in explaining the behavior of nerve impulses along nerve fibers under abnormal conditions. For example, local anesthetics prolong the least interval while they shorten the absolutely refractory period (Tasaki, 1953).

The rate at which the second impulse propagates along the nerve fiber is now discussed. It has long been known that the second impulse evoked at a short interval after the first travels at a subnormal rate (see, e.g., Gotch, 1910). Undoubtedly, this subnormal conduction rate is a reflection of the low safety factor. The low rate of conduction of the second impulse causes an increase in the spatial and temporal separation between the first impulse and the second. As the separation increases, the conduction rate of the second impulse rises. Consequently, the separation between the two impulses asymptotically approaches a constant value as they travel along a long distance.

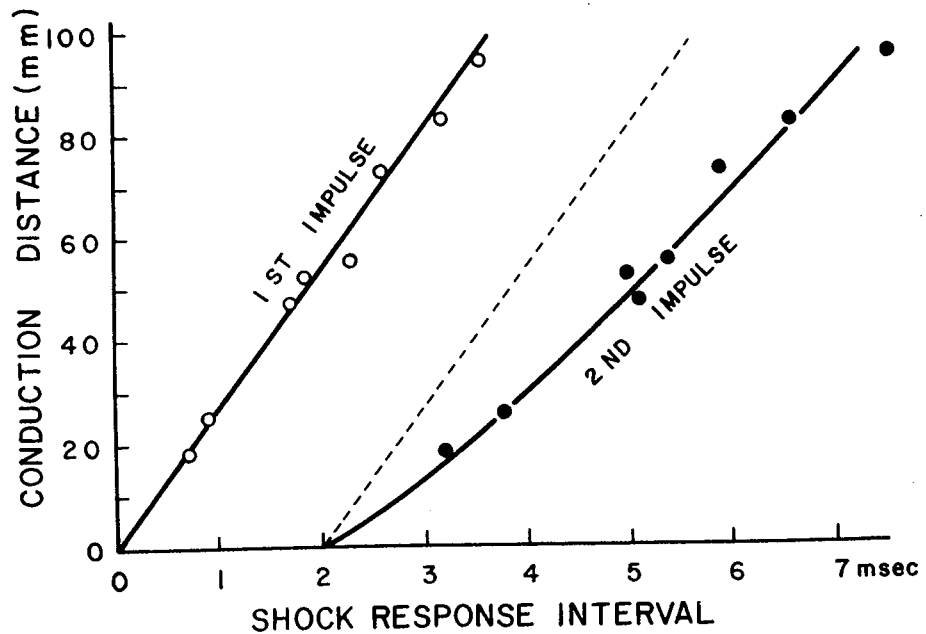


Fig. 5.10 Relation between the conduction distance and the shock-response interval for two impulses evoked at an interval of 2 msec. A motor nerve fiber of $11\mu\text{m}$ in diameter extending from the spinal cord to the toe of a toad. Temperature, 23°C . (From Tasaki, 1956; Fig. 5.)

Figure 5.10 shows an example of the experimental results showing this gradual increase in the separation between the two impulses traveling along a single nerve fiber. These two impulses were evoked at an initial interval of 2 msec. The two thick lines in the figure show the relationship between the distance that the impulses have traveled and the time required. It is seen that the first impulse travels along the entire length of the fiber at a constant rate. From the slope of the curve for the second impulse, the initial rate of conduction is found to be about one half of the normal rate. Both the spatial and the temporal separation between the two impulses increase as they travel along the fiber. As expected, the conduction rate of the second impulse gradually approaches that of the first impulse.

H. NERVE CONDUCTION IN THE ANESTHETIZED REGION OF NERVE FIBER

Local anesthetics have long been used by many neurophysiologists with a view toward clarifying the nature of the nerve impulse. When a solution of a local anesthetic (e.g., ethanol, urethane, cocaine, etc.) is applied to a portion of a nerve trunk, conduction of the nerve impulse is gradually impaired. If the concentration of the anesthetic is high enough, nerve conduction across the anesthetized region is eventually suspended. For a given anesthetic, the

higher the concentration, the shorter is the time required for suspension of conduction. The anesthetic action is obviously concentration dependent.

When large nerve trunks (of the order of 1 mm in diameter) are used for this type of experiment, the anesthetic has to diffuse into the trunk through the connective tissue and the narrow space between nerve fibers before it starts affecting the fibers located near the center of the trunk. Since diffusion through the tortuous pathways within a nerve trunk is a relatively slow process, it is difficult to study the time dependence of the action of anesthetics using nerve trunks.

When anesthetizing solutions are applied directly to isolated single nerve fibers, physiological properties of the fiber (threshold, least interval, conduction rate, action current amplitude, etc.) are found to be affected by the anesthetic *immediately* after application and to remain roughly *constant* thereafter (see Tasaki and Takeuchi, 1942; Chapter 4; Tasaki, 1953). This situation greatly simplifies analyses of the effects of anesthetics on the process of nerve conduction.

The idea that the effect of anesthetics is time independent is not new. In a monograph entitled "Die Narkose," Winterstein (1926) argued that the apparent time dependence of the effects of anesthetics can be attributed entirely to the process of diffusion.

Studies of the effects of anesthetics on electrical properties of single nodes of Ranvier (Tasaki and Takeuchi, 1942; Chapter 4) revealed the following facts. A dilute solution of cocaine or urethane raises the threshold and decreases the amplitude of the electric response. The duration of the response is reduced slightly. Although the resistance of the nodal membrane at rest is not appreciably affected, the extent of impedance loss at the peak of excitation is diminished by anesthetics. As the anesthetic concentration is raised above a certain level, the node becomes inexcitable.

In a uniformly anesthetized nerve fiber, the rate of nerve conduction is reduced. This reduction becomes increasingly severe with a rising anesthetic concentration around the fiber. Nerve conduction is suspended a long time before the response amplitude measured at the site of stimulation is reduced to a vanishingly small value. It is also to be noted that the conduction rate never approaches zero at the moment when conduction is suspended. The following observations illustrate how anesthesia brings about suspension of nerve conduction.

Figure 5.11 shows an example of the results of conduction rate measurements under the action of ethylurethane applied to a nerve trunk. It is seen that the conduction time of a particular single fiber in the nerve trunk between electrodes E_1 to E_2 was gradually increased by the anesthetic. The critical rate of conduction (i.e., the rate observed immediately before suspension of conduction) was found in this preparation to be approximately

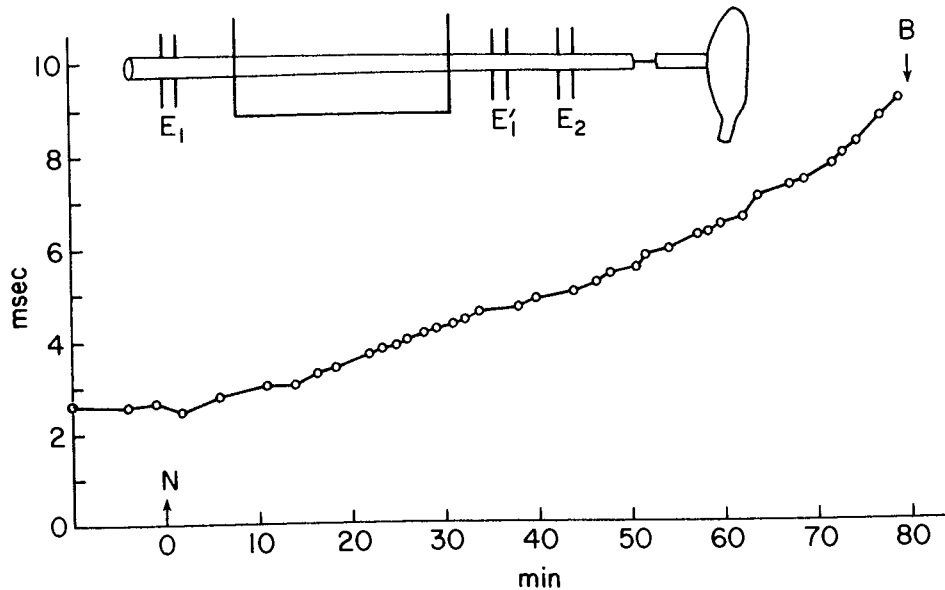


Fig. 5.11 Reduction of the conduction rate of a single motor nerve fiber in an intact nerve produced by application of a 1.8% urethane-Ringer's solution. The time required for the nerve impulse to travel between electrode pairs E_1 and E_2 was measured by taking the difference in the least interval (for production of two impulses) at the positions. The distance between E_1 and E_2 , 45 mm; the anesthetized zone, 40 mm. The conduction rates calculated from the measured intervals were 17.3 m/sec at the onset and 6.1 m/sec immediately before the conduction block. Temperature, 18°C. (From Fig. 50 in Tasaki, 1953.)

6 m/sec, or roughly 0.4 msec per internode. With this and other anesthetics, it was found that the critical internodal conduction time is always shorter than the duration of the action potential of a lightly anesthetized node.

The experimental setup shown in Fig. 5.12 (top) is designed to demonstrate a sudden change in the action current at the moment when nerve conduction is suspended (Tasaki *et al.*, 1943b). Here, the action current of a large myelinated nerve fiber of the toad was recorded across a bridge insulator between node N_1 and N_2 . Record a was obtained when all the nodes of Ranvier are immersed in normal Ringer's solution. Record b was obtained immediately after introduction of a 0.17 M ethylurethane-Ringer's solution into the distal pool; the observed change in the action current is attributed to a decrease in the amplitude of the action potential developed at node N_2 . Next, the ethylurethane-Ringer's solution was introduced also into the proximal pool where node N_1 is located within the nerve trunk. As the response of N_1 is gradually reduced by the anesthetic, the action current recorded between N_1 and N_2 became gradually more diphasic. Suddenly, the action current recorded between node N_1 and N_2 became monophasic (compare Records d and e). In these records we see that the amplitude of the action current derived from node N_1 (namely, the upward deflection) was approximately $\frac{1}{2}$ of the normal value; the loss of diphasicity indicates that the

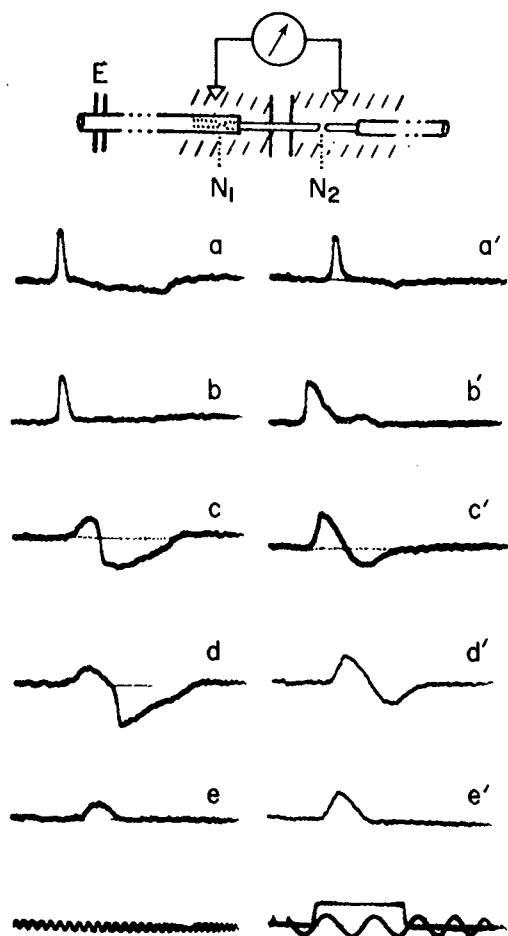


Fig. 5.12 Changes in the action current produced by application of an 1.5% urethane-Ringer solution. Records a and a': both node N_1 and N_2 in normal Ringer. Records b and b': urethane in the distal pool. Records c and c': shortly after introduction of urethane into the proximal pool. Note that conduction block was accompanied by the sudden loss of diphasicity of the action current. (From Fig. 51 in Tasaki, 1953.)

action current developed by node N_1 fell short of the threshold for node N_2 . From this and other observations, it was found that, with ethylurethane or cocaine, conduction block takes place at a concentration high enough to reduce the action potential amplitude of the node to about $\frac{1}{2}$ of the normal value (Tasaki, 1953).

A dilute urethane solution shortens the duration of a single node response slightly (Tasaki and Takeuchi, 1942; Chapter 4). It is seen in Records d and d' that at the critical stage of conduction, the response of node N_2 starts shortly after the peak of the response of node N_1 . Note that the membrane potential of node N_2 is expected to reach its maximum shortly after the upward deflection in Records c and c' passes its peak (because of the capacity of the myelin sheath). The failure of conduction from N_1 to N_2 takes place when the current generated by N_1 fails to raise the membrane potential at N_2 to its threshold level. From these considerations, it is expected that *the criti-*

cal internodal conduction time never exceeds the duration of the action potential of individual nodes.

In connection with the effects of anesthetics (or narcotics) on nerve fibers, a brief mention should be made of the phenomenon called "transitional decrement" by Davis *et al.* (1926). It has long been known that the time required for suspension of conduction with anesthetics depends on the length of the anesthetized region. When a region longer than about 10 mm is anesthetized with 0.33 M ethylurethane-Ringer's solution, for example, a desheathed sciatic nerve-muscle preparation (with its individual nerve fibers separated from one another) loses its ability to conduct impulses within 1 min. However, when the same anesthetizing solution is applied to a 3-mm-long desheathed portion of the nerve, a period of 5 min or more is required to bring about suspension of conduction. Obviously, this length dependence derived from the situation that the action current developed in the proximal, nonanesthetized region does spread along a poorly excitable or completely inexcitable region of a nerve fiber (see Chapter 4, Section E). It is interesting to note that the possibility that a nerve impulse may jump over a short anesthetized zone was recognized a long time before the role of node of Ranvier was elucidated (see Werigo, 1899; Davis, 1926).

With anesthetized regions longer than about 6 mm, the time required for suspension of conduction is practically independent of the length of the anesthetized zone (Kato, 1924, 1926). This "limit length" of Kato corresponds to the length of the portion of a large motor nerve fiber involving, on the average, two and a half nodes. The term "transitional decrement" describes the situation that a progressive decrease (i.e., decrement) in the amplitude of the spreading local current takes place only in the transitional zone between the normal and anesthetized regions of a nerve. Recently, the significance of transitional decrement was discussed elsewhere (Tasaki, 1976).

So far we have dealt exclusively with the properties of large myelinated nerve fibers. We now briefly consider the effect of anesthetics on conduction in small nerve fibers. The internodal distance is known to be roughly proportional to the fiber diameter (see Chapter 5, Section J). Hence, the length involving 2-3 nodes of Ranvier is far shorter in small fibers than in large fibers. For this reason, nerve conduction is blocked preferentially in small fibers when a short desheathed portion of a nerve trunk is exposed to an anesthetizing solution.

In relation to the action of anesthetics on nerve conduction, there is another interesting phenomenon that deserves a short comment. This phenomenon is usually referred to as the *Wedensky inhibition* (Wedensky, 1885, 1903). Adrian (1913) described the phenomenon in question in the following words: "At a certain stage of narcosis of a nerve-muscle preparation, a series of strong, rapidly recurring stimuli may produce a small initial con-

traction only, whereas a series of weak or slowly recurring stimuli produce strong sustained contractions." In these old experiments, contraction of the muscle was taken as an index of propagation of nerve impulses across the narcotized (i.e., anesthetized) region of the nerve. Wedensky's phenomenon was once regarded as a puzzling paradox in neurophysiology.

It is not difficult to explain the Wedensky inhibition based on the concept of saltatory conduction. When the depth of anesthesia is such that a single nerve impulse can barely travel across the anesthetized region of the nerve, a second impulse evoked during the relatively refractory period (left behind the first impulse) is expected to be unable to travel across the anesthetized zone. Note that the safety factor for the second impulse is reduced by both refractoriness and anesthesia. The second impulse traveling along the proximal, nonanesthetized portion of the nerve leaves a refractory period behind it; hence, the intensity of the local current associated with the third action potential (evoked during the refractory period left by the second impulse) is subnormal. Consequently, all the impulses except the first may be blocked in the anesthetized zone of the nerve. (For further discussion, see Tasaki and Takeuchi, 1942, cited in Chapter 4; Tasaki, 1953.)

I. EXPERIMENTAL DEMYELINATION

The myelin sheath is made of many layers of lipid-rich material (see Chapter 6, Section A). It has long been suspected that the role of the lipid in the myelin sheath is to electrically insulate the axis-cylinder (see, e.g., Göthlin, 1910; Chapter 4). Experimental evidence indicating that this is actually the case is presented in Chapter 4, Section B and Chapter 5, Section E. The following observations show that removal of lipids with detergents lowers the resistance of the myelin sheath and decreases the safety factor for nerve conduction (Tasaki and Ushiyama, 1950; Tasaki, 1955).

The detergent used for this purpose was either saponin or sodium oleate. It was added to Ringer's solution and was applied to a 1-mm-long portion of myelin sheath separated by a pair of bridge insulators from the rest of the nerve fiber (see Fig. 5.13, top). The electric current associated with a conducted nerve impulse was recorded from the same portion of the myelin sheath.

Before the detergent had time to dissolve the myelin sheath, the peak intensity of the observed current was approximately 10^{-9} ampere and had two maxima separated by an interval of about 0.1 msec (see Chapter 4, Section G). Soon after introduction of the detergent, the intensity of the current through the myelin sheath started to increase (see Fig. 5.13). Simultaneously, there was a progressive increase in the time interval between the two peaks.

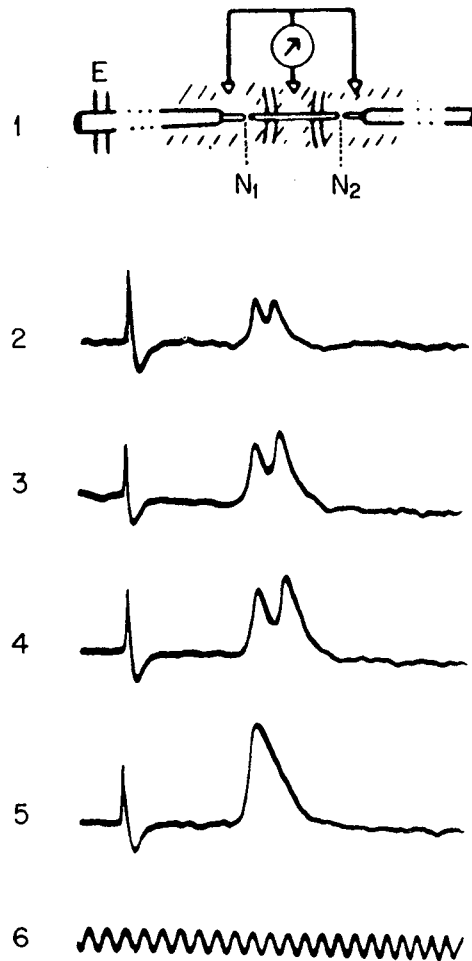


Fig. 5.13 Changes in the configuration of the membrane current recorded through a 1-mm-long myelinated portion of a nerve fiber produced by 2.5% saponine-Ringer's solution. The fiber was stimulated by a brief electric shock applied near the proximal end of the fiber. Nodes N_1 and N_2 were kept in normal Ringer's throughout the experiment. Nerve conduction across the myelinated portion of the fiber was suspended between 14 min (Record 4) and 15 min (Record 5) after introduction of the detergent solution into the middle pool. (From Tasaki and Ushiyama, 1950.)

During the following period, the quantity of electricity carried through the myelin sheath could increase 5 times or more without bringing about conduction block. Finally, the second peak of current flow was seen to drop out suddenly, indicating that nerve conduction across the demyelinated region was suspended.

Changes in the resistance and the capacity of the myelin sheath were examined by the use of the collision technique (Section E). It was found that, during the early period of detergent action, the resistance (R) falls and the capacity (C) rises in such a manner that the product, RC , remains unaltered. This finding indicates that the multilayer structure of the myelin sheath is thinned down without altering the properties of the remaining layers. The resistance of the detergent-treated zone of the myelin sheath could fall to

roughly $\frac{1}{10}$ or less of the initial value. Soon after this stage was reached, conduction block was found to set in.

The fall of the resistance of the myelin sheath could be detected also by measuring the threshold strength for stimulating current pulses. When the electrode immersed in the middle pool was connected to the cathode of the stimulating circuit and the electrode in one of the lateral pools to the anode, a marked rise in the threshold was brought about by demyelination of the portion of the fiber in the middle pool. Obviously, this rise in threshold is due to an increased leakage of the stimulating current through the myelin sheath.

When applied to a portion of a nerve fiber involving a node of Ranvier, the detergent solution was found to block nerve conduction within a very short time.

J. THE RELATION BETWEEN FIBER DIAMETER AND CONDUCTION RATE

In a sciatic nerve of the bullfrog, there are more than 3000 myelinated fibers and nearly as many nonmyelinated nerve fibers. The outside diameter of the myelinated nerve fibers range from about 2 up to 16 μm . Nonmyelinated fibers are smaller than myelinated fibers. It is possible to isolate single nerve fibers in any range of diameter and to measure their conduction rate directly. Statistically speaking, there is a simple relationship between the conduction rate and the fiber diameter measured by this direct method (Tasaki *et al.*, 1943a). At 24°C, the conduction rate, v , expressed in m/sec, and the fiber diameter, d , in micrometers, are related by

$$v = 2.5 d \quad (5.5)$$

the correlation coefficient between the two being 0.92 (see Fig. 5.14).

The existence of a simple relationship between the fiber diameter and the conduction velocity was recognized a long time before the single fiber technique was invented (Gasser and Erlanger, 1927; Chapter 4). At a time when only nerve trunks were available, the demonstration of this simple rule required complex statistical analyses of both action potential records and histological sections of the nerve trunks. The fact that smaller fibers develop action currents with smaller amplitudes and longer durations makes these analyses very tedious. Studies of this kind could not be carried out until cathode ray oscillographs became available for physiological purposes. The results of these analyses made on various nerves are treated thoroughly in a book authored by Erlanger and Gasser (1937). They called the fiber types in a nerve trunk of the bullfrog alpha, beta, gamma, B, and C; at about 23°C the

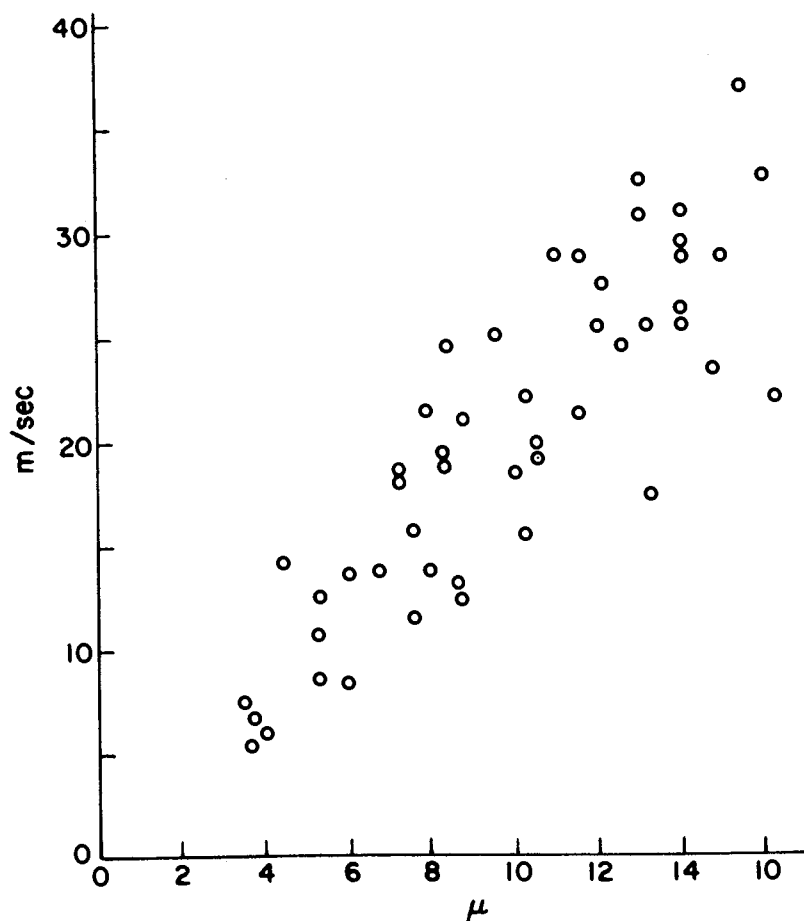


Fig. 5.14 Conduction velocity plotted against the fiber diameter. Sciatic-gastrocnemius preparations of the bullfrog were used. The outside diameters of single fibers were measured near the muscle. Temperature, 24°C. (From Tasaki *et al.*, 1943a.)

mean conduction rate of these fibers are, in m/sec, 42, 25, 17, 4.2, and 0.7, respectively (see p. 29 in Erlanger and Gasser, 1937). Type C fibers are non-myelinated. This classification of the fiber types is somewhat artificial because there is no sharp boundary between different fiber types. In other words, there is no distinction between small alpha fibers and large beta fibers. A large number of papers were written on this subject before the direct method using single fibers became available (see, e.g., Gasser and Grundfest, 1939; Hursh, 1939).

Qualitatively, it is not difficult to understand why small fibers carry nerve impulses at a lower rate. There is an approximate proportionality between the internodal distance and the fiber diameter (Boycott, 1904; Hursh, 1939). In the sciatic nerve of the bullfrog, the relationship between the internodal distance (l) and the fiber diameter (d) is given by

$$l = 1.48 \times 10^2 d \quad (5.6)$$

the correlation coefficient being only 0.62 (see Tasaki *et al.*, 1943a). From

this relationship, it follows that the internodal conduction time is roughly independent of the fiber diameter: $v/l = 0.071$ (msec).

The capacity of the myelin sheath is expected to change with the logarithm of the ratio of the outside diameter to the inside (axis-cylinder) diameter. This ratio seems to be roughly independent of the fiber diameter (see, e.g., Gasser and Grundfest, 1939); hence, the capacity per unit length of the myelin sheath (c_m) is roughly independent of the fiber diameter. The resistance per unit length of the axis-cylinder (r_i) is inversely proportional to the square of the diameter of the fiber. The spread of potential (V) along a perfectly insulated cable obeys the following differential equation:

$$\frac{\partial V}{\partial t} = \frac{1}{c_m r_i} \frac{\partial^2 V}{\partial x^2} \quad (5.7)$$

where $(c_m r_i)^{-1}$ has a dimension of cm^2/sec as diffusion constants do (see Chapter 6, Section B). [This argument is along the line first put forward by G thlin (1910; Chapter 4) except that consideration of the internodal distance is added here.] From this, it follows that the variation of the product $c_m r_i$ with fiber diameter is compensated by the change in the internodal distance, and consequently, that the time required for the spread of potential from one node to the next is expected to be roughly independent of the fiber diameter. The internodal conduction time is determined primarily by the time required for the spread of electrotonic potential from a node to the next (Hodler *et al.*, 1952). Thus we have arrived at a reasonable explanation of the linear relationship between the conduction rate and the fiber diameter.

There are differences in other properties between small and large nerve fibers. Reflecting the situation that the action potential durations of small myelinated fibers last longer than those of larger fibers, the absolutely refractory period is longer in small fibers than in large fibers (Erlanger *et al.*, 1927). However, the duration of the relatively refractory period does not differ significantly between large and small myelinated fibers. The current intensity required to excite small fibers in a sciatic nerve (trunk) is much higher than that for large fibers (Bishop and Heinbecker, 1928). When measured with brief (about 20 μsec) current pulses delivered through a pair of electrodes separated by a distance of 2.5 mm, the threshold strength for 4- μm fibers is 5 to 10 times as high as that for 15- μm fibers (Tasaki *et al.*, 1943a). The high threshold of small myelinated fibers is attributable to the high internodal resistance as well as to the short internodal distance in small fibers. The threshold for nonmyelinated fibers may be 100 times as high as that for large fibers under similar experimental conditions. The fiber size dependence of the conduction rate of small nonmyelinated nerve fibers has been analyzed and compared with that in myelinated fibers by Rushton (1951).

It is well known that the conduction rate of the myelinated nerve fiber is

strongly affected by changes in the ambient temperature. In large motor nerve fibers of the frog, the conduction rate is enhanced by a factor of 1.8 by a 10°C rise in temperature (see Lucas, 1908; Tasaki and Fujita, 1948). It is interesting to note that this temperature dependence is less marked than that of the action potential duration; the Q_{10} of the latter quantity is known to be about 3.5.

REFERENCES

- Adrian, E. D. (1913). Wedensky inhibition in relation to the "all-or-none" principle in nerve. *J. Physiol. (London)* **46**, 384–412.
- Adrian, E. D. (1921). The recovery process of excitable tissues. Part II. *J. Physiol. (London)* **55**, 193–225.
- Adrian, E. D., and Lucas, K. (1912). On the summation of propagated disturbances in nerve and muscle. *J. Physiol. (London)* **44**, 68–124.
- Adrian, E. D., and Zotterman, Y. (1926). The impulses produced by sensory nerve endings. Part 2. The response of a single end-organ. *J. Physiol. (London)* **61**, 151–171.
- Biedermann, W. (1895). "Elektrophysiologie." Gustav Fischer, Jena.
- Bishop, G. H., and Heinbecker, P. (1928). Correlation between threshold and conduction rate. *Proc. Soc. Exp. Biol. Med.* **26**, 241–243.
- Bowditch, H. P. (1871). Über die Eigenthümlichkeiten der Reizbarkeit welche die Muskelfasern des Herzens zeigen. *Ber. Saechs. Ges. Wiss. Math -Phys. Klasse* **23**, 652–689.
- Boycott, A. E. (1904). On the number of nodes of Ranvier in different stages of the growth of nerve fibers in the frog. *J. Physiol. (London)* **30**, 370–380.
- Cole, K. S., and Curtis, H. J. (1939). Electric impedance of the squid giant axon during activity. *J. Gen. Physiol.* **22**, 649–670.
- Davis, H. (1926). The conduction of the nerve impulse. *Physiol. Rev.* **6**, 547–595.
- Davis, H., Forbes, A., Brunswick, D., and Hopkins, A. McH. (1926). Studies of the nerve impulse. II. The question of decrement. *Am. J. Physiol.* **76**, 448–471.
- Erlanger, J., and Gasser, H. S. (1937). "Electrical Signs of Nervous Activity," 216 pp. Univ. of Pennsylvania Press, Philadelphia.
- Erlanger, J., Gasser, H. S., and Bishop, G. H. (1927). The absolutely refractory phase of the alpha, beta and gamma fibers in the sciatic nerve of the frog. *Am. J. Physiol.* **81**, 473–474.
- Fontana, F. (1785). "Beobachtungen und Versuche über die Natur der thierischen Körper." 336 pp. *Wegand, Leipzig*, **8**, II.
- Frankenhaeuser, B. (1957). A method for recording resting and action potentials in the isolated myelinated nerve fibre of the frog. *J. Physiol. (London)* **135**, 550–559.
- Gasser, H. S., and Grundfest, H. (1939). Axon diameters in relation to the spike dimensions and the conduction velocity in mammalian A fibers. *Am. J. Physiol.* **127**, 393–414.
- Gotch, F. (1902). The submaximal electrical response of nerve to a single stimulus. *J. Physiol. (London)* **28**, 395–416.
- Gotch, F. (1910). The delay of the electrical response of nerve to a second stimulus. *J. Physiol. (London)* **40**, 250–274.
- Gotch, F., and Burch, G. J. (1899). The electrical response of nerve to two stimuli. *J. Physiol. (London)* **24**, 410–426.

- Haller, A. (1760). "Memoires sur les parties sensibles et irritables du corps animal," Vol. 3. Sigmond d'Arnay, Lausanne.
- Hodler, J., Stämpfli, R., and Tasaki, I. (1952). Role of potential wave spreading along myelinated nerve fiber in excitation and conduction. *Am. J. Physiol.* **170**, 375-389.
- Hoff, H. E. (1942). The history of the refractory period. *Yale J. Biol. Med.* **14**, 635-672.
- Hursh, J. B. (1939). Conduction velocity and diameter of nerve fibers. *Am. J. Physiol.* **127**, 131-153.
- Kato, G. (1924). "The Theory of Decrementless Conduction in Narcotized Region of Nerve." Nankodo, Tokyo.
- Kato, G. (1926). "Further Studies on Decrementless Conduction." Nankodo, Tokyo.
- Lucas, K. (1908). The temperature coefficient of the rate of conduction in nerve. *J. Physiol. (London)* **37**, 112-121.
- Lullies, H. (1930). Über die Polarisation in Geweben, II. Die Polarisation in Nerven I, II. *Pfluegers Arch. Gesamte Physiol. Menschen Tiere* **225**, 69-97.
- Marey, E. J. (1876). Des mouvements que produit le coeur lorsqu'il est soumis à des excitation artificielles. *C. R. Acad. Sci.* **82**, 408-411.
- Rushton, W. A. H. (1951). A theory of the effect of fibre size in medullated nerve. *J. Physiol. (London)* **115**, 101-122.
- Sarnoiloff, A., and Kisseleff, M. (1925). Irreziproke Nervenleitung als Folge der Polarization kurzer Nervenstrecken. *Pfluegers Arch. Gesamte Physiol. Menschen Tiere* **209**, 476-483.
- Schaefer, H. (1936). Experimentelle Grundlagen einer Spannungstheorie der elektrischen Nervenreizung. *Pfluegers Arch. Gesamte Physiol. Menschen Tiere* **237**, 747-760.
- Takeuchi, T., and Tasaki, I. (1942). Übertragung des Nervenimpulses in der polarisierten Nervenfasern. *Pfluegers Arch. Gesamte Physiol. Menschen Tiere* **246**, 32-43.
- Tasaki, I. (1949). The excitatory and recovery processes in the nerve fiber as modified by temperature changes. *Biochim. Biophys. Acta* **3**, 498-509.
- Tasaki, I. (1953) "Nervous Transmission." Thomas, Springfield, Illinois.
- Tasaki, I. (1955). New measurements of the capacity and the resistance of the myelin sheath and the nodal membrane of the isolated frog nerve fiber. *Am. J. Physiol.* **181**, 639-650.
- Tasaki, I. (1956). Initiation and abolition of the action potential of a single node of Ranvier. *J. Gen. Physiol.* **39**, 377-395.
- Tasaki, I. (1976). Chronaxie and transitional decrement: A review of Dr. Davis' contributions to physiology of nerve fibers. p. 1-10. In "Hearing and Davis: Essays Honoring Hallowell Davis" (S. K. Hirsh, D. H. Eldredge, I. J. Hirsh, and S. R. Silverman, eds.). Washington Univ. Press, St. Louis.
- Tasaki, I., and Freygang, W. H., Jr. (1955). The parallelism between the action potential, action current, and membrane resistance at a node of Ranvier. *J. Gen. Physiol.* **39**, 211-223.
- Tasaki, I., and Fujita, M. (1948). Action currents of single nerve fibers as modified by temperature changes. *J. Neurophysiol.* **11**, 311-315.
- Tasaki, I., and Mizuguchi, K. (1949). The changes in the electric impedance during activity and the effect of alkaloids and polarization upon the bioelectric processes in the myelinated nerve fiber. *Biochim. Biophys. Acta* **3**, 484-497.
- Tasaki, I., and Ushiyama, J. (1950). The effect of saponine and several other chemicals upon the action current led through the myelin sheath. *Arch. Internz. Stud. Neurol.* **i** (Fasc. 2), 1-6.
- Tasaki, I., Ishii, F., and Ito, H. (1943a). On the relation between the conduction rate and fiber diameter and the internodal distance of the medullated nerve fiber. *Japan. J. Med. Sci. III.* **9**, 189-199.
- Tasaki, I., Yuasa, K., and Morii, I. (1943b). On the mechanism of suspension of nervous transmission by narcosis. *Japan. J. Med. Sci. III.* **9**, 183-188.

- Wedensky, N. (1885). Über einige Beziehung zwischen der Reizstärke und der Tetanushöhe bei indirecter Reizung. *Pfluegers Arch. Gesamte Physiol. Menschen Tiere* **37**, 67–72.
- Wedensky, N. E. (1903). Die Erregung, Hemmung und Narkose. *Pfluegers Arch. Gesamte Physiol. Menschen Tiere* **100**, 1–144.
- Weidmann, S. (1951). Effect of current flow on the membrane potential of cardiac muscle. *J. Physiol. (London)* **115**, 227–236.
- Werigo, Br. (1899). Zur Frage über die Beziehung zwischen Erregbarkeit und Leitungsfähigkeit des Nerven. *Pfluegers Arch. Gesamte Physiol. Menschen Tiere* **76**, 552–607.
- Winterstein, H. (1926). "Die Narkose." Julius Springer, Berlin.
- Woronzow, D. S. (1924). Ueber die Einwirkung des konstanten Stromes auf den mit Wasser, Zuckerlösung, Alkali- und Erdalkalichloridlösung behandelten Nerven. *Pfluegers Arch. Gesamte Physiol. Menschen Tiere* **203**, 300–318.

6. Electric Excitation of Single Myelinated Fibers

A. CONSIDERATION OF THE ULTRASTRUCTURE OF THE MYELIN SHEATH

A weak current pulse applied to an isolated myelinated nerve fiber alters the potential difference between the interior of the fiber and the external fluid medium. The change in the potential thus produced tends to spread along the fiber. The process of this "spread of electrotonic potential" along the nerve fiber is governed by the resistance of the axis-cylinder and by the capacities and the resistances of the nodal membrane and the myelin sheath.

In determining the resistance and capacities of the myelinated nerve fiber (Chapter 5, Section E), we have chosen the experimental condition under which the complexity of the ultrastructure of the myelinated nerve fiber does not seriously affect the results. We arrived at the following values for a bull-frog motor nerve fiber of about $14 \mu\text{m}$ in diameter:

Capacity of myelin sheath (c_m): $1.6 \times 10^{-11} \text{ F/cm}$

Resistance of myelin sheath (r_m): $2.9 \times 10^7 \Omega \cdot \text{cm}$

Capacity of nodal membrane (C): $1.5 \times 10^{-12} \text{ F}$

Resistance of nodal membrane (R): $41 \times 10^6 \Omega$

Resistance of axis-cylinder (r_i): $1.45 \times 10^8 \Omega \cdot \text{cm}$

The resistance of the axis-cylinder was estimated based on the results of DC resistance measurements of single nerve fibers combined with the consideration of the property of the resistance network shown in Chapter 4, Section D.

It is now well known that the ultrastructure of the myelinated nerve fiber is quite complex. It seems worthwhile to inquire into the relationship between the complex ultrastructure and electrical properties of the myelinated nerve fiber.

There seems little problem concerning the factor which determined the resistance of the axis-cylinder, r_i . The diameter of the axis-cylinder of a

nerve fiber of $14\ \mu\text{m}$ in outside diameter is approximately $10\ \mu\text{m}$. The observed value of r_i indicates that the specific resistance of the axoplasm is about $105\ \Omega\cdot\text{cm}$, which is roughly 30% larger than the resistivity of the external fluid medium.

The ultrastructure of the myelin sheath is not very simple. According to Geren (1954) and Robertson (1955, 1957); the myelin sheath is formed by a greatly extended Schwann cell membrane wrapping around the axis-cylinder. Examined under an electron microscope, it consists of a large number of electron-dense lamellae repeating with a period of $170\text{--}180\ \text{\AA}$; as can be seen in Fig. 6.1, the lamellar arrangement is somewhat irregular near the node (see Uzman and Nogueira-Graf, 1957; Metzuzals, 1965; Webster, 1974; Rosenbluth, 1976).

The lamellar arrangement of lipids and protein molecules in the myelin sheath strongly suggests that both the resistivity and the dielectric constant vary periodically within the sheath. The myelin sheath of a large motor

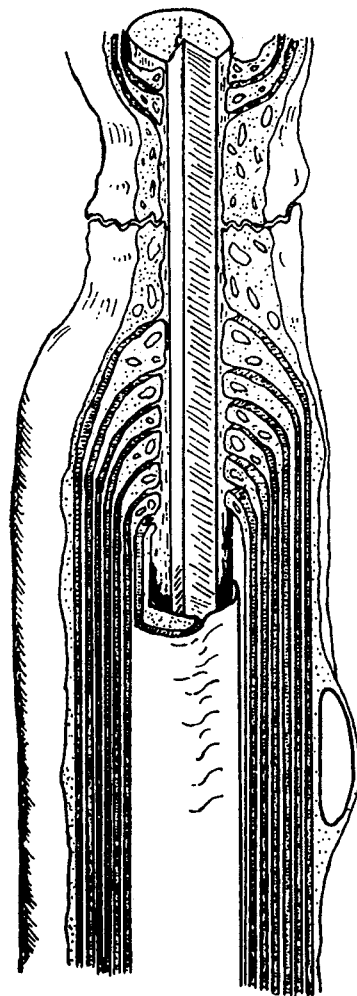


Fig. 6.1 Diagrammatic representation of cutaway view of early node of Ranvier illustrating relation between myelin lamellar endings, Schwann cell cytoplasm, and axon. The myelin lamellae are crosshatched. Cut surfaces of the Schwann cell cytoplasm are stippled and include outlines of formed cytoplasmic organelles. (From Uzmann and Nogueira-Graf, 1957.)

nerve fiber is about $2\ \mu\text{m}$ thick; it consists of about 120 lamellae. A simple calculation indicates that the uniform fluid medium, which fills a $20\text{-}\text{\AA}$ -wide space between the intraperiod lines (Revel and Hamilton, 1969), does make a significant contribution to the (radial) resistance of the myelin sheath. The surface conductivity of the myelin lamella is not known.

From the ultrastructure of the myelin sheath, it follows that the value of capacity c_m is the resultant of a series arrangement of about 120 lamellae, each having a capacity of the order of $0.5\ \mu\text{F}/\text{cm}^2$. These lamellae are separated by thin layers of conducting fluid medium. When the electric potential difference across the myelin sheath is constant along the fiber, the layers of conducting fluid medium do not carry any electric current (in the longitudinal direction). However, in dealing with the spread of the electrotonic potential along the fiber, the effect of these conducting layers may have to be taken into consideration. The effect expected from the lamellar structure is a decrease in the rapidity of the spread of potential waves along the fiber.

Reier *et al.* (1976) have shown that there is a space of $100\text{--}200\ \text{\AA}$ in thickness between the axon surface and the myelin sheath. The longitudinal resistance of the fluid medium in this periaxonal space is expected to be at least 100 times as high as that of the axis-cylinder. Hence, it is improbable that this space makes a significant contribution to the longitudinal resistance of the nerve fiber. The periaxonal space may be closed near the nodes in the normal condition of the fiber; even if this is the case, the effect of the periaxonal space on the cable properties would be toward slowing down of the spread of the electrotonic potential.

In the paranodal zones (see Fig. 6.1), the nodal membrane is covered by a small number of Schwann cell membranes (see Uzman and Nogueira-Graf, 1957; Robertson, 1957). There seems little doubt that the measured values of the resistance and the capacity of the node include some unknown contribution made by the paranodal structures.

We have pointed out in this section the structural complexity of the myelinated sheath. When a brief voltage pulse is applied to a nerve fiber, the conducting fluid medium in the interlamellar and periaxonal space is expected to carry an electric current. In dealing with spread of the electrotonic potential, the capacitative property of the myelin sheath is expected to be very complex.

B. THE CABLE EQUATION

A long time before the discontinuity in the electrical property at nodes of Ranvier was revealed, several physiologists, including Hoorweg (1898; Chapter 3); Cremer (1899); Hermann (1899); and Göthlin (1910; Chapter 4) noted the similarity between the process of spread of electricity along the

myelinated nerve fiber and the transmission of signals along a submarine cable. In fact, the mathematical equations employed by these physiologists to describe the spread of electrotonic potential in the nerve fiber are essentially the same as those derived by Lord Kelvin (Thomson, 1856) in his theory of electric telegraph. The present section deals with the age-old cable theory applied to the myelinated portion of the nerve fiber. The multilayer structure of the myelin sheath is ignored here.

In a nerve fiber immersed in a large volume of Ringer's fluid, the potential of the external fluid medium may be regarded as being constant everywhere; we choose this potential as 0. The potential inside the axis-cylinder at time t and at position x along the fiber is denoted by $V(x,t)$. We apply Kirchhoff's law to position x of the electric network illustrated in Fig. 6.2. The intensity of the longitudinal current between positions x and $(x + \Delta x)$ of the axis-cylinder is given by $[V(x,t) - V(x + \Delta x,t)]/r_i \Delta x$; similarly, the current between point $(x - \Delta x)$ and point x is given by $[V(x - \Delta x) - V(x,t)]/r_i \Delta x$. The difference between these two currents is now equated to the transmembrane current at point x , which consists of two components, ohmic and capacitive. This leads to the following equation:

$$\frac{V(x - \Delta x,t) - V(x,t)}{r_i \Delta x} - \frac{V(x,t) - V(x + \Delta x,t)}{r_i \Delta x} = c_m \Delta x \frac{\partial V(x,t)}{\partial t} + \frac{V(x,t)}{r_m/\Delta x} \quad (6.1)$$

By expanding $V(x - \Delta x,t)$ and $V(x + \Delta x,t)$ in Taylor's series and then taking the limit $\Delta x \rightarrow 0$, the differential equation describing the process of potential spread along the myelinated portion of a nerve fiber is obtained:

$$\frac{1}{r_i} \frac{\partial^2 V}{\partial x^2} = c_m \frac{\partial V}{\partial t} + \frac{1}{r_m} V \quad (6.2)$$

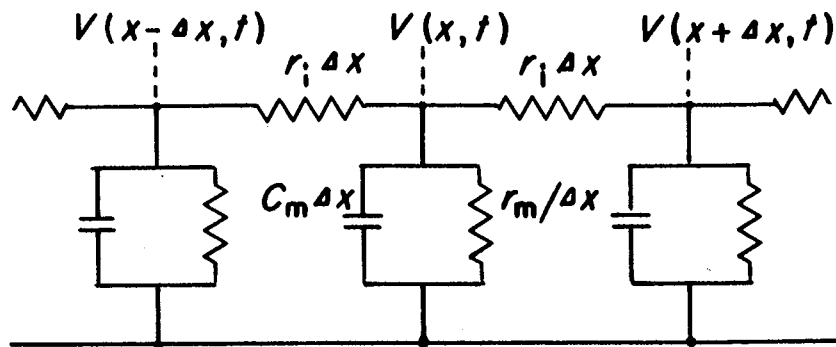


Fig. 6.2 The electric network employed to derive the "cable equation" [Eq. (6.2)] for describing the spread of the "electrotonic potential" along a myelinated fiber at rest. The resting membrane potential is omitted. The symbol r_m denotes the resistance of the myelin sheath of a unit length, c_m the capacity of the myelin sheath, and r_i the resistance of the axis-cylinder per unit length.

As is well known, this equation has the same form as that describing the conduction of heat along a rod with heat loss through the surface. Since the resistance of the myelin sheath, r_m , is very high, the last term in Eq. (6.2) may be ignored; we then arrive at Eq. (5.7) described previously.

In order to illustrate the nature of the spread of electrotonic potentials, we first examine the case in which a sinusoidally alternating voltage is applied at $x = 0$:

$$V(0,t) = V_0 \sin(2\pi ft)$$

where V_0 is the amplitude $x = 0$. In this case, the "potential wave" decays as it travels along the fiber (before it reaches the next node) according to the formula:

$$V(x,t) = V_0 e^{-x/\lambda} \sin 2\pi f \left(t - \frac{x}{\nu} \right) \quad (6.3)$$

where

$$\lambda^2 \approx \frac{1}{\pi C_m r_i f} \quad (6.3a)$$

and

$$\nu^2 \approx \frac{4\pi f}{C_m r_i} \quad (6.3b)$$

The approximate expressions for λ and ν are for the case where the leakage through r_m of the myelin sheath is ignored. It is important to note that the velocity, ν , as well as the decay (space) constant λ , depends on the frequency f ; Cremer (1900; 1932) called this kind of process a "pseudo-wave." By introducing the observed value of c_m and r_i presented in the preceding section, it is found that, at 10^4 Hz, $\lambda = 0.11$ cm and $\nu = 7.3 \times 10^3$ cm/sec.

The following alternative picture of the process of potential spread may be helpful for understanding the nature of the "delay" involved. The variation of the membrane potential produced by application of a brief rectangular voltage pulse at point $x = 0$ is analogous to the rise in temperature caused by a heat pulse delivered at one point of a long heat-conducting rod. At a finite distance away from $x = 0$, a potential (or temperature) variation appears only after a certain delay. The delay increases with the distance involved; but there is no linear relationship between the delay and the distance. In the case where r_m is so large that the last term in Eq. (6.2) can be ignored, the time, t , at which the potential variation produced by a brief shock applied at $x = 0$ reaches a maximum is given by

$$t = \frac{1}{2} C_m r_i x^2 \quad (6.4)$$

(see Cremer, 1900). Introducing $x = 0.23$ cm into Eq. (6.4) together with the values of c_m and r_i listed in the preceding section, the value of t is found to

be 0.062 msec. The value is of the same order of magnitude as the internodal conduction time.

In the calculation described above, both the discontinuity of the electric properties at nodes of Ranvier and the structural complexity of the myelin sheath are ignored. Hence, a significant discrepancy is expected between the "delay" in the real nerve fiber and the value obtained by calculation. The objective of the analysis described above is to emphasize that the pseudo-wave of potential variation spreads along the myelinated portion of a nerve fiber at a rate not very different from the conduction velocity of the nerve impulse.

C. THE STRENGTH-LATENCY RELATION

In excitation of a single nerve fiber with a long rectangular voltage pulse, the time interval between the onset of the pulse and the beginning of the electric response is known to vary with the strength of the pulse (see p. 85 in Erlanger and Gasser, 1937, Chapter 4). In this section, we describe the results of an experiment demonstrating that the relation between the pulse strength and the latency of the response is directly related to the cable property of the myelin sheath.

The arrangement used for this experiment was similar to that used by Huxley and Stämpfli (see Chapter 4, Section H). A large motor nerve fiber of the frog was pushed through a 0.6-mm-wide oil partition separating two pools of Ringer's solution. Long rectangular voltage pulses were delivered to the fiber through a pair of nonpolarizable electrodes immersed in the pools. The action current developed by the fiber was recorded through the same pair of electrodes. A Wheatstone bridge was employed to suppress the disturbance caused by the stimulating pulses in the recording system. The nerve fiber was held with a micromanipulator at its ends, so that the fiber could be displaced longitudinally from one end of an internode to the other (see Hodler *et al.*, 1952).

Figure 6.3 shows the relationship between the voltage applied and the latency of the action current (i.e., the interval between the onset of the pulse and the earliest sign of the response). In this figure, the reciprocal of the voltage applied is plotted as ordinate against the latency observed. This method of plotting the strength-latency relationship is convenient for displaying the relationship in the high voltage range. If an action potential is released immediately at (or with a constant delay after) the moment at which the membrane potential at the node reaches a definite critical level, the curve relating the reciprocal of the voltage ($1/V$) to the latency (t) is expected to represent the time course of development of the membrane potential at the node.

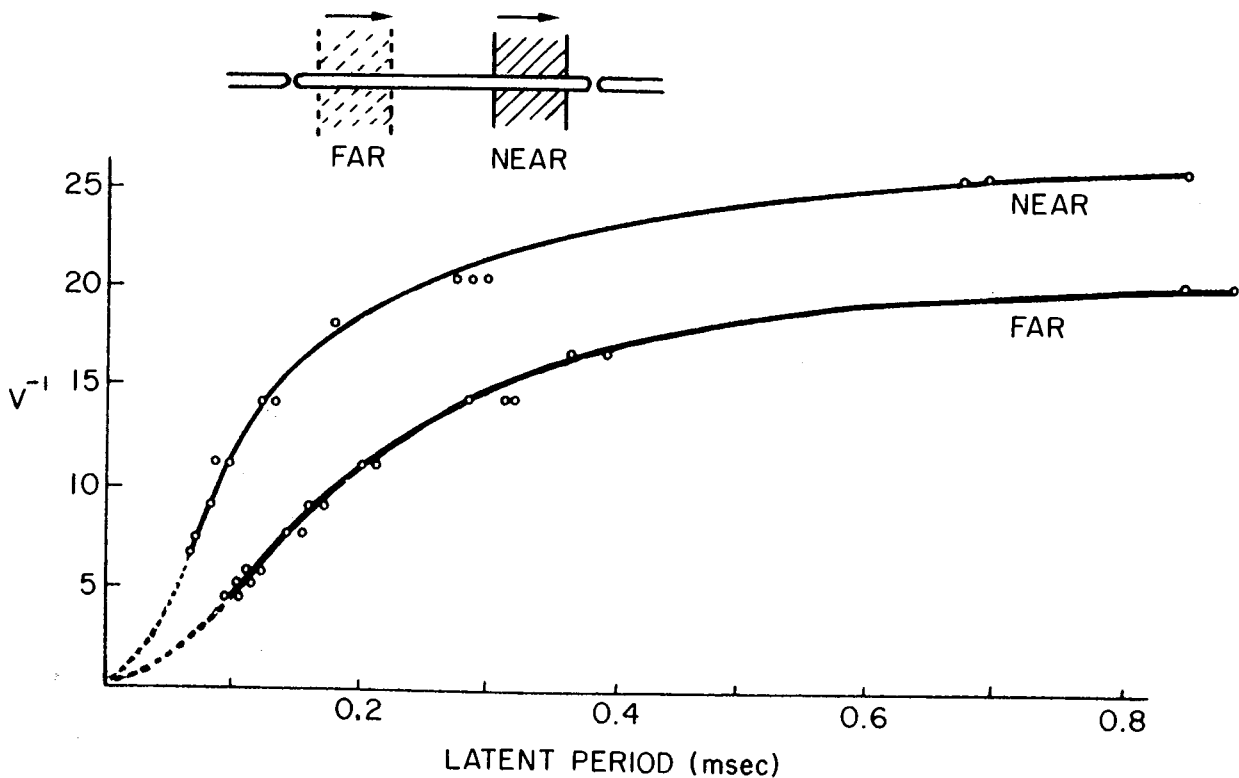


Fig. 6.3 Relation between the reciprocal of the amplitude (V) of a rectangular voltage pulse and the latency (t) of the response of a node of Ranvier. Note that the latency depends markedly on the distance between the site of stimulation and the node of Ranvier under study. 18°C . (From Hodler *et al.*, 1952.)

The curve marked "near" in the figure represents the results obtained with the node under study located very close to the oil partition. When the applied voltage is relatively low, the latency is long and variable. As the voltage is raised the latency is shortened. At every voltage level employed, the latency was definitely longer when the stimulating pulse was applied "far" from the node under study. The displacement of the fiber involved in this experiment was about 1 mm.

The latencies observed at very high voltages are extremely short and are close to the limit of reliability of these measurements. Nevertheless, since the electric resistance of the myelin sheath to DC is extremely high, the observed difference in latency between the two modes of stimulation, "near" and "far," is attributed to the effect of the capacity of the myelin sheath.

The strength-latency relation was examined also by using very brief electric pulses instead of long voltage pulses (Hodler *et al.*, 1952). Again, it was found that the latency depends on both the strength of the shock and the distance between the site of stimulation and the node of Ranvier involved. At strengths 50% above the threshold, the latency observed with stimuli applied near the node was found to be about $10\ \mu\text{sec}$ shorter than the value

observed when the stimuli were delivered far from the same node. There is little doubt that this difference is a reflection of the "delay" arising from the cable property of the myelin sheath discussed in the preceding section.

D. LATENT ADDITION

Before the turn of the century, von Kries and Sewall (1881) noted that the threshold strength for a brief electric shock is modified by another brief subthreshold shock delivered to the same point of a whole nerve at a short interval. Later on, this phenomenon was studied extensively by a large number of investigators, including Gildemeister (1908); Lucas (1910), Chapter 3; Lapique (1925).

The phenomenon under study deals with the aftereffect of an electric shock which is too weak to evoke an all-or-none response. A second shock, delivered to the same nerve before the effect left behind the first shock vanishes, could reveal the nature of the state of the membrane modified by the first shock. The term "local summation" or "l'addition latente" has been used to describe the phenomenon discussed in this section (see Katz, 1939).

Most of the theories advanced to explain the phenomenon of latent addition before the advent of the single fiber technique are at present of only historical interest. The following observations made on isolated single fibers clearly indicate that this phenomenon is directly related to the spread of electrotonic potential waves along the myelinated portion of the nerve fiber.

The electrode arrangement used to examine the phenomenon of latent addition in isolated single nerve fibers is shown schematically in Fig. 6.4. A large motor nerve fiber of the toad was mounted in a nerve chamber provided with a bridge insulator. The fiber could be excited by brief electric shocks applied to the fiber either across the bridge insulator or through a glass-pipette electrode (about $50 \mu\text{m}$ in diameter) placed directly above a node of Ranvier. Two brief electric shocks, separated by variable intervals, were used to excite the fiber. The strengths of these shocks were adjusted in such a manner that the fiber can barely be excited by these two shocks. We denote the strengths of the two shocks by s_1 and s_2 and the shock interval by z . Our task is to find the relation among these three variables, s_1 , s_2 , and z , which fulfill the *threshold condition*.

The first subthreshold shock used to modify the state of the fiber is often called the "conditioning" stimulus; and the second shock employed to examine the state of the fiber is referred to as the "test" stimulus. The interval, z , is regarded as positive when the conditioning stimulus (with strength s_1) precedes the test stimulus (s_2). It is to be noted, however, that we regularly

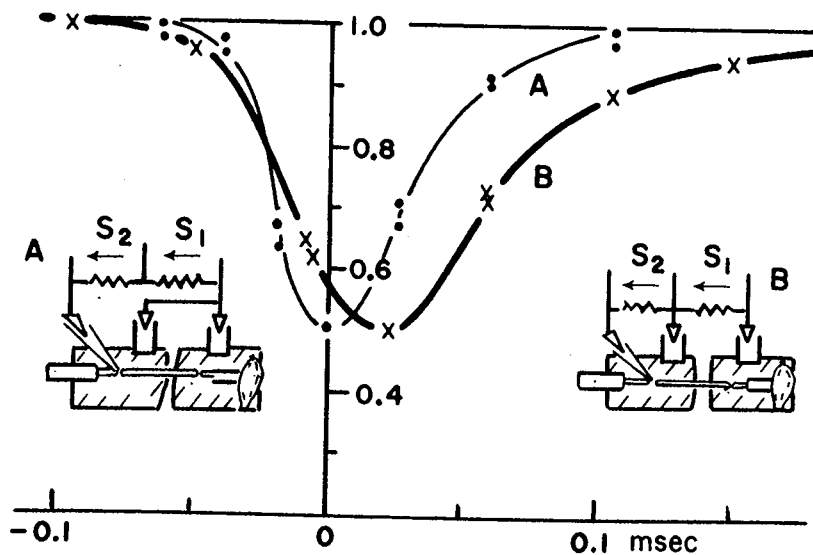


Fig. 6.4 Latent addition curves of a single nerve fiber determined by two different modes of stimulation. Curve A was obtained with two shocks applied through a glass-pipette electrode placed directly on a node of Ranvier. Curve B was taken by delivering the conditioning shocks across the bridge insulator and the test shocks through the glass-pipette electrode. 23°C. (From Tasaki, 1950b, Chapter 4.)

treat the cases where the interval, z , is negative. In all cases, the strength of the conditioning shock is fixed at a properly chosen level, and that of the test shock is varied so as to detect changes in threshold brought about by the conditioning shock.

The experimental results shown by the thin line (A) were obtained by applying the two brief shocks through the glass-pipette electrodes. The intensity of the conditioning stimulus was fixed at the level 50% below the threshold. It is seen in the figure that the threshold for the test stimulus is affected most strongly by the conditioning stimulus when the interval is zero and that the effect rapidly decreases when the separation between the two shocks is increased.

The thick line (B) was obtained when the conditioning shock was delivered across the bridge insulator and the test shocks through the glass-pipette electrode. It is seen that the strongest effect of the conditioning shock was encountered when the conditioning shock preceded the test shock by an interval of 22 μsec . Furthermore, the effect of the conditioning shock is seen to last much longer in this case than in the previous.

Based on our knowledge of the cable property of the myelin sheath, it is easy to understand the difference between the two latent-addition curves in Fig. 6.4. A subthreshold shock applied across the bridge insulator is expected to produce at the node under study a potential variation which rises and decays relatively slowly. When the shock is applied directly to the node the rise time is expected to be shorter and the decay to be faster than in the

case where the bridge insulator is used for stimulation. The potential variation produced by the second shock is superposed on that generated by the first; a nerve impulse is released when the summed potential reaches the critical level at the node under study. The additive effect should then be maximal when the conditioning shock precedes the test shock by the difference between the rise times in these two modes of stimulation. Furthermore, the effect of the conditioning shock delivered across the bridge insulator is expected to last longer than that of the shock applied directly to the node. The experimental results shown in the figure are, therefore, quite consistent with the result described in the preceding section.

Here, a brief comment is added on the significance of the portion of the latent addition curve on the negative side of the abscissa. When the test shock precedes the conditioning shock by a short interval ($z < 0$), the potential change produced by the test shock at the node under study reaches its peak during the rising phase of the potential change generated by the conditioning shock. If the strength of the conditioning shock is well below the threshold, the time at which the summed potential change reaches a maximum is determined roughly by the test shock alone. In such cases, the fall in the threshold for the test shock is a true measure of the excitatory effect of the conditioning shock. However, at relatively large (negative) intervals, the observed latent addition curve is, in general, affected by the subthreshold response evoked by the test shock. Note that a barely subthreshold shock produces a long, variable potential change which is attributed to the appearance of a subthreshold response (see Fig. 5.1). It will be repeatedly emphasized in following sections that such subthreshold responses appear only when the shock strength is very close to the threshold.

A long time before the cable property of the myelin sheath was clarified, a logical explanation of the phenomenon of latent addition in terms of a delay in the rise of the excitatory effect was given by Blair and Erlanger (1936) (see also Erlanger and Gasser, 1937, cited in Chapter 4). It should be remembered in this connection that old latent-addition curves obtained from whole nerves are always distorted by the electric capacity of the myelin sheath of the fibers surrounding the fiber under study.

E. THE LIMITING QUANTITY OF ELECTRICITY

The electric network shown in Fig. 6.2 represents the cable property of the myelinated nerve. The network is regarded as a linear system which obeys the principle of superposition. From this, it follows immediately that the time course of the potential variation produced by an extremely short pulse is independent of the shape of the applied pulse. Furthermore, the magnitude of

the potential variation is directly proportional to the quantity of electricity sent into the fiber.

It has long been known that, in determining the strength–duration relation, the product of voltage and duration is approximately constant in the range of extremely short durations (Hoorweg, 1892, see Chapter 3; Weiss, 1901, see Chapter 3; Fabre *et al.*, 1934). In isolated myelinated nerve fibers, it is easy to demonstrate the constancy of the voltage–duration product for short stimulating pulses (see Fig. 6.5).

The method of stimulating a large motor nerve fiber across a bridge-insulator was used. With rectangular voltage pulses used for stimulation, the relation between strength and duration was found to obey Weiss' empirical formula (see Chapter 3, Section D) in a limited range of durations:

$$v = \frac{a}{t} + b \quad (6.5)$$

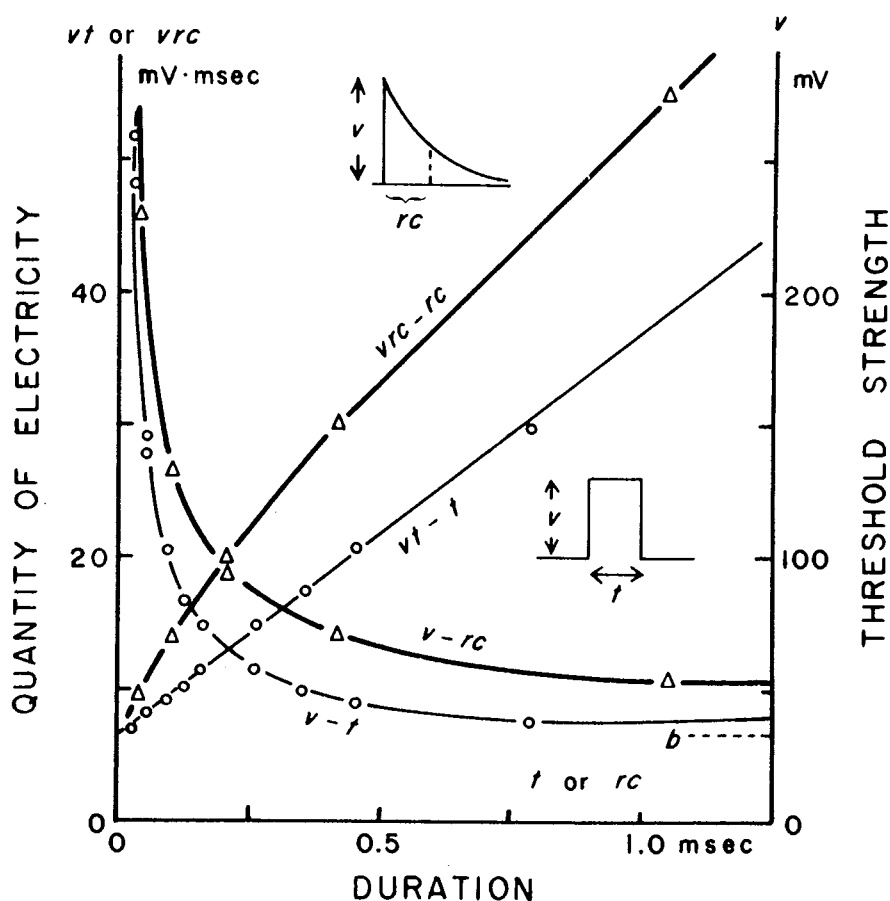


Fig. 6.5 Strength–duration relations for rectangular voltage pulse (vt) and for condenser-discharge pulses (vrc) determined on one nerve fiber using the same electrode arrangements. The same experimental data are plotted also in an alternative form, vt or vrc against t or rc . Note that the limiting value of the product vrc agrees with that of vt .

where t is the pulse duration, v the threshold voltage, and a and b are the constant required to describe the observed strength–duration relation. From this it follows immediately that

$$vt = a + bt \quad (6.6)$$

As t tends toward 0, the product vt approaches the limiting value a .

It is easy to determine the strength–duration relation for the same fiber using condenser-discharge pulses. In this case, the voltage applied to the fiber, $V(t)$, decays exponentially with time:

$$V(t) = ve^{-t/rc} \quad (6.7)$$

where v is the initial voltage and rc the resistance–capacity product (or the time constant of voltage decay). The quantity which corresponds to the product vt for rectangular pulse is given by

$$\int_0^{\infty} V(t) dt = vrc \quad (6.8)$$

It was found that the relation between the product vrc and the duration rc which fulfills the threshold condition cannot be described by a straight line. Nevertheless, the limiting value of vrc agrees very well with the limiting quantity a determined with rectangular voltage pulses.

The quantity of electricity sent into a nerve fiber is proportional to the limiting value of vt or vrc . Since the effective resistance of a nerve fiber cannot be determined readily, the limiting value of the voltage–duration product is chosen as a measure of the quantity of electricity required for excitation of a nerve fiber.

F. SUPERPOSITION OF THRESHOLD DEPRESSION

In this section, we deal with the effect of multiple brief shocks on the nerve fiber. We show that the superposition principle can be used to treat the effect of several brief shocks.

Diagram A of Fig. 6.6 is an example of the experimental results demonstrating a linear relationship between the strength of the conditioning shock and its effect on the threshold level of the test shock. Three different values were chosen as the strength of the conditioning shock. The abscissa represents the time interval, z , from the conditioning shock to the test. As ordinate, the value of $(1 - s/s_0)$ is plotted, where s is the threshold for the test pulse at interval z and s_0 is the threshold observed in the absence of the conditioning shock. For the sake of simplicity, we call $(1 - s/s_0)$ the *threshold depression*, and denote it by θ :

$$\theta = 1 - \frac{s}{s_0} \quad (6.9)$$

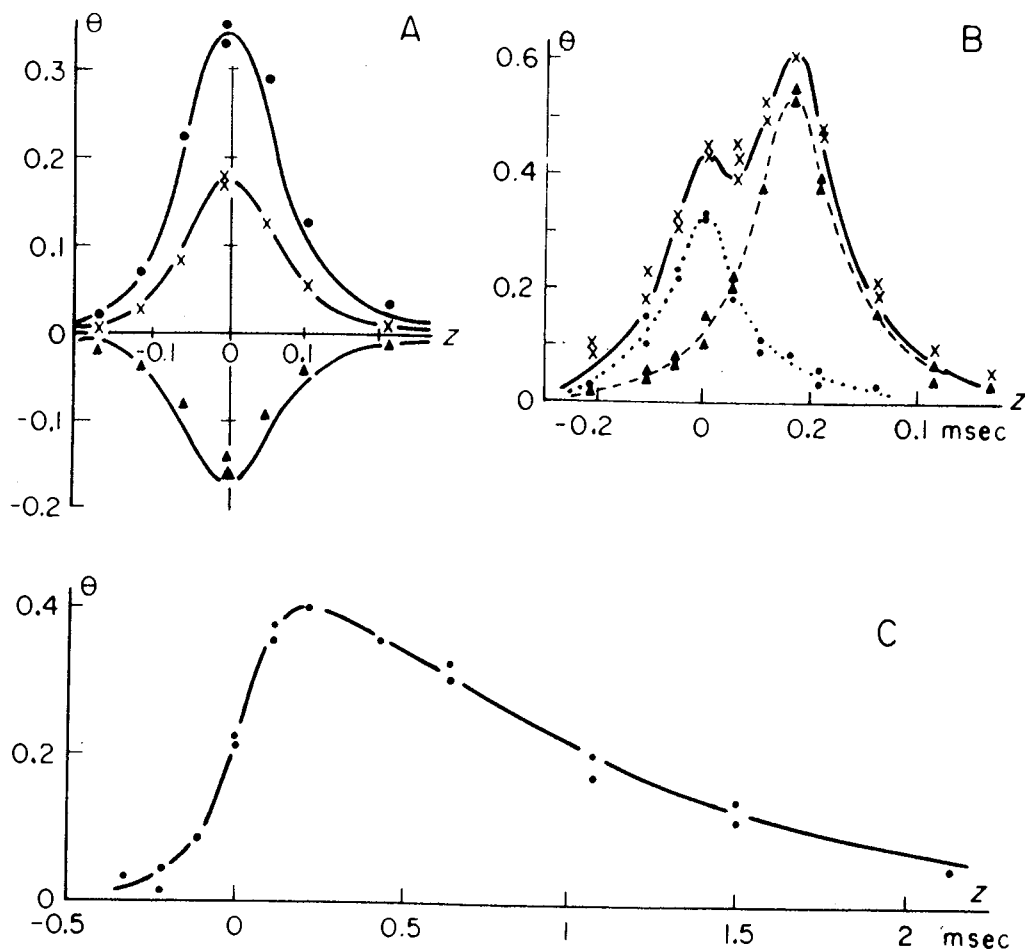


Fig. 6.6 (A) Threshold depression produced by conditioning shocks of -0.17 , $+0.17$, and $+0.34$ times the threshold. Both the conditioning and test shocks were 0.025 msec in duration. 16°C . (B) The solid line represents the threshold depression brought about by two brief conditioning shocks. The first shock was 0.35 times and the second shock 0.52 times the threshold. The interval between the two conditioning shocks was 0.162 msec. The broken line indicates the threshold depression caused by each one of the conditioning shocks. (C) Threshold depression produced by a subthreshold condenser-discharge pulse of 20 mV in amplitude and 1 msec in duration. The dots in the figure represent the observed values. The continuous line was obtained by calculation using Eq. (6.12). (From Tasaki, 1942.)

According to this definition, the threshold depression never exceeds unity. We now see that there is a very simple linear relationship between the intensity of the conditioning stimulus and this quantity.

In Fig. 6.6B, an example of the results obtained with two conditioning shocks is reproduced (see the solid line). The broken lines in the figure show the results obtained with each of these conditioning shocks. Within the accuracy of these measurements, the threshold depression obtained with two conditioning shocks is equal to the sum of the values obtained with the individual shocks.

We now generalize the experimental finding described above to include

the effect of a series of conditioning shocks. We denote the strengths of the conditioning shocks by s_1, s_2, s_3 , etc. Then, the threshold depression, θ , produced by these conditioning shocks is expected to be given simply by

$$\theta(z) = \frac{s_1}{s_0} f(z) + \frac{s_2}{s_0} f(z - t_2) + \frac{s_3}{s_0} f(z - t_3) + \dots \quad (6.10)$$

where $f(z)$ represents the normalized latent-addition relation for a single conditioning shock, z is the time from the first conditioning shock to the test shock, and t_2, t_3 , etc., are the intervals between the first shock to the second, the third, etc., respectively.

We next proceed to the consideration of the threshold depression produced by a long subthreshold pulse, either rectangular or exponentially decaying. We may regard a continuous voltage pulse as a succession of an infinite number of brief pulses. We denote the subthreshold voltage pulse by $V(t)$, a function of time t . From the argument developed above, the threshold depression produced by each of the brief pulses, $V(t) dt$, is given by

$$d\theta(z) = \frac{V(t) dt}{s_0} f(z - t). \quad (6.11)$$

The net result produced by the continuous voltage pulse tested at interval z from the onset of the long pulse is then given by integration

$$\theta(z) = \frac{1}{s_0} \int_0^z V(t) f(z - t) dt \quad (6.12)$$

When $V(t)$ represents a rectangular voltage pulse, this calculation can be carried out simply by a graphical integration of the measured curve $f(z)$. In the case of an exponentially decaying voltage pulse, the integration was carried out by approximating $f(z)$ by two exponential functions, one for the negative side of z and the other for the positive side.

The experimental result illustrated in Fig. 6.6C shows that the threshold depression calculated by the method of integration agrees with the observed values very well. In these experiments, the value of s_0 was determined by the use of short condenser-discharge pulses. Then, the normalized function $f(z)$ was determined by the double-shock method. Finally, the threshold depression produced by a long subthreshold condenser-discharge pulse was determined as a function of the time from the onset of the pulse to the test shock, z . The dots in the figure represent the observed values of threshold depression. The continuous lines represent the calculated values by using the function $f(z)$ determined on the same fiber. It should be noted that there is no adjustable parameter in the calculation. The agreement between the calculated and observed values are considered very good.

By the use of the test-pulse method, the subthreshold stimulating effect of a local current spreading beyond a site of conduction block has been demonstrated (Hodgkin, 1937, cited in Chapter 3; Tasaki, 1939b, cited in Chapter 4). The basis of this method is now clarified (see Chapter 4, Section E).

G. STRENGTH-DURATION RELATION AND LATENT-ADDITION CURVE

According to the arguments developed in the preceding sections, the normalized latent-addition curve, $f(z)$ in Eqs. (6.9) and (6.12), reflects the relative magnitude of the potential variation across the nodal membrane generated by subthreshold stimulating pulses. In the range of pulse strengths well below the threshold, the potential variation at the node changes linearly with the pulse strength. The quantity we call "threshold depression" is dimensionless because it is normalized so that excitation takes place when it reaches unity. The complications arising from the nonlinear behavior of the nodal membrane are negligible when we deal only with the rapidly rising phase of the potential variation (see Chapter 5, Section A).

We are now ready to demonstrate that the age-old strength-duration relationship for relatively short pulses can be derived directly from $f(z)$ and s_0 . We determine both the strength-duration relation for condenser-discharge pulses and the latent-addition curve on one and the same fiber. Then, by introducing the observed values of s_0 and $f(z)$ into Eq. 6.12, we calculate the relationship between v and rc which satisfies the following threshold condition:

$$\text{Maximum value of } \theta(z) = 1 \quad (6.13)$$

The value of v calculated for each duration rc can be compared with the observed value of v .

An example of such comparison is shown in Table 6.1. A good agreement was observed between the observed and calculated values over the range of duration shorter than about 0.5 msec. A similar comparison was made between the observed strength-duration relation for rectangular pulses and the values calculated by using Eq. 6.12 combined with Eq. 6.13. A satisfactory agreement was obtained in the range of duration shorter than about 0.3 msec. For durations longer than about 0.5 msec, the observed values were found to be consistently smaller than the results of calculation.

The significance of the discrepancy is as follows. With long voltage pulses of barely subthreshold strengths, a nonlinear rise in the membrane potential appears before applied voltage is terminated (see the lower records in Fig.

TABLE 6.1

The Quantity–Duration, Strength–Frequency, and Latent Addition Relations Determined on One Single Fiber Preparation^a

Quantity–duration relation			Latent addition	
<i>rc</i> (msec)	<i>vrc</i> (observed) (mV · msec)	<i>vrc</i> cal (mV · msec)	<i>z</i> (msec)	<i>f</i> (<i>z</i>)
0	(16.6)	(16.6)	−0.24	0.09
0.003	17.0	17.0	−0.21	0.17
0.012	17.6	17.4	−0.18	0.28
0.02	18.2	17.8	−0.15	0.42
0.04	19.7	19.0	−0.12	0.56
0.10	23.5	22.5	−0.09	0.71
0.20	29.5	29	−0.06	0.86
0.40	40	41	−0.03	0.97
1.00	68	78	0	1.00
2.00	108	130	0.03	0.91
Strength–frequency relation			0.06	0.82
			0.09	0.63
Frequency (kHz)	Strength observed (mV)	Strength cal (mV)	0.12	0.54
0.1	42	58	0.15	0.43
0.5	62	61	0.18	0.34
1.0	88	82	0.21	0.27
1.5	127	128	0.24	0.21
3.0	231	Above 400	0.27	0.16
5.0	455	—	0.30	0.11
7.0	770	—	0.33	0.08

^a The column "cal" shows the values calculated by the method described in the text; 11°C. The quantity is given by the product of the threshold voltage *v* and the duration *rc*. (Taken from Tasaki and Sato, 1951.)

5.1). Consequently, the threshold level of the membrane potential is reached at a pulse strength definitely below the critical level predicted from the linear behavior of the cable. This point will be discussed further in Chapter 7, Section A.

The significance of the experimental findings described in this section may be summarized in the following manner. In classical neurophysiology, analysis of the strength–duration relation was regarded as the single, most important avenue leading to the elucidation of the process of nerve excitation (see Chapter 3). We now know that, in myelinated nerve fiber, this relation is determined primarily by the cable properties of the myelin sheath.

Evidently, this conclusion had never been anticipated by the prominent physiologists who devoted themselves to studies of the strength-duration relation before World War II.

H. STRENGTH-FREQUENCY RELATION FOR HIGH-FREQUENCY AC

Studies of the effect of high-frequency AC on myelinated nerve fibers played an important role in the history of the theories of nerve excitation (see Chapter 3). Almost all classical studies on the effect of high-frequency AC were carried out on whole nerves of the frog. The facts and theories on the effects of AC known before the advent of the single fiber technique are thoroughly reviewed in a monograph written by Katz (1939). Previously, in collaboration with Hill *et al.* (1936), Katz studied the strength-frequency relation using both high-frequency AC and two-way brief shocks (see Katz, 1936). In this section, we examine how this old problem in neurophysiology has evolved after the development of the single fiber technique.

The stimulating voltage waves were applied to a large motor nerve fiber of the toad by the use of a bridge insulator (Tasaki and Sato, 1951). To avoid the excitatory effect of a sudden onset of the applied voltage (see Gildenmeister, 1929), the amplitude of the sinusoidal wave was increased exponentially at a time constant between 80 and 120 msec. In the range of frequencies between 100 and 1000 Hz, the threshold strength required for generation of sustained periodic responses was not significantly affected by the rate of rise of the amplitude. Table 6.1 includes an example of the results of measurements of the strength-frequency relation in the range of frequency between 100 and 7000 Hz. It is seen that the threshold strength increases fairly steeply with the frequency of sinusoidally varying voltages.

In these experiments, stimuli were delivered to a nerve fiber in the middle of an internode. The node of Ranvier where the process of excitation takes place is about 1 mm away from the site of delivery of the sinusoidal potential variations. Hence, there is no doubt that the effectiveness of the applied stimulus is reduced by the capacity of the myelin sheath.

The possibility of explaining the observed strength-frequency relation in terms of the simple cable property was examined by calculating the threshold strengths by using the method of integration of the latent addition curve [using Eq. (6.12) combined with (6.13)]. Both the strength-frequency and the latent-addition relations were determined on one and the same nerve fiber with the same electrode arrangement. When the strength-frequency relation was calculated under the condition that the maximum value of the threshold depression is equal to unity, a good agreement was obtained in the

range of frequency between 500 and 1500 Hz. Since no adjustable parameter was used in this calculation, this agreement between the observed and the calculated values is considered significant. However, in the range of AC frequency higher than 2000 Hz, the observed threshold strengths were found to be far lower than the values obtained by calculation.

The explanation of this discrepancy between the observed and calculated values is relatively simple. According to Gildemeister (1929), Katz (1936), and others, an alternating current applied to a frog nerve is distorted by "rectification": the quantity of electricity carried during the positive phase of a sinusoidally varying voltage is not equal to that carried during the negative phase. In artificial membranes with negative fixed charges separating two different electrolyte solutions (see Teorell, 1953), the steady-state resistance of the membrane depends both on the direction and the intensity of the current used for measurements (see Chapter 13, Section C). The asymmetric behavior is not very conspicuous when the potential difference across the membrane is smaller than about 25 mV ($= RT/F$); a pronounced asymmetry is observed when the potential difference across the membrane is increased. When there is a high concentration of divalent cation salt only on one side of the membrane, there is usually pronounced rectification. Rectification of a high-frequency AC generates a DC component superposed on the AC.

The oscillograph records of the action currents developed by a node of Ranvier exposed to a high-frequency AC of a barely subthreshold intensity is definitely weaker than that of the same node in the absence of AC. The observed reduction in the action current amplitude is a definite indication that a high-frequency AC generates a sizeable outwardly directed current through the node. The behavior of a node under cathodal polarization has been discussed in Chapter 5, Section F. The DC component is expected to lower the threshold strength below the level expected from the simple consideration of the inert electric network.

There is one more aspect which deserves a brief comment in the experimental findings described in this section. It is the fact that the strength-frequency relation obtained from single nerve fibers is very different from that predicted by Nernst (see Chapter 3, Section B). In the range of frequency higher than 2000 Hz, the threshold strength increases with frequency f at the rate steeper than $f^{1.5}$, and not with $f^{0.5}$ as Nernst's square-root law demands. We obtain a similar deviation from Nernst's law when we determine the strength-frequency relation with the stimulating electrodes placed on a single nerve fiber buried in a nerve trunk (Tasaki and Sato, 1951). The old experimental results obtained from whole nerve trunks are complicated by the presence of many fibers with different thresholds. Thus, we come to the conclusion that Nernst's theory of nerve excitation is totally inconsistent with the results of experiments carried out under well-defined conditions.

I. VARIATION OF RHEOBASE AND CHRONAXIE ALONG THE NERVE FIBER

The chronaxie is the time factor that characterizes the strength–duration relation. Here, we describe an experiment demonstrating that the chronaxie of a single myelinated nerve fiber varies widely with the distance between the site of stimulation and the node of Ranvier to be excited (Hodler *et al.*, 1952). The finding described below adduces further evidence that the major factor determining the chronaxie of a nerve fiber is the cable property of the myelin sheath, and not the intrinsic properties of the nodal membrane.

A large motor nerve fiber of the frog was used. The fiber was pushed through a 0.6-mm-wide oil partition. The threshold strengths of rectangular voltage pulses were determined at a series of points along the fiber. For pulse durations longer than 2 msec, the threshold strength was found to be practically independent of the duration: the rheobase was measured with rectangular pulses of 5 msec in duration. In addition to the rheobase, the threshold value of a very short pulse was measured at every position. The ratio of the strength–duration product for a short pulse to the rheobase (see Chapter 3, Section D) was defined as the chronaxie.

In the experimental result reproduced in Fig. 6.7, it is seen that the rheobase varies only slightly with the distance between the oil partition and the

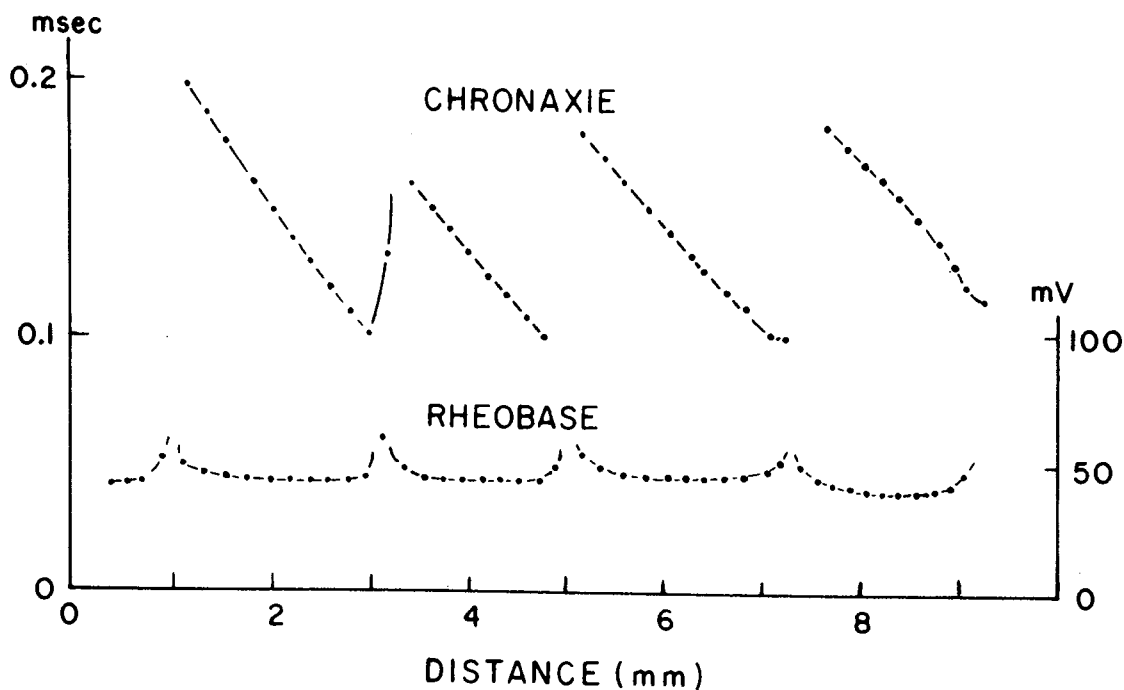


Fig. 6.7 Rheobase and chronaxie of a single myelinated nerve fiber determined at various positions along the fiber. The discontinuities in the measured values were observed when the oil partition (i.e., site of stimulation) was at the position of nodes of Ranvier. (From Hodler *et al.*, 1952.)

node of Ranvier on the cathodal side of the partition. This result is expected from the finding that the ohmic resistance of the myelin sheath is very high (see Chapter 4, Section B and Chapter 6, Section A). In contrast, the threshold strength of a short pulse was found to vary markedly within one internode of the fiber. Consequently, there is a large variation in the chronaxie along the nerve fiber. The ratio of the largest value of the chronaxie to the smallest value (about 0.1 msec) was about 2:1. Note, however, that the width of the oil partition was about 0.6 mm and the internodal distance was in the neighborhood of 2 mm. Had we used an ideally narrow partition, we would expect to have a much larger variation in chronaxie along the fiber.

It is interesting to note in this connection that Sakamoto (1933), who used glass-pipette electrodes to stimulate single fibers within a whole nerve, encountered a much larger variation in chronaxie; the smallest value of chronaxie found in those experiments was about 0.05 msec and the largest value was about 0.3 msec.

Based on the experimental finding described above, the factors which determine the threshold strength of an electric pulse applied to a whole nerve are now briefly discussed. In the experimental arrangement adopted by most physiologists, the distance between the source and the sink of the stimulation current is longer than the average internodal distance of large myelinated nerve fibers. Therefore, the electric potential gradient is distributed over several internodal segments. There are many fibers within the nerve trunk; the myelin sheath of these closely packed nerve fibers endows the medium within the nerve with a complex, anisotropic, highly frequency-dependent conductivity. The obstruction effect of the myelin sheath is particularly strong when the fibers are tightly bound together by a common connective tissue sheath called the epineurium. Late in the 1940s, there was a heated debate concerning the effect of the epineurium and perineurium on the behavior of the enclosed nerve fiber (see Lorente de Nó, 1947; Rashbass and Rushton, 1949).

REFERENCES

- Blair, E. A., and Erlanger, J. (1936). On the process of excitation by brief shocks in axons. *Am. J. Physiol.* **114**, 309–316.
- Cremer, M. (1899). Zum Kernleiterproblem. *Z. Biol. (Munich)* **37**, 550–553.
- Cremer, M. (1900). Ueber Wellen und Pseudowellen. *Z. Biol. (Munich)* **40**, 393–418.
- Cremer, M. (1932). Ein neues Erregungsgesetz. *Scientia* **51**, 145–156.
- Fabre, P., Quesnoy, P., and Berteaux, J. (1934). Vérification expérimentale de égalité des quantités d'électricité nécessaire à l'excitation liminaire par ondes rectangulaires et par décharges de condensateurs. *C. R. Soc. Biol.* **116**, 179–182.
- Geren, B. B. (1954). The formation from the Schwann cell surface of myelin sheath in the peripheral nerves of chick embryos. *Exp. Cell Res.* **7**, 558–562.

- Gildemeister, M. (1908). Über Interferenzen zwischen zwei schwachen Reizen. *Pfluegers Arch. Gesamte Physiol. Menschen Tiere* **124**, 447–461.
- Gildemeister, M. (1929). Zur Theorie des elektrischen Reizes. V. Polarisation durch Wechselstrom. *Ber. Sächs. Acad. Wissen. Math.-Phys. Klasse*, **81**, 303–313.
- Hermann, L. (1899). Zur Theorie der Erregungleitung und der elektrischen Erregung. *Pfluegers Arch. Gesamte Physiol. Menschen Tiere* **75**, 574–590.
- Hill, A. V., Katz, B., and Solandt, D. Y. (1936). Nerve excitation by alternating current. *Proc. R. Soc. London, Ser. B* **121**, 74–133.
- Hodler, J., Stämpfli, R., and Tasaki, I. (1952). Änderung der Reizschwelle und der Chronaxie langs einer einzelnen markhaltigen Nervenfasern. *Helv. Physiol. Acta* **10**, C54–55.
- Katz, B. (1936). The response of medullated nerve to alternating high-frequency stimulation. *J. Physiol. (London)* **86**, 285–289.
- Katz, B. (1939). "Electric Excitation of Nerve." Oxford Univ. Press, London and New York.
- Lapicque, L. (1925). Sur la théorie de l'addition latente. *Ann. Physiol.* **1**, 132–158.
- Lorente de Nó, R. (1947). "A Study of Nerve Physiology," Studies from the Rockefeller Institute for Medical Research, New York.
- Metuzals, J. (1965). Ultrastructure of the nodes of Ranvier and their surrounding structures in the central nervous system. *Z. Zellforsch. Mikrosk. Ana.* **65**, 719–759.
- Rashbass, C., and Rushton, W. A. H. (1949). The relation of structure to the spread of excitation in the frog's sciatic trunk. *J. Physiol. (London)* **110**, 110–135.
- Reier, P. J., Tabira, T., and Webster, H. deF. (1976). The penetration of fluorescein-conjugated and electron-dense tracer proteins into *Xenopus* tadpole optic nerve following perineural injection. *Brain Res.* **102**, 229–244.
- Revel, J. P., and Hamilton, D. W. (1969). The double nature of the intermediate dense line in peripheral nerve myelin. *Anat. Rec.* **163**, 7–16.
- Robertson, J. D. (1955). The ultrastructure of adult vertebrate peripheral myelinated fibers in relation to myelinogenesis. *J. Biophys. Biochem. Cytol.* **1**, 271–278.
- Robertson, J. D. (1957). New observations on the ultrastructure of the membranes of frog peripheral nerve fibers. *J. Biophys. Biochem. Cytol.* **3**, 1043–1051.
- Rosenbluth, J. (1976). Intramembranous particle distribution at the node of Ranvier and adjacent axolemma in myelinated axons of the frog brain. *J. Neurocytol.* **5**, 731–745.
- Sakamoto, S. (1933). Elektrische Reizung einer einzelnen Nervenfasern durch Gleichspannung. *Pfluegers Arch. Gesamte Physiol. Menschen Tiere* **231**, 489–501.
- Tasaki, I. (1942). Das Schwellenabsinken bei Reizung einer Nervenfasern mit kurzen Stromstößen. *Pfluegers Arch. Gesamte Physiol. Menschen Tiere* **245**, 665–679.
- Tasaki, I., and Sato, M. (1951). On the relation of the strength-frequency curve in excitation by alternating current to the strength-duration and latent addition curves of the nerve fiber. *J. Gen. Physiol.* **34**, 373–388.
- Teorell, T. (1953). Transport processes and electrical phenomena in ionic membranes. *Prog. Biophys. Biophys. Chem.* **3**, 305–369.
- Thomson, W. (1856). On the theory of the electric telegraph. *Philos. Mag. 4th Ser.* **11**, 146–160.
- Uzman, B. G., and Nogueira-Graf, G. (1957). Electron microscope studies of the formation of nodes of Ranvier in mouse sciatic nerves. *J. Biophys. Biochem. Cytol.* **3**, 589–597.
- von Kries, J., and Sewall, H. (1881). Über die Summierung untermaximaler Reize in Muskeln und Nerven. *Arch. Anat. Physiol. Physiol. Abt.* **1881**, 66–77.
- Webster, H. deF. (1974). Peripheral nerve structure. In "The Peripheral Nervous System" (J. I. Hubbard, ed.), pp. 3–26. Plenum, New York.

7. Accommodation in Myelinated Nerve Fibers

A. EXCITATION BY LINEARLY RISING VOLTAGE PULSES

In the present chapter, we deal with the effects of relatively long voltage pulses on the myelinated nerve fibers. Historically, long and slowly changing electric stimuli were used by physiologists a long time before brief rectangular voltage pulses became available. du Bois-Reymond noted that a slowly rising electric current fails to excite a nerve even when its intensity reaches well above the level which would excite the nerve if suddenly initiated or terminated (see p. 258 in du Bois-Reymond, 1848; Chapter 2). Later on, von Kries (1884) determined the threshold strengths of electric pulses which rose linearly and, after a certain period of time, reached a plateau. Lucas (1907), who studied the excitatory effect of linearly rising stimuli systematically, called the smallest effective rate of current rise the "*minimal gradient*."

It is not difficult to investigate the effect of linearly rising current pulses on isolated nerve fibers (Tasaki, 1950a, 1955; Frankenhaeuser, 1953). One of the experimental setups used for this purpose is illustrated schematically at the top of Fig. 7.1. Three successive nodes of Ranvier, N_0 , N_1 , and N_2 , of a large motor nerve fiber of the toad were introduced into three separate pools of Ringer's solution. The nodes in the two lateral pools, N_0 and N_2 , were rendered inexcitable with an anesthetic, and node N_1 in the middle was kept in normal Ringer's solution. Between nodes N_0 and N_1 , linearly rising voltage pulses were delivered. The change in the potential difference across the membrane at node N_1 was measured with an amplifier with a high-input impedance. With this experimental arrangement, one may regard the myelin sheath between N_1 and N_2 as acting like a micropipette for recording the potential inside node N_1 .

A few examples of oscillograph records obtained with this experimental setup are furnished in the figure. The time courses of the applied voltage pulses are shown by the upper trace interrupted at 1000 Hz. The changes in the membrane potential produced by these pulses are indicated by the

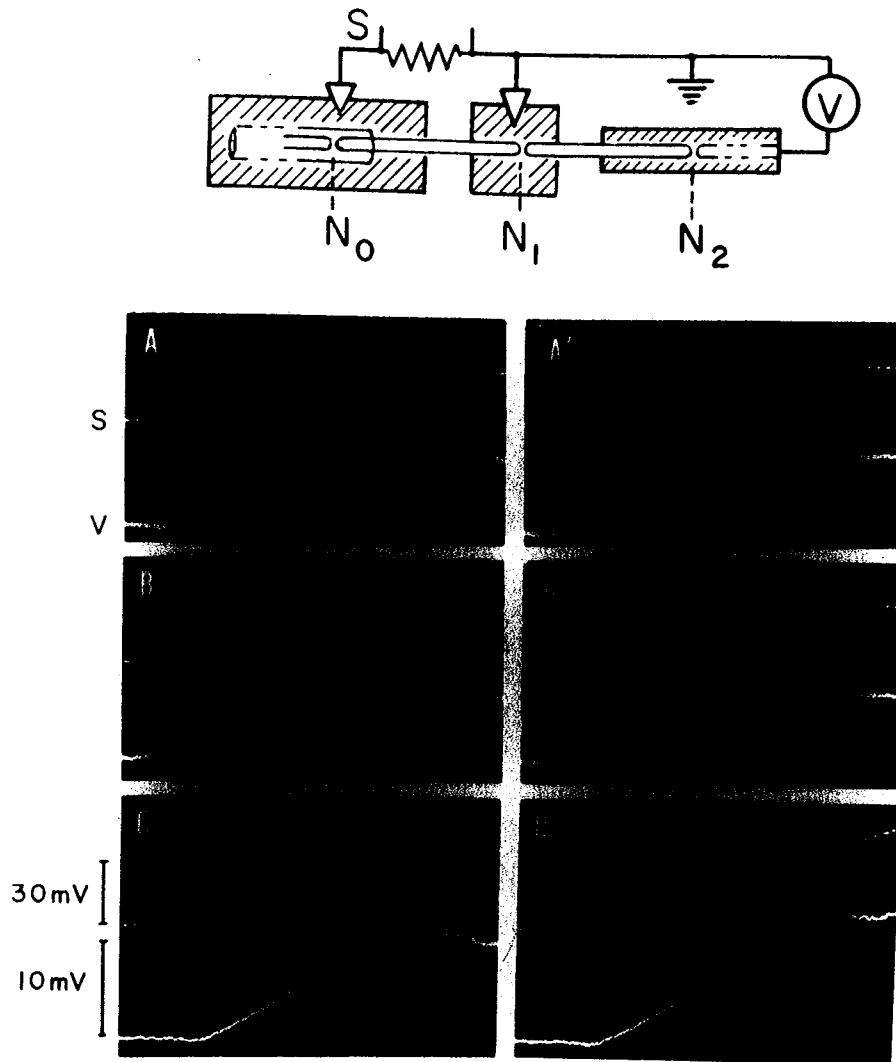


Fig. 7.1 Top: Schematic diagram illustrating the experimental arrangement used for examining the effect of linearly rising voltage pulses on a physiologically isolated node of Ranvier. The node under study (N_1) is kept in normal Ringer's solution. The two lateral nodes (N_0 and N_2) are inexcitable. S , The terminals connected to the stimulating circuit; V , a voltage follower used for recording changes in the membrane potential at N_1 . Bottom: The continuous oscillograph trace represents the changes in the membrane potential. The trace interrupted at 1000 Hz shows the time course of the applied voltage. In the upper right-hand records, the continuous trace was interrupted by production of action potentials. 11°C. (From Tasaki, 1955.)

lower, continuous trace. The right-hand column in the figure (excluding the bottom record) shows that full-sized action potentials were produced by the applied pulses. The left-hand column indicates that only subthreshold responses were observed at about the same stimulus strength. When the rate of voltage rise was below a certain critical value, a full-sized response could no longer be generated (see the bottom record). The critical rate of voltage rise corresponds to Lucas' minimal gradient.

Under the present experimental conditions, there is little or no current between nodes N_1 and N_2 . Even when the membrane conductance and the emf at N_1 change during excitation, the high resistance of the nodal mem-

brane at N_0 and of the internode between N_0 and N_1 , tends to keep the total resistance in the circuit at an approximately constant level. Hence, we conclude that a *linearly increasing current is effective in evoking an electrical response when it rises above the rheobase at a rate greater than that of the minimal gradient of the fiber.*

Now we consider the condition which the stimulating pulse, $V(t)$, has to satisfy in order to evoke an action potential. We find that, in a wide range of the rate of voltage rise, the plateau level required for excitation coincides with the rheobase (measured with a rectangular pulse). We denote the rheobase by b (expressed in mV) and the minimal gradient by m (in mV/msec). Then, the condition which a linearly rising voltage pulse, $V(t)$, has to satisfy may be formally described by the following expression:

$$\left. \frac{dV(t)}{dt} \right|_{t=t^*} \geq m \quad (7.1)$$

where t^* represents the time at which the linearly rising voltage reaches the rheobase, namely,

$$V(t^*) = b \quad (7.2)$$

In the following sections, these mathematical expressions are shown to be extremely useful in determining the threshold strengths of various types of slowly rising voltages. In the experiments described in previous sections where only brief voltage pulses were employed, the condition of Eq. (7.1) is satisfied automatically.

In classical physiology, the process responsible for the condition expressed by Eq. (7.1) is called "accommodation" (see Chapter 3, Sections B and E). Hill (1936, cited in Chapter 3) called the ratio b/m the *time constant of accommodation*. In the toad's large motor nerve fibers, the time constant of accommodation varies in the range between 10 and 300 msec. Prolonged cooling of the fiber is known to increase this time constant; rewarming of the fiber shortens the time constant after a long delay.

In experiments where whole nerves are used for measurements, the transition from the rheobase to the slope representing the minimal gradient is always smooth and gradual. Again, a wide variation in rheobase and minimal gradient among different nerve fibers within a nerve trunk is responsible for the smooth transition.

B. EXPONENTIALLY RISING VOLTAGE PULSES

Exponentially rising voltage pulses with variable time constants and final amplitudes were used for stimulation first by Gildemeister (1904) who introduced self-inductances in the stimulating circuit. It is easy to obtain expo-

nentially rising stimuli by using capacitors and resistors (Cardot and Laugier, 1913; Schriever, 1931). The time course of the voltage, $V(t)$, obtained by charging a capacity, c , through a resistor, r , is given by

$$V(t) = v(1 - e^{-t/rc}) \quad (7.3)$$

where v is the voltage level to which the capacitor is eventually charged. In determining the threshold value of v at a given value of time constant, rc , the applied voltage, $V(t)$, may be terminated when it reaches a level several times the rheobase. The procedure of stimulation may be repeated at a frequency of a few times a minute.

An example of the results obtained from a single myelinated nerve fiber mounted across a bridge-insulator is shown in Table 7.1. It is interesting to note that a linear relationship exists between the threshold value of v and the time constant rc (see Fig. 7.2). A similar linear relationship has been observed by previous investigators using whole nerves (Schriever, 1930; Solandt, 1936).

In the table, the time t^* at which exponentially rising voltages of the threshold strengths reach the rheobase, b , and the slope, $dV(t)/dt$, at $t = t^*$ are listed. It is seen that the slope at this particular moment is constant irrespective of the time constant of voltage rise, rc . The slope of the curve, $dV(t)/dt$, for a very large value of time constants is nothing but the minimal gradient, m , of the fiber, as we can readily see by expanding the right-hand side of Eq. (7.3) in Taylor's series. Thus, we find that the threshold condition for an exponentially rising voltage is given by

$$\left. \frac{dV(t)}{dt} \right|_{t=t^*} = m \quad \text{and} \quad V(t^*) = b \quad (7.4)$$

TABLE 7.1

Relation between the Rise Time (rc) and the Threshold Voltage (v) in Excitation of a Single Motor Nerve Fiber of the Toad by Exponentially Rising Voltage Pulses^a

rc (msec)	v (mV)	t^* (msec)	$\left. \frac{dV(t)}{dt} \right _{t=t^*}$
0	30-31	—	—
10	44-45	11.6	13.9
20	54-55	16.4	12.0
30	66-68	18.2	12.2
40	80-82	18.9	12.5
50	94-96	19.3	12.9
70	120-122	20.2	13.0
100	160-165	20.6	13.0

^a The bridge insulator method was used for stimulation. (From Tasaki and Sakaguchi, 1950.)

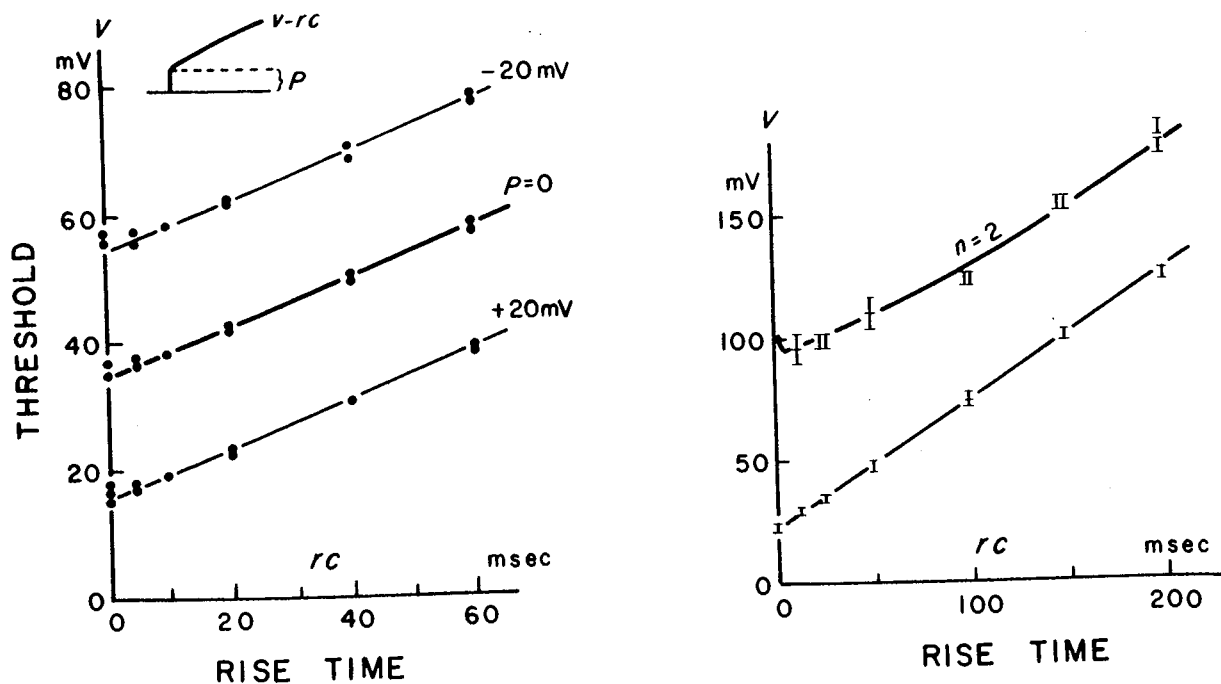


Fig. 7.2 Left: Relation between the threshold strength and the rate of rise of an exponentially rising voltage pulse superposed on a constant voltage (p). Right: Relation between threshold strength and duration of voltage pulses generated by double-condenser discharges (top). The heavy continuous curve represents the result of calculation by the rheobase and the minimal gradient of the fiber determined by simple exponentially rising pulses (bottom). (From Tazaki, 1950a.)

Again, t^* represents the time at which the voltage $V(t)$ reaches the rheobase, b . In fact, we can readily derive the well-known linear relationship between v and rc from this threshold condition.

Introducing Eq. (7.3) into Eq. (7.4) we have

$$\frac{1}{rc} ve^{-t^*/rc} = m \quad \text{and} \quad v(1 - e^{-t^*/rc}) = b \quad (7.5)$$

Elimination of t^* from these equations leads to a linear equation between v and rc :

$$v = b + mrc \quad (7.6)$$

Equation (7.6) adequately describes the observed relationship between the threshold voltage, v , and the time constant of voltage rise, rc (see the straight lines in Figs. 7.2 and 7.3). When rc is equal to 0 (namely when the applied voltage is rectangular), v is equal to the rheobase, b . With a very large value of rc , the voltage rises approximately linearly until it reaches the rheobase, in which case the rate of voltage rise coincides, as expected, with the minimal gradient of the fiber, m .

Using exponentially rising voltage pulses, the time intervals between the

onset of the stimulating pulses and the appearance of electric responses were examined. In threshold excitation, the responses were found to start a short (but variable) interval after the stimulating voltage reaches the rheobase.

C. EXPONENTIALLY RISING VOLTAGE WITH SUPERPOSED DC AND DOUBLE CONDENSER PULSES

We demonstrate in this section that the threshold condition described in the preceding section yields satisfactory results when applied to other forms of slowly rising voltage pulses. We described, in the first place, the threshold condition for exponentially rising voltage pulses on which rectangular voltage pulses are superposed. Later, the threshold conditions for double-condenser pulses are discussed.

The time course of the voltage pulses used in the first series of experiments is described by

$$V(t) = v(1 - e^{-t/rc}) + p \quad (7.7)$$

where p is the amplitude of the rectangular components. (Other notations have the same significance as those used in the preceding section.) By introducing Eq. (7.7) into Eq. (7.4), the predicted relationship between v and rc at a given value of p is found to be

$$v = b + mrc + p \quad (7.8)$$

In the experiments of which the results are illustrated on the left-hand side of Fig. 7.2 the rectangular component was initiated simultaneously with the exponential component. The observed points on the thin straight lines in the middle (marked $p = 0$) represent the linear relationship between v and rc discussed in the preceding section; both the rheobase, b , and the minimal gradient, m , of the nerve fiber are obtained from this straight line. It is seen in the figure that the observed vrc relationship for $p = \pm 20$ mV is given by straight lines with the same slope, shifted above and below the straight line in the middle by the value corresponding to p . In other words, the threshold condition for the stimulating voltage pulses given by Eq. (7.7) is described, as a rule, by Eq. (7.8).

Similar results were obtained when the rectangular component was initiated shortly (10 msec) before the onset of the exponential component. When a long period intervenes between the beginning of polarization and the onset of the exponential component, very different results are obtained. Cathodal polarization ($p > 0$) increases and anodal polarization decreases the value of m significantly.

The time course of a slowly rising voltage obtained by the use of two condensers is described by

$$V(t) = v(e^{-t/rc} - e^{-nt/rc}) \quad (7.9)$$

when n represents the ratio between the two capacitors. This form of electric stimuli was used originally by Lapicque (1908) and later by Monnier (1934). Introducing Eq. (7.9) into Eq. (7.4), we obtain the threshold condition

$$v = \frac{1}{(n-1)} \left[\frac{(nb + mrc)^n}{b + mrc} \right]^{n-1} \quad (7.10)$$

For special cases where $n = 2$, the validity of this equation was tested experimentally. We see in the figure that the agreement between the predicted and the observed values is quite satisfactory. The validity of the threshold condition, Eq. (7.4), is demonstrated again.

D. EXCITATION BY LOW-FREQUENCY AC

Since the time of von Kries (1882), it has been known that intensity of an alternating current required to excite a nerve does not vary monotonically with the frequency, but that there is a minimum in the threshold–frequency curve at about 150 Hz (see Chapter 3). The factors that determine the frequency dependence of the threshold in the high-frequency range are discussed in Chapter 6, Section H. Coppée (1934), Solandt (1936), and others showed that the factors that determine the threshold in the low-frequency range are quite distinct from those which affect the threshold in the high-frequency range. Here, we deal with the threshold–frequency relationship for isolated myelinated nerve fibers in the range of frequency below about 100 Hz.

The time courses of the stimulating voltage waves are given by

$$V(t) = v \sin(2\pi ft) \quad (7.11)$$

where v is the amplitude and f the frequency. Again, we assume that, in order to excite a nerve fiber, the applied voltage, $V(t)$, has to reach the rheobase with its derivative, $dV(t)/dt$, exceeding the minimal gradient, m . Introducing Eq. (7.11) into Eq. (7.4) we obtain

$$v \sin(2\pi ft^*) = b \quad \text{and} \quad 2\pi f v \cos(2\pi ft^*) = m$$

where t^* represents the time at which the voltage reaches the rheobase. By eliminating t^* from these simultaneous equations, we have

$$v^2 = b^2 + (m/2\pi f)^2 \quad (7.12)$$

Equation (7.12) describes the expected relationship between v and f which satisfies the threshold condition. Essentially the same equation has been derived by Hill (1936, cited in Chapter 3) on the basis of his two-factor theory (Chapter 3, Section E).

Using sciatic–gastrocnemius preparations of the bullfrog, Solandt (1936) showed that there is, in threshold excitation by low-frequency AC, a linear relationship between v^2 and $1/f^2$. Later on, Sato and Ushiyama (1950) demonstrated the validity of Eq. (7.12) by using isolated motor nerve fibers of the toad. They found that the values of b and m determined by the use of low-frequency sinusoidal waves agree very well with the rheobase and the minimal gradient on the same fiber determined with exponentially rising voltage pulses (see Fig. 7.3).

In relation to the excitatory effect of AC, there is physiologically very important phenomenon which is known as Monnier's "pararesonance" (see Coppée, 1934). A proper understanding of this phenomenon is essential in treating excitable tissues exhibiting a strong tendency toward spontaneous repetitive firing of impulses (see Chapter 10, Section F).

When a frog nerve is immersed in a medium containing a relatively low concentration of calcium salt, the latent addition curve of the nerve (see Chapter 6, Section D) does not decay monotonically following the delivery of a conditioning shock; instead, the threshold for the test shock undergoes a damped oscillation (see Monnier, 1934). Under these conditions, the threshold strength of AC shows a sharp minimum at a particular frequency which

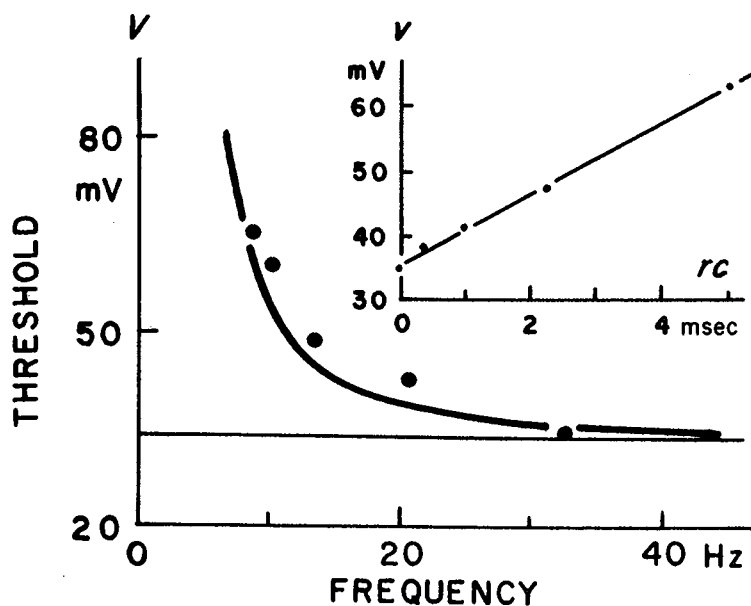


Fig. 7.3 Relation between threshold strength of low-frequency AC and the frequency. The continuous curve was obtained by calculation using the rheobase and minimal gradient determined on the same fiber (see the inset). (From Sato and Ushiyama, 1950.)

coincides with the frequency of oscillation of the latent addition curve. Subthreshold responses evoked by brief shocks also undergo a damped oscillation under these conditions (Arvanitaki, 1939). The existence of oscillatory subthreshold responses indicates that there are periodic processes taking place in the nerve membrane. The sharp minimum seen in the strength–frequency relation (at about 150 Hz) represents a kind of resonance of the stimulating AC with the intrinsic rhythm of the excitatory tissue. Quite recently, these pararesonance phenomena have been analyzed using squid giant axons (see Chapter 10, Section F).

E. REPETITIVE FIRING OF ACTION POTENTIALS

When a long rectangular voltage pulse is applied to a nerve fiber, it is seldom that action potentials are induced repetitively during the entire period of the applied pulse. Only one nerve impulse, sometimes a short train of impulse, is usually produced at the onset of the pulse (Pflüger, 1859, see Chapter 2). However, when a nerve taken from a frog kept in a cold room for some time (about 10°C) is used, a long pulse of constant current tends to produce repetitive firing of responses (von Frey, 1883, cited in Chapter 3). Nerves obtained from toads caught during their mating season tend to respond to constant current pulses with repetitive firing. It is well known that a nerve immersed in a medium with a low Ca-ion concentration tends to produce electrical responses repetitively (see Fessard, 1936; Arvanitaki, 1939). In nerve fibers which tend to fire action potentials repetitively, the minimal gradient is known to be very small, or the time constant of accommodation to be long. [Hill's time constant of accommodation is defined as the ratio b/m (see Section A).]

It is not surprising to find that the minimal gradient or the time constant of accommodation is directly related to the tendency of a nerve fiber to respond to a constant electric stimulus with repetitive firing (Katz, 1936). In a fiber with a long time constant of accommodation, a suprarheobasic voltage pulse is expected to excite the fiber every time when its excitability recovers toward the end of the relatively refractory period left behind the preceding response. Based on the concept that production of action potentials does not by itself alter the process of accommodation, Katz (1936) derived an equation relating the period of repetitive firing, T , and the time constant of accommodation, λ :

$$T = \lambda \ln \frac{I}{I_0} \quad (7.13)$$

where I represents the stimulating current intensity employed and I_0 the rheobasic intensity.

The intervals between the repeating action potentials are determined primarily by the stimulus intensity and the refractoriness (see Fessard, 1936). In this respect, the process of repetitive firing in a nerve fiber is fundamentally different from an electrical oscillation in a resonance circuit. It comes under the category of "relaxation oscillation" which represents an automatic recurrence of an essentially aperiodic phenomenon (see van der Pol and van der Mark, 1926). Based on the idea that the period of repetitive firing is governed by the relaxation time represented by the refractory period, an approximate relation can be derived relating the period of repetitive firing, $1/f$, to the voltage employed, v :

$$\frac{1}{f} = \gamma + \frac{\kappa}{\ln(v/b)} \quad (7.14)$$

where b is the rheobase, and γ and κ are constants. Constants γ and κ reflect the absolute and the relative refractory periods, respectively, with $\gamma \ll \kappa$ (Tasaki, 1950b; Sato, 1952). Qualitatively, Eq. (7.14) described the dependence of the repetition frequency on the applied voltage adequately. A prolonged exposure to an outwardly directed polarizing current is known to delay the recovery process. Therefore, the interval between successive impulses tends to increase under constant cathodal polarization.

The most direct proof that the refractory period determines the interval between successive action potentials is the demonstration of "resetting" of the rhythm of repetitive firing of responses by an "extra-stimulus." The oscillograph records shown in Fig. 7.4 illustrate the effect of "extrastimuli." Repetitive firing was induced by a DC applied at one end of the nerve and the responses of one particular fiber were recorded near the other end. A brief electric pulse, strong enough to evoke a response, was delivered randomly while the fiber was firing repetitively. It is seen that, following the extra-stimulus, the response expected from the regularity of the firing has disappeared. The important feature to be noted in these records is that the interval between the extraresponse and the following response was very close to the regular interval. (Strictly speaking, this interval is slightly longer because of the involvement of the conduction time between a stimulating electrode and the site of the pacemaker.) It is thus evident that the recovery from the refractoriness left behind every action potential plays a crucial role in determining the rhythm of repetitive firing.

The mechanism of repetitive firing of nerve impulses *in vivo* is not fundamentally different from that described above. Some time ago, Gilson (1936), working on spontaneously beating cardiac muscles, and Matthews (1933), analyzing repetitive firing of afferent impulses from a tonic sensory nerve fiber in the muscle nerve, demonstrated that an extrastimulus does reset the rhythm of repetition of action potentials originating the pacemaker. (In some instances, a nerve impulse from the pacemaker collides with the impulse ini-

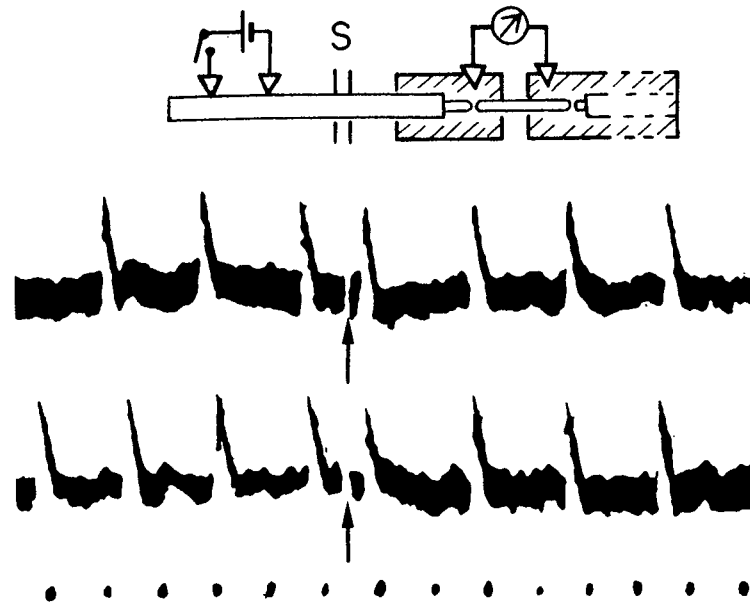


Fig. 7.4 Effect of an "extraimpulse" on the rhythm of repetitive impulse firing induced by a constant stimulating voltage. Delivery of a strong electric shock to the fiber through electrodes S is marked with the arrows in the records. Time markers, 10 msec apart. 11°C. (From Tasaki, 1950b.)

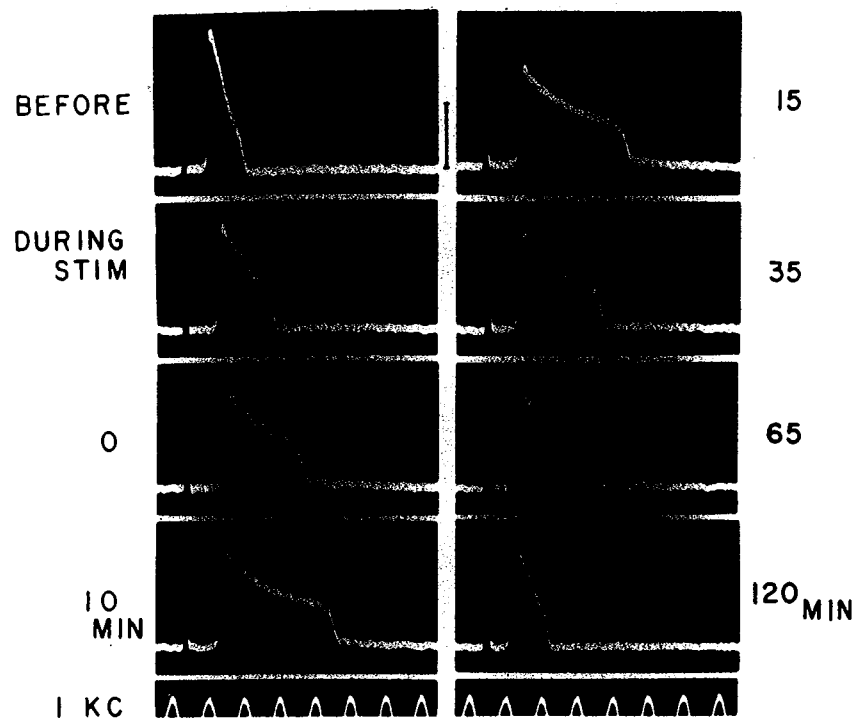


Fig. 7.5 The effect of high frequency (i.e., tetanic) stimulation on the electrical response of a single motor nerve fiber of the toad. The fiber was stimulated at 150 shocks/sec for 20 min. Note that the duration of the action current increased progressively after the cessation of repetitive stimulation. The last record shows the response to a single shock delivered 2 hr after the end of tetanic stimulation; note that the duration finally returned to the initial value. 22°C. (From Tasaki, 1955.)

tiated by the brief shock. In such instances, the rhythm of the impulses from the pacemaker is not disturbed by the applied shock except that the one impulse is annihilated by head-on collision.)

In connection with multiple responses of the myelinated nerve fiber, it is known that the action potential duration increases gradually during and after high frequency stimulation (Tasaki, 1955; Spyropoulos, 1956). The effect of long tetanic stimulation is quite dramatic (Fig. 7.5). (Note, however, that this prolongation of the action potential duration does not take place in high-frequency stimulation of normal squid giant axons.) At the time when this effect of repetitive stimulation was discovered, no clue was found that could lead to a reasonable interpretation of the effect. At present, it appears that an increased interdiffusion of cations during action potentials brings about this effect by affecting the conformational state of the protein molecules near the excitable membrane (see Chapter 9, Section E and Chapter 13, Section H).

F. CATHODAL DEPRESSION AND THE MINIMAL GRADIENT

The effects of weak currents passing through the nodal membrane on the excitability property of the node has been discussed in Chapter 5, Section F. The effects produced by a strong inward current are not qualitatively different from what has been described already. In contrast, the effects of a strong outwardly directed current (i.e., cathodal polarization) are complex and require further clarification. To illustrate the difference in the effect on the nodal membrane between strong anodal and cathodal polarization, a set of oscillograph records are presented in Fig. 7.6.

Here, a single node preparation (see Chapter 5, Section A) of a bullfrog motor nerve fiber was used. In order to study the relationship between the intensity of the applied current and the change in the membrane potential produced at the node under study (N_1 in the figure) exponentially rising voltage pulses were applied between nodes N_0 and N_1 . As usual, both N_0 and N_2 were rendered inexcitable. In order to facilitate a comparison between the effect of cathodal polarization and that of anodal polarization, oscillograph records obtained with negative voltage pulses were superposed on those obtained with positive pulses. The time course of the voltage pulses applied between N_0 and N_1 are shown by the traces interrupted at 1000 Hz.

When the applied voltage pulses are small, there is a close parallelism between the applied voltage and the observed change in the membrane potential. Note that the membrane current is proportional approximately to the applied voltage. When the applied voltage approaches the rheobase for the node (+ 25 mV in this case) at a very low rate, the membrane potential does

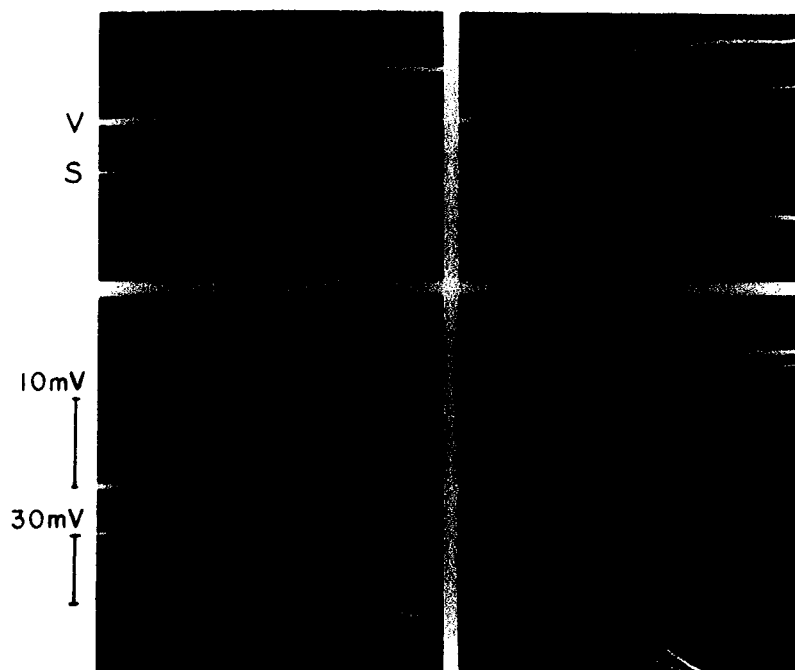


Fig. 7.6 Changes in the membrane potential (V) produced by exponential voltage pulses (S). In order to compare effects of anodal and cathodal polarization, the change in the membrane potential produced by negative pulse was recorded together with the effect of a positive pulse. Time markers, 1000 Hz. 11°C. (From Tasaki, 1955.)

not rise in proportion to the applied voltage (see the lower left-hand record). By employing the pulse method of measuring the membrane resistance, it is found that the membrane resistance falls, under such a strong cathodal polarization, below the normal level. There is also a change in the emf which tends to lower the observed membrane potential. Furthermore, the threshold for the test shocks rises and the amplitude of the response evoked by the test pulse falls under cathodal polarization of an intermediate strength. When the polarizing current is intensified further, the node becomes completely inexcitable (see the lower right-hand record).

The depressive effects of an outwardly directed current on the nerve are called by Werigo "*cathodal depression*" (Werigo, 1883, 1901). The similarity between the depressive action at the cathode of a polarizing current and the effect of potassium salts applied externally has been known for many years (Bethe, 1920). It is also well known that the effect of anodal polarization is, in some respects, similar to the action of an enhanced external Ca-ion concentration (Bethe, 1920).

Based on the finding that an outwardly directed current brings about a depressive effect on the nodal membrane, a simple interpretation of the minimal gradient is now advanced. When the applied voltage, $V(t)$, approaches the rheobase, the macromolecules at some of the excitable sites in the nodal membrane undergo a transition from their resting-state conformation to their

active-state conformation. Following the transition, a relaxation process sets in, by which the membrane sites are pushed into a cathodally depressed state. When the rate of voltage rise, $dV(t)/dt$ is small, transitions at different sites become asynchronous. We denote the relaxation time involved by τ . The condition for production of a full-sized action potential is then that at least a finite number ΔN of the sites undergo a transition within interval τ . Thus, we may write the condition as follows:

$$\frac{\partial N}{\partial V} \frac{dV}{dt} \tau \geq \Delta N \quad (7.15)$$

where $\partial N/\partial V$ represents the rate of increase in the number of active sites with the applied voltage V (see Chapter 13, Section I). Then, the minimal gradient, m , is given formally by

$$m = \Delta N / \left(\frac{\partial N}{\partial V} \tau \right) \quad (7.16)$$

The decrease in m brought about by a reduction in the external Ca-ion concentration may now be attributed to a rise in $\partial N/\partial V$. The decrease in m caused by agents which prolong the action potential (e.g., low temperature, application of nickel or cobalt salts, etc.) may be explained as arising from an increase in τ .

G. BREAK EXCITATION

It has been known since the time of du Bois-Reymond and Pflüger (see Chapter 2) that a nerve impulse is evoked when a strong current applied to nerve fibers is suddenly withdrawn. A close examination of the phenomenon of break (or opening) excitation using single nerve fiber preparations reveals that several different processes contribute to this phenomenon. The following three different processes are involved, at least.

1. *Excitation by discharge of the electricity stored on the myelin sheath.* Using the tripolar arrangement with the myelinated portion of a single nerve fiber connected to the stimulating cathode, it is possible to charge the capacity of the myelin sheath to a high voltage level. On termination of the applied voltage, an outwardly directed current is initiated transiently through the neighboring nodes of Ranvier; initiation of this current result in generation of an action potential (Tasaki, 1940).

2. *Termination of repolarizing current at a partially depolarized node.* Partial depolarization (i.e., partial loss of the resting membrane potential) may be induced by an increase in the external univalent-divalent cation

concentration ratio. A partial injury may also bring about a similar effect. An inward current through such a node brings about complete repolarization. A full-sized action potential appears on withdrawal of the current (Frankenhaeuser and Widen, 1956; see also Chapter 10, Section D, and Chapter 12, Section G).

3. *Excitation by the counter-emf generated in surrounding tissue layer.* A strong current passing through a compact layer of connective tissue and nerve fibers sets up a counter-emf in the layer. When the primary current is suddenly withdrawn, a transient current is generated, which flows in the reverse direction. This transient current is capable of exciting the nerve fibers inside.

The experimental facts known about the phenomenon of break excitation before the advent of single fiber technique are fully described in a monograph written by Lorente de Nó (1947, cited in Chapter 6). On the whole, it is far more difficult to demonstrate break excitation in isolated nerve fibers than in nerve trunks. The results of reexamination of Pflüger's rule of excitability (see Chapter 2, Section E) on single fiber preparations are described elsewhere (Tasaki, 1958, cited in Chapter 4).

REFERENCES

- Arvanitaki, A. (1939). Recherches sur la réponse oscillatoire locale de l'axone géant isolé de "sepia." *Arch. Int. Physiol.* **49**, 209–256.
- Bethe, A. (1920). Nervenpolarisationsbilder und Erregungstheorie. *Pfluegers Arch. Gesamte Physiol. Menschen Tiere* **183**, 289–302.
- Cardot, H., and Laugier, H. (1913). Efficacité des courants à croissance ou à décroissance exponentielle. *J. Physiol. Pathol. Gen.* **15**, 1134–1147.
- Coppée, G. (1934). La pararésonance dans l'excitation par les courants alternatifs sinusoidaux. *Arch. Int. Physiol.* **40**, 1–58.
- Fessard, A. (1936). "Propriétés Rhythmique de la Matière Vivante," Hermann, Paris. *Actual. Sci. In.* No. 417.
- Frankenhaeuser, B. (1953). Accommodation in single nerve fibres. *Acta Physiol. Scand.* **29**, 126–127.
- Frankenhaeuser, B., and Widen, L. (1956). Anode break excitation in desheathed frog nerve. *J. Physiol. (London)* **131**, 243–247.
- Gildemeister, M. (1904). Untersuchungen über indirekte Muskeleirregung und bemerkungen zur Theorie derselben. *Pfluegers Arch. Gesamte Physiol. Menschen Tiere* **101**, 203–225.
- Gilson, A. S. (1936). The effects upon the heart rhythm of premature stimuli applied to the pacemaker and to the atrium. *Am. J. Physiol.* **116**, 358–366.
- Katz, B. (1936). Multiple response to constant current in frog's medulated nerve. *J. Physiol. (London)* **88**, 239–255.
- Lapicque, L. (1908). Excitation par double condensateur. *C. R. Soc. Biol. Paris.* **64**, 336–339.
- Lucas, K. (1907). On the rate of variation of the exciting current as a factor in electric excitation. *J. Physiol. (London)* **36**, 253–274.

- Matthews, B. H. C. (1933). Nerve endings in mammalian muscle. *J. Physiol. (London)* **78**, 1–53.
- Monnier, A.-M. (1934). "L'excitation électrique des Tissus." Hermann & Cie, Paris.
- Sato, M. (1952). Repetitive responses of the nerve fiber as determined by recovery process and accommodation. *Jpn. J. Physiol.* **2**, 277–289.
- Sato, M., and Ushiyama, J. (1950). On the relation of strength-frequency curve in excitation by low frequency A.C. to the minimal gradient of the nerve fiber. *Jpn. J. Physiol.* **1**, 141–146.
- Schriever, H. (1931). Über Einschleichen von Strom. *J. Zitschr. Biol.* **91**: 173–195.
- Solandt, D. Y. (1936). The measurement of "accommodation" in nerve. *Proc. R. Soc. London, Ser. B* **119**, 355–379.
- Spyropoulos, C. S. (1956). Changes in the duration of the electric response of single nerve fibers following repetitive stimulation. *J. Gen. Physiol.* **40**, 19–25.
- Tasaki, I. (1940). Mikrophysiologische Untersuchungen über die Grundlage der Erregungsleitung in der markhaltigen Nervenfasern. *Pfluegers Arch. Gesamte Physiol. Menschen Tiere* **244**, 125–141.
- Tasaki, I. (1950a). Electrical excitation of the nerve fiber. I. Excitation by linearly increasing currents. *Jpn. J. Physiol.* **1**, 1–6.
- Tasaki, I. (1950b). The threshold conditions in electrical excitation in the nerve fiber. Part II. *Cytologia* **15**, 219–236.
- Tasaki, I. (1955). Études sur le processus de production du potentiel d'action d'un node de Ranvier. In "Microphysiologie Comparée des Éléments Excitables," pp. 1–27. Centre Nat. Recherche Scientifique, Paris.
- Tasaki, I., and Sakaguchi, M. (1950). Electrical excitation of the nerve fiber. II. Excitation by exponentially increasing currents. *Jpn. J. Physiol.* **1**, 7–15.
- van der Pol, B., and van der Mark, J. (1926). The heartbeat considered as a relaxation-oscillation and an electric model of the heart. *Arch. Neer. Physiol.* **14**, 418–443.
- von Kries, J. (1884). Ueber die abhängigkeit der Erregungs-Vorgänge von dem zeitlichen Verlaufe der zur Reizung dienenden Elektrizitäts-bewegungen. *Arch. Anat. Physiol., Physiol. Abt.* **1884**, 337–372.
- Werigo, Br. (1883). Die sekundären Erregbarkeitsänderungen an der Cathode eines andauernd polarisierten Froschnerven. *Pfluegers Arch. Gesamte Physiol. Menschen Tiere* **31**, 417–479.
- Werigo, Br. (1901). Die depressive Kathodenwirkung, ihre Erklärung und ihre Bedeutung für Elektrophysiologie. *Pfluegers Arch. Gesamte Physiol. Menschen Tiere* **84**, 547–618.

8. Emergence of the Squid Giant Axon

A. NONMYELINATED NERVE FIBERS

In this and following chapters, we deal mainly with physiological and physicochemical properties of nonmyelinated nerve fibers, particularly with properties of squid giant axons, examined under a variety of experimental conditions. Nonmyelinated nerve fibers are devoid of nodes of Ranvier. Hence, we consider their gross physiological properties to be uniform along their long axis and the process of nerve conduction to be continuous.

As we have discussed in Chapter 5, Section J, large and medium sized nerve fibers in the nervous system of vertebrates are all myelinated. In contrast, very small fibers in vertebrate peripheral nerves, which are often referred to as C-fibers, are nonmyelinated. Traditionally, the most popular source of vertebrate nonmyelinated nerve fibers is the olfactory tract of the freshwater fish, pike (Kühne and Steiner, 1879; Nicolai, 1901; Garten, 1903). These vertebrate nonmyelinated fibers are known to conduct nerve impulses at a velocity of the order of $\frac{1}{100}$ of that in large myelinated fibers of the frog.

Nerve fibers of invertebrates are, as a rule, all nonmyelinated. A notable exception to this rule is the system of giant myelinated fibers of the prawn (Frieländer, 1889; Retzius, 1890). To demonstrate the slowness of the nerve impulse transmitted along invertebrate nonmyelinated fibers, Fick (1863) used nerves taken from mussels; others employed nerves of lobsters, octopuses, aplysia, etc. (Frédéricq and Vendeveld, 1880; Boruttau, 1897).

Shortly after the end of World War I, when electronic amplifiers became available, studies of electrophysiological properties of individual nonmyelinated nerve fibers were initiated. It is relatively easy to isolate single nerve fibers of various species of crabs. The method described by Furusawa (1929, p. 326) is to sever a walking leg of a spider crab near the body and then to pull out the nerve from the leg. When this operation is carried out in seawater, individual nerve fibers in the leg nerve are separated from one another. Crab nerve fibers were successfully used for demonstrating the importance

of the extracellular conducting medium as the pathway of the local current (Hodgkin, 1939, cited in Chapter 4; Katz and Schmitt, 1940).

In about 1939, giant nerve fibers of the squid became available both in Plymouth, England, and Woods Hole, Massachusetts. The existence of giant fibers in the squid had been known for some time. However, for the very reason that these fibers are extraordinarily large, many anatomists were hesitant to believe that they are nerve fibers. In a monograph entitled "The Anatomy of the Common Squid," Williams (1909, p. 74) made the following brief remark: "The very size of the nerve processes has prevented their discovery, since it is well-nigh impossible to believe that such a large structure can be a nerve fiber." In 1936, Young described the anatomy and histology of the giant nerve fibers of cephalopods in detail and showed that each giant fiber is formed by fusion of the processes of 300 to 1500 nerve fibers. In the past, giant axons (0.4–1.0 mm in diameter) taken from the following squid have been used for electrophysiological investigation of the excitable membrane: *Loligo pealei*, *L. forbesi*, *L. vulgaris*, *Doriteuthis bleakeri*, *Dosidicus gigas*, etc.

B. INTRACELLULAR RECORDING OF ACTION POTENTIALS

The first important experiment carried out by using squid giant axons was direct registration of action potentials with one of the recording electrodes introduced into the axoplasm (Hodgkin and Huxley, 1939; Curtis and Cole, 1940). In the experimental setup used by Hodgkin and Huxley, axons were held vertically in seawater and a small glass-pipette electrode was introduced longitudinally into the interior of the axon. The electrodes were half cells of the Ag–AgCl type. The reference electrode was immersed in the surrounding seawater. Initially, the tip of the small electrode was also kept in the seawater. The potential observed under these conditions was marked "zero" in the oscillograph record shown in Fig. 8.1. When the small recording electrode was introduced into the axoplasm of the axon, it was found that the potential inside the axon is 45 to 60 mV below the zero level. In neurophysiology, the potential observed under these conditions is called the *resting membrane potential*.

It should be remembered that the axoplasm is a gel containing about 3% of more-or-less acidic proteins and that the electrolyte composition of the axoplasm is very different from that of seawater (see Chapter 9, Section B). Consequently, there is unavoidable ambiguity in the absolute values of the membrane potentials measured under these conditions. The uncertainty of the liquid-junction potential arising from the presence of polyelectrolytes

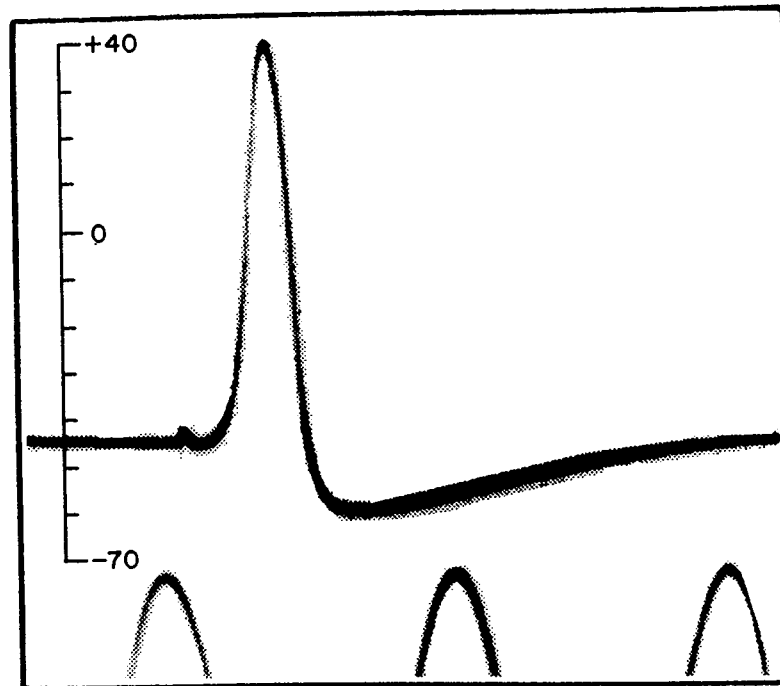


Fig. 8.1 Action potential recorded between inside and outside of axon. Time marker, 500 Hz. (From Hodgkin and Huxley, 1939.)

and polyvalent ions has been discussed by Overbeek (1953), Spiegler and Wyllie (1956), and others. Note that, in a suspension of a polyelectrolyte, the junction potential at the tip of the recording electrode cannot be eliminated by the use of a saturated KCl bridge (Overbeek, 1953).

When the axon was excited electrically by means of a pair of stimulating electrodes placed near one end of the axon, the intracellular potential was found to rise and fall in an all-or-none manner. The potential variation observed in this manner is called the *membrane action potential*. In fresh squid giant axons immersed in normal seawater, the amplitude of the membrane action potential is known to be between 110 and 115 mV. The ambiguity of the liquid-junction potential does not interfere with action potential measurements, because we deal here only with the difference between two potential levels. The difference between the resting membrane potential and the action potential amplitude is usually referred to as the *overshoot*.

The demonstration of a large (about 60 mV) overshoot in the action potential of the squid giant axon was regarded by many neurophysiologists as a very important discovery. According to Bernstein's hypothesis (see Chapter 2, Section F), the action potential is produced by "unification of the negative ions inside with the positive ions outside the membrane" (p. 105 in Bernstein, 1912; cited in Chapter 2). Hence, the membrane potential is expected to approach zero, as in the process of discharge of a Leyden jar, and not to reverse its sign at the peak of excitation.

Retrospectively, however, the great importance attached to the overshoot on the basis of Bernstein's simplistic hypothesis is unfounded. In advancing his hypothesis, Bernstein wilfully ignored his own experimental evidence suggesting the existence of the overshoot in the nerve (Fig. C in Bernstein, 1868, cited in Chapter 2; see p. 485 in Grundfest, 1965). Furthermore, Bernstein utterly neglected Cremer's theory that bioelectric potentials are generated by ion-concentration differences across multi-layer structures and that action potentials are produced by processes which create new ionized molecules or a change in the solvent (membrane). (p. 878 in Cremer, 1909, cited Chapter 2, Section F). According to the latter theory, the overshoot does not have any special significance (see Chapter 14, Section B). We shall see later that the squid axon membrane actually has a multilayer structure and that our interpretation of the mechanism of action potential production is much closer to Cremer's than to Bernstein's (see Chapter 13, Sections E and H).

Finally, it may be pointed out that the time course of the action potential of the squid giant axon is quite unusual. We have seen that the action potential developed by a node of Ranvier has a roughly triangular configuration; it usually has a more-or-less distinct "shoulder," indicating the end of the absolutely refractory period (see Chapter 5, Section A). In contrast, the action potential of the squid giant axon is very short in duration and has a distinct "undershoot," or "after-hyperpolarization"; that is to say, the membrane potential falls rapidly from the peak to a level well below the resting potential. Such a distinct undershoot is not encountered in vertebrate nerve fibers. We shall discuss the significance of the undershoot later (see Chapter 13, Section H).

C. FALL OF MEMBRANE RESISTANCE DURING EXCITATION

In 1939, Cole and Curtis made a convincing demonstration that there is a drastic fall in the membrane resistance of the squid giant axon during excitation. In this demonstration, a squid axon was introduced into a narrow trough provided with a pair of platinized-platinum electrodes on its wall. Making direct contact with the external surface of the axon, the electrodes were connected to one arm of an AC Wheatstone bridge. The output of the bridge was displayed on the screen of an oscilloscope through an amplifier properly tuned to the bridge AC. The frequency of the AC was varied over a range between about 5 and 100 kHz.

Initially, the bridge was balanced for the impedance of the axon at rest. When the axon was excited electrically by a brief shock applied to the axon

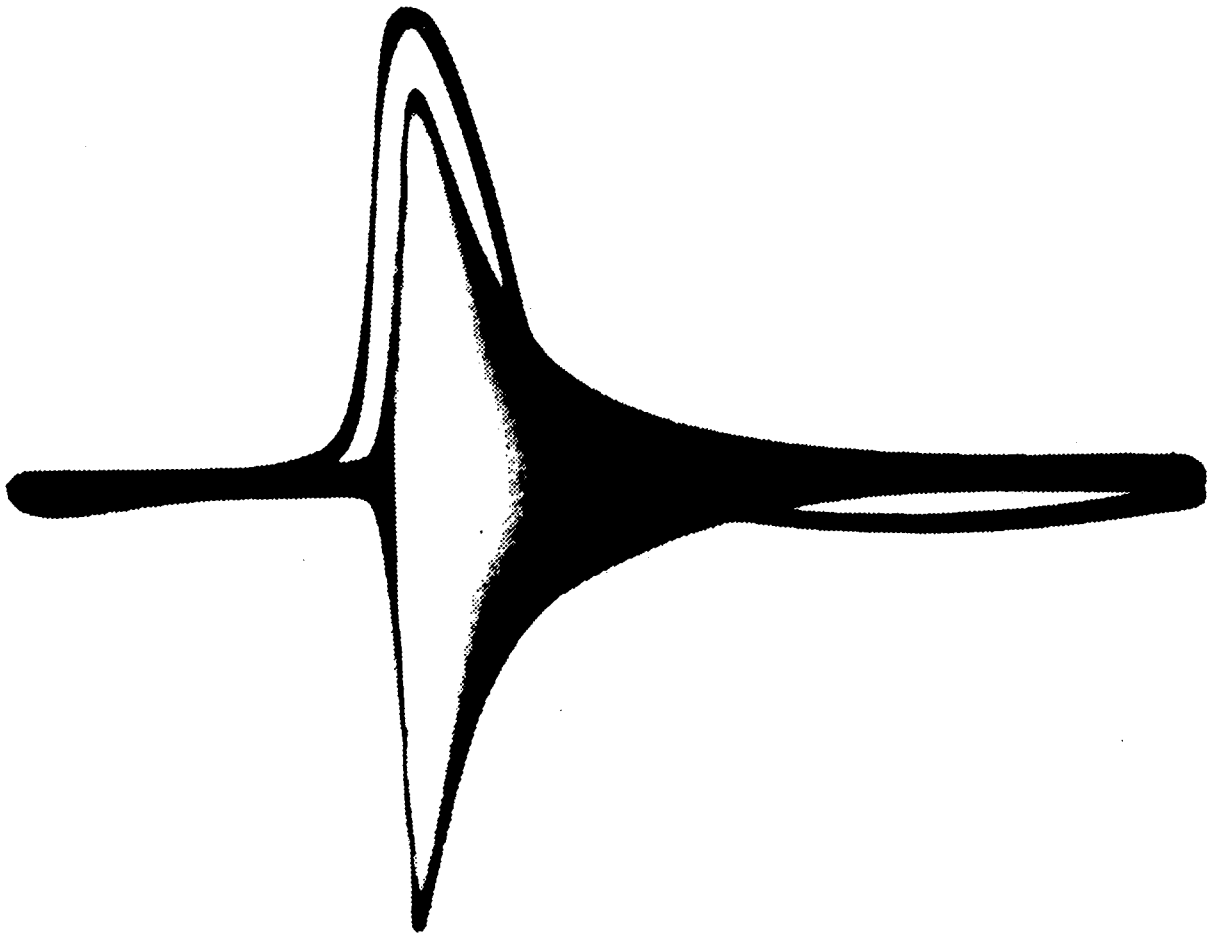


Fig. 8.2 Oscillograph records of the action potential (continuous line) and the membrane resistance decrease (band) from a squid giant axon during the passage of an action potential. (From Cole and Curtis, 1939.)

near its end, there was a transient inbalance of the bridge output at the time of arrival of the action potential at the site of measurement. Cole and Curtis extensively examined the impedance of the axon as a function of the AC frequency. Figure 8.2 is reproduced from their original article. The continuous oscillograph trace represents the extracellularly recorded action potential. The width of the impedance trace is proportional to the change of membrane impedance during excitation. The relative values of the resistance and capacity components of the change were estimated by altering the components of the known arm and obtaining the best balance of the bridge at the peak of activity. (Note that, although the width of the band of the impedance trace is proportional to the change of impedance, the width itself does not give any information as to the relative values of the resistance and capacity components of the impedance change.)

The process of quantitative analysis of the experimental data obtained was

complicated by the fact that extracellular electrodes were used in these measurements. After correction for the electrode polarization and the stray capacity of the measuring device, the observed values of the balancing parallel resistance and capacity, R_p and C_p , of the known arm were converted by calculation into series resistance and capacity R_s and C_s , which give the same impedance and phase shift. It can readily be shown that

$$(R_s - \frac{1}{2}R_p)^2 + X_s^2 = (\frac{1}{2}R_p)^2$$

where $X_s = 1/\omega C_s$, ω being the angular frequency. In the case where C_p and R_p are independent of ω , the "frequency-impedance locus," which is the path followed by X_s plotted against R_s , is a circle of radius $\frac{1}{2}R_p$ with its center located at $\frac{1}{2}R_p$ on the abscissa. If R_p changes during activity, the radius of the circle changes. A pure change in C_p would displace a point on the circle to another point on the same circle. This method of analyzing impedance changes was expanded to include the present case where extracellular electrodes were used for measurements.

By the procedure described above, the observed changes in the values of R_s and X_s were found to lie on the line expected from the assumption that the membrane resistance falls during the passage of a nerve impulse without being accompanied by a change in the membrane capacity. Thus, it was concluded that there is no significant change in the membrane capacity when a large fall in the membrane resistance takes place during nerve excitation. From appropriate analyses of the experimental data, it was inferred that the membrane resistance falls (from about $1000 \Omega \cdot \text{cm}^2$ at rest) to a level between 15 and $50 \Omega \cdot \text{cm}^2$ at the peak of excitation.

Immediately after these experimental results appeared in the *Journal of General Physiology*, another paper describing a new method of measuring the resistances of the membrane and the axoplasm appeared in the same journal (Cole and Hodgkin, 1939). The method consists of determining the longitudinal DC resistance of a cleaned axon immersed in mineral oil as a function of its effective length. Again, extracellular electrodes were used for measurements. Under these experimental conditions, the current used for measurements passes partly through an approximately $20\text{-}\mu\text{m}$ -thick layer of conducting media within the connective tissue and Schwann's cell outside the axon proper; a portion of the current is also carried through the axonal membrane and through the axoplasm. By analyzing this length dependence of the longitudinal resistance, it was found that the resistance of the membrane is approximately $1000 \Omega \cdot \text{cm}^2$ and the resistivity of the axoplasm is $29 \Omega \cdot \text{cm}$, which is about 1.4 times that of seawater.

At present, the method just mentioned for measuring the membrane resistance is rarely used. The method of intracellular wiring invented by George

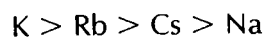
Marmont, which will be described in Section F, yields far more reliable results than the old indirect method.

D. POTASSIUM ION AND THE MEMBRANE POTENTIAL

The effect of potassium salts on the membrane potential was studied by many physiologists before squid axons became available. Since the topic of this section has not been adequately covered in preceding chapters, a brief description is made here of the facts known in classical physiology. More recently, our knowledge concerning the effects of inorganic ions on the nerve membrane advanced significantly when the technique of intracellular perfusion was introduced. The experimental findings obtained by the use of the internal perfusion technique are discussed later in Chapter 10, Section D, Chapter 11, Section F, and Chapter 12, Section G.

The discovery of a strong effect of potassium salts on the emf of the frog muscle is accredited to Biedermann (1880). He found that, when a portion of the intact surface of a muscle is brought in contact with an isotonic potassium salt solution, a large emf is developed between an electrode on the potassium-treated zone (acting as a sink) and another on the remaining surface (acting as a source). Biedermann's discovery was preceded by a less definitive observation made by Ranke (1866, p. 445). Later on, Biedermann (1895) described his findings in his voluminous monograph "Elektrophysiologie," in great detail. He noted that, as long as the duration of immersion in KCl (KNO_3 or KH_2PO_4) is not very long, the potential difference generated by potassium salts vanishes when the surface is washed with an isotonic NaCl solution (see p. 303 in Biedermann, 1895).

Much later, Höber (1905) examined the effects of a large number of inorganic salts on the muscle and found that the salts of various alkali metal ions can generate a potential difference on the surface of the muscle. He showed that the effectiveness of alkali metal ions in altering the membrane potential falls in the following sequence:



The largest potential change observed was roughly 50 mV. He also saw that anions also had definite effects on the muscle. (Note, however, that the effect of anions on the surface of a squid axon is very small except when the anions used are capable of removing free Ca-ions.) Höber noted that these effects of cations are very similar to their effects on various biocolloids. Consequently, he explained the results he obtained as being the results of alteration of the colloidal (or macromolecular) state of the muscle substance. He

also examined the effects of inorganic salts on the excitability of the frog sciatic nerve and found again a parallelism between the effects on the nerve and the influence on such biocolloids as gelatin or ovalbumine (Höber, 1905).

Macdonald (1900, 1905) and Bernstein (1902, 1912; cited in Chapter 2) appear to be the first to suggest that the bioelectricity in the nerve and muscle might be derived from a "concentration cell" involving intracellular K-salts, Macdonald (1905, p. 329) demonstrated experimentally that "potassium salts are really present at every point within the nerve-fibre in astonishing quantity." Bernstein speculated that K_2HPO_4 might be playing an important role. By using Nernst's equation, he estimated the membrane potential generated by K_2HPO_4 to be about -68 mV. He pointed out, as Cremer (1906, see Chapter 2, Section F) did, the possibility that more than one salt might contribute to the resting potential.

Shortly afterward, Loeb and Beutner (1914) emphasized the importance of lipids in the generation of bioelectricity. They confirmed Höber's observation on the effects of potassium salts of various anions. Beutner (1920) continued to gather experimental evidence for the involvement of "oil" (i.e., hydrophobic layer in modern terminology) in the generation of bioelectricity. Later on, however, Loeb seemed to have inclined toward emphasizing the importance of the Donnan potential as the source of bioelectricity (see p. 167 in Loeb, 1922).

Donnan (1911) was fully aware of the biological implication of his theory of membrane equilibrium, for the subtitle of his famous paper written in German reads "Ein Beitrag zur physikalisch-chemische Physiologie." Michaelis (1922) examined Donnan equilibria across various artificial membranes, hoping to find a physicochemical basis of generation of bioelectricity. Eventually, through his extensive experimental studies of proteinaceous membranes, Michaelis (1925) arrived at a clear notion as to the origin of the potential difference across a porous membrane. Soon, Teorell (1935) placed the general concept of membrane potentials on a quantitative basis.

In the membrane theory now known as the Teorell–Meyer–Sievers theory (see also Meyer and Sievers, 1936), the potential difference across a uniform membrane consists, conceptually, of the following three components: (1) a Donnan phase-boundary potential across the solution–membrane interface on one side, (2) an intramembrane diffusion potential, and (3) a Donnan phase-boundary potential at the solution–membrane interface on the other side. Diffusion potentials across an uncharged membrane are included in this theory as special cases. During the following two decades, through extensive studies carried out by use of Sollner's oxidized collodion membrane (see p. 57 in Sollner, 1945) and of synthetic ion-exchange membranes

(see Juda and McRae, 1950; Kressman, 1950), the validity of the basic framework of the Teorell–Meyer–Sievers theory was firmly established (see Teorell, 1953, 1956; Helfferich, 1959).

Now, the effect of potassium ions on the membrane potential of the nerve will be discussed. By using bundles of nerve fibers of the crab, Cowan (1934) carried out extensive measurements of the "injury potential" as a function of the external potassium ion concentration. In a limited concentration range, he saw that there is a linear relationship between the observed potential and the logarithm of the K-ion concentration. He also saw that the effect of potassium can be counteracted by addition of calcium or magnesium to the external medium. However, the real significance of this K–Ca ion antagonism remained unrecognized for many years to come (see Chapter 12, Section F).

In 1942, soon after it became possible to record the potential difference between the axon interior and the external medium, Curtis and Cole measured the membrane potential as a function of the external potassium ion concentration. Figure 8.3 (open circles) shows the results obtained. The membrane potential was recorded with a glass-pipette electrode filled with an isotonic KCl solution. The external potassium ion concentration was varied by replacing a part of NaCl in the external fluid with an equivalent amount of KCl, keeping the divalent cation concentrations at a constant level. It is seen that, in the range of K-ion concentration lower than about 20 mEq/liter, there is very little or no change in the membrane potential. In the

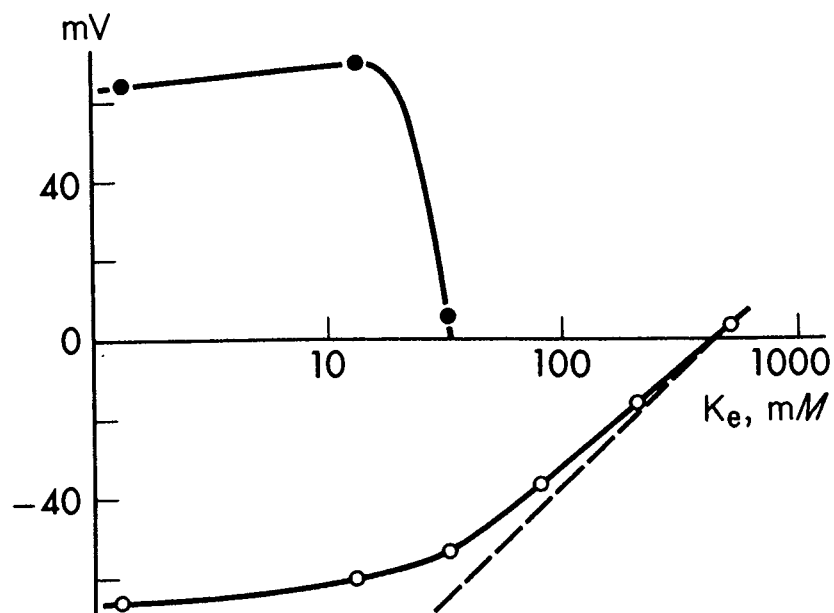


Fig. 8.3 Open circles: Membrane potential plotted against external potassium ion concentration. Solid circles: Action potential overshoot. Broken line: The potential calculated by using Eq. (8.1). (From Curtis and Cole, 1942.)

range higher than about 100 mEq/liter, the membrane potential was found to vary with a slope close to the ideal Nernst slope, i.e., 58 mV for a 10-fold change. These findings were confirmed by many other investigators.

The intracellular potassium ion concentration of a fresh squid axon is known to be 350–400 mEq/liter (Steinbach and Spiegelman, 1943). When the axon is immersed in a high potassium salt solution, potassium ions are the sole major cation species separated by the nerve membrane. Under these experimental conditions, the potential difference across a cation-exchanger membrane is expected to be close to the value of E_K described by the Nernst equation:

$$E_K = \frac{RT}{F} \ln \frac{[K]_e}{[K]_i} \quad (8.1)$$

where $[K]_e$ and $[K]_i$ represent the potassium ion concentration outside and inside the axon. At 19°C, the thermodynamic quantity RT/F is equal to 25.2 mV. (Note that $\ln 10$ times 25.2 mV is 57.96 mV.) The potassium ion concentration in the normal seawater is approximately 10 mEq/liter. The concentration ratio for an axon in normal seawater is then approximately 40; the value of E_K is therefore about 92 mV in this case. The membrane potential of a normal, excitable squid giant axon (between –45 and –60 mV) deviates significantly from the value expected from the equation above.

The deviation of the resting membrane potential from the value described by Eq. (8.1) in the range lower than the normal level was interpreted by Hodgkin and Katz (1949) as being due to the contribution of Na and Cl ions in the external medium. The observed relationship could be approximated by the following equation with $P_K:P_{Na}:P_{Cl} = 1:0.04:0.45$.

$$E = \frac{RT}{F} \ln \frac{P_K[K]_i + P_{Na}[Na]_i + P_{Cl}[Cl]_e}{P_K[K]_e + P_{Na}[Na]_e + P_{Cl}[Cl]_i} \quad (8.2)$$

Note that this equation has the same form as one of Planck's equations, mentioned in Chapter 2 (also cf. Pleijel, 1910; Goldman, 1943). In physiology, P 's in this equation are called "permeability coefficients." Later in Chapter 11, Sections E and F, it will be shown that this equation does not describe the dependence of the observed membrane potential on $[K]_i$ or $[Cl]_e$.

It is important to note that addition of potassium salts to the external medium brings about a drastic change in the excitability of the axon membrane (see Höber, 1905, cited in Chapter 3; Cowan, 1934; Curtis and Cole, 1942). The solid circles in Fig. 8.3 show the action potential overshoot affected by an increase in the external potassium concentration. It is seen that the axon is totally inexcitable in potassium-rich media. It cannot be emphasized

enough that, only when the axon is rendered incapable of developing action potentials, is the membrane potential sensitive to changes in the external potassium ions. Axons which are rendered inexcitable by addition of K-salt to the external medium are generally said to be in a "depolarized state." Normal, i.e., nondepolarized, axons are insensitive to changes in the external potassium ion concentration. The significance of these facts are discussed later in relation to the effects of divalent cations on the nerve membrane (see Chapter 10, Sections D and G).

We summarize what is discussed in this section as follows: (1) the effectiveness of alkali metal ions in altering the membrane potential of an axon immersed in a medium containing divalent cation salts is represented by the sequence $K > Rb > Cs > Na$. (2) The effect of increasing the univalent cation concentration on the membrane potential can be antagonized by addition of Ca salts to the medium. (3) The resting membrane potential of a squid giant axon in its excitable state is not significantly affected by changes in the K-ion concentration. (4) The Teorell–Meyer–Sievers theory is expected to account for the emf of the axon if the structural complexity of the membrane and the role of the external Ca-ion are taken into consideration.

E. SODIUM ION AND EXCITABILITY

The effect of Na ions on the excitability of the muscle and nerve was examined at about the turn of the century by a number of prominent physiologists, such as Ringer (1886), Loeb (1900, cited in Chapter 3), Overton (1902, 1904), and others. Ringer noted that thigh muscles of the frog cut into thin ribbons show fibrillary (rhythmical) contractions when immersed in a 0.6% NaCl solution and that addition of a small amount (about 0.02%) of $CaCl_2$ suppressed these contractions. He saw also that muscle excitability is sustained much longer in a NaCl solution to which a small amount of calcium phosphate and KCl are added.

The observations made by Loeb are often ignored in recent literature; hence, it seems worthwhile to describe his results in some detail (see also Chapter 3, Section C). In an article subtitled, "The poisonous character of a pure NaCl solution," Loeb described his findings in the following words: "I found that rhythmical contractions occur only in solutions of electrolyte, i.e., in compounds which are capable of ionization. In solutions of nonconductors (urea, various sugars, and glycerine) these rhythmical contractions are impossible" (p. 328 in Loeb, 1900, cited in Chapter 3). Then, he emphasized the importance of the coexistence of Na and Ca ions and said: "solutions of Na ions produce rhythmical contractions only if the muscle cells contain Ca ions in sufficient number. As soon as there is a lack of Ca ions in the tissue, Na ions are no longer able to cause rhythmical contractions" (p.

329). He was quite aware of the fact that rhythmical activities can be observed only in a limited range of Na–Ca concentration ratio in the medium. Loeb summarized his results in the following manner: "The poisonous effects of this (pure NaCl) solution are due to the Na-ions. . . . The poisonous effects of the Na-ions are antagonized by the addition of a small amount of Ca- and K-ions. In a pure solution of NaCl, Na-ions will gradually take the place of the Ca- and K-ions in the ion-proteids of the tissues, and this leads to a loss of contractility or irritability" (p. 338 in Loeb, 1900, cited in Chapter 3).

Shortly afterward, Overton (1902) emphasized the importance of Na-ions in the external medium for the maintenance of the muscle contractility. He also saw that a muscle immersed in an isotonic sugar solution becomes inexcitable and that it regains its ability to respond to applied electric shocks when a portion of the sugar solution was replaced with an isotonic NaCl solution. In his 1902 article, Overton reported that the sciatic nerve was different from the muscle and did not lose its excitability in a pure sugar solution for more than 10 hr. Later, he changed his view and said that the effect of Na-ions on the nerve fibers was similar to that on the muscle (Overton, 1904). He also suggested that there might be an exchange of external Na-ions with internal K-ions during excitation (p. 381 in Overton, 1902).

Much later, Lorente de Nó (1947, cited in Chapter 6) examined the effect of prolonged immersion of a sciatic nerve of the frog in an isotonic solution of choline chloride. He found that the excitability of the nerve lost in this Na-free medium can be restored within several minutes when NaCl is substituted for choline chloride. In these old experiments with intact nerve trunks, the hindrance of diffusion of various substances through the intercellular space, as well as the ion-exchange property of the fibers and connective tissue within the trunk, created serious difficulties in interpreting the results obtained. Note that conduction along an isolated frog nerve fiber is blocked within a few seconds after replacement of normal Ringer's solution outside with an isotonic sucrose solution.

In 1949, Hodgkin and Katz examined the effect of varying the external Na-ion concentration on the action potential overshoot in squid giant axons. When a portion of the seawater outside the axon was replaced with a sugar (dextrose) solution isotonic with seawater, it was found that the action potential amplitude falls rapidly and reaches a new steady state. Figure 8.4 shows an example of the records obtained. The relation between the external Na ion concentration and the action potential overshoot observed could be described within a relatively wide range, by the following formula:

$$E_a = \frac{RT}{F} \ln[\text{Na}]_e + \text{constant} \quad (8.3)$$

where E_a represents the overshoot, $[\text{Na}]_e$ the external Na-ion concentration.

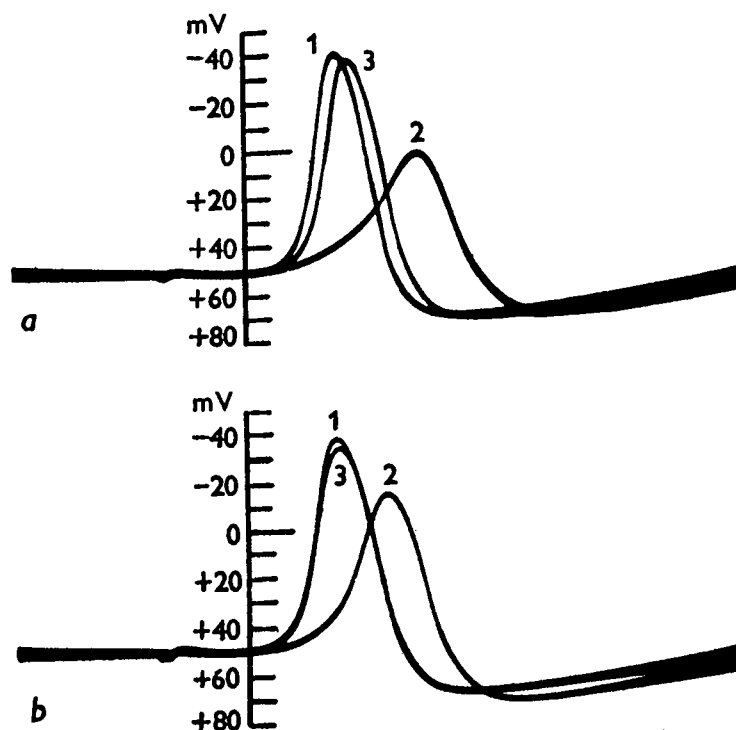


Fig. 8.4 Action of sodium-deficient solutions on the resting and action potential: (a) 1, response in seawater; 2, after 16 min in 33% seawater, 67% isotonic dextrose; 3, 13 min after reapplication of seawater; (b) 1, response in seawater; 2, after 15 min in 50% seawater, 50% isotonic dextrose; 3, 6 min after reapplication of seawater. (From Hodgkin and Katz, 1949.)

At the time when these measurements were made, it was impossible to examine the effect of altering the intracellular Na-ion concentration on the action potential overshoot. Nevertheless, Hodgkin and Katz assumed that the action potential overshoot is determined solely by the Na-ion concentration ratio across the axon membrane and described the observed results by the Nernst equation for Na-ions:

$$E_{\text{Na}} = \frac{RT}{F} \ln \frac{[\text{Na}]_e}{[\text{Na}]_i} \quad (8.3a)$$

where $[\text{Na}]_i$ represents the internal Na-ion concentration. Direct determination of sodium in the axoplasm of fresh squid giant axons indicated that $[\text{Na}]_i$ is approximately one-tenth of the level in normal seawater (Steinbach and Spiegelman, 1943). The overshoot expected from this ratio is roughly 58 mV, which is not very different from the value observed in axons immersed in normal seawater. Before the advent of the method of intracellular perfusion, therefore, Eq. (8.3a) appeared to properly describe the action potential overshoot in squid giant axons. Later, in Chapter 11, Section F, we shall see that the effect of varying the internal Na-ion concentration does not

follow Eq. (8.3a). The importance of Ca-ion in production of action potentials will be reemphasized later.

It is important to realize in this connection that there are excitable cells and tissues which do not require Na-ions in the medium to maintain their ability to develop all-or-none action potentials. At the time when the effect of Na-ions on the action potential of the squid giant axon was being examined, Fatt and Katz (1951) showed that muscle fibers of the crab develop large action potentials in the absence of Na-ions in the medium. Previously, Lorente de Nó (1947, cited in Chapter 6) found that small myelinated nerve fibers remain excitable in a mixture of divalent cation salts and tetraethylammonium ions. It is known that the blood of pupae of plant-eating insects contains a high concentration of K-ions and a very low, sometimes undetectable, concentration of Na-ions (Brecher, 1929; Tobias, 1948); the excitation processes in such organisms cannot be dependent on Na-ions. A long time ago Osterhout and Hill (1933) established that single cells of *Nitella* develop a all-or-none action potentials without any Na-ions in the medium. From the standpoint of general physiology, one might say that the validity of the sodium theory of action potential generation is somewhat limited.

We close this section by reemphasizing that excitability cannot be maintained without adding a calcium salt to the external NaCl solution. In the presence of 30–60 mM divalent cation salts in the medium, the action potential overshoot of the squid giant axon varies with the external Na-ion concentration. Some excitable cells, including small myelinated nerve fibers, do not require Na-ions in the medium to maintain their excitability.

F. INTRACELLULAR WIRING OF SQUID GIANT AXONS

George Marmont's remarkable paper describing a method of intracellular wiring of squid axons appeared in 1949. Prior to the publication of this paper, this ingenuous investigator wrote an article in which he discussed the nature of extracellularly recorded action potentials (Marmont, 1940). He showed that the potential variations observed with extracellular electrodes are nothing but the $I-R$ drops (i.e., potential drops across ohmic resistors) generated by the action current of the nerve fiber in the external electrolyte solution. Previously, the electronegativity that appears on the surface of an excited part of a nerve fiber (or a trunk) was regarded by many neurophysiologists erroneously as reflecting the appearance of negative charges of a Helmholtz double layer (see, e.g., p. 393 in Bayliss, 1924). Marmont showed that discontinuities in the cross-sectional area of the external medium create spurious electric responses when extracellular electrodes are used for recording.

The title of Marmont's article published in 1949 was, "Studies of the axon membrane. I. A new method." In the introduction, he pointed out the shortcomings of extracellular stimulating and recording electrodes. We quote his own sentences on this point: "Studies of membrane excitability, impedance, etc., which require passage of current through the membrane, have always utilized external electrodes for supplying current. This is a somewhat unsatisfactory technique because the current density through the membrane is not uniform. . . . Furthermore, if the current is large enough to make the membrane 'active,' not leaving it merely passive, the magnitude of the subsequent membrane current cannot be controlled." Next, he explained the objective of his experiments in the following words: "One would like to be able to control the current density or the potential drop across the membrane or some other parameter such as the rate of change of potential drop, regardless of whether the membrane became active or not. A technique such as this implies that the propagation will be removed from the experiment, for the area of membrane under investigation will tend to react at all points in the same manner at a given instant." One might say that this was a preliminary announcement of the arrival of the current clamp and voltage clamp era.

Figure 8.5 (top) shows the principle of the experimental method invented by Marmont. It is seen that a low resistance metal electrode, 100 μm in diameter, is inserted along the long axis of the axon. The fluid medium (seawater) outside the axon is divided into three separate pools. A metal electrode is immersed in each of these three pools. The potential difference between the central electrode and the guard (i.e., lateral) electrodes is maintained close to zero at rest, as well as during excitation of the axon. Marmont accomplished this by using a direct-coupled differential (feedback) amplifier specially designed for this purpose. To lower the electric resistance and to enhance the DC stability, he treated all the metal electrodes by a special chemical process.

An example of the action potentials recorded by this method is reproduced in Fig. 8.5 (bottom). A brief rectangular pulse of current through the axon membrane was used to evoke this response. With this barely supra-threshold stimulating pulse, the membrane potential was raised to a level roughly 20 mV above the resting potential. At the termination of the applied pulse, the membrane potential remained at a more-or-less constant level for a short period of time. Then, after an extremely variable "period of indecision," a full-sized action potential of about 110 mV in amplitude was released. This is the first record of an action potential observed under zero-net-membrane-current conditions. (Note that a propagated action potential is always associated with membrane currents. It is interesting that the time

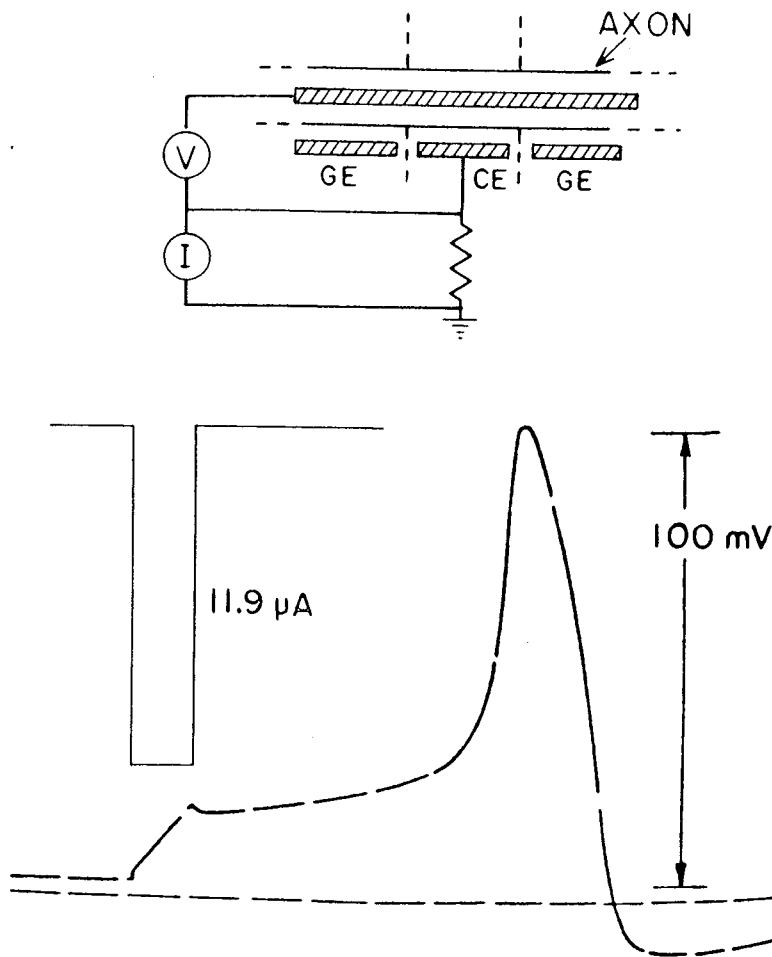


Fig. 8.5 Top: Schematic diagram showing the space clamp method invented by Marmont. CE and GE indicate the central and guard electrodes, respectively, which were kept at the same potential electronically. V and I represent the amplifiers used for recording the potential difference across the axon membrane and the membrane current, respectively. Bottom: A tracing (reproduced with the polarity reversed) of the oscillograph record of an action potential obtained by Marmont (1949). The stimulating current pulse was 0.1 msec in duration.

course of this action potential is not at all different from that of a propagated action potential.)

Unfortunately, Marmont never published Part II of his "Studies of the Axon Membrane." Nevertheless, his technique of intracellular wiring brought about a rapid revolution in the neurophysiologists' way of thinking. Furthermore, the use of DC-coupled differential amplifiers for the purpose of controlling membrane currents or potentials by the feedback mechanism became one of the standard procedures in studies of membrane excitability. Gradually, neurophysiologists were familiarized with analyses of electric circuits involving an excitable membrane. Soon, neurophysiology plunged into a new era in which the process of nerve excitation was analyzed on the basis of the equivalent electric circuit of the axon membrane.

G. THE VOLTAGE CLAMP PROCEDURE

When an electric stimulus is applied to a squid giant axon through extracellular electrodes, the major portion of the electric current passes through the tissue fluid outside the axon. Since the resistance of tissue fluid is ohmic, it makes little difference whether a pulse of constant current or a pulse of constant voltage is used for stimulation. However, the situation is quite different when a stimulating pulse is applied directly across the axon membrane, namely, when one of the stimulating electrodes is a long intracellular wire.

The axon membrane at rest behaves like a leaky capacitor. Hence, a pulse of constant current generates a linear rise in the membrane potential (see Fig. 8.5). When a pulse of constant voltage is applied across the axon membrane, an extremely brief (but strong) current is expected to be carried through the membrane "capacitatively" at the onset of the voltage pulse. Following this initial capacitative surge of current, an ohmic current passes through the membrane. As long as the membrane properties remain unaffected by the applied pulse, the ohmic current is expected to remain constant during the plateau of the pulse.

By using the experimental method developed by Marmont and by Cole (1949), the membrane current generated by constant voltage pulses through the squid axon membrane was measured by Hodgkin *et al.* (1952). The results obtained were remarkable in several respects. When the clamping voltage pulses were negative, namely, when the potential of the axon interior was made more negative by the applied voltage pulses, there were strong capacitative currents followed by approximately constant inward currents. This finding is consistent with the notion that an inwardly directed membrane current does not bring about a significant change in the emf of the system or in the resistance of the membrane. In contrast, when the applied voltage pulses were positive, namely, when the membrane potential was suddenly raised above the resting level and was maintained at a new level for a short period of time, a highly time-dependent membrane current was observed. The origin of this complex membrane current can be understood on the basis of the following consideration.

Let us denote the magnitude of the action potential (i.e., the emf at the peak of excitation) by E_a and the potential level attained during the clamping by V . We consider the case in which the level of V is only slightly below the peak of the action potential, namely, the case where the membrane potential is raised quickly to a level 80–100 mV above its resting level. Under these circumstances, we expect the axon membrane to be thrown into its excited state shortly after the onset of the applied pulse (cf. Fig. 8.7A; see also Chapter 14, Section G). Hence, the membrane current at the peak of

excitation is expected to vary linearly with V . We denote the peak value of the time-dependent membrane conductance by G_a . Ohm's law relating V to the membrane current, I , is then given by

$$I = G_a(V - E_a) \quad (8.4)$$

At the peak of excitation, E_a is close to 110 mV; since V is lower than E_a , I is inwardly directed.

In the excited state, the emf does not stay at a constant level; due to the relaxation of the system, it falls automatically. At the moment when the emf falls below the level of V , the membrane current is expected to reverse its sign. As it falls progressively, the intensity of the outwardly directed membrane current is expected to increase. These changes in the membrane current, expected from the results of impedance measurements during excitation, were actually observed by Hodgkin *et al.* (1952; see Fig. 8.6, left).

Figure 8.6 (right) shows the current intensity at 0.65 msec after the onset of the applied voltage pulse plotted against the potential level to which the

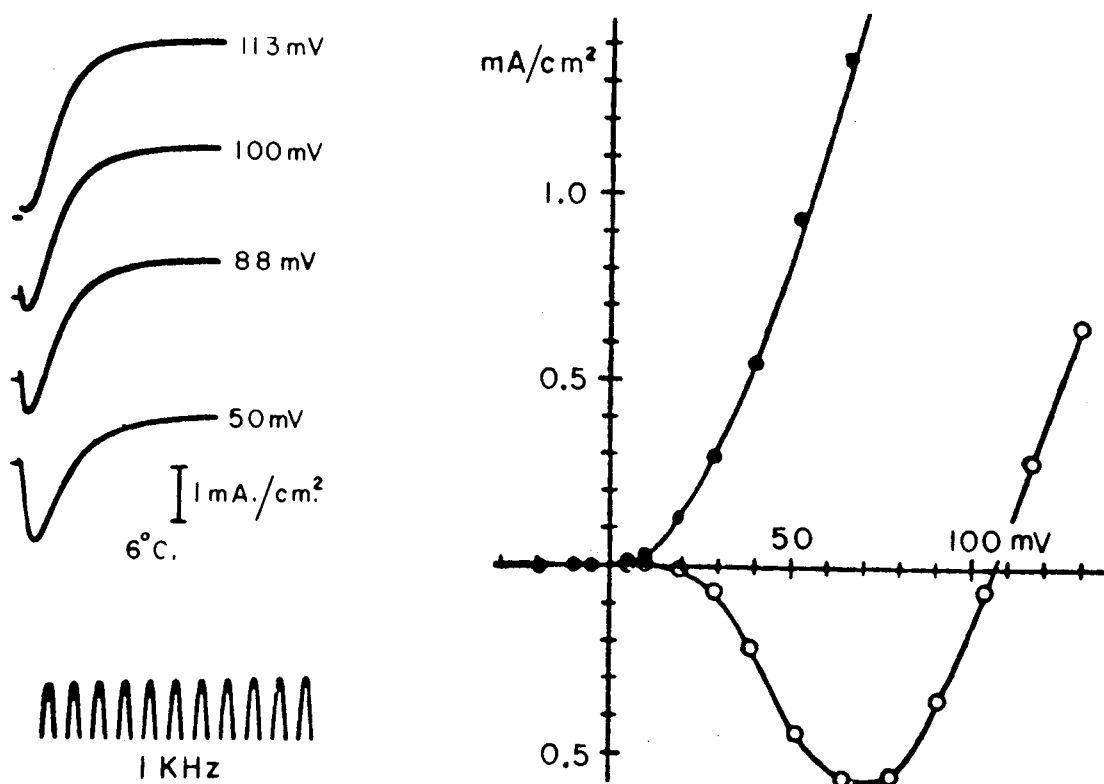


Fig. 8.6 Left: Membrane currents under voltage clamp at 6°C. Inward current is shown as a downward deflection. The numbers attached to each curve give the displacement of the membrane potential. Right: Relation between the membrane current density and membrane potential. Abscissa: displacement of the membrane potential from its resting value. Ordinate: membrane current density at 0.63 msec after beginning of voltage step (open circles) and in "steady state" (filled circles). Measurements were made at 3.8°C. (Reproduced, with the polarity reversed, from Hodgkin and Huxley, 1952a.)

membrane potential was raised. It is seen that the current–voltage curve crosses the abscissa ($I = 0$) at two different points. One of these two points represents the resting potential: when the membrane potential is not displaced at all, there is of course no (net) membrane current. The second point corresponds to the peak of the action potential, namely, approximately 110 mV above the resting potential. The slopes of the current–voltage curve at these two points represent the conductances of the axon membrane at rest and roughly at the peak of excitation. Reflecting a large rise in conductance (i.e., a large fall in resistance) during excitation, the slopes of the curve at these two points are very different.

It is seen in Fig. 8.6 that the slope of the I – V curve is negative in a limited range of voltage. In studies of the mechanism of nerve excitation, formulation of a precise interpretation of this negative slope in the I – V curve is the problem of cardinal importance. Hodgkin and Huxley (1952d) assumed the axon membrane under voltage clamp was spatially uniform. They attributed the negative slope to a particular voltage dependence of the “sodium conductance.” The significance of the sodium and potassium conductance will be discussed later on physicochemical bases (see Chapter 14, Section F). Alternatively, one may abandon the assumption of spatial uniformity of the axon membrane and attribute the negative slope of the I – V relationship to a gradual increase in the fraction of the membrane sites in their excited state (see Chapter 12, Section J, and Chapter 13, Section I).

A word of caution may be timely here against indiscriminate usage of the term “sodium current” to describe an inward current. Under normal experimental conditions, the major cation species in the external medium is sodium and that in the internal medium is potassium. When the axon membrane develops an action potential under the zero-net-current conditions, there is a large increase in the interdiffusion fluxes of potassium and sodium ions across the membrane. [Note that the interdiffusion fluxes are proportional to the membrane conductance (see Chapter 11, Section H).] The inward current observed when ($E_a - V$) is not much larger than 25 mV (i.e., RT/F) and negative should not be called a “sodium current,” because in general a decrease in the efflux of potassium ions makes a significant (and equally important) contribution to the inward current.

H. THE HODGKIN–HUXLEY THEORY OF NERVE EXCITATION

In a series of articles published in 1952, Hodgkin and Huxley (1952a,b,c,d) showed that the process of excitation of the squid axon membrane can be described by the equivalent circuit illustrated in Fig. 8.7B.

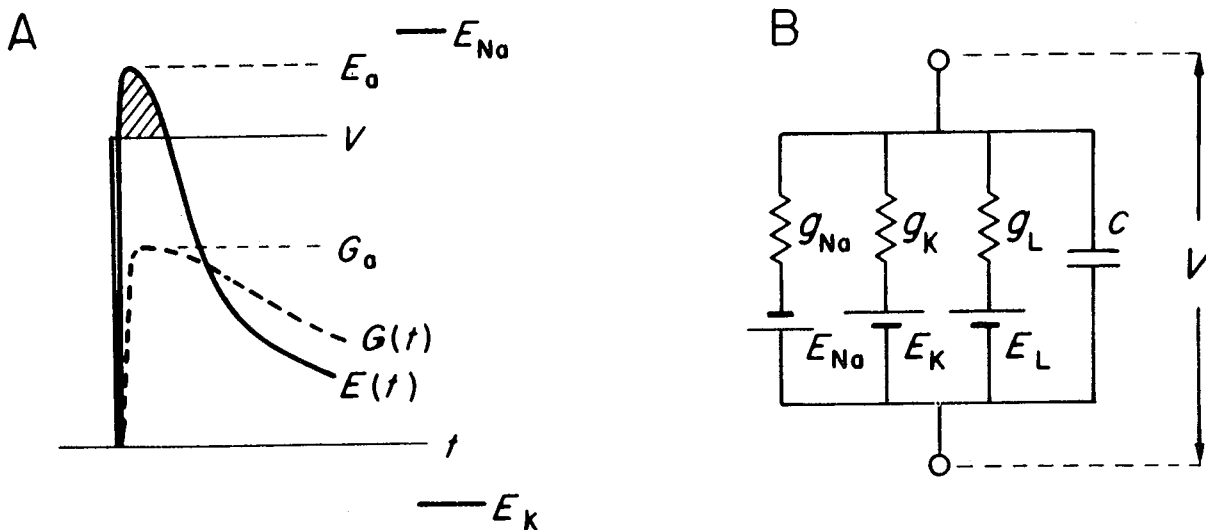


Fig. 8.7 (A) Diagram illustrating the origin of the inward membrane current observed when the membrane potential is suddenly displaced from its resting level. E_a ; Peak level of the membrane action potential. V , The potential level to which the membrane potential was displaced. G_a , Peak value of the membrane conductance. $E(t)$ and $G(t)$ show the time courses of the rise of the emf and the conductance. The shaded area under $E(t)$ roughly reproduces the time course of the inward membrane current. (B) Equivalent electric circuit introduced by Hodgkin and Huxley (see text).

Here, the membrane is considered to have three "ionic channels" and a "capacitive channel." The electric current through the capacitive channel is proportional to the variation of the membrane potential. The electric currents passing through ionic channels are assumed to be described formally by Ohm's law. For sodium ions, it is assumed that the driving force is $(V - E_{Na})$, where E_{Na} is given by Eq. (8.3a) and the conductance, g_{Na} , is a function of V and t . Similarly, E_K is given by Eq. (8.1) and g_K is also a function of V and t . The ion species transported through the "leakage channel" include Mg^{2+} , Ca^{2+} , Cl^- , and phosphate ions; the conductance of this channel, g_L , is assumed not to change during excitation.

The potential levels of E_{Na} and E_K are indicated in Fig. 8.7. It is seen that E_K is lower and E_{Na} is higher than the range of the membrane potential that varies during excitation. E_L is close to the resting level of the membrane potential, and g_L remains at a low level during excitation. Therefore, a rise in g_{Na} raises the membrane potential; a rise of g_K on the contrary lowers the potential level. Hence, it is possible to describe any potential variation that does not exceed the upper and lower limits, E_{Na} and E_K , by a proper choice of variables g_{Na} and g_K . The overall conductance of this membrane, G , is given by the sum $(g_{Na} + g_K + g_L)$. According to Kirchhoff's law applied to this electric network, the effective emf of the membrane, E , is equal to $(g_{Na}E_{Na} + g_K E_K + g_L E_L)/G$. When the time courses of G and E during the action potential are known, it is always possible to determine the values of g_{Na}

and g_K which give rise to the observed potential or current variation. During excitation, the overall membrane resistance, $1/G$, is so low that the time constant, C/G , of the membrane (15–50 μsec) is far shorter than the duration of the action potential (0.5–1.0 msec).

The procedure adopted by Hodgkin and Huxley was to control the flow of electricity through the capacitative channel by the use of the voltage clamp procedure. When the membrane potential is altered along a rectangular time course, the capacitative current vanishes except at the beginning and at the end of the voltage pulse. The time-dependent current in the equivalent circuit must then be the sum of the currents through the sodium and potassium channels. Next, this total current was divided into the sodium and potassium currents by replacing choline ions for the sodium ions in the external medium. The sodium and potassium currents thus determined were divided by $(V-E_{\text{Na}})$ and $(V-E_K)$, respectively, to obtain g_{Na} and g_K for the voltage level chosen. By repeating this procedure, the values of g_{Na} and g_K were measured experimentally as functions of time in a wide range of voltage V .

The next step in the development of the theory was to express the rise and fall of the experimentally found g_{Na} and g_K in mathematical terms. Equations (8.5), (8.6), and (8.7) were chosen on the following ground: "There are at least two general methods of describing the transient changes in sodium conductance. First, we might assume that the sodium conductance is determined by a variable which obeys a second-order differential equation. Secondly, we might suppose that it is determined by two variables, each of which obey a first-order equation. . . . The second alternative was chosen since it was simpler to apply to the experimental results" (p. 512 in Hodgkin and Huxley, 1952d). Similarly, Eq. (8.8) was chosen to describe the observed rise in the potassium conductance under voltage clamp. The voltage-dependent parameters chosen to describe the observed membrane currents are described by Eqs. (8.10–8.15). Equation (8.16) then describes the total current consisting of the capacitative component, the sodium current, the potassium current, and the leakage current.

$$g_{\text{Na}} = m^3 h \bar{g}_{\text{Na}} \quad (8.5)$$

$$\frac{dm}{dt} = \alpha_m(1 - m) - \beta_m m \quad (8.6)$$

$$\frac{dh}{dt} = \alpha_h(1 - h) - \beta_h h \quad (8.7)$$

$$g_K = \bar{g}_K n^4 \quad (8.8)$$

$$\frac{dn}{dt} = \alpha_n(1 - n) - \beta_n n \quad (8.9)$$

$$\alpha_n = 0.01(V - E_r + 10) / \left(\exp \frac{V - E_r + 10}{10} - 1 \right) \quad (8.10)$$

$$\beta_n = 0.125 \exp[(V - E_r)/80] \quad (8.11)$$

$$\alpha_m = 0.1(V - E_r + 25) / \left(\exp \frac{V - E_r + 25}{10} - 1 \right) \quad (8.12)$$

$$\beta_m = 4 \exp \left(\frac{V - E_r}{18} \right) \quad (8.13)$$

$$\alpha_h = 0.07 \exp \left(\frac{V - E_r}{20} \right) \quad (8.14)$$

$$\beta_h = 1 / \left(\exp \frac{V - E_r + 30}{10} + 1 \right) \quad (8.15)$$

$$I = C_m \frac{dV}{dt} + g_K(V - E_K) + g_{Na}(V - E_{Na}) + g_L(V - E_L) \quad (8.16)$$

The final step in the development of this theory was to calculate membrane action potentials under a variety of conditions. The results of calculation indicated that all the important characters of the action potentials observed under normal experimental conditions are properly described by the set of equations listed above. It was also possible to calculate the time course of a conducted action potential and its velocity. The success of this mathematical calculation had a great impact on neurophysiologists in the whole world. Many investigators in the field expressed the view that the mechanism of nerve excitation is perfectly elucidated by this theory. A large number of papers were published since, explaining various aspects of the behavior of excitable membranes on the basis of this theory (see Cole, 1968; Adelman, 1971).

The theory just described left the following questions unanswered: (1) Do variations of the internal sodium and potassium concentrations affect the resting and action potential as the theory demands? (2) Does the theory prove that there are two spatially separate pores or channels in the nerve membrane? (3) How can the inconsistency between the constant-field Eq. (8.2) employed previously and the equivalent circuit approach be resolved? (4) What is the role of the calcium ions which are indispensable for the maintenance of excitability? (5) What is the mechanism of action potential production in muscle and nerve fibers which remain excitable in sodium-free media? These and other related problems are discussed in subsequent chapters.

It should be emphasized in this connection that the success of this theory does not depend on the legitimacy of the assumptions made to derive the

formal mathematical Eqs. (8.5–8.16). The success derives essentially from the applicability of Kirchhoff's law to the proposed equivalent circuit. According to this law, the experimental determination of the sodium and potassium conductances in this theory may be regarded as an indirect procedure of evaluating the effective emf of the membrane which is given by $E = (g_{Na}E_{Na} + g_K E_K + g_L E_L)/G$. When this evaluation of the emf is accomplished as a function of time for all possible levels of membrane potential, calculation of the action potential (i.e., the emf for the case of zero membrane current) may be regarded as a complex process of interpolation (see Chapter 14, Section G). It is not very strange, therefore, that these equations involving a large number of experimentally determined parameters yield very reasonable results. In other words, the success of this theory does not by itself prove that the mathematical equations employed have valid physiochemical bases (see Tasaki, 1968).

REFERENCES

- Adelman, W. J. Jr. (1971). "Biophysics and Physiology of Excitable Membranes." Van Nostrand-Rheinhold, Princeton, New Jersey.
- Bayliss, W. M. (1924). "Principles of General Physiology." 1st edition published in 1915. Longmans, Green, London.
- Beutner, R. (1920). "Die Entstehung der elektrischer Ströme in lebenden Geweben." Enke, Stuttgart.
- Biedermann, W. (1880). Beiträge zur allgemeinen Nerven-und Muskel-physiologie, V. Über die Abhängigkeit des Muskelstromes von localen chemischen Veränderungen der Muskelsubstanz. *Sitzungsber, Akad. Wiss. Wien* **81**, 74–114.
- Biedermann, W. (1895). "Elektrophysiologie," 857 p. Gustav Fischer, Jena.
- Boruttau, H. (1897). Der Electrotonus und die phasischen Aktionsströme am marklosen Cephalopodennerven. *Pfluegers Arch. Gesamte Physiol. Menschen Tiere* **66**, 285–307.
- Brecher, L. (1929). Die anorganischen Bestandteilen des Schmetterlingspuppenblutes (*Sphinx-pinastri*, *Pieris brassicae*). Veränderungen in Gehalt an anorganischen Bestandteilen bei der Verpuppung (*Pieris brassicae*). *Biochem. Z.* **211**, 40–64.
- Cole, K. S. (1949). Dynamic electrical characteristics of the squid axon membrane. *Arch. Sci. Physiol.* **3**, 253–258.
- Cole, K. S. (1968). "Membranes, Ions and Impulses." Univ. of California Press, Berkeley, California.
- Cole, K. S., and Curtis, H. J. (1939). Electric impedance of the squid giant axon during activity. *J. Gen. Physiol.* **22**, 649–670.
- Cole, K. S., and Hodgkin, A. L. (1939). Membrane and protoplasm resistance in the squid giant axon. *J. Gen. Physiol.* **22**, 671–687.
- Cowan, S. L. (1934). The action of potassium and other ions on the injury potential and action current in *Maia* nerve. *Proc. R. Soc. London Ser. B.* **115**, 216–260.
- Curtis, H. J., and Cole, K. S. (1940). Membrane action potentials from the squid giant axon. *J. Cell. Comp. Physiol.* **15**, 147–157.
- Curtis, H. J., and Cole, K. S. (1942). Membrane resting and action potentials from the squid giant axon. *J. Cell. Comp. Physiol.* **19**, 135–144.

- Donnan, F. G. (1911). Theorie der Membrangleichgewichte und Membranpotentiale bei Vorhandensein von nicht dialysierenden Elektrolyten. Ein Beitrag zur physikalisch-chemische Physiologie. *Z. Elektrochem.* **17**, 572–581.
- Fatt, P., and Katz, B. (1951). Conduction of impulses in crustacean muscle fibres. *J. Physiol. (London)* **115**, 45P.
- Fick, A. (1863). "Beiträge zur vergleichenden Physiologie der irritablen Substanzen." Friedrich Vieweg & Sohn, Braunschweig, Germany.
- Frédéricq, L., and Vendeveld, G. (1880). Vitesse de transmission de l'excitation motrice dans les nerfs du Homard. *C. R. Acad. Sci.* **91**, 239–240.
- Frieländer, B. (1889). Ueber die markhaltigen Nervenfasern und Neurochorde der Crustaceen und Anneliden. *Mitt. Zool. Sta. Neapel.* **9**, 205–265.
- Furusawa, K. (1929). The depolarization of crustacean nerve by stimulation or oxygen want. *J. Physiol. (London)* **67**, 326–342.
- Garten, S. (1903). "Beiträge zur Physiologie der marklosen Nerven." Gustav Fischer, Jena, Germany.
- Goldman, D. E. (1943). Potential, impedance and rectification in membranes. *J. Gen. Physiol.* **27**, 37–60.
- Grundfest, H. (1965). Julius Bernstein, Ludimar Hermann and the discovery of the overshoot of the axon spike. *Arch. Ital. Biol.* **103**, 483–490.
- Helfferrich, F. (1959). "Ionenaustauscher." Verlag Chemie GmbH, Weinheim/Bergstrasse, Germany; (1962) "Ion Exchange." McGraw-Hill, New York.
- Höber, R. (1905). Über den Einfluss der Salze auf den Ruhestrom des Froschmuskels. *Pfluegers Arch Gesamte Physiol. Menschen Tiere* **106**, 599–635.
- Hodgkin, A. L., and Huxley, A. F. (1939). Action potentials recorded from inside a nerve fibre. *Nature (London)* **144**, 710–711.
- Hodgkin, A. L., and Huxley, A. F. (1952a). Currents carried by sodium and potassium ions through the membrane of the giant axon of *Loligo*. *J. Physiol. (London)* **116**, 449–472.
- Hodgkin, A. L., and Huxley, A. F. (1952b). The components of membrane conductance in the giant axon of *Loligo*. *J. Physiol. (London)* **116**, 473–496.
- Hodgkin, A. L., and Huxley, A. F. (1952c). The dual effect of membrane potential on sodium conductance in the giant axon of *Loligo*. *J. Physiol. (London)* **116**, 497–506.
- Hodgkin, A. L., and Huxley, A. F. (1952d). A quantitative description of membrane current and its application to conduction and excitation in nerve. *J. Physiol. (London)* **117**, 500–544.
- Hodgkin, A. L., and Katz, B. (1949). The effect of sodium ions on the electrical activity of the giant axon of the squid. *J. Physiol. (London)* **108**, 37–77.
- Hodgkin, A. L., Huxley, A. F., and Katz, B. (1952). Measurement of current-voltage relations in the membrane of the giant axon of *Loligo*. *J. Physiol. (London)* **116**, 424–448.
- Juda, W., and McRae, W. A. (1950). Coherent ion-exchange gels and membranes. *J. Am. Chem. Soc.* **72**, 1044.
- Katz, B., and Schmitt, O. H. (1940). Electric interaction between two adjacent nerve fibres. *J. Physiol. (London)* **97**, 471–488.
- Kressman, T. R. E. (1950). Ion exchange resin membranes and resin-impregnated filter paper. *Nature (London)* **165**, 568.
- Kühne, W., and Steiner, J. (1879–1880). Beobachtungen über markhaltige und marklose Nervenfasern. *Unter. Physiol. Inst. Univ. Heidelberg* **3**, 149–170.
- Loeb, J. (1922). "Proteins and the Theory of Colloidal Behavior." McGraw-Hill, New York.
- Loeb, J., and Beutner, R. (1914). Über die Bedeutung der Lipide für die Entstehung von Potentialunterschieden an der Oberfläche tierischer Organe. *Biochem. Z.* **59**, 195–201.
- Macdonald, J. S. (1900). The demarcation current of mammalian nerve. I, II and III. *Proc. R. Soc. London* **67**, 310–328.

- Macdonald, J. S. (1905). The structure and function of nerve fibres. Preliminary communication. *Proc. R. Soc. London, Ser. B* **76**, 322–331.
- Marmont, G. (1940). Action potential artefacts from single nerve fibers. *Am. J. Physiol.* **130**, 392–402.
- Marmont, G. (1949). Studies on the axon membrane. I. A new method. *J. Cell. Comp. Physiol.* **34**, 351–382.
- Meyer, K. H., and Sievers, J. F. (1936). La perméabilité des membranes I. Theorie de la perméabilité ionique. II. Essais avec des membranes selective artificieles. *Helv. Chim. Acta* **19**, 649–995.
- Michaelis, L. (1922). "Die Wasserstoffonenkonzentration." Julius Springer, Berlin.
- Michaelis, L. (1925). Contribution to the theory of permeability of membranes for electrolytes. *J. Gen. Physiol.* **8**, 33–59.
- Nicolai, G. F. (1901). Ueber die Leitungsgwindigkeit im Riechnerven des Hechtes. *Pfluegers Arch. Gesamte Physiol. Menschen Tiere* **85**, 65–85.
- Osterhout, W. J. V., and Hill, S. E. (1933). Anesthesia produced by distilled water. *J. Gen. Physiol.* **17**, 87–98.
- Overbeek, J. Th. B. (1953). Donnan-E. M. F. and suspension effect. *J. Colloid Sci.* **8**, 593–605.
- Overton, E. (1902). Beiträge zur allgemeinen Muskel- und Nervenphysiologie. II. Ueber die Unentbehrlichkeit von Natrium- (oder Lithium-) Ionen für den Contractionsact des Muskels. *Pfluegers Arch. Gesamte Physiol. Menschen Tiere* **92**, 346–386.
- Overton, E. (1904). III Studien über die Wirkung der Alkali und Erdalkalisalze auf Skelettmuskeln und Nerven. *Pfluegers Arch. Gesamte Physiol. Menschen Tiere* **105**, 176–290.
- Pleijel, H. (1910). Die Potentialdifferenz zwischen zwei elektrolytischen Lösungen. *Z. Phys. Chem.* **72**, 1–37.
- Ranke, J. (1866). "Tetanus. Eine physiologische Studie." 468 pp. Wilhelm Engelmann, Leipzig.
- Retzius, G. (1890). "Ueber myelinhaltige Nervenfasern bei Evertebraten." Biol. Untersuch. N.F.I. Stockholm.
- Ringer, S. (1886). Further experiments regarding the influence of small quantities of lime, potassium and other salts on muscular tissue. *J. Physiol. (London)* **7**, 291–307.
- Sollner, K. (1945). The physical chemistry of membranes with particular reference to the electric behavior of membranes of porous character. II. *J. Phys. Chem.* **49**, 171–191.
- Spiegler, K. S., and Wyllie, M. R. J. (1956). "Electrical potential differences." In "Physical Techniques in Biological Research," (G. Oster and A. W. Pollister, eds.), Vol. 2, 301–392. Academic Press, New York.
- Steinbach, H. B., and Spiegelman, S. (1943). The sodium and potassium balance in squid nerve axoplasm. *J. Cell. Comp. Physiol.* **22**, 187–196.
- Tasaki, I. (1968). "Nerve Excitation. A Macromolecular Approach." Thomas, Springfield, Illinois.
- Teorell, T. (1935). An attempt to formulate quantitative theory of membrane permeability. *Proc. Soc. Exp. Biol. Med.* **33**, 282–285.
- Teorell, T. (1953). Transport processes and electrical phenomena in ionic membranes. *Prog. Biophys. Biophys. Chem.* **3**, 305–369.
- Teorell, T. (1956). Transport phenomena in membranes. Eighth Speirs Memorial Lecture. *Discuss. Faraday Soc.* **21**, 9–26.
- Tobias, J. M. (1948). The high potassium and low sodium in the body fluid and tissues of a phytophagous insect, the silkworm, *Bombyx mori*, and the change before pupation. *J. Cell. Comp. Physiol.* **31**, 143–148.
- Williams, L. W. (1909). "The Anatomy of the Common Squid, *Loligo pealii*, (Leseur)," Leiden.
- Young, J. Z. (1936). The giant nerve fibres and epistellar body of cephalopods. *Q. J. Micros. Sci.* **78**, 367–386.

9. Morphology and Biochemistry of the Squid Giant Axon

A. THE ULTRASTRUCTURE OF THE SHEATH COMPONENTS

The gross anatomy of the squid giant nerve fiber has been described by Young (1936; Chapter 8). Later, using a polarizing microscope, Bear *et al.* (1937a,b,c) revealed the complexity of the "sheath" of the giant nerve fiber. They noted that the axis-cylinder (or axon) is surrounded by a positively birefringent layer (called metatropic sheath) and then by another positively birefringent layer comprising several wrappings of fibrous connective tissue. They also found that the axoplasm of a freshly excised giant nerve fiber possesses positive birefringence with the optical axis roughly along the longitudinal axis of the fiber.

The ultrastructure of the giant nerve fiber was examined with an electron microscope by Geren and Schmitt (1954), Villegas and Villegas (1960), Baker *et al.* (1962), Adelman *et al.* (1977), and others. At a magnification greater than 10,000, many components which had not been seen under optical microscopes were revealed (see Fig. 9.1).

The surface membrane of the axon proper, known as the axolemma, was found to possess a thickness of about 80 Å. This membrane is known to consist of a pair of electron dense lines, each line being about 27 Å in thickness. When a small area of the axon surface is examined, the axolemma appears to be surrounded by 3–6 layers of very thin and flat cells, called Schwann cells. The thickness of the Schwann cells varies from 0.1 to 0.2 μm, except in the region of their nuclei where it increases up to about 1 μm. According to Adelman *et al.* (1977), the surface membrane of a single Schwann cell extensively interdigitates with the neighboring cells; this situation gives rise to a false impression that there are many separate satellite cells outside the giant axon.

Outside the Schwann cell layer, there is an homogeneous layer of low electron density of 0.1 to 0.3 μm in thickness; this layer is called the base-

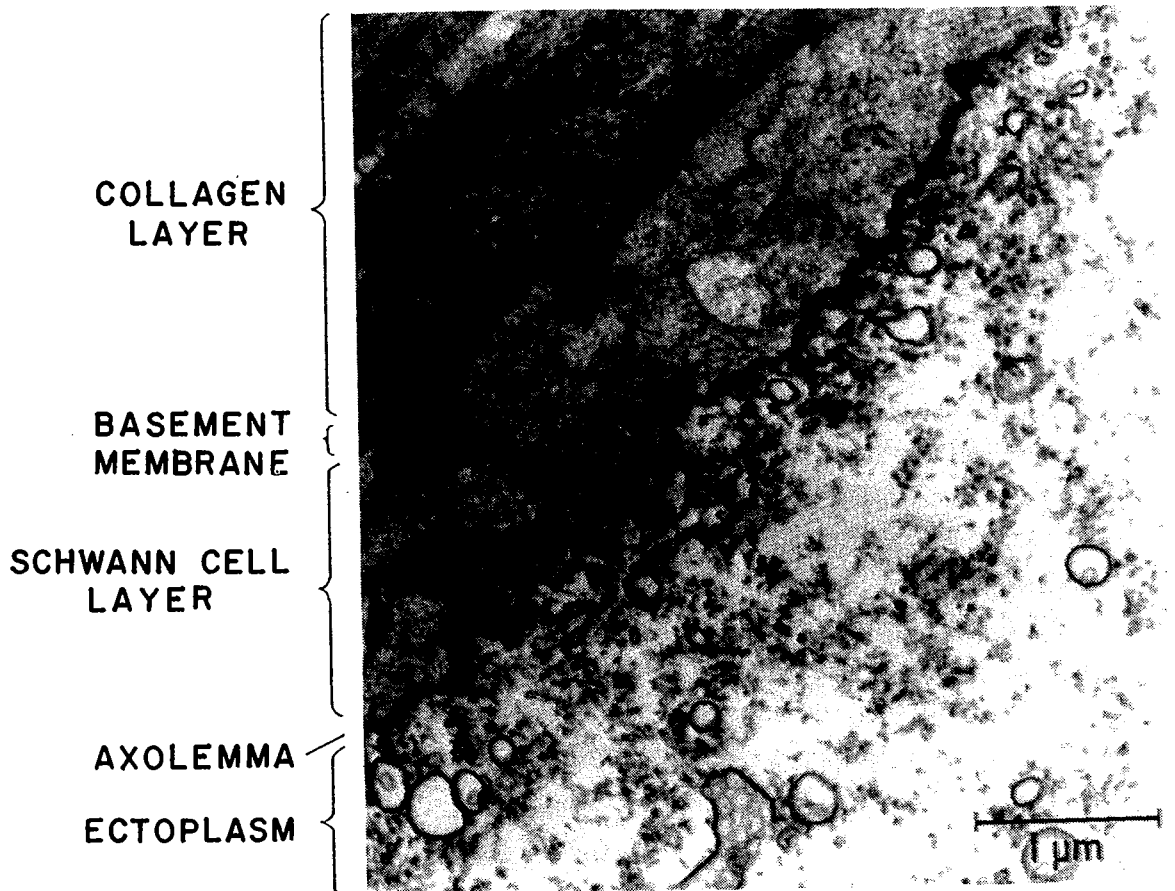


Fig. 9.1 Transmission electronmicrograph of a cross-sectioned squid giant nerve fiber. The specimen was fixed with 2% glutaraldehyde in natural seawater (for 3 hr at 22°C), postfixed with 1% osmium tetroxide in a 0.2 M sodium cacodylate buffer (for 1.5 hr at 4°C). Then it was *en bloc* stained with 1% uranyl acetate in water (for 1 hr at 22°C). After dehydration with ethyl alcohol, the specimen was embedded in Spurr's resin. (S. Terakawa, unpublished.)

ment membrane. The basement membrane is surrounded further by connective tissue cells and collagen bundles. From these findings, it follows that, even in a well-cleaned preparation of a squid giant nerve fiber, the giant axon proper (i.e., the axis-cylinder) is separated from the external bathing seawater by a "sheath" of 10–20 μm in thickness.

The complex ultrastructure of a giant nerve fiber as revealed by electron microscopy raised the following question. Is the axolemma actually the major diffusion barrier between the axoplasm and the external seawater? Can the Schwann cell and connective tissue layer be ignored in the consideration of the membrane potential?

Electron microscopic studies on this point strongly suggest that the space between the axolemma and the Schwann cell plasmalemma is directly connected to the external fluid medium through narrow channels separating individual Schwann cells. The axolemma is separated from Schwann cells by a space of 80 Å in thickness and individual Schwann cells are surrounded by a 60-Å-wide space.

There is direct experimental evidence indicating that these channels are filled with a medium with low resistivity. Villegas *et al.* (1962) and Villegas (1972) reported that in the giant nerve fiber of the squid, *Sepioeuthis sepioidea*, the Schwann cells are unusually thick and these cells could be penetrated with a hyperfine microelectrode. They could record the resting membrane potential of these cells (-33 to -46 mV) and saw that this potential level is quite distinct from that inside the giant axon. When the giant axon was stimulated to evoke a propagated action potential, the microelectrode inserted into the Schwann cell registered only a small potential variation (less than a few millivolts in amplitude) which could be interpreted as a sign of spread of electricity from the giant axon. From these observations, it seems safe to conclude that the axolemma is really the "semipermeable membrane" in the sense of Ostwald and Nernst (see Chapter 2, Section F).

The situation that the periaxonal space is only indirectly connected to the external fluid medium creates serious complications in some electric measurements. One of these complications was pointed out by Frankenhaeuser and Hodgkin (1956) who recognized the effect of a stagnant layer outside the giant axon following repetitive stimulation of the giant fiber.

We believe that the hindrance of free diffusion by Schwann cells is of special importance to the studies of transient (i.e., time-dependent) phenomena in the nerve membrane. For example, the arrangement of the Schwann cell membrane relative to the axolemma may lead to a complication in the procedure of voltage clamping. It is reasonable to assume that the Schwann cell membrane has approximately the same capacity per unit area as the axolemma. If this is the case, a sudden shift of the potential difference across the entire surface layers of the giant nerve fiber is expected to bring about a potential jump across individual Schwann cell membranes, as well as across the axolemma. The potential difference across the Schwann cell membrane is expected to dissipate rapidly. However, it is difficult to estimate the rate of this dissipation at present.

In conclusion, it is important to remember that the ultrastructure of the squid giant nerve fiber is very complex. Under certain circumstances, the sheath of the giant fiber may be treated as a simple membrane with a definite capacity and resistance. Under different circumstances, however, such treatment may lead to serious difficulties.

B. ELECTROLYTES, PROTEINS, AND LIPIDS IN THE AXOPLASM

Chemical studies of the axoplasm of the squid giant nerve fiber were undertaken first by Bear and Schmitt (1939) and by Steinbach and Spiegelman (1943, see Chapter 8). Later, Koechlin (1955) examined dialyzable anions

TABLE 9.1
Concentrations of Dialyzable Cations and Anions in the Squid Axoplasm^a

Anions	$\mu\text{Eq/gm axoplasm}$	Cations	$\mu\text{Eq/gm axoplasm}$
Chloride	140 ± 20	Potassium	344 ± 20
Phosphates	24 ± 4	Sodium	65 ± 10
Aspartic acid	65 ± 3	Calcium	7 ± 5
Glutamic acid	10 ± 3	Magnesium	20 ± 10
Fumaric acid	15 ± 5	Organic base	84 ± 20
Succinic acid	35 ± 10	(by difference)	
Sulfonate "X"	220 ± 20	Total base	520 ± 20
Isethionic acid	509 ± 20		
Total			

^a From Koechlin, *J. Biophys. Biochem. Cytol.* **1**, 521, 1955.

and cations in the extruded axoplasm by using various chemical techniques.

Table 9.1 shows the results obtained by Koechlin. In this table the concentrations of the electrolytes are expressed in micromoles per gram of wet axoplasm. It is seen that isethionic acid, $\text{HOCH}_2\text{CH}_2\text{SO}_3\text{H}$, and Cl^- are the major anion species. The main cation species in the axoplasm are potassium and sodium. According to Steinbach and Spiegelman (1943; cited in Chapter 8), the Na-ion concentration gradually rises and the K-ion concentration falls with time while the axon is kept in seawater. It is important to note that the sum of the intracellular Na- and K-ion concentrations remains constant for many hours after excision, suggesting that the axon membrane has properties of a cation exchanger. The existence of fixed negative charges in the sense of Teorell (1935, see Chapter 8) will be discussed later (see Chapter 11, Section D).

In Table 9.1, the observed value of Ca-ion concentration is misleading. Applied intracellularly, an isotonic salt solution containing Ca-ions higher than about 1 mM quickly destroys the fibrillar protein structure beneath the axolemma and suppresses the ability of the axon to develop action potentials (see Chapter 11, Section I). It is evident that the figure in the table, 7 mEq/liter, represents Ca-ions bound to the calcium-binding structure in the axoplasm (Henkart *et al.*, 1978). Recent studies suggest that the concentration of free Ca-ion in the axoplasm appears to be between 10 and 100 nM.

Proteins in squid axon axoplasm were examined first by Bear *et al.* (1937c). The solubility of the extruded axoplasm was studied using distilled water, neutral salt solution, and acidic and alkaline solutions as solvents. They found that the major protein species in the axoplasm is labile and changes into a relatively insoluble form in dilute acid. It is more soluble in isotonic neutral solutions of KCl or NaCl than in distilled water. In seawater,

extruded axoplasm was found to disintegrate immediately and go into solution (Hodgkin and Katz, 1949). Later, Maxfield (1953) made a serious attempt at characterizing axoplasmic proteins using the ultracentrifuge and electrophoresis apparatus. He isolated a protein by fractional extraction followed by differential ultracentrifugation and then characterized the properties of the proteins.

Later, the interest of the investigators in the field was directed toward characterizing two fibrillar proteins in the axoplasm, neurofilaments and microtubules. In axons fixed with glutaraldehyde, these structures are visible under the electron microscope. Huneus and Davison (1970) stated that neurofilaments, 100 Å in diameter, are assemblies of acidic proteins. They also isolated tubulin that is known to selectively bind colchicine (Davison and Huneus, 1970). Microtubules, which are formed by polymerization of tubulin molecules (55,000 and 57,000 MW), can be readily demonstrated in the axoplasm by transmission electron microscopy as tubules of about 200 Å in diameter. Actin molecules (45,000 MW) have been demonstrated in the axoplasm (Metuzals and Tasaki, 1978). It is generally believed that these fibrillar protein elements constitute the structural basis of protoplasmic flow (Weiss and Hiscoe, 1948; see Ochs, 1974, for recent progress on this subject).

Beside these fibrillar protein elements, there are a large number of proteins in the squid axoplasm. Furthermore, the molecular weight profile of proteins appears to vary with the distance from the axolemma (Yoshioka *et al.*, 1978). The total amount of axoplasm available for this type of analysis of a single giant axon is roughly 2 to 3 mm³. About 3% of the weight of this (wet) axoplasm is proteins that can be radioactively labeled with iodine-125. The Bolton–Hunter reagent for radioiodination permits detection of a fraction of a microgram of protein (Bolton and Hunter, 1973). The two-dimensional molecular weight profile has been determined by polyacrylamide gel electrophoresis following isoelectric focusing. By the silver staining method (Merril *et al.*, 1979), it is now possible to estimate both the molecular weight and the isoelectric point of polypeptide species of less than 1 ng. Small proteins in the axoplasm include calmodulin (Kakiuchi *et al.*, 1970; Cheung, 1980) and the Ca-binding acidic protein characterized by Alema *et al.* (1973). The isoelectric points of axoplasmic proteins are all between 6.5 and 4.0.

The first report on the lipids of the squid giant nerve fiber appeared in 1950 (McColl and Rossiter, 1950). They measured total lipid, cholesterol, and amino- and diamino-phospholipids in the whole giant fiber and in the extruded axoplasm, and they found that the lipid content (expressed in percent wet weight) is much higher in the nerve fiber sheath (i.e., in the fiber with its axoplasm extruded) than in the axoplasm. Later, Condrea and Rosenberg

TABLE 9.2

Phospholipids in Squid Giant Nerve Fiber, in the Sheath, and in the Axoplasm^a

Phospholipids	Total nerve fiber	Sheath	Axoplasm
Phosphatidyl-ethanolamine	31 ± 1	28 ± 1	31 ± 2
Phosphatidyl-serine	8 ± 0.3	11 ± 1	7 ± 1
Phosphatidyl-inositol	5 ± 0.2	5 ± 0.4	7 ± 1
Lecithin	45 ± 1	40 ± 2	5 ± 1
Sphingomyelin	11 ± 0.2	16 ± 1	0

^a Expressed as percentages of the total lipid phosphorus recovered. (From Condrea and Rosenberg, *Biochim. Biophys. Acta* **150**, 274, 1968.)

(1968) carried out a thorough investigation of these lipids. Table 9.2 shows the results obtained by these investigators using the method of chloroform-methanol extraction followed by thin-layer chromatography. It is to be noted that a typical lipid in the vertebrate myelin sheath, sphingomyelin, is present in the nerve fiber sheath.

In giant axons *in vivo*, the chemical composition of the axoplasm is maintained, obviously, by local and central metabolic processes. In excised giant axons, intracellular application of many metabolically active materials has no effect on the action potential of the axon (Brady *et al.*, 1958).

C. THE ULTRASTRUCTURE OF THE ECTOPLASM

The protoplasm that fills the interior of the squid giant axon is far from being a homogeneous solution of the electrolytes and proteins. Bear *et al.* (1937b) showed that the axoplasm of a freshly excised giant nerve fiber possesses positive, uniaxial birefringence with its optical axis oriented roughly along the longitudinal axis of the fiber. They noted that this birefringence vanishes almost completely when the fiber is kept in seawater for about 3 hr. Furthermore, they demonstrated that the major portion of the optical anisotropy of the axoplasm fixed with ethanol and HgCl₂ is an expression of form birefringence due to the presence of longitudinally oriented fibrillar elements.

Later, Metzuzals and Izzard (1969) and Metzuzals (1969) examined fibrillar elements in the axoplasm using differential interference microscopy as well as by the standard electron microscopic method. They showed that these elements, oriented predominantly in the longitudinal direction of the fiber, form a three-dimensional network by virtue of cross bridges. They also

found that these fibrillar elements are closely packed in the protoplasm near the axolemma, namely, in the ectoplasm. From these findings, it is evident that the birefringence of the fresh axoplasm is produced by the fibrillar elements. The gradual loss of the axoplasmic birefringence of a nerve fiber in seawater is attributable to slow disintegration of the network associated with a gradual rise of calcium and other external ions in the axoplasm.

A further advance in our understanding of this three-dimensional network of fibrillar elements near the axolemma was brought about by scanning microscopy of the axon used in conjunction with the method of intracellular perfusion (Metuzals and Tasaki, 1978). By adding a small amount of pronase, a nonspecific proteolytic enzyme, to the intracellular perfusion fluid, it is possible to mildly digest proteins in the axon interior. Under these experimental conditions, the action of pronase proceeds from a deep layer of the axoplasm toward the surface of the axon. The digestive process can be suspended by washing out the axon interior with an enzyme-free solution.

Figure 9.2 is an example of scanning microscope pictures of pronase-treated ectoplasm taken recently by S. Terakawa. The existence of longitudinally oriented fibrillar elements beneath the axolemma is clearly seen. It is to be noted that there is a small (5° to 10°) angle between the orientation of these elements and the long axis of the axon.

It is easy to demonstrate that there is a mechanical connection between the fibrillar structure in the ectoplasm and the axolemma. During the process of insertion of a beveled cannula, the fibrillar elements become visible near the posterior part of the orifice of the cannula (see Metuzals and Tasaki, 1978). The visibility of this structure is enormously increased when the giant nerve fiber is placed between two sheets of Polaroid film. Under the cross-polar conditions, the fibrillar structure appears either as a bright or dark band depending on the orientation of the polarizing axes of the polarizer and analyzer. By rotating the plane of polarization of the light used for illumination, it was possible to demonstrate that the structure is firmly attached to the surface of the axon.

The attachment of the ectoplasmic fibrillar elements can easily be broken by protease treatment. This attachment can be disrupted also by perfusion of the interior of an axon with an isotonic KCl solution. It is known that, under continuous intracellular perfusion with KCl, the axon loses its ability to develop action potentials usually within 30 min. When such an inexcitable axon is fixed and examined under an electron microscope (Metuzals and Tasaki, 1978), it is found that the major portion of the ectoplasm has been removed during perfusion. In some areas, the axolemma is found to be almost naked, indicating that the fibrillar protein elements are solubilized and washed out during perfusion with a KCl solution.

The observations described above lead to the conclusion that the compact layer of fibrillar proteins attached to the inner surface of the axolemma is

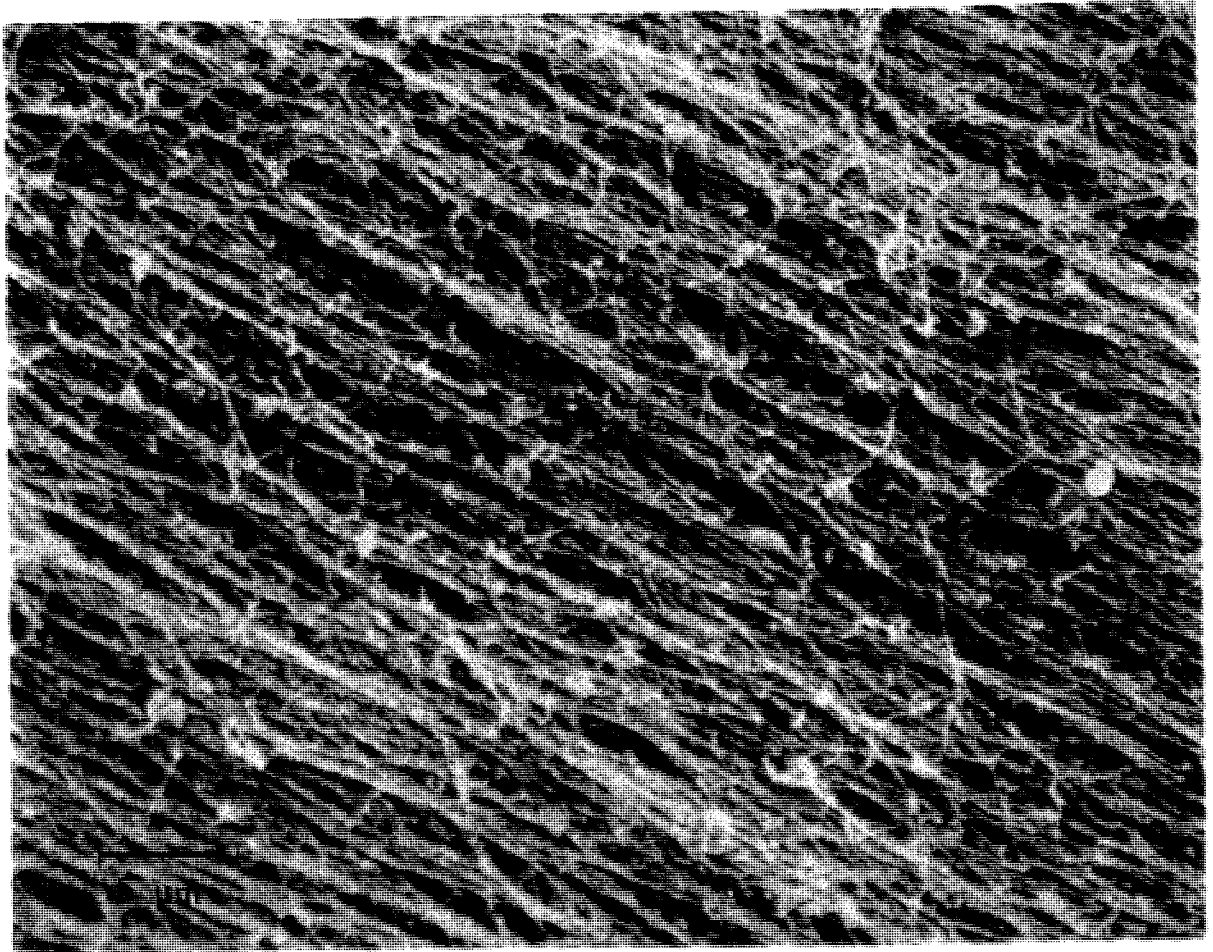


Fig. 9.2 Scanning electronmicrograph of the ectoplasm of a squid giant axon. The axon was intracellularly perfused with a 400 mM K-salt solution. During the initial 10 min period of the perfusion, the interior of the axon was treated with 0.05 mg/ml pronase dissolved in the perfusion solution. About 40 min after the pronase treatment, the axon (which showed normal excitability) was fixed with 2% glutaraldehyde added to the external seawater. After a 3-hr fixation, the axon was cut open and the structure on the inner side of the axolemma was photographed with a scanning microscope. (S. Terakawa, unpublished.)

essential for the maintenance of normal excitability of the axon. When this layer is removed by either proteolysis or solubilization by internal perfusion with various salt solutions, the axon becomes incapable of developing normal action potentials.

D. RELEASE OF SUBMEMBRANOUS PROTEINS DURING EXCITATION

The following observations show that the relatively compact layer beneath the axolemma is loosened and protein molecules in this layer are released into the axon interior during repetitive stimulation. The technique of

intracellular perfusion (see Chapter 11, Section A) was used in order to demonstrate this effect of repetitive stimulation. Initially, the major portion of the axoplasm was removed by a brief treatment of the axon interior with a dilute pronase solution. Under continuous internal perfusion with a potassium fluoride solution, protein molecules in the submembranous structure (about $1\ \mu\text{m}$ thick) are released into the perfusion fluid at a low rate. The effect of high-frequency stimulation of the axon was examined at the time when the rate of protein release was low and more-or-less constant.

Axons internally perfused with a KF solution and immersed in a mixture of Ca- and Na-salt are highly excitable; the action potential produced lasts only 1 msec or less. Figure 9.3A shows that, when such an axon was stimulated at a frequency of 60/sec, there was a marked increase in the rate of protein release. Since the total amount of proteins in the submembranous structure was limited, a high rate of protein release could not be maintained. The ability of the axon membrane to develop action potential was severely hampered when a large portion of the proteins was removed by repetitive stimulation.

The molecular weight distribution of the proteins released under these conditions was determined by the method of SDS-polyacrylamide gel electrophoresis (Pant *et al.*, 1978). The major peak in the observed molecular weight profile was located at about 12,000 daltons. Two additional peaks were seen, one at about 45,000 daltons and another at about 68,000 daltons.

The duration of the action potential can be enormously prolonged with

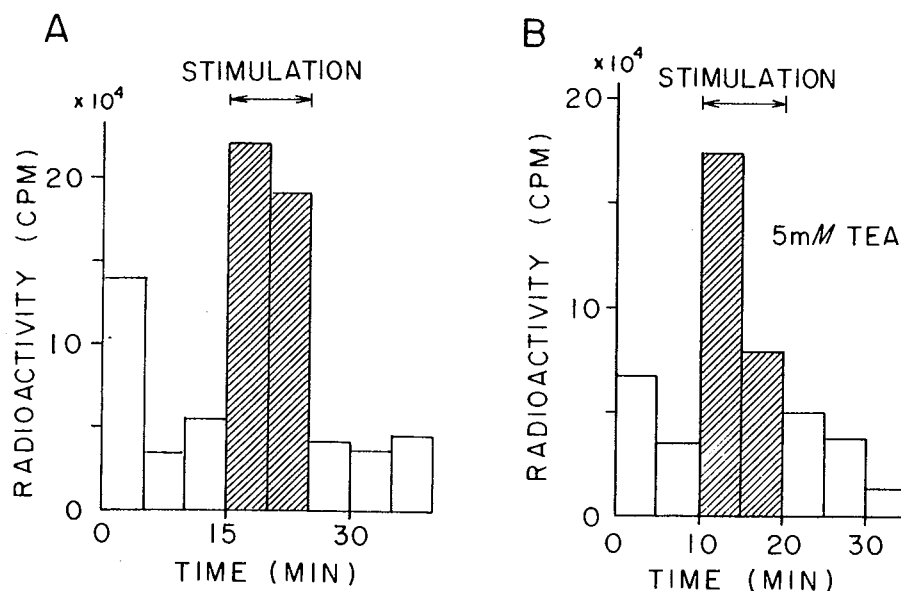


Fig. 9.3 The effect of repetitive stimulation on the rate of release of submembranous proteins into the perfusion fluid. The proteins released were detected by the radioiodination method. (From *Biochim. Biophys. Acta* 513, 136, 1978.)

tetraethylammonium salt added to the internal perfusion solution (see Chapter 10, Section B). In such TEA-treated axons, the rate of protein release could be markedly enhanced by electric stimuli repeated at about 10-sec intervals (see Fig. 9.3B). There is little doubt that the process of protein release proceeds during the plateau of the prolonged action potential.

Following replacement of a large portion of the external Na-salt with K-salt, the axon membrane remains indefinitely in its "depolarized" state (see Chapter 8, Section D). There is a large increase in the rate of protein release when about 40% of the external Na-ion is replaced with K-ion (Gainer *et al.*, 1974; Inoue *et al.*, 1976).

The experimental findings described above indicate that various types of physiological manipulation of the external membrane surface bring about a marked change in the conformational state of the submembranous protein molecules. Since the axon loses its excitability when the submembranous protein layer is destroyed by chaotropic or proteolytic reagents (see Chapter 11, Section B), the layer of ectoplasm should be treated as a part of the excitable membrane.

A possible mechanism of protein release is now considered. During repetitive stimulation of the axon, there is a marked increase in the influxes of Na- and Ca-ions (Chapter 11, Sections H and I). Under intracellular perfusion with a K-salt solution, highly mobile Na-ions derived from the external medium are expected to be promptly removed by the perfusion fluid. In the protein layer, Ca-ions are only semimobile (see Chapter 11, Section I). A rise in the Ca-ion concentration in the submembranous protein layer may therefore be regarded as the cause of protein release. We shall see in subsequent chapters that, in the external membrane layer, Ca-ions stabilize the structure by forming Ca-bridges. In the inner membrane layer, on the contrary, Ca-ions destabilize the structure, probably by weakening the electrostatic attraction (or salt linkage) between molecules.

In addition to the possible mechanism mentioned above, there is a possibility that the swelling of the axon membrane during excitation directly destabilizes the fibrillar structure in the ectoplasm (see Chapter 15, Section B).

E. CHEMICAL MODIFICATION OF PROTEINS IN THE AXON

Proteins can be modified chemically by various reagents which are known to selectively attack certain groups or bonds (see, e.g., Means and Feeney, 1971). If the protein molecules which are located at crucial sites in the axon membrane are chemically modified by such reagents, it is expected that the ability of the axon to develop normal action potentials is impaired.

By this method of chemical modification, it is possible to characterize the proteins essential for the maintenance of axon excitability. This approach was initiated by Smith (1958) and developed by Huneus *et al.* (1966), Cooke *et al.* (1968), Shrager *et al.* (1969), Shrager (1975), and others.

Quite recently, the effects of a large number of protein-modifying reagents were systematically examined using both squid giant nerve fibers and crab nerve fibers (Baumgold *et al.*, 1978). The main difficulty encountered in these studies is that the chemical reaction has to be carried out within the physiological range of pH and salt composition. The solubility of the reagents in water and lipids also imposes a great limitation to studies of this type. It is difficult to examine the effects of reagents that are poorly soluble in aqueous media, because the reagents have to be delivered by dissolving them in either artificial seawater or intracellular salt solution. When the reagents are applied intracellularly, the diffusion barrier at the surface of the nerve fiber presents no serious problem. However, the accessibility of the reagents to the prospective targets can and does complicate the interpretation.

1. Sulfhydryl Reagents

Various maleimides (*N*-ethylmaleimide, *N*-butylmaleimide, and unsubstituted maleimide) are known to form covalent bonds with sulfhydryl groups in proteins at pH higher than about 5 (p. 110 in Means and Feeney, 1971). These reagents also attack amino groups in alkaline media. When applied to squid nerve fibers intracellularly and to crab nerves extracellularly, all these reagents bring about a rapid loss of excitability.

Acrylonitrile is known to block sulfhydryl groups at pH higher than 6.5; when applied extracellularly, this reagent has little or no effect on the excitability of the nerve fibers. In contrast, 2-vinylquinoline, a highly lipid-soluble analog, is found to be effective in suppressing excitability. Acrylonitrile is not very soluble in hydrophobic solvents, such as olive oil.

Iodoacetate is known to react with various groups in proteins; it reacts most rapidly with sulfhydryl groups. Intracellular application of iodoacetate to a squid giant nerve fiber causes conduction block within a short time. When applied to crab nerves extracellularly, no distinct effect is observed. In contrast, 2-bromoacetamido-4-nitrophenol, a halide that is highly soluble in lipids, does bring about conduction block in crab nerves. The ineffectiveness of iodoacetate in crab nerves may then be attributed to its poor lipid solubility which prevents this reagent from penetrating the hydrophobic layer of the nerve membrane. A logical inference from these facts is that the sulfhydryl group we are dealing with is located on the inner (i.e., axoplasmic) side of the nerve membrane.

One of the reagents which is known to react only with sulfhydryl groups of proteins is 5,5'-dithiobis(2-nitrobenzoic acid). When applied to squid giant nerve fibers intracellularly, this reagent is found to block conduction very readily. In crab nerve (external application), this compound has no clear effect. Again, a highly lipid-soluble analog of this compound, 4,4'-dithiopyridine, is effective in blocking nerve conduction in crab nerves.

Mercurials, such as *p*-chloromercuribenzoate (PCMB), mercuric chloride, and fluorescein mercuric acetate, are very effective reagents which attack sulfhydryl groups. They are highly effective in suppressing excitability of squid giant nerve fibers and crab nerves.

Hydrogen peroxide suppresses the excitability of the squid giant axon. This effect may also be attributed to the modification of sulfur-containing amino acids, principally cysteine and methionine.

These studies with sulfhydryl reagents strongly suggest that the protein molecules at the sites critically important for the maintenance of excitability possess —SH groups. Chemical modification of these groups interferes with the process of action potential production. Furthermore, these —SH groups are accessible far more readily from the inner (i.e., axoplasmic) side of the membrane than from the outer side. These groups appear to be buried in a compact, more or less hydrophobic portion of protein molecules, because as a rule amphipathic reagents are found to be more effective in suppressing excitability than those with limited lipid solubility.

2. Amino Group Modifying Reagents

In squid nerve fibers, diketene (0.5 mM), ethyl acetimidate (2 mM), and 2,4,6-trinitrobenzene sulfonate (2 mM) were found to suppress excitability when tested by the technique of intracellular perfusion. Unfortunately, the effects of these reagents are not limited to amino groups. Since these reagents are known to attack sulfhydryl groups also, it is not safe to conclude from these observations that modification of amino groups alone leads to a loss of excitability.

3. Histidine Modifying Reagents

Photodynamic oxidation of protein after sensitization with rose bengal or methylene blue is considered to be highly selective for histidine (see Bellin and Yankas, 1968). When squid nerve fibers stained internally with these dyes are exposed to light, a rapid decline in the action potential is observed followed by complete loss of excitability. This loss of excitability by dye-sensitized photooxidation is preceded normally by subthreshold oscillation of

the membrane potential (see Chapter 10, Section E) and spontaneous firing of action potentials. In a Ca-rich medium, photooxidation can suppress excitability of squid giant nerve fibers without being preceded by spontaneous firing of action potentials. When applied extracellularly, these dyes do not produce detrimental effects on the axon excitability under strong illumination.

The harmful effect of a large number of oxidizing reagents has been demonstrated in squid giant axons by internal injection of the reagents. It is interesting to note in this connection that a strong reducing reagent, sodium sulfite, exerts no detrimental effect on excitability.

4. Cleavage of Proteins with Cyanogen Bromide

According to Gross and Witkop (1962), cyanogen bromide cleaves peptide bonds involving methionine residues selectively. This reagent quickly suppresses the excitability when applied internally by the technique of intracellular perfusion. This observation suggests that the protein molecules involved in the maintenance of excitability contain methionine.

5. Proteolytic Enzymes

The use of a proteolytic enzyme is the oldest means of altering protein molecules in the nerve fiber. When applied extracellularly, proteolytic enzymes have no effect on the excitability of the nerve fiber (Tobias, 1960). These enzymes exert strong detrimental effects on squid giant nerve fibers when introduced into the axon interior by the method of intracellular perfusion (Tasaki and Takenaka, 1964). In these early studies, an isotonic solution of potassium aspartate was used to dissolve the proteases. It is important to note that the effectiveness of the proteolytic enzyme is strongly affected by the chemical species of the anions and cations in the perfusion fluid.

Carboxypeptidase is known to attack the peptide bond next to the C-terminals of proteins. Trypsin cleaves the bonds next to lysine or arginine. The effectiveness of these proteases to suppress the excitability of the squid nerve fiber attests to the presence of both positively and negatively charged groups in the protein molecules which occupy the crucial sites (see Chapter 9, Section D). Some proteases (e.g., papain, pronase) were shown to cause a marked prolongation of the action potential duration (see also Takenaka and Yamagishi, 1966). The nature of the relaxation processes which determine the action potential duration will be discussed later (see Chapter 13, Section H). The observations described here lead to a general picture of the protein molecules which affect the axon excitability.

F. MODELS OF THE PLASMA MEMBRANE

Direct biochemical analyses of various biological membranes indicate that the membrane consists of proteins, lipids, and polysaccharides. The problem before us now is to consider how these macromolecular components are arranged and organized in the membrane. Recently, electron microscopic techniques have furnished valuable information as to the molecular organization of the plasma membrane. Due to various limitations of the techniques, however, the information obtained is insufficient to uniquely determine the relative positions of these macromolecular components in the membrane.

In the past, various investigators have proposed models of plasma membrane, postulating specific arrangements of proteins and lipids in the membrane. The oldest is the lipid bilayer model of Gorter and Grendel (1925) and of Danielli and Davson (1935). In this model, the cell surface is assumed to be completely covered by two layers of lipid molecules, with their hydrophobic terminals facing each other (see Stockenius and Engelman, 1969). Both the inner and outer surfaces of the bilayer are covered by protein molecules. This model does not account for the sidedness of the membrane and fails to explain the fact that some protein molecules can be labeled covalently on either side of the membrane (see Betscher, 1973; Rothman and Lenard, 1977).

At present, the most popular model of the plasma membrane appears to be the fluid mosaic model of Singer and Nicolson (1972). In this model, protein molecules are floating in a fluid layer made of lipid bilayer (Fig. 9.4). The term "intrinsic proteins" or "integral proteins" is used to denote the protein molecules which penetrate the bilayer partially or completely. The protein molecules attached to the inner surface of the bilayer are referred to as "peripheral proteins" (Singer, 1974). Analyses of the erythrocyte membrane is most advanced in this field of research (see Steck and Fox, 1972; Steck, 1974).

In postulating the fluid mosaic model, it is evident that the process of electrophysiological excitation has *not* been taken into consideration. However, it is easy to slightly modify this model and to incorporate Loeb's notion (see Chapter 3, Section C) of neutralization of acidic proteins with Na- and Ca-ions. We assume that the external layer of the intrinsic proteins possesses a high density of negatively charged groups. At and near the external surface of the membrane, the negative fixed charges are neutralized mainly by calcium and, to some extent, by Na-ions. The peripheral proteins of the model are assumed to be an extension of the compact layer of undercoating seen with the scanning electron microscope (see Chapter 9, Section C). The lipid bilayer is perforated by many protein molecules which are not directly in-

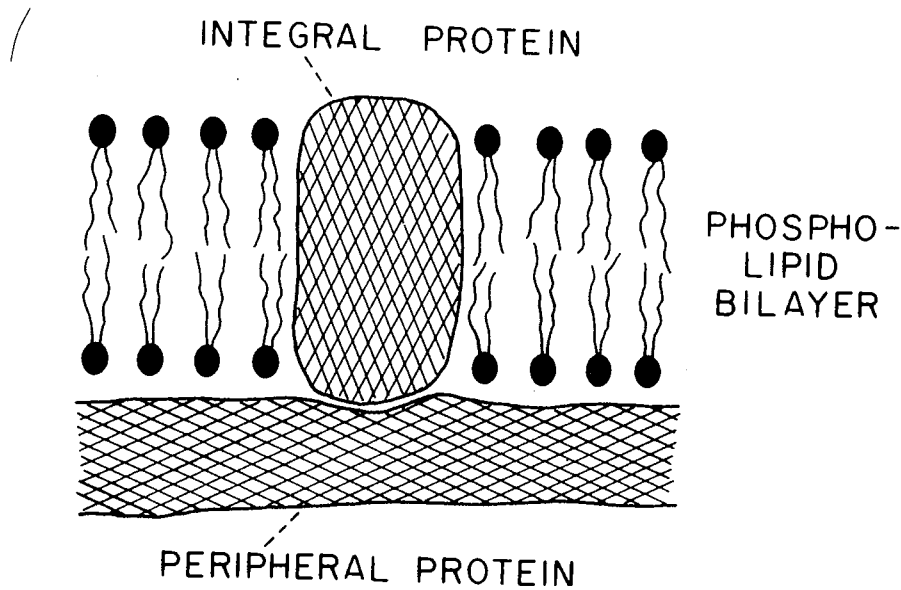


Fig. 9.4 Membrane model suggested by Singer and Nicolson slightly modified for the purpose of explaining electrophysiological properties of axons.

involved in the process of excitation. Nevertheless, these protein molecules are expected to bestow a relatively low electric resistance upon the axon membrane at rest. This version of the fluid mosaic model explains many aspects of the electrophysiological behavior of the squid axon membrane (see Chapter 13, Section E).

G. BINDING OF TETRODOTOXIN TO THE NERVE MEMBRANE

Tetrodotoxin (TTX) is a potent toxic compound found mainly in the ovary and liver of the pufferfish encountered primarily off the coast of the southern part of Japan. At an extremely low concentration, this poison is capable of suppressing excitability of most nerve fibers (see Moore *et al.*, 1967). Its molecular weight (349), formula ($C_{12}H_{19}O_9N_3$), and structure were determined in the middle 1960s, although the name "tetrodotoxin" was given to the compound much earlier (see Tahara, 1911). An authoritative historical account of this compound is given by Kao (1966). There are a number of reviews describing pharmacological actions of TTX (see, e.g., Narahashi, 1974).

Here, we shall not attempt to go into the details of numerous experiments dealing with the effects of TTX on nerve fibers; we shall discuss some aspects of TTX effects on nerve fibers in several subsequent sections (see Chapter 10, Section K, and Chapter 11, Section C). In accordance with the strata-

gem adopted consistently in this book, this section is primarily addressed to the results of chemical and physicochemical studies involving TTX.

According to Goto *et al.* (1965), pure TTX is a white crystalline powder which darkens at 220°C without melting. It shows no absorption in the visible and near UV range of light. It is soluble only in acidic media. Neutralization of TTX in 10 mM KCl solution with KOH indicates that there is a single dissociable group with pK_a 8.76. This value of pK_a reflects the property of a hydroxyl group; the pK_a of the guanidine groups is about 11.5. TTX is unstable in both alkaline and strongly acidic media; it is also unstable at high temperature. A variety of decomposition products with little or no toxicity are known (see Kao, 1966).

Hafemann (1972) showed that TTX could be tritiated by the silent electric discharge method. The radioactive preparation of TTX can be purified and utilized for studying the mode of binding of TTX to the lobster nerve membrane. The tritiated preparation of TTX was used immediately by Ritchie and collaborators (Colquhoun *et al.*, 1972; Henderson *et al.*, 1974), by Raftery and co-workers (Benzer and Raftery, 1972; Reed and Raftery, 1976), and by Villegas and others (Barnola *et al.*, 1973) to elucidate the process of TTX binding to the nerve membrane of various animals. For the purpose of carrying out similar experiments, Henderson *et al.* (1974) used tritium-labeled saxitoxin (STX), another paralytic toxin isolated from the dinoflagellate, *Gonyalax cantenella*. The results obtained by different investigators are quite consistent, indicating that this method of studying excitable membranes is sensitive and reliable.

The upper graph in Fig. 9.5 shows an example of the data obtained by Baumgold (1980) using tritiated STX. It is seen that the amount of radioactive STX bound to the nerve membrane material increases sharply with the STX concentration in the medium. When the concentration becomes higher than about 10 nM, however, there is only a small increase in STX binding, indicating that the major fraction of the binding sites is already occupied by STX. Let θ denote the fraction of the sites occupied by STX. Then, the equilibrium between the binding sites and the free STX in the medium, [STX], is given by

$$\frac{(1 - \theta)[\text{STX}]}{\theta} = K$$

where K is the dissociation constant. This equation can be rewritten in the following form:

$$\frac{1}{\theta} - 1 = K \frac{1}{[\text{STX}]}$$

The lower graph in Fig. 9.5 indicates that the observed value of $1/\theta$ varies linearly with $1/[\text{STX}]$, as expected from the equation above. This type of

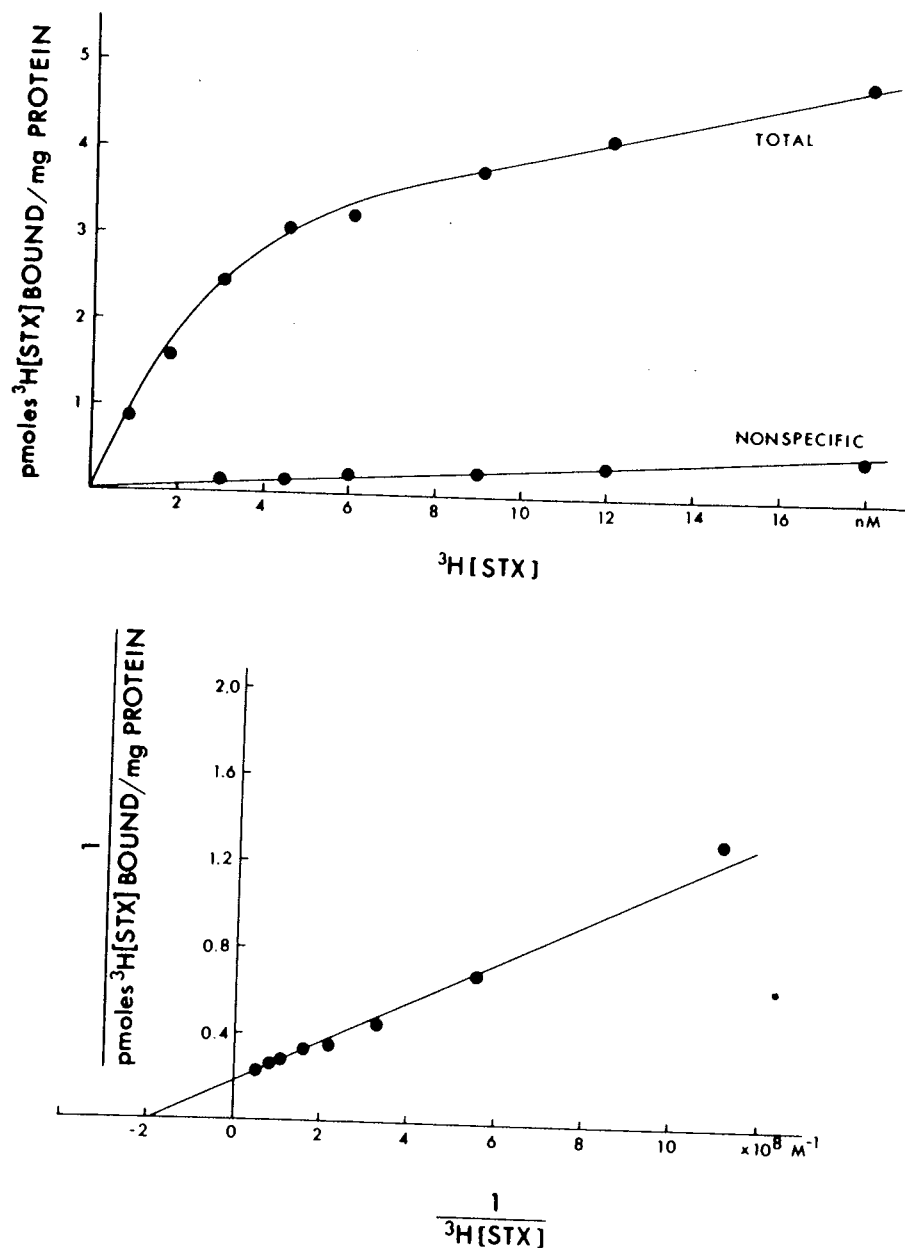


Fig. 9.5 Binding of tritiated saxitoxin to nerve membrane material. The values marked "nonspecific" indicate the results obtained in the presence of excess nonradioactive TTX. The double-reciprocal plot of the difference between the total and the nonspecific binding, shown in the lower graph, indicates that the dissociation constant of the reaction is about 2 nM. (From Baumgold, 1980.)

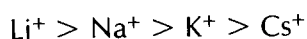
binding study has been carried out with both STX and TTX using homogenized membrane material, as well as intact axons. The dissociation constants obtained from these measurements were usually between 2 and 10 nM.

From these observations, it was found that the radioactive STX and TTX act as a faithful marker of the excitable membrane sites. It is to be noted that such TTX binding sites with a high affinity are not encountered on the sur-

face of the erythrocyte membrane or of the myelin sheath. By measuring the radioactivity per unit area of the external surface of the membrane, the surface density of the TTX molecules can be estimated. The number of TTX-binding sites estimated by this method was found to vary between about $4/\mu\text{m}^2$ (Benzer and Raftery, 1972) and $550/\mu\text{m}^2$ (Levinson and Meves, 1975) depending on the type of nerves examined. Originally, the surface density of the TTX-binding sites was estimated by an electrophysiological method by Moore *et al.* (1967). The results obtained by different methods are in general agreement.

The TTX-binding property of the membrane sites is retained even when the nerve fibers are broken down into small fragments and solubilized with a mild detergent (e.g., Triton X-100). However, mild digestion of the solubilized membrane material with proteases completely suppresses the TTX-binding activity. Therefore, there is little doubt that the TTX-binding membrane material is proteinaceous in nature. The fact that strong detergents suppress TTX-binding activity of the solubilized membrane material suggests that here we are dealing with lipoprotein complexes.

Addition of various salts of alkali metal ions to solubilized membrane material markedly reduces the amount of bound TTX. Suppression of TTX binding increases with increasing concentrations of the salts. The sequence of cations arranged according to their ability to displace TTX is as follows (Henderson *et al.*, 1974):



The apparent molecular weight of the solubilized TTX-binding component was estimated by Levinson and Ellory (1973) who used the method of irradiation inactivation of the TTX-binding sites of the pig brain; they obtained a value of about 230,000 daltons. A protein molecule of this size is expected to contain about 1000 amino acids and to penetrate the entire 80-Å-thick membrane layer when it occupies a spherical volume. It seems reasonable to assume that binding of TTX to this large protein molecule slows down conformational changes of the molecule.

Quite recently, Kao and Yeoh (1978) studied a new poison which is capable of suppressing the excitability of the squid axon at about the same concentration as TTX and competes with TTX for the same bonding sites. This new toxin, isolated from a Central American frog and called chiriquitoxin, was found to strongly suppress both the early (Na) and late (K) membrane current under voltage clamp. The complexity of pharmacological actions of TTX, saxitoxin, and chiriquitoxin was revealed by these investigators.

It eludes comprehension that the nerve fibers of the pufferfish function normally in the presence of TTX; probably, the structure of the crucial membrane protein is slightly different from that of TTX-sensitive nerve fibers. For

many years, we have known the strange fact that internal perfusion with a dilute NaF solution completely suppresses the TTX sensitivity of the squid giant axon.

In summary, tetrodotoxin (TTX) is the most potent paralytic poison known to suppress excitability of various nerve fibers. Radioactive TTX and STX have been used to estimate the surface density of the excitable membrane sites. There is good evidence that the membrane component which specifically binds TTX is a lipoprotein complex with an apparent molecular weight of about 230,000.

REFERENCES

- Adelman, W. J., Jr., Moses, J., and Rice, R. V. (1977). An anatomical basis for the resistance and capacitance in series with the excitable membrane of the squid giant axon. *J. Neurocytol.* **6**, 621–646.
- Alema, S., Calissano, P., Rusca, G., and Giuditta, A. (1973). Identification of a calcium-binding, brain specific protein in the axoplasm of squid giant axons. *J. Neurochem.* **20**, 681–689.
- Baker, P. F., Hodgkin, A. L., and Shaw, T. I. (1962). The effect of changes in the internal ionic concentrations on the electrical properties of perfused squid giant axons. *J. Physiol. (London)* **164**, 355–374.
- Barnola, F. W., Villegas, R., and Camejo, G. (1973). Tetrodotoxin receptors in plasma membranes isolated from lobster nerve fibers. *Biochim. Biophys. Acta* **298**, 84–94.
- Baumgold, J. (1980). ³H-Saxitoxin binding to nerve membranes: Inhibition by phospholipase A₂ and by unsaturated fatty acids. *J. Neurochem.* **32**, 327–334.
- Baumgold, J., Matsumoto, G., and Tasaki, I. (1978). Biochemical studies of nerve excitability: The use of protein modifying reagents for characterizing sites involved in nerve excitation. *J. Neurochem.* **30**, 91–100.
- Bear, R. S., and Schmitt, F. O. (1939). Electrolytes in the axoplasm of the giant nerve fibers of the squid. *J. Cell. Comp. Physiol.* **14**, 205–215.
- Bear, R. S., Schmitt, F. O., and Young, J. Z. (1937a). The sheath components of the giant nerve fibres of the squid. *Proc. R. Soc. London, Ser. B* **123**, 496–504.
- Bear, R. S., Schmitt, F. O., and Young, J. Z. (1937b). The ultrastructure of nerve axoplasm. *Proc. R. Soc. London, Ser. B* **123**, 505–519.
- Bear, R. S., Schmitt, F. O., and Young, J. Z. (1937c). Investigations on the protein constituents of nerve axoplasm. *Proc. Roy. Soc. London, Ser. B* **123**, 520–529.
- Bellin, J. S., and Yankus, C. A. (1968). Influence of dye binding on sensitized photooxidation of amino acids. *Arch. Biochem. Biophys.* **123**, 18–28.
- Benzer, T. I., and Raftery, M. A. (1972). Partial characterization of a tetrodotoxin-binding component from nerve membrane. *Proc. Natl. Acad. Sci. U.S.A.* **69**, 3634–3637.
- Betscher, M. S. (1973). Membrane structure: Some general principles. *Science* **181**, 622–627.
- Bolton, A. E., and Hunter, W. M. (1973). The labelling of proteins to high specific radioactivities by conjugation to a I-125-containing acylating agent. *Biochem. J.* **133**, 529–539.
- Brady, R., Spyropoulos, C., and Tasaki, I. (1958). Intra-axonal injection of biologically active materials. *Am. J. Physiol.* **194**, 207–213.
- Cheung, W. Y. (1980). Calmodulin plays a pivotal role in cellular regulation. *Science* **207**, 19–27.

- Colquhoun, D., Henderson, R., and Ritchie, J. M. (1972). The binding of labelled tetrodotoxin to non-myelinated nerve fibers. *J. Physiol. (London)* **227**, 95–126.
- Condrea, E., and Rosenberg, P. (1968). Demonstration of phospholipid splitting as the factor responsible for increased permeability and block of axonal conduction induced by snake venom. II. Study on squid axons. *Biochim. Biophys. Acta* **150**, 271–284.
- Cooke, I. M., Diamond, J. M., Grinnell, A. D., Hagiwara, S., and Sakata, H. (1968). Suppression of the action potential in nerve by nitrobenzene derivatives. *Proc. Natl. Acad. Sci. U.S.A.* **60**, 470–477.
- Danielli, J. F., and Davson, H. (1935). A contribution to the theory of permeability of thin films. *J. Cell. Comp. Physiol.* **5**, 495–508.
- Davison, P. F., and Huneus, F. C. (1970). Fibrillar proteins from squid axons. II. Microtubule protein. *J. Mol. Biol.* **52**, 429–439.
- Frankenhaeuser, B., and Hodgkin, A. L. (1956). The after-effects of impulses in the giant nerve fibers of *Loligo*. *J. Physiol. (London)* **131**, 341–376.
- Gainer, H., Carbone, E., Singer, I., Sisco, K., and Tasaki, I. (1974). Depolarization induced change in the enzymatic radio-iodination of protein on the internal surface of the squid giant axon membrane. *Comp. Biochem. Physiol.* **47A**, 477–484.
- Geren, B. B., and Schmitt, F. O. (1954). The structure of the Schwann cell and its relation to the axon in certain invertebrate nerve fibers. *Proc. Natl. Acad. Sci. U.S.A.* **40**, 863–870.
- Gorter, E., and Grendel, F. (1925). On bimolecular layer of lipoids on chromocytes of the blood. *J. Exp. Med.* **41**, 439–443.
- Goto, T., Kishi, Y., Takahashi, S., and Hirata, Y. (1965). Tetrodotoxin. *Tetrahedron* **21**, 2059–2088.
- Gross, E., and Witkop, B. (1962). Nonenzymatic cleavage of peptide bonds: The methionine residues in bovine pancreatic ribonuclease. *J. Biol. Chem.* **237**, 1856–1860.
- Hafemann, D. R. (1972). Binding of radioactive tetrodotoxin to nerve membrane preparations. *Biochim. Biophys. Acta* **266**, 548–556.
- Henderson, R., Ritchie, J. M., and Strichartz, G. R. (1974). Evidence that tetrodotoxin and saxitoxin act as a metal cation binding site in the sodium channels of nerve membrane. *Proc. Natl. Acad. Sci. U.S.A.* **71**, 3936–3940.
- Henkart, M. P., Reese, T. S., and Brinley, F. J. (1978). Endoplasmic reticulum sequesters calcium in the squid giant axon. *Science* **202**, 1300–1303.
- Hodgkin, A. L., and Katz, B. (1949). The effect of calcium on the axoplasm of giant nerve fibers. *J. Exp. Biol.* **26**, 292–294.
- Huneus, F. C., and Davison, P. F. (1970). Fibrillar proteins from squid axons. I. Neurofilament protein. *J. Mol. Biol.* **52**, 415–428.
- Huneus-Cox, F. H. L., Fernandez, H. L., and Smith, B. H. (1966). Effects of redox and sulfhydryl reagents on the bioelectric properties of the giant axon of the squid. *Biophys. J.* **6**, 675–689.
- Inoue, I., Pant, H. C., Tasaki, I., and Gainer, H. (1976). Release of proteins from the inner surface of squid axon membrane labelled with tritiated N-ethylmaleimide. *J. Gen. Physiol.* **68**, 385–395.
- Kakiuchi, S., Yamazaki, R., and Nakajima, H. (1970). Properties of a heat-stable phosphodiesterase activating factor isolated from brain extract. *Proc. Jpn. Acad.* **46**, 587–592.
- Kao, C. Y. (1966). Tetrodotoxin, saxitoxin and their significance in the study of excitation phenomena. *Pharmacol. Rev.* **18**, 997–1049.
- Kao, C. Y., and Yeoh, P. N. (1978). Different receptors for saxitoxin and tetrodotoxin. *J. Physiol. (London)* **284**, 88–89p.
- Koechlin, B. A. (1955). On the chemical composition of the axoplasm of squid giant nerve fibers with particular reference to its ion pattern. *J. Biophys. Biochem. Cytol.* **1**, 511–529.

- Levinson, S. R., and Ellory, J. C. (1973). Molecular size of the tetrodotoxin binding site estimation by irradiation inactivation. *Nature (London) New Biol.* **245**, 122–123.
- Levinson, S. R., and Meves, H. (1975). The binding of tritiated tetrodotoxin to squid giant axons. *Phil. Trans. R. Soc. London, Ser. B* **270**, 349–352.
- Maxfield, M. (1953). Axoplasmic proteins of the squid giant nerve fiber with particular reference to the fibrous protein. *J. Gen. Physiol.* **37**, 201–216.
- McCull, J. D., and Rossiter, R. (1950). Lipid of squid nerve. *Nature (London)* **166**, 185–186.
- Means, G. E., and Feeney, R. E. (1971). "Chemical Modification of Proteins," 252 pp. Holden-Day, San Francisco, California.
- Merrill, C. R., Switzer, R. C., and Van Kueren, M. L. (1979). Trace polypeptides in cellular extracts and human body fluids detected by two-dimensional electrophoresis and a highly sensitive silver stain. *Proc. Natl. Acad. Sci. U.S.A.* **76** (September) 4335–4339.
- Metuzals, J. (1969). Configuration of a filamentous network in the axoplasm of the squid (*Loligo pealii* L.) giant nerve fiber. *J. Cell. Biol.* **43**, 480–505.
- Metuzals, J., and Izzard, C. S. (1969). Spatial patterns of threadlike elements in the axoplasm of the giant nerve fiber of the squid (*Loligo pealii* L.) as disclosed by differential interference microscopy and by electron microscopy. *J. Cell. Biol.* **43**, 456–479.
- Metuzals, J., and Tasaki, I. (1978). Subaxolemmal filamentous network in the giant nerve fiber of the squid (*Loligo pealei* L.) and its possible role in excitability. *J. Cell. Biol.* **78**, 597–621.
- Moore, J. W., Narahashi, T., and Shaw, T. I. (1967). An upper limit to the number of sodium channels in nerve membrane? *J. Physiol. (London)* **188**, 99–105.
- Narahashi, T. (1974). Chemicals as tools in the study of excitable membranes. *Physiol. Rev.* **54**, 813–889.
- Ochs, S. (1974). Systems of material transport in nerve fibers (axoplasmic transport) related to nerve function and trophic control. *Ann. N.Y. Acad. Sci.* **228**, 202–223.
- Pant, H. C., Terakawa, S., Baumgold, J., Tasaki, I., and Gainer, H. (1978). Protein release from the internal surface of the squid giant axon membrane during excitation and potassium depolarization. *Biochim. Biophys. Acta* **513**, 132–140.
- Reed, J. K., and Raftery, M. A. (1976). Properties of the tetrodotoxin binding component in plasma membranes isolated from *Electrophorus electricus*. *Biochemistry* **15**, 944–953.
- Rothman, J. E., and Lenard, J. (1977). Membrane asymmetry. *Science* **195**, 743–753.
- Shrager, P. G. (1975). Specific chemical groups involved in the control of ionic conductance in nerve. *Ann. N.Y. Acad. Sci.* **264**, 293–303.
- Shrager, P. G., Strickholm, A., and Macey, R. I. (1969). Chemical modification of crayfish axons by protein crosslinking aldehydes. *J. Cell. Physiol.* **74**, 91–100.
- Singer, S. J. (1974). Molecular biology of cellular membranes with applications to immunology. *Adv. Immunol.* **19**, 1–66.
- Singer, S. J., and Nicolson, G. L. (1972). The fluid mosaic model of the structure of cell membrane. *Science* **175**, 720–731.
- Smith, H. M. (1958). Effect of sulfhydryl blockade on axonal function. *J. Cell. Comp. Physiol.* **51**, 161–171.
- Steck, T. L. (1974). The organization of proteins in the human red blood cell membrane. *J. Cell Biol.* **62**, 1–19.
- Steck, T. L., and Fox, C. F. (1972). Membrane proteins. In "Membrane Molecular Biology" (C. F. Fox and A. D. Keith, eds.), pp. 27–75. Sinauer Associates, Inc., Stamford, Conn.
- Stockenius, W., and Engelman, D. M. (1969). Current models for the structure of biological membranes. *J. Cell Biol.* **42**, 613–646.
- Tahara, Y. (1911). Über das Tetrodongift. *Biochem. Z.* **30**, 255–275.

- Takenaka, T., and Yamagishi, S. (1966). Intracellular perfusion of squid giant axons with protease solution. *Proc. Jpn. Acad.* **42**, 521–526.
- Tasaki, I., and Takenaka, T. (1964). Effects of various potassium salts and proteases upon excitability of intracellularly perfused squid giant axons. *Proc. Natl. Acad. Sci. U.S.A.* **52**, 804–810.
- Tobias, J. (1960). Further studies on the nature of the excitable system in nerve. I. Voltage-induced axoplasm movement in squid axons. II. Penetration of surviving, excitable axons by proteases. III. Effects of proteases and of phospholipases on lobster giant axon resistance and capacity. *J. Gen. Physiol.* **43**, 57–71.
- Villegas, J. (1972). Axon-Schwann cell interaction in the squid nerve fibre. *J. Physiol. (London)* **225**, 275–296.
- Villegas, R., and Villegas, G. M. (1960). Characterization of the membranes in the giant nerve fiber of the squid. *J. Gen. Physiol.* **43**, 73–103.
- Villegas, R., Gimenez, M., and Villegas, L. (1962). The Schwann-cell electrical potential in the squid nerve. *Biochim. Biophys. Acta* **62**, 610–612.
- Weiss, P., and Hiscoe, H. B. (1948). Experiments on the mechanism of nerve growth. *J. Exp. Zool.* **107**, 315–395.
- Yoshioka, T., Pant, H., Tasaki, I., Baumgold, J., Matsumoto, G., and Gainer, H. (1978). An approach to the study of intracellular proteins related to the excitability of the squid giant axon. *Biochim. Biophys. Acta* **538**, 616–626.

10. Further Electrophysiological Studies of Intact Squid Axons

A. THE RELATION BETWEEN AXON DIAMETER AND CONDUCTION VELOCITY

The term "intact axons" in the title of this chapter is used to denote axons with intact axoplasm. Most of the experimental results described here are those obtained without employing the technique of intracellular perfusion. The properties of axons examined under intracellular perfusion after removing the axoplasm will be discussed in subsequent chapters. We commence this chapter with the discussion of the relationship between the fiber diameter and the conduction velocity.

Pumphrey and Young (1938) examined the conduction velocities of squid axons between 20 and 800 μm in diameter and found that the velocity varied with the square root of the diameter. Later on, Rushton (1951, cited in Chapter 5) clarified the theoretical basis for this square root relationship between the velocity and the fiber diameter.

The data obtained by Pumphrey and Young are shown by the points in Fig. 10.1. The continuous line in the figure was obtained by calculations based on a simple equation proposed recently by Matsumoto and Tasaki (1977). The equation is given in the upper part of the figure. The derivation of this equation is far simpler and more direct than that of the equation proposed by Rushton or by Hodgkin and Huxley (1952d, cited in Chapter 8). The conduction velocity, v , is directly related to the membrane capacity, C , the membrane resistance in the excited state, R^* , the electric resistivity of the axoplasm, ρ , and the fiber diameter, d . The numerical values of the quantities used for the calculation, given in the figure, were obtained from independent measurements. We see that there is good agreement between the observed and the calculated values.

The equation was derived by applying Kirchhoff's law to the transitional zone located between the excited and resting areas of an axon carrying

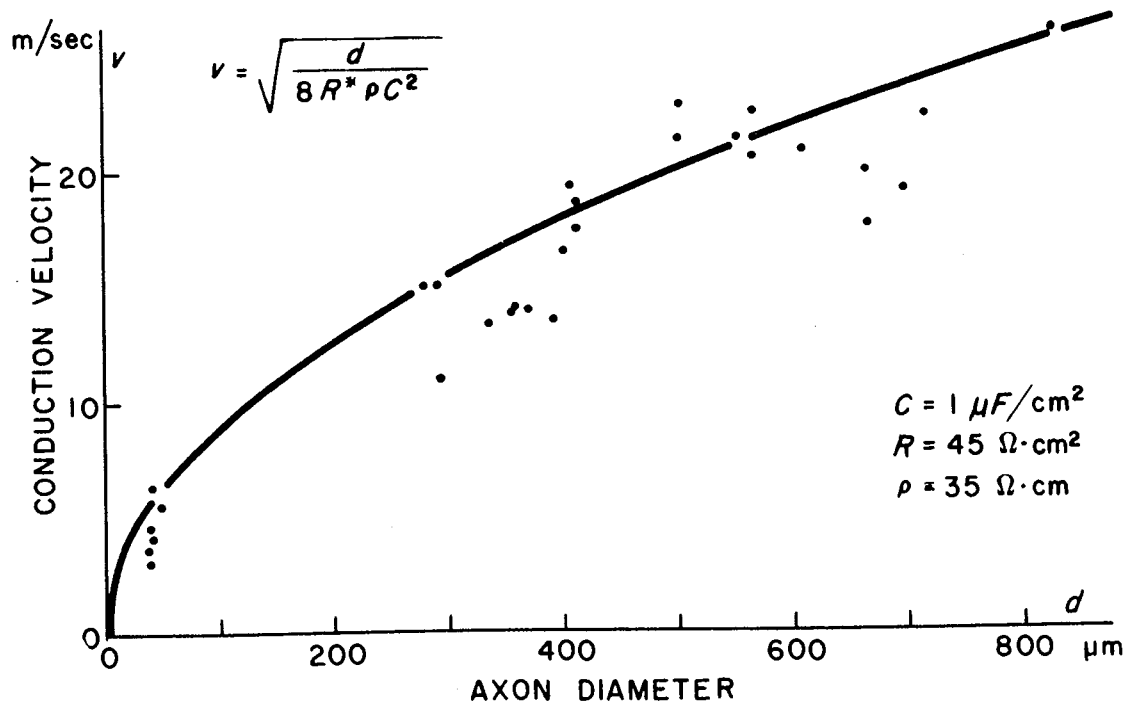


Fig. 10.1 Dependence of the conduction velocity on the axon diameter. Experimental values determined by Pumphrey and Young (1938) are shown by the points in the figure. The continuous line represents the value calculated by the use of the equation given in the figure, where C represents the membrane capacity, R^* the membrane resistance at the peak of excitation, ρ the resistivity of the axoplasm, and d the diameter of the fiber. The values chosen for calculation are given. (From *Biophys. J.* 122, 10, 1977.)

an impulse at a constant velocity. In the transitional zone, the potential gradient along the axon is assumed to be constant. When referred to the coordinate which is moving at the velocity of the nerve impulse, the transitional zone is stationary; hence, the cable properties of the excited zone can be directly related to those of the resting zone by the use of Kirchhoff's law.

Using internally perfused squid giant axons, it is possible to vary the resistivity, ρ , of the axon interior. The aforementioned equation was found to describe the dependence of the conduction velocity on ρ satisfactorily. The membrane resistance at the peak of excitation, R^* , calculated from the conduction velocity was found to agree well with the values determined by direct measurements.

In summary, one might say that the factors which determine the conduction velocity in nonmyelinated nerve fibers are well understood. It is known that both R^* and ρ increase when the axon is cooled (see, e.g., Tasaki and Spyropoulos, 1957); the temperature dependence of the conduction velocity may be attributed mainly to changes in R^* and ρ . It may be pointed out in this connection that, in highly extensible nerve fibers of the leech or the slug, the relationship between the conduction velocity and the fiber diameter appears to be very complex (see Bethe, 1908; Carlson, 1911).

B. INTRACELLULAR INJECTION OF TETRAETHYLAMMONIUM SALT

From a physicochemical point of view, tetraalkylammonium ions are of great interest because they are spherically symmetric, large, and of low electric charge. Their radii have been estimated from the N—C internuclear distance, the van der Waals radius of the methyl group and the C—C bond length and angle (see p. 124 in Robinson and Stokes, 1959). For tetraethylammonium (TEA) ion, a value of 4.0 Å is obtained from such estimation. This value is slightly greater than the radius of a hydrated sodium ion, 3.3 Å, and is comparable to that of calcium ion, 4.2 Å, estimated from Stokes' law modified by Robinson and Stokes.

The interaction between tetraalkylammonium ions and solvent molecules has been studied by measuring the electric conductivities and the diffusion coefficients of salt solutions in various solvents (see, e.g., Kay and Evans, 1966; Kay *et al.*, 1966). The structure of water molecules in the immediate vicinity of these cations is known to be very different from that in the bulk phase. It is important to note that this water structure is quite distinct from the structure of the hydration envelope around small alkali metal ions (see, e.g., Horne *et al.*, 1971). The difference in the effect between alkali metal ions and tetraalkylammonium ions on the conformational state of various macromolecules has been attributed to the disparity in the water structure (see, e.g., von Hippel and Wong, 1964).

The selective uptake of tetraalkylammonium ions by synthetic cation exchangers has been examined by Kressman and Kitchner (1949), Gregor and Bergman (1951), and others. It is known that the selectivity for these large quarternary ammonium ions over small cations (NH_4^+ , Na^+ , H^+ , etc.) increases with increasing length of the nonpolar chains of the ions. The van der Waals force acting between these nonpolar chains and the synthetic cation exchanger are regarded as the cause of the selective uptake.

Biological actions of the tetraalkylammonium salts were first studied by pharmacologists (see, e.g., Burn and Dale, 1915). Neurophysiological studies in this field were commenced by Loeb and Ewald (1916) and expanded by Cowan and Walter (1937) and others. These studies of the effects of TEA on the sciatic nerve of frog nerve—gastrocnemius preparations showed that, at relatively high concentrations, the chloride or iodide salt solutions of TEA decrease the minimal gradient (see Chapter 7, Section A) and produce repetitive firing of action potentials. In these old-time experiments, however, it is sometimes difficult to separate the effects of TEA from the results caused by a loss of Ca^{2+} or Na^+ from the nerve. In intact nerve trunks of the frog, exchange of applied TEA ion for Ca^{2+} and Na^+ in the trunk is a very slow process. In the exposed nodal membrane, exchange between Na and TEA ion is prompt (Tasaki, 1959).

The salts of tetraalkylammonium ions added to the normal external medium of a squid giant axon have very little effect on the axon excitability, as long as its concentration is not high enough to alter the ion composition of the medium drastically. In contrast, intracellularly administered TEA exerts a striking influence on the duration of the action potential and on the time course of the membrane current observed under voltage clamp (Tasaki and Hagiwara, 1957). The action potential duration can readily be prolonged by a factor of 100–1000 by intracellular injection of TEA (see Fig. 10.2). Under voltage clamp with a long positive (i.e., depolarizing) pulse, the intensity of the outwardly directed membrane current can be markedly reduced by this treatment. Much later, Armstrong (1971) explained the effect of TEA on the axon membrane in terms of the equivalent circuit concept.

In the original experiments, an isotonic solution of TEA-chloride was injected uniformly over a long stretch of the squid axon. The intracellular TEA concentration attained by this method was estimated to be approximately 20 mM. A small change in the action potential duration was recognized within a few seconds after injection. Next, there was a rapid increase in the duration. Undoubtedly this increase is associated with a gradual rise in the TEA concentration on the inner side of the major diffusion barrier near the axon surface. A final, steady state was reached in about 1 min. It is extremely instructive to follow the course of the progressive change in the "shape" of the action potential while the internal TEA concentration is continuously rising. The significance of the progressive change will be discussed later (see Chapter 13, Section H).

It is easy to inject TEA into a limited region of a squid axon and study the effect of interaction between two regions of the membrane with very different electrophysiological properties. When a TEA-treated region is electrically coupled to a normal region, there is a strong tendency toward generation of multiple action potentials in the normal region during the plateau of

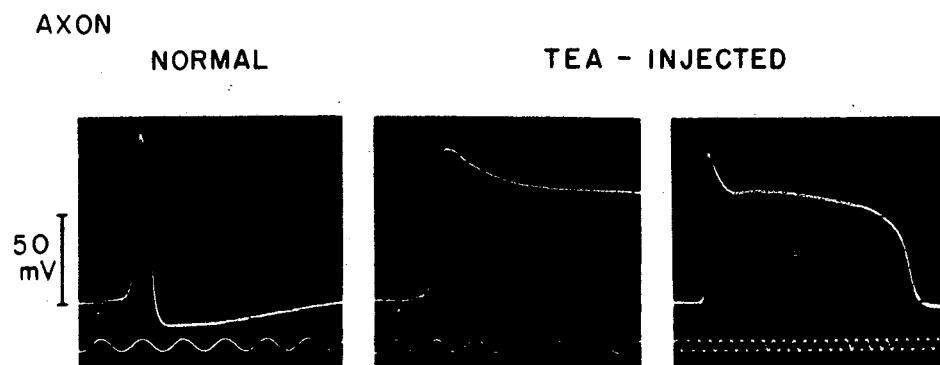


Fig. 10.2 Prolongation of the action potential duration produced by intracellular injection of tetraethylammonium (TEA) chloride. The time marker, 1000 Hz. (From *J. Gen. Physiol.* **40**, 865, 1957.)

the TEA-treated region. Simultaneously, the interaction tends to shorten the action potential of the TEA-treated region. By the use of an electronic feedback device, it was shown that the flow of electric currents between the two regions of the axon is responsible for the complex behavior of the axon near the boundary between the two regions (Oikawa, 1962).

According to the experimental results obtained recently, there is a strong interaction between TEA and the submembranous protein layer. Introduction of TEA-salt (300 mM) into the axon interior causes a release of submembranous protein molecules and also a rise in the membrane resistance (S. Terekawa, unpublished). In Chapter 13, Section H, we shall discuss how a hydrophobic interaction between TEA-ion and the submembranous protein layer brings about a marked prolongation of the action potential duration.

C. ABOLITION OF A PROLONGED ACTION POTENTIAL

In axons developing prolonged action potentials, it is easy to demonstrate "abolition of an action potential" (see Chapter 5, Section C) at any moment between the peak and shoulder (see Fig. 10.3). By employing Marmont's method of intracellular wiring (Chapter 8, Section F), we can deliver brief pulses of inward current through the axon membrane. When the electric potential inside the axon is lowered by the current pulse below a critical level, the potential falls, after termination of the pulse, rapidly to a level close to the resting membrane potential. If the pulse is not strong enough, the membrane potential rises rapidly and returns roughly to the original level. It is to be noted that the critical level of the membrane potential required for aboli-

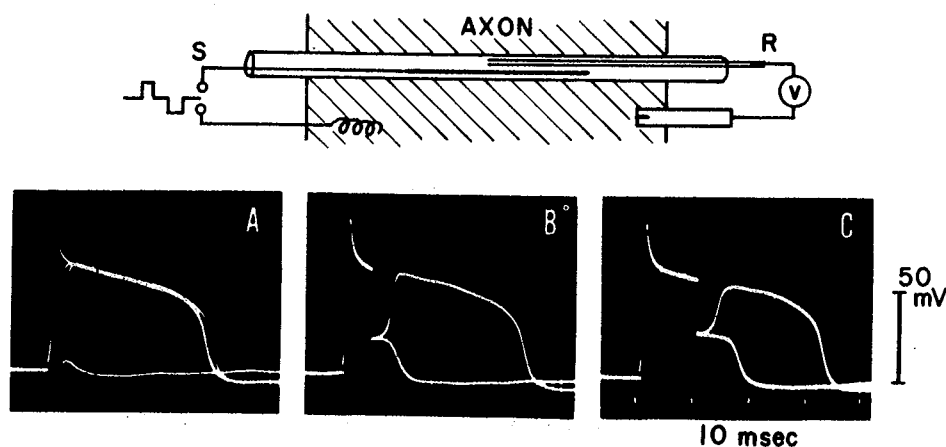


Fig. 10.3 Abolition of the prolonged action potential of a TEA-treated axon. The action potential was initiated by a brief pulse of outward current. During the plateau of the action potential, a pulse of inward current was delivered. Note that the membrane potential returned to the plateau level when the inward current pulse failed to abolish the action potential. (From *J. Gen. Physiol.* **40**, 870, 1957.)

tion rises gradually. Concomitantly, there is a gradual decrease in the current intensity required for abolition. The action potential is terminated automatically when the critical potential level reaches the plateau level of the membrane potential.

As in the case of the nodal membrane (see Chapter 5, Section C), the refractoriness vanishes completely when an action potential is abolished at its peak. A normal refractoriness is left behind by an action potential abolished near its shoulder. The significance of these facts will be clarified later in Chapter 13, Section G.

The axon membrane is said to be "stable" when a small change in the membrane potential produced by a weak current pulse decays and vanishes after the end of the pulse. During the plateau of a prolonged action potential, as well as in the resting state, the membrane is stable. We thus arrive at the view that *there are two stable states in the axon membrane and that initiation and abolition of an action potential represent transitions between the two stable states*. The objective of theories of nerve excitation is then to elucidate the physicochemical factors that determine the stability (and instability) of the macromolecular conformations of the axon membrane corresponding to the two states. Because of the slowness of the relaxation processes in the excited state, axons that develop prolonged action potentials offer an opportunity for studying excitation processes with considerable ease.

D. HYPERPOLARIZING RESPONSES IN POTASSIUM-RICH MEDIA

The natural and artificial seawater used by many investigators in Woods Hole, Massachusetts, contains the following concentrations of cations: about 10 mM potassium, 423–530 mM sodium, and approximately 60 mM divalent cations (magnesium and calcium). A variation in the chemical species of anions has very little effect on the excitability of the axons immersed, provided that the free Ca-ion concentration is not affected by the anion species used. When the potassium ion concentration in the external medium is raised to 50–100 mM at the expense of Na-ion, the ability of squid giant axons to develop propagated action potentials is immediately suppressed (see Chapter 8, Section D). Previously, it was believed that the axons immersed in such a potassium-rich medium were completely inexcitable. We now know that these axons show definite signs of excitability. It is true that no electrical responses can be elicited from such axons by application of pulses of outwardly directed membrane current. However, when pulses of inwardly directed (i.e., hyperpolarizing) current are delivered to the axons, a definite, nearly all-or-none response can be evoked.

A sign of excitability in axons immersed in a medium rich in K-ion was first noted by Segal (1958); he found "hyperpolarizing responses" in axons immersed in a medium containing a high concentration of potassium acetate.

A simple procedure for demonstrating a hyperpolarizing response is to immerse an axon in a mixture of an isotonic (about 530 mM) KCl solution and artificial seawater (Tasaki, 1959). Using double-wire electrodes introduced longitudinally, it is easy to examine the changes in the membrane potential produced by the passage of long pulses of electric current. Simultaneously, changes in the membrane impedance could be determined by inserting the axon in one arm of an AC Wheatstone bridge (see Fig. 10.4).

Axons immersed in a potassium-rich medium are referred to as being in a "depolarized" state: the potential difference across the membrane is low and the membrane resistance is subnormal. In a depolarized axon, a pulse of outward current through the membrane applied by means of a long internal metal electrode raises the level of the intracellular potential in proportion to the intensity of the current applied (see the upper records in Fig. 10.4). No significant change in the AC impedance of the membrane is produced by the application of an outward current pulse. In contrast, a pulse of inward cur-

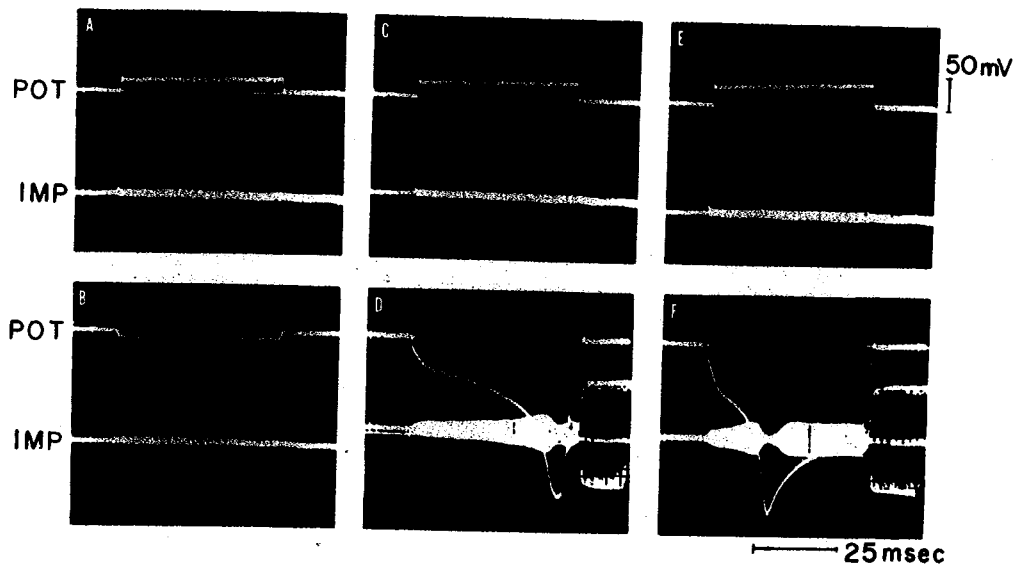


Fig. 10.4 Simultaneous recording of the change in the membrane potential (trace marked POT) and the membrane impedance (IMP) obtained from a squid giant axon immersed in a mixture of one part of isosmotic KCl solution and 4 parts of normal seawater. The bridge AC was 6 kHz, and the bridge was balanced for the impedance of the membrane at rest. Records A, C, and E show the effect of rectangular pulses of outwardly directed currents. Records B, D, and F show the responses produced by pulses of inwardly directed current. Records E and D were taken at about the same current intensity. (From *J. Physiol. (London)* **148**, 310, 1959.)

rent can produce a disproportionately large potential change associated with a large increase in the membrane impedance (see the lower records). At a critical intensity, the large potential change appears in an almost all-or-none manner. The latency (i.e., the interval between the onset of the current pulse and the beginning of the response) is shortened by an increase in the current intensity (compare Records D and F). Furthermore, the large potential change shows a definite sign of refractoriness; when two pulses of strong inward current are delivered in succession, the response of the membrane to the second pulse is smaller than that to the first pulse.

The hyperpolarizing response is associated with a large increase in the membrane resistance. There is also a definite change in the emf across the membrane. There is a close analogy between generation of a "hyperpolarizing response" and abolition of a prolonged action potential described in the preceding section (see also Chapter 12, Section G).

To demonstrate a change in the emf, single fiber preparations of the frog appear to be better suited than squid giant axons. All-or-none repolarization and depolarization of the nodal membrane were demonstrated previously by Mueller (1958) and by Stämpfli (1958). The time constant (i.e., the capacity-resistance product) of the nodal membrane at rest (see Chapter 5, Section E) is far shorter than that of the squid axon membrane; consequently, a small change in the emf in the recording circuit involving the nodal membrane can be detected without any appreciable distortion. Upon termination of the applied inward current, the membrane potential rises with two steps. Evidently, the first step of the observed potential rise represents a loss of the IR drop across the membrane. The potential level reached at the end of this rapid rise is 15–30 mV below the base line observed before the onset of the current pulse. Following an extremely variable period of time, there is another step of potential rise. Since this second step of potential rise takes place in the absence of a membrane current, it reflects a change in the emf. By an analogous (but less clear-cut) procedure, a hyperpolarizing response in the squid giant axon is found to consist of a large IR drop superposed on a small change in the emf. The change in the emf seen at the end of the applied inward current pulse (see Records D and F) is nothing but a "break response" described in a previous section (see Chapter 7, Section G). An important finding revealed by this procedure is that the discrete change in the emf still remains after complete replacement of the external Na-ion with choline ion (Tasaki, 1959).

Based on these experimental findings, we conclude that the observed curve relating the membrane potential with the external K-ion concentration (see Chapter 8, Section D, and Chapter 12, Section G) is divided into two distinct portions. In the portion corresponding to low K-ion concentrations, the axon membrane is capable of developing ordinary action potentials in

response to pulses of electric current directed outward through the membrane; pulses of inwardly directed current produce no physiological response. In the portion corresponding to high K-ion concentrations, on the contrary, inwardly directed currents produce physiological responses, but outwardly directed current pulses do not. In the intermediate portion, the axon membrane shows a sign of instability; a weak electric shock applied to the membrane produces an oscillatory potential change which decays very slowly (as in an axon immersed in a Ca-deficient medium).

To sum up, we see that a nerve fiber immersed in a potassium-rich medium is in a "depolarized state" and that an inwardly directed current produces an approximately all-or-none transition of the membrane to its "repolarized," or "resting," state.

E. CHEMICAL STIMULATION OF NERVE FIBERS

Long before the discovery of Ringer's solutions, physiologists knew that motor nerve fibers of the frog can be stimulated by various chemical agents. Eckhard (1851), for example, observed that concentrated solutions of various salts, alkalis, acids, and alcohol applied to the nerve trunk of a nerve-muscle preparation produce twitches in the muscle. He noted also that these chemical stimulants irreversibly destroy the nerve after generating nerve impulses for a limited period of time. Because of this undesirable injurious effect, the use of chemical stimulants did not yield much useful information as to the physiological properties of the nerve fiber.

Much later, Loeb recognized the importance of chemical stimulants in the study of normal physiological function of the nerve fiber (Loeb, 1907; Loeb and Ewald, 1916). He showed that excitation of the frog sciatic nerve by external application of an isotonic sodium salt solution of fluoride, oxalate, or citrate is due primarily to removal of free calcium ion in the medium. According to Loeb, the process of excitation by electric means is not fundamentally different from that induced by chemical stimulants. He postulated that electric stimuli produce a fall in the concentrations of Ca- and Mg-ions in the portion of the nerve near the cathode and that this fall in the divalent cation concentrations leads to the initiation of physiological responses (see Chapter 3, Section C).

In the mid-1930s, when it became relatively easy to record action potentials from large nonmyelinated fibers, the problem of chemical stimulation was reexamined by several prominent physiologists (see Fessard, 1936, cited in Chapter 7; Arvanitaki, 1936, 1939; Brink *et al.*, 1946). An important discovery was made during this period in relation to the origin of repetitive firing of action potentials. Arvanitaki (1936) found that generation of full-

sized action potentials is preceded by subthreshold (i.e., nonpropagated) oscillatory responses. The important characteristic of these subthreshold responses is that the frequency of oscillation is roughly the same as that of repetition of full-sized action potentials observed under similar experimental conditions.

In her early studies of subthreshold responses, Arvanitaki used for chemical stimulation the method of lowering the Ca-ion concentration in the external medium. Later on, she adopted a photochemical method of exciting sepia giant nerve fibers. When a nerve fiber stained with a dye (e.g., neutral red) is exposed to a beam of light that can be absorbed by the dye, macromolecules in the nerve membrane are oxidized and this photooxidation leads, after a short latent period, to repetitive firing of action potentials (Arvanitaki and Chalazonitis, 1955). Previously, the phenomenon of photochemical excitation was studied by Lippay (1929, 1930) using muscle fibers of the frog. As in the case of electrically induced subthreshold responses (see Chapter 3, Section F, and Chapter 8, Section F), a full-sized response is initiated when the peak of a subthreshold response reaches a critical potential level.

With the advent of the technique of intracellular perfusion, it became possible to initiate repetitive firing of action potentials by introducing various chemicals into the interior of the axon. We shall see in a subsequent section that various sulfhydryl reagents and photochemical oxidizing agents are capable of producing subthreshold responses followed by firing of full-sized action potentials. Raising the intracellular pH is also a very effective means of inducing repetitive firing.

The oscillograph records in Fig. 10.5 show examples of oscillatory subthreshold responses generated by an alkaline shift of the intracellular pH. Initially, the axon under study was immersed in artificial seawater and inter-

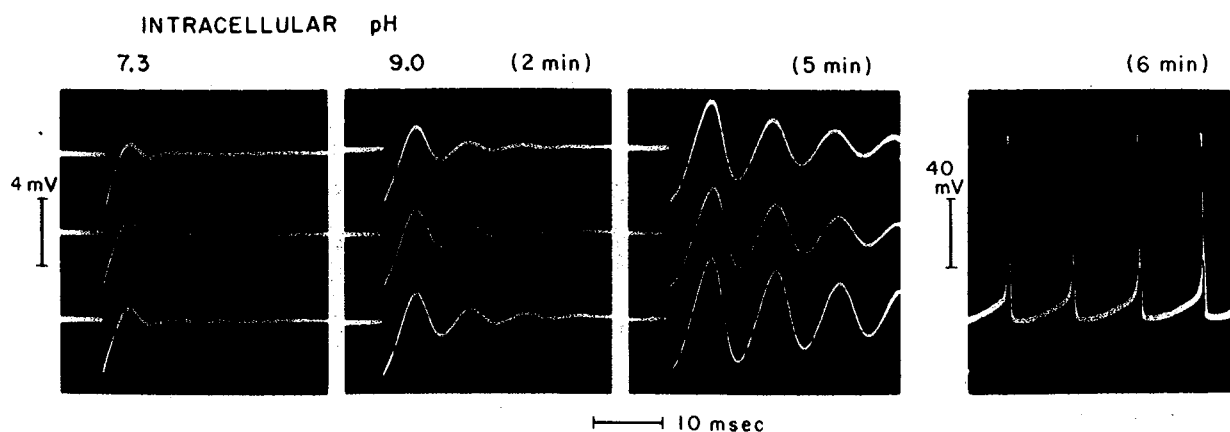


Fig. 10.5 Oscillatory subthreshold responses (the first three records) of a squid giant axon induced by an alkaline shift of the internal pH. The axon was immersed in artificial seawater. Note that the interval between the full-sized action potentials (about 9 msec at 22°C) is close to the period of the oscillatory subthreshold responses.

nally perfused with our standard potassium phosphate solution (see Chapter 11, Section B). When the internal pH was at 7.3, a brief pulse of inwardly directed current through the axon membrane produced a highly damped oscillatory potential change. Next, when the internal pH was shifted toward 9, there was a gradual decrease in the damping factor. Eventually, repetitive firing of full-sized action potentials was generated in the absence of electric stimuli. It is seen that the period of the subthreshold oscillation is very close to that of repetition of the full-sized action potentials.

F. MONNIER'S PHENOMENA OF PARARESONANCE

A collection of phenomena which come under the category of Monnier's pararesonance (Monnier, 1933) should be mentioned in connection with the effects of chemical stimulants on nerve fibers. In the 1930s, Monnier and his collaborators called attention to the following facts indicating that, in nerve fiber mildly treated with a chemical stimulant, there are physiological processes that exhibit a marked periodicity.

1. The threshold intensity measured with alternating currents (AC) shows a distinct minimum at a particular frequency (von Kries, 1882, cited in Chapter 3; Coppée, 1934, cited in Chapter 7).

2. Delivery of a weak (subthreshold) electric shock produces an oscillatory change in the threshold for the second (test) shock (Monnier and Coppée, 1939).

3. Application of a suprathreshold electric shock produces a transitory discharge of action potentials which repeat at about the same frequency (Monnier and Coppée, 1939).

4. Oscillatory subthreshold responses can be induced by a chemical stimulant and/or by a weak electric shock (Arvanitaki, 1939).

5. The membrane impedance measured with a weak AC (see Cole, 1941; Conti, 1970) shows a sharp maximum at a particular frequency (see below).

It is very easy to reproduce the phenomenon of pararesonance by measuring the membrane impedance and the threshold of a squid giant axon as a function of frequency. The left-hand graph in Fig. 10.6 shows the effect of reducing the external divalent cation concentration on the membrane impedance. When the external medium was artificial seawater which contains 60 mM divalent cations and 445 mM Na-ion, the membrane impedance showed only a small hump at about 140 Hz. In a 3:1 mixture of 530 mM NaCl solution and seawater, there was a gradual rise in the impedance at about 140 Hz and a slight fall at lower frequencies. Shortly before the onset

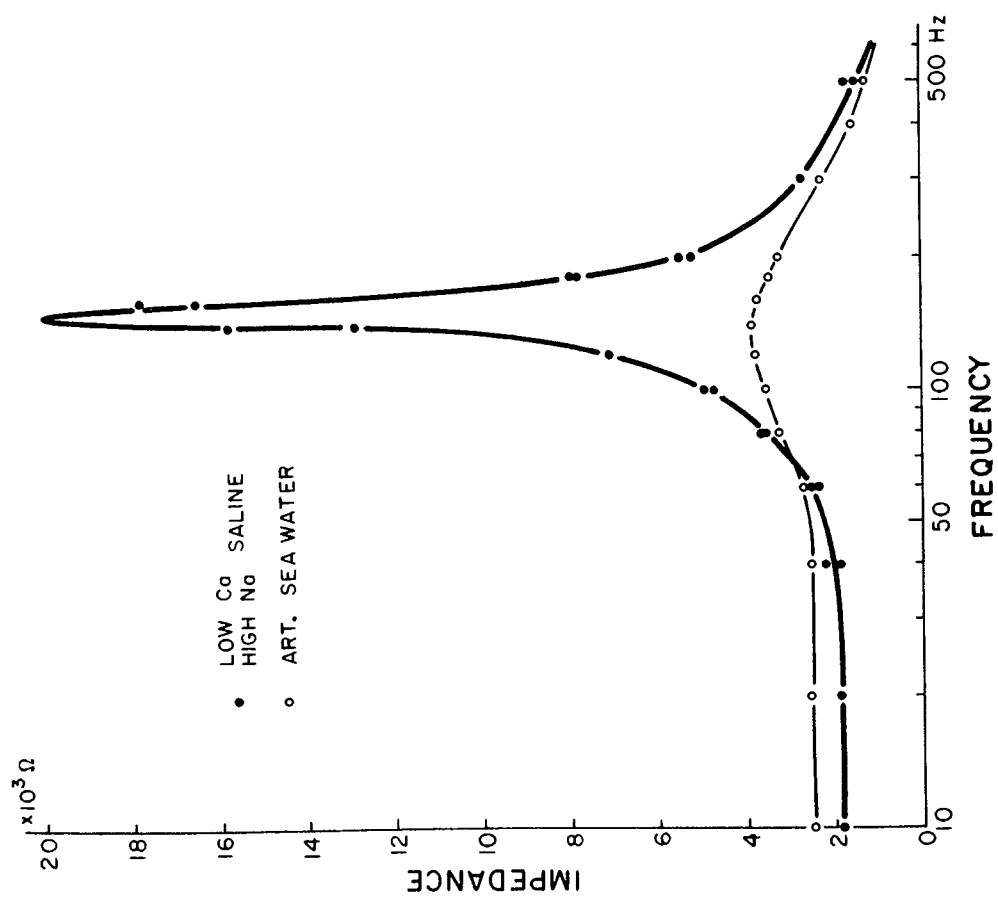
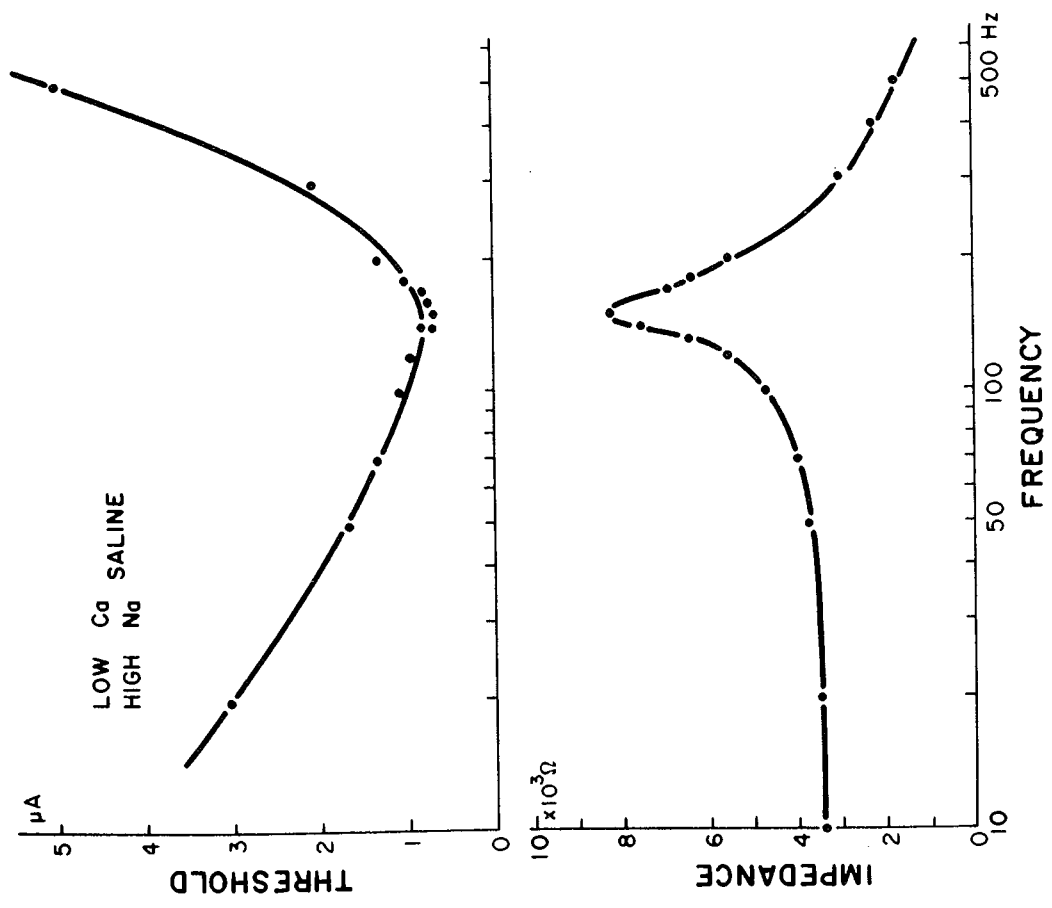


Fig. 10.6 Demonstration of pararesonance in a squid giant axon immersed in a mixture of one part of normal seawater and 3 parts of isotonic NaCl solution. Left: The membrane impedance measured before and after application of a low divalent cation medium. Right: The threshold intensity and membrane impedance determined in an intermediate stage of pararesonance. The intracellular electrode used was a 1.5-mm-long platinumized platinum wire. 19°C.

of repetitive firing of full-sized action potentials, the impedance at 140 Hz rose to an immense magnitude.

The existence of a sharp peak in the membrane impedance at a particular frequency may appear like the phenomenon of resonance in an electric circuit involving an inductor and a capacitor. However, measurements of the phase difference between the current and the voltage indicate that the phenomenon observed in the nerve membrane is very different from the behavior of an electrical or mechanical resonance system. In the axon membrane, the phase shift changed from about 0° to roughly 90° in the region of pararesonance (Matsumoto *et al.*, 1978), while in physical resonance systems, the phase can vary between plus and minus 90° .

There is one more point of interest in the phenomenon of pararesonance. In measuring the impedance of the axon membrane, it is necessary to assume that there is proportionality between the intensity of AC through the membrane and the observed potential variation. Actual measurements have shown that a significant deviation from the proportionality appears only when the peaks of the sinusoidally altering membrane potential are close to the threshold level.

We shall see in the following sections that the phenomenon of pararesonance is an indication of the existence of periodic responses localized at small spots and patches of the axon membrane. When a weak AC passes through such an axon membrane, the periodic responses at different sites of the membrane tend to be synchronized by the applied current [see van der Pol and van der Mark (1926) cited in Chapter 7]. The degree of synchronization is expected to increase with the amplitude of the applied AC, provided that the frequency of the AC is close to the frequency of the periodic responses. The frequency of the periodic responses is expected to vary, to some extent, from site to site.

The upper right-hand graph in Fig. 10.6 shows the AC threshold measured as a function of frequency during the course of gradual development of pararesonance. The lower right-hand graph in Fig. 10.6 represents the membrane impedance of the same axon. Note that the minimum of the upper curve is located at the same frequency as the maximum of the lower curve. Thus, we now have a much better understanding of the reason why there is a minimum in the threshold–frequency curve.

G. PERIODIC MINIATURE RESPONSES

Quite recently, fast Fourier transform (FFT) analyzers of a compact form became commercially available. By the use of such an instrument, spectra of small electric signals containing a large number of periodic or quasi-peri-

odic potential waves can be determined within a fraction of a second. The Fourier components of a few microvolts in amplitude can be detected with such a spectrum analyzer used in conjunction with an amplifier.

In a series of recent studies (Matsumoto *et al.*, 1978), the effects of chemical stimulants on squid giant axons were examined by using an FFT analyzer of Nicolet Scientific Corporation, New Jersey. To record potential variations in the axon interior, either a glass-pipette electrode (filled with isotonic KCl–agar gel) or a platinized platinum electrode insulated except at the tip was introduced into the axon. The potential difference across the axon membrane was led to the input of the spectrum analyzer after an appropriate amplification (see the schematic diagram in Fig. 10.7, top). A large number of chemical stimulants were examined by this method.

By the use of an FFT analyzer, a new type of electric signal was uncovered in intact axons of the squid. The new signals are far smaller in amplitude than the oscillatory subthreshold responses described in the preceding section, their Fourier components being something like 1–30 μV across the axon membrane. At this level of signal amplitude, the electric interaction between different parts of the membrane developing electric signals is very weak. Therefore, these responses may be visualized as representing regularly repeating excitation processes localized at a small number of excitable sites without being significantly affected by electric interaction between different parts of the membrane.

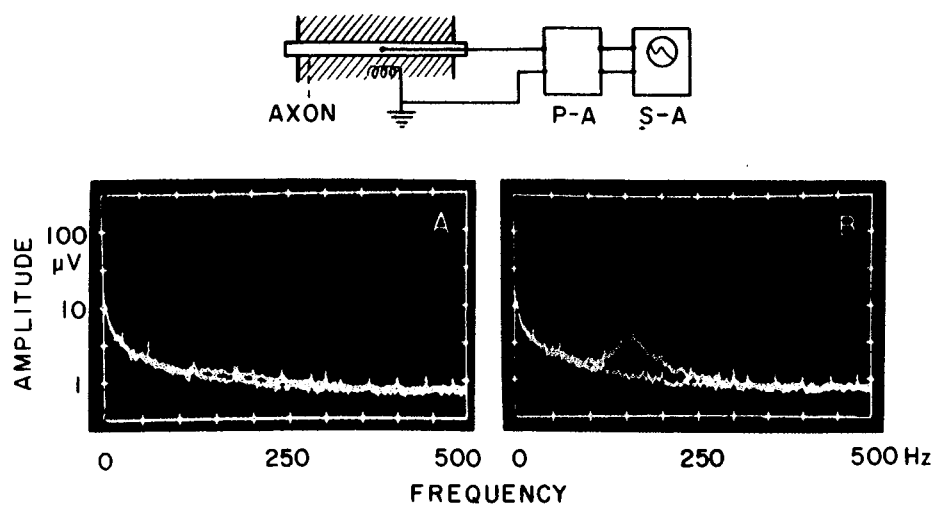


Fig. 10.7 Top: A schematic diagram of the experimental setup used for determining the frequency spectrum of the noise generated by the system, including the axon membrane, a pair of recording electrodes, a preamplifier (P-A), and a spectrum analyzer (S-A). Record A shows that a squid giant axon immersed in normal, divalent cation-rich seawater produced very small "membrane noise." Record B was taken approximately 10 min after reducing the external divalent cation concentration by a factor of 4, showing physiological responses of the axon membrane at about 150 Hz. The base line of the record was obtained with the two electrodes immersed in the external medium. (From *Jpn. J. Physiol.* **27**, 646, 1977.)

The photographic records in Fig. 10.7 show an example of the electric signals recorded from the interior of an intact axon. As indicated by the schematic diagram on the top, the potential difference between the intra- and extracellular electrodes was amplified with an AC-coupled amplifier and then led to a spectrum analyzer. First, Record A in the figure was taken from a freshly excised axon immersed in normal seawater. Next, the internal recording electrode was withdrawn from the interior of the axon and another spectral record was taken on the same photographic film with the two electrodes kept in the surrounding seawater. Usually, the two traces obtained by this procedure are superposable, indicating that the spectra obtained represent nothing more than the Fourier components of the noise generated by the electrodes, the preamplifier, and the spectrum analyzer itself. Occasionally, however, a small separation was observed between the two spectral traces, indicating that an extremely small signal is developed by the axon at around 140 Hz (as can be seen in Record A).

Record B in the figure was taken approximately 10 min after reducing the external divalent cation concentration by a factor of 4. Again, immediately after recording the signal from the axon interior, another spectral record was taken with the two recording electrodes immersed in the external medium. We see from the superposed picture in the figure that the signal generated by the axon is localized at frequencies around 140 Hz. Similar records have been obtained by using such chemical stimulants as scorpion toxin, or 4-dimethylaminopyridine, introduced into the external seawater.

The following experimental findings substantiate that the signal from the axon in Record B represents periodic physiological responses generated by the axon membrane: (1) When the temperature of the medium is lowered, the frequency of the signal falls; (2) the signal disappears when tetrodotoxin (TTX) is added to the external medium at a concentration of about 10 nM; (3) when the chemical stimulants are allowed to continue to act on the axon, the amplitude of the signal continuously increases and eventually repetitive firing of full-sized action potentials is initiated. The frequency of repetitive firing is similar to that seen in Record B.

We use the term "periodic miniature responses" to denote small electric signals which have small amplitudes and relatively broad frequency spectra. When the signal amplitude is smaller than about 30 μV , peak-to-peak, the overall spectrum of the signals is roughly independent of the amplitude.

H. THE DISCRETENESS OF MINIATURE RESPONSES

One of the salient features of the periodic miniature responses is that the spectral distribution of the Fourier components is frequently very complex and irregular. The spectrum of the signal depends to some extent on the

SCORPION VENOM IN SEAWATER

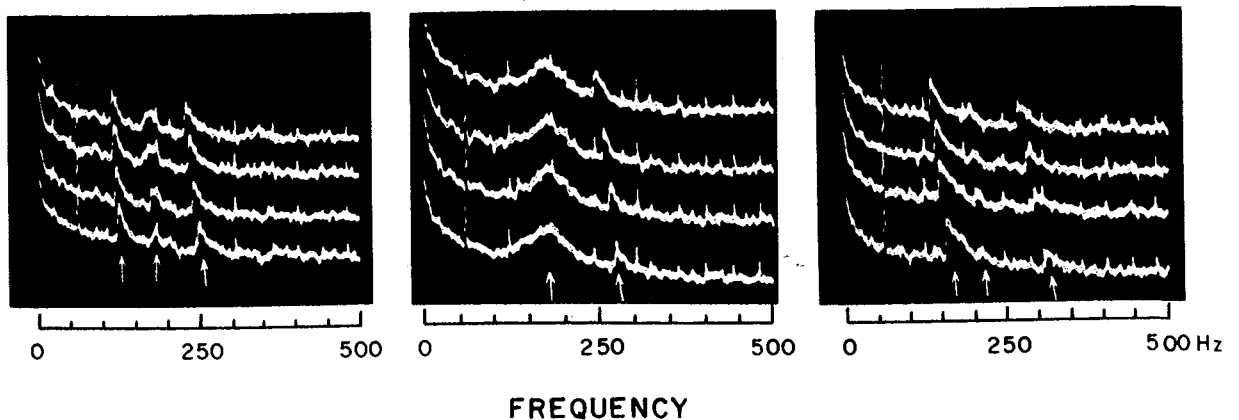


Fig. 10.8 Records of periodic miniature responses induced by external application of scorpion venom, illustrating the discrete nature of the responses. Four spectra in each record were photographed at intervals of about 20 sec starting at the bottom. The arrows at the lower margin of the photographs indicate the direction of the movement (frequency shift) of the discrete responses. The sensitivity of the recording system was the same as in the preceding figure. (From *Jpn. J. Physiol.* **28**, 97, 1978.)

class of chemical stimulants used (see later). Figure 10.8 shows three examples of the responses generated by external application of scorpion venom to squid giant axons. [The effective ingredient of scorpion venom is known to be a relatively small basic protein (Catterall, 1976).] In each column, four records taken at an interval of about 20 sec are displayed. It is seen in every spectral record that there are few prominent peaks and that these peaks slowly shift toward the left-hand side of the records (as indicated by the tilt of the arrows in the figure). The rate of frequency shift varies, within the same spectrum, depending on the position of the peak in the record.

There is little doubt that each prominent peak in the spectrum represents periodic excitation localized at a small patch of the axon membrane. The time course of the responses generated at each patch cannot be determined because only sinusoidal waves representing the fundamentals in the Fourier components can be detected by the present method. It is difficult to estimate the area of individual patches accurately; judging from the amplitude of the signal and the membrane resistance, it appears to be of the order of $1-10 \mu\text{m}^2$ (Note that, in order to produce a sinusoidal potential variation of $5 \mu\text{V}$ in amplitude at one point of an axon, an AC of about 1 nA is required; if we assume that a uniformly excited axon is capable of developing an AC of 1 mA/cm^2 , we arrive at a figure of about $10 \mu\text{m}^2$ as the effective area.) The existence of such membrane patches in the excited state has been demonstrated in internally perfused squid axons (Inoue *et al.*, 1974). We believe that such patches are formed by a cooperative process within a small area of the membrane.

It is interesting to note that the frequency of miniature responses is sensitive to changes in the temperature; cooling brings about lowering of the frequency. The temperature dependence of the frequency of miniature responses is very close to that of repetitive firing of full-sized action potentials (Tasaki, 1977).

I. CLASSIFICATION OF CHEMICAL STIMULANTS

Chemical stimulants known to produce periodic miniature responses may be divided into the following classes:

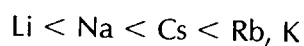
1. Small cations that are capable of displacing the divalent cations in the axon membrane. Alkali metal ions, 4-aminopyridine, 4-dimethylaminopyridine, etc., belong to this class.

2. Chemical reagents that alter the primary structure of proteins and other macromolecules in the membrane. *N*-Bromosuccinimide (which cleaves tryptophanyl peptide bonds and attacks sulfhydryl groups), glutaraldehyde (which cross-links protein molecules), photooxidation mediators like rose bengal (which attacks histidine), etc., come under this class.

3. Nerve poisons with relatively high molecular weights. Veratridine, allethrine, scorpion venoms, etc., fall under this class.

4. Raising the pH, lowering of the temperatures, etc.

The ability of externally applied alkali metal ions to generate miniature responses, measured by taking the concentration required as an index, increases in the following order:



This order is the same as the sequence determined by taking initiation of "abrupt depolarization" as an index (see Chapter 12, Section F). There is "ion antagonism" (see Chapter 3, Section C) between alkali metal ions and calcium: the critical concentration for univalent cation rises when the Calcium concentration in the medium is raised.

It is probable that the chemical stimulants under class 2 and 3 produce miniature responses also by altering the ratio of univalent-divalent cation concentration ratio within the axon membrane. The critical concentrations of these stimulants are very sensitive to a variation in the external univalent-divalent cation concentration ratio. An increase in the external divalent cation concentration always suppresses the miniature responses.

Among chemical stimulants of class 1, 4-aminopyridine was found to possess unusual properties. The ability of this compound to generate spontane-

ous discharges of full-sized action potentials was noted by Meves and Pichon (1977) and by Yeh *et al.* (1976). At concentrations of about 0.1 mM or less in artificial seawater, this compound produces miniature responses of which the frequency spreads over a very wide range (Tasaki, 1978). The peak frequency of the responses was found to vary between 8 and 230 Hz at 20°C. Such a wide variation in the frequency has not been encountered with other stimulants. The action potential duration is known to be significantly prolonged by 4-aminopyridine.

Since 4-aminopyridine is considered to be in the form of planar univalent cation, there seems little doubt that it competes with alkali and alkali earth ions for the occupancy of negatively charged membrane sites. Such competition is expected to decrease the intensity of cation interdiffusion which, in turn, slows down the relaxation processes.

It is important to note that, at the moment when barely detectable miniature responses are generated by 4-aminopyridine, 4-dimethylaminopyridine, scorpion venom, etc., there is no observable change in the resting potential of the axon. An example of the experimental results on which this finding is based is illustrated in Fig. 10.9. The records furnished in the figure were obtained by the following procedure. First, a record of both the resting and action potential was taken from an axon immersed in normal seawater. Next, the intra- and extracellular recording electrodes were connected to the

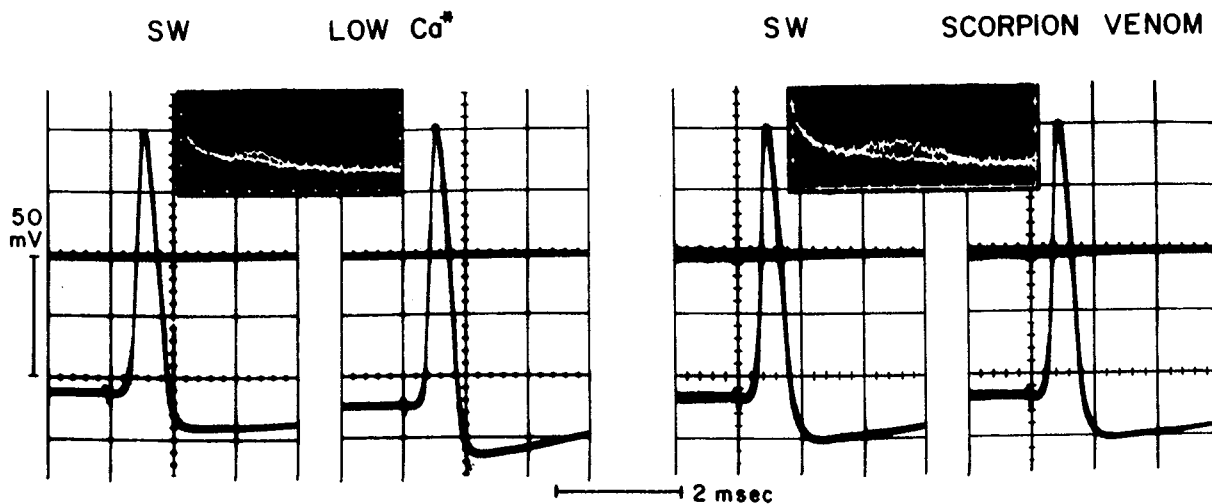


Fig. 10.9 Left: Action potentials observed before and after application of a solution with reduced divalent cation concentrations. The level of the membrane potential observed with the recording electrode kept in the surrounding medium is indicated by the heavy horizontal lines. The inset shows a superposed record of the responses of the FFT analyzer photographed immediately before the action potential records were taken. Right: Oscillograph and spectrum analyzer records showing the absence of a change in the resting potential at the moment when the miniature responses were induced by external application of scorpion venom. (From *Jpn. J. Physiol.* **28**, 94, 1978.)

FFT analyzer and the noise spectrum generated by the recording system was photographed. Then, the seawater outside the axon was replaced with one containing a chemical stimulant. When a definite sign of miniature responses was observed, a spectral record of the responses (superposed on the noise record) was taken. Immediately, the two electrodes were reconnected to the oscilloscope and a photograph of the resting and action potential was obtained. It was found by this procedure that generation of miniature responses was not preceded by a significant change in the resting membrane potential. In these cases, a decrease in the observed potential difference across the membrane cannot be regarded as the factor which triggers generation of miniature responses.

It is interesting to note in this connection that, among a large number of compounds examined, there were some that produced a fall in the membrane potential without being accompanied by generation of miniature responses. With lysolecithin or sodium dodecyl sulfate applied extracellularly, miniature responses could not be observed during the course of the gradual development of membrane depolarization.

Partial replacement of extracellular divalent cations with sodium ions generates periodic miniature responses (see Section G). There is a slight fall (a negative shift of a few millivolts) in the intracellular potential at the time when the responses are initiated (see Huxley, 1959).

In conclusion, we argue that the generation of periodic miniature responses involves changes in the conformational state of certain proteinaceous material in the axon membrane. The conformational changes involved can be induced either by chemical modification of several amino acids or simply by altering the ion species within the proteinaceous material.

J. MINIATURE RESPONSES GENERATED BY ELECTRIC CURRENTS

We now address ourselves to the question: What is the role of periodic miniature responses in electrical stimulation of the nerve membrane? We first demonstrate that miniature responses can be generated by pulses of outwardly directed current through the membrane. We then seek common physiochemical factors that contribute to the generation of responses by electrical and chemical stimuli.

The experimental setup used to investigate the effects of electrical stimuli are shown schematically at the top of Fig. 10.10. The electrodes used for delivering electric currents to the axon were made of two long glass pipettes separated by a distance of about 3 mm at the ends. The tip of the electrode for recording changes in the membrane potential was placed halfway be-

tween the two tips of the current electrodes. To reduce the sudden potential change generated by an abrupt onset of a current, the intensity of the applied current was raised linearly until it reached its final value. In addition, the artifact produced by the current was reduced by introducing a linearly rising voltage pulse to the second input of a differential amplifier simultaneously. The single-ended output of the amplifier was led to the spectrum analyzer. The external medium used in these experiments was a mixture of isotonic NaCl and CaCl₂ solutions, with the Ca-ion concentration (20 mM) high enough to suppress the generation of miniature responses in the absence of applied current.

Two examples of the spectral records obtained by the experimental setup described above are furnished in Fig. 10.10. The records on the left were taken approximately 10 sec after the onset of the current. It is seen that miniature responses are evoked by pulses of outwardly directed currents stronger than about 1 μ A and that the amplitude of the responses increases sharply with the intensity of the applied current. As the amplitude of the responses exceeds about 30 μ V (peak-to-peak), there is a marked reduction of the bandwidth of the response spectrum. When the amplitude exceeds about 300 μ V, the axon may soon be thrown into a state of repetitive firing of full-sized action potentials.

When the current intensity is maintained at a constant level, there is a gradual fall in the response amplitude (see the right-hand column in the figure). It seems quite natural to associate this gradual fall with the phenomenon of accommodation in classical physiology (see Chapter 7, Section A). Therefore, changes in the ionic composition of the surrounding medium are expected to greatly influence the rate of fall. Under the experimental conditions described above, the amplitude of the miniature responses fell to about $\frac{1}{3}$ in 1 min.

The effects of inwardly directed current through the membrane were examined using the same experimental setup. As expected, no responses could be evoked by a current which hyperpolarizes the membrane. The effects of an inward current were also tested in axons immersed in a medium with a reduced Ca-ion concentration. In axons developing miniature responses, application of an inward current through the membrane immediately suppressed the responses. Upon termination of the applied inward current, the responses promptly reappeared and grew to a level much larger than the initial amplitude. Frequently, full-sized action potentials were induced following withdrawal of an inwardly directed membrane current. Here we see an obvious link between the phenomenon of break excitation (see Chapter 7, Section G) and the rebound of the miniature responses.

The effective impedance of the membrane under the present experimental conditions was roughly 6000 Ω at about 150 Hz. The potential drop gen-

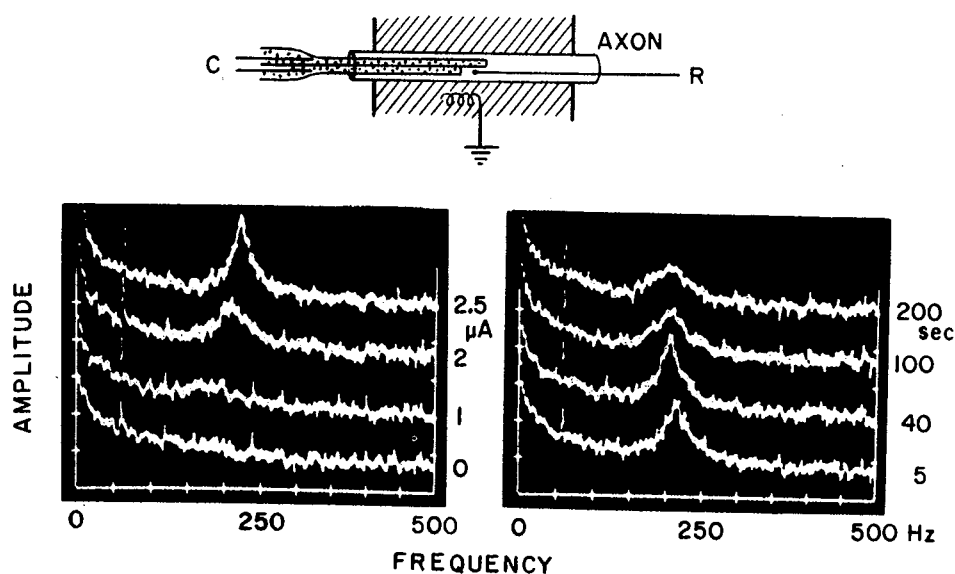


Fig. 10.10 Top: Schematic diagram showing the arrangement of the current (C) and recording (R) electrodes employed to study the effect of electric currents on the squid axon membrane. Bottom: Spectra of periodic miniature responses induced by outwardly directed membrane currents. Left records show the dependence of the response amplitude on the current intensity; each photograph was taken approximately 10 sec after the onset of the current. Right records show a gradual change in the response amplitude after the onset of an outwardly directed current of $2 \mu\text{A}$. These records were taken from an axon immersed in a medium containing 17 mM CaCl_2 and 503 mM NaCl (pH 8.1) for approximately 20 min. (From *Jpn. J. Physiol.* **27**, 650, 1977.)

erated by a current of $2 \mu\text{A}$ (used in the experiment shown in Fig. 10.10, right) was of the order of 16 mV at the site of recording. This value is slightly smaller than the familiar thermodynamic quantity RT/F (about 25 mV at room temperature).

From a physicochemical standpoint, it is desirable to find a link between the voltage changes generated by applied current and generation of miniature responses. The fact that there is a high concentration of potassium in the axon interior constitutes an obvious link. We have seen in the preceding section that potassium is the most powerful chemical stimulant among alkali metal ions. Its ability to initiate miniature responses is so strong that the external CaCl_2 concentration had to be raised to about 20 mM to study the phenomenon (Tasaki, 1978). An interesting aspect of the miniature responses produced by external application of a potassium-rich solution is that the amplitude falls gradually while the K-ion concentration is kept constant. A similar fall in amplitude is observed when an electric current is used instead of a potassium-rich solution (see Fig. 10.10, right). The peak frequency of the responses generated by a potassium-rich solution is about 150 Hz and is very close to that of the responses generated by an electric current.

An outwardly directed current through the membrane enhances the efflux

of potassium ions. When the voltage change generated by the applied current becomes comparable to the familiar value of RT/F , there should be a small rise in the intramembrane concentration of potassium ions. Since the external surface of the axon membrane is covered by Schwann cells and connective tissue, even the external layer of the axon membrane is expected to become, to some extent, potassium-rich. This rise in the potassium ion concentration must be accompanied by a fall in the intramembrane Ca-ion concentration. Thus, we arrive at a reasonable picture of how miniature responses are generated by an outwardly directed current through the axon membrane. Undoubtedly, this picture is not very different from what Loeb (1907), Bethe, (1920, cited in Chapter 7), and others suggested a long time ago.

K. EFFECTS OF TTX AND TEA ON MINIATURE RESPONSES

This section is devoted to the effects of tetrodotoxin (TTX) and tetraethylammonium (TEA) on the miniature responses of the axon. The effects of these pharmacological agents on the full-sized action potential has been discussed already (see Chapter 9, Section G, and Chapter 10, Section B). Since generation of periodic miniature responses is regarded as an electric manifestation of the excitation process taking place at a small number of membrane sites, it is interesting to investigate how these responses are affected by TTX and TEA.

Figure 10.11 furnishes a set of records showing the effects of TEA and TTX on the miniature responses. The spectral record on the lower left was taken approximately 10 min after external application of 4-dimethylaminopyridine. It is shown in the middle record that intracellular application of a dilute solution of TEA brings about an immediate lowering of the frequency of the miniature responses. As expected, the action potential duration is prolonged by this procedure (see the inset). Finally, when TTX (at a concentration of about 50 nM) was added to the surrounding artificial seawater, the miniature responses were completely suppressed within 1 min. It is seen that the action potential (generated by an electric shock applied to the axon near its end) was not yet completely eliminated at this moment. This is an example of our repeated experiences that miniature responses are far more sensitive to the action of TTX than propagated action potentials.

In a separate series of experiments, the effects of TTX were examined in axons without TEA pretreatment. In all the cases examined, suppression of miniature responses was prompt and complete at the level of about 5 nM. The chemical stimulants used to evoke miniature responses for this purpose

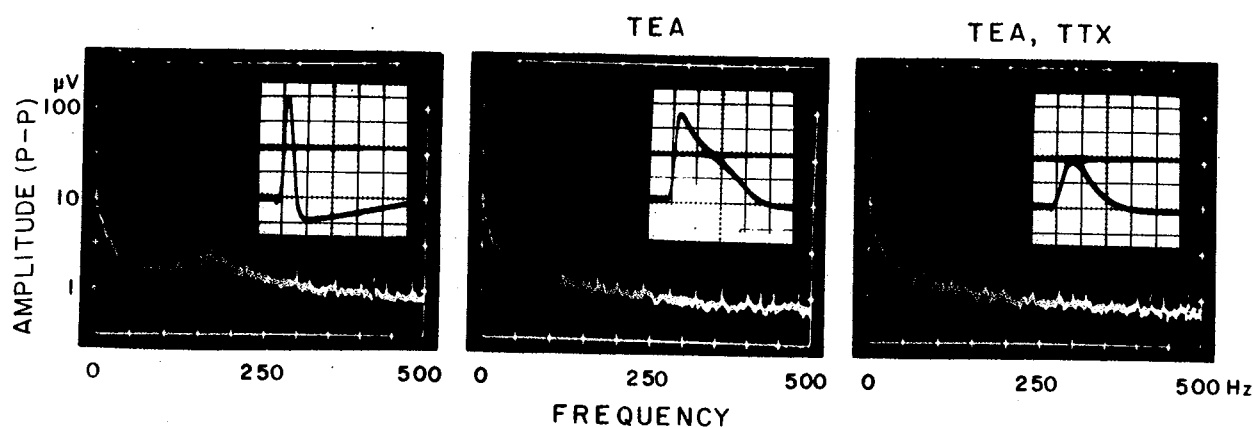


Fig. 10.11 Effects of intracellular injection of tetraethylammonium (TEA) followed by extracellular application of tetrodotoxin (TTX) on periodic miniature responses. The squid giant axon under study was treated with 4-dimethylaminopyridine dissolved in artificial seawater (2 mM). Note that the frequency of the miniature responses was lowered by TEA and that subsequent application of TTX suppressed the responses completely. The insets show the action potentials recorded within 1 min after the corresponding miniature responses were photographed. (From *Jpn. J. Physiol.* **28**, 96, 1978.)

include allethrin, 4-aminopyridine, *N*-bromosuccinimide, 4-dimethylaminopyridine, glutaraldehyde, low calcium seawater, scorpion venoms, and veratridine. The chemical nature of substances which generate miniature responses is manifold. Nevertheless, TTX was found to be effective in suppressing the responses evoked without exception.

The effects of TEA on miniature responses were examined under a variety of conditions. Without exception, TEA injection was found to lower the frequency of miniature responses. The chemical stimulants used to evoke miniature responses for this purpose include allethrin, 4-dimethylaminopyridine (Fig. 10.11), low calcium seawater, scorpion venoms, and veratridine.

In recent years many neurophysiologists have used TTX and TEA for the sole purpose of diagnosing the involvement of the "sodium channels" or the "potassium channels" in electrophysiological events under study. It has been assumed frequently that sodium and potassium channels occupy spatially distinct loci in the membrane and also that TTX specifically blocks the sodium channel and TEA suppresses the current through the potassium channel. It is true that under voltage clamp the inward membrane current is separated on the time axis from the outward current (see Chapter 8, Section G) and that TTX eliminates the inward current without affecting the outwardly directed component. From this suggestive evidence, the assumption of two separate and independent channels was derived. Because of its simplicity, this assumption gained great popularity.

Let us assume for a moment that TTX specifically blocks the "sodium

channels" and TEA affects the "potassium channels" exclusively. This assumption of two separate and independent channels combined with the experimental finding illustrated in Fig. 10.11 leads us syllogistically to the following self-contradictory conclusion: (1) Production of miniature responses involves Na channels because it is readily suppressed by TTX. (2) Blockade of K channels lowers the frequency of the miniature responses. (3) Therefore, the processes taking place in the Na channels must be strongly affected by the state of the K channels. In other words, the two channels cannot be separate and independent.

Under the voltage clamp conditions, the two channels are inseparably linked to the common voltage controlled by the experimenter. Under the conditions of the experiment illustrated in Fig. 10.11, however, no change takes place in the average (DC) potential difference across the membrane. The field of potential generated by a current passing through one ion channel must then fall very sharply with the distance. At a distance several times the diameter of the channel, the potential field must completely vanish. Therefore, the two types of channels cannot be widely separated, if the interaction between different parts of the membrane is mediated by an electric field.

The demonstration of miniature responses that have discrete spectra (see Chapter 10, Section H) strongly suggests the existence of a long-range chemical force contributing to a cooperative conformational change of membrane macromolecules. In the presence of a cooperative phenomenon, a simplistic picture of the axon membrane with two types of "ion channels" would not be useful in explaining the process of nerve excitation.

In the past, the assumption of the presence of two types of ion channels in the axon membrane has been questioned from time to time. In 1967, Watanabe *et al.* discovered that, under intracellular perfusion with a dilute CsF solution, axons maintain their ability to develop all-or-none action potentials in a medium containing CaCl_2 as the sole electrolyte (see Chapter 12, Section A). Since these action potentials produced in the absence of Na-ion could be suppressed very readily by TTX, an objection was raised against the use of TTX as a diagnostic tool for identifying the Na channels (Watanabe *et al.*, 1967). In response to this objection, the advocates of the two-channel hypothesis answered in the following words (see Moore *et al.*, 1967): "This (voltage-clamp experiment using TTX) leads us to point out that there were two operationally distinct channels. It is not yet clear how to devise an experiment that would conclusively determine whether two distinct functions are separated spatially as well."

In 1968, Mullins emphasized that the evidence for the presence of two independent ion conductances is only circumstantial and suggested the possibility that there is only one type of channel of which the selectivity changes with time (Mullins, 1968). In a letter to the editor, Narahashi and Moore

(1968) admitted that they do not see any experiment that could help them choose definitively between a single channel or a pair of independent channels. They said that it is "more convenient to conceive of separate channels because fewer additional assumptions are required."

It is true that, when the nerve membrane is assumed to possess two separate channels, the voltage clamp technique is a convenient means of investigating the properties of the membrane (see Chapter 8, Section G). Consequently, investigators who use this technique prefer the assumption of two separate channels. Nevertheless, the results of separation of the membrane currents into two components along the time axis can equally be interpreted as reflecting a gradual change in the emf and the conductance as functions of time (see Chapter 8, Section G and Chapter 14, Section G). Since the assumption of two separate channels has never been on a firm experimental basis, it is thoroughly logical to explain the new findings described in this section without rigidly adhering to the old assumption.

In a later chapter, an attempt will be made to explain the origin of the periodicity of miniature responses on the basis of physical chemistry of polyelectrolytes (see Chapter 13, F and H).

L. MEMBRANE NOISE AND MINIATURE RESPONSES

The experimental setup employed for demonstrating miniature responses described in the preceding sections is very similar to that employed by a number of investigators in studying membrane noise (Derksen and Verveen, 1966; Verveen and de Felice, 1974; Fishman, 1973; Fishman *et al.*, 1975, 1977; Conti and Wanke, 1975). We have seen that, in axons immersed in normal, divalent cation-rich seawater, the membrane voltage noise derives predominantly from the recording instrument. When an outwardly directed current is applied to the axon membrane, periodic miniature responses appear immediately. Within a few minutes after the onset of the current, however, the periodicity of the responses becomes unclear. A record taken with an FFT analyzer from an axon under the action of steady current may contain aperiodic physiological responses of the membrane which may be affected by TEA or TTX. In detection of small aperiodic responses, it is important to use special, low noise amplifiers (see Conti and Wanke, 1975).

When variations in the membrane potential is suppressed by the voltage clamp procedure, physiological responses are expected to appear in the form of "current noise." The current noise is related to the voltage noise by Ohm's law written in complex numbers. As has been emphasized by Wanke *et al.* (1974) it follows that

$$\begin{aligned} & \text{(Voltage noise power density)} \\ & = (\text{membrane impedance})^2 \times (\text{current noise power density}) \end{aligned}$$

The membrane impedance sharply rises to a maximum at the peak frequency of the periodic miniature responses (see Chapter 10, Section F). Consequently, it is difficult to detect a sign of periodic miniature responses by measuring current noise.

The absence of a sign of periodic responses in current noise data may also be explained in the following manner. When we determine the current–voltage relationship (the I – V curve of the type discussed in Chapter 8, Section G) for an axon under the action of a chemical stimulant, we immediately find that the slope, dI/dV , at $I = 0$ decreases with time. The reason for this decrease in the slope is that a small rise in the membrane potential is capable of throwing small membrane patches into their excited state (see Chapter 13, Section I). The appearance of a patch in the excited state makes a negative contribution to slope dI/dV ; the net result is that the slope becomes vanishingly small at the time when the axon is ready to generate subthreshold responses. When dI/dV is very small, a voltage variation, dV , can be much more easily detected than dI .

In order to carry out current noise measurements, the membrane potential has to be clamped with a relatively long axial wire; otherwise, the responses of the poorly clamped portion of the axon membrane near the end of the axial wire could make a significant contribution to the results obtained. Detection of noise derived from a large membrane area is less sensitive than that from a small area.

It is customary to present the result of a noise measurement in the form of a "log-log" plot (see Fishman, 1973; Conti and Wanke, 1975). An example of the data plotted in this manner is presented in Fig. 10.12 (right). The axon under study was chemically stimulated with glutaraldehyde dissolved in

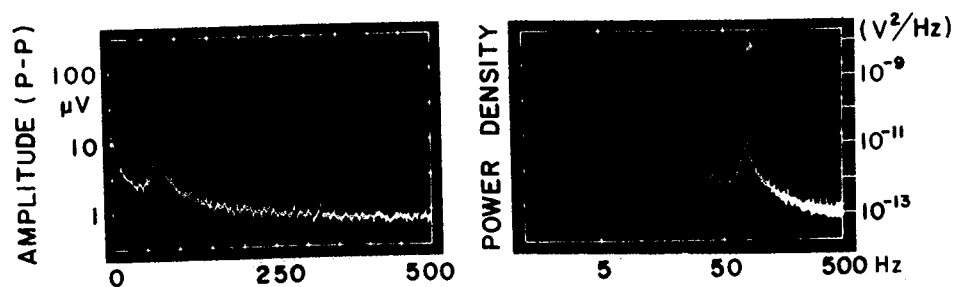


Fig. 10.12 Periodic miniature responses induced by external application of 8 mM glutaraldehyde dissolved in artificial seawater. The left-hand record was taken at about 75 min after application of the stimulant. The right-hand record was taken about 6 min before the left-hand record. Note that the peak frequency of the responses fell gradually and reached about 65 Hz before repetitive firing of full-sized action potentials was initiated. The vertical axis of the right-hand record was calibrated with a random-noise generator; the horizontal axis is on a logarithmic scale. 20°C.

seawater. The ordinate was calibrated with a random-noise generator and is expressed in the unit of power-density, V^2/Hz . The spectral record on the left-hand side of the figure is displayed on a semilogarithmic scale for comparison. An example of the data plotted in the linear scales (both axes) is given in a later chapter (see Fig. 11.10).

When we are dealing with the results of random-noise measurements, it is reasonable to express the magnitude of noise in power-density units. However, when we deal with steady, sinusoidal waves, we cannot adopt this unit because the power-density becomes infinitely large at the frequency of a sinusoidal wave. The experimental results discussed in Section H strongly suggest that the physiological responses of individual domains of the axon membrane are repeating at nearly constant frequency. This is the reason why we have expressed the amplitude of the miniature responses in the unit of microvolts rather than in V^2/Hz .

REFERENCES

- Armstrong, C. M. (1971). Interaction of tetraethylammonium ion derivatives with the potassium channels of giant axons. *J. Gen. Physiol.* **58**, 413–437.
- Arvanitaki, A. (1936). Variations lente de potentiel, associées au fonctionnement rythmique des nerfs non myélinisés, isolés. *J. Physiol. Pathol.* **34**, 1182–1197.
- Arvanitaki, A. (1939). Recherches sur la réponse oscillatoire locale de l'axon géant isolé de "sepia." *Arch. Int. Physiol.* **49**, 209–256.
- Arvanitaki, A., and Chalazonitis, N. (1955). Phase descendante a "palier" de la pointe axonique (sepia). In "Microphysiologie comparée de elements excitables." Colloques Internationaux Centre National de la Recherche Scientifique, Gif-Sur-Yvette, Paris.
- Bethe, A. (1908). Ein neuer Beweis Für die leitende Funktion der Neurofibrillen, nebst Bemerkungen über die Reflexzeit, Hemmungszeit und Latenzzeit des Muskels beim Blutegel. *Pfluegers Arch. Gesamte Physiol. Menschen Tiere* **122**, 1–36.
- Brink, F., Bronk, D. W., and Larrabee, M. C. (1946) Chemical excitation of nerve. *Ann. N.Y. Acad. Sci.* **47**, 457–485.
- Burn, J. H., and Dale, H. (1915). The action of certain quaternary ammonium base. *J. Pharmacol. Exp. Ther.* **6**, 417–438.
- Carlson, A. J. (1911). The effects of stretching the nerve on the rate of conduction of the nervous impulse. *Am. J. Physiol.* **27**, 323–330.
- Catterall, W. A. (1976). Purification of a toxic protein from scorpion venom which activates the action potential Na^+ ionophore. *J. Biol. Chem.* **251**, 5528–5536.
- Cole, K. S. (1941). Rectification and inductance in the squid giant axon. *J. Gen. Physiol.* **25**, 29–51.
- Conti, F. (1970). Nerve membrane electrical characteristics near the resting state. *Biophysik (Berlin)* **6**, 257–270.
- Conti, F., and Wanke, E. (1975). Channel noise in nerve membranes and lipid bilayers. *Q. Rev. Biophys.* **8**, 451–506.
- Cowan, S. L., and Walter, W. G. (1937). The effects of tetra-ethylammonium iodide on the electrical response and the accommodation of nerve. *J. Physiol. (London)* **91**, 101–126.

- Derksen, H. E., and Verveen, A. A. (1966). Fluctuations of resting membrane potential. *Science* **151**, 1388–1389.
- Eckhard, C. (1851). Die chemische Reizung der motorischen Froschnerven. *Z. Rat. Med.* **1**, 303–328.
- Fishman, H. M. (1973). Relaxation spectra of potassium channel noise from squid axon membrane. *Proc. Natl. Acad. Sci. U.S.A.* **70**, 876–879.
- Fishman, H. M., Poussart, D. J. M., and Moore, L. E. (1975). Noise measurements in squid axon membranes. *J. Membr. Biol.* **24**, 281–304.
- Fishman, H. M., Poussart, D. J. M., Moore, L. E., and Siebenga, E. (1977). K⁺ conduction description from the low frequency impedance and admittance of squid axon. *J. Membr. Biol.* **32**, 255–290.
- Gregor, H. P., and Bregman, J. I. (1951). Studies on ion-exchange resins. IV. Selectivity coefficients of various cation exchangers towards univalent cations. *J. Colloid Sci.* **6**, 329–347.
- Horne, R. A., Almeida, J. P., Day, A. F., and Yu, N-T. (1971). Macromolecule hydration and the effect of solutes on the cloud point of aqueous solutions of polyvinyl methyl ether: A possible model for protein denaturation and temperature control in homeothermic animals. *J. Colloid Interface Sci.* **35**, 77–84.
- Huxley, A. F. (1959). Ion movements during nerve activity. *Ann. N.Y. Acad. Sci.* **81**, 221–246.
- Inoue, I., Tasaki, I., and Kobatake, Y. (1974). A study of the effects of externally applied sodium ions and detection of spatial non-uniformity of the squid axon membrane under internal perfusion. *Biophys. Chem.* **2**, 116–126.
- Kay, R. L., and Evans, D. F. (1966). The effect of solvent structure on the mobility of symmetrical ions in aqueous solution. *J. Phys. Chem.* **70**, 2325–2335.
- Kay, R. L., Vituccio, T., Zawoyski, C., and Evans, D. F. (1966). Viscosity B coefficients for the tetraalkylammonium halides. *J. Phys. Chem.* **70**, 2336–2341.
- Kressman, T. R. E., and Kitchner, J. A. (1949). Cation exchange with a synthetic phenolsulphonate resin. III. Equilibrium with large organic cations. *J. Chem. Soc.* **1949**, 1208–1210.
- Lippay, F. (1929). Über Wirkungen des Lichtes auf den quergestreiften Muskel. 1. Versuche mit sichtbarem Licht an sensibilisierten Kaltblütermuskeln. *Pfluegers Arch. Gesamte Physiol. Menschen Tiere* **222**, 617–639 (see also **224**, 587–599, 1930).
- Loeb, J. (1907). Ueber die Ursache der elektronische Erregbarkeitsänderung im Nerven. *Pfluegers Arch. Gesamte Physiol. Menschen Tiere* **116**, 193–202.
- Loeb, J., and Ewald, W. F. (1916). Chemical stimulation of nerves. *J. Biol. Chem.* **25**, 377–389.
- Matsumoto, G., and Tasaki, I. (1977). A study of conduction velocity in nonmyelinated nerve fibers. *Biophys. J.* **20**, 1–13.
- Matsumoto, G., Tasaki, I., and Inoue, I. (1978). Oscillatory subthreshold responses and potential fluctuation observed in squid giant axons. *J. Phys. Soc. Jpn.* **44**, 351–352.
- Meves, H., and Pichon, Y. (1977). The effect of internal and external 4-aminopyridine on the potassium currents in intracellularly perfused squid giant axons. *J. Physiol. (London)* **268**, 511–532.
- Monnier, A. M. (1933). Phénomènes de "para-résonance" et théorie chronologique du système nerveux. *C. R. Soc. Seances Biol. Ses. Fil.* **114**, 1295–1297.
- Monnier, A. M., and Coppée, G. (1939). Nouvelles recherches sur la résonance des tissue excitables. I. Relation entre la rythmicité de la réponse nerveuse et la résonance. *Arch. Int. Physiol.* **48**, 129–180.
- Moore, J. W., Narahashi, T., Anderson, N. C., and Blaustein, M. P. (1967). Tetrodotoxin: Comments on effects on squid axons. *Science* **157**, 220–221.
- Mueller, P. (1958). Prolonged action potentials from a single node of Ranvier. *J. Gen. Physiol.* **42**, 137–162.
- Mullins, L. J. (1968). A single channel or a dual channel mechanism for nerve excitation. *J. Gen. Physiol.* **52**, 550–552; 555–556.

- Narahashi, T., and Moore, J. W. (1968). A single channel or a dual channel in nerve membrane? *J. Gen. Physiol.* **52**, 553–555.
- Oikawa, T. (1962). Electrical interaction between normal and TEA-treated zones of squid axon. *Am. J. Physiol.* **202**, 865–871.
- Pumphrey, R. J., and Young, J. Z. (1938). The rate of conduction of nerve fibres of various diameters in cephalopods. *J. Exp. Biol.* **15**, 453–466.
- Robinson, R. A., and Stokes, R. H. (1959). "Electrolyte Solutions," 559 pp. Butterworths, London.
- Segal, J. R. (1958). An anodal threshold phenomenon in the squid giant axon. *Nature (London)* **182**, 1370–1372.
- Stämpfli, R. (1958). Die Strom-Spannungs-Charakteristik der Erregbaren Membran eines einzelnen Schnürrings und ihre Abhängigkeit von der Ionenkonzentration. *Helv. Physiol. Acta* **16**, 127–145.
- Tasaki, I. (1959). Demonstration of two stable states of the nerve membrane in potassium-rich media. *J. Physiol. (London)* **148**, 306–331.
- Tasaki, I. (1977). Properties of excitable sites in the squid axon membrane as revealed by use of chemical stimulants and a spectrum analyzer. *Jpn. J. Physiol.* **27**, 643–655.
- Tasaki, I. (1978). Further studies of periodic miniature responses in squid giant axons. *Jpn. J. Physiol.* **28**, 89–108.
- Tasaki, I., and Hagiwara, S. (1957). Demonstration of two stable potential states in the squid giant axon under tetraethylammonium chloride. *J. Gen. Physiol.* **40**, 859–885.
- Tasaki, I., and Spyropoulos, C. S. (1957). Influence of change in temperature and pressure on the nerve fiber. In "The Influence of Temperature and Pressure on Biological Systems" (F. S. Johnson, ed.), pp. 201–220. Waverly Press, Baltimore, Maryland.
- Verveen, A. A., and de Felice, L. J. (1974). Membrane noise. *Prog. Biophys. Mol. Biol.* **28**, 189–265.
- von Hippel, P. H., and Wong, K.-Y. (1964). Neutral salts: The generality of their effects on the stability of macromolecular conformations. *Science* **145**, 577–580.
- Wanke, E., de Felice, L. J., and Conti, F. (1974). Voltage noise, current noise and impedance in space clamped squid giant axon. *Pfluegers Arch. Gesamte Physiol. Menschen Tiere* **347**, 63–74.
- Watanabe, A., Tasaki, I., Singer, I., and Lerman, L. (1967). Effects of tetrodotoxin on excitability of squid giant axons in sodium-free media. *Science* **155**, 95–97.
- Yeh, J. Z., Oxford, G. S., Wu, C. H., and Narahashi, T. (1976). Dynamics of aminopyridine block of potassium channels in squid axon membrane. *J. Gen. Physiol.* **68**, 519–535.

11. Squid Giant Axons under Internal Perfusion

A. TECHNIQUES OF INTRACELLULAR PERFUSION

The techniques of intracellular perfusion were invented with a view to experimentally manipulating the chemical composition of the internal milieu of the squid giant axon. The techniques were developed along two distinct approaches. In Plymouth, England, the procedure used was to remove the axoplasm by mechanical pressure applied to the axon and then to refill the axon interior with an artificial salt solution (Baker *et al.*, 1961.; Baker *et al.*, 1962, see Chapter 9). In Woods Hole, Massachusetts, and in Misaki, Japan, the technique was developed by modifying the method of intracellular injection so as to permit continuous flow of an artificial salt solution through the axon interior (Oikawa *et al.*, 1961; Tasaki *et al.*, 1962). Generally, there seems to be little difference between the results obtained by the two different techniques.

The double cannulation technique developed in this laboratory is suited for biochemical and physicochemical studies of the axon membrane. The procedure of double cannulation is illustrated schematically in Fig. 11.1.

An axon, about 40 mm in length, is mounted in a 30-mm-wide nerve chamber filled with seawater. The two ends of the axon are raised about 0.5 mm above the floor of the chamber by means of two sidepieces which are separated from the chamber by 2-mm-wide air gaps (see Diagram 1). An incision is made in the axon membrane near the top of one of the sidepieces and a glass cannula is inserted into the axon. Next, another incision is made near the other end of the axon and the other cannula is introduced into the axon interior.

Fabrication and alignment of the two cannulae demand special care. The outlet cannula is usually 250–300 μm in outside diameter and about 35 mm in length. The tip of this cannula is beveled and rounded. The other end of the cannula is connected to a polyethylene tube for the purpose of sucking the axoplasm into the cannula while it is pushed into the axon interior. The inlet cannula is usually about 100 μm in outside diameter and

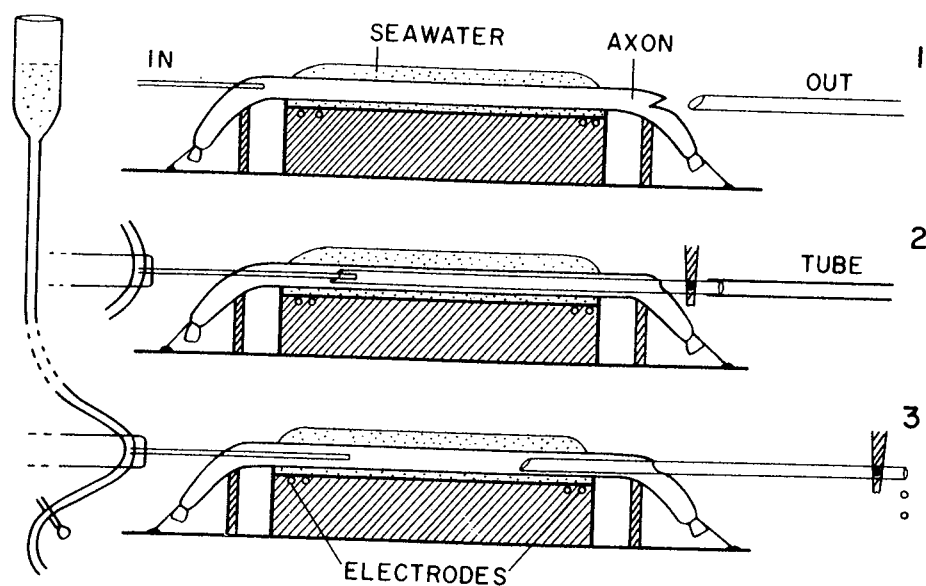


Fig. 11.1 Schematic diagram illustrating the double-cannulation method of intracellular perfusion of squid giant axons. IN and OUT represent inlet cannula and outlet cannula, respectively. The extracellular electrodes for monitoring propagated action potentials are indicated. Diagram 1 shows how the tips of the cannulae are introduced into the axon. Diagram 2 shows how the tip of the inlet cannula is inserted into the lumen of the outlet cannula. Diagram 3 shows that the interior of the axon is exposed to a continuous flow of the perfusion solution.

roughly 15 mm in length; it is connected to a reservoir of internal perfusion solution by means of a polyethylene tubing. Each of these cannulae is fixed to a plastic rod held by a micromanipulator. The two cannulae are accurately aligned so that they move along the axis of the axon as they are introduced into the axon.

By advancing the two cannulae along the axis of the axon, the tip of the inlet cannula is eventually pushed into the lumen of the outlet cannula inside the axon (Diagram 2). A flow of the solution from the inlet to the outlet cannula is initiated by applying a mild hydrostatic pressure (30–50 mm H₂O) to the solution. When the axoplasm within the outlet cannula is completely washed out by this flow, the two cannulae are separated. The interior of the axon is now exposed to the continuously flowing artificial salt solution. The length of the perfusion zone, namely, the distance between the tips of the two cannulae in their final positions, is usually between 12 and 20 mm. During the entire period of this manipulation, the threshold and the conduction time of the action potential are continually monitored by using two pairs of extracellular electrodes.

By the technique described above, it is possible to maintain the ability of the axon to develop normal action potentials for more than 10 hr under continuous intracellular perfusion if the pH, the osmolarity and the electrolyte composition of the internal solution are properly chosen (see the next sec-

tion). Frequently, however, the flow of the perfusion fluid is suspended when a mass of detached axoplasm clogs the outlet cannula. This problem can be avoided by pretreating the axon interior briefly with a dilute pronase solution. Electrophysiological properties of the axon are not affected by intracellular perfusion with a 400 mM KF solution containing 0.05 mg/ml pronase for a period of about 30 sec.

The technique of intracellular perfusion opened up the possibility of studying the physiological functions of the nerve fiber under complete control of intra- and extracellular milieu. Prior to the discovery of this method, measurements of various electrochemical quantities of the axon were of a more-or-less indirect nature. In the following sections, properties of the squid giant axon as revealed by the use of this method are described.

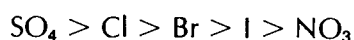
With some modification, this technique has been applied to crayfish axons (Shrager *et al.*, 1969), barnacle muscle fibers (Hagiwara *et al.*, 1969), and single cells of *Nitella* (Tazawa *et al.*, 1976). Brinley *et al.* (1975) devised a method of dialyzing the interior of the squid giant axon.

B. EFFECTS OF ANIONS INSIDE THE AXON

During the very early stage of perfusion experiments, we employed an isotonic KCl solution to perfuse the interior of the axon. It was our repeated experience that axons lost their excitability within 15 to 40 min when they were intracellularly perfused with a KCl solution at pH 7.3. Since a complete loss of excitability was preceded by a gradual fall in the action potential amplitude, it was difficult to study physiological properties of the axon membrane in a quasi-stationary state (Oikawa *et al.*, 1961).

Soon, we noticed that the survival time of axons under perfusion varies widely with the chemical species of intracellular anions. In addition, we reached a better understanding of the dependence of the survival time on the intracellular pH and ionic strength (Tasaki *et al.*, 1962). Much later, various factors which determine the survival time of the axon were analyzed from a physicochemical point of view (Tasaki *et al.*, 1965; Yoshioka *et al.*, 1978). We found that both anions and cations in the intracellular perfusion solution strongly affect the solubility of the protoplasmic and submembranous proteins.

The effects of inorganic salts on the solubility of proteins and biocolloids are well known. In his pioneering work, Hofmeister (1888) determined the critical concentrations of various salts required for "salting out" of various proteins in water and found the following series:



Later on, Bruins (1932) devised a method of putting this so-called "lyotropic series" on a quantitative basis and introduced the concept of lyotropic numbers. When we determined the lyotropic numbers of many potassium salts used for intracellular perfusion, we found an excellent correlation between the survival time of squid axons under intracellular perfusion and the lyotropic number of the anions (Tasaki *et al.*, 1965).

The sequence of anions arranged in accordance with their favorability for maintaining excitability under intracellular perfusion is

F > HPO₄ > glutamate, aspartate > citrate > tartrate
> propionate > SO₄ > acetate > Cl > NO₃ > Br > I > SCN

The lyotropic numbers determined in this laboratory for these anions are: F, 4.8; phosphate, 5.9; glutamate and aspartate, 6.6; citrate, 7.2; tartrate, 7.4; propionate, 9.8; SO₄, 6.8; acetate, 8.7; Cl, 10.0; NO₃, 10.3; Br, 10.8; I, 11.2; SCN, 12.3.

It is remarkable that an axon which has just lost its ability to develop action potentials under intracellular perfusion with a 400 mM KCl solution regains excitability when the KCl solution is quickly switched to a KF solution. Figure 11.2 shows an example of such observations.

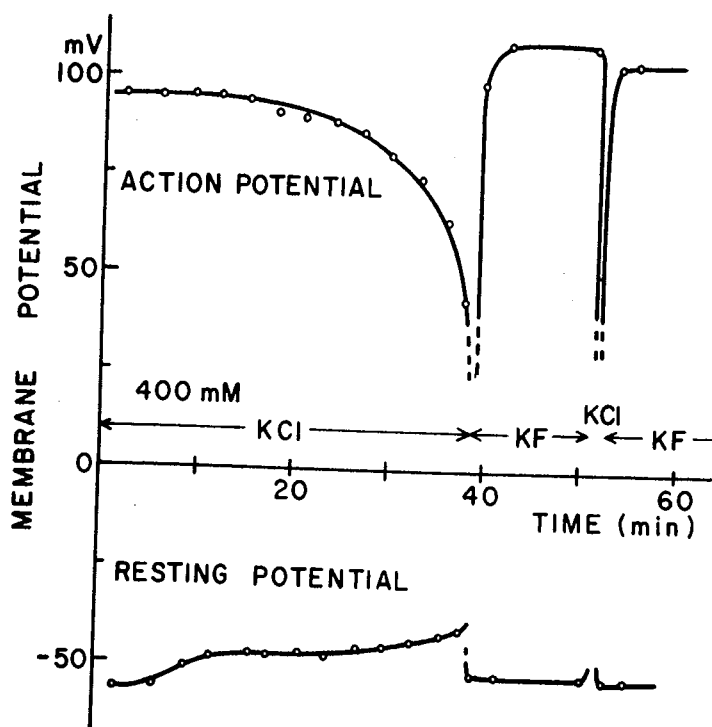


Fig. 11.2 Effect of intracellular anions on the resting and action potentials of a squid giant axon. Initially, the axon was internally perfused with a 400 mM KCl solution. At about 40 min after the onset of internal perfusion, the axon lost its ability to generate propagated action potentials. It is seen that the axon excitability was restored when a 400 mM KF solution was introduced immediately after the conduction block. (From *J. Gen. Physiol.* **48**, 1104, 1965.)

We have pointed out in a previous section (Chapter 9, Section C) that intracellular perfusion with an isotonic KCl solution produces an increased release of proteins into the perfusion fluid. There is little doubt that the loss of protein molecules from the layer beneath the axolemma is the major factor leading to the suppression of excitability caused by KCl inside. Replacement of chloride ions in the intracellular fluid with fluoride ions promptly reduces the rate of protein release. Re-formation of a compact protein layer beneath the axolemma, resulting from the decrease in the solubility of the remaining submembraneous proteins, appears to be the factor that brings about restoration of excitability by perfusion with KF. It may be pointed out in this connection that initiation of intracellular perfusion with a mixture of KF and potassium phosphate frequently restores the excitability of unperfused axons of which the excitability has been severely depressed by prolonged repetitive stimulation.

Although the survival time of squid axons under intracellular perfusion is enormously prolonged by the use of KF and potassium phosphate, it should be kept in mind that the conformational state of the protein molecules near and in the axonal membrane is somewhat different from that of an intact axon or of an axon internally perfused with, say, a potassium glutamate solution. We have seen that intracellularly applied proteolytic enzymes dissolved in the KF solution suppress the excitability of the axon far more slowly than when the same enzyme is dissolved in an isotonic potassium glutamate solution. Under intracellular perfusion with a solution containing a mixture of KF and potassium phosphate, the membrane macromolecules appear to be more compact and less vulnerable to the action of proteolytic enzymes.

C. SUBSTITUTION OF EXTERNAL Na-ION WITH POLYATOMIC UNIVALENT CATIONS

During the last several decades, physiologists have learned a great deal about the process of nerve excitation by examining the effects of modifying the external electrolyte composition. In this section, the effects of substituting one univalent ion species in the external medium for another are discussed.

Chloride ion constitutes the major portion of the extracellular anions; sulfate is also quite abundant in seawater.

Complete substitution of the external anions with bromide or ethylsulfate does not affect electrophysiological properties of a freshly excised, highly excitable axon. The effect of replacement of an extracellular anions species

with another is very small, except when the new anion species affects the concentration of free calcium ion. The low sensitivity of the resting and action potentials of the squid axon to the extracellular anions is in striking contrast to the high sensitivity to cations. In this respect, there is a close similarity between a cation-exchanger membrane and the external surface of the squid axon membrane.

The major cation species in seawater is sodium (425–534 mM). The effect of replacement of the external sodium ion with choline was examined a long time ago by Hodgkin and Huxley (see Chapter 8, Section H). The action potential amplitude is profoundly reduced by this replacement, while the resting membrane potential is hardly affected. Lorente de Nó and associates (1957) substituted various nitrogenous univalent cations for the external sodium ion and found that the action potential of the frog nerve trunk is *not* seriously affected (see also Larramendi *et al.*, 1956). We now systematically examine the Na-substituting ability of various univalent cations.

In squid giant axons under intracellular perfusion with favorable electrolyte solutions, a large number of univalent cations were found to be able to replace sodium ions without suppressing excitability (Tasaki *et al.*, 1965, 1966). Figure 11.3 shows an example of the results obtained with hydrazin-

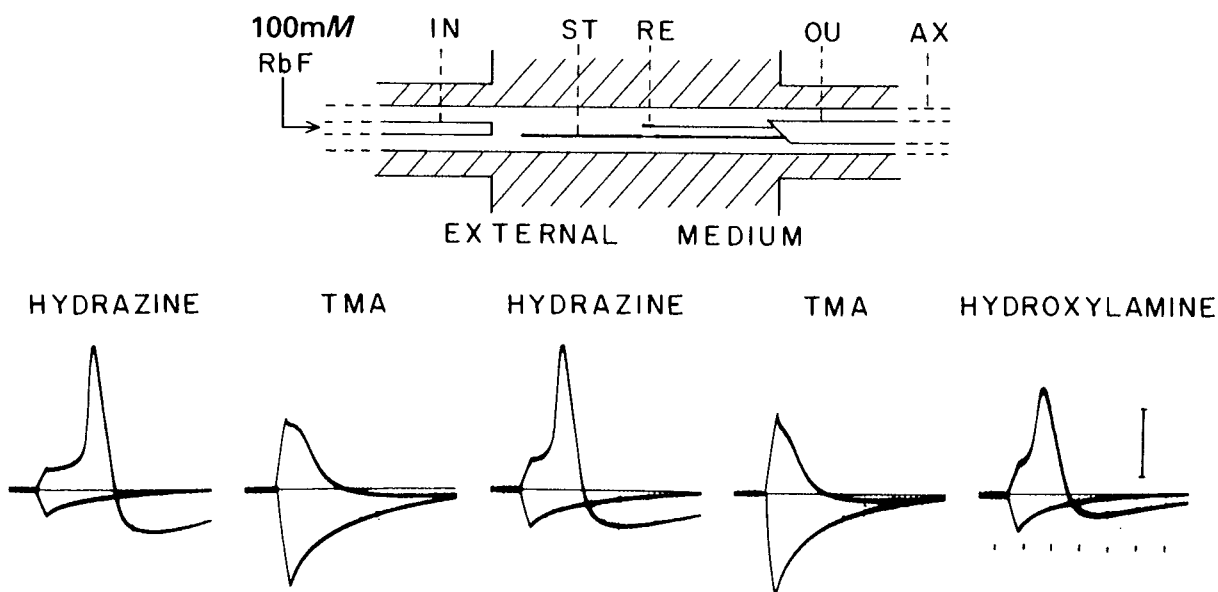


Fig. 11.3 Top: Experimental arrangement used for demonstration of excitability of squid giant axon in Na-free medium (not to scale). AX, giant axon; RE, recording electrode; ST, internal stimulating electrode; IN, inlet cannula; OU, outlet cannula. The axon was under intracellular perfusion with a 100 mM RbF solution with its pH adjusted to 7.3 with a small amount of rubidium phosphate. The external CaCl_2 concentration was kept at 200 mM. Bottom: Demonstration of action potentials in the presence of 300 mM hydrazine chloride outside (Records 1 and 3) or hydroxylamine (Record 5). Replacement of tetramethylammonium for hydrazine suppressed action potential production. (From *Proc. Natl. Acad. Sci. U.S.A.* **54**, 767, 1965.)

ium ion, $\text{H}_2\text{N}\cdot\text{NH}_3^+$. It is seen in the figure that hydrazinium is more favorable for the axon to maintain its excitability than tetramethylammonium ion. Beside hydrazinium ion, hydroxylamine, guanidine, and aminoguanidine ions can be used to replace external sodium ion without suppressing excitability. In these experiments it is important to increase the external divalent cation concentrations to a level high enough to prevent membrane depolarization.

The process of excitation in these sodium-free media is not fundamentally different from that of an axon immersed in normal seawater. There is a significant fall in the membrane impedance at the peak of excitation. Under voltage clamp, it is easy to demonstrate a membrane current that can be suppressed by application of tetrodotoxin (TTX). Quantitatively, however, there is some difference in behavior between polyatomic cations and Na-ions in axons. With a relatively large polyatomic cation externally, the membrane conductance at the peak of excitation does not increase as much as in axons immersed in sodium-rich media. Particularly when one of the hydrogen atoms of these polyatomic cations is replaced with a methyl or ethyl group, the ability of the cation to replace sodium is greatly reduced. This fact can be understood in the following manner: The mobilities of the cations within the axonal membrane in its excited state decrease as the size and the hydrophobicity of the side chains increase. The membrane conductance at the peak of excitation is determined by the mobilities and concentrations of the univalent cations (see Chapter 11, Section H).

Finally, the behavior of ammonium ion added to their external medium is briefly mentioned. In a medium containing normal divalent cation concentrations, ammonium ion behaves more-or-less like potassium or rubidium ion: when a large portion of sodium ion is replaced with ammonium, there is a decrease in the potential difference across the membrane and a rise in the membrane conductance. However, when the external calcium concentration is raised to about 100 mM, the ammonium ion concentration can be raised to about 100 mM without bringing about membrane depolarization. Under these conditions, ammonium ion (mixed with tetraalkylammonium ions to maintain the tonicity) behaves like sodium ions: the axon gives rise to action potentials of about 80 mV in the absence of Na-ion in the medium.

In dealing with the results of ion substitution experiments, it is important to realize that the sequence of univalent cations arranged in accordance with their Na-substituting ability is quite different from that arranged in the order of their depolarizing power. It will be shown later that membrane depolarization is caused by displacement of calcium ion in the axonal membrane (see Chapter 12, Section F). The effectiveness of univalent cations as Na-substitutes is determined by the mobilities and selectivities of the cations in the depolarized state of the membrane.

D. SUBSTITUTION AND DILUTION OF EXTERNAL DIVALENT CATION SALTS

Magnesium ion is the major divalent cation species in seawater. Complete replacement of magnesium ion with calcium ion does not affect the ability of the axon to develop normal action potentials. Similarly, complete replacement of the external calcium ion with magnesium brings about no immediate change in the axon excitability. If, however, this substitution of Mg^{2+} for Ca^{2+} is accompanied by addition of about 2 mM ethyleneglycol-bis(β -aminoethylether)- N,N' -tetraacetic acid (EGTA), there is a gradual fall in the action potential amplitude. (Note that EGTA is a strong chelating agent for calcium ion.) This finding suggests that the presence of magnesium ion alone is not sufficient to maintain the axon excitability. The difference, as well as the similarity, between the physiological action of calcium ion and that of other divalent cations has long been recognized by many previous investigators (see, e.g., Höber, 1920; see also Chapter 12, Section A).

It is well known that biological tissue contains an appreciable amount of bound calcium which can slowly be converted into the ionized form. In an excitable tissue that was immersed in a medium free of calcium ion, this conversion could raise the free calcium ion concentration to a level high enough to sustain excitability (see, e.g., Arima, 1914). Squid giant axons are surrounded by Schwann cells and connective tissue which are capable of releasing calcium. Therefore, when a small amount of EDTA (ethylenediaminetetraacetic acid) is added to an isotonic NaCl solution, the "poisonous effect of Na-ion in the medium" (Loeb, see Chapter 3, Section C) is enormously enhanced.

Axons intracellularly perfused with the standard KF solution lose their ability to carry nerve impulses when immersed in a mixture of isotonic sucrose (or glycerol) and $MgCl_2$ (or $CaCl_2$) solutions. The potential difference across the axonal membrane is maintained in such media. Figure 11.4 shows that the membrane potential observed under these conditions can be altered reversibly by changing the external divalent cation concentration. It is seen in the figure that the potential difference—measured with a glass-pipette electrode inside the axon referred to a calomel electrode in the external medium—increases when the external divalent cation concentration is reduced by dilution with an isotonic nonelectrolyte solution. Such an increase in the intracellular negativity is expected if the axonal membrane is assumed to possess cation-exchange properties.

In the absence of univalent cations in the medium, the superficial layer of the potential-determining sites of the axonal membrane is considered to be occupied solely by divalent cations. Furthermore, when co-ions (chloride in

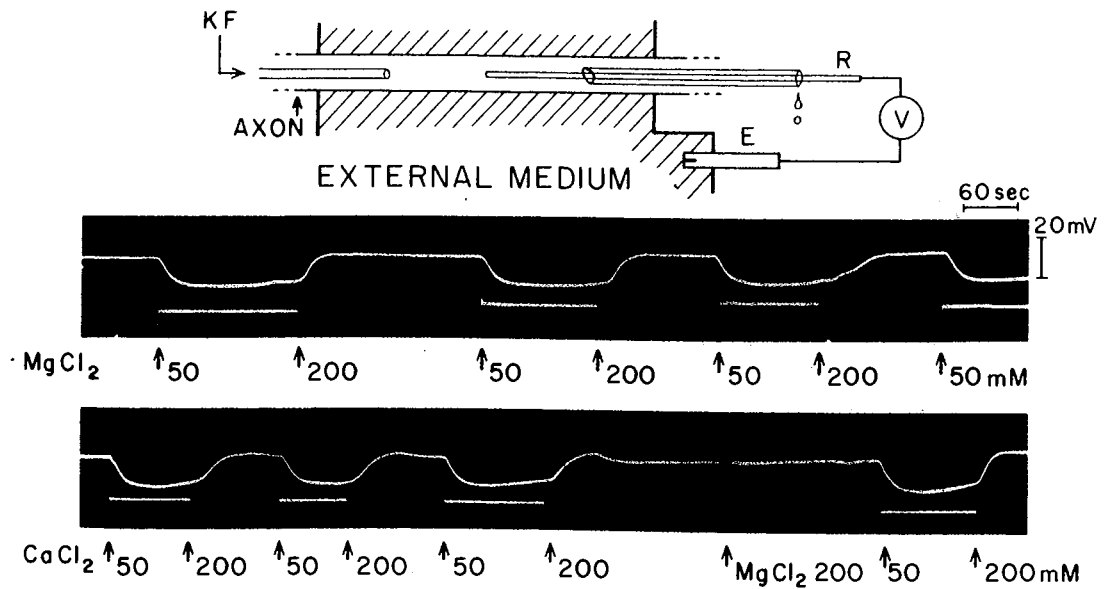


Fig. 11.4 Dependence of the membrane potential of an internally perfused squid giant axon on the concentration of the external $MgCl_2$ (upper record) and $CaCl_2$ (lower record) concentrations. The rapidly flowing external solution was alternated between 200 mM and 50 mM. The upward deflection of the oscillograph beam indicates a rise (i.e., a decreased negativity) of the intracellular potential. (From *Am. J. Physiol.* **213**, 1467, 1967.)

this case) are excluded from this layer, the potential difference across the interface between the medium and the membrane—the Donnan phase-boundary potential (see Teorell, 1953, cited in Chapter 8; Helfferich, 1962, cited in Chapter 8)—is expected to vary directly with the logarithm of the external divalent cation concentration. In the range between 50 and 200 mM, the observed values of the potential changes, ΔV , was found, in fact, to agree well with the theoretical value:

$$\Delta V = \frac{RT}{2F} \ln \frac{[Ca]_1}{[Ca]_2} \quad (11.1)$$

where the subscripts, 1 and 2, represent the two levels of the external Ca-ion concentration.

It is well known that co-ion exclusion becomes imperfect as the salt concentration in the medium is increased to a level comparable to the density of the fixed negative charges in the membrane. This explains why the observed potential change is smaller than the value expected from Eq. (11.1) in the concentration range higher than 200 mM. It is interesting to note that, in axons subjected to mechanical or chemical injuries, the observed potential changes are always smaller than the value expected from Eq. (11.1).

E. DILUTION OF THE INTRACELLULAR POTASSIUM SALT SOLUTION

We have previously discussed (see Chapter 8, Section D) the effect of varying the extracellular potassium ion concentration on the electrophysiological properties of the squid giant axon. We have seen that the potential difference across the axonal membrane is quite insensitive to a variation in the potassium ion concentration within the concentration range which is insufficient to suppress the normal excitability. When the potassium ion concentration is raised to a level high enough to depolarize the membrane, the membrane potential varies directly with the logarithm of the external potassium ion concentration with a slope close to 58 mV for a 10-fold change.

We are now ready to discuss the effect of varying the intracellular potassium ion concentration. In the standard internal perfusion solution, potassium is the only cation species present. The potassium ion concentration can be varied simply by mixing the standard solution with an isotonic glycerol (or sucrose) solution. Under these circumstances, the axon excitability is maintained in the entire range of potassium ion concentration as long as the K-ion concentration in the external seawater is kept at a low level (0–20 mM).

The data presented in Fig. 11.5 show the effect of dilution of the intracellular potassium ion concentration on the membrane potential measured recently by Ohki and Aono (1979). The potential difference across the membrane is seen to decrease by about 10 mV as the K-ion concentration is reduced from 500 to 50 mEq/liter. The value expected from the Nernst equation is about 58 mV for this 10-fold dilution. We thus find that the inner side of an intracellularly perfused axon does not behave like a potassium-sensitive membrane electrode. This finding is quite consistent with those obtained previously by Tasaki *et al.* (1962) and by Baker *et al.* (1962, cited in Chapter 9).

Ohki and Aono examined further the effect of variation of external K-ion concentration on the membrane potential at a series of internal K-ion concentrations. They showed that, independently of the internal K-ion concentration, the membrane potential changes with a slope about 50 mV for a 10-fold change in the external K-ion concentration in the range higher than about 50 mEq/liter. This finding indicates that the properties of the external layer of the axon membrane are very different from those of the inner layer, and also that the potentials generated on two sides of the membrane are more-or-less additive.

Studies of the squid giant axon under intracellular perfusion by means of transmission electron microscopy reveal that the axolemma is covered with a thick layer of axoplasm (Baker *et al.*, 1962). Examination of the axoplasmic

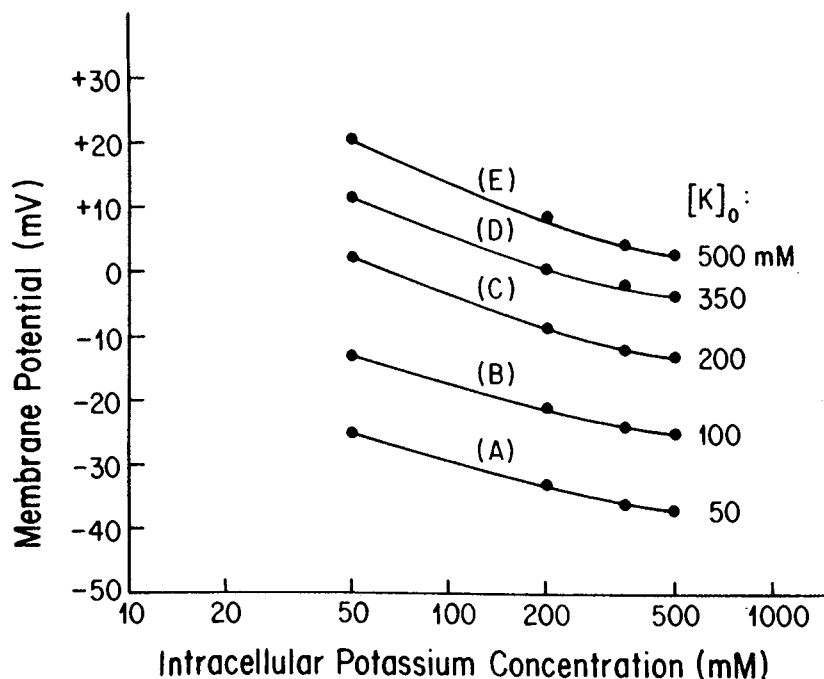


Fig. 11.5 Dependence of the membrane potential (ordinate) on the intracellular K-ion concentration (abscissa) at 5 different levels of the extracellular K-ion concentrations. The internal perfusion solution was prepared by mixing isotonic solutions of KF and glucose and the pH was maintained at 7.4 using potassium phosphate buffer. The extracellular solutions contained 20 mM of CaCl_2 and 550 mM of NaCl plus KCl. (From Ohki and Aono, 1979.)

surface of the membrane by scanning electron microscopy shows the existence of a longitudinally oriented fibrillary structure imbedded in soluble protein molecules (see Chapter 9, Section C). The isoelectric points of all these protein molecules are in the range between 6.5 and 4.5. Since the pH of the standard perfusion solution is 7.3, the protein molecules must carry fixed negative charges. We have seen, however, that intracellular anions (Cl^- , Br^- , etc.) invade the submembranous protein layer and alter the solubility of the protein molecules therein (Chapter 11, Section B). Therefore, it is evident that the volume density of the negative fixed charges of these proteins is not high enough to exclude co-ions. It is well known that a cation-exchange membrane covered with a thick layer of biocolloids does not behave like a cation-sensitive membrane electrode (see p. 47 in Tasaki, 1968, cited in Chapter 8).

F. SUBSTITUTION OF Na FOR INTERNAL K ON MEMBRANE POTENTIAL

In squid giant axons under intracellular perfusion, a large portion of K-ion in the internal perfusion solution can be replaced with Na-ion without bringing about suppression of the axon excitability. Total substitution of an iso-

tonic K-salt solution inside an axon with an Na-salt solution frequently causes a progressive suppression of excitability. The unfavorable effect of the internal Na-ion is markedly reduced when the salt solution is diluted with an isotonic glycerol (or sucrose) solution. For this reason, the effect of extensive substitution of Na-ion for the intracellular K-ion has been examined by keeping the total univalent cation concentration in the axon at a relatively low level.

The results obtained by the use of this procedure showed that the resting potential of the axon was hardly affected by a nearly total replacement of Na-ion for the intracellular K-ion (Tasaki and Takenaka, 1963; Ohki and Aono, 1979). An example of the results is furnished in Fig. 11.6. The external medium used was artificial seawater. It is seen that the change in the resting membrane potential produced by a nearly 10-fold reduction of the internal K-ion by this procedure was about 5 mV when the total univalent cation concentration was kept at 400 mEq/liter. At a lower total concentration, there was a smaller change of the resting membrane potential. This finding, together with the experimental results described previously (Chapter 8, Section D, and Chapter 11, Section E), completely invalidates the age-old myth that the resting potential is determined solely by the intracellular potassium

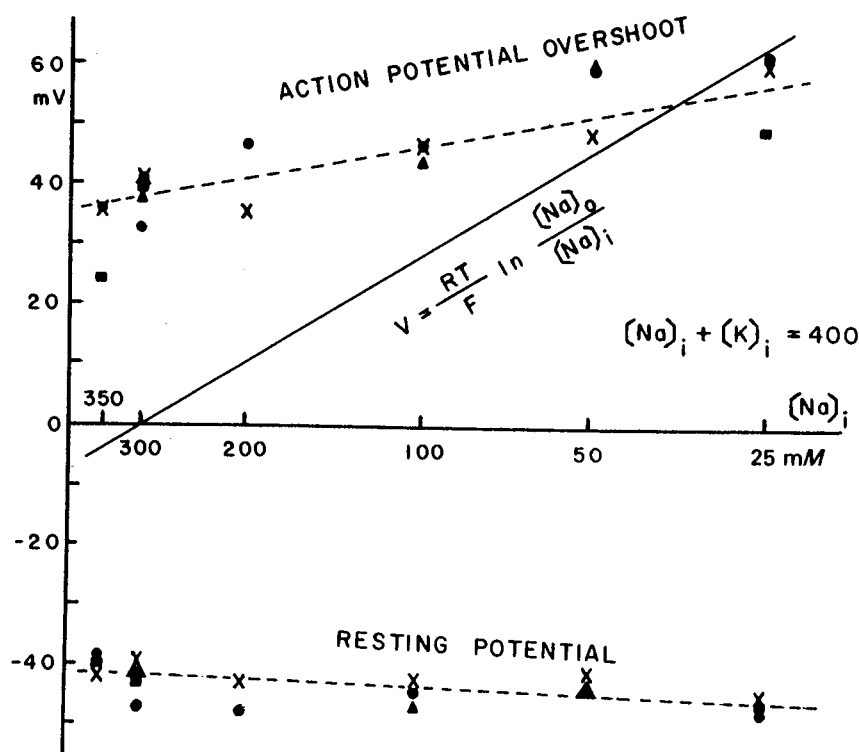


Fig. 11.6 Dependence of the resting membrane potential (bottom) and the action potential magnitude (top) on the intracellular concentration of Na- and K-ion. The sum of the internal Na- and K-ion concentrations was held at a constant level of 400 mEq/liter throughout. The perfusion fluid contained 470 mM glycerol besides Na- and K-salts in the glutamate form. The external medium containing 300 mM NaCl, 45 mM MgSO₄, and 22 mM CaCl₂. (From *Proc. Natl. Acad. Sci. U.S.A.* 50, 622, 1963.)

ions. In the resting (i.e., nondepolarized and excitable) state, the membrane potential is *not* affected appreciably by the potassium ion concentrations inside and outside the axon. On slightly different grounds, Stämpfli (1959), and Arhem *et al.* (1973) came to the same conclusion. Under intracellular perfusion, the resting membrane potential of a squid giant axon is determined by the selectivities and mobilities of uni- and divalent cations inside and outside the axon. It comes under the category of multi-ionic potential across a cation exchange membrane.

Figure 11.6 also shows the effect of replacement of internal K-ion with Na-ion on the amplitude of the action potential. There is a definite decrease in the amplitude when a large portion of the intracellular potassium ion is replaced with sodium (Tasaki and Takenaka, 1963; see also Fig. 11.7). However, it is evident that the action potential amplitude is not determined solely by the sodium ion concentration ratio across the membrane. Note that the observed dependence of the action potential on the internal Na-ion significantly deviates from the Nernst slope.

We have seen in Chapter 8, Section E, that the dependence of the action potential amplitude on the external Na-ion is close to that described by the Nernst slope in a relatively wide concentration. Again we see that there is a large difference between the electrochemical effects of ions on the external membrane layer and those on the inner layer.

Substitution of Na-ion for intracellular K-ion is expected to decrease the interdiffusion fluxes of these cations at the peak of excitation. Qualitatively, the observed slight decrease in the action potential may be explained as being brought about by a decrease in the intramembrane diffusion potential on the assumption that the selectivity-mobility product of Na-ion is slightly

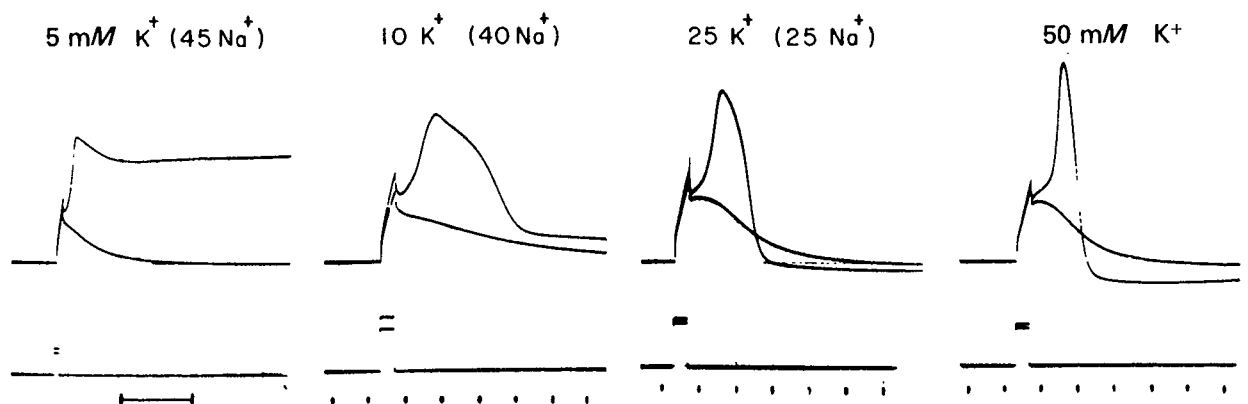


Fig. 11.7 Changes in action potential amplitude and duration produced by changes in the Na-K-ion concentration ratio of the internal perfusion fluid. The sum of the internal Na- and K-ion concentrations is kept at 50 mM; the anion was phosphate. The external medium contained 150 mM NaCl and 100 mM CaCl₂. The lower oscillograph trace represents the intensity of the electric current applied to the 18-mm-long perfusion zone. The dotted time markers are 1 msec apart; the bar is 10 msec long. (From *Am. J. Physiol.* **216**, 135, 1969.)

higher than that of K-ion (see Section G). This explanation is supported by the finding that replacement of internal K-ion with Rb-ion slightly increases the action potential amplitude. At the peak of excitation, the selectivity-mobility product of Rb-ion is considered to be smaller than that of K-ion.

G. PROLONGATION OF ACTION POTENTIAL DURATION BY SUBSTITUTION OF Na FOR INTERNAL K

Substitution of Na-ion for intracellular K-ion brings about a profound change in the time course of the action potential. Figure 11.7 shows an example of the action potential records taken from an axon intracellularly perfused with various mixtures of Na- and K-salt solutions. It is seen that, in a wide range of concentration ratio, the duration of the action potential increases continuously with the internal Na-K-ion concentration ratio. There is, however, a critical Na-ion concentration at which a *discontinuously large increase in the action potential duration* takes place. The action potentials produced by an axon with a high Na-ion concentration internally have a pronounced plateau followed by a distinct "shoulder." The duration of the plateau phase frequently exceeds 30 sec.

The effect of changing the intracellular Na-K-ion concentration ratio mentioned above is interpreted on the basis of the process of cation interdiffusion across the axon membrane during excitation. With the increasing Na-ion concentration inside, the intensities of the cation fluxes are expected to decrease. The reduction of the rate of potential fall in the excited state is linked to the decrease in the interdiffusion fluxes (see Chapter 13, Section H). The discontinuous increase in the action potential duration at a critical Na-K-ion concentration ratio is of special theoretical interest. An interpretation of this effect is presented in Chapter 13, Section G.

H. THE RESISTANCE-FLUX PRODUCT

The electric resistance of the axon membrane is determined by the mobilities and concentrations of the ions within the membrane. In an axon internally perfused with a K (or Rb)-salt solution and immersed in a mixture of Ca- and Na-salt solutions, the resistance is governed primarily by the internal and external univalent cations interdiffusing through the membrane. The experimental evidence that divalent cations are only semimobile in the axon membrane will be presented in the following section. When the fluxes of divalent cations and anions are negligibly small, the resistance r of the membrane of a unit area is given simply by integrating $dx/(u_1C_1 + u_2C_2)F^2$ from

one side of the membrane to the other, where u 's and C 's represent the mobilities and concentrations of the interdiffusing univalent cations, respectively.

It is important to note that the electrochemical factors which determine the magnitude of ion fluxes are also the mobilities and concentrations of the ions in the membrane. When the fluxes of divalent cations and anions are neglected, the influx of the external univalent cation must be equal to the efflux of the internal univalent cations. The magnitude of these ion fluxes observed in the absence of net membrane current, known as the "interdiffusion flux" (see e.g., p. 357 in Helfferich, 1962, cited in Chapter 8), is an important quantity which characterizes a cation exchanger membrane.

It can be shown by integrating the Nernst-Planck equations that the interdiffusion flux, J , is inversely proportional to the membrane resistance, r , the proportionality constant being given by the following universal constant:

$$r \cdot J = RT/F^2 = 2.6 \times 10^{-7} \Omega \cdot \text{Eq} \cdot \text{sec}^{-1} \quad (11.2)$$

where R , T , and F have the usual thermodynamic significance. It is important to note that Eq. 11.2 is valid even when the fixed charge density in the membrane is a function of the coordinate normal to the surface. Kobatake and Tasaki (1968) have demonstrated the validity of this equation extensively by using oxydized collodion membranes and commercially available cation exchanger membranes. In the range of membrane resistance between 10 and 10,000 $\Omega \cdot \text{cm}^2$, the interdiffusion fluxes involving Li-, Na-, and Rb-ion were found to agree with the values expected from the membrane resistance within about 10%. The limit of the applicability of this equation is discussed by Gottlieb and Sollner (1968).

We now apply this $r \cdot J$ relationship to the membrane of an internally perfused axon (Tasaki *et al.*, 1967). The standard solution used for perfusing squid axons intracellularly contains only K-ion. These axons remain excitable when they are immersed in a solution containing 450 mM NaCl and about 60 mM CaCl_2 . The efflux of potassium ion through the axon membrane is expected to be very close to the influx of sodium ion under these conditions.

The efflux of potassium ion across the membrane of intracellularly perfused squid axons was determined by radioactively labeling the internal perfusion solution with potassium-42. Since there was no potassium in the extracellular medium, the efflux could readily be measured by counting the radioactivity appearing in the external medium. The potassium efflux found by this method was between 1.25 and $2.25 \times 10^{-10} \text{ Eq} \cdot \text{cm}^{-2} \cdot \text{sec}^{-1}$. The membrane resistance of axons under these conditions was between 1.5 and 2 times $10^3 \Omega \cdot \text{cm}^2$. Thus, the values of the $r \cdot j$ product observed in intracellularly perfused squid axons were found to be between 2.5 and $3.3 \times 10^{-7} \Omega \cdot \text{Eq} \cdot \text{sec}^{-1}$; this value is very close to the theoretically expected value given

by Eq. (11.2). The influx of Na ion measured under similar experimental conditions yielded results consistent with the $r \cdot j$ product described above.

[Note that such a simple relationship between the resistance and flux does not exist in intact (i.e., internally nonperfused) axons immersed in normal seawater, because the concentrations of Na- and K-ion are finite on both sides of the membrane. Furthermore the existence of actively metabolizing protoplasm in the axon interior also complicates physicochemical analyses of ion fluxes (see Chapter 14, Section D).]

Cation interdiffusion fluxes were also measured in axons internally perfused with a Rb-salt solution and immersed in a mixture of CaCl_2 and guanidinium (Gu) chloride solutions. An example of the results obtained from axons in such sodium-free, potassium-free media is presented in Fig. 11.8 (right). The resistance-flux (rj) products determined in these axons were not very different from the values expected from Eq. 11.2.

Qualitatively, the $r \cdot j$ relationship described above may be applied to the axon membrane at the peak of excitation. It is seen in Fig. 11.8 that the efflux of K- (or Rb)-ion is markedly enhanced during repetitive stimulation of the axon. Since the extra-efflux of potassium is roughly proportional to the frequency of stimulation, the cation efflux associated with a single propagated nerve impulse can readily be determined. The value thus determined is roughly $12 \times 10^{-12} \text{ Eq} \cdot \text{cm}^{-2}$ per impulse. Because of the requirement of electroneutrality, approximately the same quantity of Na-ion has to be transported from the K-free external medium into the Na-free internal perfusion solution. The previous estimates of Na-K exchange per nerve impulse carried out by using intact giant axons are somewhat smaller than the value mentioned above (Hodgkin and Keynes, 1955; Hodgkin, 1958). [Note that determination of net cation fluxes in intact axons requires a very complex procedure (see Chapter 14, Section D).]

Associated with the process of action potential production, there is a drastic fall in the membrane resistance; the resistance returns to its resting level approximately 1 msec after the onset of the action potential. At the peak of excitation, the membrane resistance falls to about $\frac{1}{100}$ of the resting level. According to the $r \cdot j$ relation mentioned above, it is expected that the flux rises by a factor of about 100. The approximate peak level of the observed K-efflux, estimated by dividing the extra-efflux per impulse by about 0.5 msec, is roughly $240 \times 10^{-10} \text{ Eq} \cdot \text{cm}^{-2} \cdot \text{sec}^{-1}$; this is close to the value expected from Eq. (11.2). Thus, we find that the enhancement of the cation interdiffusion at the peak of excitation is directly related to the rise of the membrane conductance (see Tasaki *et al.*, 1967). (The existence of membrane capacitance does not affect the present analysis significantly, because the capacitative component of charge transfer across the membrane is less than $\frac{1}{10}$ of the charge transported by the alkali metal ions.)

In summary, interdiffusion fluxes of univalent cations have been deter-

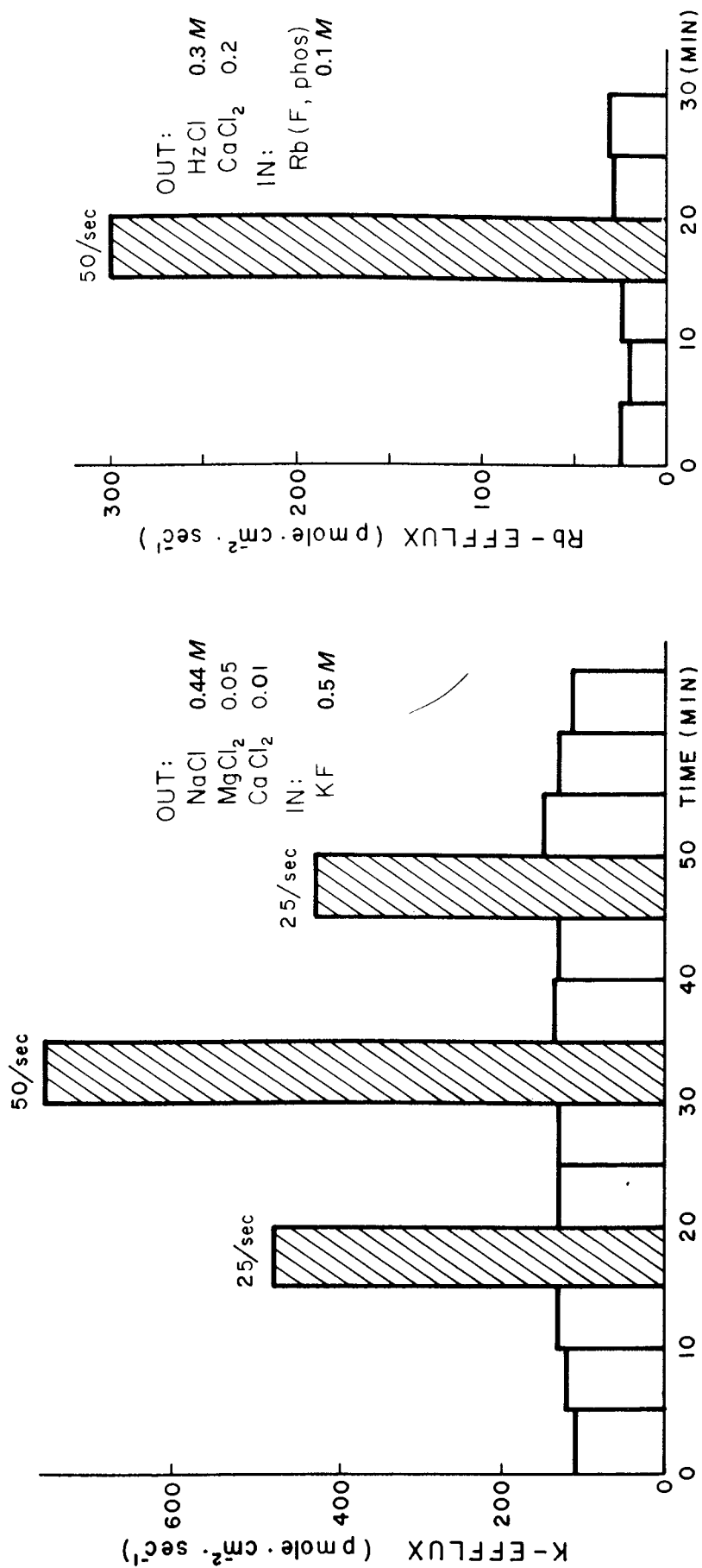


Fig. 11.8 Left: Potassium effluxes through the membrane of an axon internally perfused with a 0.5 M KF solution and immersed in a medium containing both NaCl and divalent cation salts. The effects of repetitive stimulation of the axon at 25 and 50/sec on the K efflux are shown. Right: Rubidium effluxes through the membrane of an axon internally perfused with a 0.1 M Rb phosphate. The axon was immersed in a medium containing 0.2 M CaCl₂ and 0.3 M hydrazinium chloride. The effects of repetitive stimulation of the axon at a rate of 50 impulses/sec are shown by the crosshatched area. (From *J. Gen. Physiol.* **50**, 993, 1967.)

mined in squid giant axons which are immersed in a mixture of Na- and Ca-salt solutions and intracellularly perfused with a solution containing only K-salts. In the resting state of the axon, the cation fluxes are related to the membrane resistance by Eq. (11.2). Enhancement of cation interdiffusion during excitation is a reflection of a fall of the membrane resistance.

I. INFLUX OF CALCIUM ION

Before the technique of intracellular perfusion was invented, the influx of calcium ion into intact giant axons was determined by the method of radioisotope incorporation (Hodgkin and Keynes, 1957). Using cleaned giant axons immersed in seawater to which calcium-45 was added, it was found that the rate of incorporation of radioactive calcium was enhanced by repetitive stimulation of the axons.

It is desirable to determine the influx of Ca-ion across the membrane by the use of the technique of intracellular perfusion. Particularly, the effect of repetitive stimulation on the Ca-flux into the internal perfusion fluid is expected to furnish new information concerning the mobility of Ca-ion in the membrane during excitation. When an attempt was made to measure Ca-influx in an axon with a relatively thick layer of axoplasm remaining beneath the axonal membrane, it was found impossible to detect an increase in influx during repetitive stimulation (Luxoro *et al.*, 1965). Transport of Ca-ion through the axoplasm is very slow.

Later on, measurements of Ca-influx were repeated using axons pretreated intracellularly with pronase (Tasaki *et al.*, 1967). The thickness of the axoplasm remaining beneath the axolemma was estimated to be about 1 μm . We now know that, in such axons, repetitive stimulation brings about a large increase in the rate of solubilization of protein molecules in the remaining axoplasm (Chapter 9, Section D). Nevertheless, it was possible to demonstrate a marked increase in Ca-influx during high-frequency stimulation (see Fig. 11.9). (There was gradual deterioration in the excitability of the axon under these conditions.)

Under internal perfusion with a pure potassium salt solution, the total influx of Ca-ion could be determined directly from the levels of radioactivity in the external medium and in the collected samples of perfusion fluid. The external medium contained 50 mM CaCl_2 , 400 mM NaCl, and 42,000 counts $\cdot\text{min}^{-1}\cdot\text{mm}^{-3}$ radioactivity. The calcium influx thus determined was 0.17 pmole $\cdot\text{cm}^{-2}\cdot\text{sec}^{-1}$. In the resting state of the axon membrane, the contribution of calcium ion to the total cation influxes (see Chapter 11, Section H) is very small.

The extra Ca-influx associated with repetitive stimulation of the axon was

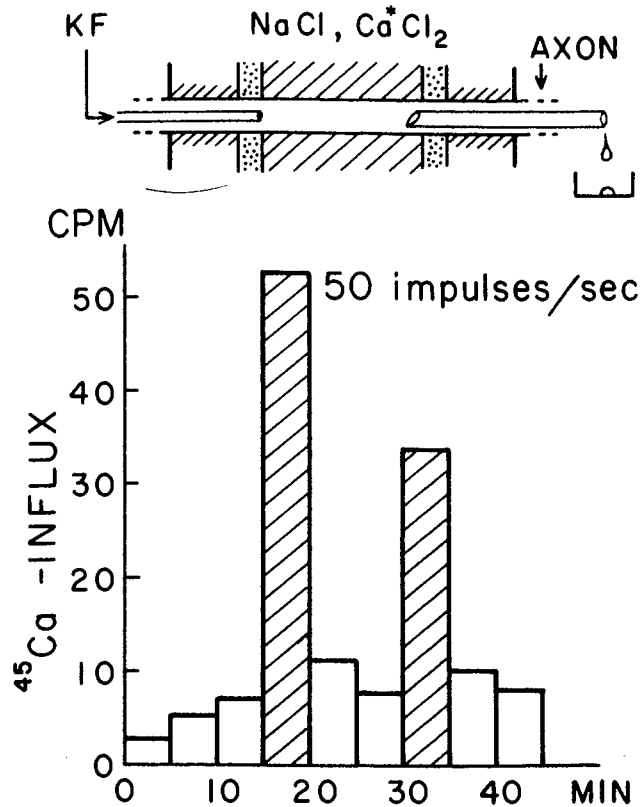


Fig. 11.9 Top: Schematic diagram representing the experimental arrangement used for measuring calcium influx across the squid axon membrane. The external medium contained 400 mM NaCl and 50 mM CaCl_2 . The internal perfusion fluid, containing 400 mM KF and glycerol, was collected continuously as it flowed from the outlet pipette. Bottom: Ca-influx at rest and during repetitive stimulation at 50 shocks/sec. The ordinate represents the radioactivity in the internal perfusion fluid collected during 5-min periods. The abscissa represents the time after introduction of radioactive calcium into the pool of external fluid medium. The cross-hatched bars represent periods of repetitive stimulation. The lower radioactivity during the second stimulation period is due to gradual deterioration of the axon. 19°C . (From *Am. J. Physiol.* 213, 1472, 1967.)

roughly $0.025 \text{ pmole}\cdot\text{cm}^{-2}$ per impulse. Assuming that the influx rises and falls along a triangular time course of about 1 msec duration, the peak Ca-influx is estimated to be more than 200–300 times as high as that at rest. The ratio of the peak influx to the influx at rest appears to be *much larger for Ca-ion than for Na-ion*. This finding indicates that there is an enormous increase in the mobility of Ca-ion during excitation. The low mobility in the resting state may be attributed to binding of the divalent cations to two negatively charged sites. During nerve excitation, such Ca bridges may be broken by the invasion of univalent cations (see Chapter 10, Section J; Chapter 12, Section A; and Chapter 13, Section F).

From a physicochemical point of view, analyses of membrane phenomena involving both uni- and divalent counterions are not easy. There are only a limited number of comprehensive studies of artificial membrane

involving Ca-ions (see, e.g., Gregor and Wetstone, 1956; Helfferich and Ocker, 1957). From the results of these studies, the following general rules may be extracted (see pp. 103, 156, and 305 in Helfferich, 1962). (1) There are strong electrostatic interactions between polyvalent counterions and fixed charges of the membrane; this interaction raises the selectivity and lowers the mobility of polyvalent counterions. (2) The ion mobilities usually vary with the content of water within the membrane matrix. Counterions of a high valency bound to the membrane lower the water content. (3) Both a reduction in the cross-linking within the membrane and an increase in the water content enhance the mobilities of counterions and alter the ion selectivity of ion-exchange membranes (see Boyd and Soldano, 1953; Lagos and Kitchener, 1960).

The effects of divalent cations on properties of biocolloids and synthetic polymers have been examined by a number of physical chemists. Clowes (1916) and Waterman (1928) showed that the colloidal state of oil-water mixture is affected strongly by a change in the ratio of Ca- to Na-ion in the mixture. The electric resistance of the mixture was found to increase sharply at a critical Ca-Na ratio (see also Matijevic *et al.*, 1966). Smidsrod and Haug (1967) analyzed the process of precipitation of acidic polysaccharides by uni- and divalent cations. Ikegami and Imai (1962) showed that polyacrylic acid neutralized partially with NaOH can be readily precipitated by calcium salt but not by magnesium; the difference in behavior between Ca and Mg is attributed to the strong tendency of Ca-ion to diminish the hydration sphere around the synthetic polyacid. As we shall see later (Chapter 13, Section E), Ca-ions play a central role in our macromolecular theory of nerve excitation.

J. EFFECTS OF CHANGING THE INTERNAL pH

In an early study of the effects of varying the internal pH on axon excitability (Tasaki *et al.*, 1962), a 225 mM K_2SO_4 solution was used for internal perfusion. The range of pH examined was varied between 5 and 10. With the internal pH adjusted to 7.3 ± 0.1 , squid giant axons immersed in natural seawater were found to be able to maintain their excitability for more than 4 hr under continuous intracellular perfusion. When the internal pH widely deviated from 7.3, the axons lost their ability to develop action potentials in a relatively short period of time.

The effects of an acidic perfusion solution on the electrophysiological properties of the axon are very different from those of an alkaline perfusion solution. Under internal perfusion with an alkaline solution, the axon tends to plunge into a state of repetitive firing of full-sized action potentials before

the axon excitability starts to deteriorate. Acidic internal perfusion solutions do not usually induce repetitive firing of action potentials. Instead, the axons behave as if they are anesthetized or stabilized by excess calcium in the external medium. On either side of the most favorable pH, the effects of unfavorable pH on the electrophysiological properties of the axon are progressive. These changes cannot be completely reversed by initiating perfusion with a favorable solution unless perfusion with an unfavorable solution is terminated within a few minutes (Terakawa *et al.*, 1978). There seems little doubt that denaturation of protein molecules located in and near the axon membrane is the major factor which limits the reversibility of the observed pH effects.

More recently, the effects of the internal pH on the rate of protein release into the perfusion solution were examined by S. Terakawa (unpublished). By using the method of radioactively labeling the proteins released, it was found that perfusion with an alkaline solution profoundly enhances the rate. When the pH of the perfusion solution (containing a mixture of KF and phosphate) was shifted from 7.3 to approximately 10, the rate of protein release was enhanced by a factor of about 5. The major portion of the proteins released had their molecular weight around 60,000 and 12,000. There was little or no increase in the rate when the internal pH was shifted to the acidic side.

A small alkaline shift of the internal perfusion fluid is a very effective means of generating "periodic miniature responses." Figure 11.10 shows that a pH rise of about half a unit can lead to the generation of distinct miniature responses when the external Ca-ion concentration is barely sufficient to keep the axon membrane in the quiescent state.

We have seen that lowering of the external Ca- to Na-ion concentration ratio is a forceful means of generating miniature responses (see Chapter 10, Section G). A slight shift of the pH of the internal perfusion fluid toward the acidic side of 7.3 was found to suppress the miniature responses generated by lowering of the Ca-Na ratio.

It is well known that the degree of swelling (or water content) of a polyelectrolyte is very sensitive to the hydrogen ion concentration. Lowering of the pH brings about a loss of water from the polyelectrolyte phase (see, e.g., Michaeli and Katchalsky, 1957). The similarity between the effect of lowering of the pH and that of raising the Ca-ion concentration may be attributed to (1) enhancement of the degree of neutralization of fixed negative charges and (2) lowering of the degree of swelling.

Finally, it should be pointed out that, in internally perfused axons, the effect of changing the pH of the external medium is less pronounced than that of the intracellular solution. This difference in the pH effect may be attributed to the multilayer structure of the axonal membrane. The external layer

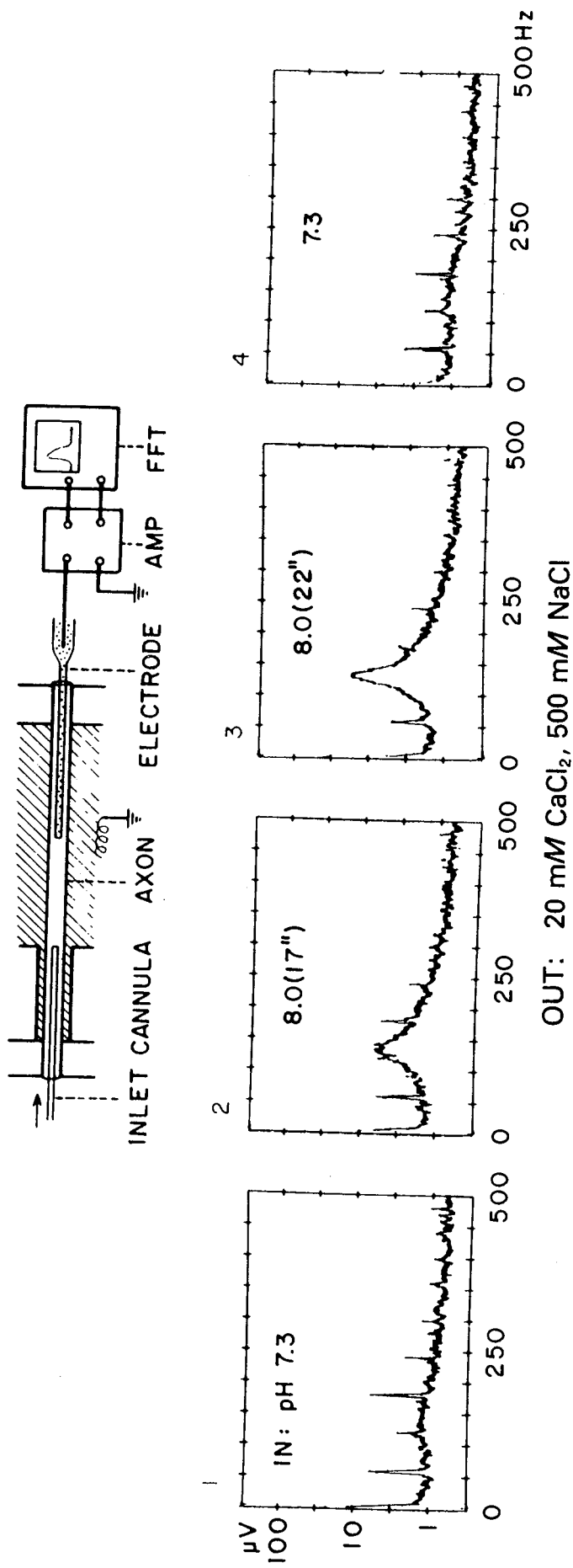


Fig. 11.10 Generation of periodic miniature responses by a small alkaline shift of the intracellular pH. Records 1 and 4 were taken when the intracellular pH was maintained at 7.3. Records 2 and 3 were obtained 17 and 22 sec, respectively, after the introduction of an internal perfusion solution at pH 8.0. The composition of the external medium is given.

of the excitable membrane sites has a high negative charge density, while the inner layer seems to possess a low density of ionic groups (cf. Chapter 11, Section E).

In excitable cells *in vivo*, the variation of the intracellular pH caused by metabolic processes may be an important factor which influences the rhythmical activity of the cells.

K. EFFECTS OF Ca-ION ON THE DURATION OF PROLONGED ACTION POTENTIALS

The duration of the action potential of an intact axon is markedly increased by intracellular application of tetraethylammonium (TEA) salt (see Chapter 10, Section B). The duration of a prolonged action potential is sensitive to the extracellular Ca-ion concentration. When the external Ca-ion concentration is raised, there is always a reduction in the duration. In the absence of divalent cations in the external medium, the axon membrane stays indefinitely in its "depolarized" (i.e., low-resistance) state.

A long time ago, Spyropoulos (1961) showed in this laboratory that a prolonged action potential of a frog nerve fiber can be prematurely terminated by a sudden rise in the external Ca-ion concentration. Since the area of the nodal membrane is very small (see Chapter 6, Section A), the external Ca-ion concentration can be raised uniformly over the entire surface of the excitable membrane. In the case of the squid axon membrane with a large surface area, it is not possible to alter the chemical composition outside the excitable membrane uniformly within the time comparable to the duration of the action potential.

Quite recently, it was found that a rise in the intracellular Ca-ion concentration is effective in shortening the duration of a prolonged action potential (Terakawa *et al.*, 1977). An example of the results showing the effect of the internal Ca-ion concentration on the prolonged action potential is shown in Fig. 11.11. A squid giant axon under study was immersed in artificial seawater and internally perfused with a solution containing 100 mM potassium glutamate, 5 mM TEA-Cl, and 0.1 mM K-EDTA. The duration of the action potential observed was approximately 3 sec under these conditions. Next, 0.3 mM CaCl₂ was introduced to the internal perfusion fluid in place of K-EDTA. When the internal Ca-ion concentration reached the steady level, there was a distinct decrease in the action potential duration. So long as the Ca-containing perfusion solution was not allowed to stay inside the axon for more than 1 min, there was no detectable deterioration of the axon excitability; the action potential duration returned to its original value when the Ca-ion in the internal perfusion solution was completely removed. Pro-

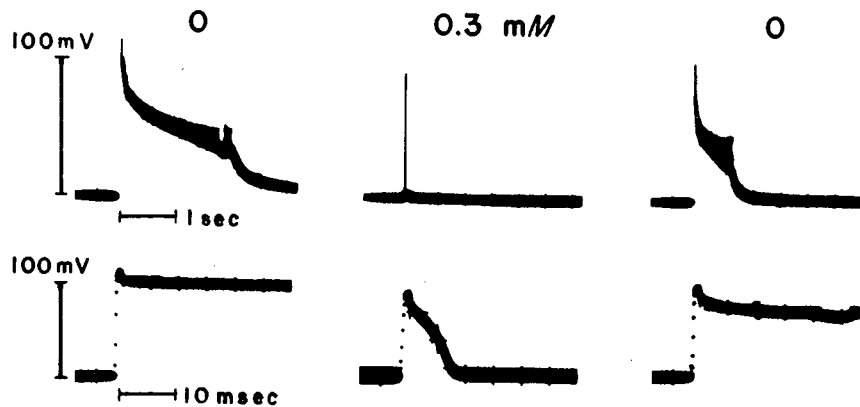


Fig. 11.11 Shortening of the duration of the action potential of a TEA-treated squid axon produced by intracellular application of a 0.3 mM Ca glutamate solution. Records A and C were taken from an axon internally perfused with a solution containing 100 mM K glutamate, 5 mM TEA-chloride, 0.1 mM K-EDTA and 2 mM Tris-glutamate. Record B was obtained about 50 sec after replacement of K-EDTA in the internal perfusion fluid with CaCl_2 . (From Terakawa *et al.*, 1977.)

longed exposure of the Ca-rich perfusion solution suppresses axon excitability irreversibly.

All the experimental facts mentioned above can readily be understood on the assumption that termination of a prolonged action potential is triggered by a rise of the Ca-ion concentration within the membrane macromolecules. In our macromolecular theory of nerve excitation, all of these experimental facts will be taken into consideration (Chapter 13, Section G).

REFERENCES

- Arhem, P., Frankenhaeuser, B., and Moore, L. E. (1973). Ionic currents at resting potential in nerve fibres from *Xenopus laevis*, potential clamp experiments. *Acta Physiol. Scand.* **88**, 446–454.
- Arima, R. (1914). Über Spontanerholung des Froschherzens bei unzureichender Kationenspeisung. *Pfluegers Arch. Gesamte Physiol. Menschen Tiere* **157**, 531–540.
- Baker, P. F., Hodgkin, A. L., and Shaw, T. I. (1961). Replacement of the protoplasm of a giant nerve fibre with artificial solutions. *Nature (London)* **190**, 885–887.
- Boyd, G. E., and Soldano, B. A. (1953). Self-diffusion of cations in and through sulfonated polystyrene cation-exchange polymers. *J. Am. Chem. Soc.* **75**, 6091–6099.
- Brinley, F. J., Jr., Spangler, S. G., and Mullins, L. J. (1975). Calcium and EDTA fluxes in dialyzed squid axons. *J. Gen. Physiol.* **66**, 223–250.
- Bruins, E. M. von (1932). Die numerische Festlegung der lyotropen Reihe. *Proc. R. Acad. Amsterdam.* **35**, 107–115.
- Clowes, G. H. A. (1916). Protoplasmic equilibrium. *J. Phys. Chem.* **20**, 407–451.
- Gottlieb, M. H., and Sollner, K. (1968). Failure of the Nernst-Einstein equation to correlate electrical resistance and rates of ionic self-exchange across certain fixed charge membranes. *Biophys. J.* **8**, 515–535.

- Gregor, H. P., and Wetstone, D. M. (1956). Specific transport across sulphonic and carboxylic interpolymer cation-selective membranes. *Discuss. Faraday Soc.* **21**, 162–173.
- Hagiwara, S., Hayashi, H., and Takahashi, K. (1969). Calcium and potassium currents of the membrane of a barnacle muscle fibre in relation to the calcium spike. *J. Physiol. (London)* **205**, 115–129.
- Helfferich, F., and Ocker, H. D. (1957). Ionenaustauschermembranen in bi-ionischen Systemen. *Z. Phys. Chem. Neue Folge.* **10**, 214–235.
- Höber, R. (1920). Zur Analyse der Calciumwirkung. *Pflügers Arch. Gesamte Physiol. Menschen Tiere* **182**, 104–113.
- Hodgkin, A. L. (1958). Ionic movements and electrical activity in giant nerve fibres. *Proc. R. Soc. London Ser. B* **148**, 1–37.
- Hodgkin, A. L., and Keynes, R. D. (1955). The potassium permeability of giant nerve fibre. *J. Physiol. (London)* **128**, 61–88.
- Hodgkin, A. L., and Keynes, R. D. (1957). Movement of labelled calcium in squid giant axons. *J. Physiol. (London)* **138**, 253–281.
- Hofmeister, F. (1888). Zur Lehre von der Wirkung der Salze. *Naunyn-Schmiedeberg Arch. Exp. Pathol. Pharmacol.* **24**, 247–260.
- Ikegami, A., and Imai, N. (1962). Precipitation of polyelectrolytes by salts. *J. Polym. Sci.* **56**, 133–152.
- Kobatake, Y., and Tasaki, I., see Tasaki, I. (1968). "Nerve Excitation: A Macromolecular Approach." Thomas, Springfield, Illinois.
- Lagos, A. E., and Kitchener, J. A. (1960). Diffusion in polystyrenesulphonic acid ion-exchange resins. *Trans. Faraday Soc.* **56**, 1245–1251.
- Larramendi, L. M. H., Lorente de Nó, R., and Vidal, F. (1956). Restoration of sodium-deficient frog nerve fibres by an isotonic solution of guanidinium chloride. *Nature (London)* **178**, 316–317.
- Lorente de Nó, R., Vidal, F., and Larramendi, L. M. (1957). Restoration of sodium-deficient frog nerve fibres by onium ions. *Nature (London)* **179**, 737–738.
- Luxoro, M., Canessa, M., and Vargas, F. (1965). Physiological properties of the giant axon from *Dosidicus gigas*. *23rd Int. Cong. Physiol. Sci. Tokyo* **83**, 60. (Abstr.)
- Matijevic, E., Leja, J., and Nemeth, R. (1966). Precipitation phenomena of heavy metal soap in aqueous solutions. I. Calcium oleate. *J. Colloid Interface Sci.* **22**, 419–429.
- Michaeli, I., and Katchalsky, A. (1957). Potentiometric titration of polyelectrolyte gels. *J. Polym. Sci.* **23**, 683–696.
- Ohki, S., and Aono, O. (1979). Membrane potential of squid axons: Effects of internal and external ion concentrations. *Jpn. J. Physiol.* **29**: 373–382.
- Oikawa, T., Spyropoulos, C. S., Tasaki, I., and Teorell, T. (1961). Methods for perfusing the giant axon of *Loligo pealii*. *Acta Physiol. Scand.* **52**, 195–196.
- Shrager, P. G., Macey, R. I., and Strickholm, A. (1969). Internal perfusion of crayfish giant axons: Action of tannic acid, DDT and TEA. *J. Cell. Physiol.* **74**, 77–90.
- Smidsrod, O., and Haug, A. (1967). Precipitation of acidic polysaccharides by salts in ethanol-water mixtures. *J. Polym. Sci. C* **16**, 1587–1598.
- Spyropoulos, C. S. (1961). Initiation and abolition of electric response of nerve fiber by thermal and chemical means. *Am. J. Physiol.* **200**, 203–208.
- Stämpfli, R. (1959). Is the resting potential of Ranvier node a potassium potential? *Ann. N.Y. Acad. Sci.* **81**, 265–284.
- Tasaki, I., Singer, I., and Takenaka, T. (1965). Effects of internal and external ionic environment on excitability of squid giant axon. A macromolecular approach. *J. Gen. Physiol.* **48**, 1095–1123.
- Tasaki, I., Singer, I., and Watanabe, A. (1965). Excitation of internally perfused squid giant axons in sodium-free media. *Proc. Natl. Acad. Sci. U.S.A.* **54**, 763–769.

- Tasaki, I., and Takenaka, T. (1963). Resting and action potential of squid giant axons intracellularly perfused with sodium-rich solutions. *Proc. Natl. Acad. Sci. U.S.A.* **50**, 619–626.
- Tasaki, I., Watanabe, A., and Takenaka, T. (1962). Resting and action potential of intracellularly perfused squid giant axon. *Proc. Natl. Acad. Sci. U.S.A.* **48**, 1177–1184.
- Tasaki, I., Singer, I., and Watanabe, A. (1966). Excitation of squid giant axons in sodium-free external media. *Am. J. Physiol.* **211**, 746–754.
- Tasaki, I., Singer, I., and Watanabe, A. (1967). Cation interdiffusion in squid giant axons. *J. Gen. Physiol.* **50**, 989–1007.
- Tasaki, I., Watanabe, A., and Lerman, L. (1967). Role of divalent cations in excitation of squid giant axons. *Am. J. Physiol.* **213**, 1465–1474.
- Tazawa, M., Kikuyama, M., and Shimmen, T. (1976). Electric characteristics and protoplasmic streaming of Characeae cells lacking tonoplast. *Cell Struct. Funct.* **1**, 165–176.
- Terakawa, S., Nagano, M., and Watanabe, A. (1977). Intracellular divalent cations and plateau duration of squid giant axons treated with tetraethylammonium. *Jpn. J. Physiol.* **27**, 785–800.
- Terakawa, S., Nagano, M., and Watanabe, A. (1978). Intracellular pH and plateau duration of internally perfused squid giant axon. *Jpn. J. Physiol.* **28**, 847–862.
- Waterman, N. (1928). Colloid chemistry and malignant tumor. Vol. 2. In "Colloid Chemistry" (J. Alexander, ed.), pp. 877–892. Chem. Catalog. Co., New York.
- Yoshioka, T., Pant, H. C., Tasaki, I., Baumgold, J., Matsumoto, G., and Gainer, H. (1978). An approach to the study of intracellular proteins related to the excitability of the squid giant axon. *Biochim. Biophys. Acta* **538**, 616–626.

12. Macromolecular Transitions

A. BI-IONIC ACTION POTENTIALS

Normal seawater contains a large number of uni- and divalent ion species. It is not easy to analyze the membrane properties of an axon in such a complex medium from a physicochemical point of view. The important question arises: How far can we simplify the electrolyte composition of the surrounding medium without eliminating the ability of the axon to develop all-or-none action potentials?

Soon after the inception of the method of intracellular perfusion, serious attempts were made to simplify the ionic compositions on the inner and outer sides of the membrane. It is now known that the salt of a single divalent cation species outside and the salt of a single univalent cation species inside are sufficient to maintain the ability of the axon to develop action potentials. Calcium and its substitutes (strontium or barium) are favorable external cations. Without being accompanied by Ca- or Sr-ions, sodium and other univalent cations in the external medium are totally *inadequate* to keep the axon excitable. The internal cation can be any one of the alkali-metal cations, tetramethylammonium, tetraethylammonium, choline, hydrazine, and many other polyatomic cations (see Tasaki *et al.*, 1969; Terakawa, 1978). The anion species in the external medium (chloride, ethylsulfate, etc.) are chosen so as to maintain Ca-ion in a free form. The selection of intracellular anions is made with the purpose of delaying the loss of protoplasmic protein molecules by dissolution (see Chapter 9, Section D).

Figure 12.1 shows that magnesium ion alone is inadequate to replace the external Ca-ion. The internal perfusion fluid of the axon under study was a cesium fluoride solution made isotonic by addition of glycerol. The axon was shown to lose its ability to generate prolonged action potentials when immersed in a pure magnesium salt solution. However, it remained excitable in a solution containing a 5:1 mixture of Mg- and Ca-salts.

The classical interpretation of the fact that Mg-ion cannot completely replace Ca-ion is as follows: Ca-deficiency, as well as K-enrichment, brings about *Auflockerung* (loosening or swelling) of the colloidal material (polyelectrolytes in the membrane); Ca, Sr, and Ba, but not Mg, produce *Verdich-*

ting (making compact) (see p. 294 in Bethe, 1920, cited in Chapter 7; Höber, 1920, cited in Chapter 11). The inability of Mg-salt to make the membrane compact may be interpreted as arising from the greater tendency toward hydration (see Ikegami and Imai, 1962, cited in Chapter 11).

The all-or-none responses involving only two potential-determining cation species, with one species internally and the other externally, are referred to as "bi-cationic" or simply as "bi-ionic" action potentials. The properties that are common to all the known bi-ionic action potentials are as follows: (1) The duration is very long, being usually between 100 msec and 30 sec, (2) the termination is relatively abrupt and is marked by a pronounced "shoulder," and (3) the membrane resistance at the peak of excitation is not as low as that in intact axons; the ratio of the resistance at rest to that at the peak of excitation is in the range between 3 and 10.

The properties of the bi-ionic action potentials are very different from those of the action potentials observed under ordinary, i.e., multi-ionic conditions. However, it is important to note that brief, nearly normal, action potentials reappear when seawater is introduced externally and a K-salt solution internally. This fact indicates that there is no irreversible alteration of the membrane macromolecules in axons under the bi-ionic conditions. From a

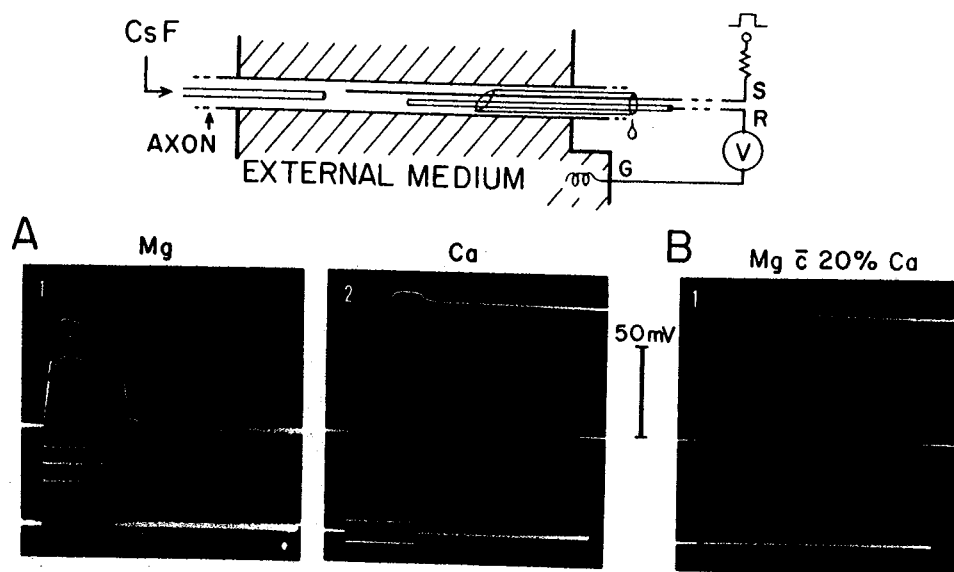


Fig. 12.1 Top: Experimental setup used for demonstrating all-or-none action potentials of squid giant axons immersed in external media free of univalent cation. S, 20-mm-long Ag-AgCl wire (50 μ m diameter); R, glass-pipette electrode filled with 600 mM KCl; G, large coil of Ag-AgCl electrode. (A) Alternate suppression and recovery of action potential production with $MgCl_2$ and $CaCl_2$ externally. The axon was internally perfused with a 25 mM CsF solution. The external divalent cation concentration was 200 mM. The duration of rectangular stimulating pulses (shown by the lower trace) was 100 msec. (B) Demonstration of an action potential in a medium containing 40 mM $CaCl_2$ and 160 mM $MgCl_2$. (Adapted from *Am. J. Physiol.* **213**, 1468, 1967.)

physicochemical point of view, analysis of a bi-ionic action potential is much easier than that of a normal, i.e., multi-ionic, action potential (see Chapter 13, Section H).

The mechanism of excitation of an axon under bi-ionic conditions may be interpreted in the following manner: In the resting state of the axon, the negatively charged sites of the membrane macromolecules are cross-linked by Ca-ions. This type of cross-linking is often referred to as "calcium bridges" (see, e.g., Katchalsky, 1954; Williams, 1970). A certain fraction of the calcium bridges are broken when an applied electric current transports intracellular univalent cations into the membrane. As the consequence, the macromolecules become unstable and cooperatively undergo a transition from a "compact" to a "loose" state (see Chapter 3, Section C, and Chapter 13, Section E). In this new, i.e., excited, state, the mobilities of cations in the system are higher than in the resting state; hence, the membrane resistance is reduced and the interdiffusion fluxes are enhanced.

Properties of the axons under bi-ionic conditions are discussed further in the following sections.

B. ACTION POTENTIALS OBSERVED WITH Na-ION INTERNALLY

Axons internally perfused with a sodium salt solution remain excitable in a medium containing a mixture of Na- and Ca-salt. Furthermore, the external Na-salt can be completely replaced with glycerol without eliminating the ability of the axon to develop all-or-none action potentials (Watanabe *et al.*, 1967; Meves and Vogel, 1973). The action potentials observed under these conditions deserve further explanation.

Figure 12.2 shows an example of the records of action potentials taken from an axon internally perfused with a dilute solution of Na-salt. The procedure of this observation was as follows: With two perfusion cannulae introduced into the axon interior, seawater outside the axon was replaced with a rapidly circulating solution containing 100 mM CaCl_2 and glycerol (for maintaining the tonicity). Conduction of the action potential was suspended within a few minutes after the onset of circulation. Next, intracellular perfusion was initiated with a 30 mM NaF solution with its pH adjusted to 7.3 with sodium phosphate buffer. At the onset of internal perfusion, the axon developed no distinct action potential in response to a pulse of outwardly directed current. During the following period of 5 to 15 min, the axon was found to regain its ability to generate all-or-none responses.

The amplitude of the action potentials observed under these conditions was usually between 40 and 60 mV. The resting membrane potential re-

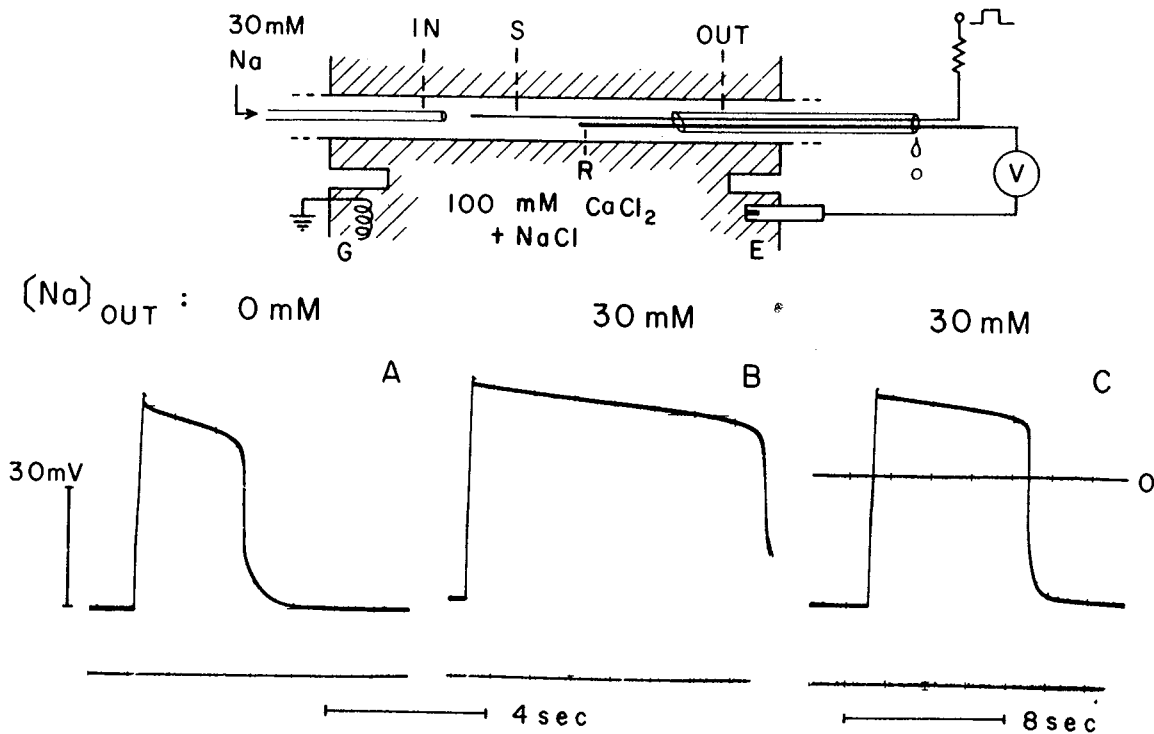


Fig. 12.2 Top: Schematic diagram showing the experimental arrangement used for determining the resting and action potentials of axons internally perfused with sodium salt solutions. The inlet cannula (IN), outlet cannula (OUT), stimulating wire electrode (S), recording glass-pipette electrode (R), external calomel electrode (E), and Ag-AgCl ground electrode (G) are indicated. The recording electrodes (R and E) are connected to the differential input stage of an oscilloscope via a high-impedance amplifier. The axon is represented by two horizontal lines enclosing the cannulae. Bottom: Resting and action potentials recorded from an axon internally perfused with a 30 mM sodium salt solution. The composition of the external medium is indicated. (From *Proc. Natl. Acad. Sci. U.S.A.* **58**, 2249, 1967.)

mained in the range between 25 and 30 mV (inside negative). It is shown in Fig. 12.2 that addition of a small amount of NaCl to the external medium enhanced the amplitude and prolonged the duration of the action potential. The observation described above is significant in view of the fact that the influx of Na-ion has been regarded by some investigators (see Baker, 1966; p. 940 in Bockris and Reddy, 1970) as the cause of the action potential production. At the time when this observation was made, several physiologists suggested that the observed action potentials might be generated by the influx of free Na-ions derived from the layers of connective tissue and Schwann cells outside the axon proper. Such a possibility is precluded by the fact that the action potential grows gradually under rapid and continuous circulation of the external Na-free medium. It is obvious that the external Na-ion concentration does not rise during continuous perfusion of the axon interior with a Na-free solution. The observed gradual rise in the action potential amplitude is attributed to a continuous fall in the residual K-ion concentration in the axon interior (see Section C).

It is clear that the experimental finding described above cannot be explained in terms of the postulate that the influx of Na-ions is the cause of action potential production. The Na-ions are located on the "wrong" side of the membrane; therefore, the potential variation produced when the alleged Na channels are opened up is expected to be "upside down." Actually, however, the sign of the observed potential change is the same as that of a normal action potential.

The concentration of the Na-salt used in the experiments mentioned above is very close to the level that is present in the interior of a freshly excised axon. We conclude this section by emphasizing that complete replacement of both the intracellular K-salt and the extracellular Na-salt with a nonelectrolyte does not suppress axon excitability.

C. BI-IONIC ACTION POTENTIAL OBSERVED WITH K-IONS INTERNALLY

In early studies of squid giant axons under bi-ionic conditions, it was not possible to demonstrate all-or-none action potentials with the salt of K-ions internally and the salt of Ca-ions externally. Quite recently, Terakawa (1978) succeeded in demonstrating bi-ionic action potentials in axons internally perfused with a K-salt solution and immersed in a Ca-salt solution. The reason for this success was that the external Ca-salt concentration used in the recent experiments was much lower than in previous experiments.

An example of the oscillograph records obtained by Terakawa is furnished in Fig. 12.3. The experimental procedure employed in obtaining the left-hand action potential record in the figure was as follows: With one cannula inserted into each end of a giant axon, the major portion of the axoplasm was removed by briefly perfusing the axon interior with a dilute protease solution (0.1 mg of pronase in 1 ml). Next, the axon was internally perfused with a protease-free 50 mM KF solution of which the pH was adjusted to 7.3 with potassium buffer. Finally, the seawater outside the axon was replaced with a rapidly circulating 12% (by volume) glycerol containing 2 mM CaCl_2 . Stimulating current pulses (1 msec in duration) were applied through a long metal wire electrode in the perfusion zone and the electric responses were recorded by means of an electrode in the middle of the perfusion zone.

It is seen in the figure that the electrical responses of the axon observed under these experimental conditions were roughly all-or-none. The amplitude of the action potentials developed was usually between 20 and 30 mV and the duration between 50 and 100 msec in most cases. The right-hand record in the figure indicates that the observed action potential was accompanied by a simultaneous fall in the membrane impedance. The ratio of the

membrane resistance at rest to that at the peak of excitation (measured by the voltage clamp technique) was between 2 and 4.

Again, it should be noted that treatment of the axon membrane with a dilute Ca-salt solution does not bring about any irreversible alteration of the membrane macromolecules. When the dilute Ca-salt solution outside is replaced with normal seawater, the action potential of the axon becomes nearly normal.

Physiologists who assume the existence of two kinds of spatially separate ion channels in the axon membrane, one for Na- and the other for K-ions (see Chapter 10, Section K), might be tempted to interpret the experimental results described above as indicating fluxes of Ca-ions through the Na channels. The commonly accepted criterion for the involvement of Na channels is to demonstrate suppression of the observed responses by tetrodotoxin (see Chapter 10, Section K). It was found that, under the experimental conditions indicated, the excitability of the axons is not affected by the toxin at all. It is very interesting, however, to find that the axon regains its tetrodotoxin sensitivity when NaCl (about 10 mM) is added to the external medium. It is probable that the added Na ions alter the conformational state of the external layer of the membrane macromolecules by complex formation. Here, we see another example of experimental results indicating the complexity of the action of this pufferfish poison.

At present, it is not clear why the Ca-salt concentration has to be lowered

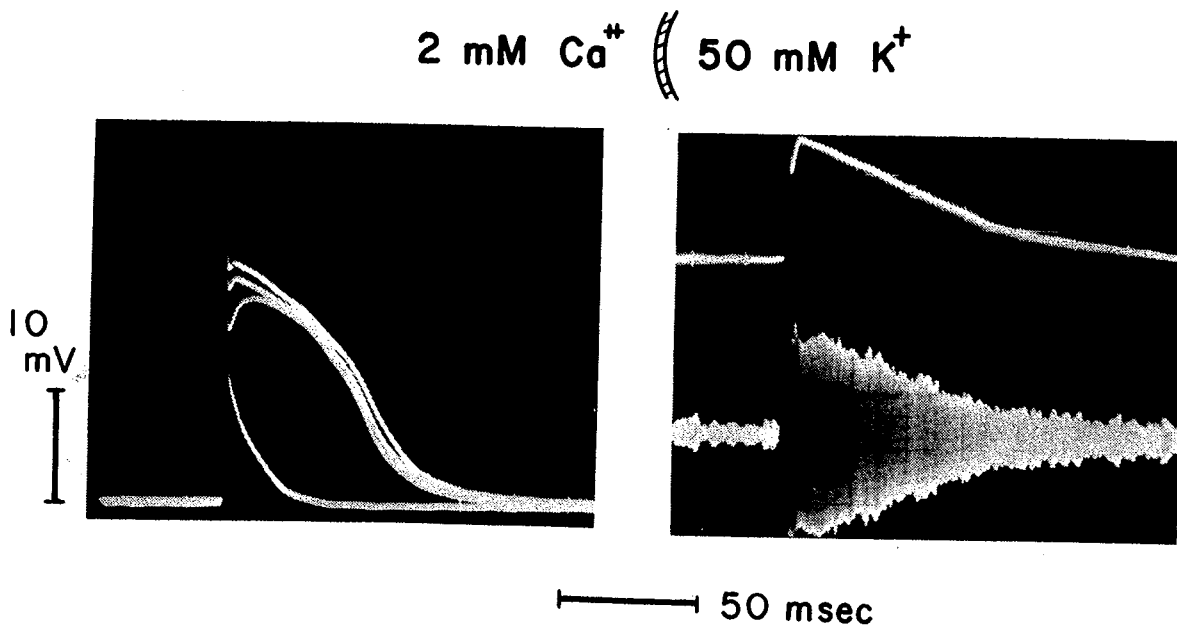


Fig. 12.3 Action potentials observed in an axon internally perfused with a 50 mM KF solution. The external medium was a diluted CaCl_2 solution. Record 1 shows the effect of four different strengths of stimulating current pulses. Record 2 shows loss of membrane impedance during excitation. The resting membrane potential was about -30 mV at 20°C . (Terakawa, 1978.)

in order to demonstrate Ca–K bi-ionic action potentials. A possible explanation is that a reduction in the external Ca-salt concentration decreases the rate of cation interdiffusion across the membrane and shifts the Ca–K concentration ratio within the membrane macromolecules toward the range which gives rise to instability of the system (see Chapter 13, Section F).

D. POLYATOMIC UNIVALENT CATIONS IN THE AXON INTERIOR

Axons immersed in a 100–200 mM Ca-salt solution remain highly excitable when they are internally perfused with a dilute salt solution of the following polyatomic cations: tetramethylammonium (TMA), tetraethylammonium (TEA), tetrapropylammonium (TPA), choline, guanidinium, methylguanidinium, ethylamine, ethanolamine, trimethylamine, etc. Among the univalent cations mentioned above, TMA was found to give rise to the largest action potentials; with a 25 mM TMA-phosphate internally, a resting membrane potential between -10 and $+5$ mV and action potentials between 90 and 135 mV in amplitude have been observed (see Fig. 12.4). Action potentials observed with guanidinium phosphate internally were relatively small. Interestingly, excitation was not possible when internal perfusion with tetrabutylammonium (TBA) salt was employed. The salts of monomethylamine, dimethylamine, propylamine, etc., gave rise only to graded responses (Tasaki *et al.*, 1969).

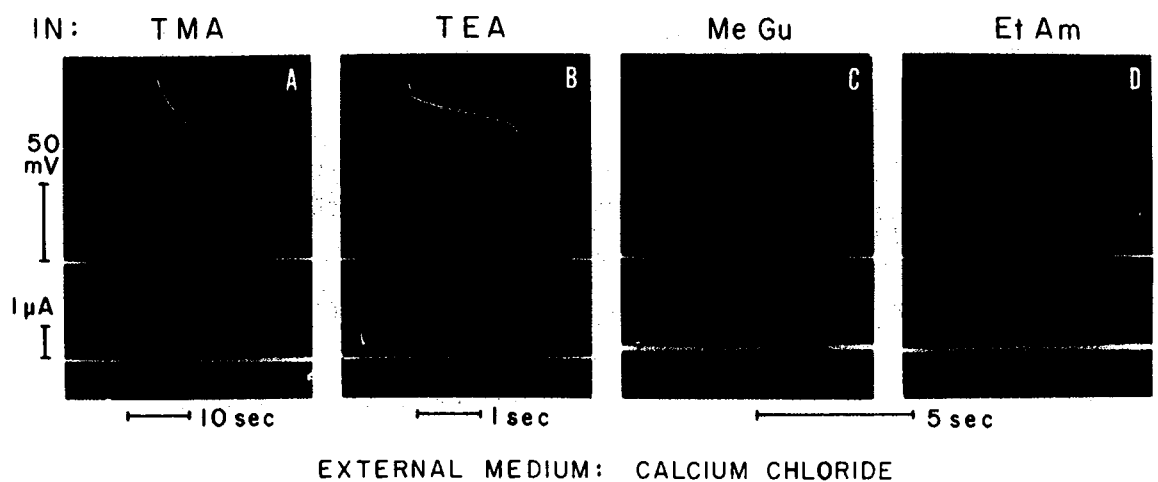


Fig. 12.4 Bi-ionic action potential of squid giant axons internally perfused with a phosphate salt solution containing 25 mM tetramethylammonium (TMA), tetraethylammonium (TEA), guanidinium (Gu), or ethanolamine (Et Am). The external medium contained 100 mM CaCl_2 for the experiments cited in (A), (C), and (D) and 200 mM CaCl_2 for (B). (From *Am. J. Physiol.* **216**, 132, 1969.)

These findings indicate that both the size and the hydrophilicity of the internal univalent cations play an important role in generating action potentials. According to Robinson and Stokes (1959, cited in Chapter 10), the corrected Stokes radii of tetraalkylammonium ions in water (expressed in Å) are 2.04 for TMA, 2.81 for TEA, 3.22 for TPA, and 4.71 for TBA. The pathway of ions within the intramembrane protein molecules seems to be unable to accommodate particles larger than about 9 Å in diameter.

Axons internally perfused with the salts of cations with hydrophilic side groups (guanidinium, ethanolamine, etc.) were found to give rise to small action potentials or only graded responses. When added to the external, Ca-containing medium, these cations are capable of enhancing the action potential amplitude. These facts can easily be understood on the assumption that the selectivity–mobility products of these cations (see p. 173 in Tasaki, 1968, cited in Chapter 8) are markedly enhanced in the excited state of the nerve membrane. When the major portion of Ca bridges within the intramembrane protein molecules are broken (see Chapter 13, Section E), a number of negatively charged sites are newly exposed and these sites prefer cations with hydrophilic side groups to those surrounded by hydrophobic hydrocarbon chains. Addition of the salts of TMA, TEA, choline, etc., to the external (Ca-containing) medium does not enhance the action potential amplitude because they are not preferred. For the same reason, TMA and other cations with hydrophobic side groups give rise to large action potentials when introduced intracellularly.

In summary, studies of bi-ionic action potentials with polyatomic cations intracellularly strongly suggest that a transition of the nerve membrane to its excited state is accompanied by a marked increase in the selectivity for univalent cations of a hydrophilic nature.

E. THE EFFECT OF EXTERNAL Na-SALT ON BI-IONIC ACTION POTENTIALS

In axons internally perfused with a dilute solution of Na- or Cs-salt, the amplitude of the action potential varies with the concentration of Ca-salt in the external medium. The amplitude is increased also by addition of Na-salt to the medium. The effects of varying the concentrations of the salts of di- and univalent cations in the external medium are now considered on a quantitative basis.

The dependence of the amplitude on the external Ca-ion concentration, $[Ca]_e$, was found to follow, with a fair degree of accuracy, the equation

$$E_a = E_a^0 + (RT/2F) 1n[Ca]_e \quad (12.1)$$

where E_a is the peak level of the action potential, E_a^0 is a constant which depends on the internal ionic composition. The value of $(1/n - 1)RT/(2F)$ is approximately equal to 29 mV at 19°C. When the action potential overshoot is plotted on a semilogarithmic scale, the observed values fall on a straight line with a slope of roughly 29 mV for a 10-fold change in the external Ca-ion concentration (I. Inoue, unpublished).

In Fig. 12.5, the effects of NaCl added to the external CaCl_2 solution are shown. In all the cases examined, the action potential amplitude was increased monotonically with the concentration of NaCl added. In the experimental results illustrated in the left-hand diagram, the NaCl concentration was fixed and the Ca-salt concentration was varied (by replacing the glycerol in the medium with CaCl_2). It is seen that the effect of addition of NaCl is great when the CaCl_2 concentration is low. In the right-hand diagram, the Ca-ion concentration was fixed, and the Na-ion concentration was varied. In the range where the Ca-ion concentration is smaller than the Na-ion concentration, the dependence of the action potential amplitude on the external Na-ion concentration approaches the Nernst slope for univalent cations, namely, 58 mV for a 10-fold change.

The experimental data described above can be expressed by the following formula:

$$E_a = E_a^0 + (RT/F) \ln\{[\text{Ca}]_e^{1/2} + Q[\text{Na}]_e\} \quad (12.2)$$

where Q can be treated as a constant within a limited range of the Na-ion concentration. The approximate values of E_a^0 and Q chosen to fit the observed data in Fig. 12.5 (left) are -38 mV and $0.061 \text{ mM}^{-1/2}$, respectively. Note that, when the external Na-ion concentration approaches zero, Eq. (12.2) tends toward Eq. (12.1). For the data shown on the right (obtained with Cs-ion internally), the values of E_a^0 and Q chosen to fit the observed data were -19 mV and $1.1 \text{ mM}^{-1/2}$, respectively.

It is interesting to note that Eq. (12.2) for the case with Na-ion internally can be derived on the basis of the Teorell–Meyer–Sievers theory applied to a cation-exchanger membrane with a high fixed charge density and a low divalent cation mobility (see Eq. A.42 in Tasaki and Kobatake, 1968). The significance of this equation is that both Ca- and Na-ions compete for the same negatively charged sites in the external layer of the axon membrane. The contribution of Na-ions in the inner membrane layer to the overall membrane potential is included in E_a^0 . Here, we see that the membrane sites responsible for the production of action potentials do not possess absolute specificity for a particular cation species. The peak value of the action potential is determined, under these experimental conditions, by the distribution of Na- and Ca-ions at and near the external surface at the critical membrane sites. The factor Q , which reflects the difference in mobilities and

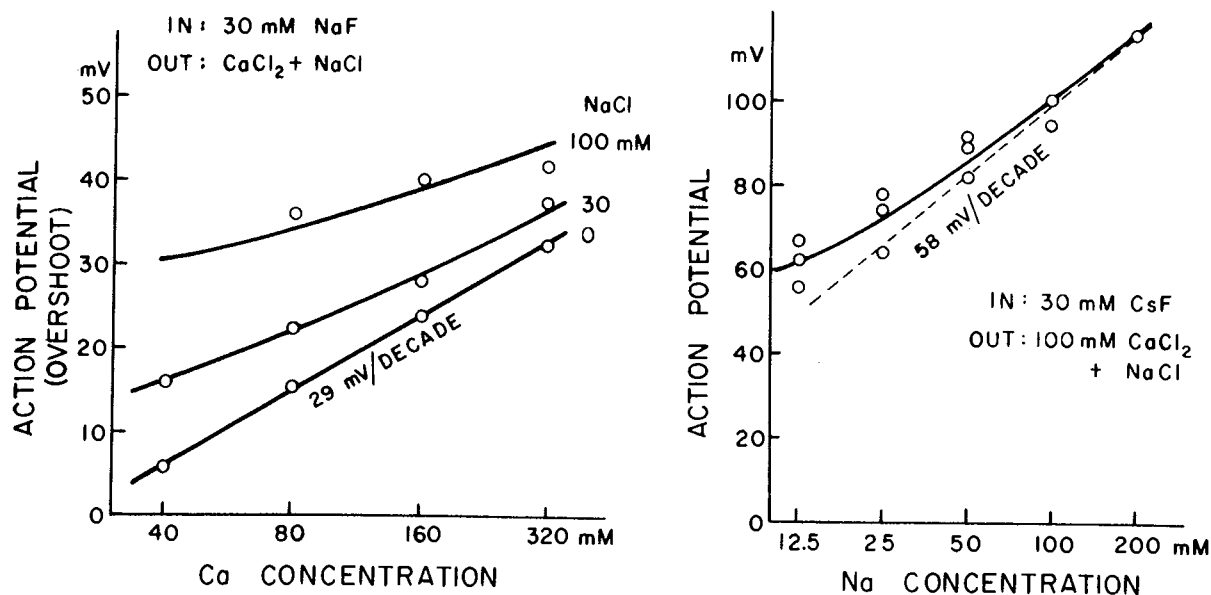


Fig. 12.5 Left: Effect of addition of NaCl to the external medium on the action potential observed in an axon internally perfused with a 30 mM NaF solution. The overshoot of the action potential was plotted against the external CaCl_2 concentration. Right: The action potential overshoot plotted against the external NaCl concentration. The axon was internally perfused with a 30 mM CsF solution. The external CaCl_2 concentration was kept at 100 mM. (I. Inoue, unpublished.)

selectivities of the cations in the superficial layer of the membrane sites, is a measure of the effectiveness of Na-ions as compared with that of Ca-ions in determining the potential. This factor has a dimension of $M^{-1/2}$; it should not be called "permeability ratio" because it does not reflect the ratio of the rates of ion permeation across the membrane.

It is interesting to note that mathematical expressions similar to Eq. (12.2) have been employed to describe the behavior of Ca-sensitive electrodes immersed in a mixture of uni- and divalent cation salts (Garrels *et al.*, 1962; Ross, 1967). It has long been known that in a glass electrode, a potential difference is developed on each surface independently of the other (see p. 259 in Dole, 1941; p. 173 in Kratz, 1950). The situation is more complex in the nerve membrane, because we are dealing with potential changes associated with transitions of the state of the membrane macromolecules.

The observations described above may be summarized as follows. (1) Under intracellular perfusion with a dilute solution of Na- or Cs-salts, addition of a sodium salt to the external calcium salt solution augments the action potential amplitudes. (2) In the range of external Na-salt concentrations higher than the Ca-salt concentration, the action potential amplitude changes with the Na-ion concentration roughly at a rate of 58 mV/decade. (3) When the external Na-ion concentration is low, the action potential amplitude varies with the Ca-ion concentration with a slope of approximately

29 mV/decade. Action potentials cannot be observed in the absence of Ca-ions in the external medium. It is concluded that both Na- and Ca-ions pass through the same macromolecular sites in the axon membrane.

F. ABRUPT DEPOLARIZATION

In axons internally perfused with a solution of Na- or Cs-salt, addition of a sufficiently large amount of the salt of univalent cations is known to produce an abrupt rise in the intracellular potential accompanied by a fall in the membrane resistance. Analyses of this phenomenon, which we call "abrupt depolarization," yield important information as to the nature of physicochemical processes taking place at the excitable membrane sites. The significance of this phenomenon is now considered in some detail.

Abrupt depolarization was first demonstrated in excitable plant cells by Hill and Osterhout (1938) a long time before its existence was recognized in the myelinated nerve fibers (Tasaki, 1959, cited in Chapter 10) and in perfused squid giant axons (Tasaki *et al.*, 1968).

In order to demonstrate abrupt depolarization, it is required that the axon membrane is in the resting, but electrically excitable, state. Axons which are internally perfused with a dilute solution of NaF (or CsF) and glycerol with its pH adjusted to 7.3 with sodium phosphate are best suited for the demonstration. The diagram on the top of Fig. 12.6 illustrates the experimental setup employed by I. Inoue (unpublished) in this laboratory. Initially, an axon under internal perfusion was immersed in a medium containing only CaCl_2 and glycerol. Although the axon remains electrically excitable under these conditions, no electric stimuli were used in the following observations. At the time when the axon reached a steady state, the rapidly circulating external medium containing CaCl_2 was switched to a solution containing both CaCl_2 and NaCl solutions. As is shown by the uppermost oscillograph trace in the figure, a large abrupt rise in the intracellular potential was observed while the concentration of the univalent cation salt was continuously rising.

It is seen in the figure that the magnitude of the potential jump, as well as the threshold concentration of the univalent cation, varies widely with the cation species employed. When NaCl is used, the magnitude of the potential jump is very large, and the threshold concentration required to induce the potential jump is relatively high. With KCl and RbCl, the potential jump induced is small, and the threshold concentration is very low. With CsCl, the potential jump is small and the threshold concentration is high. Thus, we find that the physicochemical factors which determine the magnitude of the potential jump are quite distinct from those that influence the threshold concentration.

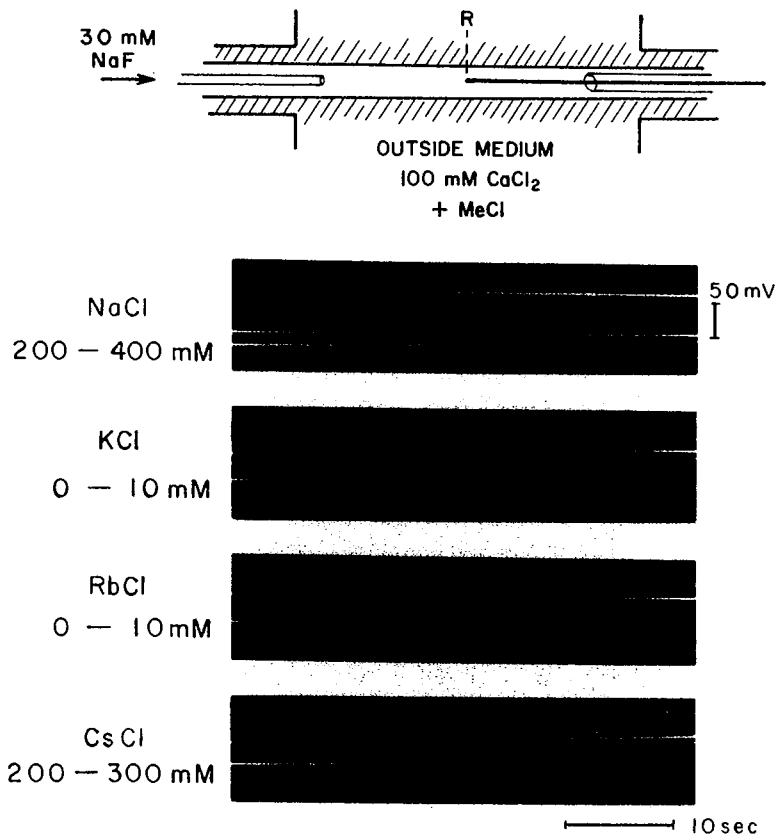


Fig. 12.6 Abrupt depolarization observed in axons internally perfused with a 30 mM NaF solution. The potential difference between the internal glass-pipette electrode (R) and the external calomel half-cell was recorded on a slowly moving photographic film. The external Ca-ion concentration was kept at 100 mM. The concentration of the univalent cation salts in the external medium was slowly raised in the range indicated. (I. Inoue, unpublished.)

The significance of "abrupt depolarization" was clearly recognized by Hill and Osterhout (1938) who discovered the phenomenon. They arrived at the conclusion that the potential jump observed is nothing but the onset of an action potential. We see that the magnitude of the potential jump is very close to the amplitude of an action potential induced electrically under the same ionic environment. The rate of the potential decay following the onset of the potential jump is also very similar to that of an action potential evoked by an electric shock.

The essential difference between an electrically induced action potential and an abrupt depolarization is the absence of a potential jump in the reverse direction (i.e., termination of the action potential) in a chemically induced response. We have ample grounds for attributing this absence of repolarization to the continuous rise in the external univalent cation concentration. In the case of an electrically evoked action potential, the external divalent cation concentration is kept at a level high enough to ensure the appearance of the repolarized (i.e., resting) state. During the depolarized

state of the axon membrane, addition of a divalent cation salt to the medium does bring about abrupt repolarization.

It is important to note that the threshold concentration of a univalent cation salt varies with the Ca-ion concentration in the external medium. Since we assume that both Ca- and univalent cations occupy the same negatively charged sites in the axon membrane, the fraction of the univalent cations in the membrane site is expected to depend approximately on the level of $C_1/(C_2)^{1/2}$, where C_1 and C_2 represent the concentrations of the uni- and divalent cations in the external medium, respectively (see Chapter 13, Section F). We expect that the ratio of the uni- and divalent cations in the membrane sites remains unaltered when the Na-ion concentration is doubled and, simultaneously, the Ca-ion concentration is quadrupled. The uni- and divalent cation concentration ratio required for production of abrupt depolarization appears to follow this expected pattern.

The difference in the threshold concentration among alkali metal ions is attributed to their ability to disrupt the "compact" structure of the membrane macromolecules. The sequence of cations arranged in accordance with their "depolarizing power" is



This sequence is not determined simply by the "permeability" of the univalent cations involved (see Chapter 14, Section D). The great depolarizing power of K-ion probably derives from the similarity between Ca- and K-ion in their stereochemical properties (see Williams, 1970). Both of these cations have a coordination number of 8; Na-ion, which has a coordination number of 6, is less effective in displacing Ca-ion in the intramembrane protein molecules. Old information about the coordination numbers of other alkali-metal ions is given by Martell and Calvin (1956).

G. HYPERPOLARIZING RESPONSES IN INTERNALLY PERFUSED AXONS

Electrophysiological properties of axons internally perfused with a dilute solution of NaF or CsF are discussed further in this section. When a small amount of the salt of univalent cations is added to the external Ca-salt solution, the amplitude of an action potential that can be evoked by an electric stimulus is augmented (see Fig. 12.5). As the concentration of the added univalent cation salt is increased step by step, the axon eventually undergoes a transition to its depolarized state. Following the appearance of abrupt depolarization, the axon becomes totally unresponsive to pulses of outwardly directed current applied to the axon membrane.

Figure 12.7 shows the effect of KCl added to the external medium upon the membrane potential of an axon internally perfused with a dilute solution of NaF. The membrane potential was affected very little by the added salt when the external univalent cation concentration was insufficient to produce abrupt depolarization. In a medium containing 100 mM CaCl_2 , abrupt depolarization was observed when the external KCl concentration reached 20 mM. Following the appearance of abrupt depolarization, the membrane potential became highly sensitive to the external KCl concentration. In the concentration range higher than about 100 mM, the dependence of the membrane potential upon the KCl concentration approached the Nernst slope, namely, approximately 58 mV for a 10-fold change in the concentration.

The oscillograph record furnished in the figure indicated that the axon exhibits a distinct sign of excitability in the range of KCl concentration above the threshold for abrupt depolarization. Pulses of inwardly directed current through the axon membrane are required to demonstrate the existence of excitability. When the current intensity is low, the axon membrane behaves like an ohmic resistor (with a capacitor connected in parallel). As the intensity exceeds a critical (i.e., threshold) value, the membrane responds to the applied pulse with a disproportionately large hyperpolarization (i.e., a large

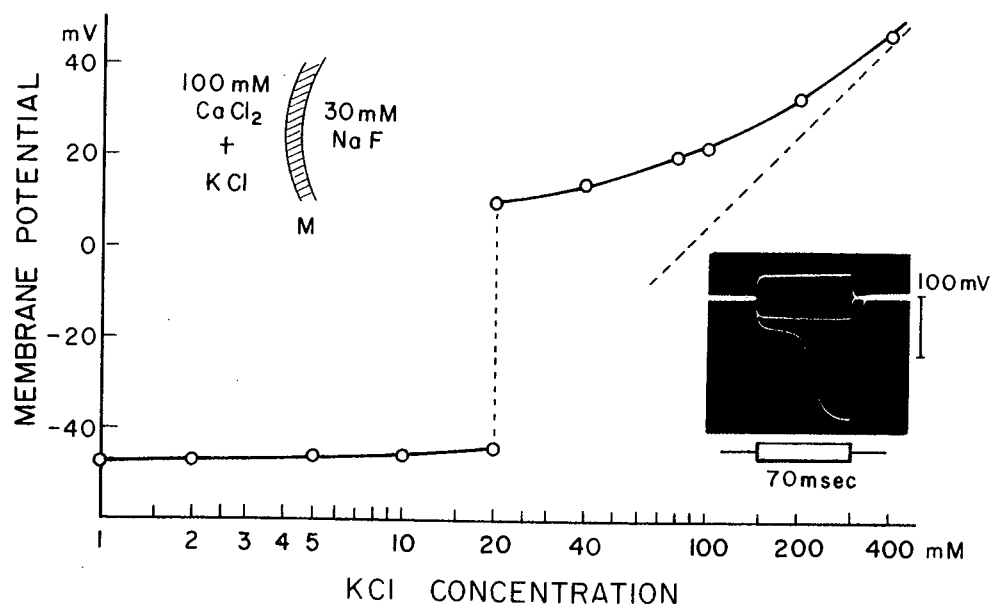


Fig. 12.7 Effect of addition of KCl to the external medium on the membrane potential of an axon internally perfused with a 30 mM NaF solution and immersed in a 100 mM CaCl_2 solution. Note a discontinuous rise in the membrane potential at 20 mM. The oscillograph record inserted shows that an inwardly directed current applied to the membrane immersed in a 100 mM KCl solution produced a large potential variation which is known as hyperpolarizing response. (I. Inoue, unpublished.)

negative shift of the intracellular potential). This large potential variation is nothing but a "hyperpolarizing response" discussed previously in Chapter 10, Section D. Again, it is emphasized that pulses of electric current passing *inward* through the membrane are required to evoke hyperpolarizing responses and that these responses can be observed only in the depolarized state of the axon membrane. In the resting state, on the contrary, the axon responds to pulses of *outward* current through the axon membrane, but not to pulses of inward current.

The origin of a hyperpolarizing response is now explained on a physicochemical basis. In an aqueous medium, the mobility of Ca-ion is not very different from the mobilities of Na- or K-ion. [Note that the limiting equivalent conductances of Ca-, Na-, and K-ion at 18°C are 50.7, 42.8, and 63.9 $\text{mho}\cdot\text{Eq}^{-1}\cdot\text{cm}^2$, respectively (see Landolt and Börnstein, 1960).] In the matrix of the axon membrane, however, the Ca-ion mobility is about two orders of magnitude smaller than the mobility of Na- or K-ion (see Chapter 11, Section I). As a consequence of this discontinuous change in the mobility ratio at the external surface of the axon membrane, the passage of an inward current through the membrane brings about a drastic rise of the Ca-ion concentration within the membrane matrix. When the concentration ratio of uni- to divalent cations falls below a critical level, the membrane macromolecules undergo a transition from its "loose" (i.e., depolarized) conformational state to the "compact" (i.e., repolarized) state. This macromolecular transition is accompanied by a large increase in the membrane resistance and a small change in the emf. We conclude, therefore, that generation of a hyperpolarizing response is nothing but the reverse of the normal process of action potential production (see Chapter 13, Section G for further discussion).

H. CYCLIC CHANGES IN MEMBRANE PROPERTIES—HYSTERESIS

In axons internally perfused with a dilute solution of an alkali metal salt, cyclic changes in the external univalent-divalent cation concentration ratio produce multiple transitions. A fall in the divalent cation (Ca-ion) concentration produces a transition from the resting state of the axon membrane (characterized by a high membrane resistance and a low internal potential) to the depolarized state (namely, to the state with a low membrane resistance and a high intracellular potential). A subsequent rise in the divalent cation concentration brings about a transition in the reverse direction. It is important to note that, in such a cyclic change in the external ionic composition, the concentration of the divalent cation required for repolarization is definitely

higher than that needed to produce depolarization. In other words, roughly time-independent hysteresis is observed when the axon is exposed to such a cyclic change in the fraction of divalent cations in the external medium (Tasaki *et al.*, 1968). This phenomenon of hysteresis plays an important role in formulating our physicochemical theory of nerve excitation.

As we shall see later (Chapter 13, Section E), we treat the aforementioned phenomenon in the axon membrane analogously as Weisbuch and Neumann's (1973) treatment of hysteresis in polynucleotides. We assume that the negatively charged sites along strands of fibrous protein molecules are cross-linked extensively by Ca bridges in the resting state of the axon. The breakage of the first bridge by introduction of a pair of univalent cations into the macromolecule is energetically unfavorable. As the number of broken bridges increases, the separation between strands increases. When all the bridges are broken, the formation of the first bridge is difficult because of the large separation between the binding sites. The origin of hysteresis can thus be explained by using Ca bridges instead of H bonds in the theory of Weisbuch and Neumann.

When the external Ca–Na concentration ratio is kept within a proper range, macromolecular transitions can be induced by a variety of means. Lowering of the ambient temperature is a convenient means of bringing about abrupt depolarization (Inoue *et al.*, 1973). Figure 12.8 is an example of the oscillograph records showing the response of the membrane potential

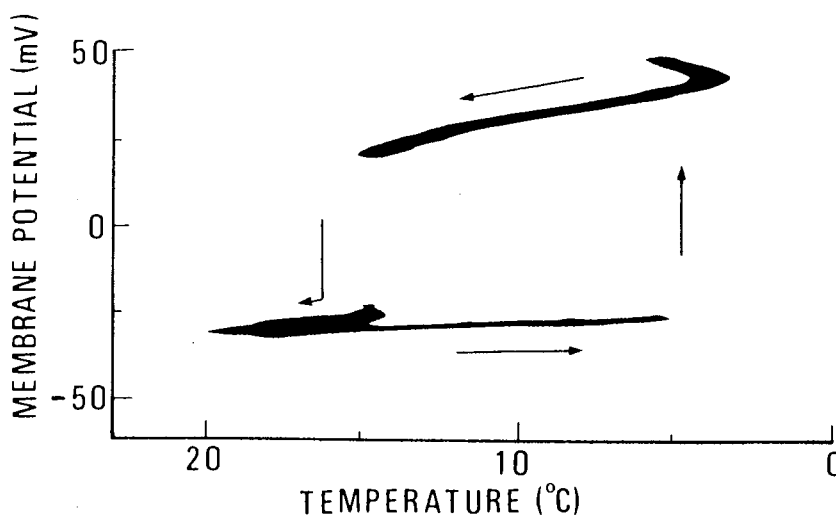


Fig. 12.8 Oscillograph record showing hysteresis in the membrane potential associated with a cyclic change in the temperature. The squid giant axon under study was internally perfused with a 15 mM NaF solution and immersed in a medium containing 100 mM CaCl_2 , 100 mM NaCl, and glycerol. A period of about 3 min was required to complete a cycle. (From *Biochim. Biophys. Acta* **307**, 474, 1973.)

to a cyclic change in the temperature. It is seen that the membrane was depolarized abruptly at about 5°C when the axon was cooled slowly. Repolarization took place at about 15°C.

It is not difficult to explain the effect of temperature changes on the membrane potential and conductance. In inanimate cation exchangers, it is known that substitution of Ca-ions in the exchanger with Na- or K-ions is associated with a decrease in enthalpy of 1.5 – 3.0 kcal/Eq (Coleman, 1952; Flett and Meares, 1966; Sherry, 1968). Swelling of a compact gel is exothermic. Consistent with this fact is the finding that the initiation of an action potential is accompanied by a small rise in the temperature (Abbott *et al.*, 1958; Howarth *et al.*, 1968). The termination of the action potential, as well as replacement of univalent cations in the exchanger with Ca-ions, is endothermic. In accordance with Le Chatelier–Braun's law, replacement of Ca-ion in the exchanger with Na-ion is favored by lowering the temperature.

The effect of raising the temperature of the axon is explained as the result of replacement of Na-ions at the negatively charged sites with Ca-ions. Since the free energy of the entire system has to decrease in order for this endothermic process to proceed, it must be accompanied by a simultaneous increase in the entropy. The disappearance of an ordered layer of water molecules around the macromolecular strands with negatively charged sites has been suggested as the process that contributes to the required increase in entropy (Tasaki, 1968, cited in Chapter 8).

Hysteresis can be observed when the pH of the intracellular perfusion solution is varied in a cyclic fashion (I. Inoue, unpublished). An increase in the hydrogen ion concentration is expected to stabilize the axon membrane in its resting state by neutralizing the negative charges and/or by forming hydrogen bonds between macromolecular strands. The theory of Weisbuch and Neumann (1973) was designed to explain the origin of hysteresis produced by cyclic change in pH.

I. INSTABILITY OBSERVED NEAR THE CRITICAL POINT FOR TRANSITION

In the preceding sections we have seen ample evidence indicating that macromolecules in the axon membrane undergo a transition from one stable conformational state to another. In the terminology of modern thermodynamics (see Glansdorff and Prigogine, 1971), the excited (or depolarized) state of the axon membrane represents a new "structure" which is formed and maintained through the effect of exchange of energy and matter in non-equilibrium conditions. *The formation of a new structure is preceded by the appearance of an instability. At the critical point where a new structure is*

formed, the instability is so enhanced that the fluctuations are amplified and reach a macroscopic level. There is a parallelism between instability and phase transition (see pp. xiv, xv, and 104 in Glansdorff and Prigogine, 1971).

It is easy to find the sign of instability near the critical point for a transition in the axon membrane. Fluctuations of the membrane potential at a "macroscopic level" have been observed in axons internally perfused with a dilute solution of NaF or CsF (Inoue *et al.*, 1973). As in the experiments described in the preceding sections, abrupt depolarization was induced by a slow, continuous increase in the external univalent cation concentration. The CaCl_2 concentration was kept at a constant level throughout the experiment.

In an axon immersed in a Ca-rich medium, the membrane potential shows very little fluctuation. The random noise generated by the recording device is the major source of the observed potential variations. As the concentration of a univalent cation salt added to the external medium rises, the membrane starts to develop detectable fluctuations (see Chapter 10, Section G). Eventually, the amplitude of the potential fluctuation becomes very large and a transition to the depolarized state starts from the peak of the potential fluctuation (see Fig. 12.9).

The stability of a steady state of an axon membrane may be tested by examining the effect of small perturbations. A weak pulse of current through the membrane may be used to perturb the axon. The time dependence of a

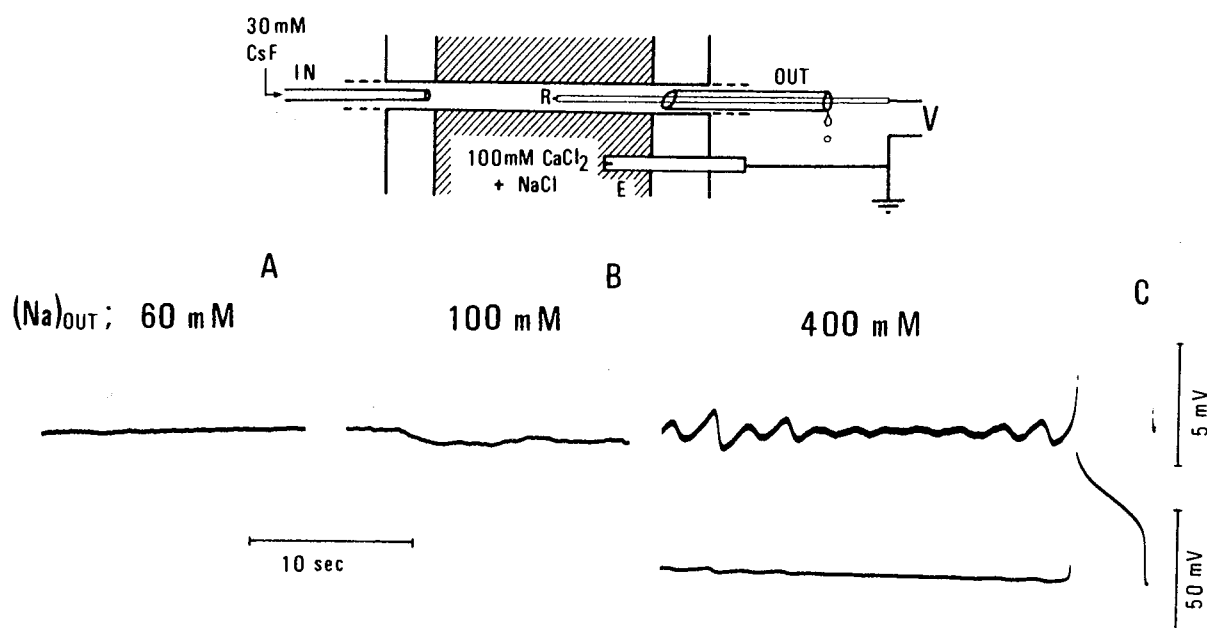


Fig. 12.9 Oscillograph records showing fluctuations in the membrane potential produced by addition of NaCl to the external medium. The axon was internally perfused with a 30 mM CsF solution. The concentrations of NaCl added to the external 100 mM CaCl_2 solution are indicated. Note that the axon was abruptly depolarized near the end of Record C. (From *Biochim. Biophys. Acta* **307**, 475, 1973.)

mode of evolution of the membrane potential is of the form $\exp(\gamma + j\omega)t$, where γ is the real part and ω is the imaginary part of a complex number. In a stable state of the axon membrane γ is negative. As the axon approaches the critical point for transition, γ approaches zero. Eventually when γ becomes positive, the deviation from the initial steady state increases with time and a new steady state is reached. Electrical signs of instability produced by various chemical stimulants (see e.g., Chapter 10, Section F) may be properly described by the aforementioned formulation.

J. MACROMOLECULAR TRANSITIONS UNDER VOLTAGE CLAMP

The technique of voltage clamp has been extremely popular among physiologists. Since transistorized operational amplifiers became commercially available, the instrumentation of voltage clamping became very simple. With this method, the overall potential difference between the internal and external recording electrodes can be maintained at a constant level. In principle, the voltage clamping is equivalent to introducing the axon membrane between two metal electrodes kept at a preselected potential level.

The overall potential difference consists, conceptually, of (1) the difference in the liquid junction potential between the two recording electrodes, (2) the phase-boundary potential at the external surface of the membrane, (3) the intramembrane diffusion potential, and (4) the phase-boundary potential at the inner surface of the membrane. When the equivalent fraction of the external divalent cation is altered, components (1), (2), and (3) are expected to change. At the moment when a small change in the overall potential difference is generated, the feedback device generates a current through the membrane. The IR drop thus produced brings the overall potential difference back to the original level. When a small number of excitable sites of the membrane undergo a transition to the depolarized state, the feedback generates a strong inward current through these sites and suppresses a further increase in the number of excited sites.

Figure 12.10 shows examples of the results obtained by I. Inoue in this laboratory, demonstrating the effect of decreasing the external divalent–univalent cation concentration ratio on squid axons under voltage clamp. The potential difference across the membrane was clamped at the resting level of the axon, namely, at the level observed when the axon was immersed in a normal, Ca-rich medium. As the concentration of the univalent cation salt (NaCl, KCl, RbCl, or CsCl) was raised gradually, a weak inward membrane current was generated. When the external univalent cation concentration reached a level high enough to completely depolarize the membrane, the

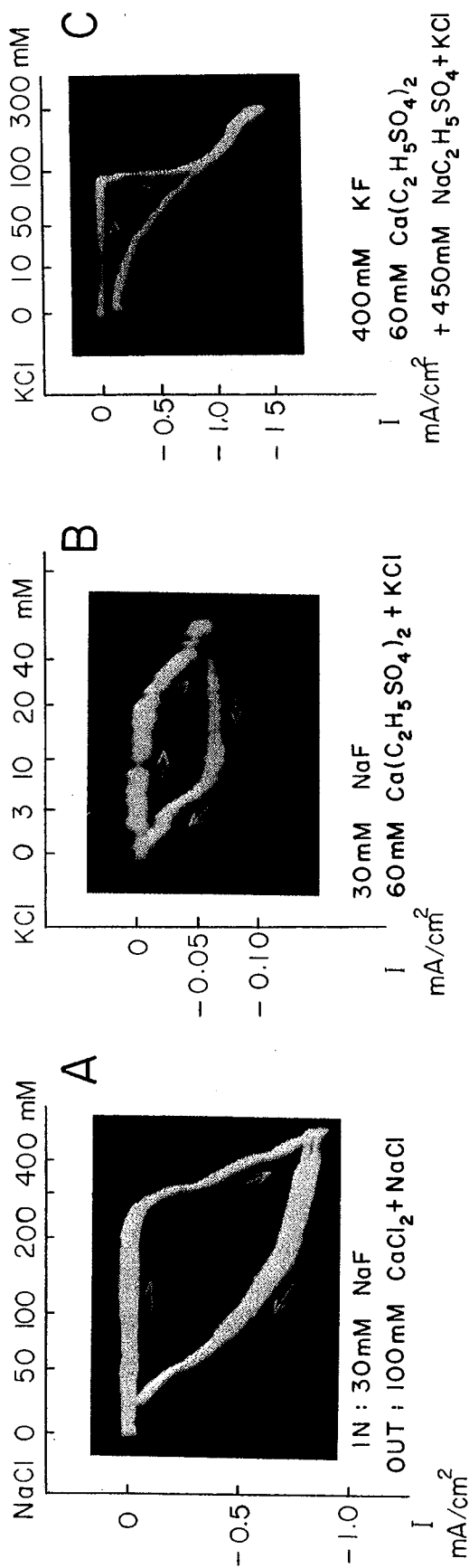


Fig. 12.10 Oscillograph records showing hysteresis, observed under voltage clamp, associated with a cyclic change in the external univalent cation salt concentrations. The membrane current is displayed as a function of the univalent cation concentration in the external medium. Records A and B were taken from axons internally perfused with 30 mM NaF solution; Record C, from an axon under internal perfusion with 400 mM KF solution. The electrolyte compositions of the external media (containing ethylsulfate salts of Ca- and Na-ion) are indicated. A period of approximately 3 min was required to complete a cyclic change in the external univalent cation concentration. (I. Inoue, unpublished.)

intensity of the inward current was sharply enhanced. Finally, when the concentration of the external univalent cation salt was slowly lowered, the inward current decreased gradually. In response to a cyclic change in the external univalent cation concentration, a pronounced hysteresis loop was formed by the intensity of the observed inward current plotted against the external univalent cation concentration.

We believe that abrupt transition from one state to the other is one of the basic properties of a single "domain" of the membrane (see Chapter 10, Section H). When the domains are arranged in such a way that there is a strong electric interaction among them, all the domains may undergo transitions simultaneously. The voltage clamp procedure is an effective means of suppressing electric interactions. As Neumann stated some time ago, "*an assembly of domains which have different stabilities, the distribution of transition points leads to an apparently smooth hysteresis curve*" (p. 358 in Neumann, 1973).

We see in Fig. 12.10 that the shape of the hysteresis loop observed is smooth; it is very different from that observed without voltage clamping. The difference observed derives from the situation that the inward current generated by the feedback device tends to increase the divalent cations within the membrane (see Section G). (The pathway of the current arising from a "domain" of the membrane is discussed further in Chapter 13, Section I). Since the potential difference between the electrodes is kept at the level of the resting state, the current through the portion of the membrane at rest is almost completely suppressed by the clamping device. This suppression of the outward current through the resting area is the reason why an abrupt transition is absent in Fig. 12.10.

K. DEMONSTRATIONS OF DOMAINS IN EXCITED AND RESTING STATES

In an iron wire immersed in a concentrated nitric acid (Ostwald-Lillie nerve analog), it is easy to demonstrate potential variations that resemble prolonged action potentials described in the early part of this chapter. In this nerve membrane analog, the existence of spots and patches in the active state surrounded by the surface in the passive state can be recognized simply by examining the surface of the wire under a microscope (see Chapter 3, Section F).

Attempts at demonstrating similar spots and patches of the nerve membrane in different electrophysiological states were made using squid axons internally perfused with a dilute (15 mM) NaF solution (Inoue *et al.*, 1973). The external medium used contained 400 mM NaCl and 100 mM CaCl₂.

Under these conditions, the amplitude of the action potential was between 70 and 80 mV; the membrane resistance was roughly $1500 \Omega \cdot \text{cm}^2$ at rest and about $100 \Omega \cdot \text{cm}^2$ at the peak of excitation. Hyperfine glass-pipette microelectrodes (less than $0.5 \mu\text{m}$ in diameter at the tip) were used for detecting small electrical signals from the external surface of the axon membrane.

The axon under study was excited at a regular interval (of about 5 sec) and the action potential of the axon was recorded with a large glass pipette electrode (about $100 \mu\text{m}$ in diameter) located in the middle of the perfusion zone. The hyperfine microelectrode was held with a micromanipulator and its tip was brought in contact with the axon surface at an angle of about 30° with the surface. The tip of the microelectrode was then slowly advanced toward the axon surface. As soon as there was penetration of the axon membrane, the microelectrode was quickly withdrawn. The search for small electric signals was repeated many times over a wide area of the membrane.

Two examples of the records of small potential variations obtained by this procedure are reproduced in Fig. 12.11. The upper oscillograph trace in the figure represents the output of the voltage follower connected to the intracellular electrode. The lower trace shows the small potential variations recorded with the extracellular microelectrode. As can be seen in the figure, the time courses to the small potential variations are very different from that of the action potential recorded with the intracellular electrode. These potential variations are characterized by a sudden rise or fall of the potential of less than 1 mV in amplitude. These rectangular potential variations ap-

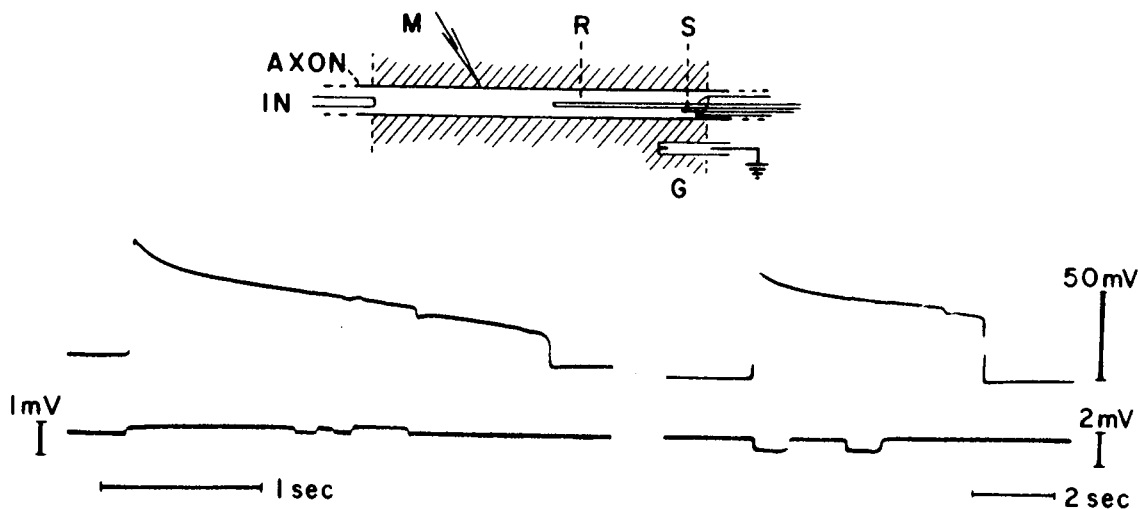


Fig. 12.11 Top: Schematic diagram showing the experimental setup used for demonstrating transitions of domains of the axon membrane between two discrete states. The axon was internally perfused with a dilute sodium salt solution. M, microelectrode; S, stimulating electrode; R, large internal electrode; S, stimulating metal electrode; G, calomel electrode. Bottom: Records of potential variations observed with the large internal electrode (upper trace) and with the microelectrode (lower trace). (From Inoue *et al.*, 1973.)

peared repeatedly during the plateau of the intracellularly recorded action potential. The duration of these small rectangular responses was extremely variable.

It should be noted that small rectangular responses appear even when there is no detectable variation in the intracellular potential recorded at the center of the axon. This fact indicates that the small rectangular responses derive from a very small portion of the membrane. In fact, small responses were found to disappear when the microelectrode was moved away from a favorable site of recording by a distance of a few micrometers. At a favorable site, records similar to those in the figure could be obtained for many minutes.

From the findings described above, we conclude (1) that the membrane sites responsible for production of action potentials (or ion channels) are capable of undergoing transitions between two discrete states, and (2) that the overall behavior of the axon membrane is determined by the fraction of the sites in one state. We have already interpreted various electrophysiological properties of the axon membrane by assuming the existence of two discrete states (Chapter 10, Sections B and H, and Chapter 12, Section A). This aspect of the axon membrane will be discussed further in Chapter 13, Sections E and F.

It is interesting that transitions between two discrete states have been observed in various macromolecules incorporated in a lipid bilayer (Bean *et al.*, 1969; Ehrenstein *et al.*, 1970). The overall behavior of a membrane containing a number of such macromolecules was treated on a statistical basis.

REFERENCES

- Abbott, B. C., Hill, A. V., and Howarth, J. V. (1958). The positive and negative heat production associated with a nerve impulse. *Proc. R. Soc. London Ser. B.* **148**, 149–187.
- Baker, P. F. (1966). The nerve axon. *Sci. Am.* **214**, 74–82.
- Bean, R. C., Shepherd, W. C., Chan, H., and Eichner, J. (1969). Discrete conductance fluctuations in lipid bilayer membranes. *J. Gen. Physiol.* **53**, 744–757.
- Bockris, J. O'M., and Reddy, A. K. N. (1970). "Modern Electrochemistry," Vol. 2. Plenum, New York.
- Coleman, N. T. (1952). A thermochemical approach to the study of ion exchange. *Soil Sci.* **74**, 115–125.
- Dole, M. (1941). "The Glass Electrode," 332 pp. Wiley, New York.
- Ehrenstein, G. H., Lecar, H., and Nosal, R. (1970). The nature of the negative resistance in bimolecular lipid membrane containing excitability-inducing material. *J. Gen. Physiol.* **55**, 119–133.
- Flett, D. S., and Meares, P. (1966). Thermodynamics of cation exchange. Part 4. Uni-, bi- and tervalent ions on Dowex 50. *Trans. Faraday Soc.* **62**, 1469–1481.
- Garrels, R. M., Sato, M., Thompson, M. E., and Truesdell, A. H. (1962). Glass electrodes sensitive to divalent cations. *Science* **135**, 1045–1048.

- Glansdorff, P., and Prigogine, I. (1971). "Thermodynamic Theory of Structure, Stability and Fluctuations," 301 pp. Wiley (Interscience), New York.
- Hill, S. E., and Osterhout, W. J. V. (1938). Calculations of bioelectric potentials. *J. Gen. Physiol.* **21**, 541–556.
- Howarth, J. V., Keynes, R. D., and Ritchie, J. M. (1968). The origin of the initial heat associated with a single impulse in mammalian non-myelinated nerve fibres. *J. Physiol.* **194**, 745–793.
- Inoue, I., Kobatake, Y., and Tasaki, I. (1973). Excitability, instability and phase transitions in squid axon membrane under internal perfusion with dilute salt solutions. *Biochim. Biophys. Acta* **307**, 471–477.
- Katchalsky, A. (1954). Polyelectrolyte gels. *Prog. Biophys. Biophys. Chem.* **4**, 1–59.
- Kratz, L. (1950). "Die Glasselektrode und ihre Anwendungen." Dietrich Steinkopf, Frankfurt/Main.
- Landolt, H. H., and Börnstein, R. (1960). "Zahlenwerte und Funktionen aus Physik, Chemie, Astronomie, Geophysik und Technik," 6th ed., Vol. 11, Part 7, p. 258. Julius Springer, Berlin.
- Martell, A. E., and Calvin, M. (1956). "Chemistry of the Metal Chelate Compounds," 613 pp. Prentice-Hall, Englewood Cliffs, New Jersey.
- Meaves, H., and Vogel, W. (1973). Calcium inward currents in internally perfused giant axons. *J. Physiol. (London)* **235**, 225–265.
- Neumann, E. (1973). Molecular hysteresis and its cybernetic significance. *Angew. Chem.* **12**, 356–369.
- Ross, J. W. (1967). Calcium-selective electrode with liquid ion exchanger. *Science* **156**, 1378–1379.
- Sherry, H. A. (1968). The ion-exchange properties of zeolites. IV. Alkali earth ion exchange in the synthetic zeolites Linde X and Y. *J. Phys. Chem.* **72**, 4086–4094.
- Tasaki, I., and Kobatake, Y. (1968). Appendix in *Nerve Excitation* (Tasaki, 1968, cited in Chapter 8)
- Tasaki, I., Takenaka, T., and Yamagishi, S. (1968). Abrupt depolarization and bi-ionic action potentials in internally perfused squid giant axons. *Am. J. Physiol.* **215**, 152–159.
- Tasaki, I., Lerman, L., and Watanabe, A. (1969). Analysis of the excitation process in squid giant axons under bi-ionic conditions. *Am. J. Physiol.* **216**, 130–138.
- Terakawa, S. (1978). Ca-K bi-ionic action potentials in squid giant axons. *Biol. Bull.* **155**, 469–470.
- Watanabe, A., Tasaki, I., and Lerman, L. (1967). Bi-ionic action potentials in squid giant axons internally perfused with sodium salts. *Proc. Natl. Acad. Sci. U.S.A.* **58**, 2246–2252.
- Weisbuch, G., and Neumann, E. (1973). Molecular field theory of hysteresis in helix-coil transitions of polynucleotides. *Biopolymers* **12**, 1479–1491.
- Williams, R. J. P. (1970). The biochemistry of sodium, potassium, magnesium, and calcium. *Q. Rev.* **24**, 331–365.

13. A Physicochemical Approach and a Model

A. EARLY RELATION BETWEEN PHYSICAL CHEMISTRY AND PHYSIOLOGY

The early tradition preserved in physiology is the belief that, for elucidation of physiological processes, a deep understanding of the laws of physical chemistry is essential. On this point, one of the great physiologists of the last century, Claude Bernard (1865) says: "Previous knowledge of the physicochemical sciences is decidedly not, as is often said, an accessory to biology, but, on the contrary, is essential to it and fundamental. That is why I think it proper to call the physicochemical sciences allied sciences, and not sciences accessory to physiology" (translation by Greene, 1927, see p. 95).

In this connection, it should be noted that a number of important contributions to the development of physical chemistry were made by workers with biological or medical training. The foundation of the first law of thermodynamics was laid by young doctors of medicine, Julius R. Mayer (1842) and Hermann Helmholtz (1847, cited in Chapter 2). The well-known Hagen-Poiseuille law describing the quantity of fluid flowing through a small tube was described by a physician who was interested in the elucidation of the cause of blood flow in capillaries (Poiseuille, 1840). The law of diffusion was discovered by a neurophysiologist, Adolf Fick (1855), who wanted to solve the problem of transport of substances in glands. Van't Hoff's law of osmotic pressure (Van't Hoff, 1887) was built on the extensive experimental work on osmosis through artificial and biological membranes by plant physiologists Wilhelm Pfeffer (1877) and Hugo de Vries (1884). The sensitivity of glass electrodes to acid was discovered by a neurophysiologist, Max Cremer, who wanted to understand the origin of bioelectricity (see p. 601 in Cremer, 1906, cited in Chapter 2). Leonor Michaelis (1922, cited in Chapter 8), who made great contributions to the modern concept of charged porous membranes, started his investigation with medical training and interest. The foundation of the modern theory for ionic mem-

branes was laid first by a doctor of medicine, Torsten Teorell (1935, cited in Chapter 8).

During the past 50 years, however, the old tradition of emphasizing the importance of physical chemistry has gradually lost its weight. Physiologists were fascinated by the rapid advancement of electronic engineering which took place during this period. Consequently, young investigators in the field of neurophysiology became thoroughly proficient in designing and constructing complex electronic circuits used for their electrical measurements. At the same time, there was a great advancement in electro-anatomy and the distribution of electric potential, resistance, and capacitance inside and outside the nerve fiber was clarified (see, e.g., Chapters 4 and 8). [The term "electro-anatomy" was coined by Bekesy (1951).] Eventually, it became a standard approach for physiologists to describe the results of electrochemical measurements in terms of changes in various parts of the electrical circuit representing the state of the nerve fiber (Chapter 8, Section H).

In the early 1960s, when the technique of intracellular perfusion was developed, the need for physicochemical approaches became evident again. It is extremely difficult, if not impossible, to explain many of the new findings in terms of the conventional equivalent electrical circuit. Excitation in a medium devoid of univalent cation (Chapter 12, Section A) and demonstration of hysteresis (Chapter 12, Section H) and rhythmical responses localized at an extremely small membrane area (Chapter 10, Section H, and Chapter 12, Section K) are some of these new findings. An immediate question that arises is how to treat these new findings.

Strange as it may seem, the new findings mentioned above are something that could have been expected from the knowledge of classical physiology. A long time ago (see Chapter 3 Section C), Jacques Loeb and Rudolf Höber held the view that the colloidal state of the surface layer of the nerve and muscle fiber is regulated by a change in the ratio of the concentration of Ca-ions to that of univalent cations. They proposed that the process of nerve excitation involves a rapid change from a compact, Ca-rich state to a swollen, Ca-deficient state. Qualitatively, all the new findings are consistent with the old colloid chemical theory.

Since the time of Loeb and Höber, there has been considerable progress in the field of colloid and polymer chemistry. Electrochemistry of charged membranes has also made great strides during this period. The main task before us is then to "translate" the phenomenon of nerve excitation into meaningful physicochemical concepts (see Katchalsky, 1973). In carrying out such a task, "we must be bold and free in setting forth our ideas. . . . We must be able to attack questions even at the risk of going wrong" (see p. 40 in Claude Bernard, 1865).

B. UNSTIRRED DIFFUSION LAYER

In order to understand physiological properties of the nerve membrane on an electrochemical basis, it is necessary to familiarize ourselves with several basic facts about the behavior of inanimate membranes. One of the important properties which is often overlooked by physiologists is the existence of an unstirred diffusion layer on the surface of the membrane proper. The effects of such an unstirred layer on various membrane phenomena are now considered.

The effect of a stagnant solution layer on the rate of chemical reaction involving solutes and particles was discussed originally by Nernst (1904). The influence of the unstirred solution layer on the fluxes and the potential difference across cation-exchange membranes was investigated by Helfferich (1955), Scatchard and Helfferich (1956), Mackay and Meares (1959), and others. These investigators revealed that, under violent stirring of the aqueous solution in contact with solid particles or a membrane, there is a 30–50- μm thick immobile layer of solution and that the process of diffusion across this layer becomes the rate-limiting step under a variety of conditions. When the stirrer is stopped, the stagnant layer becomes thick and indefinite.

In the case of an ion-exchange membrane separating two different electrolyte solutions, the rate of the ion interdiffusion is inversely proportional to the membrane resistance (see Chapter 11, Section H). If the resistance of the membrane proper is much higher than that of the stagnant layer, neither the membrane potential nor the ion fluxes across the membrane are seriously affected by the rate of diffusion through the stagnant layer. If, on the contrary, the resistance of the membrane proper is low and close to that of the stagnant solution layers, the rate of interdiffusion across the membrane is strongly influenced by the processes taking place in the stagnant layers. Under these conditions, the diffusion potentials across the layers make a large contribution to the overall membrane potential.

The importance of the stagnant solution layer on studies of membrane phenomena is illustrated by an example of the records furnished in Fig. 13.1 (obtained by S. Terakawa). A cation-exchange membrane (polyethylene membrane impregnated with polystyrene sulfonate) separating a 10 mM CaCl_2 solution from a 20 mM KCl solution was used. The electric impedance of the membrane was measured with an AC Wheatstone bridge operated at an arm ratio of 1:10, with a frequency of 5 KHz and an amplitude of 6 mV rms. The output of the bridge was recorded with an inkwriter after rectification. The membrane potential was led off with a pair of calomel electrodes and was recorded simultaneously with the impedance changes.

It is easy to understand, at least qualitatively, the results shown in the figure. When the stirrer in the Ca-salt solution is stopped, there is a fall in the

Ca-ion concentration in the membrane; this results in a decrease in the membrane impedance. Cessation of the stirrer on the side of the K-salt solution produced a fall in the intramembrane concentration of K-ions and a rise in the Ca-ion; this brings about a rise in the membrane impedance. The intramembrane diffusion potential is the greatest when both stirrers are in operation. Cessation of stirring on either side produces a fall in the membrane potential.

Note that the overall potential difference across the membrane includes also two Donnan phase-boundary potentials and the diffusion potentials across the stagnant solution layers. The effect of cessation of stirring on the measured potential difference is sometimes very complex. Scatchard and Helfferich (1956) have shown that the sign of the potential difference across an ion-exchange membrane could be reversed simply by cessation of stirring.

There is good reason to believe that the stagnant layers on both sides of the squid axon membrane exert a profound influence on the process of nerve excitation. In the resting state of the axon, the membrane resistance is high; hence the effect of the stagnant layers is relatively small. During excitation, the membrane resistance falls drastically and the fluxes of interdiffusing cations are markedly enhanced. There is a compact layer of protein mol-

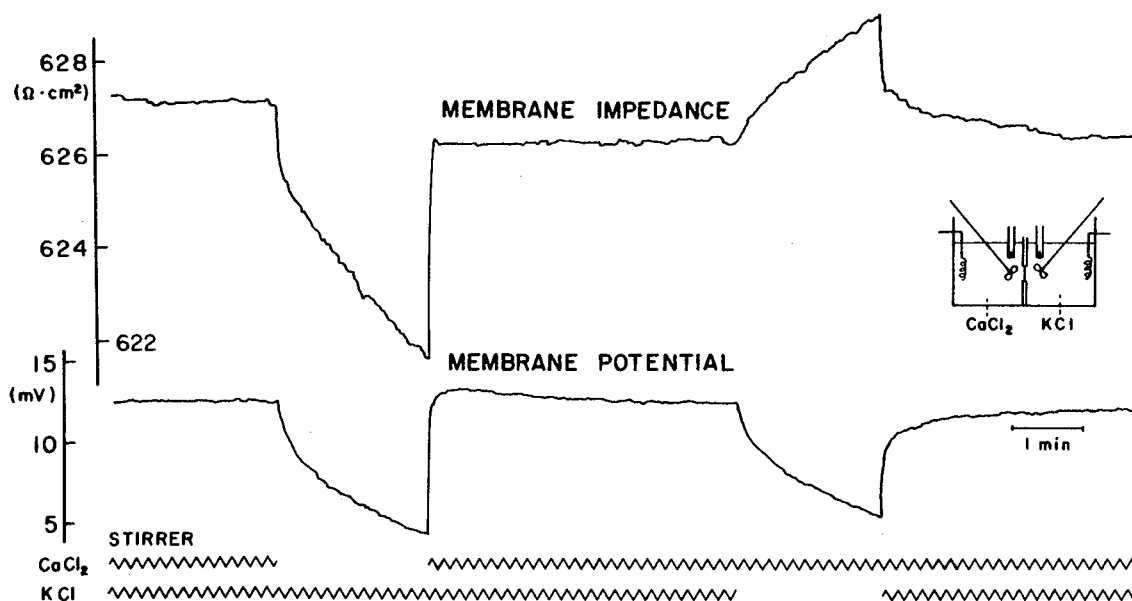


Fig. 13.1 Effect of cessation of stirring on the membrane impedance and on the bi-ionic potential. The cell under study consists of a 10 mM calcium chloride, an artificial cation-exchange membrane, and a 20 mM KCl solution. A 0.2-mm-thick polyethylene membrane containing polystyrene sulfonic acid was used. The breaks of the lower traces indicate the periods during which stirring of the solution in one of the two compartments was stopped. (S. Terakawa, unpublished.)

ecules beneath the axolemma. The external surface of the axolemma is surrounded by a layer of Schwann cells and connective tissue. Following the onset of excitation, the concentration profiles of the interdiffusing cations in the stagnant layers are expected to change rapidly. The effect of this progressive change in the cation concentration profile will be discussed later in Sections G and H.

In comparing the results of observations on artificial membranes with those obtained from biological membranes, it is important to keep marked differences between the two kinds of membranes in mind. Biological membranes are labile; they readily undergo reversible (or sometimes irreversible) structural changes when the temperature, the electrolyte composition, the pH, etc., of the surrounding medium are varied in a wide range. In contrast, commercially available membranes are stable against changes in the medium. Usually, artificial membranes are much thicker than natural membranes. Therefore, various time-dependent phenomena proceed at a rate several orders of magnitude slower in artificial membranes than in the nerve membrane.

C. AN EXAMPLE OF CURRENT-VOLTAGE RELATIONS

As a model of a squid axon under bi-ionic conditions, we consider an inanimate cation-exchanger membrane separating a solution of the salt of a divalent cation species (Ca-ion) and a solution containing the salt of a univalent cation species (Na-ion). We assume that the density of the negative fixed charges in the membrane is uniform and high enough to completely exclude co-ions (i.e., anions). Furthermore, assuming that the membrane is very compact, we ignore flows of water through the membrane. If the selectivity of the membrane for one counterion over the other does not change within the membrane, it is easy to calculate the steady-state fluxes of cations across such a membrane as a function of the voltage (see Schlögl, 1954; Helfferich and Ocker, 1957, cited in Chapter 11; Tasaki, 1968).

Figure 13.2 shows an example of such calculation. Here, the fluxes of cations are calculated as functions of the ion mobilities, the fixed charge density, and the intramembrane potential drop. The "net outward currents" are evaluated by

$$I = F(J_1 - 2J_2)$$

where J_1 and J_2 present the fluxes of Na- and Ca-ions (expressed in mole \cdot cm $^{-2}$ \cdot sec $^{-1}$), respectively, and F is the Faraday constant. When the ratio of the mobility of Na-ion to that of Ca-ion is taken to be 4 and 40, the intramembrane potential drops at $I = 0$ were found to be 27 and 77 mV,

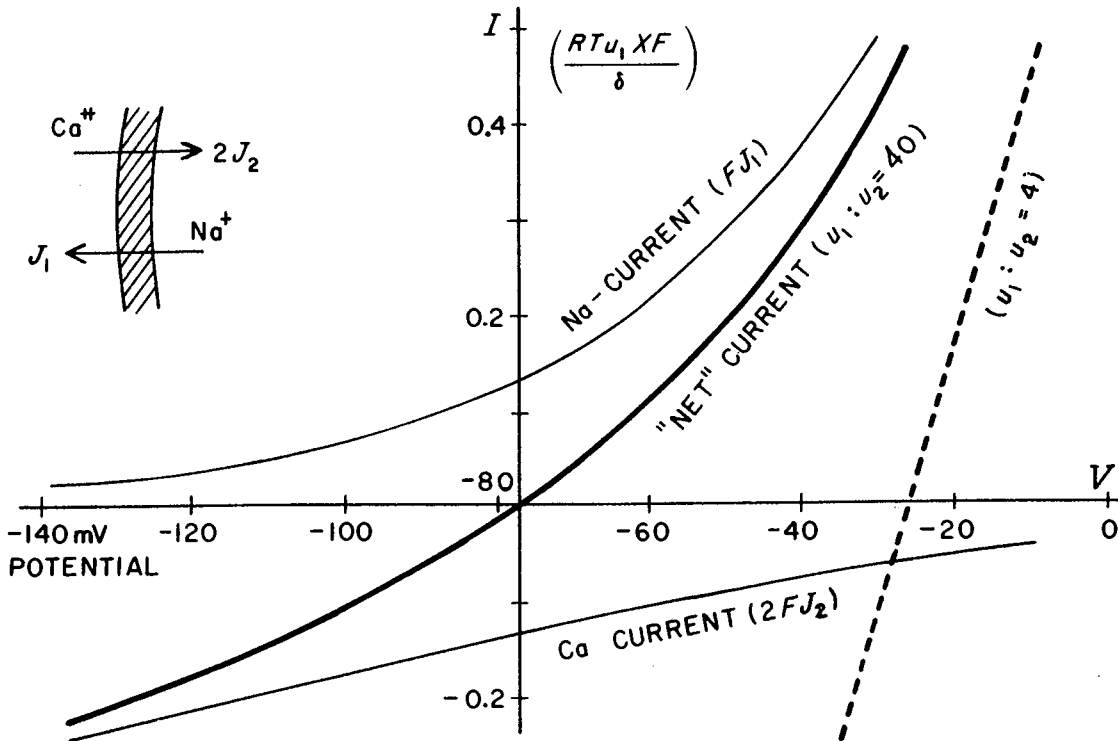


Fig. 13.2 Theoretical membrane current (thick lines), "Na-current" and "Ca-current" (thin lines) plotted against the intramembrane diffusion potential. Equation A.61 in Tasaki (1968) was used for calculation with the mobility ratio taken as 4 and 40. The unit of the ordinate is indicated.

respectively, The current-voltage relations determined by actual measurements on oxidized collodion membranes are similar to that shown in Fig. 13.2.

The following general properties of a charged (ionic) membrane emerge from this type of calculation:

1. When there is no net current through the membrane (i.e., $I = 0$), the influx of external cations ($2J_2$) is equal in magnitude to the efflux of internal cations (J_1). Unless the membrane potential is shifted by several times RT/F (by an external current source), the membrane current cannot be carried only by one cation species.

2. The membrane potential (at $I = 0$) is determined primarily by the mobility ratio, u_1/u_2 . The greater the ratio, the more negative is the potential of the solution containing the univalent cation salt (relative to the potential of the other solution).

3. The relationship between the (net) membrane current and the voltage is roughly linear only within about ± 25 mV (namely, RT/F). When the voltage exceeds this range, the current-voltage relation deviates significantly from Ohm's law. In other words, the membrane behaves like a "rectifier."

4. The membrane current is carried in general by both divalent and univalent cations. When the mobility of the divalent cation is very low, changes in the univalent cation flux make a greater contribution to the (net) membrane current than changes in the divalent cation flux.

5. The effects of an applied current on the membrane are governed by the voltage (IR drop) produced by the current. The flux-voltage curve, plotted in the manner shown in Fig. 13.2, is totally independent of the membrane thickness (δ), as long as the IR drop and the mobility ratio (u_1/u_2) are kept unaltered.

In the absence of a (net) membrane current, the process of generation of a membrane potential may be described in the following manner: The high mobility of Na-ion tends to make the Na-salt solution electronegative relative to the solution of Ca-salt. "This does not mean that, in either the ion-exchanger membrane or the salt solutions, deviations from electroneutrality detectable by chemical analyses can occur" (p. 134 in Helfferich, 1962 cited in Chapter 8). The membrane potentials are adequately described by the Nernst-Planck electrodiffusion equations solved under the condition of *strict electroneutrality*. In order to avoid accumulation of charges anywhere in the system, the movement of Na-ions has to be slowed down and the movement of Ca-ions has to be speeded up by virtue of the potential field developed within the membrane. For this reason, one might say that "the existence of a potential field is a consequence of the electroneutrality requirement" (p. 368 in Helfferich, 1962). [Concerning deviations from electroneutrality, see, e.g., Hafemann (1965); p. 267 in Helfferich (1962).]

When a pair of calomel electrodes is introduced, one in each solution, an electric current can be drawn from the system indefinitely as long as the composition of the solution remains practically unaltered. The emf observed between the two electrodes can of course do work. The energy source is the free energy of mixing of the two solutions.

Finally, the factors which determine the membrane conductance are considered. Figure 13.2 shows that the slope of the current-voltage curve varies with the intramembrane potential difference. At every potential, the slope of the thick line is equal to the sum of the slopes of the thin lines. For this reason, it is not erroneous to say that the membrane conductance is the sum of the "Na conductance" and the "Ca conductance." However, it is important to realize that the Na conductance defined in this manner is a function of the mobilities of both Ca- and Na-ion.

In the model of the nerve membrane described in this section, several restrictive assumptions were made in order to simplify mathematical treatment of the problem. However, the qualitative aspects of the conclusions are expected to remain valid even when co-ions are not perfectly excluded from the membrane or when cations are transported only at restricted membrane

sites. In the recent literature of physiology, inward membrane currents observed in axons under bi-ionic conditions are often referred to as "calcium currents." There is little doubt that the major portion of the inward currents observed in such axons under voltage clamp represents a reduction of the sodium (or univalent cation in general) effluxes.

D. INTRAMEMBRANE CONCENTRATION PROFILES

With a view toward gaining insight into the behavior of the axon membrane exposed to a pulse of electric current, we now consider the distribution of ions within ion-exchanger membranes. Because of its extreme thinness, the concentration profile of the ions within the axon membrane will never be measured directly. Even in much thicker artificial membranes, experimental determination of the intramembrane concentration profiles is not easy. In this section, therefore, we proceed with our mathematical analysis of uniform, ideally permselective cation-exchanger membrane separating a Ca-salt solution from a Na-salt solution. The profiles of Ca- and Na-ions within the membrane can be obtained by solving the Nernst-Planck equations under steady-state conditions (Schlögl, 1954; Helfferich and Ocker, 1957, cited in Chapter 11).

In calculating the concentration profiles, it is assumed that the negatively charged sites on one side of the membrane are occupied solely by Ca-ions and on the other side only by Na-ions. This assumption is necessary because the concentration profiles of the ions within a membrane immersed in unstirred media are ill defined. Within the membrane, the condition of electroneutrality is satisfied:

$$2[\text{Ca}^{2+}] + [\text{Na}^+] = X$$

where X represents the density of the fixed negative charges in the membrane. It is also assumed that X is constant and is independent of the coordinate x across the membrane. (In the axon membrane, it is not safe to assume the negative charge density to be constant; however, the qualitative aspects of the conclusions of the following argument are expected to be applicable to the axon membrane.)

The heavy lines in Fig. 13.3 show the results of calculation performed by taking the ratio of the mobility of Na-ions in the membrane to that of Ca-ions to be either 40 (left) or 4 (right). As is well known, the concentration profiles vary with the mobility ratio. In the absence of a transmembrane electric current, the profiles are steeper on the side facing the faster ions (see p. 360, Helfferich, 1962). In other words, the counterions with a low mobility and a high valency are enriched in the membrane at the expense of counterions

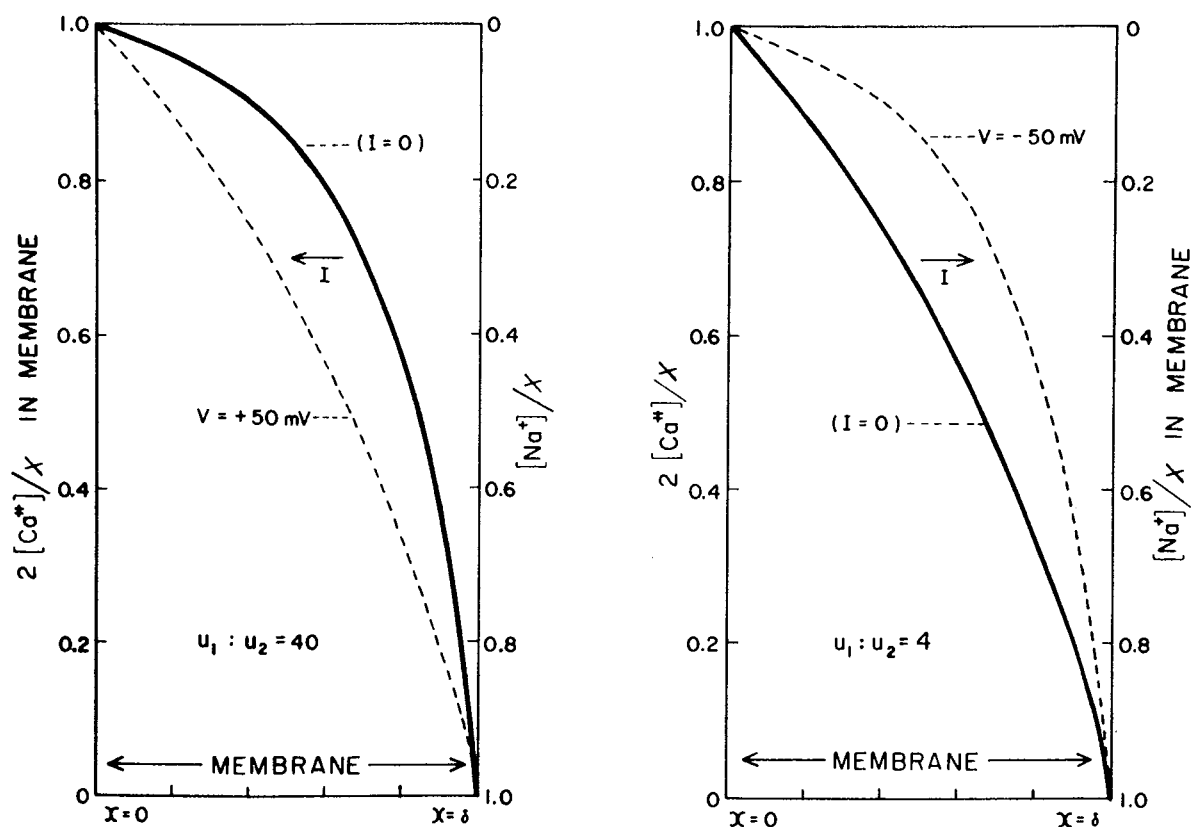


Fig. 13.3 Intramembrane concentration profiles calculated by using Schlögl's time-independent integral of Nernst-Planck equations for electrodiffusion. The Na-Ca mobility ratio was taken as 40 (left) or 4 (right). The broken lines indicate the profiles displaced by electric currents.

with a high mobility and a low valency. Because of the difference in valency between the two counterions, the concentration profile cannot be linear. The deviation from linearity becomes more marked as the mobility ratio becomes greater.

The broken lines in Fig. 13.3 show changes in the concentration profiles brought about by a transmembrane current which produces a potential shift of 50 mV. As expected, a current which enhances transport of highly mobile Na-ions into the membrane is seen to decrease the amount of sluggish Ca-ions in the membrane (see the left-hand graph). The rise in the membrane conductance seen on the right-hand branch of the current-voltage curve in Fig. 13.2 is the consequence of this change in the concentration profile.

The membrane resistance (i.e., the reciprocal of conductance) is given by integration of $dx/[u_1 C_1(x) + 4u_2 C_2(x)]F^2$, where u_1 and u_2 are the mobilities, and $C_1(x)$ and $C_2(x)$ are the concentrations of the two cations in the membrane. When $u_1 \gg u_2$, there is a marked enrichment of divalent cations at the negatively charged membrane sites. A rise in the divalent cation concentration in the membrane is invariably accompanied by a fall in the univalent

cation concentration. It is obvious, therefore, that the overall membrane conductance is *not* determined by the cations with a high mobility (or permeability) alone; rather, it is "controlled" by the slow cation species.

The right-hand graph in Fig. 13.3 shows the effect of transporting Ca-ions across the membrane. The resulting increase in the occupancy of the membrane sites by Ca-ions brings about a significant fall in the slope conductance of the membrane.

In heavily anesthetized squid axons, it is known that the slope conductance of the membrane rises significantly when a long pulse of outwardly directed electric current is applied. An inwardly directed current produces an opposite effect. This behavior of axons in their inexcitable state may be attributed to changes in the concentration profiles of the divalent cations in the membrane. The nonlinearity of the current-voltage relation can be demonstrated by measuring the intensities of currents produced by rectangular voltage pulses applied to the axon membrane. The difference between the current intensity produced by a depolarizing voltage pulse and that generated by a hyperpolarizing pulse of the same amplitude seems to be related, in some ways, to the "gating current" studied by Armstrong and Bezanilla (1973) and Keynes and Rojas (1974).

E. A MACROMOLECULAR MODEL OF TWO DISCRETE STATES OF NERVE MEMBRANE

According to the experimental results described in Chapter 12, Section F, the membrane macromolecules undergo an abrupt conformational transition when the external univalent cation concentration is raised to a certain critical level. The critical concentration is strongly dependent on the concentration of the divalent cation salt in the external medium. The transition is characterized by a fall in the membrane impedance and a rise in the intracellular potential. In the "depolarized" state that appears following a transition, a gradual rise in the external divalent cation concentration can bring about a reverse transition.

There are a few inanimate electrochemical systems that are capable of producing abrupt transitions between two discrete potential and conductance levels. In the case of the Ostwald-Lillie nerve model (see Chapter 3 Section F), the oxidized and reduced states of the surface of an iron wire (immersed in nitric acid) correspond to the two discrete states; a transition can be induced by varying the concentration of the nitric acid as well as by electric currents. In the hydraulic model of Teorell (1959), the existence of stable salt-concentration profiles in the pores of a sintered glass or a glass capillary provides the basis of observed transitions. Some protein molecules

are known to be capable of undergoing transitions between two discrete states (Bean, 1969, cited in Chapter 12). The physicochemical nature of the two discrete states in one nerve model is quite different from that in other model systems.

These questions arise at once: What is the nature of the two discrete states in the nerve membrane? How does the nerve membrane become unstable at a certain divalent–univalent cation concentration ratio?

There is good reason to believe that protein molecules in the membrane play a crucial role in determining electrochemical properties of the nerve fiber. Let us recapitulate the experimental findings indicating the involvement of protein molecules in the process of nerve excitation: (1) Intracellularly administered proteases (including trypsin, chymotrypsin, aminopeptidase, carboxypeptidase, pronase, etc.) eliminate the ability of the axon to undergo transitions (Chapter 9, Section E). (2) The nerve membrane can be excited chemically by a variety of reagents (parachloromercuribenzoate, cyanogen bromide, dyes which mediate photo-oxidation, etc.) that react with proteins (Chapter 10, Section I). (3) Reagents that attack lipids (such as phospholipases, sodium dodecyl sulfate, etc.) do not induce periodic electric responses. (4) Both tetrodotoxin and saxitoxin, powerful nerve poisons, bind to large protein molecules of about 230,000 daltons in the membrane (Chapter 9, Section G).

Based on the experimental finding that the electrical properties of the nerve membrane are hardly affected by replacement of one anion species in the external medium with another, we assume the existence of a high density of fixed negative charges in the membrane protein molecules (see Chapter 11, Sections C, E, and H). When the nerve fiber is immersed in a Ca-rich medium, many of these negatively charged sites are expected to be cross-linked by Ca-ions (see, e.g., p. 15 in Katchalsky, 1954; p. 344 in Williams, 1970, cited in Chapter 12). Upon addition of a large quantity of the salt of univalent cation to the external medium, many of these cross-links between strands of protein molecules are broken, and the strands are separated from one another by virtue of electrostatic repulsion and of increased hydration. Hence, substitution of Na-ions for Ca-ions in the protein molecules results invariably in expansion of the molecules. Expansion ceases when the electrostatic force and the osmotic pressure are counterbalanced by the "contractile" pressure (see Gregor, 1951; Katchalsky and Michaeli, 1955). Thus, we identify the "compact" and "swollen" states of the nerve membrane (see Chapter 3, Section C) as the states of the protein molecules with and without extensive cross-linking by Ca-ions, respectively.

It is assumed that the intramembrane protein molecules penetrate the lipid layer. These molecules are held by a hydrophobic interaction with the lipid. We assume further that there is a large number of acidic amino acids near

the external surface of the protein molecules. On the assumption that the molecular weight of this acidic protein is about 230,000 (see Chapter 9, Section G), the number of carboxyl groups in the molecule is estimated to be on the order of 300. Many of the acidic groups are considered to be located in such positions that can be cross-linked by Ca-ions.

The state of the membrane heavily cross-linked by Ca-ions is stable. In this compact state of the nerve membrane, the selectivity for highly hydrated cations (e.g., Na-ions) is low. A transition to the swollen state brings about a sudden rise in the selectivity and the mobility of hydrated cations. Consequently, a large change in the membrane potential and a marked increase in the membrane conductance are expected when the membrane undergoes a transition from the compact to the swollen state.

The macromolecular model of the two discrete states of the nerve membrane helps toward the understanding of a great number of experimental facts. Swelling of the axon membrane, which had been anticipated since the time of Loeb and Höber (see Chapter 3, Section C), was actually shown to take place concurrently with action potential production (see Chapter 15, Section B). In the following section, an attempt is made to "translate" the qualitative description of the model presented above into a quantitative form.

Finally, the historical background of the concepts incorporated in the present model of the excitable membrane is now briefly discussed. The notion that Ca-ions play a crucial role in nerve excitation originated with Loeb and was extended by Höber, Heilbrunn (see Chapter 3), Brink (1954), Tobias (1964), and many others. The importance of the cooperative ion-exchange processes in excitation has been emphasized by Nachmansohn (1955), Segal (1958), Ling (1962), Nasanow (1962), Troshin (1966), Karreman (1973), and, more recently, by Chang (1979). The possibility of formation of two stable states of the membrane by virtue of ion-exchange processes involving uni- and divalent cations was discussed previously by Tasaki (1963) and by Adam (1968).

F. A PHYSICOCHEMICAL THEORY OF CONFORMATIONAL TRANSITION

We denote the ratio of the number of cross-linked pairs of negatively charged sites to the total number of pairs available for cross-linking by f . We assume that the free energy required to form a single cross-link is dependent on f :

$$(a - bf)kT \qquad (13.1)$$

where kT has the usual physicochemical significance and where a and b are regarded as being independent of f . When f is small, namely, when the majority of the pairs are in their unlinked state, much work is required, because the polypeptide chains are widely separated by electrostatic repulsion ($b > 0$). The work done when the fraction increases from 0 to f is then

$$(a - \frac{1}{2}bf)fNkT \quad (13.2)$$

where N is the number of pairs of sites available for the formation of Ca bridges. The free energy of the whole molecule, F , may then be written in the following form:

$$\begin{aligned} (F - F_0)/NkT = & (a - \frac{1}{2}bf)f \\ & + f \ln f + (1 - f) \ln(1 - f) \\ & + 2f \ln \lambda_1 - f \ln \lambda_2 \end{aligned} \quad (13.3)$$

where F_0 represents the portion of the free energy which is independent of f , and λ_1 and λ_2 are the absolute activities of the univalent and the divalent cations, respectively. When the protein molecules are in their compact state, cation fluxes through the molecules are small; the absolute activities of the cations in the superficial layer of the macromolecules are not different from their values in the external medium. The second and third terms on the right-hand side of Eq. (13.3) represent the mixing entropy of the pairs of sites available for cross-linking. The last two terms denote the free energy change associated with replacement of univalent cations with divalent cations.

Equation (13.3) has the same general form as Eq. (4) in Weisbuch and Neumann's paper (cited in Chapter 12). Hence, depending on a , b , and C_1^2/C_2 , we find one minimum or two minima in the value of F when f is varied from 0 to 1. In equilibrium, only those states represented by the minima are realized. The equilibrium values of f are determined by the condition $\partial F/\partial f = 0$, namely, by

$$a - bf + \ln[f/(1 - f)] + \ln[KC_1^2/C_2] = 0 \quad (13.4)$$

where the absolute activities were replaced with the external concentrations: $\lambda_1^2/\lambda_2 = KC_1^2/C_2$ where K is a constant. This is the desired equation relating the equilibrium value of f to the variable of the system C_1^2/C_2 .

Quite recently, K. Iwasa has shown in this laboratory that Eq. (13.4) can be derived, besides by the procedure described above, by the following two alternative methods: (1) by treating the cation-exchange process as a chemical reaction of which the equilibrium depends on f (also see Tasaki, 1963), and (2) by describing the system under study in terms of a grand canonical partition function.

The mode of dependence of the fraction of cross-linked pairs, f , on the value of C_1^2/C_2 in the medium varies with the choice of b and $(\ln K + a)$.

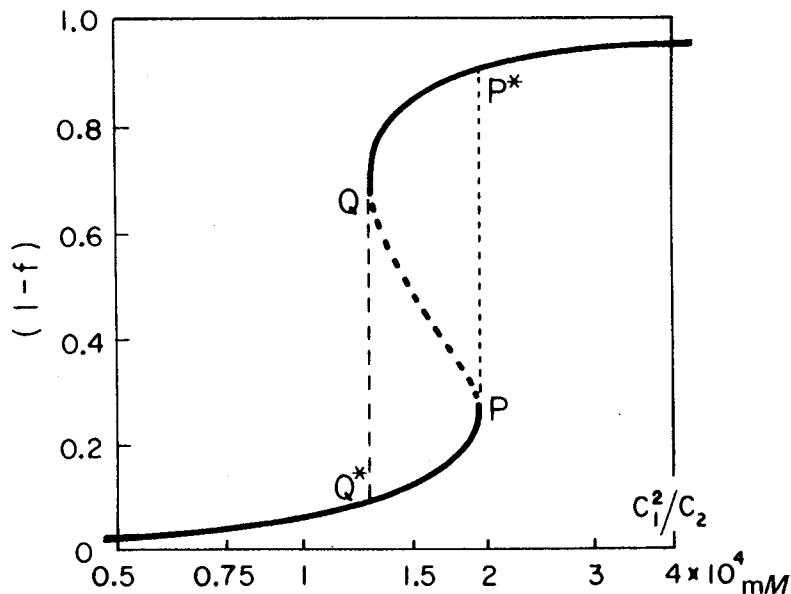


Fig. 13.4 The relationship between the value of C_1^2/C_2 in the external medium and the fraction of broken Ca bridges, $1 - f$, calculated by the use of Eq. (13.4) in the text. In calculation, b is chosen to be equal to 5 and $[5 - a - \ln K]$ to be approximately 12. This diagram indicates that, when C_1 (univalent cation concentration) is 500 mM, transition P to P^* takes place as C_2 (divalent cation concentration) is reduced to 12 mM.

When b is larger than 4, the relationship between f and C_1^2/C_2 is represented by an S-shaped curve. Figure 13.4 shows the results of calculation carried out with b chosen to be 5. The next step in our argument is to use this S-shaped curve for explaining the phenomena of abrupt depolarization and hysteresis.

G. INITIATION, TERMINATION, ABOLITION, AND REPETITIVE FIRING OF ACTION POTENTIALS UNDER BI-IONIC CONDITIONS

It is easy to see that the macromolecular model described in the preceding sections offers a satisfactory explanation to the process of electric excitation of an axon under bi-ionic conditions. In order to excite the axon membrane electrically, a potential drop of about kT/e (approximately 25 mV) has to be generated by an outwardly directed current through the axon membrane which is initially in the resting state. Such a current is capable of increasing the concentration of the univalent cations in the intramembrane protein molecules (see Section E). This in turn raises the fraction of the non-cross-linked pairs of the negatively charged sites. When this fraction reaches the critical level, there is a conformational transition of the macromolecule

from its "compact" to the "swollen" state. The transition brings about a large increase in the intramembrane Ca-ion mobility (see Section C), and consequently, a jump in the overall membrane potential (see Chapter 12, Sections A–D). This is the process of initiation of an action potential in this model.

Next, we consider what happens during the excited state of the axon membrane. A sudden loss of Ca bridges within the macromolecules brings about a large increase in the cation fluxes across the membrane. We have seen in Section B that the effect of "unstirred layers" at the two surfaces of the membrane proper becomes vastly enhanced when the membrane resistance is reduced. When the concentration gradients of the cations in the membrane decreases, the overall membrane potential is expected to fall. There is little doubt that the observed fall of the membrane potential is the consequence of the enhanced cation interdiffusion in the excited state of the membrane (see p. 126 in Tasaki, 1968).

The submembranous protein layer is considered to play a significant role in determining what happens during the excited state of the axon membrane. We have seen that the rate of potential fall is markedly reduced when the submembranous layer is partially removed by various proteases (see Chapter 9 Section E). Since this layer appears to be compact, it is reasonable to assume that the position of the major diffusion barrier in the axon shifts toward this layer during the excited state. Consequently, there is a gradual rise in the Ca-ion concentration within the intramembrane protein molecules. In proteins, Ca-ions are only semimobile (see, e.g., Williams, 1970, cited in Chapter 12; see also Gregor and Wetstone, 1956, cited in Chapter 11). Hence, the process of re-formation of Ca bridges is expected to be relatively slow. When the number of cross-linked pairs of negatively charged sites reaches a critical level, there is a conformational transition which terminates the excited state of a prolonged action potential (see Chapter 11, Section K).

We now turn to the phenomenon of abolition of the action potential. In aqueous media, the equivalent conductivity of Ca-ion is not very different from those of alkali-metal ions; within membrane macromolecules, univalent cations are highly mobile, while Ca-ions are not. Consequently, a strong pulse of inwardly directed current through the membrane tends to enhance the Ca-ion concentration within the intramembrane protein molecules. Accumulation of Ca-ions within the intramembrane particle increases the number of Ca bridges. When such a pulse is applied during the plateau of a prolonged action potential, the action potential can be prematurely terminated. The intensity of the current pulse required for abolition of the action potential is expected to decrease with time and to tend to zero as the system approaches the point of spontaneous termination.

Finally, we discuss the process of spontaneous firing of action potentials on the basis of our macromolecular model. The axon considered here is under intracellular perfusion with a dilute solution of the salt of an alkali-metal ion, say Na-ion. When the extracellular Ca-ion concentration is high (about 100 mM), the membrane is stabilized in its resting state. When a Na-salt solution is added to the external medium step by step, a state of sustained repetitive firing of prolonged action potentials is eventually reached.

In the left-hand graph of Fig. 13.5, the critical univalent cation concentration for initiation of an action potential is represented by point *P*. The state of the system immediately after the onset of an action potential is represented by point *P**. In the excited state of the membrane, the interdiffusion fluxes are intensified and the position of the lowest ion mobilities is shifted toward the submembranous protein layer. Then, there is a gradual rise in the Ca-ion concentration within the intramembrane protein molecules. The effect of this rise is analogous to that of an increase in the extracellular Ca-ion concentration; consequently, the fraction of the broken Ca bridges decreases along line *P*Q*. When the system reaches point *Q*, there is a transition to *Q**. Since the external univalent cation concentration is high enough, the system is expected to move gradually toward *P*. The membrane conductance (measured with high-frequency AC) is expected to reflect the fraction of the non-cross-linked pairs of negatively charged sites; therefore, the expected changes in the membrane conductance associated with a cyclic change of the system along the loop *PP*QQ** is represented by the right-hand graph in the figure. The source of energy required for the maintained cyclic changes is the free energy of mixing Ca- and Na-salt solutions.

In this section, we have seen that many aspects of the electrophysiological behavior of the axon membrane under bi-ionic conditions can be explained on the basis of our macromolecular model. The essential feature of this model is that the cooperative processes of forming and breaking Ca bridges

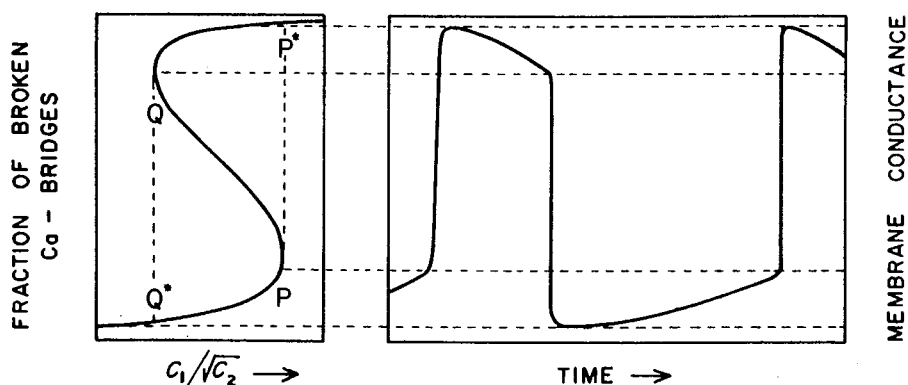


Fig. 13.5 Relation between hysteretic structural changes in the membrane macromolecules (left) and periodic firing of action potentials (right). See text.

are controlled by long-range electrostatic forces and by water molecules around the protein strands. The model gives us a reasonable physicochemical basis for the presence of two stable states of the membrane macromolecule separated by an unstable state.

H. A MACROMOLECULAR INTERPRETATION OF EXCITATION PROCESSES IN INTACT AXONS

In intact (i.e., internally nonperfused) giant axons of the squid, the action potential, evoked either chemically or electrically, lasts for only 1 msec or less at room temperature. In this section, the mechanism of production of such a brief action potential is considered. Analyses of such highly time-dependent changes in the membrane potential are in general very difficult. Note that, in most treatises on inanimate membranes, a discussion of highly time-dependent phenomena is carefully avoided (see e.g., p. 343 in Helfferich, 1962). Admittedly, the following analysis of the brief action potentials in intact axons is somewhat indirect and the conclusions are only qualitative.

Axons internally perfused with a K-salt solution also develop very brief action potentials when immersed in a medium containing both Na- and Ca-salt. Both the amplitude and the duration of the action potential of these axons are very similar to those observed in intact axons. Furthermore, cation fluxes have been determined using radiotracer under these simplified ionic conditions (Chapter 11, Section H). Therefore, we regard the process of action potential production in these well-defined ionic environments as the prototype of the process that occurs in intact axons.

In the presence of both Na- and Ca-ions at a proper ratio, many pairs of negatively charged sites in the intramembrane protein molecules are cross-linked by Ca-ions. A pulse of outwardly directed current, strong enough to generate a potential drop of the order of kT/e (approximately 25 mV), drives internal K-ions into the membrane. We have seen already that K-ions have the strongest tendency toward displacing Ca-ions in the axon membrane (see Chapter 12, Section F). When a critical number of Ca bridges in the intramembrane protein molecules are broken by invading K-ions, a transition to the excited state is triggered and the major portion of the Ca bridges are broken cooperatively. Thus, the intramembrane protein molecules are thrown into their swollen state. A large fall in the membrane resistance (measured with a weak high-frequency AC) ensues from this swelling.

The fall in the membrane resistance greatly enhances the effect of "unstirred diffusion layers," and the interdiffusing cations progressively accumulate on two sides of the axolemma (see Section B). Again, the position of

the maximum resistivity is expected to shift toward the submembranous protein layer. Up to this point, the process in an intact axon is not different from that involving only two cations.

The important feature of the excitation process involving these three cations is that the Na–K interdiffusion is far more intense than that involving only two cations of which one is Ca ion. Immediately following the transition, the interdiffusion fluxes are increased by a factor of 100 (Chapter 11, Section H). This brings about a progressive change in the distribution of Na- and K-ions, followed by a gradual rise in the Ca-ion concentration in the intramembrane protein molecules. The electrical behavior of the axon membrane is determined by the distribution of cations in and around the diffusion barrier between the axon interior and the external medium. As in many inanimate ion exchangers (see p. 188 in Helfferich, 1962), the membrane macromolecules appear to be "irregular" in that the ion selectivity is strongly affected by the ionic composition. There is an indication that the negatively charged sites prefer counterions that are present at a high concentration.

There is little doubt that the rapid fall of the membrane potential from the peak of an action potential is directly related to the high rate of the Na–K interdiffusion. Replacement of Rb-ions for the intracellular K-ions roughly doubles the action potential duration. Intracellularly administered Cs-ions enormously prolong the action potential duration. This prolongation of the action potential is attributed to the marked reduction in the interdiffusion associated with replacement of Rb- or Cs-ion for internal K-ion (Tasaki, 1963). The intramembrane mobilities of the large alkali cations must be lower than that of the K-ion. In general, the counterions that are strongly preferred by the charged sites have low mobilities (see, e.g., p. 304 in Helfferich, 1962).

The important single factor which affects the ion mobility is the water content or the degree of swelling (see, e.g., Gregor and Sollner, 1946; Lagos and Kitchner, 1960, cited in Chapter 11). The shortening of the action potential duration produced by a slight dilution of the external medium with distilled water is likely to be due to the enhancement of interdiffusion fluxes resulting from an increase in the water content.

We have seen that the membrane conductance (measured with a high-frequency AC) is still very high at the moment when the membrane potential reaches the lowest point toward the end of the action potential (Chapter 8, Section C). It is reasonable to assume that the majority of the Ca bridges still remain broken at this moment. The major diffusion barrier must then be located in the submembranous protein layer. The shape of the action potential of the squid giant axon is very different from that of other nerve fibers: the "shoulder" of the action potential, which is present in almost all other nerve

fibers, is missing in the squid axon. The shoulder is regarded as the onset of a macromolecular transition to the high-impedance (Ca-rich) state of the membrane. The following observation is designed to illustrate the difference (and similarity) between the action potential in the squid axon and that in other nerve fibers.

We have seen in Chapter 10, Section B, that intracellular injection of tetraethylammonium (TEA) salt solution brings about a marked prolongation of the action potential. When a small amount of TEA-salt solution is introduced along the axis of the axon, there is a progressive change in the duration of the action potential, reflecting a gradual rise in the TEA concentration at the axon membrane. The tracings in Fig. 13.6 show the course of such a progressive change. It should be noted that the tracing marked "2" in the figure is very similar to the record of an action potential taken from a single node of Ranvier of the frog nerve fiber (see Chapter 5, Section A). The tracings marked "3" and "4" are similar to the action potential of the cardiac muscle (see Weidmann, 1956). From these tracings, it is found that the lowest point in the action potential of the squid axon corresponds to the "shoulder" of the frog fiber action potential. During the undershoot, incorporation of Ca-ions into the membrane macromolecules proceeds rapidly because the membrane resistance is still low and the intracellular potential is negative.

A similar progressive change in the time course of the action potential can be produced by successively increasing substitution of Na-ions for the intracellular K-ions (see Chapter 11, Section G). There is no doubt that replacement of K-ions in the axon interior with Na-ions suppresses both the influx of Na-ions and the efflux of K-ions in the excited state of the axon. This suppression of counterion interdiffusion is regarded as the cause of the observed action potential prolongation. TEA ions in the axon interior are considered to prolong the action potential duration by a similar mechanism. When the

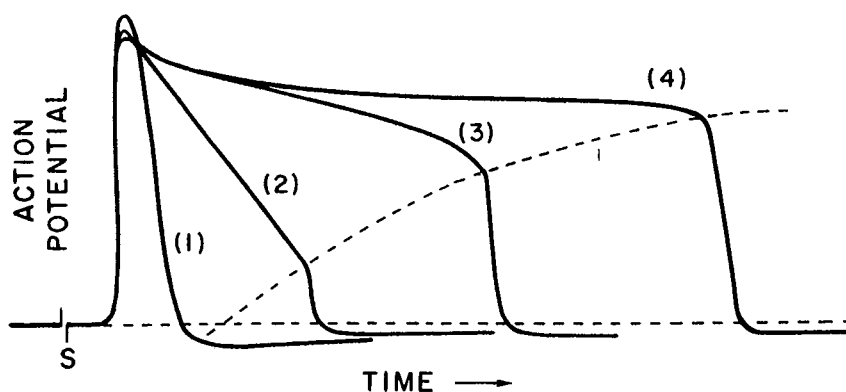


Fig. 13.6 Comparison of the action potential of the squid giant axon (1) with that of the frog nerve fiber (2) and with the responses of the cardiac muscle fiber (3) and (4). See text.

compact layer of submembranous protein molecules takes up TEA-ions, the mobility of K-ions in this layer is expected to fall and suppresses the interdiffusion fluxes.

In summary, we find that the electrochemical processes which underlie action potential production in intact axons are far more complex than the excitation processes involving Ca-ions and a single univalent cation species. The existence of two highly mobile univalent cations, Na- and K-ions, is the factor that determines the duration of the action potential in intact axons.

I. DOMAINS OF THE MEMBRANE IN ITS EXCITED STATE

In the preceding sections, we have repeatedly remarked that the nerve membrane is capable of undergoing transitions between two stable conformational states. The demonstration of cooperative transitions automatically leads us to anticipate the existence of a domain structure in the axon membrane (see Chapter 12, Section K).

In inanimate systems which are capable of undergoing transitions between two stable states, the appearance of domains in one state mingled with the zone in the other state is a phenomenon of common occurrence. The oldest known example is the Barkhausen effect encountered in magnetization of ferromagnetic material (Barkhausen, 1919). The phenomena of hysteresis (Ewing, 1885) and propagation of discontinuous state changes at a finite speed (see Sixtus and Tonks, 1931) have also been known in ferromagnetic materials for a long time.

In the case of the Ostwald–Lillie analog of the nerve membrane (see Chapter 3, Section F), a transition from the high-resistance (passive) state of the iron–acid interface to the low-resistance (activated) state may be induced by a pulse of electric current. A “subthreshold” current pulse produces activated spots and domains. Since there is a difference in the emf between the two parts, local microcurrents (Hermann’s *Strömchen*) are generated between the activated sites and the neighboring passive area. When the intensity of the local microcurrent reaches a critical level, a wave of activation is initiated and the entire surface is thrown into its activated state.

There is close similarity between the properties of domains in the nerve membrane and those in inanimate systems. By the term “domain” in the nerve membrane, we mean a portion of the membrane in which all the functional units (i.e., intramembrane protein molecules) change their state cooperatively. The existence of such domains in the excited state is evidently the consequence of the existence of the two stable states of the axon membrane separated by an unstable, unrealizable, state. There is a finite variation in the

threshold concentrations of chemical stimulants for different domains (Chapter 10, Section H). In view of the fact that the axon membrane is surrounded by such spatially nonuniform structures as Schwann's cells, mitochondria, etc., a variation is expected in the threshold membrane potential for different domains of the axon membrane.

When a domain in the excited state is surrounded by the membrane area in the resting state, there is a local microcurrent which is inwardly directed through the excited domain and outwardly directed through the resting area. When there is no net current through the whole membrane, the surface integral of the inward current is equal in magnitude to that of the outward current. When a net current is allowed to pass through the membrane, the ratio of the outward to the inward component is altered. The emf responsible for the local microcurrent is equal to the difference between the membrane potential in the excited state and that at rest (approximately 110 mV). As long as the average potential difference across the whole membrane is kept well below the peak level of the action potential, the net current through the whole membrane is always far weaker than the sum of the local microcurrents.

Analogous situations are known to exist in artificial membranes. From his studies of the phenomenon of electroosmosis, Sollner says that, in a system in which two parts of a membrane yielding different membrane potentials are arranged to interact electrically, the current flowing in the macrosystem would be several orders of magnitude weaker than the sum of all the local microcurrents (p. 44 in Sollner, 1976).

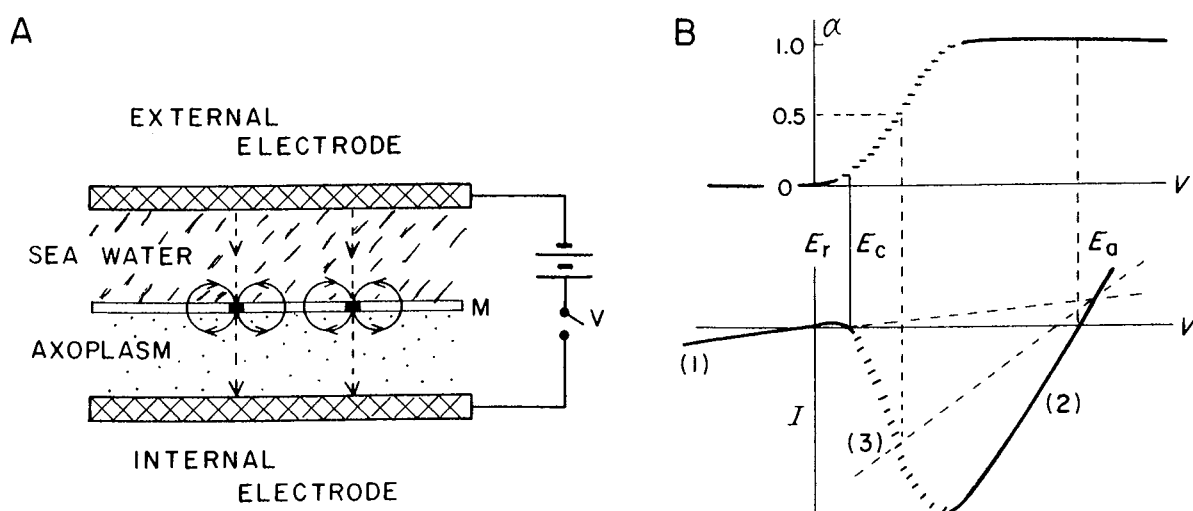


Fig. 13.7 Interpretation of the current-voltage (I - V) relation based on the domain structure of the axon membrane. (A) Diagram illustrating the principle of voltage clamp procedure. (B) Top: The fraction of the membrane area in the excited state plotted against voltage V . Bottom: Current-voltage relations calculated by using Eqs. (13.5-13.7).

We now consider the behavior of the squid axon membrane under the experimental manipulation known as the voltage clamp procedure. The principle of this procedure is illustrated schematically in Fig. 13.7, left. Along the axis of an axon, a long metal electrode (e.g., platinized platinum wire) is introduced. Between this intracellular electrode and a similar electrode outside, a source of constant voltage is suddenly connected. When the imposed voltage raises the intracellular potential slightly above the threshold level for electric excitation, domains of the membrane in the excited state are formed. The portion of the membrane for which the applied voltage is subthreshold remains in the resting state under these conditions. Through the domains in the excited state, there are inwardly directed currents. A portion of the local microcurrent flows through the resting membrane area in the immediate vicinity of the domains in the excited state. The potential field around a domain in the excited state is expected to decay sharply with distance.

When the applied voltage is below the threshold for excitation, the membrane remains in the resting state. The relationship between the current through the membrane and the applied voltage is given roughly by

$$I = G_r(V - E_r) \quad (13.5)$$

where G_r and E_r are the conductance and the membrane potential for $I = 0$ in the resting state, respectively. This roughly linear relation between I and V is represented by the straight line marked (1) in Fig. 13.7B.

When the level of applied voltage is high, the area of the membrane in the excited state is increased. When the entire membrane becomes excited, the electric current, I , at the onset of excitation is described roughly by Ohm's law written in the following form:

$$I = G_a(V - E_a) \quad (13.6)$$

where E_a is the membrane potential in the excited state (in the absence of current) and G_a the membrane conductance. The straight line marked (3) in the Fig. 13.7B represents this relationship between V and I at the onset of excitation. In the excited state, E_a falls with time (see Section H).

In the intermediate range of applied voltage, the current flows through both the resting area and the domains in the excited state. We describe the fraction of the membrane area in the excited state by α . The current at the onset of excitation is then given formally by

$$I = (1 - \alpha)G_r(V - E_r) + \alpha G_a(V - E_a) \quad (13.7)$$

The fraction α increases monotonically with the applied voltage. The dependence of α on the voltage, V , is shown in the upper part of Fig. 13.7B. This dependence has been determined by the use of a high-frequency AC super-

posed on the rectangular voltage, V (Tasaki, 1968). Using the observed dependence of α on V , the observed N-shaped relationship between I and V can be described by Eq. (13.7).

The voltage clamp procedure is a powerful means of suppressing the electric interaction between different parts of the axon membrane. On the assumption that the electric interaction has been completely eliminated, we infer that the slope, $\partial\alpha/\partial V$, of the curve approximately represents the variation of the threshold membrane potential among different domains.

Under voltage clamp, it is difficult to detect signs of spatial nonuniformity of the axon membrane by electrical means. The membrane potential is artificially equalized over a wide area, and only the membrane current averaged over the entire membrane area under study can be recorded. For this reason, most physiologists assume that the axon membrane is spatially uniform. Since, however, electric currents are known to produce domain structures even in chemically pure systems (see, e.g., p. 578 in Stephenson and Bartlett, 1954), we emphasize here that it is unrealistic to ignore spatial nonuniformity of the axon membrane. In a macromolecular system in which the conformation state changes by virtue of cooperative processes, the average level of the potential difference across the membrane can not uniquely determine the conformational state (see Chapter 12, Section K). In the axon membrane under voltage clamp, the inward current through the sites in the excited state (see Fig. 13.7) tends to bring about a transition of the site to the resting state.

In summary, we have explained in this section the properties of the axon membrane under voltage clamp on the basis of our theory which infers the existence of a domain structure of the axon membrane. Most present day axonologists explain the I - V relationship in terms of an equivalent electric circuit and variable single ion conductances. The significance of this commonly accepted explanation will be discussed later in Chapter 14, Sections F and G.

REFERENCES

- Adam, G. (1968). Theory of nerve excitation as a cooperative cation exchange in two-dimensional lattice. In "Physical Principles of Biological Membranes" (F. Snell, ed., pp. 35-68. Gordon Breach, New York.
- Armstrong, C. M., and Bezanilla, F. (1973). Currents related to movement of the gating particles of the sodium channels. *Nature (London)* **242**, 459-461.
- Barkhausen, H. (1919). Zwei mit Hilfe der neuen Verstärker entdeckte Erscheinungen. *Physik. Z.* **20**, 401-403.
- Bekesy, G. von (1951). The coarse pattern of the electrical resistance in the cochlea of the guinea pig (electro-anatomy of the cochlea). *J. Acoust. Soc. Am.* **23**, 18-28.
- Bernard, C. (1865). "Introduction a l'Etude de la Médecine Expérimentale." J. B. Bailliere et

- Fils, Paris. Translation by H. C. Greene (1927). "An Introduction to the Study of Experimental Medicine." Macmillan, New York.
- Brink, F. (1954). The role of calcium ions in neural processes. *Pharmacol. Rev.* **6**, 243–298.
- Chang, D. C. (1979). A physical model of nerve axon-II: Action potential and excitation currents. Voltage-clamp studies of chemical driving forces of Na and K in squid giant axon. *Physiol. Chem. Phys.* **11**, 263–288.
- de Vries, H. (1884). Eine Methode zur Analyse der Turgorkraft. *Jahrbüch. Wiss. Bot. (N. Pringsheim)* **14**, 427–601.
- Ewing, J. A. (1885). Experimental researches in magnetism. *Philos. Trans. R. Soc. London* **176**, 523–640.
- Fick, A. (1855). On liquid diffusion. *Philos. Mag.*, **10**, 30–39. See also *Ann. Phys. (Leipzig)* **170**, 59–86.
- Gregor, H. P. (1951). Gibbs–Donnan equilibria in ion exchange resin systems. *J. Am. Chem. Soc.* **73**, 642–652.
- Gregor, H. P., and Sollner, K. (1946). Improved methods of preparation of electropositive permselective protamine collodion membranes. *J. Phys. Chem.* **50**, 88–96.
- Hafemann, D. R. (1965). Charge separation in liquid junctions. *J. Phys. Chem.* **69**, 4226–4231.
- Helfferrich, F. (1955). Berücksichtigung anhaftender Flüssigkeitsfilme bei Messungen an Ionenaustauschermembranen. *Z. Phys. Chem. (Neue Folge)* **4**, 386–387.
- Helfferrich, F. (1962). "Ion Exchange," 624 pp. McGraw-Hill, New York.
- Karremen, G. (1973). Towards a physical understanding of physiological excitation as a cooperative specific adsorption phenomenon. *Bull. Math. Biol.* **35**, 149–171.
- Katchalsky, A. (1954). Polyelectrolyte gel. *Prog. Biophys. Biophys. Chem.* **4**, 1–59.
- Katchalsky, A. (1973). (See Neumann, 1973, cited in Chapter 12). Molecular hysteresis and its cybernetic significance. *Angew. Chem.* **12**, 356–369.
- Katchalsky, A., and Michaeli, I. (1955). Polyelectrolyte gels in salt solutions. *J. Polym. Sci.* **15**, 69–86.
- Keynes, R. D., and Rojas, E. (1974). Kinetics and steady-state properties of the charged system controlling sodium conductance in the squid giant axon. *J. Physiol. (London)* **239**, 393–434.
- Ling, G. (1962). "A Physical Theory of the Living State: The Association Induction Hypothesis." Ginn (Blaisdell), Boston, Massachusetts.
- Mackay, D., and Meares, P. (1959). On the correction for unstirred solution films in ion-exchange membrane cells. *Kolloid Z.* **167**, 31–39.
- Mayer, J. R. (1842). *Liebigs Ann. Chem.* **42**, 233–240. See remarks on the mechanical equivalent of heat. *Philos. Mag. J. Sci. Suppl.* **25**, 495–522, 1863.
- Nachmansohn, D. (1955). "Metabolism and Function of the Nerve Cell," *Harvey Lect. Ser. XII*, 1953–1954. Academic Press, New York.
- Nasanov, D. N. (1962). "Local Reaction of Protoplasm and Gradual Excitation." National Science Foundation, Washington, D.C. (translated from Russian).
- Nernst, W. (1904). Theorie der Reaktionsgeschwindigkeit in heterogenen Systemen. *Z. Phys. Chem.* **47**, 52–55.
- Pfeffer, W. (1877). "Osmotische Untersuchungen" 236 pp. Verlag von W. Engelmann, Leipzig.
- Poiseuille, J. L. M. (1840). Recherches expérimentales sur le mouvement des liquides dans les tubes de très petits diamètres. *C. R. Acad. Sci. Paris* **11**, 961–967 and 1041–1048.
- Scatchard, G., and Helfferrich, F. (1956). The effect of stirring on cells with cation exchanger membranes. *Discuss. Faraday Soc.* **21**, 70–82.
- Schlögl, R. (1954). Elektrodifffusion in freier Lösung und geladenen Membranen. (Das allgemeine, zeitunabhängige Integral der Nernst–Planckschen Ionenbewegungsgleichungen für beliebige Elektrolyte.) *Z. Phys. Chem.* **1**, 305–339.

- Segal, J. (1958). "Die Erregbarkeit der lebenden Materie," 239 pp. Veb. Gustav Fischer, Jena, Germany.
- Sixtus, K. J., and Tonks, L. (1931). Propagation of large Barkhausen discontinuities. *Phys. Rev.* **37**, 930-958.
- Sollner, K. (1976). The early developments of the electrochemistry of polymer membranes. In "Charged Gels and Membranes," E. Selegny, pp. 3-55. D. Reidel Co., Dordrecht-Holland.
- Stephenson, L., and Bartlett, J. H. (1954). Anodic behavior of copper in HCl. *J. Electrochem. Soc.* **101**, 571-581.
- Tasaki, I. (1963). Permeability of squid axon membrane to various ions. *J. Gen. Physiol.* **46**, 755-772.
- Tasaki, I. (1968). "Nerve Excitation." Thomas, Springfield, Illinois.
- Teorell, T. (1959). Electrokinetic membrane processes in relation to properties of excitable tissues. II. Some theoretical considerations. *J. Gen. Physiol.* **42**, 847-862.
- Tobias, J. M. (1964). A chemically specified molecular mechanism underlying excitation in nerve: A hypothesis. *Nature (London)* **203**, 13-17.
- Troshin, A. S. (1966). "The Problem of Cell Permeability." Pergamon, Oxford (translation by M. G. Hell; translation edited by W. F. Widdas).
- Van't Hoff, J. H. (1887). Die Rolle des osmotischen Druckes in der Analogie zwischen Lösungen und Gasen. *Z. Phys. Chem.* **1**, 481-508.
- Weidmann, S. (1956). "Elektrophysiologie der Herzmuskelfaser," 100 pp. Hans Huber, Bern and Stuttgart.

14. Electrochemical Considerations of the Classical Membrane Theory

A. ELECTROCHEMICAL PROPERTIES OF THE SQUID AXON: RECAPITULATION

We have seen in the preceding chapters that our knowledge of electrochemical properties of the squid giant axon is derived mainly from observations carried out under intracellular perfusion. Squid axons remain highly excitable with the salt of a divalent cation externally and the salt of a univalent cation internally. Electrochemical data obtained under these extremely simple experimental conditions are far easier to understand and less vulnerable to misinterpretation than those collected under normal physiological conditions. Starting with the analyses of the resting and action potentials of such axons, we have proceeded to clarify the effects of adding the salt of univalent cations to the external medium. Immersed in a mixture of Ca- and Na-salt solutions, squid axons internally perfused with a solution of K-salts are shown to develop electric responses with the appearance of a normal action potential. By such logical steps, we have arrived at a reasonable understanding of electrochemical properties of the normal, intact axon.

The electrochemical properties of the axon, as revealed by the technique of intracellular perfusion, may be summarized as follows:

1. In the resting state, the membrane macromolecules are stabilized by the divalent cations (Ca-ions) derived from the external medium.
2. The resting membrane potential is a multi-ionic potential determined by the mobilities and selectivities of cations in the potential-determining macromolecules.
3. Transition of the axon membrane from the resting to the excited state is triggered by substitution of the semimobile divalent cations in the membrane macromolecules with highly mobile univalent cations.
4. The membrane potential at the peak of excitation is an emf deter-

mined primarily by the mobilities and selectivities of cations in the membrane macromolecules in their swollen, univalent cation-rich state.

5. In an axon immersed in a mixed solution of Ca- and Na-salt and internally perfused with a K-salt solution, the production of an action potential is associated with the enhanced interdiffusion involving Na- and K-ions. The fall in the membrane potential from the peak of an action potential is a consequence of the enhanced cation interdiffusion associated with the decrease in membrane resistance.

6. The restoration of the resting state is accompanied by reoccupation of the macromolecules by divalent cations.

In our description of electrochemical properties of the excitable membrane, the membrane macromolecules play the principal role. Under a given environment, both the membrane potential (emf) and conductance are determined by the conformational state of the macromolecules. The difference in behavior among univalent cations is taken into consideration through the variance of their mobilities and selectivities in the macromolecules. Movements of cations through the macromolecules are considered to proceed without violating the condition of macroscopic electroneutrality.

A question now arises: What is the relationship between classical membrane theory and the present approach to the problem of nerve excitation?

We see, in most textbooks of physiology, that the axon membrane is depicted as a thin layer with positive charges on one side and negative charges on the other. Is it reasonable to interpret the membrane potential as being generated by the electric charges accumulated on the membrane capacity? Can the influx of extracellular cations (Na- or Ca-ions) be regarded as the cause of the rise of the intracellular potential during the process of excitation? Does the concept of "ion permeability" fit in with the macromolecular description of the axon membrane? What is the significance of "ion pumps" which many biologists adopt in explaining K-ion accumulation in the protoplasm? How is the concept of specific ion channels reconciled with the macromolecular concept?

In the following sections, attempts are made to answer the questions raised above. For readers who are uninterested in the formal logic of classical membrane theory, however, the arguments expounded in the remainder of this chapter may be superfluous.

B. POLARIZATION OF THE AXON MEMBRANE

The origin of the term "polarization" can be traced back to the time of du Bois-Reymond when polarizable metal electrodes were used for stimulating

nerve trunks and for recording action currents (see Chapter 2, Section B). Much later, Bernstein introduced the physiological term "membrane polarization" to describe the state of his membrane model with negative charges accumulated on the inner surface and positive charges on the outer surface (see p. 93 in Bernstein, 1912, cited in Chapter 2). He believed that the net charges on the surfaces of the membrane were responsible for generation of the emf which could be observed between a pair of nonpolarizable electrodes placed effectively across the membrane (See Chapter 2, Section F). He further explained changes in the membrane potential produced by an electric current from an external source in terms of an increase or a decrease of the electric charges on the membrane (see p. 133 in Bernstein, 1912).

For the majority of students of biology and medicine, this model of the nerve membrane (as well as Galvani's capacitor model of the muscle) may appear very simple and easy to understand. At the same time, the orthodox method of calculating the emf of an electrochemical cell with transference by evaluating a change in the Gibbs free energy (see, e.g., p. 238 in MacInnes, 1961) or by solving the Nernst-Planck equations for a multi-ionic diffusion potential under the electroneutrality condition (see Schlögl, 1954; Tasaki, 1968, cited in Chapter 8) may appear unnecessarily complicated. Because of its illusory simplicity, Bernstein's model of the nerve membrane became very popular. Reflecting the long-standing popularity of this simple model, most present-day physiologists use the terms "depolarization" and "hyperpolarization" to denote a rise and fall, respectively, of the intracellular potentials and to indicate changes in the electric charge of the axon membrane.

At present, we have a rather poor understanding of the nature of the capacity of the axon membrane (see, e.g., Tien and Diana, 1967; Takashima, 1976). Nevertheless, since the nerve membrane is immersed in electrolyte solutions, Bernstein's diagram (Fig. 2.5 in Chapter 2) of the membrane carrying positive and negative charges on its two surfaces is totally unrealistic. Instead, a picture with one electric double layer (see Gouy, 1910; Chapman, 1913; Overbeek, 1952) on each surface of the nerve membrane is undoubtedly close to reality. Actually, such a double layer exists on each side of the membrane in the Teorell-Meyer-Sievers theory (see Fig. 5 in Teorell, 1953, cited in Chapter 8) and, in order to calculate the (total) membrane potential, the potential differences across the double layers are added to the intramembrane diffusion potential.

As has been mentioned already (see Chapter 2, Section F), Bernstein explained the process of nerve excitation by assuming "unification" of the positive and negative charges on the membrane. He believed that the presence of charges on the membrane (namely, the existence of a potential difference across the membrane at rest) is imperative for generation of action

currents. Although Bernstein's hypothesis on the process of nerve excitation was shown to be erroneous (Hodgkin and Huxley, 1939, cited in Chapter 8), the old notion remained prevalent among electrophysiologists that the nerve membrane without a normal resting potential is inexcitable. As a warning against unrestrained use of the old notion, we now describe a simple observation indicating the presence of all-or-none action potentials in an axon of which the resting potential is either vanishingly small or slightly positive inside (see Fig. 14.1).

Here, a squid giant axon was intracellularly perfused with a solution containing 25 mM choline phosphate. In the presence of a 100 mM CaCl_2 solution externally, the axon was found to develop all-or-none action potentials of about 100 mV in amplitude when a pulse of an outwardly directed current is delivered. The point of interest is that the resting membrane potential of the axon is very close to zero or slightly positive (inside). In such an axon, the effect of electric shunting near the cut end or around a severed branch is very small.

From a physicochemical point of view, it is not difficult to understand the experimental finding described above (at least qualitatively). Because of their large size, choline ions are expected to have a low mobility in the nerve membrane as compared with small alkali-metal ions (Tasaki and Spyropoulos, 1961). Intracellular cations with a low mobility tend to shift the potential inside in the positive direction; this may explain why the rest-

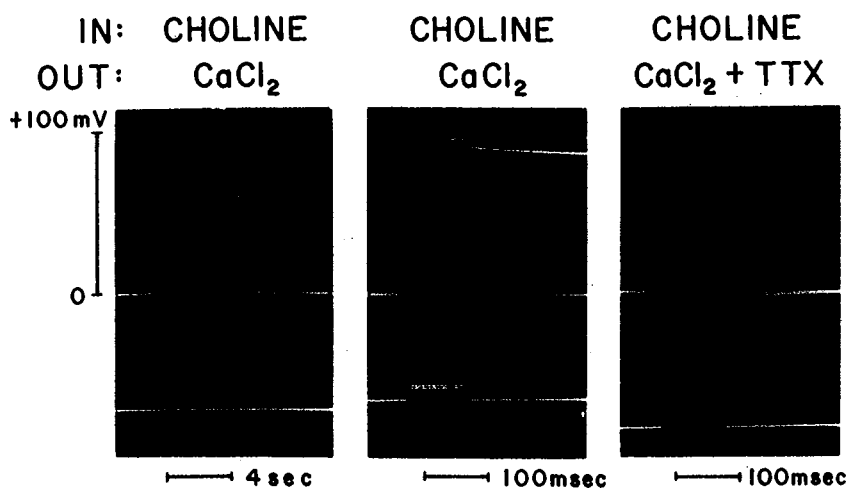


Fig. 14.1 Oscillograph records showing the resting and action potential of a squid giant axon internally perfused with a 25 mM choline phosphate solution and immersed in a 100 mM calcium chloride solution. Note that the membrane potential at rest (shown by the base line in the left-hand record) is very close to the potential level measured with the recording electrode kept in the external medium. The middle record was taken on an expanded time base. The right-hand record shows that tetrodotoxin (about 10 nM) suppressed the response (A. Watanabe, L. Lerman, and I. Tasaki, unpublished).

ing potential is close to zero. Upon excitation of the axon, the mobility of Ca-ions rises more profoundly than that of choline ions; this change in the mobility ratio can bring about a large rise in the intracellular potential in response to a pulse of outward current.

In summary, we have discussed in this section how the term "polarization" has been used by physiologists. We have cited an experiment indicating that the membrane of an axon whose resting membrane potential is eliminated by intracellular perfusion with a choline-salt solution is highly excitable (in spite of the absence of a measurable potential difference across the membrane at rest). It is illogical (or misleading) to denote the process of action potential production in such an axon as "depolarization" of the membrane.

C. SODIUM INFLUX AND PRODUCTION OF AN ACTION POTENTIAL

On the basis of the capacitor model of the nerve membrane (see Section B), some books of physiology and electrochemistry explain that the rising limb of an action potential is caused by an influx of Na-ions (see, e.g., p. 940 in Bockris and Reddy, 1970, cited in Chapter 12). We now examine whether or not an influx of Na-ions is an obligatory step in the process of action potential production.

It is easy to show that the potential variation associated with excitation of the nerve membrane represents a change in the emf of the system. By the use of the voltage clamp technique, we raise the membrane potential from the resting level suddenly to a new level slightly below the peak of the action potential. We have seen that the axon membrane is traversed, under these conditions, by a transient surge of inward current (see Chapter 8, Section G, and Chapter 13, Section I). We denote the new voltage level by V and the peak of the action potential by E_a . The intensity of the maximum inward current, I , is known to vary roughly with the voltage level V :

$$I = G_a(V - E_a) \quad (8.4)$$

where G_a is the proportionality constant representing the membrane conductance. It should be noted that E_a is also a constant which is independent of I . Experimentally, it can be shown that the linear relation between the voltage, V , and the inward current, I , extends down to the range of V about 50 mV below the peak of the action potential. Near the lower end of the voltage range, the inward current is carried predominantly by the influx of Na-ions. Thus, we find that E_a is the emf of the system which is independent of the influx of Na-ions.

We now examine the relation between Na influx and the action potential from a slightly different angle. We know the fact that, under intracellular perfusion of an axon with a dilute salt solution, action potentials can be evoked in the absence of Na-ions in the external medium (Chapter 12, Sections A and B). Obviously, there is no possibility that an influx of Na-ions precedes the process of action potential production in such an axon.

In an intact axon immersed in seawater, a pulse of strong outward current, strong enough to raise the membrane potential promptly to 120 mV or more above the resting level, throws the membrane into the excited state after an extremely short latency. In this case, there is undoubtedly no Na influx before a full-sized action potential is produced.

Next, we consider the case where the current pulse is barely sufficient to raise the intracellular potential to the threshold for excitation (see Fig. 14.2). After the end of the applied pulse, the membrane potential stays at a roughly constant level for a short period of time before an action potential is generated. Sometimes the membrane potential falls to the resting level without initiating a full-sized response. It should be thoughtfully noted here that the situation described above is exactly what has been discussed by Rushton (see Chapter 3, Section F) based on Hermann's principle of electric self-stimulation (*Selbstreizung*). The state of the axon membrane subjected to a current pulse of the threshold strength is illustrated in Fig. 14.2. Initially, the axon membrane (M in the figure) is in its resting state. At the end of the current pulse, a small fraction of the membrane is thrown into its excited state. There is an inwardly directed current in the domains of the membrane in the

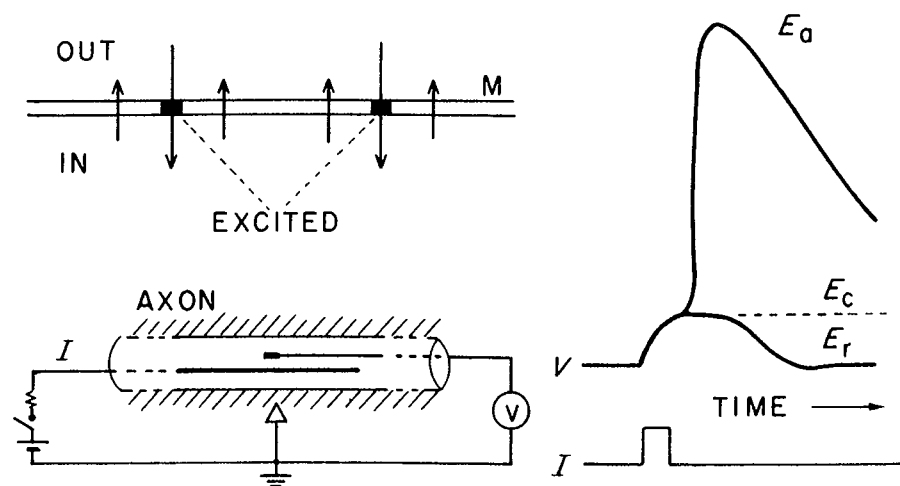


Fig. 14.2 Left top: Diagram illustrating the appearance of "domains" of the axon membrane in the excited state (black zones in the figure) surrounded by the resting area. The arrow indicates the flow of local microcurrent (*Strömchen*). Left bottom: The experimental setup (drawn schematically) and the electric responses of an axon to a current pulse of the threshold strength (I) are shown. Right: E_a , E_c , and E_r represent, respectively, the peak level of the action potential, the critical (threshold) membrane potential, and the resting membrane potential.

excited state. The pathway of the local microcurrent (*Strömchen*) is closed by the flow of electricity outward through the portion of the membrane in the resting state. There is no net current through the membrane under these conditions.

There is little doubt that the inwardly directed component of the local microcurrent is carried by Na-ions because the mobilities of the divalent cations are far smaller than those of univalent cations (Chapter 11, Section I). The inwardly directed component of the local microcurrent tends to bring about a transition of the membrane from its excited to the resting state (see Chapter 5, Sections C, and Chapter 10, Section D). On the other hand, the outwardly directed component, carried mainly by K-ions, is the factor which brings about a transition of the membrane from the resting to the excited state.

In summary, we have reexamined in this section the relationship between inwardly directed membrane currents through the axon membrane and the process of nerve excitation. We have shown that it is illogical to regard the influx of the Na-ions as the cause of action potential production.

D. MEASUREMENTS OF ION PERMEABILITY WITH RADIOISOTOPES OF Na- AND K-IONS

Radioisotopes of alkali-metal ions became available for biological studies shortly before World War II. Immediately, the importance of radioisotopes for studies of transport was recognized (see Hevesy and Hahn, 1941; von Euler *et al.*, 1948). On this point, Krogh (1946) remarked: "Although permeability of the cell surface is of course a necessary corollary of the ion transport taking place, quantitative determination of such permeabilities, in the generally accepted sense of the term, can be made only by means of isotopes. . . ."

Krogh was quite aware of the fact that the distribution of radiotracers across the membrane is affected by the process of "active" transport. When a small amount of radiotracer of an ion species is introduced into the external medium of a living (metabolizing) cell, the radioactivity in the protoplasm rises with time. The influx of the radiotracer vanishes when the ratio of the radioactivity inside the cell to that outside becomes equal to the concentration ratio of the cold species. Krogh's equation describing the influx of the radiotracer, J_γ , has substantially the following form:

$$J_\gamma = P[C'_\gamma - (C'/C'')C''_\gamma] \quad (14.1)$$

where C' and C'_γ represent the concentrations of the cold and hot species inside, respectively, and C'' and C''_γ are the corresponding values outside.

The proportionality constant, P , is Krogh's permeability coefficient. The rate of rise of the intracellular radioactivity is proportional to the influx.

The validity of Eq. (14.1) was tested using squid giant axons (Tasaki *et al.*, 1961). Cleaned giant axons were immersed in seawater labeled with radioisotopes of Na- and K-ions. After a varied period, the radioactivity in the interior was determined by extruding the axoplasm of the axon. The results obtained are reproduced in Fig. 14.3, where the ratio of the radioactivity of the axoplasm per unit volume to that of the seawater was plotted against the time of immersion. There is a large difference in the distribution of the radioactivity between Na- and K-ions.

We recall (see Chapter 9, Section B) that the ratio of the nonradioactive Na-ions inside and outside an intact axon is about 1:7 and the corresponding value of K-ions is roughly 20:1. Since the Na-K ion concentration ratio is known to rise slowly with time (Steinbach and Spiegelman, 1943, cited in Chapter 8), these excised axons are not in a perfectly stationary state. Nevertheless, the main feature of the results obtained is consistent with Eq. (14.1). In the case of Na-ions which exist at a low concentration inside, the radioactivity in the axoplasm was found to stop rising rapidly within 1 hr after the onset of immersion. On the other hand, the concentration of the radioactive K-ions is seen to rise continuously to a level well above that in the external seawater.

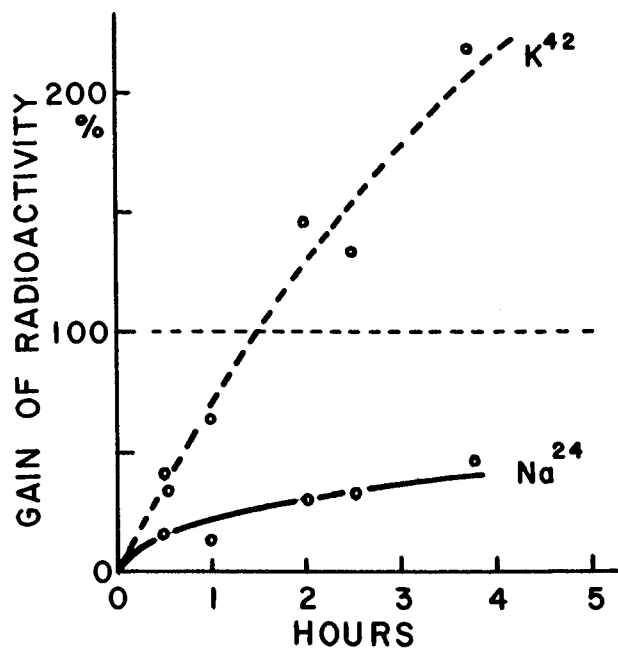


Fig. 14.3 Accumulation of radioactive K- and Na-ions in the axoplasm of axons immersed in seawater containing both Na-24 and K-42. The ordinate represents the concentration of the radioactive ions expressed in percentage of the concentration in the bathing seawater; the abscissa is the time of immersion. (*Am. J. Physiol.* **200**, 17, 1961).

Krogh's permeability coefficient can be determined by the rate of rise of the radioactivity at the onset of immersion. It is not easy to determine the rate of rise at $t = 0$ accurately. Nevertheless, it is evident that the permeability coefficient for K-ions defined in this manner is not vastly different from that for Na-ions.

We now turn to thermodynamics of irreversible processes for gaining a better understanding of the fluxes of radiotracers. We emphasize that the driving force for the radiotracer flux, J_γ , is the gradient of the electrochemical potential of the radioactive species, $d\eta_\gamma/dx$. Note that mixing two different isotopes of the same chemical substance produces an increase in the entropy (see reference books of thermodynamics or statistical mechanics, e.g., p. 209 in Mayer and Mayer, 1950; p. 187 in Guggenheim, 1957; p. 98 in Kirkwood and Oppenheim, 1961). Although two isotopes can be distinguished from each other by the use of a radiation detector, the difference between the two isotopes in all other physical and chemical properties (e.g., electric charges, mobilities, binding constants, etc.) is assumed to be negligibly small. The product of the force by the flux is equal to the rate of production of entropy (Prigogine, 1955; de Groot, 1951).

The flux of the tracer, J_γ , across the membrane in a quasi-stationary state may be written in the following form:

$$J_\gamma = -\omega_{\gamma\gamma} d\eta_\gamma/dx - \sum_{i \neq \gamma} \omega_{\gamma i} d\eta_i/dx \quad (14.2)$$

where ω 's represent phenomenological coefficients and the summation extends over all the mobile, normally existing, species in the system (see Kirkwood, 1954). Formally, the second term on the right-hand side of Eq. (14.2) represents the effects of the sustained chemical processes (i.e., metabolism) taking place in the cell. On the assumption that the quantity of the radiotracer added to the medium is extremely small, it is possible to derive Eq. (14.1) from this equation (Tasaki, 1960). In this formalism, the concentration ratio of the nonradioactive species, C'/C'' , is determined by the fluxes of metabolites, as well as by the electric potential and the ion activity coefficient in the protoplasm (see Section E). The permeability coefficient depends on the intramembrane ion mobility, the selectivity and the ratio C'/C'' of the nonradioactive species. Although this formalism does not give any concrete picture of the mechanism involved, it clearly points out the problems encountered in permeability measurements using radiotracers.

There is a huge amount of experimental data dealing with fluxes of Na- and K-ions in axons (see, e.g., Mullins and Brinley, 1969). Most of these data are treated on the basis of a simple kinetic notion that a radiotracer can be used for "tracing" the movement of the nonradioactive ions of the same chemical species. There is no question that, under intracellular perfusion,

the flux of the extracellular Na-ions into the axon interior can be traced by the use of radioactive Na-ions (see Chapter 11, Section H). In an intact axon, however, the influx of the "cold" species cannot be measured readily by this method. The difficulty of such measurements stems from the basic fact that mixing of two isotopic species is an irreversible process and, consequently, is associated with production of entropy. This difficulty has been recognized by Edwards and Harris (1955) and was emphasized by Nimms (1959) and others. When a radiotracer is used in studies of biochemical reactions, this difficulty does not arise because the ratio of the hot species to the cold is uniform in the reaction mixture.

We have seen in this section that the radiotracer method gives useful information about the permeability of the axon membrane to the ion species under study. Although the radiotracer method can be used for determining the fluxes of "cold" ion species across the axon membrane under internal perfusion, it is not simple to interpret the results obtained from intact axons by this method. Krogh's permeability coefficient in intact axons for K-ion is not vastly different from that for Na-ion.

E. ACCUMULATION OF K-SALTS IN PROTOPLASM

The protoplasm of plant and animal cells contains a high concentration of potassium salts. Toward the end of the last century, various methods for quantitative analysis of alkali metals and alkali earth metals were established (see, e.g., Treadwell, 1907), and it was shown that the K content of the muscle is nearly 10 times as high as that of Na content (Katz, 1896). Much later, Cowan (1934, cited in Chapter 8), Steinback and Spiegelman (1943, cited in Chapter 8), and others thoroughly examined the potassium ion concentration in invertebrate nerve fibers (see Chapter 8, Section D).

The electrolyte composition of the blood of animals is similar to that of seawater, being rich in Na-ions and poor in K-ions. In fact, based partly on this similarity, Bunge (1894), Quinton (1897), and Macallum (1910) pointed out that the composition of the blood of land animals might be an inheritance from the life in the sea of a vastly remote past. According to "Formulae and Methods, IV," edited by the Marine Biological Laboratory, the cation content of Woods Hole seawater is (expressed in millimole per liter): 534 Na, 18.2 K, 56.2 Mg, and 5.8 Ca. It has been stated that a favorable blood substitute for vertebrates can be made simply by diluting seawater with distilled water by a factor of four to five.

Attempts to explain the process of accumulation of K-salts in the protoplasm (and simultaneous expulsion of Na-salts from the cell interior) have been made by many physiologists, physical chemists, and biochemists. It is

practically impossible to review the wide range of phenomena encompassed by the term "active transport." The objective of this section is to outline a very general way of understanding the phenomena on a physicochemical basis. Biochemical studies of the phenomena deal mainly with Mg-Na-activated adenosine triphosphatase (Skou, 1960). Readers interested in the role of this membrane enzyme are referred to a recent book edited by Skou and Norby (1979).

One of the most elegant physicochemical analyses of the process of salt accumulation in the cell interior is that of Longworth (1933). Prior to this analysis, Osterhout and Stanley (1932) constructed an ingenious cell model capable of accumulating K-salts. This model mimics the process of K-ion accumulation in large plant cells. In the vacuolar sap of the marine alga, *Valonia*, the concentrations of K- and Cl-ions are about 500 mM; the protein concentration of the sap is very low and the electric conductivity is not very different from that of seawater (Osterhout, 1922).

The model constructed by Osterhout and Stanley is illustrated schematically in Fig. 14.4. The large compartment corresponding to the external medium contained a saturated K-salt solution of a weak acid, guaiacol (sometimes together with Na-salt). The membrane was prepared by mixing guaiacol and *p*-cresol. The small compartment representing the cell interior was filled with distilled water initially. As CO₂ was bubbled in the small compartment, there was a gradual accumulation of K-salt in this compartment. In the steady state the K-salt concentration inside was more than 10 times as high as that in the external medium. Longworth carefully analyzed this model system and accurately described the time course of the observed K-salt accumulation by using measured values of the partition coefficients and the mobilities of the diffusing chemical species.

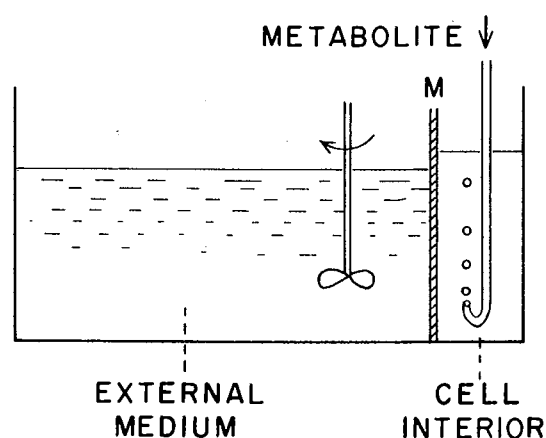


Fig. 14.4 Diagram of a cell model used to demonstrate the phenomenon of potassium accumulation in the cell interior.

A similar observation was made using either NH_3 or monomethylamine bubbles as a "metabolite," and a commercially available cation exchanger as the membrane (Tasaki and Singer, 1968). Initially, the two chambers were filled with a 1:1 mixture of NaCl and KCl solutions. After acidifying the solution in the large chamber by addition of glutamic acid (powder), bubbling of the gas was initiated in the small chamber. This continuous "metabolism" was found to markedly alter the Na-K ratio in the small chamber. The concentration ratio achieved in the stationary state was about 3:1 in this model.

The processes taking place in this type of cell model can be described qualitatively by the following expressions based on thermodynamics of irreversible processes. We choose Eq. (6) in Kirkwood's article as the starting point (Kirkwood, 1954):

$$d(RT \ln a_i + z_i F \phi)/dx = -\sum R_{ij} J_j \quad (14.3)$$

where a_i represents the activity of the ion species under study, ϕ the electric potential, and R_{ij} the phenomenological coefficients at position x within the membrane. The summation extends over all the fluxes of "metabolites" maintained in the final, stationary state. Since J_j is independent of x , the last equation can be integrated from one side of the membrane to the other. We now have

$$RT \ln (a_i''/a_i') + z_i F (\phi'' - \phi') = -\sum W_{ij} J_j \quad (14.4)$$

where the single and double primes indicate the quantities on the right and left side of the membrane, respectively, and W_{ij} represents the integral of R_{ij} . When we rewrite this equation in the following form, we immediately see the factors which determine the concentration ratio across the membrane:

$$RT \ln(C_i''/C_i') = -RT \ln(f_i'/f_i'') - z_i F (\phi'' - \phi') - \sum W_{ij} J_j \quad (14.5)$$

The first term on the right-hand side represents the ratio of the activity coefficients in the two aqueous phases. When the "intracellular" phase contains polyelectrolytes, the coefficient in this phase for some ion species could be very different from that in the external aqueous phase. The second term denotes the effect of the electric potential difference. The third term represents the effect of the "metabolism." The effects of metabolism in living cells are undoubtedly more complicated than in the models. In fact, Williams (1966), Katchalsky and Spangler (1968), and others developed a much more complex theory describing active transport in living cells.

The importance of specific ion accumulation by intracellular polyelectrolytes in the muscle has been repeatedly emphasized by a large number of investigators including Ling (1955, 1962), Nasonov (1962), Troshin (1966), Jones and Karreman (1969), and Gulati (1973). According to Jones and Karreman, for example, the process of K-ion accumulation in the arterial

smooth muscle under metabolically supported condition exhibits several properties of an interaction between ions and a proteinaceous fixed charge system. Saturation behavior is one such property. Cooperative interaction between K- and Na-ions is another property. The properties are consistent with Ling's "association-induction theory" for explaining the origin of specific interactions between cations and anionic sites of proteins (Ling, 1962). Probably, this theory can be used for explaining the state of K-ions in the protoplasm of fresh water amoebae. In the protoplasm of *Amoeba proteus* and *Chaos chaos*, the intracellular K-ion concentration is more than 150 times as high as that in the surrounding medium; the mobility of these ions is less than $\frac{1}{20}$ of that in water and the osmotic coefficient is apparently very small (Tasaki and Kamiya, 1964). There is little doubt that these cations are acting as the counterions of acidic proteins in the protoplasm.

We shall not pursue these arguments any further, because the purpose of the present discussion is simply to destroy some of the myths surrounding the term "ion pump."

F. SINGLE ION CONDUCTANCES IN EQUIVALENT CIRCUIT MEMBRANE MODEL

Equivalent electrical circuits are frequently used by physiologists to describe the behavior of excitable membranes. In this approach, the contribution of every permeant ion species to the membrane potential is represented by its "equilibrium potential" and "ion conductance" (see Fig. 14.5). The equilibrium potentials are evaluated from the ratio of the single ion activities by the use of the Nernst equation:

$$E_i = (RT/z_i F) \ln(a_i''/a_i') \quad (14.6)$$

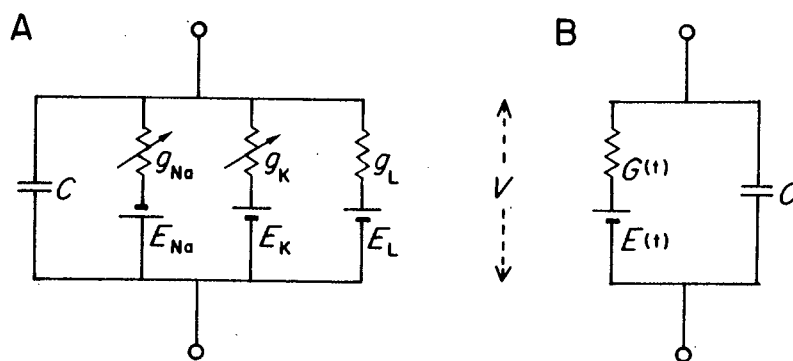


Fig. 14.5 (A) The electric circuit model of the axon membrane used by Hodgkin and Huxley. (B) An electrical circuit that is indistinguishable from the circuit shown in (A). See text.

The electric current through the i th ion channel, I_i , is given simply by Ohm's law:

$$I_i = g_i(V - E_i) \quad (14.7)$$

where g_i is the conductance and V the potential difference across the membrane. The total flow of electricity through the membrane is given, in accordance with Kirchhoff's law, by addition of the currents through all the channels. We now consider the physicochemical significance of this equivalent circuit approach to studies of membrane phenomena.

The equivalent circuit approach is expected to yield meaningful results when applied to a mosaic membrane consisting of several patches with different electrical properties. If each of these patches is assumed to be permeable specifically to one ion species, the behavior of the membrane may be described properly by an equivalent circuit of this type. The well-known uncertainty of using single ion activities presents difficulties in a quantitative study of such a system, however. In the presence of divalent cations and polyelectrolytes, there is inevitable arbitrariness in estimating activities of individual ions (see Spiegler and Wyllie, 1956; p. 378 in Guggenheim, 1957). There is a continuous flow of electricity in such a membrane: this flow may also give rise to some difficulty. The unstirred layers on the surfaces of the membrane (see Chapter 13, Section B) may also present difficulties in estimating the equilibrium potentials.

It is unlikely that ion channels in the squid axon membrane have such a high specificity to individual ion species. The results of analyses of periodic miniature responses indicate that alkali-metal ions compete for the binding sites of Ca-ions (Chapter 10, Sections G and I). Both the early inward current and the late outward current observed under voltage clamp are affected by changes in the external Ca-ion concentration (see, e.g., Frankenhaeuser, 1957). The acidic protein molecules in the axon membrane are expected to bind both uni- and divalent cations to varying degrees. We now examine the meaning of an equivalent circuit model applied to this type of membrane.

Let us describe ion fluxes through the membrane in terms of the Nernst-Planck equations:

$$J_i = -u_i C_i d(RT \ln a_i + z_i F \phi)/dx \quad (14.8)$$

here J_i represents the flux, u_i the mobility, C_i the concentration of the i th ion, and ϕ the electrical potential, at position x within the membrane. The fluxes of ions are not all independent since the total membrane current is given. The ion concentrations in the membrane have to satisfy the condition of electroneutrality (see below).

When we integrate Eq. (14.8) from one side of the membrane to the other *without taking the interdependence of the ion fluxes and concentrations into*

consideration, we immediately obtain Eq. (14.7). We have, in this treatment, $I_i = Fz_i j_i$, and $V = \phi'' - \phi'$, and g_i is given by the reciprocal of the integral of $dx/(z_i^2 F^2 u_i C_i)$. Thus, we see that the equivalent electrical circuit approach comes under the category of "discontinuous" treatment (see Schlögl, 1956), in which the driving forces are regarded as the *differences* in the electrochemical potentials (rather than their local gradients). Kirkwood regarded flux equations of the discontinuous type as best suited for describing transport of ions through biological membranes, because this approach can be applied to cell membranes of microscopic thickness (p. 122 in Kirkwood, 1954).

In spite of the apparent simplicity of Eqs. (14.6) and (14.7), a judicious caution has to be exercised when these integrated equations are used in a quantitative treatment of membrane phenomena. These equations are "*only apparently linear with respect to the forces,*" since the conductances depend not only on the membrane properties but also on the applied forces (see pp. 48 and 118 in Schlögl, 1956). The pitfall that catches users of a discontinuous approach is now discussed.

The dependence of the single ion conductance, g_i , on the ion concentrations and the potentials may be understood on the following ground. The condition of electroneutrality demands that the concentrations of ions in the membrane must satisfy the relation

$$\sum_i z_i C_i = X \quad (14.9)$$

where X represents the local concentration of the negative fixed charges. When the concentration of one cation species increases, the concentrations of other ion species in the membrane are immediately altered. Particularly, a rise and fall in the Ca-ion concentration in the external media are bound to produce far-reaching effects on the concentrations and mobilities of all the univalent cations in the membrane (see Chapter 12, Section F). Changes in the membrane potential imposed by an external source of current are also expected to alter the concentration profiles of ions within the membrane (Chapter 13, Section D). We thus find that single ion conductances defined by Eq. (14.7) are not independent of one another. In other words, each of these g 's depends on the concentrations of all mobile ions and the electric potential difference. "This dependence deprives these coefficients (conductances) of their practical value" (p. 118, Schlögl, 1956).

We may conclude this section by saying that, from a physicochemical point of view, the use of an equivalent circuit to describe electrical properties of the nerve membrane is of limited value. The ion conductances in this model depend on all the mobile ion species in the system as well as on the membrane potential.

G. DETERMINATION OF EMF BY VOLTAGE CLAMPING

In the absence of a transmembrane electric current, the electromotive force (emf) of an electrochemical cell, consisting of a pair of electrodes (e.g., calomel electrodes with salt bridges) placed across an axon membrane, can be determined simply by connecting the electrodes to a potential measuring device (e.g., to an oscilloscope). When the membrane is traversed by a current, the observed potential difference between the electrodes includes the IR drop associated with the current. If the membrane resistance is known from the result of a simultaneous AC impedance measurement, the emf can be determined by subtracting the IR drop from the observed potential difference. Alternatively, separation of the potential difference into the two components, an emf and an IR drop, can be accomplished by measuring the potential difference at more than one level of current intensity.

When the membrane potential of a squid giant axon is "clamped" at a number of (depolarizing) voltage levels, a series of records can be obtained, representing the current-time curves at different levels of the applied voltage. The question arises: Can the emf and the membrane resistance be determined from such records?

In Chapter 8, Section H, we have discussed that Hodgkin and Huxley (1952) described the current-voltage-time relationship in a squid axon membrane by a set of empirical equations. They adopted the equivalent circuit illustrated in Fig. 14.5A and treated the conductances, g 's, as functions of voltage and time. They assumed that the emf's of the batteries remained unaltered when g 's underwent drastic changes. With a proper choice of the arbitrary constants in the empirical equations, the observed current-time curves could be described fairly accurately by the equations.

We now note that the electric circuit shown in Fig. 14.5A is totally indistinguishable from that in Fig. 14.5B, where both the emf and the conductance are variable. The emf of the circuit in Fig. 14.5B is related to the conductances and emf's in Fig. 14.5A by the following equation:

$$E(t) = (g_{\text{Na}}E_{\text{Na}} + g_{\text{K}}E_{\text{K}} + g_{\text{L}}E_{\text{L}})/C(t) \quad (14.10)$$

where

$$C(t) = g_{\text{Na}} + g_{\text{K}} + g_{\text{L}} \quad (14.11)$$

It is emphasized that no electrochemical justification is required to deduce the indistinguishability of the circuit of Fig. 14.5A from that of Fig. 14.5B. For the present argument, it is quite irrelevant whether or not Ohm's law is rigorously obeyed or the emf's in each channel remain constant in the axon under voltage clamp. As long as the empirical equations describe the observed current-time data faithfully, $E(t)$ calculated by Eq. (14.10) is ex-

pected to represent the emf measured with a pair of electrodes placed across the axon membrane.

Figure 14.6 shows the results of a computer calculation of $E(t)$ carried out by Akira Watanabe of Tokyo Medical and Dental University. In this calculation, he used the experimental data described by the set of empirical equations published by Hodgkin and Huxley. Those equations are cited in Chapter 8, Section H.

It is seen in Fig. 14.6 that, in response to a series of rectangular voltage pulses ranging from 20 to 120 mV in amplitude; the emf quickly rises to a peak and then falls slowly toward the level observed before the onset of voltage clamping. Special attention should be focused on the fact that the peak level of the emf is practically independent of the applied voltage in the range

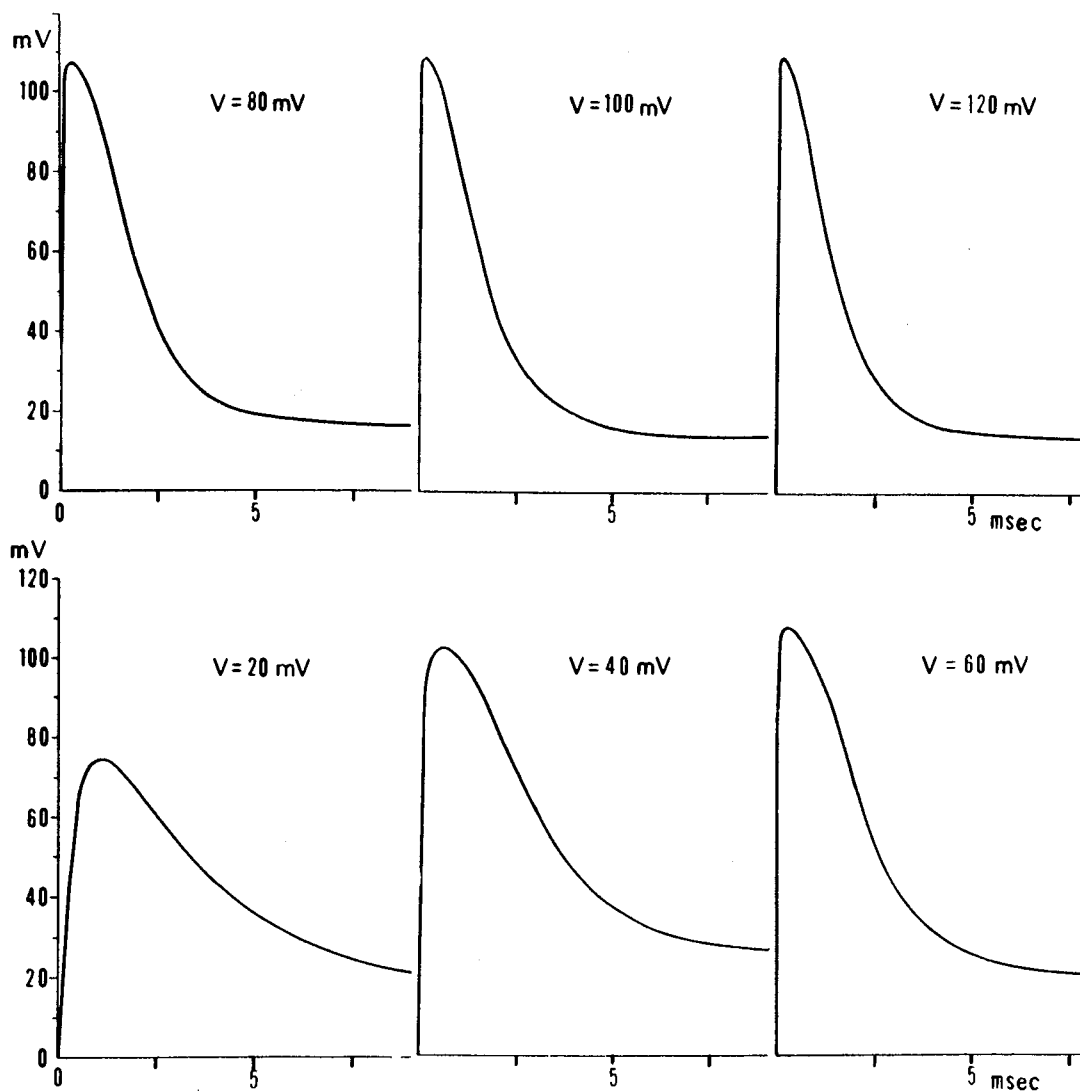


Fig. 14.6 The emf across the squid axon membrane under voltage clamp calculated by the use of Eqs. (14.10) and (14.11). V represents the voltage used to clamp the membrane potential. In calculation, the numerical values described by the empirical equations published by Hodgkin and Huxley (*J. Physiol. (London)* **117**, 518, 1952) were used. (A. Watanabe, unpublished.)

greater than about 40 mV. Furthermore, this peak level coincides very accurately with the peak of the action potential (observed under the condition of zero current). The duration of the emf variation is seen to change to a considerable extent with the pulse amplitude. With a clamping pulse of 20 mV in amplitude, the amplitude of the induced emf variation is definitely smaller than those obtained with larger voltage pulses.

Essentially the same results have been obtained using a high-frequency sinusoidal wave superposed on rectangular voltage pulses (see p. 138 in Tasaki, 1968, cited in Chapter 8). Again, the emf changes were found to be independent of the amplitude of the clamping voltage pulses in a wide range. The time from the onset of the clamping pulse to the peak of the emf change was found to decrease as the amplitude of the applied voltage pulse was increased.

There is no doubt that the variation in the emf observed under voltage clamp in the range above 40 mV represents the production of a full-sized action potential. Under these experimental conditions, the critical stage for triggering a transition from the resting state of the membrane to the excited is reached within a short period of time after the onset of the applied pulse. The peak level of the emf should then be practically independent of the amplitude of the applied voltage pulse, because transition is practically all-or-none. The falling limb of the action potential is known to be strongly affected by the current through the membrane (see Chapter 5, Section F). The dependence of the time course of the emf change on the voltage is attributed to the current effect. The small emf change observed at 20 mV has to be attributed to the appearance of a partially excited, spatially nonuniform state of the membrane (see Fig. 14.2). Voltage clamping is a powerful means of suppressing the electric coupling between the excited and resting states of the membrane (see Chapter 12, Section J, and Chapter 13, Section I).

In the procedure of determining the emf by the voltage clamp technique, the empirical equations cited in Chapter 8, Section H, play the role of a bridge between $E(t)$ and the observed membrane current. Using the empirical equations cited above, it was found possible to describe the electrophysiological properties of the axon membrane under a variety of experimental conditions. In studying the interdependence of the membrane potential and the current, the equivalent circuit treatment of the experimental data yields self-consistent results, because the electrical behavior is determined exclusively by the emf and the conductance.

H. LIQUID MEMBRANES AND POROUS MEMBRANES

We have depicted the excitable sites of the axon membrane as an assembly of flexible strands of protein molecules which are capable of undergoing

conformational transitions between a compact and a swollen state. We know, however, that such a structure alone is insufficient for explaining the membrane permeability to neutral organic molecules. In this section, we are concerned mainly with membrane properties that are not directly involved in the process of excitation and are probably common to most biological cells.

Many years ago, an extensive study of osmotic properties of the frog muscle was conducted by Overton (1902). After establishing the fact that the weight of a muscle remains practically unaltered when it is immersed in 0.65% (111 mM) NaCl solution, he saw that immersion of a muscle in 0.4% NaCl solution brings about a distinct increase in the weight as the result of water uptake. Overton was quite aware of the fact that the interior of a muscle is not a simple aqueous solution, and he emphasized that some of the water molecules taken up by the muscle are bound to proteins. Subsequently, he examined the effects of adding a variety of chemicals to isotonic and hypotonic salt solutions on the amount of water taken up by the muscle and arrived at the following general rule: "Substances which are soluble in organic solvents (such as olive oil or long-chain alcohols) penetrate the surface membrane of the muscle." For example, a muscle immersed in a solution containing both 0.2% NaCl and 3% (652 mM) ethanol swells as fast as a muscle in 0.2% NaCl (without adding alcohol). Overton's viewpoint is known as "the lipid solubility theory."

Much later, Collander and Bärlund (1933) tested the validity of the lipid solubility theory by using large plant cells, *Chara*. With these large cells it is possible to chemically analyze the content of the vacuole and determine how much a substance outside has reached the cell interior in a given period of time. For the majority of the nonelectrolytes examined by this direct method, an excellent correlation was found between the penetrating power and the oil-water partition coefficient. They also noted that small, highly water-soluble substances (formamide, ethylene glycol, urea, etc.) penetrate at rates much faster than what is expected from their oil-water partition coefficients. Based on these findings, Collander and Bärlund viewed the plasma membrane as having a mosaic structure, being composed of lipid areas and sievelike portions. Large lipophilic molecules penetrate the lipid area and small hydrophilic molecules pass through the porous, sievelike portions of the membrane. This viewpoint is known as "the lipid-sieve theory."

The concept of "sieve" is as old as the membrane theory itself. Both Traube (1867) and Ostwald (1890) regarded a copper ferrocyanide membrane as a porous, sievelike structure. Höber (1945), Michaelis (1926), Sollner (1930), and others considered hydrophilic colloid (collodion, gelatin, etc.) as also having a porous structure. The modern concept of fluid membranes perforated by intramembrane particles (see Singer and Nicol-

son, 1972, cited in Chapter 9) may be regarded as a revival of the age-old lipid-sieve concept of the membrane.

Both in artificial and natural membranes, the effective pore sizes of the sievelike portion can be estimated by using a series of molecules with different sizes. Höber emphasized that the effective pore size can be altered reversibly by swelling or shrinking of the colloidal material (see p. 233 in Höber, 1945). Rigid pores in the membrane proposed by some physiologists (see, e.g., Mullins, 1959; p. 650 in Hille, 1972) may be regarded as a highly schematized picture of a sievelike structure.

We now turn to general properties of lipid (oil) membranes. This subject has been reviewed authoritatively by Sollner (1971). The dielectric constants of the "oils" used in these artificial membrane studies are usually in the range between 10 and 20; they are much larger than those of common organic solvents (2–3). Nevertheless, the difference between the dielectric constant of the oil and that of water (about 80) is large enough to exclude small ions from the oil phase. As Born (1920) has pointed out, the electrostatic energy, U , required to transfer an ion of radius r to a medium with dielectric constant D_1 from another with D_2 is given by

$$U = \frac{e^2}{2r} \left(\frac{1}{D_1} - \frac{1}{D_2} \right)$$

where e is the electronic charge (4.8×10^{-10} esu). When an ion with a radius of 2 Å (e.g., tetramethylammonium) is transferred from water to 2-butanol (D_1 approximately 20), the energy required is 2.16×10^{-13} erg. The Boltzmann factor calculated from this energy, $\exp(U/kT)$, is of the order of 200; this explains why ions are expelled from the oil phase. Ions can be transferred into the oil phase in the form of a complex with a liquid ion exchanger.

In this context, it must be realized that the potential difference between oil and water can never be measured by electrochemical means. Guggenheim (1957) says on this point: "The electric potential difference between two points in different media can never be measured and has not yet been defined in terms of physical reality."

The significance of this statement can be illustrated by the example just mentioned. By definition, the potential difference between two points is equal to the mechanical work per unit charge which is done in moving a charge from one point to the other. The work done in moving an ion from oil to water depends on the radius of the ion, as well as on the square of the charge. Hence, the potential difference between oil and water cannot be defined in terms of such work. [Note that, to define the electrostatic potential field within a solid dielectric, it is necessary to consider an imaginary procedure of creating, within the solid, an empty cavity which serves as a means of eliminating the work discussed here (see, e.g., p. 20 in Smythe, 1939).]

Even in the case of a phase of hydrophilic colloid immersed in a phase of dilute salt solution, there is a knotty problem in treating the potential difference between the two phases. According to Overbeek (1953), the junction potential at the tip of the calomel electrode in the colloidal phase plays a decisive role in generating the potential difference.

Finally, as an example of mosaic membranes, an interesting artificial membrane which shows a sign of excitability may be quoted (Mueller *et al.*, 1963; Mueller and Rudin, 1967). A lipid bilayer membrane formed between two aqueous solutions of uni-univalent salts is highly permeable to water. However, the membrane has an extremely high electric resistance. When a proteinaceous material called EIM is incorporated in the membrane, it was found that the resistance becomes much lower and potential variations which resemble the action potential of the nerve fiber can be evoked. The significant difference between the excitability in this model and that in the nerve fiber appears to be the fact that this model system does not require Ca-ions. As far as we know, nerve fibers are not excitable when they are immersed in a medium devoid of Ca-ions (see, e.g., Frankenhaeuser, 1957; Tasaki *et al.*, 1967).

REFERENCES

- Born, M. (1920). Volumen und Hydrationswärme der Ionen. *Z. Phys.* **1**, 45–48.
- Bunge, G. (1894). "Lehrbuch der Physiologischen und Pathologischen Chemie," 447 pp. F. C. W. Vogel, Leipzig. (See p. 120).
- Chapman, D. L. (1913). A contribution to the theory of electrocapillarity. *Philos. Mag.* **25**, 475–481.
- Collander, R., and Bärlund, H. (1933). *Permeabilitätstudien an Chara Ceratophylla*. II. Die Permeabilität für Nichteinktrolyte. *Acta Bot. Fenn.* **11**, 3–114.
- de Groot, S. R. (1951). "Thermodynamics of Irreversible Processes," 242 pp. North-Holland Pub., Amsterdam.
- Edwards, C., and Harris, E. J. (1955). Do tracers measure fluxes? *Nature (London)* **175**, 262.
- Frankenhaeuser, B. (1957). The effect of calcium on the myelinated nerve fibre. *J. Physiol. (London)* **137**, 245–260.
- Gouy, G. (1910). Sur la constitution de la charge électrique à la surface d'un électrolyte. *J. Phys. (Orsay, Fr.)* **9**, 457–468.
- Guggenheim, E. A. (1957). "Thermodynamics. An Advanced Treatment for Chemists and Physicists," 3rd ed., 475 pp. (Wiley Interscience), New York.
- Gulati, J. (1973). Cooperative interaction of external calcium, sodium, and ouabain with the cellular potassium in smooth muscle. *Ann. N.Y. Acad. Sci.* **204**, 337–357.
- Hevesy, G., and Hahn, L. (1941). "Exchange of Cellular Potassium," 27 pp. Copenhagen, Ejnar Munksgaard.
- Hille, B. (1972). The permeability of the sodium channel to metal cations in myelinated nerve. *J. Gen. Physiol.* **59**, 637–658.
- Höber, R. (1945). "Physical Chemistry of Cells and Tissues," 659 pp. McGraw-Hill (Blakiston) New York.
- Jones, A. W., and Karreman, G. (1969). Potassium accumulation and permeation in the canine carotid artery. *Biophys. J.* **9**, 910–924.

- Katchalsky, A., and Spangler, R. (1968). Dynamics of membrane processes. *Q. Rev. Biophys.* **1**, 127–175.
- Katz, J. (1896). Die mineralischen Bestandtheile des Muskelfleisches. *Pfluegers Arch. Gesamte Physiol. Menschen Tiere* **63**, 1–85.
- Kirkwood, J. G. (1954). Transport of ions through biological membranes from the standpoint of irreversible thermodynamics. In "Ion Transport Across Membranes" (H. T. Clarke, ed.), pp. 119–127. Academic Press, New York.
- Kirkwood, J. G., and Oppenheim, I. (1961). "Chemical Thermodynamics," 261 pp. McGraw-Hill, New York.
- Krogh, A. (1946). The active and passive exchanges of inorganic ions through the surface of living cells and through living membranes generally. *Proc. R. Soc. London* **133**, 140–200.
- Ling, G. (1955). Muscle electrolytes. *Am. J. Phys. Med.* **34**, 89–101.
- Ling, G. (1962). "A Physical Theory of the Living State," 680 pp. Blaisdell Co., Waltham, Mass.
- Longworth, L. G. (1933). The theory of diffusion in cell models. *J. Gen. Physiol.* **17**, 211–235.
- Macallum, A. B. (1910). The inorganic composition of the blood in vertebrates and invertebrates, and its origin. *Proc. R. Soc. London* **82B**, 602–624.
- MacInnes, D. A. (1961). "The Principle of Electrochemistry," 487 pp. Dover, New York.
- Mayer, J. E., and Mayer, M. G. (1950). "Statistical Mechanics," 495 pp. Wiley, New York.
- Michaelis, L. (1926). Die Permeabilität von Membranen. *Naturwissenschaften* **14**, 33–42.
- Mueller, P., and Rudin, D. O. (1967). Action potential phenomena in experimental bimolecular lipid membranes. *Nature (London)* **213**, 603–604.
- Mueller, P., Rudin, D. O., Tien, H. T., and Wescott, W. C. (1963). Reconstitution of cell membrane structure *in vitro* and its transformation into an excitable system. *Nature (London)* **194**, 979–980.
- Mullins, L. J. (1959). The penetration of some cations into muscle. *J. Gen. Physiol.* **42**, 817–829.
- Mullins, L. J., and Brinley, F. J. (1969). Potassium fluxes in dialyzed squid axons. *J. Gen. Physiol.* **53**, 704–740.
- Nasonov, D. N. (1962). "Local Reaction of Protoplasm and Gradual Excitation" (translated from Russian by the National Science Foundation, Washington, D.C.).
- Nims, L. F. (1959). Membranes, tagged components, and membrane transfer coefficient. *Yale J. Biol. Med.* **31**, 373–386.
- Osterhout, W. J. V. (1922). Some aspects of selective absorption. *J. Gen. Physiol.* **5**, 225–230.
- Osterhout, W. J. V., and Stanley, W. M. (1932). The accumulation of electrolytes. V. Models showing accumulation and a steady state. *J. Gen. Physiol.* **15**, 667–689.
- Ostwald, W. (1890). Elektrische Eigenschaften halbdurchlässiger Scheidewände. *Z. Phys. Chem.* **6**, 71–82.
- Overbeek, J. Th. G. (1952). Electrochemistry of the double layers. In "Colloid Science" (H. R. Kruyt, ed.), Vol. I, pp. 151–193. Elsevier, Amsterdam.
- Overbeek, J. Th. G. (1953). Donnan E. M. F. and suspension effect. *J. Colloid Sci.* **8**, 593–605.
- Overton, E. (1902). Beiträge zur allgemeinen Muskel- und Nervenphysiologie. *Pfluegers Arch. Gesamte Physiol. Menschen Tiere* **92**, 115–280.
- Prigogine, I. (1955). "Introduction to Thermodynamics of Irreversible Processes," 115 pp. Thomas, Springfield, Illinois.
- Quinton, R. (1897). Hypothèse de l'eau de mer, milieu des organisme élevés. *C. R. Soc. Biol.* **49**, 935–936.
- Schlögl, R. (1956). The significance of convection in transport processes across porous membranes. *Discuss. Faraday Soc.* **21**, 46–52.
- Skou, J. C. (1960). Further investigation on Mg–Na-activated adenosine-triphosphatase, possibly related to the active, linked transport of Na and K across the nerve membrane. *Biochim. Biophys. Acta* **42**, 6–23.

- Skou, J. C., and Norby, J. G., eds. (1979). "Na, K-ATPase. Structure and Kinetics," Proc. 2nd Int. Conf. on the Properties and Functions of Na, K-ATPase, Sondeberg, Denmark, 1978. Academic Press, New York.
- Smythe, W. R. (1939). "Static and Dynamic Electricity," 560 pp. MacGraw-Hill, New York.
- Sollner, K. (1930). Zur Erklärung der abnormen Osmose an nichtquellbaren Membranen. (I. Teil). *Z. Elektrochem.* **36**, 36–47.
- Sollner, K. (1971). The basic electrochemistry of liquid membrane. In "Proc. Thomas Graham Memorial Symposium," (J. N. Sherwood, A. V. Chadwick, W. M. Muir, and F. L. Swinton, eds.) Gordon & Breach, London.
- Spiegler, K. S., and Wyllie, M. R. T. (1956). Electrical potential difference. In "Physical Techniques in Biological Research" (G. Oster and A. W. Pollister, eds.), Vol. 2, p. 301–392. Academic Press, New York.
- Takashima, S. (1976). Membrane capacity of squid giant axon during hyper- and depolarizations. *J. Membr. Biol.* **27**, 21–39.
- Tasaki, I. (1960). Thermodynamic treatment of radio-tracer movements across biological membranes. *Science* **132**, 1661–1663.
- Tasaki, I., and Kamiya, N. (1964). A study on electrophysiological properties of carnivorous amoebae. *J. Cell. Comp. Physiol.* **63**, 365–380.
- Tasaki, I., and Singer, I. (1968). Some problems involved in electric measurements of biological systems. *Ann. N.Y. Acad. Sci.* **148**, 36–53.
- Tasaki, I., and Spyropoulos, C. S. (1961). Permeability of the squid axon membrane to several organic molecules. *Am. J. Physiol.* **201**, 413–419.
- Tasaki, I., Teorell, T., and Spyropoulos, C. S. (1961). Movement of radioactive tracers across squid axon membrane. *Am. J. Physiol.* **200**; 11–22.
- Tasaki, I., Watanabe, A., and Lerman, L. (1967). Role of divalent cations in excitation of squid giant axons. *Am. J. Physiol.* **213**, 1465–1474.
- Tien, H. T., and Diana, A. L. (1967). Black lipid membranes in aqueous media: The effect of salts on electrical properties. *J. Colloid Interface Sci.* **24**, 287–296.
- Traube, M. (1867). Experimente zur Theorie der Zellbildung und Endosmose. *Arch. Anat. Physiol. Ana. Abt.* **1867**, 87–165.
- Treadwell, F. P. (1907). See p. 120. In "Kurzes Lehrbuch der Analytischen Chemie," 639 pp. 2. Band, Franz Deuticke, Leipzig u. Wien.
- Troshin, A. S. (1966). "Problems of Cell Permeability, 549 pp. Pergamon Press, Oxford (translated by M. G. Hell; translation edited by W. F. Widdas).
- von Euler, H., von Euler, U. S., and Hevesy, G. (1948). The effect of excitation on nerve permeability. *Acta Physiol. Scand.* **12**, 261–267.
- Williams, R. J. P. (1966). The selectivity of metal-protein interactions. In "Protides of the Biological Fluids" (H. Peeters, ed.), Vol. 14, p. 25–36. Elsevier, Amsterdam.

15. Optical Studies of the Axon Membrane

A. NONELECTRICAL SIGNS OF NERVE EXCITATION

From a physicochemical point of view, the rapid rise in the membrane potential associated with initiation of a nerve impulse is an electrical manifestation of a macromolecular conformational change occurring in the axon membrane. This conformational change is accompanied by various physicochemical processes which take place in and around the axon membrane. The search for nonelectrical signs of nerve excitation is directed toward gaining full and independent information as to the nature of these physicochemical processes.

The inception of studies of nonelectrical signs of nerve excitation is old. Due to technical difficulties involved, the progress in this field of investigation has been slow. However, recent advancements in technology of chemical and physical micromasurements lead us to speculate that there will be a rapid expansion of our knowledge.

The oldest research in this field appears to be the detection of heat production. Claude Bernard observed that, when two junctions of a thermopile were placed on a rabbit nerve at rest, there was no current flow through the galvanometer connected to the pile; however, there was a deflection of the galvanometer when the region of the nerve under one of the junctions was excited. From these observations, Claude Bernard concluded: ". . . the nervous activity is the source of heat" (see p. 163, Bernard, 1876). In 1912, Hill wrote a paper entitled "The absence of temperature changes during the transmission of a nerve impulse." He erroneously contended that the process of nerve conduction was a reversible change of a purely physical nature. Following the publication of this paper, many physiologists believed that previous demonstrations of heat production were artifacts. Much later, Downing *et al.* (1926), using an improved method, succeeded in demonstrating a temperature rise during nerve excitation and made a quantitative estimation of the heat produced. More recent studies on bundles of nonmyelinated nerve fibers indicated that the problem is more complex than previ-

ous observations have suggested. It was shown that there is positive heat production during the early phase of the action potential and negative heat production (cooling) in the later phase (Abbott *et al.*, 1958, cited in Chapter 12; Howarth *et al.*, 1968, cited in Chapter 12). The time resolution of measurements of temperature changes has been quite limited.

The second oldest demonstration of nonelectrical signs of nerve excitation seems to be the discovery of CO₂ production associated with nerve stimulation (Tashiro, 1913). Unfortunately, Tashiro's paper was published when leading physiologists believed that the process of nerve conduction was a "purely physical phenomenon." Reflecting this situation, Bayliss insisted, in all four editions of *Principles of General Physiology* (Bayliss, 1915–1924, cited in Chapter 8), that Tashiro's finding was an artifact. In the following years, however, the evidence for enhanced metabolism during excitation became overwhelmingly strong and convincing (see Gerard, 1932, 1937).

In the middle of the 1930s, it was shown that there is a loss of intracellular potassium salt during nerve excitation (Cowan, 1934, cited in Chapter 8). Later, when radioisotopes of alkali metal ions became available, the existence of exchange between intracellular K-ions and extracellular Na-ions was established (Keynes, 1951; Hodgkin, 1951).

In 1968, optical studies of the nerve fiber were commenced. Changes in the turbidity and birefringence were demonstrated (Cohen *et al.*, 1968) and a method of detecting optical signals from vitally stained nerve fibers was invented (Tasaki *et al.*, 1968). Prior to this, we knew that slow changes in turbidity and volume of the nerve can be detected after a long period of repetitive stimulation. (Hill and Keynes, 1949; Hill, 1950; Bryant and Tobias, 1952). We now can record various types of optical signals simultaneously with electrical signals. Several types of such optical signals are discussed and the possible physicochemical bases of these signals are analyzed in the following sections.

To sum up, a variety of nonelectrical concomitants of the process of nerve excitation and conduction are known at present. The time resolution of the recording of optical signals is practically unlimited.

B. SMALL MOVEMENTS OF THE AXON SURFACE DURING ACTION POTENTIAL

Quite recently, a discovery was made indicating that the production of an action potential in the squid giant axon is accompanied by small, very rapid movements of the axon. The present section deals with this newly discovered phenomenon.

The suggestion that nerve fibers might swell when excited is very old.

During the early part of this century, Loeb and Höber (see Chapter 3, Section C) postulated that changes in the colloidal state of the fiber underlay the process of nerve excitation, and suggested that nerve became loosened during excitation. Later on, based on the results of the investigation of his electrohydraulic nerve analog, Teorell (1962) rightly contended that there must be changes in water movement during excitation. He said: "It is not likely that biological membranes are rigid; they may rather be distendable and elastic. . . . Different layers in the composite membrane may have varying charge densities and hydraulic permeability. . . . It might perhaps be possible that this (membrane) structure can be subject to swelling or shrinkage. . . ." Only recently, Teorell's prediction was verified by direct experiments.

In the 1950s, several investigators made attempts at detecting rapid mechanical changes of the nerve induced by repetitive stimulation (see, e.g., Kayushin and Lyudkovskaya, 1955). However, the sensitivity of the optical devices available at that time was insufficient for recording movements of the nerve during action potentials.

The left-hand diagram on the top of Fig. 15.1 illustrates the experimental setup employed in one series of our recent experiments. A squid axon was introduced into a Lucite chamber which was provided with two partitions separated by a distance of about 5 mm. Using a pair of extracellular electrodes placed across one of the partitions, the axon was excited electrically.

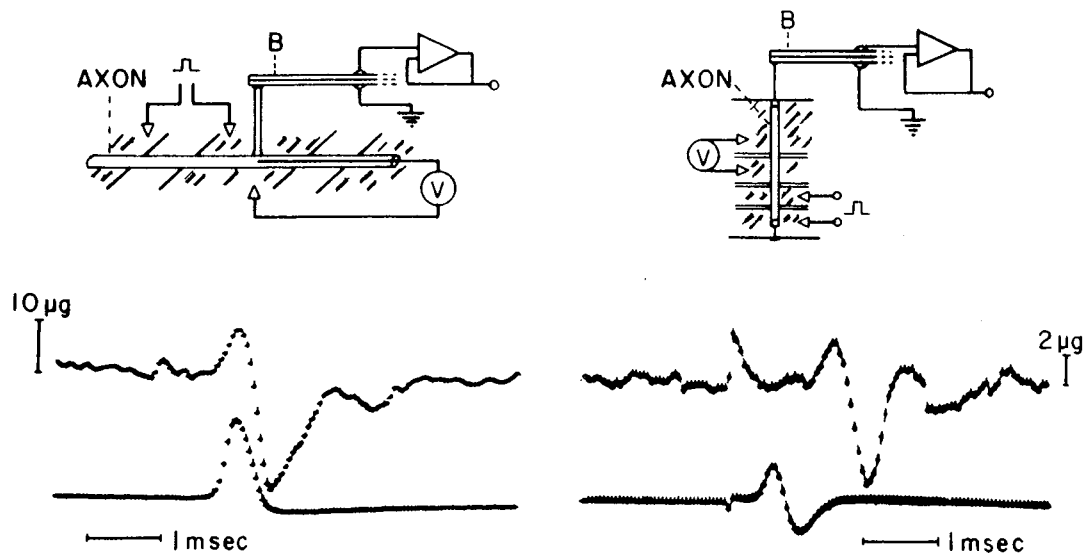


Fig. 15.1 Left top: Schematic diagram of the setup used for detecting mechanical responses of the squid axon. B, a Gulton bender. Left bottom: Mechanical response (upper trace) and internally recorded action potential (lower trace). Right top: Experimental arrangement employed for demonstrating an increase (followed by a decrease) of the tension of the squid axon associated with action potential propagation. The portion of the axon in the uppermost pool of seawater was about 15 mm long. 21°C.

The action potential of the axon was recorded with an intracellular metal electrode from the middle portion of the axon immersed in seawater. On the axon surface, above the tip of the recording electrode, was placed a stylus attached to a piezoceramic bender (a mechanoelectric transducer manufactured by Gulton Industries, Inc.). The output of the voltage follower connected to the bender was amplified and transient changes in the output were recorded with a signal averager. The upper trace in the left-hand record shows an example of the mechanical responses of the axon recorded by this technique.

It is seen in the figure that, during the rising phase of the action potential (shown by the lower trace), there was a rapid rise in the force exerted by the axon on the bender. The peak of the mechanical response was found to coincide with the peak of the action potential fairly accurately. Interestingly, the falling phase of the action potential was accompanied by an exaggerated fall in the mechanical force. The small downward deflection of the mechanical trace that follows the main diphasic response appears to be real. The area of the stylus in contact with the axon surface was roughly 10^{-3} cm². The pressure exerted by the axon upon this area was estimated to be 2–10 dyn/cm².

The right-hand half of the Fig. 15.1 shows that there is a transient increase, followed by a decrease, in the tension (longitudinal) of the axon when an action potential travels along the axon.

The findings obtained with the piezoceramic bender were confirmed and extended by the use of an optical method of detecting small displacements of the axon surface. During the rising phase of the action potential, the axon surface was found to move outwards; the displacement of the surface was roughly 10Å at the peak of excitation.

Qualitatively similar records of mechanical responses were obtained also from various crustacean nerve fibers. It is now beyond question that there is an expansion (not contraction) of the fiber diameter at the time when the action potential is generated in crab or lobster axons (Iwasa and Tasaki 1980; see Hill *et al.*, 1977).

The effects of various physicochemical, biochemical, and pharmacological agents on the mechanical responses of nerve fibers have been studied by using the same mechanoelectric and optical methods. The results of those studies will be published elsewhere.

The following simple calculation indicates that the process of Na–K ion-exchange associated with production of an action potential does not account for the swelling of the axon described above. The difference between the molar volume of Na-ion and that of K-ion is known to be of the order of 23 cm³ (see Gregor, 1951, cited in Chapter 13). An exchange of 15 pmoles/cm² of alkali metal ions across the axon membrane can bring about

a swelling on the order of only 0.04 \AA . Furthermore, such an exchange process does not explain why the axon diameter falls below the initial value toward the end of the action potential.

We have seen that the solubility of cytoskeletal protein molecules is increased when the axon is repeatedly excited (see Chapter 9, Section D). It is expected that such an increase in solubility is accompanied by invasion of water into the axon. Thus, we see that the experimental finding described above lends good support to the macromolecular theory of nerve excitation (see Chapter 3, Section C, and Chapter 13, Section E). The negative phase of the diphasic mechanical response appears to have the same origin as that of the birefringence response (see below).

C. ECTOPLASM AND BIREFRINGENCE RESPONSE

The superficial layer of the axon proper consists of the axolemma and the ectoplasm. The endoplasm, which occupies the major portion of the axon interior, contains a relatively low density of filamentous material—neurofilaments and microtubules. In contrast, the ectoplasm is densely packed with longitudinally oriented filamentous material (see Chapter 9, Section C). There is little doubt that these longitudinally oriented filamentous elements endow the protoplasm with positive (uniaxial) birefringence. In this section, we describe an experiment strongly suggesting that the birefringence of the ectoplasm undergoes a rapid, reversible change during the action potential.

The procedure of the experiment was as follows. Into a squid giant axon, a potassium phosphate buffer containing a high concentration of hydrophilic dye was repeatedly infused. After infusion, the axon appeared completely black when examined with quasi-monochromatic light at the wavelength of absorption maximum of the dye. The intracellular dye concentration was such that the light transmitted through the center of the axon was attenuated by a factor of 1000 or more. The surface layer of such a heavily stained axon was found to remain unstained and birefringent. Optical responses could easily be demonstrated under the cross-polar conditions when such an axon was electrically excited. In fact, the amplitude of the optical response (relative to the background light) of such axons was found to be roughly 10 times as large as that observed in unstained axons.

Figure 15.2 (top) shows the experimental setup used for recording birefringence responses. The light source employed was a 200-W mercury-xenon lamp. The white light from the source (S) was converted into a collimated, quasi-monochromatic light beam by the use of a lens (L) and a mercury line filter (F). A squid giant axon was placed in a 1-mm-thick layer of seawater in the pathway of the light beam to a photodetector. A polarizer (Polaroid, HN) was inserted between the light source and the axon with its polarizing axis

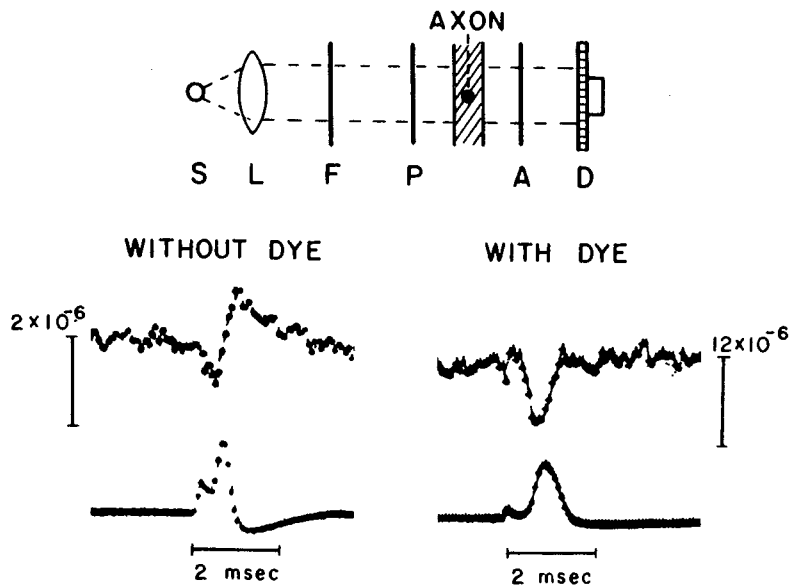


Fig. 15.2 Top: Schematic diagram showing the experimental setup used for recording changes in birefringence from a squid giant axon. S, light source; L, lens; F, filter; P and A, polarizer and analyzer; D, photodetector (connected to a signal averager). Bottom: Birefringence responses recorded from an unstained axon (left) and from an axon stained heavily by internal applications of chlorphenol red (dissolved in potassium phosphate buffer). The vertical bars indicate the magnitude of the response (decrease of the light intensity) relative to the background light intensity. The lower traces represent action potentials recorded extracellularly. (I. Tasaki and A. Watanabe, unpublished.)

fixed at 45° to the long axis of the axon. An analyzer (Polaroid, HN) was placed between the axon and the photodetector at a right angle to the polarizer (cross-polar). Two black Lucite plates, one on each side of the axon, kept the thickness of the seawater uniform around the fiber. Brief stimulating current pulses were delivered to the axon through a pair of platinum electrodes placed near one end of the axon. Action potentials were detected extracellularly with another pair of electrodes near the other end. An example of birefringence responses taken from unstained axons is shown in the figure for comparison.

It is well known (see Cohen *et al.*, 1968) that the birefringence responses recorded from unstained giant axons are diphasic: the first phase, representing a decrease in light intensity (downward deflection in the figure), is followed by a large second phase (upward deflection). The ratio of the amplitude of the downward deflection to that of the upward deflection varies usually between 1:1.5 and 1:2. In axons heavily stained with a hydrophilic dye, the responses observed were purely monophasic or only slightly diphasic. In other words, the second phase of the birefringence response was almost completely eliminated by the dye molecules in the axoplasm.

The dyes used in the experiment mentioned above (chlorphenol red, xylene cyanol, etc.) are insoluble in hydrophobic media (e.g., in olive oil). We therefore expect the dye molecules in the axoplasm not to pass through the

superficial layer of the axon. At the two edges of the axon, this superficial layer is traversed by the quasi-monochromatic, polarized light. The positive birefringence of this layer is thought to make a significant contribution to the background light detected in the resting state of the axon. It is reasonable to assume that the birefringence response (i.e., a change in the light intensity produced by stimulation of the axon) is a reflection of a reversible structural change taking place in the superficial layer of the axoplasm.

We have seen that microtubules and neurofilaments in the ectoplasm are readily converted into their constituent monomers when the axon is internally perfused with a solution containing KBr, KI, or a mild detergent (Baumgold *et al.*, 1980). Repetitive stimulation of the axon is known to accelerate solubilization of these cytoskeletal elements into their monomeric forms (see Chapter 9, Section D). Birefringence responses may then be interpreted as being produced by a fast, reversible, partial depolymerization of microtubules and neurofilaments in the ectoplasm. Colchicine, which is known to bind to tubulin, alters the time course and suppresses birefringence responses (Watanabe *et al.*, 1973; I. Tasaki and A. Watanabe, unpublished).

For the sake of simplicity, let us assume that the ectoplasm is free of dye molecules and the endoplasm is uniformly stained with the dye. Partial depolymerization of the filamentous elements in the ectoplasm is expected to bring about a decrease in the light intensity observed under the cross-polar condition: this decrease then corresponds to the first phase of the birefringence response. During the falling phase of the action potential, the reverse process, namely, polymerization, proceeds. The second phase of the response (observed in the absence of dyes in the protoplasm) may be attributed to an overshoot of the reverse process. The suppression of the second phase in heavily stained axons may be explained as a result of the interruption of the light passing through the diffuse boundary between the ectoplasm and endoplasm.

The experimental findings described above are quite consistent with those reported by Watanabe *et al.* (1973) and Sato *et al.* (1973), and emphasize the crucial role played by the cortical layer of the axoplasm in the production of birefringence responses. An alternative explanation of these responses is given by Cohen *et al.* (1971).

D. OPTICAL RESPONSES PRODUCED BY EXPANSION OF DYE-LOADED ENDOPLASM

In squid axons loaded with chlorphenol red (or with other dyes) and exposed to a light beam at the wavelength of maximum absorption of the dye, it was found possible to record optical responses without using a polarizer or

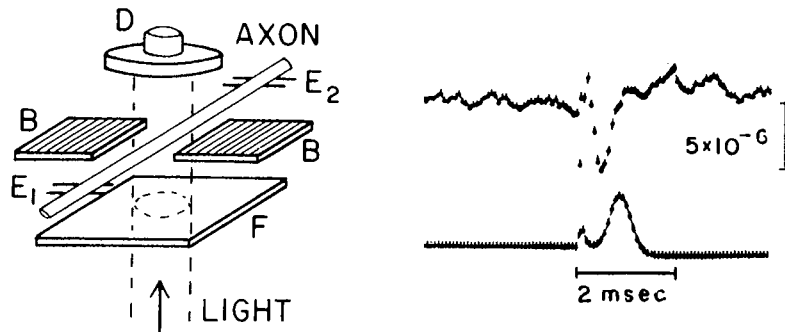


Fig. 15.3 Left: Schematic diagram of the experimental setup used for demonstrating changes in the intensity of light transmitted through the ectoplasm during the action potential. S, light source; F, interference filter with its center wavelength located near the absorption maximum of the dye; B, black Lucite plates; D, photodetector used in conjunction with a signal averager. Right: Optical response obtained from a squid giant axon heavily stained with chlorphenol red. The dye was dissolved in a potassium phosphate solution (pH 7.3) and was infused into the axon. The downward deflection represents a fall in the light intensity. The lower trace represents the action potential recorded extracellularly. (I. Tasaki and A. Watanabe, unpublished.)

analyzer. After repeated infusion of a dye (dissolved in a potassium phosphate buffer) solution, the axon was mounted on a nerve chamber as shown schematically in Fig. 15.3. With the analyzer or both the polarizer and analyzer removed from the optical setup, a distinct decrease in the light intensity was produced in the axon. The fall in the light intensity at the peak of the action potential was found to be $1-5 \times 10^{-6}$ times the intensity of the background light. No clear optical response was observed when an unstained giant axon was used in this experiment. (Note that, under these experimental conditions, the signals produced by turbidity changes are far smaller than the responses described above.)

The optical responses described above may be explained on the assumption that there is a small expansion of the dye-loaded endoplasm during the process of nerve excitation. Under the conditions of the present experiment, the intensity of the background light is determined primarily by the width of the space outside the axon through which the light beam from the source directly reaches the photodetector. The record furnished in the figure was taken with the width of the seawater-filled space chosen to be 0.3–0.4 mm. By multiplying the peak value of the optical responses into this width, the displacement of the boundary between the ectoplasm and endoplasm was estimated to be on the order of 10\AA .

The demonstration of optical responses described above gives strong support to our interpretation of the origin of birefringence responses discussed in the preceding section. It is possible that the turbidity of the axon is enhanced when the microtubules, neurofilaments, and actin filaments are par-

tially depolymerized. Hence, the early portion of the light scattering signal of the axon (which can be detected in the direction away from 0°) may also be explained on the same structural basis. The process of production of extrinsic fluorescence responses will be explained later on the basis of the structural change described above.

A question arises at once. How does a rise or fall of the membrane potential affect the conformational state of the filamentous elements in the ectoplasm? We may assume that the ectoplasm is compact and its electric resistivity is high. It is possible, therefore, that a change in the membrane potential strongly affects the distribution of electric charges at and around the interface between the endo- and ectoplasm. This change in the charge distribution may, in turn, alter the equilibrium distribution of tubulin, neurofilament proteins, actin molecules, etc., across the interface. Alternatively, invasion of extracellular cations into the ectoplasm across the labile layer of axolemma may be regarded as responsible for the conformational changes. The large difference in mobility between Na- and Ca-ions in macromolecules complicates diffusion and transport of these ions.

E. TRANSIENT CHANGE IN LIGHT ABSORPTION ASSOCIATED WITH EXCITATION OF VITALLY STAINED NERVE

The optical setup required for the demonstration of changes in the absorption spectra of dyes in the membrane during nerve excitation is relatively simple (Ross *et al.*, 1974; Tasaki *et al.*, 1974). The setup used most frequently in this laboratory is similar to that schematically illustrated in Fig. 15.3 (left). A light beam from a 100-W quartz-iodine lamp is focused on the nerve by means of a lens. Before the light reaches the nerve, it is converted into a quasi-monochromatic light with an interference filter and is linearly polarized by the use of a polarizer. The light which does not pass through the nerve is blocked by a thin plate of black Lucite placed on each side of the nerve. The output of the photodetector, either a photomultiplier or a photodiode, is led to a signal averager through a condenser-coupled amplifier.

The procedure of staining a crab nerve with a dye is as follows: A claw nerve of a crab, *Libinia emarginata* or *Callinectes sapidus*, is dissected out by the method described elsewhere (Tasaki and Sisco, 1975). The connective tissue sheath around the nerve is removed under a dissecting microscope and individual fibers in the nerve are separated with dissecting needles into small bundles, so that the dye can readily penetrate into the interior of the nerve bundle when the nerve is immersed in a staining solution. The

staining solution is prepared by either dissolving or suspending a dye in artificial seawater at a level of 20–50 μM .

The technique of staining squid giant axons is as follows: Giant axons are isolated from *Loligo pealei*. After the adhering connective tissue and small fibers are removed from the portion of the axon used for optical measurements, the axon is immersed in the staining solution for a period between 20 and 100 min, depending on the stainability of the dye used. The staining time for a dye is chosen by the criterion that the transmission of light through the axon is reduced by the dye to a level between 20 and 80% of the initial level.

The main advantage of using squid giant axons for optical studies is that various dyes can be applied intracellularly. For internal staining of the axon, the following techniques are used. Ordinarily, the dye is dissolved (or suspended) in a mixture containing potassium phosphate (pH 7.3) and potassium fluoride and is injected into the axon by using a small glass pipette (of about 100 μm in diameter). Alternatively, the dye may be suspended in a viscous medium which contains 25% (w/w) dextran, potassium phosphate (pH 7.3), and potassium fluoride. The dye suspension is infused into the axon, after removal of the axoplasm, with a glass pipette (about 300 μm in diameter). The latter technique is useful for dyes with very low solubility in salt solutions.

The stained nerve is mounted in a chamber filled with artificial seawater. Since stained nerves frequently lose their excitability when exposed to intense light in the presence of oxygen by virtue of the photodynamic action (see Blum, 1932), it is desirable to use seawater which has been deoxygenated by bubbling with nitrogen gas.

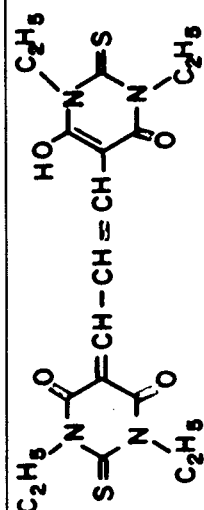
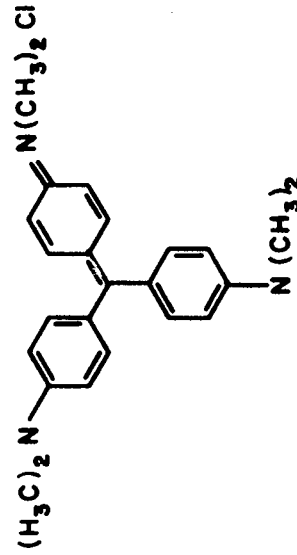
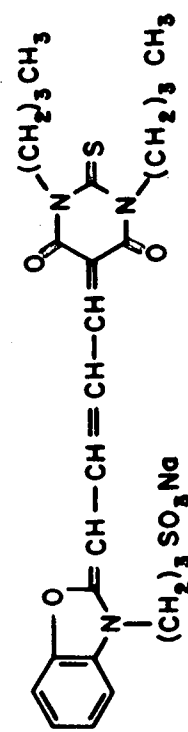
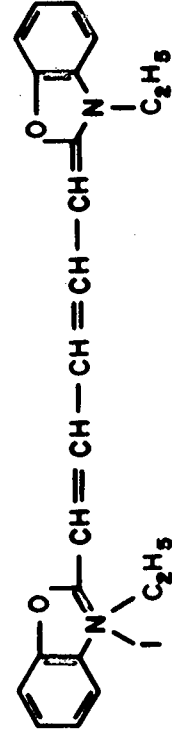
The dyes used in the absorption experiments described in the following sections are listed in Table 15.1. The molecular structures as well as the absorption maxima, both in water and ethanol, are given.

We have encountered many cases in which the time course of the absorption response is approximately the same as that of the action potential. With some dyes, however, the absorption responses observed are either prolonged or diphasic, indicating that the optical responses have time courses significantly different from that of the action potential. With many dyes studied, the peak value of the response, expressed in terms of $\Delta I/I$, was of the order of 10^{-5} for squid axons and of the order of 10^{-4} for crab nerves. (The symbol ΔI represents the change in the light intensity detected and I the light intensity observed in the resting state of the nerve.) Although the value of the ratio $\Delta I/I$ varies with the degree of staining, it is a very convenient quantity in a theoretical analysis of the present problem.

Once a nerve stained with a dye is found to give rise to a measurable response at a certain wavelength, we can readily map out the spectrum of the

TABLE 15.1

Structural Formulas of the Dyes Used for Studying Optical Responses in Crab Nerves and in Squid Giant Axons

	λ max	
	Water	Ethanol
I	540 nm	539 nm
Bis-(1,3-diethyl-2-thiobarbituric acid-(5)) trimethinoxonol		
II	590 (550)	590
Crystal Violet		
III	500 (535)	560
Merocyanine 540		
IV	576	581
3,3'-Diethyloxadicyarbocyanine iodide		

response by changing the wavelength of the incident light. This can be done by choosing a series of interference filters and determining the value of $\Delta I/I$ at every wavelength.

The absorption responses obtained from a crab nerve stained with merocyanine-540 (dye III in Table 15.1) at several wavelengths are shown in Fig. 15.4. In recording these responses, the intensity of incident light was adjusted at every wavelength so that the intensity of the transmitted light at rest (I) remained constant. At each wavelength, measurements were carried out with the lightwave polarized in the directions both parallel (the upper trace) and perpendicular to the long axis of the nerve (the lower trace).

In these records of absorption responses, the following points should be noted: (1) the range of wavelengths where the optical responses are observed coincides with the range where the dye strongly absorbs light when dissolved in water or in ethanol. (2) The sign of the optical response is reversed at a certain wavelength (which is called the "reversal point"). (3) The amplitude of the response varies depending on the direction of light polarization, whereas the intensity of the transmitted light at rest (I) is only slightly affected by a change in polarization.

In Fig. 15.4, the response measured with a 540-nm light wave polarized in the parallel direction is larger than the response obtained with a perpendicularly polarized light at the same wavelength. At 580 nm, the relative sizes of these two responses are reversed. A similar behavior was frequently seen in crab nerves and squid axons stained with many other dyes. In some cases, however, no clear reversal of the sign of the response within the spectrum is observed. In addition, there are cases in which the polarization of the incident light has no effect on the sign of the response observed (see later).

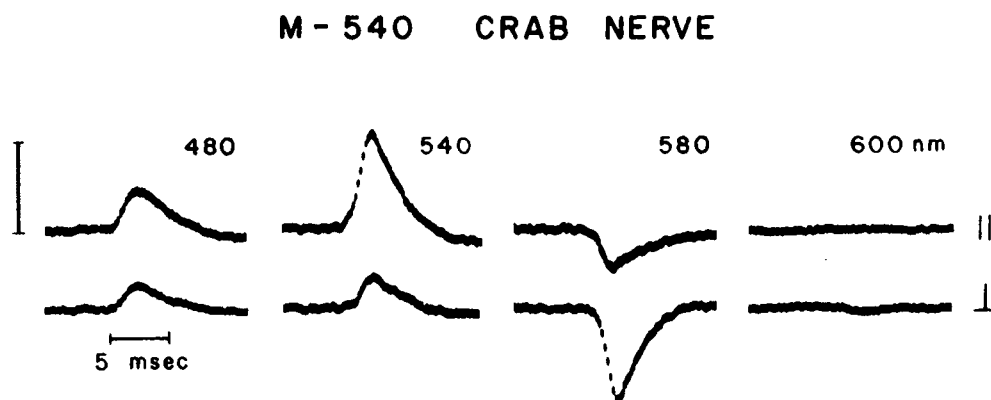


Fig. 15.4 Absorption responses obtained from a crab nerve stained with merocyanine-540 at four different wavelengths. Upper trace, responses obtained with the light polarized in the direction parallel to the nerve. Lower trace, responses obtained with perpendicularly polarized light. The vertical bar indicates 3×10^{-4} times the transmitted light intensity. (From *Photochem. Photobiol.* **24**, 194, 1976.)

The contribution of fluorescence to the response observed under these experimental conditions can be estimated by inserting a cut-off filter between the stained nerve and the photodetector. In most cases examined (see below), the contribution of fluorescence to the absorption response does not exceed 10% of the observed response (ΔI). However, with dyes having extremely high quantum yield of emission in both aqueous solutions and organic solvents (e.g., rhodamine B), changes in fluorescent light may contribute to the observed signal much more than 10%. In such cases, insertion of another interference filter between the nerve and the detector, as has been done by Ross *et al.* (1974), serves as a means of reducing the contribution of the fluorescent light.

In connection with the polarization of the light used for measuring absorption responses, a brief comment may be made on the possible effect of multiple scattering of light by the nerve. The degree of polarization of the transmitted light can be determined by inserting an additional Polaroid sheet (analyzer) between the nerve and the photodetector in such a fashion that the analyzer is perpendicular to the polarizer. The result of such examinations has indicated that the transmitted light is highly polarized and that the degree of polarization of the incident light is not appreciably affected by the light scattering within the nerve.

F. SPECTRA OF LIGHT ABSORPTION RESPONSES

The spectra of the transient absorption changes associated with nerve excitation can be constructed by plotting the response amplitude against the wavelength of the light used. We have examined the spectra of responses with a number of dyes. A few examples of such spectra are presented here.

Figure 15.5A shows the spectra of absorption responses obtained from the edge of a squid giant axon internally stained with dicarbocyanine (dye IV in the table). The curve marked with \parallel was obtained with the electric vector of the lightwave directed parallel to the long axis of the axon. The curve marked with \perp was determined by using a perpendicularly polarized lightwave. The reversal points of these two curves were found to be approximately 570 nm. The difference in polarization of the light employed for measurements did not change the spectrum significantly.

A few examples of the records of the absorption responses obtained from a crab nerve stained with merocyanine-540 are shown in Fig. 15.4. When the spectra for this dye were constructed by plotting the response amplitude as a function of wavelength, a marked influence of the polarization of the light became evident (see Fig. 15.5B). The reversal points of the two spectra, ΔI_{\parallel} and ΔI_{\perp} , did not coincide with each other in this case (Warashina and

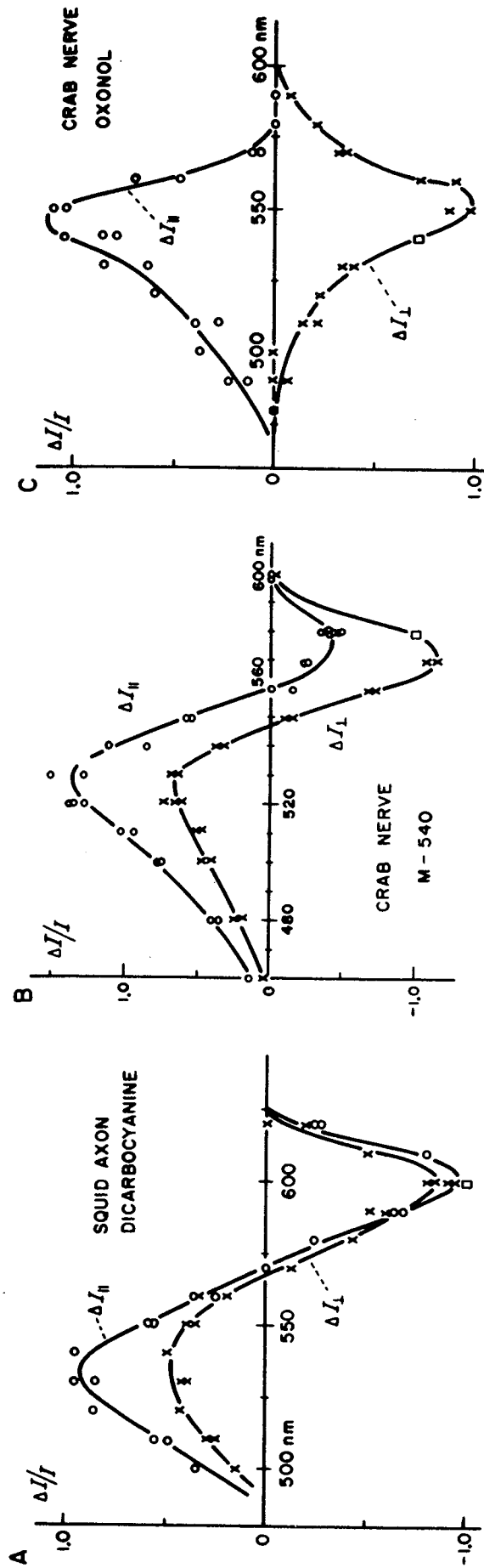


Fig. 15.5 (A) Spectra of absorption responses obtained from a squid axon internally stained with dicarboyanine. The light used was polarized either in the parallel or in the perpendicular direction to the nerve. Unity on the ordinate indicates a change of 6×10^{-5} times the transmitted light intensity. (B) Spectra of absorption responses obtained from a crab nerve stained with merocyanine-540. The polarization of the light is indicated. Unity on the ordinate indicates a change of 3×10^{-4} times the transmitted light intensity. (C) From crab nerves stained with oxonol. Unity on the ordinate indicates a change of 5×10^{-4} times the transmitted light intensity. (*Photochem. Photobiol.* **24**, 195-196, 1976.)

Taskai, 1975). When the same dye was introduced into the interior of a squid axon by the infusion technique mentioned before, we observed a very similar wavelength dependence of the responses, but with the sign completely reversed.

The polarization of the light used for measurements has a still more remarkable effect on the spectra of the responses shown in Fig. 15.5C. We see in this case that the parallel component ΔI_{\parallel} is positive (representing a transient decrease in the light absorption) and the perpendicular component ΔI_{\perp} is negative. There is no reversal point anywhere and the responses are highly dichroic in the entire range of wavelength examined.

We have presented, above, several types of spectra indicating the wavelength dependence of transient changes in absorbency of the dye molecules in the nerve. We now consider the relationship between the physicochemical properties of the dyes used and the observed spectra of the absorption responses. We infer (see below) that a shift of the absorption spectrum and a change in the angular distribution of the dye molecules within or near the nerve membrane are the immediate causes for the production of these responses. We attribute the diphasicity in a response spectrum to the shift in the absorption spectrum associated with nerve excitation; subtraction of the absorption spectrum in the resting state from that in the excited state of the nerve gives rise to a diphasicity in the response spectrum.

We now examine the effect of a change in the angular distribution of the absorption oscillators of the dye molecules. The following consideration indicates that this change leads to a dichroism of the response. The absorption of light by a dye molecule reaches a maximum when the orientation of the absorption oscillator of the molecule coincides with that of the electric vector of the incident light wave. When a number of dye molecules, which are randomly oriented in the nerve initially, rotate and assume a new distribution in which the absorption oscillators are more-or-less perpendicular to the long axis of the nerve, absorption of the light polarized in the perpendicular direction is expected to increase; simultaneously, absorption of the light polarized in the parallel direction is expected to decrease. In the following section, this notion is examined quantitatively.

G. MATHEMATICAL EXPRESSIONS FOR SPECTRA OF OPTICAL RESPONSES

The probability of absorption of light by a dye molecule is proportional to the square of the cosine of the angle between the electric vector of the incident lightwave and the direction of the absorption oscillator (or the transition moment) of the dye molecule (see, e.g., Feofilov, 1961). Figure 15.6 il-

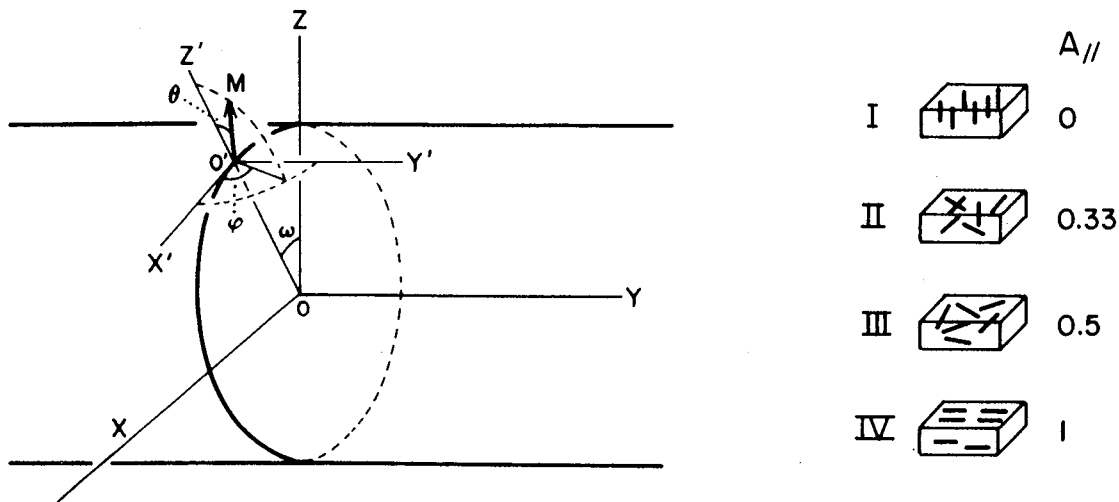


Fig. 15.6 Left: Diagram illustrating three angles, θ , φ , and ω used in theoretical consideration of the distribution of transition moments of dye molecules in the nerve membrane. Axis OY represents the long axis of a single fiber in the nerve trunk. Right: A schematic diagram illustrating the dye molecules in the membrane; in Case I, all the dye molecules are oriented in the direction perpendicular to the membrane surface; in Case II, the molecules have a random spatial distribution; in Case III, they are two-dimensionally random with their transition moments parallel to the membrane surface; in Case IV, the orientation of the dye molecules is parallel to the long axis of the nerve. The degree of parallel orientation, defined by Eq. (15.2), for each case is indicated. (*Proc. Jpn. Acad.* **51**, 613, 1975).

illustrates the spatial relationship between the nerve membrane and a dye molecule in or near the membrane. Axis OY represents the long axis of a particular single fiber in the nerve trunk under study. The direction of propagation of the incident light is along axis OZ and the electric vector of the incident lightwave is directed either along axis OY (parallel polarization) or along axis OX (perpendicular polarization). The angle which the axis of the oscillator ($O'M$) makes with the direction ($O'Z$) normal to the membrane surface is denoted by θ . As illustrated in the figure, two additional angles, φ and ω , are required to denote the orientation of $O'M$ relative to the electric vector of the incident light. The cosine of the angle between $O'M$ and $O'Y'$ is given by $\sin \omega \sin \varphi$.

The angular distribution function of the absorption oscillators relative to the membrane surface may be denoted by $f(\theta, \varphi)$. The depth of penetration of dye molecules into the membrane is unquestionably an important factor in determining the spectral shift and the orientation of dye molecules. However, since the method of measuring absorption of polarized light tells nothing about the depth directly, this variable is not explicitly treated here. Function $f(\theta, \varphi)$ is normalized, namely

$$\int_0^{2\pi} \int_0^{\pi} f(\theta, \varphi) \sin \theta \, d\theta \, d\varphi = 1 \quad (15.1)$$

so that $f(\theta, \varphi) \sin \theta d\theta d\varphi$ represents the probability of finding a dye molecule with its orientation in the range between θ and $(\theta + d\theta)$ and between φ and $(\varphi + d\varphi)$.

The molar extinction coefficient of the dye in the membrane is now denoted by $\epsilon(\lambda)$. Then, the contribution of these dye molecules to absorption of light polarized along OY is proportional to the product $\epsilon(\lambda)A_{\parallel}$, where A_{\parallel} is a geometric factor representing the *degree of parallel orientation* of the dye molecules defined by

$$A_{\parallel} = \iint f(\theta, \varphi) [\sin \theta \sin \varphi]^2 \sin \theta d\theta d\varphi \quad (15.2)$$

The quantity in the bracket represents the cosine of the angles between $O'M$ and $O'Y'$. Again, the integration extends from 0 to π for θ and from 0 to 2π for φ . In an analogous manner, the geometric factor representing the *degree of perpendicular orientation* of the dye molecules, A_{\perp} , is defined by

$$A_{\perp} = \frac{1}{2\pi} \iiint f(\theta, \varphi) [\cos \theta \sin \omega + \sin \theta \cos \varphi \cos \omega]^2 \sin \theta d\theta d\varphi d\omega \quad (15.3)$$

the limits of integration with respect to ω being from 0 to 2π . By comparing Eq. (15.3) with Eqs. (15.1) and (15.2), it is easily found that A_{\parallel} and A_{\perp} are related to each other by the relation

$$A_{\parallel} + 2A_{\perp} = 1 \quad (15.4)$$

With particular distributions of absorption oscillators, these geometric factors can easily be calculated. For a completely random spatial distribution (Case II in Fig. 15.6), namely, for $f(\theta, \varphi) = 1/(4\pi)$, A_{\parallel} is equal to $\frac{1}{3}$. In the case of two-dimensionally random distribution on the surface of the nerve (Case III), $A_{\parallel} = \frac{1}{2}$. When the absorption oscillator of every dye molecule is oriented perpendicularly to the surface of the nerve (Case I), $A_{\parallel} = 0$. When all the dye molecules are arranged with their oscillators parallel to axis OY (Case IV), $A_{\parallel} = 1$. These values are given in Fig. 15.6. The value for A_{\perp} in the corresponding cases can be determined by Eq. (15.4).

In the case of the crab nerve, there are many fibers in the light path. The contribution of the dye molecules in the membrane to the optical density measured under the conditions of parallel and perpendicular polarization is equal to $3N\epsilon(\lambda)A_{\parallel}$ and $3N\epsilon(\lambda)A_{\perp}$, respectively, where N represents the average dye concentration times the thickness of the nerve. The factor of 3 is required, because when the dye distribution is completely random, namely, when $A_{\parallel} = A_{\perp} = \frac{1}{3}$, the optical density is given by $N\epsilon(\lambda)$, irrespective of the polarization of the incident light.

Let us now consider the case in which the incident light is absorbed by the

dye molecules existing in two distinct states in the membrane. These two states, determined by the environment of the dye molecules, are distinguished by the extinction coefficients, $\epsilon_1(\lambda)$ and $\epsilon_2(\lambda)$, and the angular distributions, $f_1(\theta, \varphi)$ and $f_2(\theta, \varphi)$, without any implication as to the physiochemical nature of the two states involved. The geometric factors in the second state of the nerve membrane, B_{\parallel} and B_{\perp} , are different from the factor in the first state, A_{\parallel} and A_{\perp} , because the distribution of dye molecules is, in general, different in the two states of the membrane. Again, $B_{\parallel} + 2B_{\perp} = 1$.

The intensities of the light transmitted through a stained nerve at rest are given by

$$I_{\parallel} = I_0 K \exp[-N_1 A_{\parallel} \epsilon_1(\lambda) - N_2 B_{\parallel} \epsilon_2(\lambda)] \quad (15.5)$$

under parallel polarization, and

$$I_{\perp} = I_0 K \exp[-N_1 A_{\perp} \epsilon_1(\lambda) - N_2 B_{\perp} \epsilon_2(\lambda)] \quad (15.6)$$

under perpendicular polarization. Here, the intensity of the incident light is denoted by I_0 , and the reduction of light intensity due to dye molecules bound to nonresponsive sites (connective tissue, Schwann's cells, endoplasms, etc.) by factor K , and the amount of dyes in the first and second states of the nerve by N_1 and N_2 , respectively. (We assume that the dye molecules bound to nonresponsive sites are randomly oriented. Since natural logarithm is used in the equations above, a corresponding modification of the unit of concentration is required.)

We now discuss the changes in the light intensity associated with small alterations in N_1 and N_2 . On account of mass conservation, the condition that $N_1 + N_2 = \text{constant}$ is satisfied, or $\Delta N_1 = -\Delta N_2 = \Delta N$ for small changes. (This relation holds even when we are dealing with a monomer-dimer conversion, as long as the monomeric concentration unit is used to express the concentration of dimers.) Therefore, the changes in the light intensity, ΔI_{\parallel} and ΔI_{\perp} , are given by

$$-\frac{\Delta I_{\parallel}}{I_{\parallel}} = [A_{\parallel} \epsilon_1(\lambda) - B_{\parallel} \epsilon_2(\lambda)] \Delta N_1 \quad (15.7)$$

and

$$-\frac{\Delta I_{\perp}}{I_{\perp}} = [A_{\perp} \epsilon_1(\lambda) - B_{\perp} \epsilon_2(\lambda)] \Delta N_1 \quad (15.8)$$

We now see how various patterns in the absorption response spectra are produced. Three *basic patterns of the spectra* are obtained based on the following consideration:

Case A. We first consider the case in which the spectral shift is a sole cause of the production of responses. Since there is, in this case, no change

in the distribution of absorption oscillators, the following relations hold: $A_{\parallel} = B_{\parallel}$ and $A_{\perp} = B_{\perp}$. Thus Eqs. (15.7) and (15.8) become

$$-\frac{\Delta I_{\parallel}}{I_{\parallel}} = A_{\parallel}[\epsilon_1(\lambda) - \epsilon_2(\lambda)]\Delta N \quad (15.9)$$

$$-\frac{\Delta I_{\perp}}{I_{\perp}} = A_{\perp}[\epsilon_1(\lambda) - \epsilon_2(\lambda)]\Delta N \quad (15.10)$$

It is seen from these equations that the spectra of ΔI_{\parallel} and ΔI_{\perp} are determined only by the difference spectrum $\epsilon_1(\lambda) - \epsilon_2(\lambda)$, indicating that the two spectra possess a common reversal point. The ratio of the amplitudes of the two responses at any wavelength depends only on the angular distribution of absorption oscillators that remain unaltered during nerve excitation.

The curves in Fig. 15.7A represent the result of calculation of the two spectra based on these equations. In this calculation, the wavelength dependence of the molar extinction coefficient, $\epsilon_1(\lambda)$, is approximated by a Gaussian function which has a halfwidth of 1.5 in an arbitrary wavelength unit. The other extinction coefficient, $\epsilon_2(\lambda)$, is given by equation $\epsilon_2(\lambda) = \epsilon_1(\lambda - 2.5)$, namely, a spectrum that is red-shifted by 2.5 units with no change in the shape. The numerical values for A_{\parallel} and A_{\perp} are given by $\frac{1}{2}$ and $\frac{1}{4}$, respectively, corresponding to the case of a two-dimensionally random distribution of absorption oscillators.

Case B. Next we consider the case in which the spectral shift is associated with a reorientation of dye molecules. The curves shown in Fig. 15.7B are calculated by the use of Eqs. (15.7) and (15.8) with the same values of $\epsilon_1(\lambda)$ and $\epsilon_2(\lambda)$ as those adopted in Case A and with $A_{\parallel} = \frac{1}{2}$, $A_{\perp} = \frac{1}{4}$, $B_{\parallel} = \frac{1}{4}$, and $B_{\perp} = \frac{3}{8}$. This implies that a two-dimensionally random distribution of the absorption oscillators is converted to a distribution in which the absorption os-

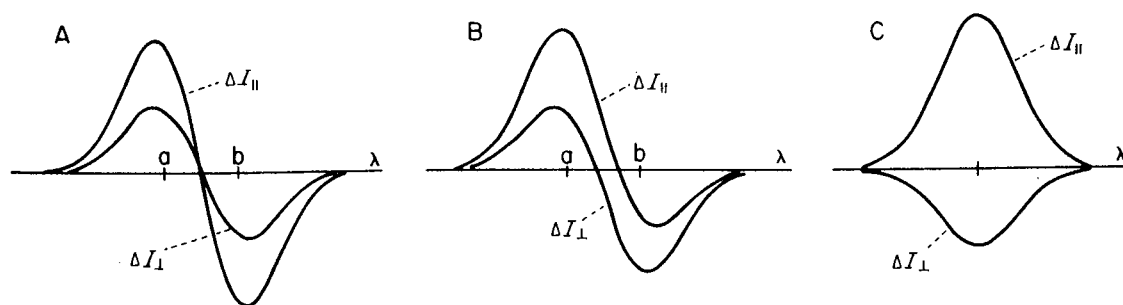


Fig. 15.7 Diagram illustrating three basic patterns of the wavelength dependence of absorption responses. The spectra were obtained from the mathematical equations described in the text. (A) The responses are generated by a spectral shift alone. (B) Both spectra shift and reorientation of dye molecules contribute to the responses. (C) Reorientation of dye molecules alone produces the responses. The wavelengths of the absorption maxima before and after the spectral shift are marked by *a* and *b* on the abscissa. (*Photochem. Photobiol.* **24**, 198, 1976.)

cillators are preferentially oriented in the radial direction of the axon. As seen in Fig. 15.7B, the reversal points for the two spectra do not coincide with each other in this case.

Case C. Finally, the case in which reorientation of the dye molecules is the sole cause of response production. In this case, the equations are given by

$$-\frac{\Delta I_{\parallel}}{I_{\parallel}} = (A_{\parallel} - B_{\parallel})\epsilon_1(\lambda)\Delta N \quad (15.11)$$

$$-\frac{\Delta I_{\perp}}{I_{\perp}} = (A_{\perp} - B_{\perp})\epsilon_1(\lambda)\Delta N \quad (15.12)$$

Because of the relations between the geometric factors, i.e., $A_{\parallel} + 2A_{\perp} = 1$ and $B_{\parallel} + 2B_{\perp} = 1$, the amplitude ratio between the two components $(A_{\perp} - B_{\perp})/(A_{\parallel} - B_{\parallel})$ is invariably equal to $-\frac{1}{2}$ at every wavelength, irrespective of the modes of distribution of the dye molecules. This means that the responses observed under the perpendicular conditions must have a half of the amplitude of the responses under the parallel conditions with its sign reversed.

A pattern similar to that in Fig. 15.7C may be encountered in an extreme example of Case B where, for example, the absorption oscillators are shifted from an all-parallel distribution to an all-random distribution, namely, when the values $A_{\parallel} = 1$, $A_{\perp} = 0$, $B_{\parallel} = 0$, and $B_{\perp} = \frac{1}{2}$ are introduced into Eqs. (15.7) and (15.8). However, as the result of the spectral shift assumed in Case B, the peak wavelength of the spectrum obtained under the perpendicular conditions must be different from that of the spectrum observed under the parallel conditions.

H. ANALYSES OF LIGHT ABSORPTION RESPONSES

When we compare the spectra obtained experimentally with the spectra obtained from the aforementioned theoretical calculations, we immediately find that the two factors, spectral shift and reorientation of dye molecules in the nerve, are sufficient to account for the patterns of observed spectra. We now compare the result of calculation shown in Fig. 15.7B with the pattern of response spectra shown in Fig. 15.5B obtained from a crab nerve stained with merocyanine-540. In this case, a further analysis has been made based on the result of a physicochemical study of this dye (Tasaki *et al.*, 1976).

By mounting a stained crab nerve in a special chamber, the absorption spectrum of merocyanine-540 in the crab nerve at rest was determined with a Beckman spectrophotometer; the solid line in Fig. 15.8 (left) shows the result of the determination. In this absorption spectrum, there are two maxima,

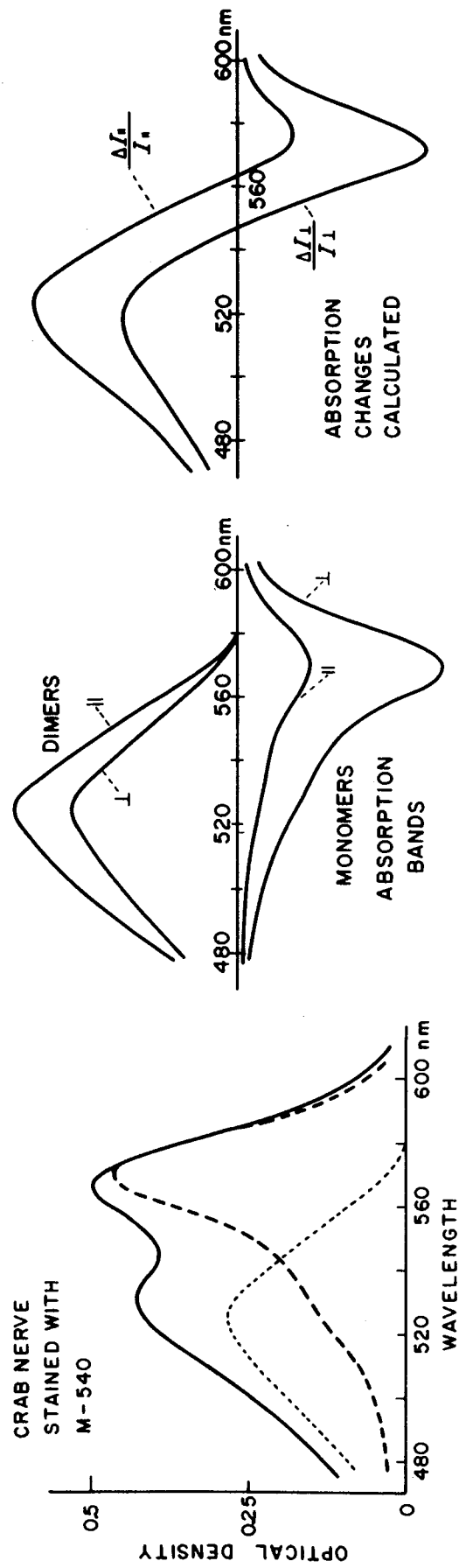


Fig. 15.8 Diagrams illustrating an example of the procedure of reconstructing the spectra of absorption changes during nerve excitation (see text). (*Proc. Jpn. Acad.* 51, 611, 1975.)

one at 528 nm and the other at about 565 nm. The dashed line in this figure represents the corrected *fluorescence excitation spectrum* of the dye in the crab nerve at rest. This spectrum has a single maximum at about 568 nm.

If the light energy absorbed by a single species of dye molecules is converted into fluorescent light by a simple process of fluorescence emission, the fluorescence excitation spectrum is expected to coincide with the absorption spectrum (except for the dimension of the ordinate). The existence of an additional maximum in the absorption spectrum indicates that there is a nonfluorescent species of dye molecules which have a different absorption spectrum. Based on the effect of dilution of the dye solution, the absorption band with a maximum of about 530 nm is attributed to dimers of the dye molecules. The dotted line in Fig. 15.8 (left) represents the absorption spectrum of the dimers obtained by subtraction of the monomer spectrum (shown by the dashed line) from the total absorption band (the solid line).

It has been proposed that in the nerve membrane stained with merocyanine-540 optical responses are produced by conversion of dimers into monomers during action potentials (Tasaki *et al.*, 1974; Ross *et al.*, 1974). Figure 15.8 indicates that the observed spectrum of the optical responses (shown in Fig. 15.5B) can adequately be interpreted as being nothing but linear combinations of the monomer and dimer spectra. The absorption spectra shown on the right-hand side of Fig. 15.8 are constructed by subtracting the dimer absorption bands from the monomer absorption bands in the center. The absorption bands in the middle are obtained from the monomer and dimer bands shown in the left-hand diagram (by multiplying proper factors). The spectra obtained by this calculation reproduce all the essential characteristics of the observed spectra of the optical responses shown in Fig. 15.5B.

From the ratio between the amplitudes of the two monomer bands in the diagram, it is found that $A_{\perp} : A_{\parallel}$ is roughly 2.8, indicating that A_{\parallel} is approximately 0.15. [Note the relation between A_{\parallel} and A_{\perp} given by Eq. (15.4).] Similarly, from the relative amplitudes of the two dimer bands in the diagram, the ratio of B_{\perp} to B_{\parallel} is found to be 0.74. From this it follows that B_{\parallel} is roughly 0.40.

As the result of this analysis, the following scheme is proposed for the process of response production with merocyanine-540 in crab nerve. During nerve excitation, the number of monomers increases at the expense of the dimers which are more or less randomly oriented in the nerve. The monomer molecules are oriented preferentially in the direction perpendicular to the long axis of the nerve. These molecules absorb the light with perpendicular polarization much more strongly than the light with parallel polarization.

It has already been noted that this dye gives rise to very different spectra when applied *intracellularly*. The reversed spectra obtained under these

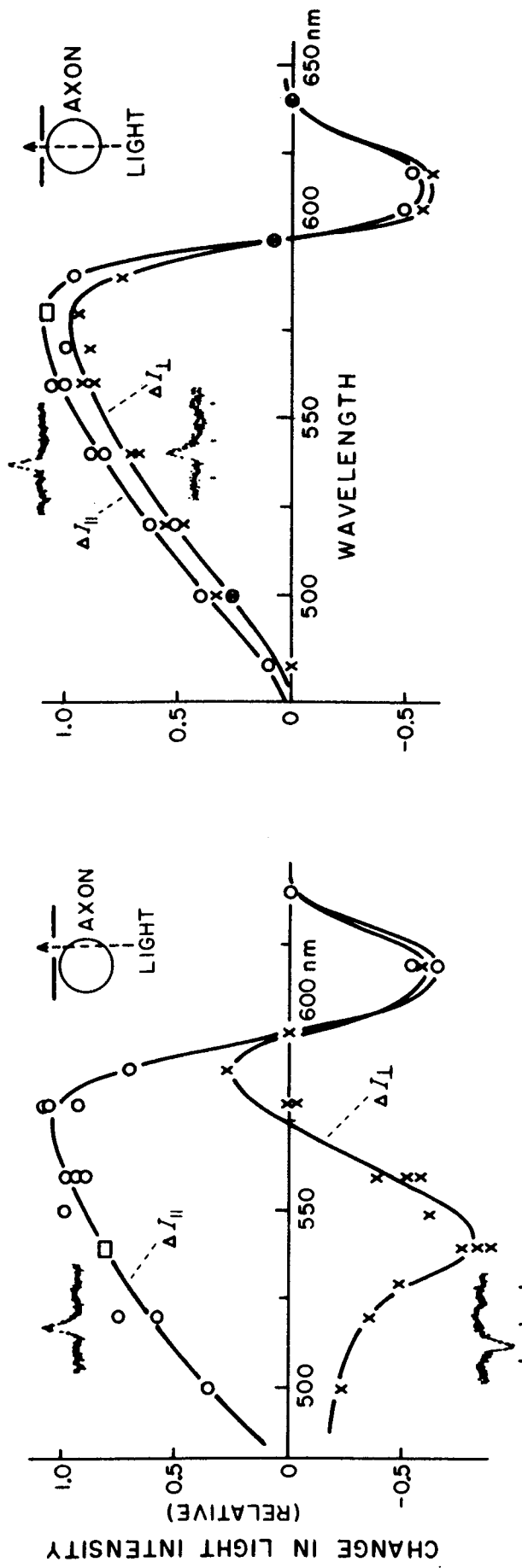


Fig. 15.9 Wavelength dependence of the optical responses of squid axons stained externally with crystal violet determined at the edge (left) and at the center (right). The light used was polarized in the direction either parallel or perpendicular to the long axis of the axon. Samples of the records of optical responses taken at 540 nm are shown; the time markers below the records are 5 msec. μ art. Unity on the ordinate indicates a change of 1.7×10^{-5} times the transmitted light intensity. (*Proc. Jpn. Acad.* 52, 38, 1976.)

conditions may adequately be interpreted as indicating that the number of dimer molecules increases and that of monomer molecules decreases during an action potential in the inner layer of the axon membrane.

In the squid axon membrane stained externally with a dye, spectral analysis based on the aforementioned mathematical equations is not expected to yield correct results. In this case the attenuation of the incident light varies depending on which portion of the axon the light beam passes through. We have demonstrated this property of a squid axon by placing a narrow (0.1–0.2 mm wide and 3–4 mm long) slit on various parts of the axon. A beam of light passing through the slit placed at the edge of the axon is absorbed much more strongly than a beam traversing the middle part of the same axon.

The response spectra shown in Fig. 15.9 were obtained from squid axons stained externally with crystal violet (Tasaki and Warashina, 1976b). In the case where the edge of the axon was examined, it is seen that the polarization of the light beam has a strong effect on the spectrum of the optical response in the region of wavelengths shorter than 570 nm. In addition to this distinct dichroism of the response, a reversal of the response at about 600 nm is seen. In the middle portion of the axon (see the right-hand diagram), the effect of polarization of the light beam is almost absent. It is well known that the absorption spectra of crystal violet *in vitro* indicates more than one species of molecules (Barker *et al.*, 1959); this would explain the behavior of the dye in the axon membrane.

The presence or absence of the dichroic responses in squid giant axons can be understood on the basis of the following consideration. The geometrical factor A_{\parallel} , given by Eq. (15.2), is still applicable to the dye molecules in squid giant axons. However, the expression for the factor A_{\perp} given by Eq. (15.3) cannot be used to describe the behavior of the dye molecules in the squid axon membrane. In the *middle* of the axon A_{\perp} is given by

$$A_{\perp} = \iint f(\theta, \varphi) [\sin^3 \theta \cos^2 \varphi] d\theta d\varphi \quad (15.13)$$

For the light beam passing ideally through the *edge* of an axon, the factor A_{\perp} is given by

$$A_{\perp} = \iint f(\theta, \varphi) [\cos^2 \theta \sin \theta] d\theta d\varphi \quad (15.14)$$

In the case where the distribution is independent of φ , the relation between the geometrical factors is given by $A_{\parallel} = A_{\perp}$ in the middle of the axon, and by $2A_{\parallel} + A_{\perp} = 1$ at the edge of the axon. The corresponding relations exist between B_{\parallel} and B_{\perp} . At least on the external surface of the squid axon, the dependence of $f(\theta, \varphi)$ on φ appears to be very small.

The absence of dichroism in the absorption response in the middle of the axon is expected even when there is reorientation of the dye molecules in the membrane during nerve excitation. (Note that $A_{\parallel} \approx A_{\perp}$ in this case.) On the other hand, reorientation of the absorption oscillators can be detected at the edge of an axon by virtue of the marked dichroism of the response. It is important to note that the absorption oscillators oriented to the direction perpendicular to the membrane surface are detected efficiently by a perpendicularly polarized light at the edge of the axon. This is not the case in the middle. Thus, it is concluded from the measurement at the edge of the axon (Fig. 15.9, left) that the absorption oscillators of the crystal violet molecules in the nerve membrane rotate during excitation and assume preferentially a perpendicular orientation.

I. RELATION BETWEEN OPTICAL RESPONSES AND THE MEMBRANE POTENTIAL

We have noted already that a transient absorption change associated with nerve excitation has, in some cases, the same duration as the change in the membrane potential. With a view toward elucidating the relationship between the optical response and the membrane potential, the following observations were made using squid axons treated internally with TEA (tetraethylammonium salt). The reasons for this TEA treatment is that the membrane potential can be controlled much more easily under these conditions than in normal axons (see Tasaki and Hagiwara, 1957, cited in Chapter 10). To avoid passage of a strong current at the onset of voltage pulses, a trapezoid configuration of clamping voltage pulses was chosen (see Fig. 15.10, bottom). Furthermore, by using a special device constructed by Hauser, the sign of trapezoidal voltage pulses was changed alternately without changing the amplitude.

In Fig. 15.10, three examples of the records obtained by this technique are presented. Symbol “-” in the figure indicates that the records were obtained with a train of negative (hyperpolarizing) pulses; “+” signifies that the record was taken by using positive (depolarizing) pulses of the same amplitude and the same predetermined number. Symbol “±” shows that “+” and “-” pulses of the same number and amplitude were presented alternately to the same axon. In Record A obtained from a squid axon stained internally with dicarbocyanine, the response obtained with “+” pulses was close to that obtained with “-” pulses, so that only a small response was obtained under the “±” conditions. In record B obtained from squid axons stained internally with crystal violet, the response obtained under the “±” conditions was large and positive, indicating that depolarizing pulses gave

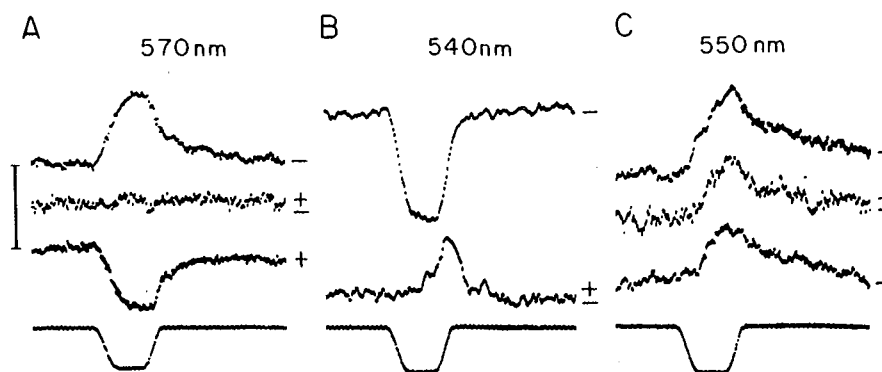


Fig. 15.10 Absorption responses observed under voltage clamp with trapezoid voltage pulses. The squid axon under study was stained internally with dicarbocyanine (A), internally with crystal violet (B), and externally with oxonol (C). The records marked "±" in the figure was obtained by superposing the optical responses to hyperpolarizing voltage pulses on the responses to depolarizing pulses of the same amplitude and duration. The record marked "--" was obtained by the use of hyperpolarizing voltage pulses. The light used was polarized in the parallel direction. The amplitudes of the trapezoid pulses were 100 mV for (A), and 90 mV for (B) and (C). The duration of the trapezoid was 6 msec at the base. The vertical bar indicates a change of 6×10^{-5} times the transmitted light intensity for (A), and 3×10^{-5} for (B) and (C). (*Photochem. Photobiol.* **24**, 201, 1976).

rise to definitely larger responses. Record C was obtained from an axon externally stained with oxonol: in this case, the response to depolarizing pulses was so small that the response obtained under the "±" conditions was not significantly different from that taken under the "--" conditions.

The experimental finding described above indicates that there is in general no simple relationship between the change in the membrane potential and the observed absorption responses.

J. OPTICAL SETUP FOR DETECTION OF TRANSIENT CHANGES IN EXTRINSIC FLUORESCENCE

When a nerve stained with a proper fluorescent membrane probe is electrically stimulated, there is a transient change in the intensity of the fluorescent light derived from the probes (Tasaki *et al.*, 1968, 1969; Cohen *et al.*, 1974). The optical setup used to observe such a fluorescence response is schematically shown in Fig. 15.11. This setup consists of a device to optically excite the fluorescent probe in a nerve (bottom) and an arrangement to collect the emitted fluorescent light from the nerve (top). The light source is a 200-W Xe-Hg or Xe lamp operated with a stabilized power supply. Cylindrical quartz lenses are used to condense the incident light on a 10-mm-long portion of the nerve. The white light from the source is turned into a quasi-

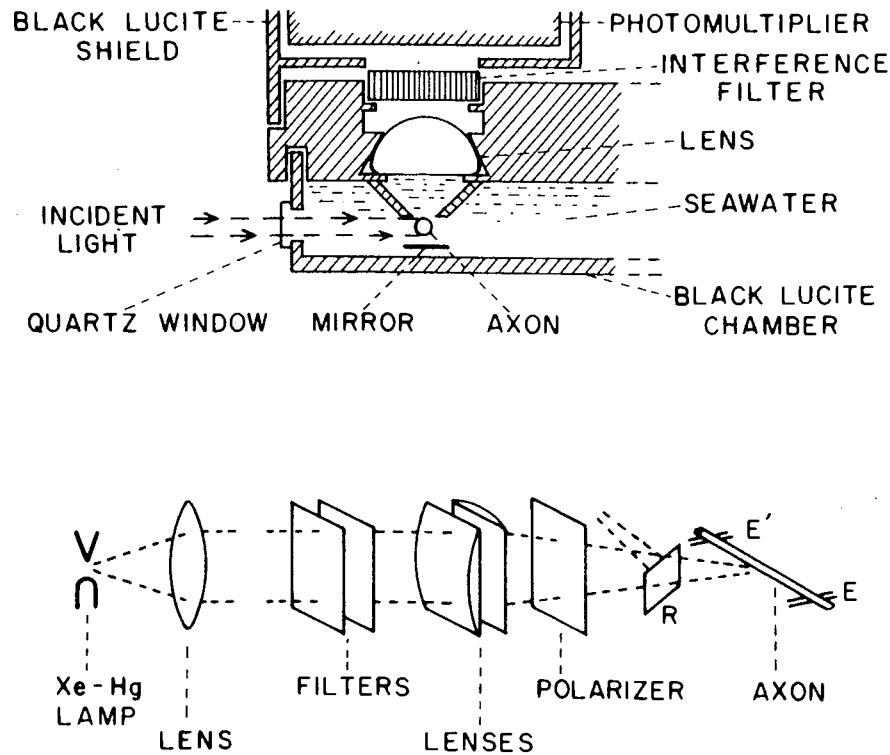


Fig. 15.11 Schematic diagram of spectrofluorometer used for determining emission spectra of an axon stained with a fluorescent probe. R represents a quartz cover slip for reflecting a small portion of the incident light to the reference photomultiplier tube. E and E' represent electrodes for stimulating the axon and for recording the action potential extracellularly. (*Biochim. Biophys. Acta* **323**, 221, 1973.)

monochromatic lightwave by inserting an interference filter between the lenses and the nerve. When polarization of the incident light is required, a polarizer (Polaroid, KN or HN series) is placed between the filter and the nerve. The light emitted by the stained nerve is collected with a lens placed on the top of the nerve chamber. The portion of the incident light scattered by the nerve is effectively eliminated by the use of a secondary filter, either a cut-off filter or an interference filter. To measure the degree of polarization of the emitted light, a Polaroid sheet inserted between the secondary filter and the photomultiplier is used.

The intensity of the Xe or Xe-Hg lamp may fluctuate in the range of frequencies required to analyze fluorescence responses. Since the observed changes in the fluorescence intensity are far smaller than 1%, it is necessary to suppress the response of the detector system to this fluctuation. This can be accomplished by reflecting a small portion of the incident light onto a reference photomultiplier. The phase of the output of the reference photomultiplier is inverted and is added to the output of the fluorescence-detecting photomultiplier. The techniques used to eliminate mechanical and elec-

trical disturbances in detection of fluorescence responses are discussed elsewhere (Tasaki and Sisco, 1975).

Giant axons of the North Atlantic squid (*Loligo pealei*), claw nerves of the spider crab (*Libinia emarginata*), and walking leg nerves of the American lobster (*Homarus americanus*) have been used in these experiments. The staining techniques used are the same as those mentioned in the previous section.

K. PHYSICOCHEMICAL FACTORS AFFECTING PRODUCTION OF AmNS FLUORESCENCE RESPONSES

There are 14 positional isomers in aminonaphthalene sulfonate (AmNS). When these isomers were used for detecting fluorescence responses of squid axons and of crab nerves, it was found that very different results are obtained depending on the positions of amino and sulfonate groups in the naphthalene ring. Figure 15.12A shows the relative sizes of these fluorescence responses expressed in terms of the ratio $\Delta I/I$, where ΔI denotes the change in the intensity of fluorescent light associated with nerve excitation and I repre-

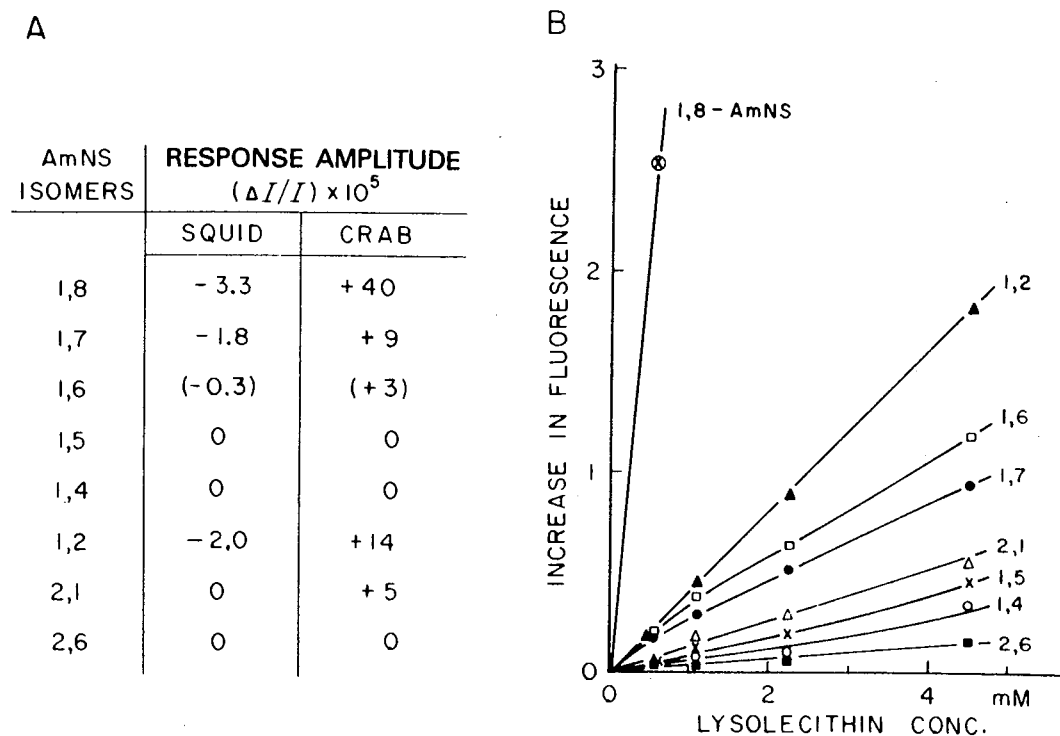


Fig. 15.12 (A) Amplitudes of fluorescence responses obtained from squid axons and crab nerves stained with various isomers of aminonaphthalene sulfonate (AmNS). (B) Increments in the intensity of fluorescence emission by the addition of lysolecithin to aqueous solutions of AmNS isomers. (*Photochem. Photobiol.* **24**, 202-203, 1976.)

sents the intensity of the fluorescent light emitted from the stained nerve at rest. The plus sign (+) in the table indicates that the observed signal represents a transient increase in the fluorescence intensity; “-” signifies that there is a transient decrease in the fluorescent light intensity during nerve excitation. In squid axons stained internally with these isomers, relatively large responses were observed with 1-aminonaphthalene-8-sulfonate (1,8-AmNS). With other isomers injected into squid axons, a change in fluorescence associated with nerve excitation was hardly detectable. When the isomers were applied *extracellularly* to crab claw nerves, it was found that the sign of the responses was opposite to that seen in *intracellularly* stained squid axons. In addition to 1,8-AmNS, 1,2-AmNS was also found to produce detectable responses.

We now examine what physicochemical factors are responsible for the difference in ability among AmNS isomers in the nerves to produce a fluorescence response. We consider, first, the effect of solvent polarity on fluorescence emission of AmNS. The polarity dependence of the quantum yield of many AmNS isomers was examined previously by Turner and Brand (1968); we have confirmed the major portion of their findings and expanded our examination to include three more isomers (1,5-, 1,2-, and 2,1-AmNS). According to these results (Tasaki and Warashina, 1976a), the fluorescence emission from 1,8-AmNS is highly sensitive to the solvent polarity, while the emissions of 2,6-AmNS and of 1,6-AmNS are practically unaffected by this factor. Such isomers as 1,7-AmNS, 1,6-AmNS, 1,2-AmNS, and 2,1-AmNS are, roughly speaking, moderately sensitive to the solvent polarity. These facts seem to explain the mechanism of production of responses with most of these AmNS isomers. In the case of 1,5-AmNS, however, the fluorescence emission is rather sensitive to a change in the solvent polarity; but no fluorescence response has been detected with this isomer.

In order to account for this behavior of 1,5-AmNS, it is postulated that the binding of dye molecules to the membrane macromolecules is an additional factor required for production of fluorescence responses. To give experimental support to this postulate, the effect of addition of lysolecithin or of bovine serum albumin to aqueous solutions of AmNS isomers on the fluorescence emission was examined. Upon addition of lysolecithin, the intensity of fluorescent light emitted by an aqueous solution of AmNS was enhanced. The magnitude of this effect was very different for different isomers. The integrated intensity of the fluorescence emission from each of the AmNS isomers in water (Φ_w) was compared with the corresponding value observed after the addition of lysolecithin (Φ_L) by determining the increment, $\Delta\Phi$, defined by the following equation:

$$\Delta\phi = \frac{\phi_L - \phi_w}{\phi_w}$$

The values of increment were plotted against the concentration of lysolecithin used. It is seen in Fig. 15.12B that the effect on 1,8-AmNS fluorescence was very large. With isomers 1,2-, 1,6-, 1,7-, and 2,1-AmNS, a sizable increase in fluorescence was observed. With 1,5-, 1,4-, and 2,6-AmNS, very little or no detectable increase was observed. The order of these isomers arranged according to the magnitude of $\Delta\Phi$ is roughly the same as that arranged in accordance with the size of the fluorescence response. A qualitatively similar result was obtained when bovine serum albumin (BSA) was used for increasing the fluorescence emission of aqueous solutions of AmNS.

The increase in fluorescence intensity observed in these experiments is thought to be brought about by a decrease in the polarity of the microenvironment of the dye molecules resulting from binding of AmNS molecules to the added macromolecules. Then, the fact that addition of the macromolecules does not enhance the fluorescence emitted by 1,5-AmNS has to be attributed to a relatively weak tendency of this compound to bind to the macromolecules. In 1,5-AmNS molecules, the two hydrophilic groups, $-\text{NH}_2$ and $-\text{SO}_3^-$, are attached to the opposite sides of the naphthalene ring. Probably, this arrangement prevents a hydrophobic bonding of 1,5-isomer with various macromolecules.

We conclude therefore that a change in the state of binding of AmNS and/or a change in the number of AmNS molecules bound to the membrane macromolecules take place during nerve excitation. A transient change in the intensity of the fluorescent light (i.e., a fluorescence response) is produced as the consequence of a change in the microenvironment of the probe molecule. Because of the negative electric charge carried by the dye molecules, externally applied AmNS tends to enter into the low-polarity sites of the axon membrane during the action potential; the positive fluorescence signals observed in crab nerves are explained in this manner. The origin of the negative signals observed with 1,8-AmNS in the axon interior will be discussed later.

L. SPECTRAL ANALYSIS OF FLUORESCENCE RESPONSES

Anilidonaphthalene sulfonate (ANS) and toluidinylnaphthalene sulfonate (TNS) are favorable membrane probes for detecting fluorescence responses. The fluorescence emission of these compounds exhibits a high polarity sensitivity. When dissolved in water, neither ANS nor TNS emits strong fluorescent light; they fluoresce intensely when dissolved in organic solvents (Weber and Laurence, 1954; McClure and Edelman, 1966). Light absorption

by these compounds is rather insensitive to changes in solvent polarity; changes in fluorescence emissions are brought about by changes in quantum yield. An increase in quantum yield is usually accompanied by a blue shift in the wavelength of emission maximum. Taking advantage of these properties, ANS and TNS have been widely used to study physicochemical properties of binding sites for these compounds in various macromolecules (e.g., Stryer, 1968).

By using squid giant axons internally stained with 2,6-TNS, attempts to determine the emission spectrum of the fluorescence response have been made (Tasaki *et al.*, 1972, 1973). In these experiments, 2,6-TNS molecules in the axon were excited with polarized quasi-monochromatic lightwave (365 nm) with its electric vector directed parallel to the longitudinal axis of the axon. In Fig. 15.13 (left) the intensity (I) of fluorescent light emitted by the stained axon in the resting state was plotted against the center wavelength of the interference filter placed between the axon and the photomultiplier. The spectrum of the component of the TNS fluorescent light that changes at the peak of the action potential (ΔI) was determined by the following procedure: fluorescence responses were recorded at 440 nm and an-

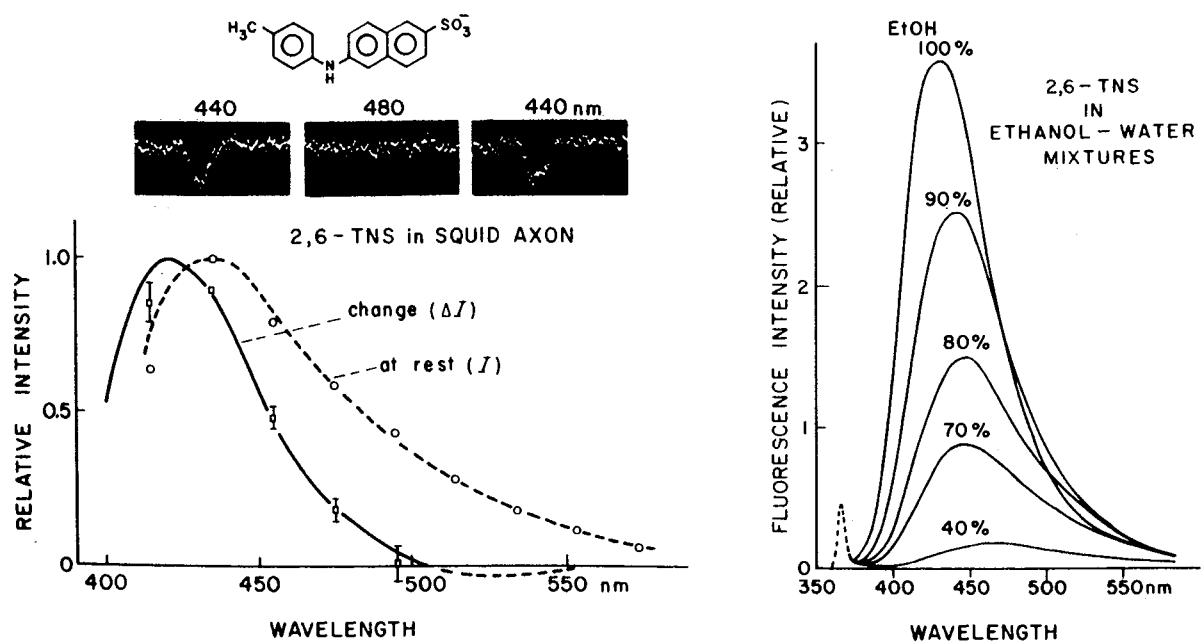


Fig. 15.13 Left: Emission spectrum of 2,6-TNS in squid giant axons at rest, and spectrum of the portion of the fluorescent light that changes during nerve excitation. Records (taken from one and the same axon) showing fluorescence changes associated with action potentials are presented at the top of the figure. The center-band wavelength (for normal incidence) of the secondary filter used is indicated above each record. The number of trials averaged was the same for the three records. The vertical lines indicate 4-msec intervals. Temperature, 6°C. Right: Corrected emission spectra of 2,6-TNS in ethanol-water mixtures. (*Biochim. Biophys. Acta* 323, 225, 1973.)

other wavelength alternately under constant illuminating and recording conditions and the magnitude of responses at these two wavelengths were compared. (Examples of such records are shown at the top of Fig. 15.13, left.) By repeating this procedure of measuring the ratio of the response amplitudes at two different wavelengths, the entire spectrum of ΔI could be determined.

The spectrum of 2,6-TNS determined by taking a transient change in fluorescence as an index (ΔI) is strikingly different from the emission spectrum in the resting state of the axon (I). The spectrum of the fluorescence response (ΔI) is sharp and narrow, having a maximum at about 420 nm and terminating abruptly at about 485 nm. It was impossible to find such a sharp and narrow spectrum from the spectra of 2,6-TNS bound to commonly available macromolecules, while the spectrum at rest is not very different from the spectra of TNS *in vitro*.

It is possible to reconstruct this sharp and narrow spectrum by taking the difference between two spectra. For example, when the emission spectrum of 2,6-TNS in 80% ethanol is subtracted from that in 100% ethanol (see Fig. 15.13, right), the resultant (difference) spectrum agrees very well with the observed response spectrum (ΔI) shown by the continuous line in Fig. 15.13 (left). The agreement between these two spectra is meaningful since the wavelength of maximum emission and the bandwidth of the 2,6-TNS spectrum are determined almost entirely by the solvent polarity (Turner and Brand, 1968). We believe, for this reason, that the transient decrease in fluorescence intensity from squid axons internally stained with 2,6-TNS is brought about by an abrupt increase in the polarity of the environment of the probe molecules.

A similar analysis was made by using crab nerves externally stained with 2-*p*-Cl-anilinonaphthalene-6-sulfonate (*p*-Cl-ANS). A crab nerve stained with this probe gave rise to negative fluorescence responses in the range of wavelengths longer than 420 nm with its maximum (absolute value) at about 453 nm. The spectrum of the portion of the fluorescent light which changes during nerve excitation (ΔI) is again sharp and narrow, and is red-shifted relative to the spectra at rest (I). By determining the fluorescence emission spectra of *p*-Cl-ANS in various organic solvents, we found that the spectrum at rest (I) is very similar to that in ethylene glycol, the wavelength of maximum emission being about 432 nm and the half-bandwidth about 77 nm. The difference between the emission spectrum of *p*-Cl-ANS in ethanol and that in ethylene glycol was found to agree with the observed spectrum of the fluorescence response (ΔI) fairly accurately. Based on these findings, it was concluded that there is a distinct fall in the polarity of the microenvironment of the *p*-Cl-ANS molecules in crab nerves during nerve excitation. Through studies of fluorescence polarization, it was inferred that these dye molecules

are partially buried in the axon membrane, with their transition moment oriented nearly perpendicular to the surface and with the sulfonate groups exposed to the aqueous phase (Tasaki *et al.*, 1976).

M. FLUORESCENCE POLARIZATION STUDIES

The orientation of probe molecules at or near the nerve membrane can be determined by studying the polarization of the fluorescent light. In these studies, an analyzer (A) was placed in the lightpath between the axon and the photodetector. Symbols A_{\perp} and A_{\parallel} are used to denote the polarizing axes of the analyzer perpendicular and parallel, respectively, to the long axis of the nerve fiber; symbols P_{\perp} and P_{\parallel} are used to denote the two alternative positions of the polarizer.

When an axon internally stained with 2,6-TNS was illuminated by a polarized light of 365 nm with its electric vector parallel to the long axis of the axon (P_{\parallel}), a transient decrease in fluorescence intensity (i.e., a negative fluorescence response) was observed during nerve excitation. The portion of the light contributing to the production of this response was highly polarized with its electric vector oriented along the long axis of the axon. With the polarizing axis of the analyzer oriented parallel to the axon (A_{\parallel}), a distinct fluorescence response was observed; but when the analyzer was rotated through 90° (A_{\perp}) under the same experimental conditions, only a record of random noise was obtained (Fig. 15.14, left).

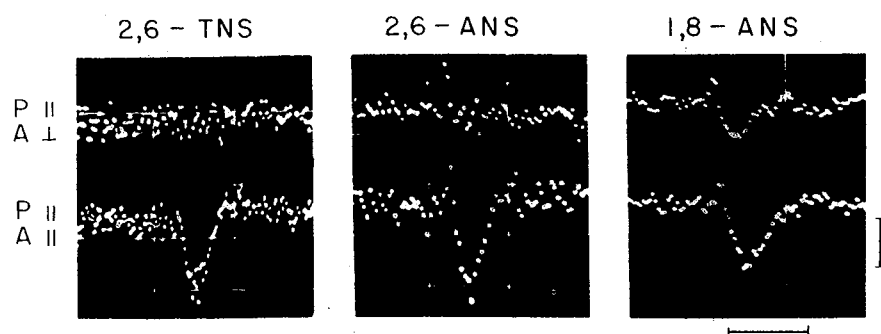


Fig. 15.14 Signal averager records showing a transient decrease in the intensity of fluorescence deriving from squid giant axons internally labeled with three different probes of anilino-naphthalene derivatives. P and A indicate the axes of the polarizer and analyzer relative to the longitudinal axis of the axon used. Two records in each column were taken from one and the same axon under the same illuminating and recording conditions. For the lower records, one vertical division represents 4.3×10^{-5} times the intensity at rest for 2,6-TNS, 3.4×10^{-5} times for 2,6-ANS, and 8×10^{-5} times for 1,8-ANS. Each horizontal division represents approximately 7.8 msec. Temperature, 7°C . (*Biophys. Chem.* 2, 319, 1974.)

The degree of polarization, P , is calculated formally by using the formula

$$P = \frac{\Delta I_{\parallel} - \Delta I_{\perp}}{\Delta I_{\parallel} + \Delta I_{\perp}}$$

where ΔI_{\parallel} and ΔI_{\perp} represent the fluorescence response amplitudes observed with the analyzer axis parallel and perpendicular, respectively, to the direction of the electric vector of the incident light. The value of P for this type of 2,6-TNS response was found to be greater than about 0.7.

Similar experiments were carried out by using squid axons internally stained with two positional isomers of anilinonaphthalene sulfonate, 2,6-ANS and 1,8-ANS. It is seen in Fig. 15.14 that, with 2,6-ANS in the axon interior, no distinct response was observed under the "parallel (polarizer)–perpendicular (analyzer)" condition. This is in sharp contrast to the behavior of 1,8-ANS with which clear signals were obtained under both the "parallel–parallel" and "parallel–perpendicular" conditions.

The upper row of Table 15.2 shows the relative sizes of the fluorescence signals in axons stained with 2,6-ANS at various combinations of orientations of the polarizer and analyzer. The lower row shows the relative sizes of responses obtained using 1,8-ANS under similar conditions. A formal calculation of P for 1,8-ANS observed with the electric vector of the incident light parallel to the long axis of the axon yielded a value of approximately 0.35. The corresponding value for 2,6-ANS was found to be larger than about 0.74. These results clearly indicate that there is a significant difference in polarization behavior between 1,8-ANS and its 2,6-isomer.

Before considering the orientation of the probe molecules in the nerve membrane, we examine the direction of the two vectors, the absorption and emission oscillators, relative to the molecular axis of the probe. When 2,6-TNS molecules are embedded in a stretched sheet of polyvinyl alcohol

TABLE 15.2

Relative Sizes of the Fluorescence Signals of Squid Giant Axons Labeled Internally with 2,6-ANS, as Compared with the Signals of the Axons Labeled with 1,8-ANS Internally^a

	$P_{\parallel}, A_{\parallel}$	P_{\parallel}, A_{\perp}	P_{\perp}, A_{\parallel}	P_{\perp}, A_{\perp}
2,6-ANS	(1)	<0.15	<0.17	0.25
1,8-ANS	(1)	0.48	0.24	0.23

^a The polarizing axes of the polarizer (P) and that of the analyzer (A) relative to the long axis of the axons are indicated. The signal amplitudes are expressed as values relative to that observed under the P_{\parallel} and A_{\parallel} conditions. The signs of the signals were all negative except the sign observed in 2,6-ANS stained axons under the P_{\perp} and A_{\perp} conditions which was positive. (From *Biophys. Chem.* 2, 319, 1974.)

(PVA) by the method described by Nishijima *et al.* (1966) and McGraw (1970), a high degree of alignment of the probe molecules can be produced (Tasaki *et al.*, 1974). A theoretical analysis of the polarized fluorescent light from 2,6-TNS in a stretched PVA sheet indicated that the absorption and emission oscillators of this molecule exist roughly in the direction of stretching of the PVA sheet. The molecular orientation axis, which tends to coincide with the direction of stretching of the PVA sheet, is considered to be close to the straight line connecting the two side groups of 2,6-TNS. Similar results were obtained from 2,6-ANS in a stretched PVA sheet. In sharp contrast to these 2,6-derivatives, the polarization of the fluorescent light emitted by 1,8-ANS in a stretched PVA sheet was imperfect.

The difference between 1,8- and 2,6-derivatives mentioned above may be explained in the following manner: Unlike 2,6-ANS, there is no clear long axis in the molecular structure of 1,8-ANS. According to the result of a theoretical calculation (Suzuki *et al.*, 1973), the lowest energy absorption band of 1-aminonaphthalene (α -naphthylamine) corresponds to two types of electronic transition moments separated by an angle of 40°; the corresponding two absorption bands are widely separated in 2-aminonaphthalene (β -naphthylamine). The pattern of light absorption by 2,6-ANS is very similar to that of 2-aminonaphthalene, while the absorption band of 1,8-ANS is comparable to that of 1-aminonaphthalene. Therefore, it is probable that the lowest energy absorption band of 1,8-ANS corresponds also to two separate electronic transitions.

From these considerations, it may be concluded that the molecules of 2,6-TNS and 2,6-ANS which contribute to the production of fluorescence responses are aligned inside the axons with their orientation axes along the long axis of the axon. The high degree of alignment of either 2,6-TNS or 2,6-ANS is considered as evidence for binding of the probe molecules to a highly ordered macromolecular structure at or near the membrane. It is probable that the assembly of threadlike elements in the ectoplasm described by Metzals and Izzard (1969) and by Metzals and Tasaki (1978) is the structure which brings about a high degree of alignment of 2,6-TNS and 2,6-ANS. A transient increase in the solubility of the protein molecules in these elements (see Chapter 9, Section D, and Chapter 15, Sections B and D) is expected to be accompanied by a change in the microenvironment of the dye molecules. Such a change could account for the process of production of fluorescence responses described above.

N. GENERAL COMMENT ON OPTICAL STUDIES

The structure of the axon membrane is very complex. We have seen in Chapter 9, Sections D and E, that the excitability of the axon is suppressed when the proteinaceous undercoating of the axolemma is removed or chem-

ically modified. We may regard, therefore, the layer that we call ectoplasm as a part of the physiological membrane. The macromolecular components of the physiological membrane are highly sensitive to physicochemical changes of their environment. The dye molecules incorporated into the nerve membrane are capable of informing us about the nature of the changes taking place during nerve excitation.

In this chapter, a brief survey was made of a variety of nonelectrical responses of nerve fibers to electric stimuli. The types of the responses surveyed are (1) responses reflecting structural changes of nerve fibers (Figs. 15.1–15.3), (2) responses generated by changes in the absorption spectrum and/or in the orientation of the dye molecules near and in the nerve membrane (Figs. 14.4–14.10), and (3) responses produced by changes in the quantum yield of dye fluorescence resulting from a disturbance of the interaction between the membrane macromolecules and dye molecules (Figs. 15.12–15.14). Other types of optical responses, e.g., those indicating the existence of fast and slow rotation of dye molecules or demonstrating energy transfer between two fluorescent molecules in the nerve membrane, were not covered in this chapter; the reader is referred to the original papers (Tasaki and Warashina, 1976b; Tasaki *et al.*, 1976).

In recent years, optical responses are treated as mere reflections of the overall potential difference across the physiological membrane (cf. Cohen *et al.*, 1974; Conti, 1975). It is quite true that many of the optical responses described in this article have a time course very similar to that of an action potential. However, we have encountered many cases where the time course of an optical response is quite dissimilar to that of the voltage pulse applied across the nerve membrane. In general, there is no simple relationship between the membrane potential and optical responses.

We regard the overall potential difference across the axon membrane as consisting of potential jumps at the phase boundaries and an intramembrane diffusion potential. Evidently, the membrane has a multilayer structure. We have noted that there are multiple binding sites in the nerve membrane for a single species of probe molecules. In order to decipher the information given to us by a dye, it is essential to understand the behavior of the dye molecules in various solvents and biological macromolecules. We now know that the mode of interaction between individual binding sites and the dye molecules can be revealed at least partly by polarization studies of the optical responses. Furthermore, we have seen that analyses of the spectra of optical responses can yield detailed information about the nature of the interaction. We thus emphasize that an attempt to explain absorption and fluorescence responses recorded without a polarizer and monochromator is almost hopeless.

The dyes which are known to give rise to absorption or fluorescence responses are amphipathic. Undoubtedly, the ionized dye molecules in the

external medium are exposed to the electric field in the Stern layer (see Verwey, 1950). A change in the field strength in this layer during the action potential may be responsible for the alteration of the angular distribution of the dye molecules. We have seen that intracellularly administered dye molecules strongly interact with the filamentous components in the ectoplasm. Absorption and fluorescence responses described in this chapter are a reflection of a transient, reversible alteration of the state of the macromolecular components of the ectoplasm.

Various aspects of nervous activity can now be correlated with physicochemical changes taking place in membrane macromolecules. Discoveries of new nonelectrical concomitants of the action potential could unquestionably brighten the future of the physiology and electrochemistry of nerve fibers.

REFERENCES

- Barker, C. C., Bride, M. H., and Stamp, A. (1959). Steric effects in di- and tri-arylmethanes. Pt. 1. Electronic absorption spectra of methyl-derivatives of Michler's hydrol blue and crystal violet; conformational isomers of crystal violet. *J. Chem. Soc.* **4**, 3957-3963.
- Baumgold, J., Terakawa, S., Iwasa, K., and Gainer, H. (1980). Membrane-associated cytoskeletal proteins in squid giant axons. *J. Neurochem.* **36**, 759-764.
- Bernard, C. (1876). "Leçons sur la Chaleur Animale, sur les Effets de la Chaleur et sur la Fièvre," 471 pp. Baillière, Paris. see p. 163.
- Blum, H. F. (1932). Photodynamic action. *Physiol. Rev.* **12**, 23-55.
- Bryant, S. H., and Tobias, J. M. (1952). Changes in light scattering accompanying activity in nerve. *J. Cell. Comp. Physiol.* **40**, 199-219.
- Cohen, L. B., Keynes, R. D., and Hille, B. (1968). Light scattering and birefringence changes during nerve activity. *Nature (London)* **218**, 438-441.
- Cohen, L. B., Hille, B., Keynes, R. D., Landowne, D., and Rojas, E. (1971). Analysis of the potential-dependent changes in optical retardation in the squid giant axon. *J. Physiol. (London)* **218**, 205-237.
- Cohen, L. B., Salzberg, B. M., Davila, H. V., Ross, W. N., Landowne, D., Waggoner, A. S., and Wang, C.-H. (1974). Changes in axon fluorescence during activity: Molecular probes of membrane potential. *J. Membr. Biol.* **19**, 1-36.
- Conti, F. (1975). Fluorescent probes in nerve membranes. *Annu. Rev. Biophys. Bioeng.* **4**, 287-310.
- Downing, A. C., Gerard, R. W., and Hill, A. V. (1926). The heat production of nerve. *Proc. Ry. Soc. (London)* **100B**, 223-251.
- Feofilov, P. P. (1961). "The Physical Basis of Polarized Emission." Consultants Bureau, New York.
- Gerard, R. W. (1932). Nerve metabolism. *Physiol. Rev.* **12**, 469-592.
- Gerard, R. W. (1937). The metabolism of brain and nerve. *Annu. Rev. Biochem.* **6**, 419-444.
- Hill, A. V. (1912). The absence of temperature changes during the transmission of a nerve impulse. *J. Physiol. (London)* **43**, 433-440.
- Hill, B. C., Schubert, E. D., Nokes, M. A., and Michelson, R. P. (1977). Laser interferometer measurement of changes in crayfish axon diameter concurrent with action potential. *Science* **196**, 426-428.

- Hill, D. K. (1950). The volume change resulting from stimulation of a giant nerve fibre. *J. Physiol. (London)* **111**, 304–327.
- Hill, D. K., and Keynes, R. D. (1949). Opacity changes in stimulated nerve. *J. Physiol. (London)* **108**, 278–281.
- Hodgkin, A. L. (1951). The ionic basis of electrical activity in nerve and muscle. *Biol. Rev.* **26**, 339–409.
- Iwasa, K., and Tasaki, I. (1980). Mechanical changes in squid giant axons associated with production of action potentials. *Biochem. Biophys. Res. Commun.* **95**, 1328–1331.
- Kayushin, L. P., and Lyudkovskaya, R. G. (1955). Elastic and electrical phenomena in nerve in the propagation of excitation. *Doklady Akad. Nauk SSSR.* **102**, 727–728.
- Keynes, R. D. (1951). The leakage of radioactive potassium from stimulated nerve. *J. Physiol. (London)* **113**, 99–113.
- McClure, W. O., and Edelman, G. M. (1966). Fluorescent probes for conformational states of proteins. I. Mechanism of fluorescence of 2-*p*-toluidinylnaphthalene-6-sulfonate, a hydrophobic probe. *Biochemistry* **5**, 1908–1918.
- McGraw, G. E. (1970). Study of molecular orientation in poly(ethylene terephthalate) fibers by fluorescence polarization. *J. Polym. Sci. A.* **8**, 1323–1336.
- Nishijima, Y., Onogi, Y., and Asai, T. (1966). Methods for studying molecular orientation in polymer solids. *J. Polym. Sci. C* **15**, 237–250.
- Ross, W. N., Salzberg, B. M., Cohen, L. B., and Davila, H. V. (1974). A large change in dye absorption during the action potential. *Biophys. J.* **14**, 983–986.
- Sato, H., Tasaki, I., Carbone, E., and Hallett, M. (1973). Changes in axon birefringence associated with nerve excitation: Implications for the structure of the axon membrane. *J. Mechanochem. Cell. Motil.* **2**, 209–217.
- Stryer, L. (1968). Fluorescence spectroscopy of proteins. *Science* **162**, 526–533.
- Suzuki, S., Fujii, T. and Baba, H. (1973). Interpretation of electronic spectra by configuration analysis absorption spectra of monosubstituted naphthalenes. *J. Mol. Spectros.* **47**, 243–251.
- Tasaki, I., Carbone, E., Sisco, K., and Singer, I. (1973). Analyses of extrinsic fluorescence of the nerve membrane labeled with aminonaphthalene derivatives. *Biochim. Biophys. Acta* **323**, 220–233.
- Tasaki, I., Carnay, L., and Watanabe, A. (1969). Transient changes in extrinsic fluorescence of nerve produced by electric stimulation. *Proc. Natl. Acad. Sci. U.S.A.* **64**, 1362–1368.
- Tasaki, I., and Sisco, K. (1975). Electrophysiological and optical methods for studying the excitability of the nerve membrane. *Methods Membr. Biol.* **5**, 163.
- Tasaki, I., Sisco, K., and Warashina, A. (1974). Alignment of anilinonaphthalene-sulfonate and related fluorescent probe molecules in squid axon membrane and in synthetic polymers. *Biophys. Chem.* **2**, 316–326.
- Tasaki, I., and Warashina, A. (1976a). Dye-membrane interaction and its changes during nerve excitation. *Photochem. Photobiol.* **24**, 191–207.
- Tasaki, I., and Warashina, A. (1976b). Fast and slow rotation of dye molecules in squid axon membrane during excitation. *Proc. Jpn. Acad. Sci.* **52**, 37–41.
- Tasaki, I., Warashina, A., and Pant, H. (1974). Energy transfer between fluorescent probe molecules in and across nerve membrane. *Biol. Bull.* **147**, 501.
- Tasaki, I., Warashina, A., and Pant, H. (1976). Studies of light emission, absorption and energy transfer in nerve membranes labelled with fluorescent probes. *Biophys. Chem.* **4**, 1–13.
- Tasaki, I., Watanabe, A., and Hallett, M. (1972). Bioenergetics of nerve excitation. *J. Membr. Biol.* **8**, 109–132.
- Tasaki, I., Watanabe, A., Sandlin, R., and Carnay, L. (1968). Changes in fluorescence, turbidity and birefringence associated with nerve excitation. *Proc. Natl. Acad. Sci. U.S.A.* **61**, 883–888.

- Tashiro, S. (1913). Carbon dioxide production from nerve fibers when resting and when stimulated. *Am. J. Physiol.* **32**, 107–136.
- Teorell, T. (1962). Excitability phenomena in artificial membranes. *Biophys. J.* **2**, 27–52.
- Turner, D. C., and Brand, L. (1968). Quantitative estimation of protein binding site polarity. Fluorescence of *N*-arylamino-naphthalene-sulfonates. *Biochemistry* **7**, 3381–3390.
- Verwey, E. J. W. (1950). Theory of the electric double layer of stabilized emulsions. *K. Akad. Wet., Amsterdam* **53**, 376–385.
- Warashina, A., and Tasaki, I. (1975). Evidence for rotation of dye molecules in membrane macromolecules associated with nerve excitation. *Proc. Jpn. Acad.* **51**, 610–615.
- Watanabe, A., Terakawa, S., and Nagano, M. (1973). Axoplasmic origin of the birefringence change associated with excitation of a crab nerve. *Proc. Jpn. Acad.* **49**, 470–475.
- Weber, G., and Laurence, D. J. R. (1954). Fluorescent indicators of adsorption in aqueous solution and on the solid phase. *Biochem. J.* **56**, 31.

INDEX

- A**
- Absorption oscillator, 318
 - A.C. stimulation, 23, 24
 - high frequency, 25, 109
 - low frequency, 120
 - Accommodation process, 26, 31, 114, 196
 - time constant, 116
 - Acrylonitrile, 165
 - Actin, 159
 - Action current, discovery of, 9
 - Action potential
 - abolition of, 66, 181, 270
 - bi-ionic, 232
 - definition, 54, 58, 131, 143, 298
 - fall of membrane resistance during, 69, 113
 - intracellular recording of, 131
 - overshoot, 132
 - recovery after abolition, 68
 - repetitive firing, 122, 191, 196, 271
 - shoulder, 66, 133, 219, 233, 264, 273
 - undershoot, 133
 - of single node, 64
 - recorded under space-clamp, 145
 - under zero resting potential, 284
 - Active patches, spots, iron-wire nerve model, 33
 - Active transport, 287, 291
 - Adrian's rule on refractoriness, 65
 - After-potential, 78
 - Amino-group modifying reagents, 166
 - Aminonaphthalene-sulfonate, 331
 - 4-Aminopyridine, effect of, 193
 - Ammonium ion, 212
 - Ampère's galvanometer, 8
 - Anelectrotonus, 15
 - Anesthetics, effect on nerve conduction, 81
 - Anilinonaphthalene-sulfonate (ANS), 333, 336
 - Animal electricity, discovery of, 8
 - Anions, effect on excitability, 208
 - Anisotropic resistivity of nerve, 37
 - Anodal block, 15
 - Anodal polarization, 38
 - Apáthy neurofibril hypothesis, 19, 38
 - Auflockerung (loosening) of membrane macromolecules, 28, 232
 - Arvanitaki's subthreshold oscillation, 122, 187
 - Axis cylinder, resistance of, 93
 - Axolemma, 155, 157
 - Axon
 - chemical modification of proteins in, 164
 - diameter and conduction velocity, 177
 - membrane
 - cooperative process in, 200, 271, 272, 275
 - critical point for transition, 249
 - domains, 252, 275
 - instability, 248–250
 - pores, 300
 - spatial nonuniformity, 275
 - water content, 273
 - squid, chemical stimulation of, 185

surface, displacement of, 307
 Axon sheath, ultrastructure of, 155, 156
 Axoplasm, electrolytes in, 158

B

Barkhausen effect, 275
 Basement membrane, 156
 Bean's discrete conduction states, 254, 266
 Bernstein's membrane hypothesis, 18, 132, 283
 Bethe's membrane polarization, 126, 198, 233
 Bi-ionic conditions, electric excitation under, 269
 Bimetallic arc (Galvani), 6
 Birefringence
 of axoplasm, 160
 of ectoplasm, 308
 responses, 308, 309
 Blood, of vertebrates, 290
 Break excitation, 15, 127, 184, 196
 Bunge-Quinton-Macallum hypothesis, 290

C

Cable equation, derivation of, 96
 Cable properties, 26, 30, 34
 Ca-bridges, 234, 247, 267, 272
 Ca-cross link, 267, 272
 Ca-ion
 concentration, lowering of, 187, 190, 193
 effect on membrane current, 294
 in excitable tissues, 27, 158, 228
 influx across axon membrane, 224
 intracellular, 158, 228
 Carboxypeptidase, 167
 Catelectrotonus, 15
 Cation, polyatomic univalent, 211, 238
 Cation-exchange membrane, 260, 263
 Cation salts, divalent
 in cation-exchange membrane, 225
 external, dilution of, 214
 Cathodal depression (Werigo), 125
 C fibers, 88
 Chemical stimulants, classification of, 193
 Chiriquitoxin, 172
 Chronaxie, 29, 111
 Colchicine, 310
 Colloid chemical theory, 27, 257

Concentration profiles, 263
 Condenser discharge pulses, 24, 31, 106
 Conditioning stimulating pulse, 100
 Conduction
 of impulse along anesthetized region, 80
 restoration, by D.C. polarization, 77
 Conduction time, internodal, 54, 73, 98
 Conduction velocity, dependence on
 fiber diameter, 87, 117
 internodal distance, 89
 Constant field equation, 17, 139
 Cooperativity, 234
 Core-conductor properties, 30
 Co-salt, 127
 Cremer's membrane hypothesis, 17, 133
 Critical point for transition, axon membrane, 249
 Cs-ions, 273
 Curare, 30
 Current-voltage relations, 260
 Cyanogen bromide, 167

D

Davis' transitional decrement, 84
 Demyelination, experimental, 85
 Depolarization, 283, 285
 abrupt, 242
 Dicarboyanine, 314, 317
 Diffusion in
 stagnant solution layer, 258
 unstirred layers, 258, 270, 272
 Double condenser stimulating pulse, 120
 du Bois-Reymond's galvanometer, 9
 du Bois-Reymond's theory of excitation, 13, 22
 Dye, *see also* specific compounds
 angular distribution of molecules, 319
 degree of parallel orientation, 320
 degree of perpendicular orientation, 320
 mathematical expressions for absorption responses, 318

E

Ectoplasm, 161, 308
 release of proteins, 162
 scanning electron microscopy, 162
 ultrastructure, 160
 Electricity, limiting quantity, 102

Electric self-stimulation (Selbstreizung), 286
 Electrode, hyperfine glass-pipette, 58
 internal metal-wire recording, introduction of, 143
 nonpolarizable, 10
 Electrolytes in axoplasm, 158
 Electroneutrality, 16, 18, 262, 292
 Electrotonic current, potential, spread of, 45, 93
 Electrotonic potential, spread of, 93
 Endoplasm, dye-loaded, optical signals, 311
 Enthalpy changes, 248
 Entropy change, 248
 Erlanger-Gasser nerve-fiber types, 88
 Excitation, nonelectrical signs of, 304

F

Fiber diameter, conduction velocity, 87
 Fiber types, A, B, and C, 88
 Fluorescence, extrinsic, 329
 Fontana's analog of all-or-none law, 62
 Frankenhaeser-Hodgkin stagnant layer, 157
 Frog nerve, cold, 122

G

Galvani's experiment, with bimetallic arc, 7
 "Gating current," 265
 Glutaraldehyde, effect of, 202

H

Helmholtz's experiments on nerve, 12
 Hermann's local current theory, 32
 Hermann's principle of self-stimulation, 32, 286
 Hill's theory of nerve excitation, 26, 31
 Histidine modifying reagents, 166
 Hodgkin-Huxley theory, 148
 Hofmeister series, 28, 208
 Hoorweg's equation, 24
 Hydration, of membrane macromolecules, 267
 Hydrogen peroxide, 166
 Hyperpolarization, 15, 283
 Hyperpolarizing responses, 182, 245
 Hysteresis, 247, 252, 275
 under voltage clamp, 252

I

Injury currents, injury potential, 9, 138
 Instability, axon membrane, 248-250
 Integral membrane proteins, 168
 Interdiffusion flux across axon membrane, 219
 Internodal conduction time, 54, 73, 98
 critical, 83
 Internodal distance, 88
 Intramembrane concentration profiles, 263
 Iodoacetate, 165
 Ion-antagonism (Loeb), 27, 138, 140, 141, 193
 Ion-exchanger, "irregular", 273
 Ion-permeability, 287
 Ion-pump, 293

J

Jump of nerve impulse from one fiber to another, 52

K

Kato's limit length, 83
 Katz equation on repetitive firing, 122
 K-Ca bi-ionic action potential, 236
 KCl, internal perfusion with, 161
 K depolarization, 140
 K-ion
 Ca-bridges, 272
 effect on nerve membrane, 136, 140
 efflux measurement, 220
 intracellular, dilution of, 216
 K-salts, accumulation of, 290
 Krohg's permeability coefficient, 287

L

Lapicque's chronaxie, 29
 Latent addition, 100
 Least interval between two impulses, 79
 Light absorption signal, response, 312-329
 Light scattering signal, 312
 Light polarization, in optical studies, 315, 317, 319, 322
 Lillie's iron wire analog, 33
 Ling's hypothesis, 293
 Lipid-sieve theory, 299

- Lipids of giant nerve fiber, 160
 Lipid solubility theory, 299
 Local circuit theory, 51
 Local microcurrent (Strömchen), 275, 276, 287
 Loeb's theory of nerve excitation, 27, 140, 185
 Lyotropic numbers, 209
 Lyotropic series, 28, 209
- M**
- Macromolecular transitions, 234
 Macromolecular model of axon membrane, 268
 Maleimides, 165
 Matsumoto-Tasaki equation, 177
 Membrane, *see also* Axon membrane
 cation-exchange, 260, 263
 fraction in excited state, 277
 multi-layer structure, 18
 semipermeable, 16, 24
 Membrane current observed under voltage clamp, 146
 Membrane hypotheses, 16
 Membrane impedance, 69, 133
 Membrane macromolecules
 expansion of, 266
 hydration of, 267
 loosening (Auflockerung), 28
 swelling, 272
 tightening (Verdichtung), 28
 Membrane noise, 201
 Membrane polarization, 282
 Membrane proteins,
 integral, 168
 intrinsic, 168
 peripheral, 168
 Membrane resistance, during action potential, 69, 133
 Merocyanine-540, 315, 317, 324
 Methylene blue, 166
 Microelectrode
 recording from myelinated fiber, 58
 study of Schwann cell, 157
 Microtubules, 159
 Minimal gradient, current, 114, 179
 Mg-ion, 232
 versus Ca-ion, 233
 Monnier's pararesonance, 121, 187
- Muscle twitch, without metal, 8
 Myelin sheath
 capacitative flow of current through, 54
 resistance and capacity of, 19, 71, 93
 time constant, 73
- N**
- Na-Ca ion-mixture, externally applied, 240
 Na current, 148, 285
 Na-free media, excitation in, 143
 Na ion, effect of, 140
 Na-K ion-exchange, 307
 Na-K ion interdiffusion, 273
 Na-K substitution inside, 216, 218
 Na oleate, effect of, 85
 Na salt solution, internally applied, 217, 234
 Negative variation, nerve response to electric stimuli, 10
 Nerve
 anisotropic resistivity, 37
 conduction
 during refractory period, 77
 safety factor, 79
 Nerve excitation, two-factor theory, 30
 Nerve fiber
 isolation, 37
 mechanical changes in, 305
 movement, 305
 nonmyelinated, 130
 Nerve impulse
 collision of, 71, 86, 125
 conduction along anesthetized region, 80
 high frequency, effect of, 125
 isolated conduction, 53
 jump, 52
 propagation across inexcitable nodes, 47
 Nerve membrane, swelling, 267, 270
 Nerve stimulation, tripolar, 43
 Neurofibrils, 19
 Neurofibril theory, 38
 Neurofilaments, 159
 Nernst equation, 16, 26
 Nernst's theory of excitation, 24
 Nerve conduction during refractory period, 77
 Ni-salt, 127
 Nodal membrane, 44, 45

capacity, 93
 resistance and capacity of, 73, 93
 time constant, 73
 Node of Ranvier, 94
 all-or-none property, 62
 gun-powder analogy, 62
 ultrastructure of, 94

O

Optical responses, 310–341
 membrane potential and, 328
 Oscillatory subthreshold responses, 186
 Ostwald-Lillie nerve analog (model), 265, 275
 Overton's lipid solubility theory, 299

P

Pacemaker, 123
 Pararesonance (Monnier), 121, 187
 Patches
 active, 33
 in excited state, 33, 192, 202
 PCMB (Parachloromercuribenzoate), 166
 Perfusion, intracellular, of giant axons, technique, 206
 Periodic miniature responses, 187, 191
 effect of TEA on, 198
 of TTX on, 198
 induced by electric currents, 195
 intracellular pH, 226
 Pflüger's rule of excitability, 15, 128
 pH
 intracellular, 226
 alkaline shift, 186
 Phase-boundaries, 17, 137, 214, 250
 Phase transition, 246, 249, 270
 Planck equation, 17
 Plasma membrane model, 168
 Polarization of light in optical studies, 315, 317, 319, 322
 Polarizing current
 effect, 74, 76
 unidirectional conduction produced by, 76
 Polyatomic univalent cations, 211
 salts, internally applied, 238
 Pores, in axon membrane, 300

Potential field in two-dimensional fluid medium, 40, 42
 Pouillet's method, 11
 Proteases, action of, 270
 Proteins
 in axoplasm, 158
 chemical modification of, in axon, 164
 Proteolytic enzymes, 167

R

Ranvier's illustration, 39
 Rb-ion, 211, 219, 222, 273
 Recovery, supernormal phase of, 78
 Recovery curve, 77
 of node, 66
 Rectification of A.C. by nerve membrane, 110
 Refractory period, 65
 relatively, 65
 Relaxation oscillation, 123
 Repetitive firing
 of action potentials, 122, 191, 196, 271
 resetting of rhythm, 123
 Resistance
 of axis-cylinder, 93
 of myelin sheath, 93
 of nodal membrane, 93
 Resistance-flux product, 219
 Re-stimulation by local currents (Hermann), 32
 Rheobase, 29, 111
 Rose bengal, 166, 193
 Rushton's liminal length, 32

S

Saponin, effect of, 85
 Saxitoxin (STX), 170
 Scanning electron microscopy of ectoplasm, 162
 Schwann cells of squid giant nerve fiber, 155
 Scorpion venom, effect of, 191, 192, 193
 Singer Nicolson membrane model, 168
 Sollner's oxidized collodion membrane, 137
 Squid axon, see axon, squid
 Stable state, definition, 182, 249, 252, 269
 Strength-duration relation, 28, 31, 107
 Strength-frequency relation, 109

- Strength-latency relation, 98
Strömchen (Hermann), 32, 275
Subthreshold response, 33, 63, 115, 186
 local summation of effects, 100
Sulphydryl reagents, 165
Swelling
 of membrane macromolecules, 272
 of nerve membrane, 267, 270
- T**
- Temperature change, 74, 78, 90, 178, 191,
 193, 198, 247, 248
Teorell's hydraulic model, 265
Teorell–Meyer–Sievers theory, 137, 283
Test stimulating pulse, 100
Tetanic stimulation, 124
Tetraethylammonium (TEA), 164, 179, 198,
 238, 274
Tetrodotoxin (TTX), 169, 191, 198, 212, 237
Threshold along myelinated fiber, 40
Threshold depression, 104–110
 produced by blocked impulse, 50
 superposition of, 105
Threshold strength, 22, 24
Time constant
 of accommodation, 116
 of myelin sheath, 73
 of nodal membrane, 73
Toluidinylnaphthalene-sulfonate (TNS), 334,
 336
Transitional decrement (Davis), 84
Trypsin, 167
- Tubulin, 159
Two-stable states of axon membrane, 268,
 272, 275
- U**
- Unstirred diffusion layers, 258, 270, 272
Ultrastructure
 of axon sheath, 155, 156
 of ectoplasm, 160
 of node of Ranvier, 94
- V**
- Verdichtung (tightening), membrane macro-
 molecules, 28, 233
2-Vinylquinoline, 165
Voltage-clamp
 membrane domains, 276, 278
 procedure, 146, 287, 296
Voltage pulse, exponentially rising, 116
von Kries' experiment on A.C. stimulation,
 23
- W**
- Water
 content of axon membrane, 273
 molecules in membrane, 248, 272, 273
Wedensky inhibition, 84
Weiss' formula, 29
Weisbuch-Neumann theory of hysteresis,
 247

